

UC Irvine

UC Irvine Electronic Theses and Dissertations

Title

Strategies for the Syntheses of Complex Molecules

Permalink

<https://escholarship.org/uc/item/3gs810th>

Author

Mills, Riley Brigdon

Publication Date

2022

Peer reviewed|Thesis/dissertation

UNIVERSITY OF CALIFORNIA,
IRVINE

Strategies for the Syntheses of Complex Molecules

DISSERTATION

submitted in partial satisfaction of the requirements
for the degree of

DOCTOR OF PHILOSOPHY

in Chemistry

by

Riley Bridgon Mills

Dissertation Committee:
Professor Christopher D. Vanderwal, Chair
Professor Scott D. Rychnovsky
Professor Sergey V. Pronin

2022

DEDICATION

To

My Parents

Laura

and

George Mills

TABLE OF CONTENTS

	Page
LIST OF SCHEMES	vii
LIST OF FIGURES	ix
LIST OF TABLES	x
LIST OF EQUATIONS	xi
ACKNOWLEDGEMENTS	xv
VITA	xvii
ABSTRACT OF THE DISSERTATION	xix
Chapter 1: Development of Isocyanoterpene Analogues for the Treatment of Malaria	1
1.1 Introduction	1
1.2 Malaria	1
1.2.1 An Introduction to Malaria	1
1.2.2 Genus Plasmodium and Their Biological Effects	2
1.2.3 Early Therapies for Malarial Infections	3
1.2.4 Artemisinin and its Derivatives	4
1.2.5 Combination Therapies	5
1.2.6 Isocyanoterpenes: Investigations of Bioactivities and Syntheses	6
1.3 Synthesis of Artemisinin-Isonitrile	7
1.3.1 Project Considerations	7
1.3.2 Synthetic Considerations	7
1.3.3 Previous Synthetic Efforts	8
1.3.4 Initial Synthetic Efforts	9
1.3.5 Completed Synthesis of Artemisinin-Isonitrile	10
1.3.6 Biological Assays	10
1.3.7 Conclusions	11
1.4 Synthesis of MK-109 and MK-110	12
1.4.1 Introduction	12
1.4.2 Previous Syntheses	12
1.4.3 Efforts Toward a Concise Synthesis of MK-109 and MK-110	13
1.4.4 Synthetic Reconsiderations	14
1.4.5 Completed Syntheses	14
1.4.6 Biological Assays	15
1.4.7 Conclusions	15
1.5 Project Conclusions	16
1.6 Distribution of Credit and Contributions	16
1.7 Experimental Information	17
1.7.1 Materials and Methods	17
1.7.2 Experimental Procedures	18
1.8 References	26
Chapter 2: Introduction to the Curvulamine Family of Natural Products	30
2.1 Introduction	30
2.2 Isolation	30
2.2.1 Antibiotic Resistance	30
2.2.2 Isolation of the Curvulamine Family	31

2.3 Biological Considerations	31
2.3.1 Bioactivity of the Curvulamines	31
2.3.2 Biosynthetic Studies	32
2.3.3 Efforts Toward High Scale Isolation of the Curvulamines	33
2.3.4 Genome Modifications Resulting in Novel Products	34
2.4 Structural Considerations and Synthetic Efforts	35
2.4.1 Structural Analysis	35
2.4.2 Synthetic Considerations	36
2.4.3 <i>Previous Synthetic Efforts by the Vanderwal Lab</i>	37
2.4.4 <i>Maimone and Coworkers' Total Synthesis</i>	39
2.5 Conclusions	40
2.6 References	40
Chapter 3: Efforts Toward the Synthesis of the Curvulamines and Investigations of Novel Pyrrole Annulation Chemistry	43
3.1 Introduction	43
3.2 Synthesis of the Curvulamides Piperidine Cores	43
3.2.1 Justification for the Synthesis of the Curvulamides	43
3.2.2 Initial Synthetic Efforts from a Previously Synthesized Intermediate	44
3.2.3 Reconsideration of Approach	45
3.2.4 Successful Synthesis of The Core of Curvulamide A	46
3.2.5 Efforts Toward the Core of Curvulamide B	46
3.2.6 Revised Synthesis to Afford the Piperidine Cores in a Divergent Manner	47
3.3 Efforts Toward the Curvulamides via Pyrrole Annulation	48
3.3.1 Heterocycle Synthesis via C–H Bond Insertion Reactions	48
3.3.2 Previously Reported Heterocycle Annulation Methods	49
3.3.3 Attempted Applications of Pyrrole Annulation Chemistry to Afford Curvulamide A	51
3.3.4 Strategy for the Development of a Novel Pyrrole Annulation Methodology	52
3.3.5 Aza-Michael Addition Strategies	53
3.3.6 α -Carbamyl Radical Strategy	55
3.4 Conclusions	56
3.5 Distribution of Credit and Contributions	57
3.6 Experimental Information	57
3.6.1 <i>Materials and Methods</i>	57
3.6.2 Experimental Procedures	58
3.7 References	66
Chapter 4: Efforts Toward the Total Synthesis of the Curvulamines	69
4.1 Introduction	69
4.2 Radical Bicyclization Route	69
4.2.1 Synthetic Considerations	69
4.2.2 Aza-radical Bicyclization	70
4.2.3 Retrosynthetic Analysis	72
4.2.4 Precursor Syntheses	72
4.2.5 Efforts Toward Bicyclization	74
4.3 Enolate Alkenylation Strategy	77
4.3.1 Retrosynthetic Considerations	77
4.3.2 Optimization of Piperidinone Synthesis	78

4.3.3 Amine Fragment Synthesis	80
4.3.4 Bimolecular Enolate Vinylation Efforts	80
4.3.5 Imine Condensation Efforts	81
4.4 Conclusions	82
4.5 Distribution of Credit and Contributions	83
4.6 Experimental Information	83
4.6.1 Materials and Methods	83
4.6.2 Experimental Procedures	84
4.7 References	94
Chapter 5: Progress Toward the Total Synthesis of the Arcutine Family of Natural Products	97
5.1 Introduction	97
5.2 Discovery and Biological Evaluations of the Arcutines	97
5.2.1 Diterpene Alkaloids	97
5.2.2 Discovery of the Arcutines	98
5.2.3 Biosynthesis	99
5.2.4 Structural Analysis	100
5.3 Previous Total Syntheses	100
5.3.1 Qin's Total Synthesis	100
5.3.2 Li's Total Synthesis	102
5.3.3 Sarpong's Total Synthesis	103
5.4 Efforts Toward the Total Synthesis of the Arcutines	104
5.4.1 Synthetic Analysis	104
5.4.2 Amine Fragment Synthesis	106
5.4.3 Key Transformation Model System	106
5.4.4 Biocatalytic Dearomative Dihydroxylation	107
5.4.5 Retrosynthetic Reconsiderations	108
5.4.6 Phenol Synthesis	109
5.4.7 Reductive Ozonolysis Strategy	110
5.4.8 Chemoselective Acryloylation	111
5.4.9 Dearomative Oxidation	112
5.4.10 Preliminary Investigations into Enantioselective Oxidative Dearomatization	113
5.4.11 Electronically Mismatched Intramolecular Diels-Alder Cycloaddition	114
5.4.12 Optimization of Ketone Reduction	116
5.4.13 Acetate Pyrolysis	117
5.4.14 Fragment Convergence	118
5.4.15 Attempts at Derivatization	120
5.4.16 Revised Fragment Convergence and Future Directions	120
5.5 Conclusions	121
5.6 Distribution of Credit and Contributions	122
5.7 Experimental Information	122
5.7.1 Materials and Methods	122
5.7.2 Experimental Procedures	123
5.8 References	135
Chapter 6: Investigations into Alkene Metathesis in the Presence of Iron-Tricarbonyl Complexed Diene Systems	140
6.1 Introduction	140

6.2 Previous Work on Iron-Tricarbonyl Complexed Dienes	140
6.2.1 History of Diene-Iron Tricarbonyl Complexes	140
6.2.2 Methods of Iron-Diene Complexation	141
6.2.3 Decomplexation Methodologies	142
6.2.4 Iron-Tricarbonyl Diene Complex Reactivity	142
6.2.5 Stability of Iron-Diene Complexes	143
6.3 Alkene Metathesis in the Presence of Iron-Diene Systems	143
6.3.1 Alkene Metathesis Off-site Reactivity and Relay	143
6.3.2 Project Considerations	145
6.3.3 Model Studies	146
6.3.4 Cross-Metathesis Studies	146
6.3.5 Expansion of Scope	147
6.3.6 Synthesis of Bridged Bicyclic Systems	148
6.4 Applications of this Strategy Toward Transannular Diels-Alder Adducts	149
6.4.1 Substrate Synthesis	149
6.4.2 Investigations of Macrocyclization	152
6.5 Conclusions	153
6.6 Distribution of Credit and Contributions	154
6.7 Experimental Information	154
6.7.1 Materials and Methods	154
6.7.2 Experimental Procedures	155
6.8 References	171
APPENDIX A: NMR Spectra	174
APPENDIX B: X-Ray Crystallographic Data	294

LIST OF SCHEMES

	Page
Scheme 1.1: Completed synthesis of tetralone intermediate.	13
Scheme 1.2: Retrosynthetic considerations.	14
Scheme 2.1: Initial proposal of the biosynthesis of the curvulamines.	32
Scheme 2.2: Revised biosynthetic proposal.	33
Scheme 2.3: Curandolazine and its proposed biosynthesis.	33
Scheme 2.4: Synthetic analysis of the curvulamines and curvulamides.	36
Scheme 2.5: Retrosynthetic elaboration to the core.	37
Scheme 3.1: Retrosynthetic considerations.	44
Scheme 3.2: Tetrahydropyridine strategy.	45
Scheme 3.3: Investigations into diastereoselective epoxidation by Marazano and coworkers.	46
Scheme 3.4: Diastereocontrolled epoxidation via N-oxide directing.	47
Scheme 3.5: Proposed synthesis of the core of curvulamide B.	48
Scheme 3.6: General pathway for C-H activated heterocycle formation.	49
Scheme 3.7: Proposed mechanism for Yoshida's pyrrole annulation methodology.	49
Scheme 3.8: Retrosynthetic analysis of proposed annulation.	52
Scheme 3.9: Synthon derivitization.	53
Scheme 3.10: Proposed aza-Michael/Brook pyrrole annulation methodology.	53
Scheme 3.11: Proposed a-carbamyl radical pyrrole annulation sequence.	55
Scheme 4.1: Intramolecular amination strategy.	70
Scheme 4.2: Synthesis of 5-methylene pyrrolidinones from N-aryloxycarbamates.	71
Scheme 4.3: Radical cyclization developed by Leonori and coworkers.	75
Scheme 4.4: Narasaka-Heck cyclization developed by Bower and coworkers.	75
Scheme 4.5: Proposed 1,5-HAT disrupting the desired reaction pathway.	77
Scheme 4.6: Enolate vinylation retrosynthesis.	77
Scheme 4.7: Model for predicted diastereoselectivity of enolate alkenylation.	78

Scheme 4.8: Proposed enamine cyclization strategy.	81
Scheme 5.1: Proposed biosynthesis of arcutinidine and atropurpuran from hetidine scaffold.	99
Scheme 5.2: Proposed biosynthesis of hetidine scaffold from GGPP.	99
Scheme 5.3: Qin's key aza-Wacker cyclization and intramolecular Diels-Alder cyclization.	100
Scheme 5.4: Li's key cationic cascade reaction.	102
Scheme 5.5: Li's completed synthesis of arcutinidine.	102
Scheme 5.6: Retrosynthetic analysis of arcutinidine via central fragmentation.	104
Scheme 5.7: Retrosynthetic analysis for the synthesis of arcutinidine.	105
Scheme 5.8: Proposed bicyclization cascade.	105
Scheme 5.9: Precedented biocatalytic dearomative dihydroxylation vs. desired enantiomer.	105
Scheme 5.10: Model system developed to test Dieckmann alkylation cascade.	106
Scheme 5.11: Reconsidered retrosynthetic analysis of the eastern fragment.	108
Scheme 5.12: Regioselectivity challenge of dearomative oxidation.	111
Scheme 5.13: Screen of hypervalent iodine reagents in acidic medium.	112
Scheme 5.14: Proposed intramolecular Diels-Alder cycloaddition.	114
Scheme 5.15: Proposed electronically-matched intramolecular Diels-Alder transform.	114
Scheme 5.16: Necessary functional group interchange.	116
Scheme 5.17: Efforts to attenuate the primary alcohol nucleophilicity.	120
Scheme 5.18: Future directions for fragment convergence.	121
Scheme 5.19: Proposed Future Directions for Completion of the Synthesis.	121
Scheme 6.1: Initial synthesis of iron-tricarbonyl butadiene and common representations.	140
Scheme 6.2: Relay ring-closing metathesis.	144
Scheme 6.3: Project goals.	145
Scheme 6.4: Proposed formal synthesis to brascilicardin A.	145
Scheme 6.5: Retrosynthetic analysis of iron-diene complexed TADA precursor.	149

LIST OF FIGURES

	Page
Figure 1.1: Quinine and quinidine.	3
Figure 1.2: Chloroquine and hydroxychloroquine.	3
Figure 1.3: Artemisinin and common derivatives.	4
Figure 1.4: Bioactive isocyanoterpenes.	6
Figure 1.5: Structural similarities of artemisinin and known ICTs.	7
Figure 1.6: Unambiguous structural determination of formyl triazene via x-ray crystallography.	9
Figure 1.7: Unambiguous structural determination of artemisinin analogue.	10
Figure 1.8: Targeted analogues.	12
Figure 2.1: Members of the curvulamine family.	30
Figure 2.2: The curvulamines.	35
Figure 2.3: The curvulamides.	35
Figure 3.1: The curvulamides.	43
Figure 3.2: Tetrahydropyridine structural analysis.	45
Figure 4.1: Members of the curvulamine family.	69
Figure 4.2: Targeted core of curvulamine A.	69
Figure 5.1: The arcutine family of natural products.	97
Figure 5.2: Aconicarmicharcutinium A.	98
Figure 5.3: Structural analysis of arcutinidine.	100
Figure 5.4: Unambiguous structural determination of cycloaddition product via X-ray crystallography.	115
Figure 5.5: Unambiguous structural determination of reduction product via X-ray crystallography.	116
Figure 5.6: Unambiguous structural determination of pyrolysis product via X-ray crystallography.	117
Figure 6.1: Advances in tricarbonyl-iron complexation of conjugated π -systems.	141
Figure 6.2: Isolated dimerized product.	152

LIST OF TABLES

	Page
Table 1.1: Bioactivity data of analogue compared to artemisinin.	11
Table 1.2: Benzylic oxidation conditions screen.	13
Table 2.1: Curvulamine antimicrobial activity.	31
Table 2.2: Curvulamide ACEI activity.	32
Table 2.3: Curindolizine anti-inflammatory data.	34
Table 2.4: Bipolamine G antimicrobial potency.	34
Table 3.1: Conditions tested to promote bond insertion.	54
Table 4.1: Efforts toward dehalogenative N-centered radical initiated bicyclization cascade.	76
Table 4.2: Optimization of piperidinone synthesis.	79
Table 4.3: Conditions screen for model enolate alkenylation.	80
Table 5.1: Conditions screen to induce the Dieckmann-alkylation transformation.	107
Table 5.2: Efforts toward biocatalytic dearomative dihydroxylation.	108
Table 5.3: Screen of common conditions to induce dearomative oxidation.	112
Table 5.4: Optimization of lead acetate-mediated dearomative oxidation.	112
Table 5.5: Ketone reduction solvent screen.	116
Table 5.6: Conditions screen to induce acetate pyrolysis.	117
Table 5.7: Acetate pyrolysis optimization.	117
Table 5.8: Optimization of acetate pyrolysis of silylated substrate.	118
Table 6.1: Efforts toward iron-diene complexation.	150
Table 6.2: Efforts toward diallylation.	151
Table 6.3: Conditions screening for macrocyclization.	152

LIST OF EQUATIONS

	Page
Equation 1.1: C-H oxidation of artemisinin.	8
Equation 1.2: C-H azidation of artemisinin.	8
Equation 1.3: Efforts toward isocyanation from the tertiary alcohol.	8
Equation 1.4: Precedented Staudinger reduction on artemisinin scaffold.	9
Equation 1.5: Unproductive application of Staudinger conditions.	9
Equation 1.6: Synthesis of the undesired formyltriazene.	9
Equation 1.7: Successful synthesis of artemisinin-isonitrile.	10
Equation 1.8: Literature precededented synthesis of desired tetralone.	13
Equation 1.9: Completed synthesis of the tetralone intermediate.	14
Equation 1.10: Completed synthesis of MK-109 and MK-110.	15
Equation 2.1: Efforts by Dr. Brian Atwood toward the piperidine core.	37
Equation 2.2: Synthesis of the piperidine core with desired stereochemistry.	38
Equation 2.3: Attempted elaboration toward the core.	38
Equation 2.4: Maimone's construction of the curvulamine core structure.	39
Equation 2.5: Maimone's furan ring closure and elaboration to a penultimate intermediate.	39
Equation 2.6: Completed synthesis of curvulamine and its epimer.	39
Equation 3.1: Efforts toward elaborating previously synthesized piperidenol.	44
Equation 3.2: Iodolactonization efforts.	45
Equation 3.3: Marazano's route to desired tetrahydropyridine.	45
Equation 3.4: Successful synthesis of (+)-iminodeoxydigitoxose.	46
Equation 3.5: Successful route to the piperidine core of curvulamide B.	48
Equation 3.6: Divergent synthesis of the protected core of curvulamide A.	48
Equation 3.7: Dihydropyrrole formation via N-H bond insertion from secondary amines.	50
Equation 3.8: Synthesis of benzofurans via C-H bond insertion.	51

Equation 3.9: Successful pyrrole annulation onto the core of curvulamide A.	51
Equation 3.10: Attempted reduction of curvulamide A precursor.	52
Equation 3.11: Efforts toward pyrrole annulation via tosyl hydrazone.	53
Equation 3.12: Aza-Michael addition into propargylic acylsilane.	54
Equation 3.13: Dong and coworkers reactivity with notable byproduct.	54
Equation 3.14: Efforts toward the dihydropyrrole adduct via acylsilane chemistry.	55
Equation 3.15: α -carbamyl alkylation and elaboration to the pyrrolidine.	56
Equation 3.16: Efforts toward pyrrole installation via α -carbamyl alkylation.	56
Equation 4.1: Alkene hydroamidation developed by Knowles and coworkers.	71
Equation 4.2: Amino-alkyne fragment synthesis.	73
Equation 4.3: Synthesis of 7-exo-trig cyclization fragment.	73
Equation 4.4: Synthesis of N-centered radical induced polycyclization precursors.	73
Equation 4.5: Efforts toward N-centered radical initiated polycyclization.	74
Equation 4.6: Efforts to replicate precedented bicyclization reaction.	74
Equation 4.7: Attempted synthesis of N-aryloxy carbamate N-centered radical precursor.	75
Equation 4.8: Efforts towards N-chloro carbamate synthesis, bicyclization, and derivitization.	76
Equation 4.9: Previous synthesis of piperidinone intermediate.	78
Equation 4.10: Precedented piperidinone synthesis.	79
Equation 4.11: Improved multi-gram synthesis of enolate alkenylation precursor.	79
Equation 4.12: Synthesis of alkenyl halide coupling fragment.	80
Equation 4.13: α -dimethylation to confirm enolate formation.	81
Equation 4.14: Efforts toward intramolecular enamine alkenylation.	81
Equation 4.15: Attempted cyclic enamine carbamate formation.	82
Equation 4.16: Efforts toward enecarbamate formation.	82
Equation 5.1: Qin's core construction and derivatization to arcutinine.	101
Equation 5.2: Li's rapid skeletal construction.	102
Equation 5.3: Diels-Alder cycloaddition utilizing an oxopyrrolium dienophile.	103
Equation 5.4: Sarpong's synthesis of the bridged bicyclic intermediate.	103
Equation 5.5: Radical coupling to afford arcutine skeleton and completed synthesis.	104

Equation 5.6: Enantioselective nitro-Michael addition and path forward.	106
Equation 5.7: Successful synthesis of the protected western fragment.	106
Equation 5.8: Key-step model system synthesis.	107
Equation 5.9: First generation synthesis of the phenol alcohol intermediate.	109
Equation 5.10 Attempted synthesis of the benzofuranone intermediate via Friedal-Crafts acylation.	109
Equation 5.11: Precedented synthesis of ozonolysis precursor and proposed reductive ozonolysis.	110
Equation 5.12: Successful phenoethanol synthesis.	110
Equation 5.13: Investigations into chemoselective acylation.	111
Equation 5.14: Dearomative oxidation and scalability data.	112
Equation 5.15: Enantioselective oxidative dearomatization using chiral hypervalent-iodine reagent.	113
Equation 5.16: Synthesis of aryl-lead oxidant.	113
Equation 5.17: Oxidative dearomatization via aryl-lead oxidant.	114
Equation 5.18: Dienone reduction resulting in rearomatization.	115
Equation 5.19: Successful intramolecular Diels-Alder cycloaddition.	115
Equation 5.20: Silyl ether synthesis and subsequent acetate pyrolysis	118
Equation 5.21: Attempts at nucleophilic fragment conversion.	118
Equation 5.22: Efforts toward lactone opening.	118
Equation 5.23: Attempted lactone opening via nucleophilic iodide substitution.	119
Equation 5.24: Efforts to afford ring-opened thioester.	119
Equation 5.25: Convergence of the eastern and western fragments.	119
Equation 5.26: Attempted ketal deprotection.	120
Equation 5.27: Eastern fragment derivatization.	120
Equation 6.1: Iron-transfer reagents facilitate diene complexation.	141
Equation 6.2: Experiments testing substrate stability in the presence of metathesis catalysts.	146
Equation 6.3: First successful alkene cross-metathesis in the presence of an iron-diene complex.	147
Equation 6.4: Successful cross-metathesis with relay prone alkenes.	147
Equation 6.5: Successful ring-closing metathesis on an iron-diene complexed substrate.	147

Equation 6.6: Successful alkene metatheses in the presence of acyclic iron-diene complexes.	148
Equation 6.7: Successful ring-closing metathesis in the presence of acyclic iron-diene complex.	148
Equation 6.8: Synthesis of bridged-bicyclic ring systems.	148
Equation 6.9: Synthesis of racemic allylic alcohol.	149
Equation 6.10: Efforts toward cross-coupling substrate via Keck allylation.	149
Equation 6.11: Successful synthesis of enantiopure cross-coupling fragment.	150
Equation 6.12: Successful homodimerization.	150
Equation 6.13: Macrocyclization precursor synthesis.	151
Equation 6.14: Macrocyclization precursor syntheses.	153
Equation 6.15: Progress towards TADA utilizing iron-diene protection.	153

ACKNOWLEDGEMENTS

First, I must thank Professor Christopher D. Vanderwal. Chris, your guidance, drive, and intuition have made me over these five years into the chemist I am today. You were a motivating force that pushed us to create and problem-solve, recognizing every challenge as an opportunity to be inventive. The time I spent in your lab was one of the most creatively rewarding times of my life. You gave your students freedom; the freedom to create our own routes, the freedom to test our own hypotheses. With your experience and knowledge, you guided me to invent for myself and to prove myself right or wrong. This thesis is built from ideas that you and I worked through and crafted together. I feel so much gratitude that I was given the ability to really create in my time in graduate school. Your continuous assurance, kindness, and motivation drove me to continue to grow stronger.

To the members of the Vanderwal lab who had graduated before me, thank you for all that you did for me. You all taught me how a chemist really thinks, and that critical thinking is a better tool than a perfect memory can ever give you. To Brian Atwood, your mentorship was so impactful, and it elevated me from undergraduate to graduate researcher faster than I could have ever hoped. You once told me “grad school is a marathon, not a race” and I think that one piece of advice you gave me four years ago saved me more than once. Your patience for my idiotic questions and the time you took to teach me made me feel hopeful that I could become great instead of ashamed that I was not. To Ryan Kozlowski, you were the greatest friend I made in graduate school. I think our daily conversations about the most unimportant things in the world kept us distracted when times were toughest. I look forward to moving a mile away from you and playing D&D in person again.

To the current members of the Vanderwal lab, I think the best reflection of our group was when we were outside of the lab. By the end of my time here, I had my head down and my focus on producing, but every time we got together for a barbecue or a drink, I enjoyed every conversation I had with each one of you. There’s a lot of drive and a lot of passion in the lab right now. Keep that spirit. To Bonnie Pak, you were also the best friend I made in grad school that I already kind of had, but I really don’t like how you made me write that. Your optimism regarding your graduation date and that you can bicyclize things always made me smile. Really, thank you, we were two kids who came up at the same time, through the same system and were there for each other the entire time.

To the friends I’ve made at UCI, having not lived on campus I never chose to spend much of my free time here, until you all made it extremely worthwhile. I came to UCI with a dream that I could run a game of D&D with some nerds I met at grad school. A few campaigns later and you nerds are all some of my closest friends. Thank you all for being so kind, understanding, and willing to participate in whatever shenanigans I threw your way.

To my parents. The day before I started at UCI, I panicked so my dad encouraged me to get up and walk with him around the neighborhood. We had a conversation about what grad school was and what I could do to manage my future there. I’ll never forget how that one moment set these five years up as an opportunity rather than an obligation. In that same week, my mom reassured me that I wasn’t doing this alone, but that we were all earning this degree together. This proved to be entirely true. Every single day of my graduate school career both of my parents offered at least one thing that would help me that day. That made these challenging years just that much more manageable. You know people really love you when they are always consciously, selflessly giving just to improve your well-being. Also, the fact that they were very nice about me living with them for five years, which, let’s be honest, I wouldn’t even want to do. I love you both and this degree is ours.

To my brothers, I think becoming adults has made us respect and enjoy each other more than we ever had as kids. Nelson, your passion and intellect had such a profound impact on me that I think it is apparent in this thesis. Connor your charisma and drive are also wedged into these pages. I never

would have gotten to this point without both of you. Also, both of your senses of humor were combined to give me some kind of objectively perfect sense of humor, which I will always appreciate the both of you for.

To the rest of my family, just growing up with such a broad support system brought me to this point. It was embarrassingly late in my life that I realized that not everyone's family lives in the same city and gets together for birthdays, holidays, and just for fun. That privilege helped me develop a value-system I'm extremely proud of. To the Lowe's, you're in this paragraph because you have become a part of my family. Thank you all so much for your kindness and acceptance. You have never treated me with anything, but love and respect and I valued that so much because I had a full new group of people on which I could rely in these past five years.

Laura, you may never know how important you have been to me in these past five years. Your support has brought me through this thesis, the other four and a half years of graduate school, and the five years before that. Your drive and spirit not only make you a nightmare to play Monopoly with but are what motivated me to turn my life onto this path. Your kindness and empathy make me strive to be a better person every single day. You cannot comprehend how proud I am of your accomplishments, not only as your partner, but as an observer who saw your dreams from 10 years ago become a reality by sheer determination and grit. Those attributes put my laziness to shame so terribly I had to go get a PhD about it. I love you and I'm so excited for the direction both of our lives are heading together.

VITA

Riley Brigdon Mills

EDUCATION

University of California, Irvine, Irvine, CA

Doctor of Philosophy in Chemistry, 2022

Research Advisor: Dr. Chris Vanderwal

University of California, San Diego, La Jolla, CA

Bachelor of Science in Molecular Synthesis, 2016

RESEARCH EXPERIENCE

University of California, Irvine

The Vanderwal Group: December 2017 – 2022

Graduate Student Researcher

Focused mainly on the total synthesis of complex natural products with interesting bioactivities for biological assays. Also, developed a series of novel drug analogues for the treatment of drug-resistant strains of malaria. Developed a protecting group strategy to allow for alkene cross metathesis in the presence of labile dienes to produce Diels-Alder cycloaddition precursors.

Takeda Pharmaceuticals

Medicinal Chemistry Department: June 2015 – September 2015, June 2016 – August 2017

Research Associate

Development of pharmaceuticals directed toward the treatment of diseases that affect the central nervous system. Worked on the development of a frontline drug that reached clinical trials.

The Scripps Research Institute

The Baran Group: January 2016 – June 2016

Student Research Assistant

Developed methodologies focused on metal-catalyzed radical generation from activated esters. Utilized nickel catalysis for radical trapping to forge challenging carbon-carbon bonds.

UCSD Medical Center

The Parsons Group: November 2014 – January 2016

Student Research Assistant

Performed biochemical research focused on connecting protein and ionic biomarkers to urinary diseases such as interstitial cystitis and overactive bladders syndrome. Developed HPLC methods to isolate, characterize, and quantify biomarkers in patient samples.

TEACHING EXPERIENCE

University of California Irvine

Undergraduate Teaching Assistant: 2017 – 2022

Instructed teaching labs and lectures in both lower division and upper division undergraduate chemistry courses.

Instructor of Record: 2021

Acted as instructor for a number of organic chemistry laboratory courses for undergraduates. Aided in the design of a flipped, online class setting to accommodate during the COVID-19 pandemic.

Undergraduate Mentorship: 2019 – 2022

Mentored two undergraduate student researchers in a laboratory setting. Developed high level laboratory technique with a focus on the fundamentals of academic research.

PUBLICATIONS

Qin, T.; Edwards, J. T.; Merchant, R. R.; Novak, A. J. E.; Zhong, J. Z.; Mills, R. B.; Yan, M.; Yuan, C.; Eastgate, M. D.; Baran, P. S. "Nickel-Catalyzed Barton Decarboxylation and Giese Reactions: A Practical Take on Classic Transforms" *Angew. Chem. Int. Ed.* **2017**, *56*, 260-265.

AFFILIATIONS

American Chemical Society, Member, 2014 – Present

ACTIVITIES

Vanderwal Group Leaps, Community Outreach Coordinator, 2017 – 2022.

ABSTRACT OF THE DISSERTATION

Strategies for the Syntheses of Complex Molecules

By

Riley Brigdon Mills

Doctor of Philosophy in Chemistry

University of California, Irvine, 2022

Professor Christopher D. Vanderwal, Chair

This thesis highlights a multitude of projects all with the goal of synthesizing complex molecules, either to probe their biological activity or as a proof-of-concept for novel synthetic strategies. The first of these projects discussed is the development of novel drug analogues based on the isocyanoterpene family of natural products. The first compound is an artemisinin-derivative with an installed isocyanide functionality. With the core structure of artemisinin and the motif resembling isocyanoterpenes, this drug was developed to fight malaria by employing multiple mechanisms of actions. The second part of this project is the syntheses of a pair of diastereomers, MK-109 and MK-110, whose promising bioactivities are still under investigation by collaborating groups. The synthetic efforts produced a viable convergent route to afford both compounds in appreciable scale for biological assays. The syntheses of these analogues afforded the desired compounds in appreciable scale and in an efficient manner, allowing for deeper investigations into their bioactivities and pharmacokinetics.

The second project discussed over three chapters of this thesis is the Vanderwal lab's efforts toward the synthesis of the curvulamine family of natural products. These dipyrrole alkaloids were targeted with the strategy of installing the electron-rich pyrroles late in the synthesis, which led to a

series of investigations into novel pyrrole annulation reactions. Efforts toward the bicyclic curvulamides resulted in the total synthesis of two other natural products in the most concise manner reported. Efforts toward synthesizing the tetracyclic curvulamines involved a radical bicyclization strategy and a strategy invoking enolate alkenylation chemistry. Although the syntheses of the targeted natural products were not achieved, our efforts did result in a greater understanding of the application of modern methodologies to complex systems.

Our ongoing efforts toward the synthesis of the arcutine family of natural products our focused on a convergent route to arcutinidine to avoid the pitfalls noted in previously reported syntheses. The development of a route to two fragments of the natural product was achieved and optimized to be highly scalable. Investigations of converging these fragments are currently underway and may act as a proof-of-concept for a very concise synthesis of the arcuitines. The efforts detailed within highlight the challenges of developing a synthesis on large scale and the problem-solving required to overcome these challenges.

The final project of this thesis is the use of iron-tricarbonyl complexation to protected relay-prone dienes when subjected to alkene metathesis conditions. This novel strategy allows for selective dienophile metathesis in the presence of a diene to synthesize novel Diels-Alder cycloadducts. These efforts led to a focus on the development of transannular Diels-Alder cycloaddition precursors using this method, which resulted in a novel method of synthesizing diene dimers. These new discoveries in the application of iron-diene complexes have opened a path for multiple future projects, including novel methods and total syntheses.

Chapter 1: Development of Isocyanoterpene Analogues for the Treatment of Malaria

1.1 Introduction

Malaria is one of the main causes of disease and death in the world with over 200 million cases and over 430 thousand deaths reported yearly.¹ The prevalence of malaria is due to its ease of transmission as it is spread through endemic species of mosquitoes via infection by the unicellular protozoan *Plasmodium falciparum*.² Treatments for malaria have been developed since the 18th century; however, many of these treatments have decreased in efficacy due to evolving resistances in *Plasmodia* parasites.¹ Since the discovery of artemisinin in 1972 by Tu and coworkers, artemisinin combination therapy (ACT) has become the most effective treatment for drug-resistant malaria and is widely prescribed.^{3,4} Recently, isocyanoterpene (ICT) natural products have been discovered to exhibit high efficacy in the treatment of drug-resistant *Plasmodium*, prompting an investigation into analogues derived from ICTs. Herein are described the syntheses of novel drug analogues, which contain both isonitrile functional groups and motifs reminiscent of compounds known to treat malaria. This project aims to elucidate the mechanistic pathway of *P. falciparum* growth inhibition by isocyanoterpene containing natural products while also developing novel bioactive compounds aiming to exhibit multiple mechanisms of action for the treatment of malaria.

1.2 Malaria

1.2.1 An Introduction to Malaria

Malaria is an infectious disease that can cause symptoms of fevers, headaches, vomiting and in more extreme cases coma, seizures, and death.⁵ Those who survive malaria are subject to reinfection, although with milder symptoms, as natural immunity grants partial resistance that has been shown to

wane over months without continuous exposure. Infection is caused by transmittance of the *Plasmodium* parasite via the saliva of *Anopheles* mosquitos into human blood.⁶ *Anopheles* mosquitos carrying the *Plasmodium* parasite are predominantly found in Sub-Saharan Africa. Although mosquitoes carrying *Plasmodium* parasites have been eradicated in all first-world nations, members of the *Anopheles* family can be found in every continent except for Antarctica, prompting the CDC to warn of the risk for reintroduction of malaria to any region of the world.⁷

1.2.2 Genus *Plasmodium* and its Biological Effects

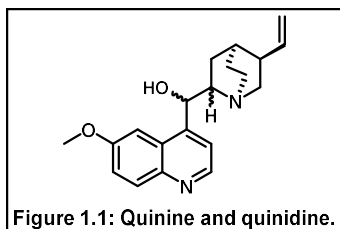
Plasmodium is a genus of unicellular eukaryotes capable of infecting vertebrates and insects.⁸ Within the family, 14 subgenera have been classified based on their morphology and potential hosts; however, only five species of *Plasmodium* are capable of infecting humans: *P. vivax*, *P. malariae*, *P. ovale*, *P. knowlesi*, and *P. falciparum*, the latter being responsible for about 50% of all cases of malaria and nearly all fatal cases.⁸

These species of *Plasmodium* are merozoites, infectors of red blood cells, and cause detrimental symptoms via destruction of erythrocytes. *Plasmodial* digestion of haemoglobin results in the release of insoluble β -hematin crystals, haemozoin, which when ingested by phagocytes, induce a chain of inflammatory responses resulting in the characteristic fever seen in most cases of malaria.⁹ Deposition of haemozoin in the spleen, liver, kidneys, and lungs results in enlargement and discoloration of these organs, causing lasting health complications.¹⁰ Most species of *Plasmodium* infect erythrocytes in periodic intervals allowing for treatment to be predictable and manageable. *P. falciparum* is capable of infecting a large number of red blood cells without coordinated intervals resulting in rapid infection and irregular fevers.¹¹ *P. falciparum* also sequesters groups of infected erythrocytes into clusters, while also changing the adhesion properties of cellular membranes producing masses that occlude blood circulation resulting in organ dysfunction and long-term complications.¹² For these reasons, most cases of severe and fatal

malaria are a result of infection by *P. falciparum*, and therefore, the largest focus of research into malarial treatment is in the treatment of *P. falciparum*.

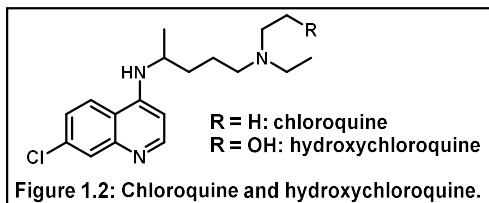
1.2.3 Early Therapies for Malarial Infections

The treatment of malaria spans back many centuries, with its origins rooted in South American folk medicine. The Quechua people, a group of indigenous people from the area that is now modern Peru, discovered the bark of the cinchona tree was an effective treatment for shivering.¹³ Spanish Jesuit missionaries were the first to bring the cinchona tree to Europe, and its attempted use to control the shivering caused by malaria-induced fever led to the fortuitous discovery of its ability to treat malaria. French scientists Pierre Joseph Pelletier and Joseph Bienaimé Caventou isolated quinine (**Figure 1.1**) from extracts of the cinchona tree in 1820 and its use as a prophylactic for malaria infection became common



place in the mid-19th century.¹⁴ Although it was the most effective available treatment for malaria, quinine's toxicity results in an abundance of drug-induced disorders.¹⁵ Liver failure, kidney failure, neurodegeneration, and blindness are only a few noted side effects of quinine overdose. According to the FDA, 23 deaths between 1969 to 1992 can be directly attributed to quinine treatments.¹⁶ Quinine derivatives, namely the diastereomer quinidine (**Figure 1.1**), are still used in some countries today; though, these are recommended only for severe cases of malaria and are no longer being manufactured for use in the United States.¹⁷

Because of quinine's apparent toxicity, alternative treatments were developed, which were



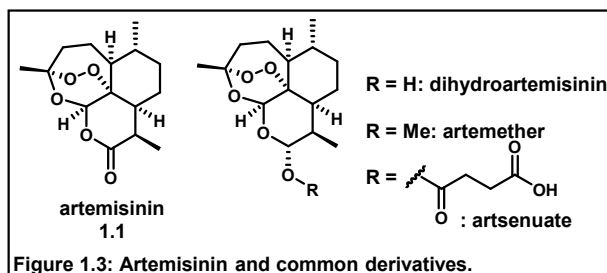
shown to exhibit similar efficacy with decreased toxicity. The first alternative to quinine treatment was chloroquine (**Figure 1.2**), a synthetic analogue developed by Hans Andersag and his coworkers at Bayer laboratories in 1934. This medication was introduced into clinical treatment as a

malaria prophylactic in 1947.¹⁸ Chloroquine still exhibits some toxicity, leading to the development of analogues, such as hydroxychloroquine, amodiaquine, mefloquine and many others, all of which maintain the quinoline ring of their predecessor quinine.¹⁹ All of these quinoline-containing compounds are hypothesized to function via inhibition of haemozoin biocrystallization, resulting in the accumulation of insoluble heme, leading to parasite death.²⁰

Many other antimalarial compounds have been developed for wide-spread treatment of malaria, largely due to the appearance of drug-resistant strains of *Plasmodium* that have disallowed for the complete eradication of malaria.²¹ One notable family of drugs is the tetracyclines, including doxycycline, one of the most widely distributed antimalarial pharmaceuticals in the world.²² The tetracyclines exhibit high effectiveness in prophylaxis of malaria but are ineffective in the treatment of acute cases of malaria.²³ This class of drugs has been shown to inhibit protein synthesis in erythrocytic stages of *P. falciparum* but shows no effect against gametocytes of *P. falciparum*.²⁴ It is generally recommended to use in combination with either artemisinin-derived artesunate or quinine for effective treatment.

1.2.4 Artemisinin and its Derivatives

One of the most profound medical discoveries of the 20th century was the isolation of artemisinin (1.1) and its application to the treatment of malaria (Figure 1.3). Extraction of the sweet wormwood herb, used in traditional Chinese medicine, resulted in the discovery of artemisinin (1.1) by Tu Youyou and coworkers in 1972.²⁵ The sesquiterpene lactone contains an endoperoxide bridge, which is not commonly found in natural products and has been theorized to be vital for the mechanism of action.²⁶



Haemoglobin digestion by *Plasmodium* results in the formation of haem, which catalyzes homolytic cleavage of the endoperoxide. The resultant alkoxy radicals react with vital proteins resulting in cell

death.²⁷ Although the exact mechanism of action is undetermined, recent studies have indicated that the radical/protein interactions are non-specific, allowing for cytotoxicity of *Plasmodium* at all life cycle stages.²⁸

Although artemisinin is a highly effective antimalarial drug, its limitations include high cost of production, credited to its complex structure, as well as poor pharmacokinetics and bioavailability.²⁹ To increase availability of this treatment, synthetic efforts have been the subject of intense research efforts, including biosynthesis of an artemisinin precursor via modified yeast cells, as well as efficient and scalable total syntheses.³⁰ Development of a series of analogues of artemisinin has resulted in a multitude of drugs with improved pharmacological characteristics.³¹ Research into artemisinin derivatization has resulted in a wide-array of pharmaceuticals with high efficacy and good pharmacokinetics, the most prevalent of which are dihydroxyartemisinin, artemether, and artesunate (**Figure 1.3**).³²

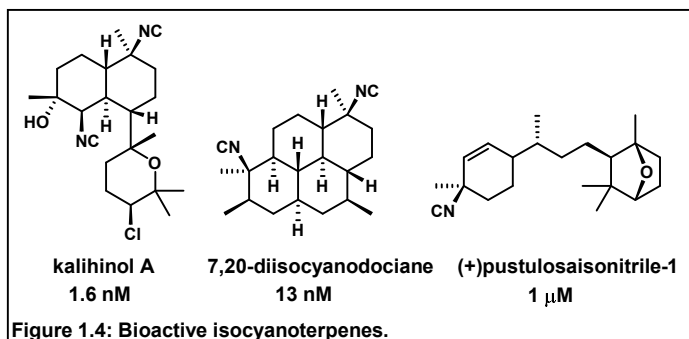
1.2.5 Combination Therapies

All of the previously discussed medications are effective in the treatment of malaria, but the use of these drugs as monotherapies has been phased out and replaced by multidrug combination therapies to prevent the evolution of drug-resistant strains of *Plasmodium*.³³ Combination therapy involves the employment of two or more drugs with differing mechanisms of actions. This greatly increases the probability that any strain of *Falciparum*, that would otherwise survive due to evolved resistance to a single drug, is eradicated.³⁴ Although many drug combinations are prescribed, the most common modern treatment method is Artemisinin Combination Therapies (ACTs), which involves one artemisinin-derived drug combined with a non-artemisinin derived drug. This has shown high success in the treatment of drug-resistant strains of malaria as artemisinin has a very different mechanism of action from other classes of antimalarials.³⁵ Artemisinin resistance is extremely rare in wild-type strains of *Plasmodium*, though artemisinin-resistance is becoming more prevalent.³⁶

1.2.6 Isocyanoterpenes: Investigations of Bioactivities and Syntheses

Isocyanoterpenes (ICTs) are a relatively new category of natural products that have exhibited high antiplasmodial potency against drug-resistant strains of *P. falciparum*. Some ICTs exhibit up to a two-fold increase in potency relative to that of artemisinin (**Figure 1.4**).³⁷ ICTs are characterized by their isocyanide functionalities, which are rarely observed in natural products, and generally contain complex carbocyclic skeletons.³⁸ Although these compounds show very promising anti-malarial efficacy, only a few have been

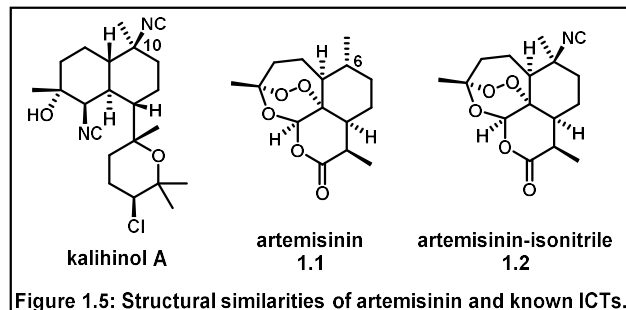
tested for antiplasmodial activity, limited by the difficulty of procuring appreciable amounts for assays.³⁹ In an effort to investigate the efficacy of these natural products as antimalarial treatments, as well as gain knowledge of the currently unknown mechanism of action, the Vanderwal Lab has engaged in the total syntheses of ICTs since 2014, when the group first published its efforts towards the synthesis of a highly complex ICT, 7,20-diisocyanoadociane (DICA)⁴⁰. Since then, the Vanderwal Lab has published multiple syntheses of naturally occurring ICTs, including two concise syntheses of DICA, and the development of a number of analogues.⁴¹ In collaboration with the Le Roch Lab at UC Riverside, our synthetic efforts have revealed many ICT natural products and analogues with high cytotoxicity against chloroquine-resistant strains of *P. falciparum*. Collaborations between the Vanderwal Lab and multiple research groups are currently underway to probe the mechanism of action of ICT induced *Plasmodium* growth inhibition, while also probing their efficacy for the treatment of other diseases. The Vanderwal lab continues to pursue total syntheses of natural ICTs, while also developing novel drug analogues in search for highly potent antimalarial compounds with drug-like qualities.



1.3 Synthesis of Artemisinin-Isonitrile

1.3.1 Project Considerations

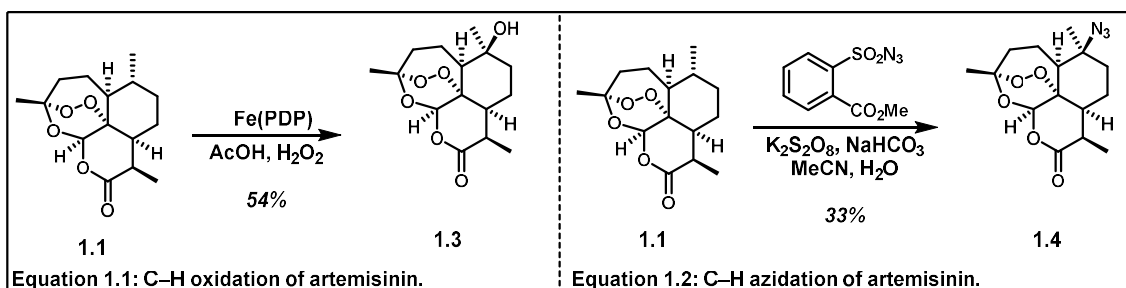
An analysis of reported ICTs revealed structural similarities that were prevalent in nearly all members of the family, namely the isonitrile attached to a fully substituted sp^3 carbon at a sterically hindered site. An example is the



isonitrile functionality at the C10 position of kalihinol A (**Figure 1.5**). When considering potential isocyanoterpene analogues that could be synthesized and examined for their bioactivity, it was recognized that a similar structural motif was present at the C6 position of artemisinin. Functionalization of this carbon center to produce the isonitrile containing compound (**1.2**) was a very attractive prospect. This artemisinin analogue would contain functionalities that could grant multiple distinct mechanisms of action, which was hypothesized to increase potency while dismissing the need for multidrug combination therapies. For these reasons, the synthesis of artemisinin-isonitrile (**1.2**) was pursued.

1.3.2 Synthetic Considerations

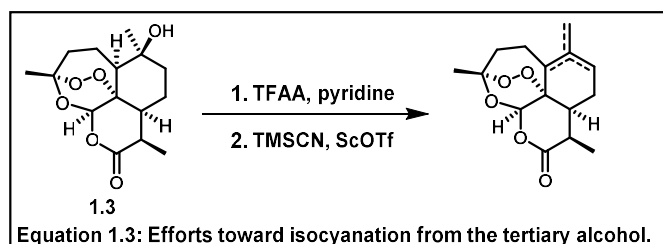
Methodologies targeting the functionalization of unactivated aliphatic carbons have grown in prevalence in the last decade. In 2013 White and coworkers developed a regioselective C–H oxidation, allowing for the formation of tertiary alcohols on unactivated tertiary carbons.⁴² Similarly, Tang and coworkers developed an oxidative azidation methodology using mild conditions to afford regioselective



azidation of many complex substrates with high functional group tolerance.⁴³ Both the White Lab (**Equation 1.1**) and Tang Lab (**Equation 1.2**) have demonstrated their methodologies on artemisinin, affording the C–H functionalized products (**1.3**, **1.4**) at the C6 position. Alcohol **1.3** could be converted to the isonitrile via stereoinvertive isocyanation chemistry developed by Shenvi and coworkers.⁴⁴ Azide **1.4** could also be converted to the isonitrile via reduction to the primary amine and further functionalization. Both sequences have been used in previous syntheses of isocyanide containing products by the Vanderwal lab.⁴¹

1.3.3 Previous Synthetic Efforts

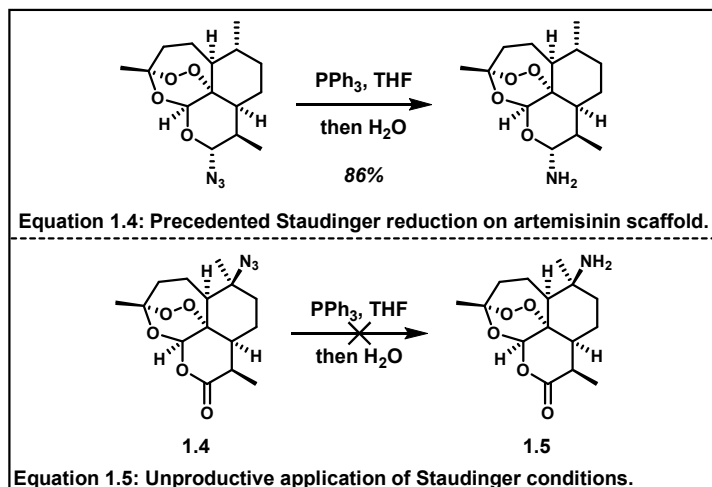
Initial studies by previous graduate students in the Vanderwal Lab found that both the White and Tang chemistry were reproducible in yields equivalent to those reported to afford **1.3** and **1.4**. Unfortunately, previous efforts by Dr. Alex



Karns revealed that substitution of **1.3**, via the isocyanation chemistry developed by the Shenvi lab, produced a complex mixture of elimination products (**Equation 1.3**). A series of reduction conditions of **1.4** were also investigated but resulted in either no reaction or decomposition products, likely caused by reductive cleavage of the endoperoxide bond. Based on these preliminary results, it became apparent that screening mild azide reduction conditions would be necessary to produce **1.2**.

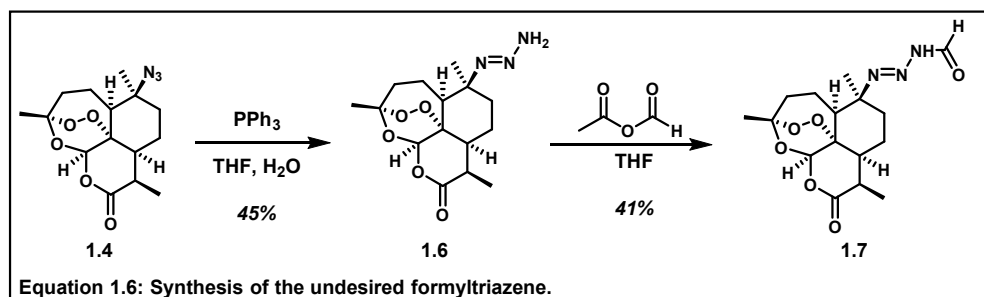
1.3.4 Initial Synthetic Efforts

My efforts toward the synthesis of artemisinin-isonitrile (**1.2**) were dedicated toward investigations of the Staudinger reaction to convert azide **1.4** to the primary amine **1.5**. Literature precedent indicated the Staudinger reaction could be applied to azide containing artemisinin-

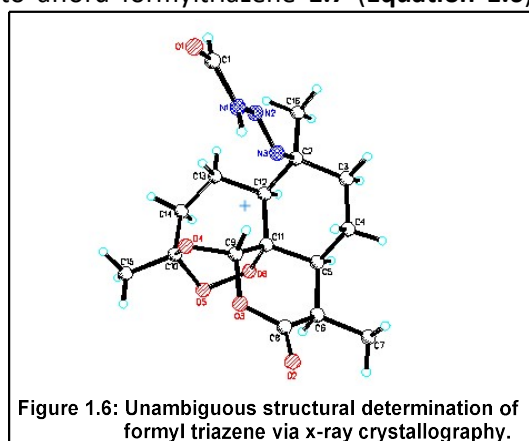


analogues in moderate yields with no effect on the endoperoxide bridge (**Equation 1.4**).⁴⁵ Application of standard Staudinger conditions yielded no reactivity (**Equation 1.5**). Addition of water to the initial reaction mixture allowed for full consumption of the starting material and isolation of a new product, which was later revealed to be the triazine (**1.6**) (**Equation 1.6**). ¹H NMR, ¹³C NMR and IR spectroscopy

indicated the presence of a primary amine; though, mass

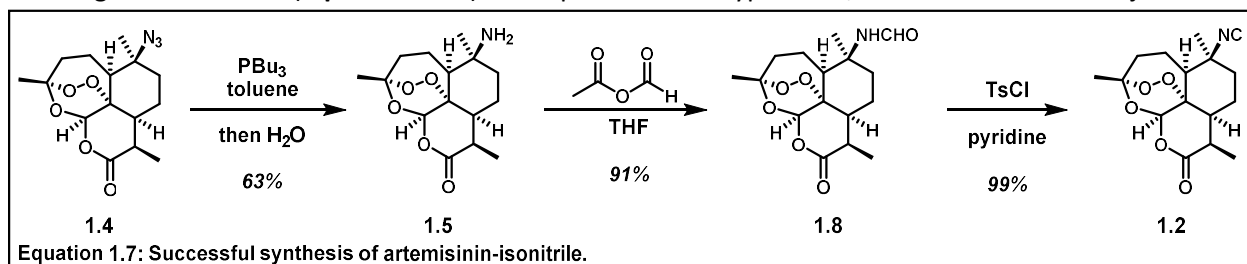


spectrometry did not corroborate the desired product (initially credited to endoperoxide instability under ionization conditions). This new product was formylated to afford formyltriazene **1.7** (**Equation 1.6**), which was found to be crystalline. X-ray crystallographic analysis of the formylated product confirmed **1.7** was the formylated triazene (**Figure 1.6**). Isolation of **1.7** indicated that Staudinger conditions successfully interacted with the azide but the resultant intermediate was unable to convert to the amine.

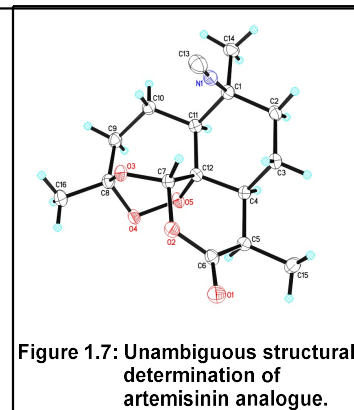


1.3.5 Completed Synthesis of Artemisinin-Isonitrile

Standard Staudinger reaction conditions were revisited but were nonproductive as the use of more forcing conditions resulted in decomposition of the starting material. Characterization of **1.6** as the triazene led to the hypothesis that the steric congestion surrounding the tertiary azide prohibited the formation of the four-membered ring intermediate. This hypothesis was corroborated by the formation of the triazene **1.6**, as reduction of the azide occurred but the substrate was unable to undergo the pericyclic rearrangement necessary nitrogen gas elimination. It was hypothesized that replacing triphenylphosphine with another phosphine with less steric bulk could allow for completion of the Staudinger reduction (**Equation 1.7**). To probe this hypothesis, azide **1.4** was subjected to



tributylphosphine and conversion to a new product was observed before addition of water. Primary amine **1.5** was isolated corroborating the hypothesis that the steric bulk of triphenylphosphine disallowed reaction conversion. Formylation of **1.5** produced formamide **1.8** in good yields, which was subjected to dehydration conditions afforded the desired analogue **1.2** in quantitative yields. The isonitrile analogue was found to be highly crystalline allowing the structure to be confirmed via X-ray crystallography (**Figure 1.7**).



1.3.6 Biological Assays

Compound **1.2** was assayed for growth inhibition against multiple strains of drug-resistant *P. falciparum* by the Le Roch Lab at the University of California, Riverside. The analogue was tested in both

clonal and non-clonal cell lines of *P. falciparum* as well as strains that exhibited chloroquine resistance (**Table 1.1**). Unfortunately, it was found that the analogue was found to be less potent than the

STRAIN	ART-Isonitrile	ART-Control
3D7	76.2 nM	13.4 nM
Dd2	351 nM	36.4 nM
HB3	76.2 nM	6.5 nM

Table 1.1: Bioactivity data of analogue compared to artemisinin.

artemisinin control and was also less active in the chloroquine-resistant strain. This indicated that the inclusion of the isonitrile group did not impart the growth inhibition activity against drug-resistant *Plasmodia* that other ICTs tend to exhibit. Although disappointing, the result does that the sterically hindered isocyanide motif may not be the only important structural feature of ICTs.

1.3.7 Conclusions

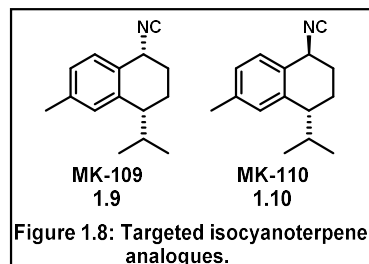
Artemisinin-isonitrile (**1.2**) was synthesized from known azide **1.4** in three steps in 58% overall yield and four steps from commercially available artemisinin (**1.1**). Although the analogue proved less efficacious than hoped, the results do impart interesting information in considering the mechanism of action of isocyanoterpenes. The challenging reduction of the sterically congested azide in the presence of highly labile functional groups, led to synthetic insights that can be applied to the functionalization of other complex starting materials. It has been demonstrated that utilizing C–H azidation on secondary metabolites with sensitive functionalities, and derivatizing to the isocyanide is a feasible strategy to afford complex isocyanoterpene analogues. Applying this strategy to commercially available, drug-like compounds could lead to the development of novel isocyanoterpene analogues with potential for clinical use in the treatment of malaria.

1.4 Synthesis of MK-109 and MK-110

1.4.1 Introduction

In an effort to synthesize novel isocyanoterpene analogues, previous Vanderwal post-doctoral associate Dr. Milandip Karak developed a route toward a number of isocyanide containing analogues that have been tested for their bioactivity in *P. falciparum* growth inhibition. These assays revealed two

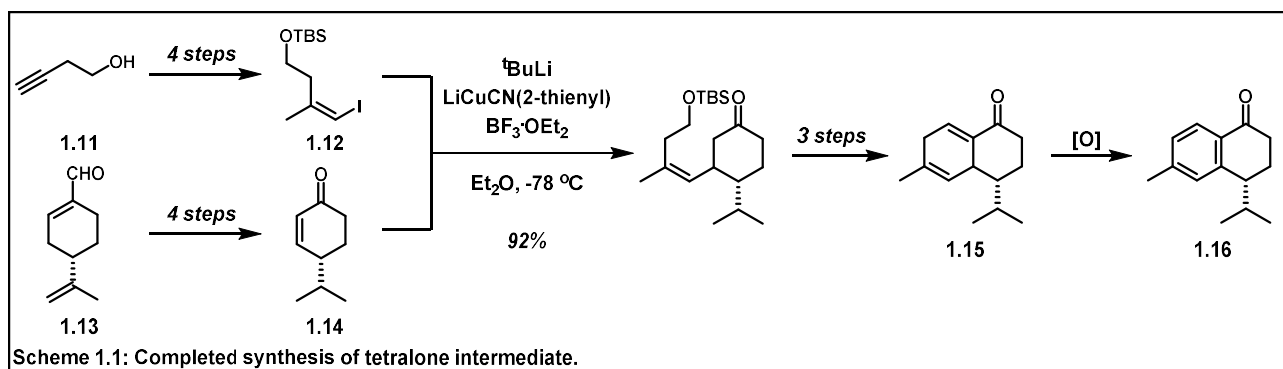
diastereotopic isocyanoterpenes with high potency, which were given the names MK-109 (**1.9**) and MK-110 (**1.10**) (Figure 1.8). The promising results of the bioactivity studies created a demand for these compounds in large quantities for further testing. The syntheses of these



compounds were lengthy and low yielding on multigram scale, producing the desired compounds only in small quantities; therefore, efforts were made to develop a new route to synthesize **1.9** and **1.10** in appreciable amounts.

1.4.2 Previous Syntheses

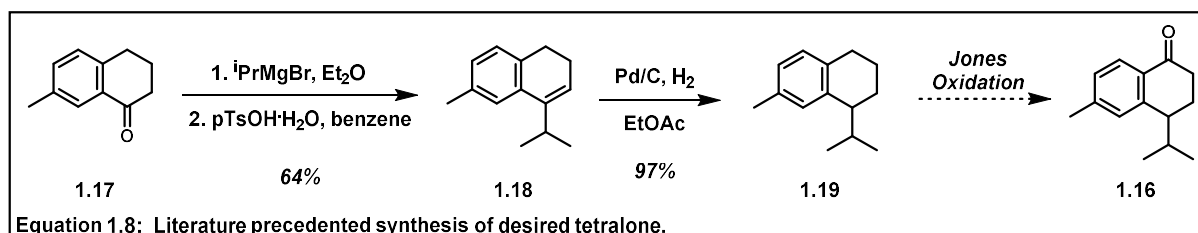
The initial syntheses of **1.9** and **1.10** were developed to produce a series of novel isonitrile containing compounds through a divergent route. This route involved a convergence of vinyl iodide **1.12** with cryptone (**1.14**). The synthesis of **1.12** involves the use of multiple equivalents of AlMe_3 , an extreme pyrophore, to carboaluminate 3-butyne (**1.11**), followed by iodination and silyl protection, a lengthy process that proved hazardous to run on large scale.



(*R*)-cryptone (**1.14**) is synthesized from (*R*)-perillaldehyde in a four-step sequence. The total step count of the synthesis of tetralone **1.16** is 13 steps and, due to the lengthy sequence, only a few milligrams of each analogue were synthesized by Dr. Karak.

1.4.3 Efforts Toward a Concise Synthesis of MK-109 and MK-110

Analyzing the initial syntheses of **1.9** and **1.10**, it was believed this route could be intercepted at tetralone **1.16**, as the synthesis of racemic **1.16** had been achieved in four steps from commercially available starting materials (**Equation 1.8**).⁴⁶ Alkyl addition to commercially available tetralone **1.17**



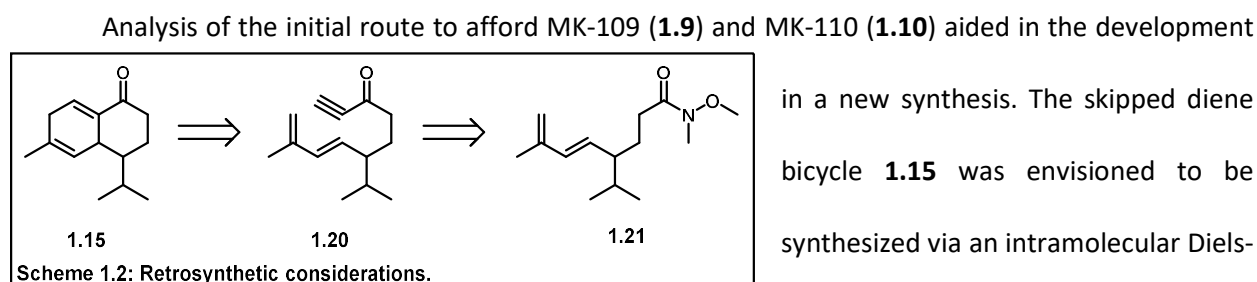
followed by acid-catalyzed dehydration produced **1.18** in yields similar to those previously reported. Hydrogenation of the styrene occurred in good yields to produce the racemic tetralin **1.19**. Jones oxidation at the secondary benzylic site, reported without specific conditions, proved problematic. A screen of common Jones oxidation conditions (**Table 1.2**) yielded modest amounts of **1.16** on small scale and proved to be

Oxidant	Solvent	Amount	Conversion
K ₂ CrO ₃ , H ₂ SO ₄ , H ₂ O	acetone	10 mg	35%
K ₂ CrO ₃ , H ₂ SO ₄ , H ₂ O	acetone	150 mg	8%
K ₂ CrO ₃ , H ₂ SO ₄ , H ₂ O	DCM	10 mg	0%
K ₂ CrO ₃ , H ₂ SO ₄ , H ₂ O	THF	10 mg	0%
K ₂ CrO ₃ , H ₂ SO ₄ , H ₂ O	EtOAc	10 mg	4%
K ₂ CrO ₃ , H ₂ SO ₄ , H ₂ O	Neat	10 mg	0%
CrO ₃ , AcOH	AcOH	10 mg	64%
CrO ₃ , AcOH, H ₂ O	AcOH	10 mg	48%
CrO ₃ , AcOH	AcOH	50 mg	>5%

Table 1.2: Benzylic oxidation conditions screen.

ineffective when over 10 mg of **1.19** were subjected to these conditions. After screening a series of conditions at modest scale, we were unable to produce tetralone **1.16** in usable amount. Alternative benzylic oxidation conditions were briefly investigated but produced no product. This strategy was abandoned, and a new route was considered.

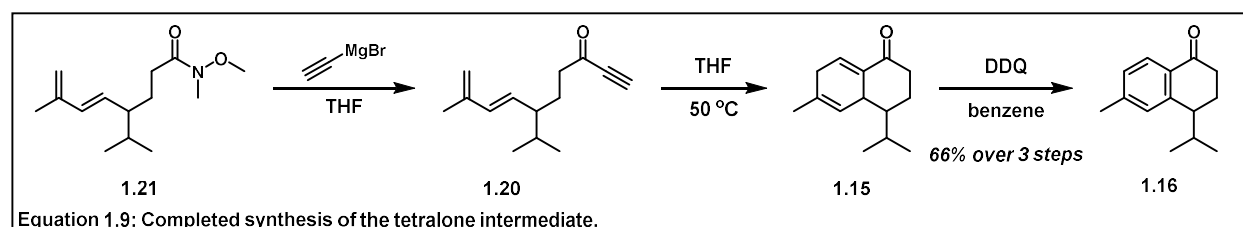
1.4.4 Synthetic Reconsiderations



Weinreb amide **1.21** was made in three steps from commercially available materials via the precented route.⁴⁵ **1.21** was alkynylated to afford ynone **1.20** (Equation 1.9). In the product mixture, a minor product was observed, which was confirmed by comparison to Dr. Karak's previously acquired spectroscopic data to be **1.15**, produced by spontaneous IMDA cycloaddition. **1.20** was subjected to mild heating to drive the remainder of the material to undergo IMDA cycloaddition, resulting in complete conversion to the desired bicyclic intermediate (**1.15**). Once more, a minor product was observed, which was confirmed

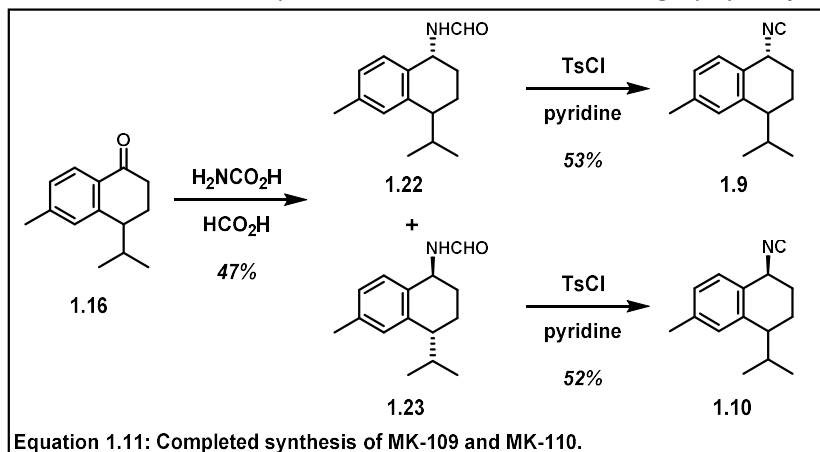
1.4.5 Completed Syntheses

Weinreb amide **1.21** was made in three steps from commercially available materials via the precented route.⁴⁵ **1.21** was alkynylated to afford ynone **1.20** (Equation 1.9). In the product mixture, a



minor product was observed, which was confirmed by comparison to Dr. Karak's previously acquired spectroscopic data to be **1.15**, produced by spontaneous IMDA cycloaddition. **1.20** was subjected to mild heating to drive the remainder of the material to undergo IMDA cycloaddition, resulting in complete conversion to the desired bicyclic intermediate (**1.15**). Once more, a minor product was observed, which was confirmed

to be the aromatized tetralone **1.16**, likely oxidized via trace amounts of O₂ in the reaction mixture. The material was oxidized to the desired tetralone (**1.16**), via conditions developed by Dr. Karak. Subjecting **1.16** to Leuckart reaction conditions afforded the expected mixture of formamide diastereomers (**1.22**, **1.23**), which were separated via column chromatography (**Equation 1.10**). The formamides were



subjected to dehydration conditions to afford **1.9** and **1.10** in modest yields, resulting in 90 mg and 73 mg of MK-109 and MK-110, respectively, isolated for evaluation.

1.4.6 Biological Assays

MK-109 and MK-110 were subjected to assays by the Le Roch group at UC Riverside and the Mamoun group at Yale. The Le Roch group reported modest activity in the growth inhibition of drug-resistant *P. falciparum*, and the investigations of these compounds as anti-malarials were no longer studied. Assays for undisclosed novel biological activity by the Mamoun group are currently ongoing.

1.4.7 Conclusions

The synthesis of MK-109 and MK-110 were completed in eight steps from commercially available materials. Initial synthetic efforts unveiled scalability issues with benzylic oxidation conditions previously reported in the literature. The utilization of an intramolecular Diels-Alder cycloaddition of dienyne system **1.20** intercepted intermediate **1.15** in five synthetic steps from commercially available starting materials, while the previous synthesis required a total of 12 synthetic steps. Having produced an appreciable amount of material, bioactivity studies are currently underway to evaluate the bioactivities of these novel isocyanoterpenes analogues.

1.5 Project Conclusions

The successful syntheses of these drug analogues highlight several viable strategies to produce other analogues modeled on the isocyanoterpenes. The lessons learned in overcoming the challenging azide reduction to form artemisinin-isonitrile may prove useful in future efforts toward isocyanation of drug-like molecules at sterically congested sites. This work may allow for the development of a series of isocyanide containing analogues beginning with complex starting materials with sensitive functional groups. The development of the new syntheses of MK-109 and MK-110 allowed for access to appreciable amounts of these bioactive compounds, which show promise as potent candidates for treatment of disease.

1.6 Distribution of Credit and Contributions

I would like to give credit to Dr. Alex Karns for his early investigations the formation of artemisinin-isonitrile. These efforts led to a greater understanding of the lability of the endoperoxide bridge of artemisinin and allowed me to focus my efforts in the correct direction. I would also like to acknowledge Dr. Milandip Karak for his initial synthesis of MK-109 and MK-110. The development of conditions to produce and isolate the isocyanide containing compounds from the tetralone intermediate were fundamental in the completion of this product. Further, his characterization of the final intermediates and products were fundamental in the completion of these syntheses.

1.7 Experimental Information

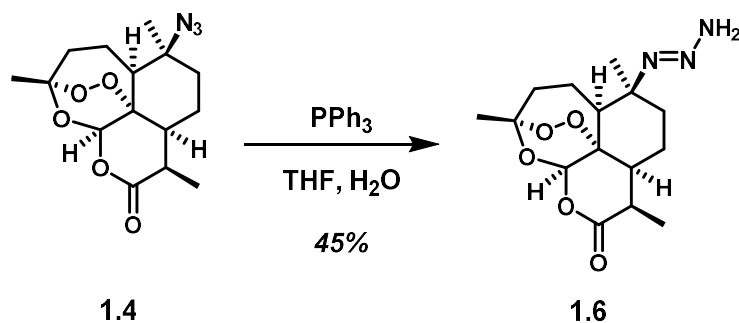
1.7.1 Materials and Methods

All reactions were carried out in oven-dried (140 °C) or flame-dried glassware under an atmosphere of dry argon unless otherwise noted. Dry dichloromethane (CH_2Cl_2), tetrahydrofuran (THF), diethyl ether (Et_2O), acetonitrile (MeCN), toluene (PhMe), and dimethoxyethane (DME) were obtained by percolation through columns packed with neutral alumina and columns packed with Q5 reactant, a supported copper catalyst for scavenging oxygen, under a positive pressure of argon. Solvents used for liquid-liquid extraction and chromatography were: Ethyl acetate, (EtOAc, Sigma-Aldrich, ACS grade) hexanes (Sigma-Aldrich, ACS grade), dichloromethane (CH_2Cl_2 , Fisher, ACS grade), acetone (Sigma-Aldrich, ACS Grade), diethyl ether (Et_2O , Fisher, ACS grade), and pentane (Sigma-Aldrich, ACS grade). Reactions that were performed open to air utilized solvent dispensed from a wash bottle or solvent bottle, and no precautions were taken to exclude water. Column chromatography was performed using EMD Millipore 60 Å (0.040–0.063 mm) mesh silica gel (Sigma-Aldrich). Analytical thin-layer chromatography (TLC) was performed on Merck silica gel 60 F254 TLC plates. Visualization was accomplished with UV (210 nm), and potassium permanganate (KMnO_4) or *p*-anisaldehyde staining solutions.

^1H NMR and ^{13}C NMR spectra were recorded at 298 K on Bruker GN500 (500 MHz ^1H ; 125 MHz, ^{13}C) and Bruker CRYO500 (500 MHz ^1H ; 125 MHz, ^{13}C) spectrometers. ^1H and ^{13}C spectra were referenced to residual chloroform (7.26 ppm ^1H ; 77.00 ppm, ^{13}C) or residual methanol (3.31 ppm, ^1H ; 49.00, ppm ^{13}C). Chemical shifts are reported in ppm and multiplicities are indicated by: s (singlet), d (doublet), t (triplet), q (quartet), p (pentet), hept (heptet), m (multiplet), and br s (broad singlet). Coupling constants, are reported in Hertz. The raw fid files were processed into the included NMR spectra using MestReNova 11.0, (Mestrelab Research S. L.). Infrared (IR) spectra were recorded on a Varian 640-IR instrument on NaCl plates and peaks are reported in

cm⁻¹. Mass spectrometry data was obtained from the University of California, Irvine Mass Spectrometry Facility. High-resolution mass spectra (HRMS) were recorded on a Waters LCT Premier spectrometer using ESI-TOF (electrospray ionization-time of flight) or a Waters GCT Premier Micromass GC-MS (chemical ionization), and data are reported in the form of *m/z*).

1.7.2 Experimental Procedures



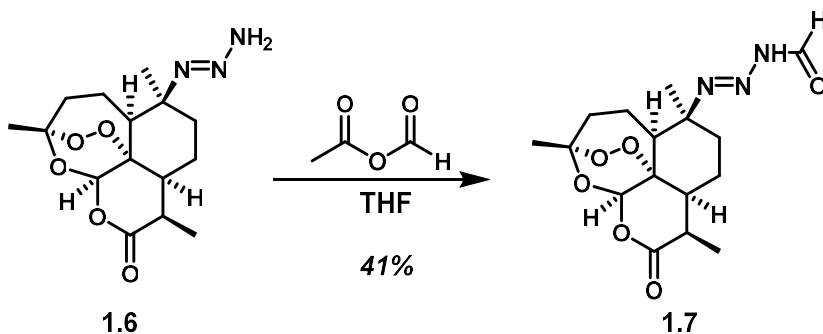
(**3**,5a**S**,6**S**,8a**S**,9**R**,12**R**,12a**S**)-3,6,9-Trimethyl-6-(**E**)-triaz-1-en-1-yl)octahydro-12H-3,12-

epoxy[1,2]dioxepino[4,3-*i*]isochromen-10(**B**)-one (**1.6**):

A 10 mL round bottom flask was charged with azide **1.4**⁴⁴ (44 mg, 0.14 mmol, 1 equiv), triphenylphosphine (62.0 mg, 0.20 mmol, 1.5 equiv), THF (0.35 mL) and **10** (0.10 mL). The solution was heated to 60°C and stirred for 16 h. After cooling to room temperature, the reaction mixture was diluted with CH₂Cl₂ (5.0 mL) and H₂O (5.0 mL). The phases were separated, and the aqueous phase was extracted with CH₂Cl₂ (2 x 5.0 mL). The combined organic extracts were dried over MgSO₄ and concentrated *in vacuo*. The residue was purified by chromatography on silica gel, eluting with hexanes/EtOAc/NEt₃ 85:14:1 (*v/v*), to afford 18 mg (45% yield) **1.6** as a white solid.

¹H NMR (500 MHz, CDCl₃): δ 9.63 (*d*, *J* = 13.7 Hz, 1H), 9.12 (*d*, *J* = 10.8 Hz, 1H), 6.20 (*s*, 1H), 3.45 – 3.39 (*m*, 1H), 2.52 – 2.39 (*m*, 1H), 2.08 (*dd*, *J* = 14.9 Hz, 1H), 1.97 (*dd*, *J* = 12.1, 7.1 Hz, 3H), 1.81 (*dd*, *J* = 27.2, 13.8 Hz, 4H), 1.56 (*s*, 3H), 1.44 (*s*, 3H), 1.29 – 1.23 (*m*, 4H).

¹³C NMR (125 MHz, CDCl₃): δ 172.5, 105.3, 95.0, 80.1, 65.4, 52.8, 45.6, 38.9, 35.8, 33.0, 29.8, 25.3, 25.2, 20.0, 19.4, 12.7.

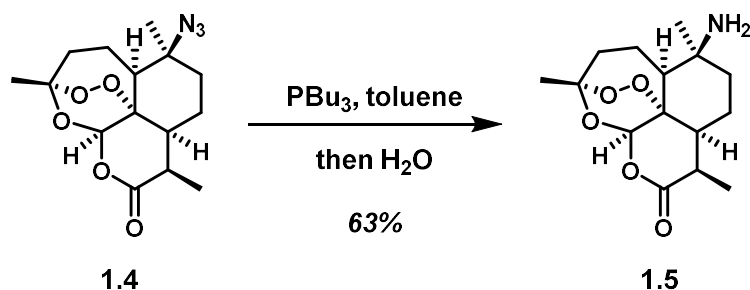


(E)-3-((R,3aS,6S,8aS,9R,12R,12aS)-3,6,9-Trimethyl-10-oxodecahydro-12H-3,12-

epoxy[1,2]dioxepino[4,3-i]isochromen-6-yl)triaz-2-ene-1-carbaldehyde (1.7) A 10 mL round bottom flask was charged with solid triazene **1.6** (18 mg, 0.06 mmol, 1 equiv) and dry THF (0.5 mL). The solution was cooled to 0 °C and acetyl formyl anhydride (20 mg, 0.11 mmol, 2 equiv) was added dropwise via syringe addition. The mixture was warmed to room temperature and stirred for 6 h. The reaction was quenched with saturated aqueous ammonium chloride (5 mL) and extracted with EtOAc (3 x 5 mL). The combined organic extracts were dried over Na₂SO₄ and concentrated *in vacuo*. The residue was purified by chromatography on silica gel, eluting with hexanes/EtOAc 95:5 (v/v), to afford 8 mg (41% yield) **1.7** as a white solid.

¹H NMR (500 MHz, CDCl₃): δ 9.93 (d, = 10.4 Hz, 1H), 9.13 (d, = 10.4 Hz, 1H), 6.25 (s, 1H), 3.47 – 3.39 (m, 1H), 2.49 – 2.40 (m, 1H), 2.12 – 2.03 (m, 2H), 1.96 (s, 3H), 1.86 – 1.75 (m, 2H), 1.62 (dd, = 16.8, 7.2, 3.4 Hz, 2H), 1.44 (s, 3H), 1.28 (s, 3H), 1.22 (dd, = 12.9, 4.4 Hz, 4H).

¹³C NMR (126 MHz, CDCl₃): δ 172.1, 164.4, 105.4, 94.6, 79.8, 68.5, 52.6, 45.5, 39.0, 35.7, 33.0, 25.3, 24.9, 20.0, 19.6, 12.6.



(*R*,5*aS*,6*S*,8*aS*,9*R*,12*R*,12*aS*)-6-Amino-3,6,9-trimethyloctahydro-12*H*-3,12-

epoxy[1,2]dioxepino[4,3-*i*]isochromen-10(3*H*)-one (**1.5**) 10 mL round bottom flask was

charged with solid azide **1.4** (84 mg, 0.26 mmol, 1 equiv), toluene (1.5 mL), and

tributylphosphine (0.12 mL, 0.39 mmol, 1.50 equiv). The reaction mixture was stirred for 4 h at

room temperature. H₂O (0.2 mL, 1.3 mmol, 5 equiv) was added and the reaction mixture was

stirred at room temperature for 16 h. The reaction mixture was diluted with CH₂Cl₂ (5 mL) and

H₂O (1 mL), then extracted with CH₂Cl₂ (3 x 5 mL). The combined organic extracts were dried

over MgSO₄. The filtrate was concentrated in vacuo and the residue was purified by

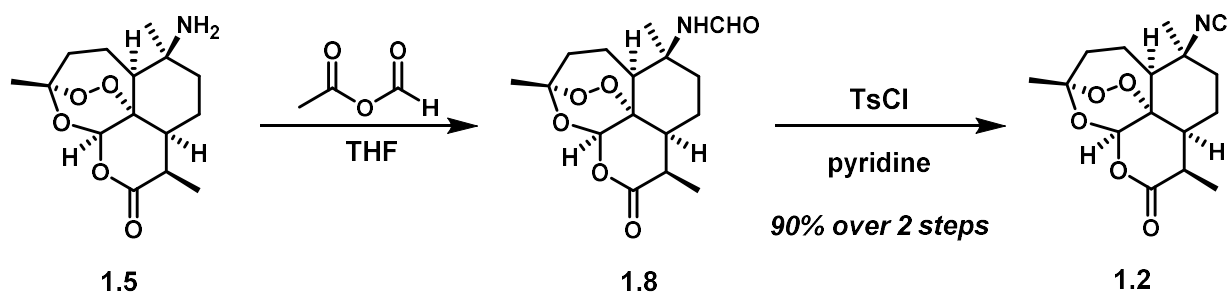
chromatography on silica gel, eluting with hexanes/EtOAc/NEt₃ 85:14:1 (v/v), to afford 47 mg

(63% yield) of **1.5** as a white solid.

¹H NMR (600 MHz, CDCl₃): δ 7.04 (s, 1H), 3.39 – 3.31 (m, 1H), 2.49 – 2.40 (m, 1H), 2.13 – 2.05 (m, 1H), 1.82 (dd, *J* = 7.0, 3.4 Hz, 1H), 1.76 (ddd, *J* = 14.4, 10.0, 4.2 Hz, 2H), 1.69 (dd, *J* = 13.3, 3.4 Hz, 1H), 1.62 (dd, *J* = 11.9, 7.1 Hz, 2H), 1.45 (s, 3H), 1.25 (s, 3H), 1.21 (s, 3H), 0.89 – 0.82 (m, 4H).

¹³C NMR (125 MHz, CDCl₃): δ 172.6, 105.0, 94.6, 80.0, 51.7, 45.9, 40.9, 35.7, 33.9, 32.9, 29.7, 25.3, 19.8, 19.5, 12.7.

HRMS (ES+) *m/z* calc'd for C₁₅H₂₃NO₅ [M+H]⁺: 298.1654; found: 298.1649.



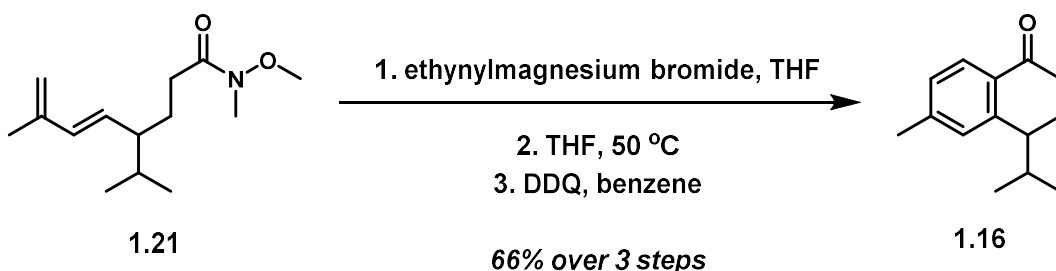
(*R*,5*aS*,6*S*,8*aS*,9*R*,12*R*,12*aS*)-6-Isocyano-3,6,9-trimethyloctahydro-12*H*-3,12-

epoxy[1,2]dioxepino[4,3-*i*]isochromen-10(3*H*)-one (1.2) 10 mL round bottom flask was charged with solid amine **1.5** (47 mg, 0.16 mmol, 1 equiv) and dry THF (2 mL). The solution was cooled to 0 °C and acetyl formyl anhydride (204 mg, 1.58 mmol, 10 equiv) was added dropwise via syringe addition. The mixture was warmed to room temperature and stirred for 1 h. The reaction mixture was concentrated *in vacuo*. The residue was dissolved in CH₂Cl₂ (2.0 mL), and pyridine (0.40 mL, 1.41 mmol, 10 equiv) and tosyl chloride (450 mg, 1.58 mmol, 10 equiv) was added to the solution. The mixture was stirred at room temperature for 1 h. The reaction mixture was diluted with CH₂Cl₂ (10 mL), then washed with water (5 mL) and brine (5 mL). The organic phase was dried over Na₂SO₄ and concentrated *in vacuo*. The residue was purified by chromatography on silica gel, eluting with hexanes/EtOAc 80:20 (v/v), to afford 43 mg (90% yield over 2 steps) of **1.2** as a white solid.

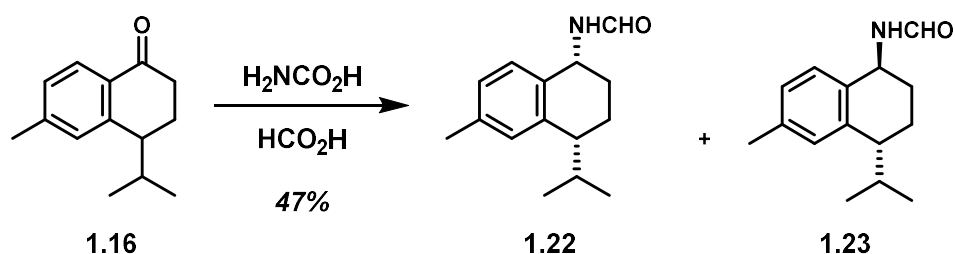
¹H NMR (500 MHz, CDCl₃): δ 6.30 (s, 1H), 3.36 (dd, *J* = 7.2, 6.1 Hz, 1H), 2.46 (ddd, *J* = 14.7, 13.2, 4.2 Hz, 1H), 2.24 – 2.16 (m, 2H), 2.12 – 2.03 (m, 1H), 2.01 – 1.94 (m, 1H), 1.94 – 1.89 (m, 1H), 1.83 – 1.77 (m, 1H), 1.70 – 1.63 (m, 1H), 1.55 – 1.53 (m, 4H), 1.49 (t, *J* = 7.8 Hz, 3H), 1.25 (d, *J* = 10.8 Hz, 4H).

¹³C NMR (125 MHz, CDCl₃): δ 171.3, 159.9 (t, *J* = 3.8 Hz), 105.4, 92.9, 78.9, 61.7 (t, *J* = 4.9 Hz), 50.9, 45.0, 39.5, 35.2, 32.7, 29.6, 25.2, 20.5, 19.7, 12.6.

HRMS (ES+) *m/z* calc'd for C₁₅H₂₃NO₃ [M+Na]⁺: 330.1317; found 330.1306.



4-Isopropyl-6-methyl-3,4-dihydronaphthalen-1(1*H*)-one (**1.16)** A 25 mL round bottom flask was charged with a solution of **1.21** (100 mg, 0.42 mmol, 1 equiv) in THF (6.0 mL). The solution was cooled to 0 °C and a 0.35 mM solution of ethynylmagnesium bromide in THF (6.0 mL, 2.10 mmol, 5 equiv) was added dropwise over 5 min. The solution was warmed to room temperature and stirred for 2 h. The reaction mixture was quenched with 1M HCl (5 mL) and extracted with EtOAc (3 x 5 mL). The combined organic phases were dried with Na₂SO₄ and concentrated *in vacuo*. The residue was dissolved in dry THF, warmed to 50 °C, and stirred for 4 h. The reaction mixture was cooled to room temperature. The solvent was removed *in vacuo* and the reaction flask was charged with benzene (2.5 mL) and had DDQ (237 mg, 1.04 mmol, 2.5 equiv) added portionwise. The reaction mixture was stirred at room temperature for 4 h. The solution was concentrated *in vacuo* and the residue was purified by chromatography on silica gel, eluting with hexanes/EtOAc 90:10 (v/v), to afford 55 mg (66% yield) of **1.16** as a clear, colorless oil. ¹H and ¹³C NMR spectra were consistent with those previously reported.⁴⁷



***N*-((1*R*,4*R*)-4-Isopropyl-6-methyl-1,2,3,4-tetrahydronaphthalen-1-yl)formamide (**1.22**)** and ***N*-((1*S*,4*R*)-4-Isopropyl-6-methyl-1,2,3,4-tetrahydronaphthalen-1-yl)formamide (**1.23**)** A 25 mL

Schlenk tube was charged with tetralone **1.16** (770 mg, 3.81 mmol, 1 equiv), carbamic acid (4.60 mL, 114.01 mmol, 30 equiv), and formic acid (2.90 mL, 76.20 mmol, 20 equiv). The reaction vessel was evacuated and filled with Ar, sealed, and was heated to 180 °C for 2 h. The reaction mixture was cooled to room temperature and was diluted with hexanes (10 mL). The solution was washed with saturated aqueous sodium bicarbonate (10 mL). The organic phase was dried with Na₂SO₄ and concentrated *in vacuo*. Crude NMR indicated a 5:3 ratio of diastereomers favoring **1.22** as the major product. The residue was purified by chromatography over silica gel, eluting with hexanes/EtOAc 70:30 (v/v) to afford 187 mg of **1.22**, 153 mg of **1.23** both a clear colorless oils. 77 mg of a mixture of **1.22** and **1.23** was also isolated (combined yield of 47%).

1.22

¹H NMR (500 MHz, CDCl₃): δ 8.16 (s, 1H), 7.13 (J_d, 7.8 Hz, 1H), 7.08 (s, 1H), 6.97 (J_d, 7.8 Hz, 1H), 5.97 (d, J = 6.0 Hz, 1H), 5.19 – 5.05 (m, 1H), 2.71 – 2.59 (m, 1H), 2.40 – 2.33 (m, 1H), 2.31 (d, J = 6.2 Hz, 3H), 2.01 – 1.91 (m, 1H), 1.86 (dd_d, 14.1, 8.1, 3.9 Hz, 1H), 1.82 – 1.72 (m, 1H), 1.69 – 1.59 (m, 1H), 1.05 (J_d, 6.9 Hz, 3H), 0.74 (d, J = 6.9 Hz, 3H).

¹³C NMR (125 MHz, CDCl₃): δ 160.2, 140.5, 137.4, 133.4, 129.5, 128.6, 127.1, 46.6, 42.7, 30.9, 27.7, 21.4, 21.2, 18.5, 17.2.

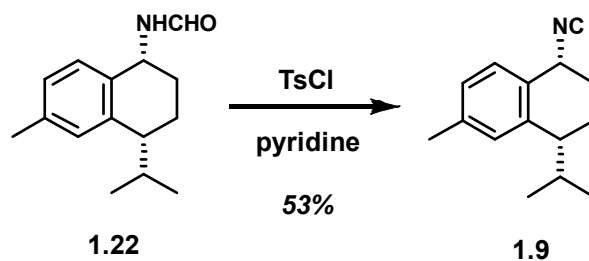
HRMS (ES+) m/z calc'd for C₁₅H₂₁NO [M+Na]⁺: 254.1521; found: 254.1521.

1.23

¹H NMR (500 MHz, CDCl₃): δ 8.27 (s, 1H), 7.14 (J_d, 7.9 Hz, 1H), 7.05 (s, 1H), 6.98 (J_d, 7.9 Hz, 1H), 5.81 (d, J = 6.8 Hz, 1H), 5.18 (dd, J = 14.2, 8.7 Hz, 1H), 2.72 (dd, J = 13.4, 6.0 Hz, 1H), 2.30 (s, 3H), 2.29 – 2.23 (m, 1H), 2.23 – 2.15 (m, 1H), 1.88 – 1.80 (m, 1H), 1.70 – 1.53 (m, 3H), 1.04 (d, J = 6.8 Hz, 3H), 0.69 (d, J = 6.8 Hz, 3H).

¹³C NMR (125 MHz, CDCl₃): 160.6, 140.5, 136.7, 134.4, 128.9, 126.9, 126.9, 46.7, 43.1, 31.6, 29.5, 21.3, 21.2, 20.5, 17.1.

HRMS (ES^+) m/z calc'd for $C_{15}H_{21}NO$ $[M+Na]^+$: 254.1521; found: 254.1521.

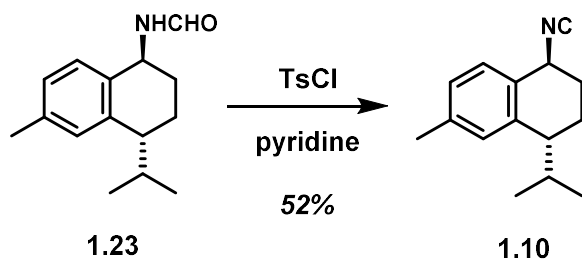


(**1R,4R**)-1-isocyano-4-isopropyl-6-methyl-1,2,3,4-tetrahydronaphthalene (**1.9**) 10 mL round bottom flask was charged with formamide **1.22** (187 mg, 0.81 mmol, 1 equiv) and pyridine (2.5 mL). Tosyl chloride (1.54 g, 8.10 mmol, 10 equiv) was added portionwise. The reaction mixture was stirred for 12 h at room temperature. The reaction mixture was diluted with CH_2Cl_2 (5 mL) and saturated aqueous ammonium chloride (5 mL). The phases were separated, and the aqueous phase was extracted with CH_2Cl_2 (2 x 5 mL). The combined organic extracts were dried over Na_2SO_4 and concentrated *in vacuo*. The residue was purified by chromatography over silica gel, eluting with hexanes/EtOAc 85:15 (v/v) to afford 90 mg (53% yield) **1.9** as a colorless oil.

1H NMR (500 MHz, $CDCl_3$): δ 7.23 (*d*, $J = 7.8$ Hz, 1H), 7.13 (*s*, 1H), 7.03 (*d*, $J = 7.7$ Hz, 1H), 4.73 (*s*, 1H), 2.77 – 2.68 (*m*, 1H), 2.40 (*d*, $J = 5.0$ Hz, 1H), 2.34 (*s*, 3H), 2.27 – 2.17 (*m*, 1H), 2.00 – 1.87 (*m*, 2H), 1.85 – 1.76 (*m*, 1H), 1.08 (*d*, $J = 6.9$ Hz, 3H), 0.76 (*d*, $J = 6.9$ Hz, 3H).

^{13}C NMR (125 MHz, $CDCl_3$): δ 155.04 (*t*, $J = 4.8$ Hz), 139.66, 138.44, 130.00, 129.03, 128.77, 127.14, 52.54 (*t*, $J = 5.5$ Hz), 42.39, 31.57, 28.62, 21.42, 21.09, 17.85, 16.80.

HRMS (Cl^+) m/z calc'd for $C_{15}H_{19}N$ $[M]^+$: 213.1517; found: 213.1526.



(S,4R)-1-isocyano-4-isopropyl-6-methyl-1,2,3,4-tetrahydronaphthalene (1.10) A 10 mL round bottom flask was charged with formamide **1.23** (153 mg, 0.66 mmol, 1 equiv) and pyridine (2.0 mL). Tosyl chloride (1.26 g, 6.61 mmol, 10 equiv) was added portionwise and the reaction mixture was stirred for 12 h at room temperature. The reaction mixture was diluted with CH₂Cl₂ (5 mL) and saturated aqueous ammonium chloride (5 mL). The phases were separated, and the aqueous phase was extracted with CH₂Cl₂ (2 x 5 mL). The combined organic extracts were dried with Na₂SO₄ and concentrated *in vacuo*. The residue was purified by chromatography over silica gel, eluting with hexanes/EtOAc 85:15 (v/v) to afford 73 mg (52% yield) of **1.10** as a colorless oil.

¹H NMR (500 MHz, CDCl₃): δ 7.40 (t, *J* = 7.8 Hz, 1H), 7.11 – 6.99 (m, 2H), 4.72 (s, 1H), 2.80 (J dd, 13.4, 6.1 Hz, 1H), 2.39 – 2.35 (m, 1H), 2.34 (s, 3H), 2.26 (J dd, 1.9, 6.8 Hz, 1H), 1.97 (ddd, = 23.4, 13.8, 8.8 Hz, 2H), 1.63 – 1.56 (m, 1H), 1.02 (J t, 6.9 Hz, 3H), 0.67 (d, = 6.9 Hz, 3H).

¹³C NMR (125 MHz, CDCl₃): δ 155.2 (t, *J* = 4.9 Hz), 139.0, 137.8, 130.2, 128.9, 127.2, 126.9, 53.3 (t, *J* = 6.2 Hz), 42.6, 31.8, 30.2, 21.3, 21.0, 20.0, 17.0.

HRMS (Cl⁺) *m/z* calc'd for C₁₅H₁₉N [M]⁺: 213.1517; found: 213.1514.

1.8 References

- ¹ World Malaria Report. *World Health Organization* **2015**. World Health Organization, Geneva
- ² Rich, S. M.; Leendertz, F. H.; Xu, G.; LeBreton, M.; Djoko, C. F.; Aminake, M. N.; Takang, E. E.; Dikko, J. L. D.; Pike, B. L.; Rosenthal, B. M.; Formenty, P.; Boesch, C.; Ayala, F. J.; Wolfe, N. D. "The Origin of Malignant Malaria." *Proc. Natl. Acad. Sci. USA* **2009**, *106*, 14902–14907.
- ³ Tu, Y. "The Discovery of Artemisinin and Gifts from Chinese Medicine" *Nat. Med.* **2011**, *17*, 1217–1220.
- ⁴ Muangphrom, P.; Seki, H.; Fukushima, E. O.; Murunaka, T. "Artemisinin-Based Antimalarial Research." *Nat. Med.* **2016**, *70*, 318–334.
- ⁵ Caraballo, H.; King, K. "How Not to Miss a Case of Malaria in Emergency Department in Malaria Non-Endemic Areas? Practical Approach & Experiences in Hong Kong." *Emerg. Med. Pract.* **2014**, *16*, 1–23.
- ⁶ "Malaria Fact Sheet No. 94." *World Health Organization* **2014**.
- ⁷ Centers for Disease Control and Prevention, **2018**. *CDC - malaria - about malaria - history*. Centers for Disease Control and Prevention.
- ⁸ a) Perkins, S. L. "Malaria's Many Mates: Past, Present and Future of the systematics of the order of Haemosporida." *J. Parasitol.* **2014**, *100*, 11–25. b) Perkins, D. J.; Were, T.; Davenport, G. C.; Kempaiah, P.; Hittner, J. B.; Ong'Echa, J. M. "Severe Malarial Anemia: Innate Immunity and Pathogenesis." *Int. J. of Bio. Sci.* **2011**, *7*, 1427–1442; c) Perlmann, P.; Troye-Blomberg, M. "Malaria Blood-Stage Infection and Its Control By The Immune System." *Folia Biologica.* **2000**, *46*, 210–218.
- ⁹ a) Coronado, L. M.; Nadovich, C. T.; Spadafora, C. "Malarial Hemozoin: From Target to Tool." *Biochimica et Biophysica Acta* **2014**, *1840*, 2032–2041; b) Tyberghein, A.; Deroost, K.; Schwarzer, E.; Arese, P.; Van den Steen, P. E. "Immunopathological effects of malaria pigment or hemozoin and other crystals." *BioFactors* **2014**, *40*, 59–78.
- ¹⁰ a) Deroost, K.; Lays, N.; Noppen, S.; Martens, E.; Opdenakker, G.; Van den Steen, P. E. "Malaria Resurgence: A Systematic Review and Assessment of Its Causes." *Malaria Journal*, **2012**, *166*, 1-11; b) Pek, R. H.; Yuan, X.; Rietzschel, N.; Zhang, J.; Jackson, L.; Nishibori, E.; Ribeiro, A.; Simmons, W.; Jagadeesh, J.; Sugimoto, H.; Alam, M. Z. "Hemozoin Produced by Mammals Confers Heme Tolerance." *eLife* **2014**, *8*.
- ¹¹ Crutcher, J. M.; Hoffman, S. L. *Medical Microbiology* **2016**, *8*, 120–135.
- ¹² Dondorp, A. M.; Pongponratn, E.; White, N. J. "Reduced Microcirculatory Flow in Severe Falciparum Malaria." *Acta. Trop.* **2004**, *89*, 309–317.
- ¹³ Flückiger, F. A.; Daniel, H. *Pharmacographia "A History of the Principal Drugs of Vegetable Origin, Met with in Great Britain and British India."* **1874**, *1*, 302–331.

- ¹⁴ a) Pelletier P. J.; Caventou J. B. *Annales de Chimie et de Physique* **1820**, *15*, 337–365; b) Briquet, P. “*Traité thérapeutique du quinine et de ses préparations.*” **1853**.
- ¹⁵ Liles, N. W.; Page, E. E.; Liles, A. L.; Vesely, S. K.; Raskob, G. E.; George, J. N. “Diversity and Severity of Adverse Reactions to Quinine: A Systematic Review.” *Am. J. Hemat.* **2016**, *91*, 461–466.
- ¹⁶ *FDA Consumer Magazine*. U.S. Food and Drug Administration “*FDA Orders Stop to Marketing of Quinine for Night Leg Cramps.*” **1995**.
- ¹⁷ “*CDC: Artesunate Now First-Line Treatment for Severe Malaria in the United States.*” www.cdc.gov. **2019**.
- ¹⁸ a) Kouznetsov, V. V.; Amado T.; Diego, F. “Antimalarials: Construction of Molexular Hybrids Based on Chloroquine.” *Universitas Scientiarum*. **2008**, *13*, 306–320; b) “*The History of Malaria, an Ancient Disease*” Centers for Disease Control, **2019**.
- ¹⁹ Markus, M. B. “Biological Concepts in Recurrent Plasmodium Vivax Malaria.” *Parasitology* **2018**, *145*, 1765–1771.
- ²⁰ Fitch, C. D.; Kanjananggulpan, P. “The State of Ferriprotoporphyrin IX in Malaria Pigment.” *J. Biol. Chem.* **1987**, *262*, 15552-15555.
- ²¹ Centers for Disease Control and Prevention. *CDC - malaria - about malaria - history*. Centers for Disease Control and Prevention, **2018**.
- ²² Geneva: World Health Organization. “Guidelines for the treatment of malaria.” **2015**, 246. ISBN 978-92-4-154912-7.
- ²³ Tan, K. R.; Arguin, P. M. “Malaria: Yellow Book Travelers' Health.” *CDC*. **2018**, *3*.
- ²⁴ “*Doryx- doxycycline hyclate tablet, delayed release.*” *DailyMed*. **2020**.
- ²⁵ a) Wang, J.; Xu, C.; Wong, Y. K.; Li, Y.; Liao, F.; Jiang, T.; Tu Y. “Artemisinin, the Magic Drug Discovered from Traditional Chinese Medicine.” *Engineering* **2018**, *5*, 32–39; b) Yu, T. “Artemisinin – A Gift from Traditional Chinese Medicine to the World.” *Angew. Chem. Int. Ed.* **2016**, *55*, 10210–10226.
- ²⁶ Brown, G. “Artemisinin and a New Generation of Antimalarial Drugs.” *RSC Advances* **2006**, *43*, 97–99.
- ²⁷ a) Tilley, L.; Straimer, J.; Gnädig, N. F.; Ralph, S. A.; Fidock, D. A. “Artemisinin Actions and Resistance in Plasmodium Falciparum.” *Trends Parasitol.* **2016**, *32*, 682–696; b) Winzeler, E. A.; Manary, M. J. “Drug Resistance Genomics of the Anitmalarial Drug Artemisinin.” *Genome Biology* **2014**, *15*, 544–555.
- ²⁸ Wang, J.; Zhang, C. J.; Chia, W. N.; Loh, C. C.; Li, Z.; Lee, Y. M. “Haem-Activated Promiscuous Targeting of Artemisinin in Plasmodium Falciparum.” *Nat. Commun.* **2015**, *6*, 10111–10121.
- ²⁹ Rawat, D. “*Development of Novel Antimalarials.*” *Malaria World* **2010**.

- ³⁰ a) Arsenault P. R.; Wobbe K. K.; Weathers P. J. "Recent Advances in Artemisinin Production Through Heterologous Expression." *Curr. Med. Chem.* **2018**, *15*, 2886–2896. b) Zhu, C.; Cook, S. P. "A Concise Synthesis of (+)-Artemisinin." *J. Am. Chem. Soc.* **2012**, *134*, 33, 13577–13579.
- ³¹ a) Liu, G.; Song, S.; Shu, S.; Miao, Z.; Zhang, A.; Ding, C. "Novel Spirobycyclic Artemisinin Analogues (Artemalogues): Synthesis and Antitumor Activity." *Eur. J. Med. Chem.* **2015**, *103*, 17–28; b) Cloete, T. T.; Breytenbach, J. W.; Kock, C.; Smith, P. J.; Breytenbach, J. C.; N'Da, D. D. "Synthesis, Antimalarial Activity and Cytotoxicity of 10-aminoethylether Derivatives of Artemisinin." *Bioorg. Med. Chem.* **2012**, *20*, 4701–4709.
- ³² "Guidelines for the Treatment of Malaria Geneva: World Health Organization." **2015**, *3*.
- ³³ "WHO calls for an immediate halt to provision of single-drug artemisinin malaria pills." WHO. **2006**, *19*.
- ³⁴ Antony, H. A.; Parija, S. C. "Antimalarial Drug Resistance: An Overview." *Trop. Parasitol.* **2016**, *6*, 30–41.
- ³⁵ Krieger, J.; Smeilus, T.; Kaiser, M.; Seo, E. J.; Efferth, T.; Giannis, A. "The Antimalarial Activity of Artemisinin is Not Stereospecific." *Angew. Chemie.* **2018**, *57*, 8293–8296.
- ³⁶ a) Lim, P.; Alker, A. P.; Khim, N. "Pfm1r Copy Number and Artemisinin Derivatives Combination Therapy Failure In Falciparum Malaria In Cambodia." *Malar. J.* **2009**, *8*, 1-15; b) White, N. J. "Emergence of Artemisinin-Resistant Plasmodium Falciparum in East Africa." *N. Engl. J. Med.* **2021**, *385*, 1231–1232.
- ³⁷ Wright, A. D.; König, G. M.; Angerhofer, C. K.; Greenidge, P.; Linden, A.; Desqueyroux-Faundez, R. "Antimalarial Activity: The Search for Marine-Derived Natural Products with Selective Antimalarial Activity." *J. Nat. Prod.* **1996**, *59*, 710–716.
- ³⁸ Basco, L. K.; Le Bras, J. "In Vitro Activity of Artemisinin Derivatives Against African Isolates and Clones of *Plasmodium Falciparum*." *Am. J. Trop. Med. Hyg.* **1993**, *49*, 301–307.
- ³⁹ Daub, M. E.; Prudhomme, J.; Mamoun, C. B.; Le Roch, K. G.; Vanderwal, C. D. "Antimalarial Properties of Simplified Kalihinol Analogues." *ACS Med. Chem. Lett.* **2017**, *8*, 355–360.
- ⁴⁰ Roosen, P. C.; Vanderwal, C. D. "Investigations into an Anionic Oxy-Cope/Transannular Conjugate Addition Approach to 7,20-Diisocyanoadociane." *Org. Lett.* **2014**, *16*, 4368–4371.
- ⁴¹ a) Daub, M. E.; Prudhomme, J.; Le Roch, K.; Vanderwal, C. D. "Synthesis and Potent Antimalarial Activity of Kalihinol B." *J. Am. Chem. Soc.* **2015**, *137*, 4912–4915; b) Daub, M. E.; Roosen, P. C.; Vanderwal, C. D. "General Approaches to Structurally Diverse Isocyanoditerpenes." *J. Org. Chem.* **2017**, *82*, 4533–4541; c) White, A. M.; Dao, K.; Vrubliauskas, D.; Konst, Z. A.; Pierens, G. K.; Mándi, A.; Andrews, K. T.; Skinner-Adams, T. S.; Clarke, M. E.; Narbutas, P. T.; Sim, D. C.-M.; Cheney, K. L.; Kurtán, T.; Garson, M. J.; Vanderwal, C. D. "Catalyst-Controlled Stereoselective Synthesis Secures the Structure of the Antimalarial Isocyanoterpene Pustulosaisonitrile-1." *J. Org. Chem.* **2017**, *82*, 13313–

13323; d) Roosen, P. C.; Vanderwal, C. D. "A Formal Enantiospecific Synthesis of 7,20-Diisocyanoadociane." *Angew. Chem. Int. Ed.* **2016**, *55*, 7180–7183; e) Karns, A. S.; Ellis, B. D.; Roosen, P. C.; Chahine, Z.; Le Roch, K. G.; Vanderwal, C. D. "Concise Synthesis of the Antiplasmodial Isocyanoterpene 7,20-Diisocyanoadociane." *Angew. Chem. Int. Ed.* **2019**, *58*, 1–5.

⁴² Gormisky, P. E.; White, M. C. "Catalyst-Controlled Aliphatic C–H Oxidations with a Predictive Model for Site-Selectivity." *J. Am. Chem. Soc.* **2013**, *135*, 14052–14055.

⁴³ Zhang, X.; Yang, H.; Tang, P. "Transition-Metal-Free Oxidative Aliphatic C–H Azidation." *Org. Lett.* **2015**, *17*, 5828–5831.

⁴⁴ Pronin, S. V.; Reiher, C. A.; Shenvi, R. A. "Stereoinversion of tertiary alcohols to tertiary-alkyl isonitriles and amines." *Nature* **2013**, *501*, 195–199.

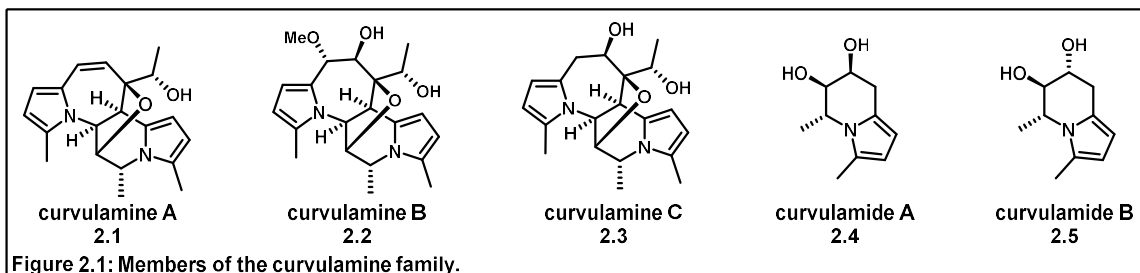
⁴⁵ Ha, V. T.; Kien, V. T.; Binh, L. H.; Tien, V. D.; My, N. T. T.; Nam, N. H.; Baltas, M.; Hahn, H.; Han, B. W.; Thao, D. T.; Vu, T. K. "Design, Synthesis and Biological Evaluation of Novel Hydroxamic Acids Bearing Artemisinin Skeleton." *Bioorg. Chem.* **2016**, *66*, 63–71.

⁴⁶ Tse-Lok, H.; Yang, P. "Synthesis of Phenolic Sesquiterpenes via Oxidative Cleavage of Benzocycloalkenols." *Tetrahedron* **1995**, *51*, 181–192.

Chapter 2: Introduction to the Curvulamine Family of Natural Products

2.1 Introduction

Five alkaloid natural products, named the curvulamines (**Figure 2.1**), were isolated and characterized in 2014 by Tan and coworkers. Biological testing indicated that the tetracyclic members of the curvulamine family exhibited potent and selective microbial growth inhibition. The highly complex,



unprecedented tricyclic core with two fused electron-rich pyrroles has drawn the attention of synthetic chemists. Herein is described the notable work published on the curvulamine family and structural considerations necessary for pursuing the total synthesis of these natural products. Synthetic efforts toward the synthesis of the core of curvulamine A by previous Vanderwal lab member Dr. Brian Atwood as well as the successful synthesis of curvulamine A by Maimone and coworkers are discussed in detail.

2.2 Isolation

2.2.1 Antibiotic Resistance

With the longstanding practice of antibiotic prescription for treatment of infectious diseases, pathogenic drug-resistance has become a prevalent issue, prompting the continued search for natural products with selective antimicrobial properties.¹ Antibiotics that are broad spectrum and operate via mechanisms of action different than those commonly prescribed are of great interest to the pharmaceutical industry.² Production of novel antibiotics has become more necessary as drug-resistance continues to evolve in disease causing bacteria.³ Growth inhibition selectivity is also highly valued, as selective antibiotics maintain homeostasis of the human gut biome and have lower levels of toxicity.⁴

For these reasons, research in the discovery and synthesis of natural products with potent antimicrobial activity and minimal off-target effects is a vast field in modern science.

2.2.2 Isolation of the Curvulamine Family

In 2014, anecdotal evidence of a species of fish, native to the Sea of China, that was noted to feed on rotten carrion, led Tan and coworkers to investigate the white croaker (*Argyrosomus argentatus*).⁵ It was discovered that extracts from the fungus (*Curvularia sp.*) found thriving in the fish's gut had potent antibiotic properties. Isolation and characterization of compounds found in these extracts led to the discovery of five novel natural products, deemed the curvulamine family (**Figure 2.1**), named for the fungus from which it was isolated. Three tetracyclic alkaloid natural products were identified by mass spectrometry and their structure was determined via rigorous NMR experiments and diffraction experiments, denoted as curvulamines A (**2.1**), B (**2.2**), and C (**2.3**). Two indolizidine alkaloids were also discovered and assigned the structures of **2.4** and **2.5**, deemed curvulamides A and B, respectively. Due to the structural similarities, the bicyclic curvulamides were hypothesized to be biosynthetic precursors to the tetracyclic members of the curvulamine family.

2.3 Biological Considerations

2.3.1 Bioactivity of the Curvulamines

In the initial publication disclosing the discovery of the curvulamine family, Tan and coworkers reported potent antimicrobial bioactivity of the large members of

	Curvulamine A	Tinidazole
<i>Veillonella parvula</i>	0.37 μ M	0.49 μ M
<i>Actinomyces israelii</i>	>10 μ M	>10 μ M
<i>Streptococcus sp.</i>	0.37 μ M	1.01 μ M
<i>Bacteroides vulgatas</i>	0.37 μ M	2.02 μ M
<i>Peptostreptococcus sp.</i>	0.37 μ M	2.02 μ M

Table 2.1: Curvulamine antimicrobial activity.

the family.⁵ Curvulamine A was tested against a panel of infectious species of bacteria (**Table 2.1**) and was shown to exhibit high levels of potency in growth inhibition. Curvulamine A was found to be more efficacious and was also exhibited a higher level of selectivity than commercially prescribed antibiotic tinidazole.⁶ Curvulamine A proved inert toward the growth of *Actinomyces israelii*, indicating antimicrobial selectivity. Curvulamine A also displayed no antifungal properties, while tinidazole has been

shown to exhibit high levels of non-specific efficacy against fungi.^{6b} No reports have been published on the mechanism of action for the antibiotic activity of the curvulamines.

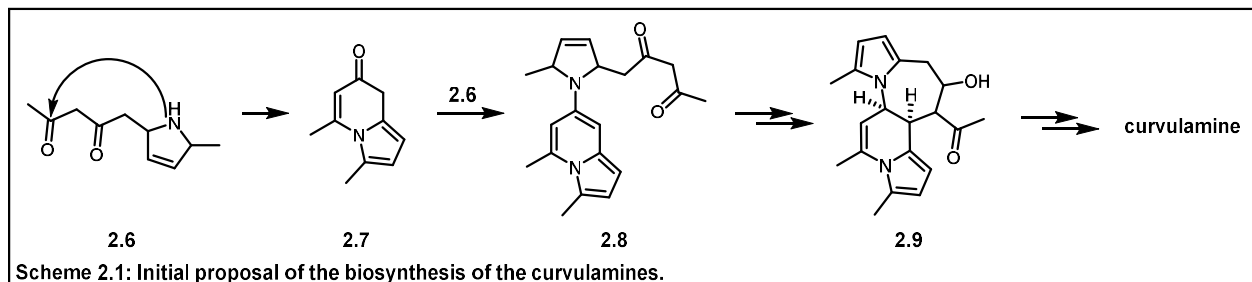
Relative to the curvulamines, the curvulamides exhibit decreased antibiotic activity; however, the curvulamides have been found to exhibit moderate potency as acetylcholine esterase inhibitors (ACEIs) **Table 2.2**.⁷ Although the activity is modest when compared to commercially prescribed ACEI tacrine, its efficacy is promising enough to have led Tan and coworkers to patent the use of the curvulamides as ACEIs. Within the patent, Tan and coworkers cite their intention to investigate the use of the curvulamides in the prevention of developing symptoms caused by Alzheimer's disease.⁸ No mechanism of action for the curvulamides' biological activity has been published.

Compound	IC ₅₀ (μM)
Curvulamine A	68.37
Curvulamine B	64.33
Curvulamine C	76.91
Curvulamide A	6.91
Curvulamide B	4.33
Tacrine	0.17

Table 2.2: Curvulamide ACEI activity.

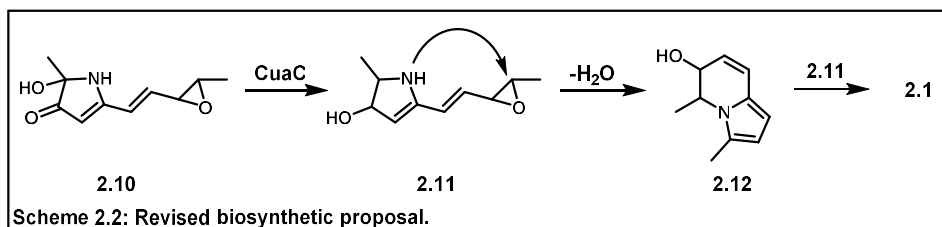
2.3.2 Biosynthetic Studies

Feeding studies indicated the involvement of the polyketide synthase pathway in biosynthesis of the curvulamine family, leading the authors to propose a biosynthetic pathway to the curvulamines (**Scheme 2.1**).⁵ They propose a cyclization of dihydropyrrole **2.6** to form indolizinone **2.7**, which could be



envisioned as a precursor of the curvulamides. Condensation of a second molecule of **2.6** would allow for cyclization to form the seven-membered ring (**2.9**), which was proposed to be elaborated through further oxidation and dehydration events to afford **2.1**. Although this proposal did account for the involvement of the polyketide synthesis pathway and the formal dimerization of curvulamide precursor **2.7**, there was no evidence for the proposed transformations.

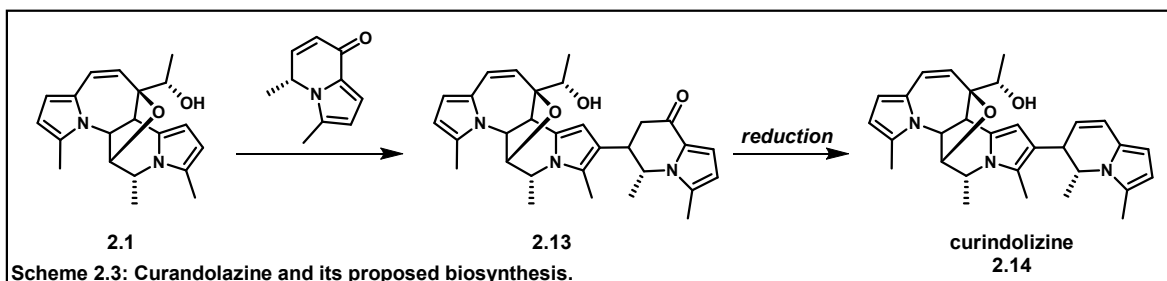
Tan and coworkers investigated the biosynthetic pathway more deeply, focusing on a gene cluster that they discovered was vital for the biosynthesis.



This led Tan and coworkers to propose a different biosynthesis, which still involved the polyketide synthase pathway, but invoked the reduction of vinyllogous amide **2.10** with CuaC to precursor **2.11**, which undergoes intramolecular cyclization to afford **2.12** (Scheme 2.2).⁹ This pathway was corroborated by noted accumulation of congener **2.10** in modified *Curvularia* that had the gene for CuaC production deleted. Indolizolinol **2.12** can be formally hydrated to afford curvulamides A and B (**2.4**, **2.5**). It is proposed that **2.12** and **2.11** are combined and further elaborated to afford the large members of the family, though no pathway forward is proposed as investigations of the late stages of curvulamine biosynthesis are still underway.

2.3.3 Efforts Toward High Scale Isolation of the Curvulamines

The potential for the use of the curvulamines as a selective antibiotic led multiple labs to pursue scalable methods of generating the natural products via growth of *Curvularia sp.*¹⁰ These studies afforded the natural products in modest yields, the most successful of which resulted in isolating 210 milligrams of a mixture of the curvulamines from a five liter fermentation.^{10b} The production of compound was noted to decrease drastically with respect to the scale of the bioreactor, proving a major limitation in large scale isolation efforts.^{10b} Unexpectedly, large scale isolation resulted in the isolation of a previously undiscovered member of the curvulamine family, **2.14**, named curindolazine (Scheme 2.3).¹¹



It was proposed that the synthesis of **2.13**, occurred via incorporation of a third indolizine subunit via Michael–type addition of the nucleophilic pyrrole of curvulamine A to a cyclic Michael acceptor.⁹

Curindolizine (**2.14**) has not been found to exhibit the antibiotic efficacy of the other family members. Curindolazine does exhibit anti-inflammatory properties, with efficacy moderately equivalent to commercially prescribed dexamethasone.¹² This anti-inflammatory activity is not exhibited by any of the previously reported members of the curvulamine family (**Table 2.3**). A more in-depth study on the mechanism of action for this antiinflammatory pathway hypothesizes curindolizine reduces the production of nitric oxide, a known inflammatory agent.¹³ It is also proposed that curindolizine inhibits expression of genes associated with the inflammatory response, though further investigations into the mechanism of action are needed. Recent work by Maimone and coworkers developed a synthetic route to afford curindolizine from curvulamine A.¹⁴

	IC ₅₀ (μM)	survival rate (%)
curindolazine	5.31 ± 0.21	97.60 ± 3.42
dexamethasone	2.17 ± 0.15	96.33 ± 2.11

Table 2.3: Curindolizine anti-inflammatory data.

2.3.4 Genome Modifications Resulting in Novel Products

Investigations of the gene cluster vital to the synthesis of the curvulamines revealed multiple dormant proteins capable of modifying the secondary metabolites.⁹ Overexpression of a putative transcription factor responsible for the

	curvulamine A (2.1)	bipolamine G (2.15)
<i>Veillonella parvula</i>	0.37	0.32
<i>Actinomyces Israelii</i>	>10	>10
<i>Streptococcus sp.</i>	0.37	0.32
<i>Bacteroides vulgatas</i>	0.37	0.32
<i>Peptostreptococcus sp.</i>	0.37	0.32

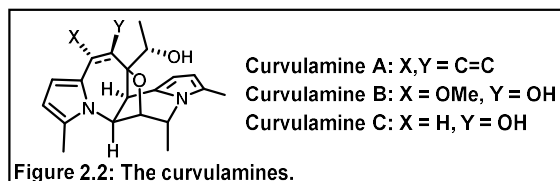
Table 2.4: Bipolamine G antimicrobial potency.

promotion of these dormant genes resulted in the biosynthesis of nine new members of the family. The structural variations of these newly discovered compounds included alterations of the curvulamides as well as changes in the skeletal structure of the curvulamines. These compounds were tested for biological activity, and it was discovered that one of these newly discovered alkaloids, bipolamine G (**2.15**) exhibited greater antimicrobial efficacy than curvulamine A (**Table 2.4**).

2.4 Structural Considerations and Synthetic Efforts

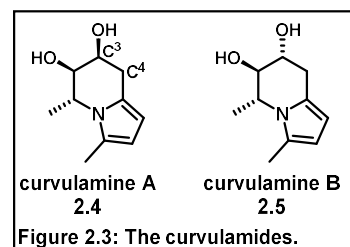
2.4.1 Structural Analysis

A three-dimensional representation of the curvulamines (**Figure 2.2**) highlights many of the synthetic challenges posed by these natural products.



The curvulamines differ only by the oxygenation pattern of seven-membered ring system. All three compounds exhibit a [7–6–5] tricyclic core, bridged by a five-membered tetrahydrofuran ring. This is the first example reported of this skeletal arrangement in any isolated natural product.⁵ Fused to the core are two electron-rich pyrroles.¹⁵ The piperidine ring also contains an array of chemical complexity. The caged structure and pyrrole ring force the six-membered ring into a boat-like conformation. The piperidine has substitution at each carbon center and contains four contiguous stereocenters, three of which have their substituents on the same face leading to large steric constraints. The α -substituted pyrrole induces allylic strain onto the methyl group, forcing these stereocenters into pseudo-axial conformation. Curvulamine A (**2.1**) contains a total of five stereogenic centers, one of which is a secondary alcohol distal to the core structure, while curvulamines B and C (**2.2** and **2.3**) contain seven and six stereocenters, respectively, which arise from oxidation events at the seven-membered ring alkene.

Curvulamides A and B (**2.4**, **2.5**) are comprised of a highly substituted piperidine core and an electron-rich pyrrole (**Figure 2.3**).⁷ These alkaloids differ only at the stereochemistry of the alcohol at the C3 carbon. The curvulamides mirror the piperidine core of the curvulamines but lack the

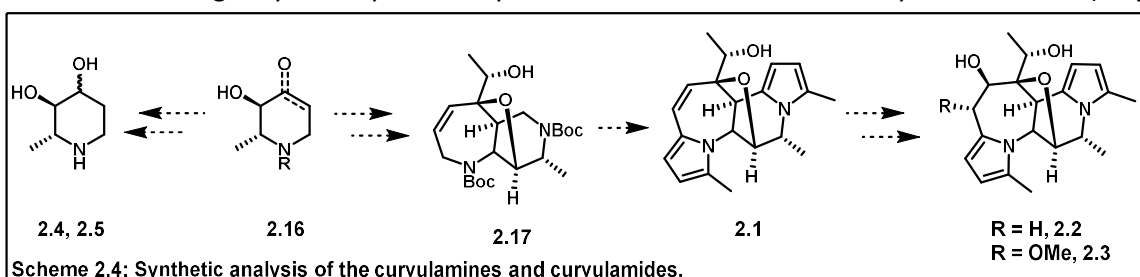


high complexity of the tricyclic core. The piperidine ring contains three contiguous stereocenters subjected to steric constraint via allylic strain induced by the pyrrole α -substitution.¹⁶ This conformation forces all three stereocenters of **2.5** into pseudoaxial positions due to their alternating stereochemical

relationship and two of the stereocenters of **2.4** into this pseudoaxial arrangement. The major difference noted between the curvulamides and the curvulamines is the lack of substitution at C4 on **2.4** and **2.5**, presumed to be the point of connection of the dimeric compounds.

2.4.2 Synthetic Considerations

When evaluating a synthetic approach toward the curvulamine family, curvulamine A (**2.1**) was believed to be biologically and synthetically converted to the other tetracyclic members (**2.2**, **2.3**)



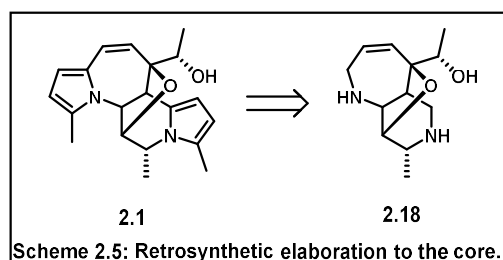
(Scheme 2.4). With potential reactivity issues posed by electron-rich pyrroles, the core lacking pyrroles (**2.17**) was targeted, with the strategy of installing the pyrroles at a late stage. The high complexity piperidine ring system was believed to be the major challenge of the core synthesis, leading us to target piperidine congener **2.16**. Dr. Brian Atwood targeted multiple piperidine systems that mapped on to **2.16**, as it was believed that the preinstalled stereochemistry could be used to leverage diastereocontrol when appending the seven-membered ring. It was also believed to be easily derivatized to the curvulamides (**2.4**, **2.5**).

One of the most apparent challenges posed by the synthesis was the electron-rich pyrroles in all members of the family. Electron-rich pyrroles are challenging functionalities to have present over multiple synthetic steps due to their highly nucleophilic nature, sensitivity to acidic and oxidative conditions, and propensity to dimerize.¹⁷ Pyrrole-containing natural products are a distinct synthetic challenge; although many total syntheses of pyrrole-containing natural products have been completed, most of these syntheses result in electron-poor pyrroles or pyrroles conjugated with aromatic systems, both of which exhibit attenuated reactivity.¹⁸ The nucleophilic nature of pyrroles causes them to undergo undesired side reactivity in the presence of oxidants and electrophiles. Pyrroles have also been

found to eject neighboring leaving groups via gramine-type fragmentation, to form the reactive aza-fulvenium cation.¹⁹ Pyrroles have also been observed to polymerize in oxidative conditions.²⁰ Generally, these issues are avoided in total synthesis by using electron-poor pyrroles; however, all members of the curvulamine family contain electron-rich pyrroles. In our retrosynthetic analysis, any route employing electron-poor pyrroles, to be converted at the end of the synthesis, was non-obvious.²¹ The large members of the curvulamine family contain two electron-rich pyrrole rings, complicating any synthetic strategies involving carrying the pyrroles through multiple synthetic steps.

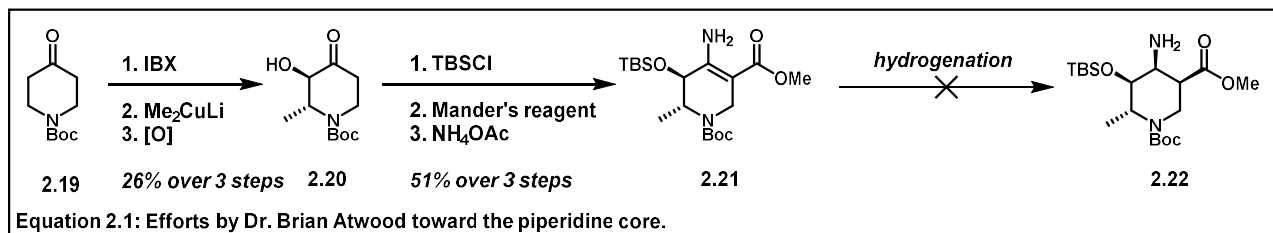
2.4.3 Previous Synthetic Efforts by the Vanderwal Lab

With the synthetic challenges in mind, it was decided that an effective synthesis to the tricyclic core of curvulamine A (**2.18**, **Scheme 2.5**) would provide a scaffold to perform a late-stage pyrrole installation. This strategy



would access the natural product while avoiding the promiscuous reactivity of pyrroles throughout the synthesis. Initial efforts toward the synthesis of the curvulamine family of natural products in the Vanderwal lab began in 2015 by Dr. Brian Atwood.²² Although many routes were devised and pursued, herein we will focus on two routes, as the results were pertinent to our later synthetic efforts.

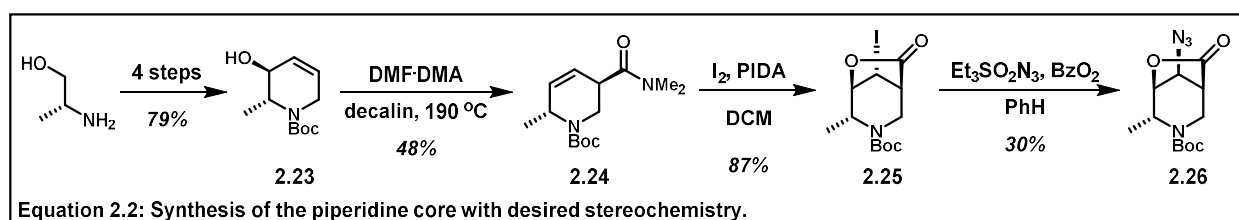
The formation of the three *cis* stereocenters on the piperidine ring was thought to be one of the key challenges in the formation of the core. This was initially approached via formation of piperidinone **2.20** from commercially available **2.19**, which was further elaborated to vinylogous amide **2.21** (**Equation 2.1**). It was hoped that **2.22** could be obtained by hydrogenation; however, all hydrogenation



conditions were unsuccessful and hydride reduction conditions afforded only the undesired

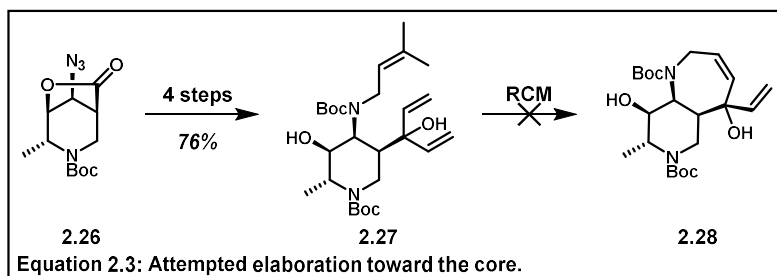
diastereomer, directed by steric congestion caused by the pseudoaxial methyl group.²³ These efforts unveiled the challenge of forming the three cis stereocenters on the piperidine ring, especially highlighting the high steric congestion of the pseudoaxial methyl group. This work also provided a synthetic route to intermediate **2.20**, which will be discussed in chapter 4 (Section 4.3.2).

The most successful synthetic attempt pursued by Dr. Atwood utilized piperidinol (**2.23**), synthesized in four steps from commercially available alaninol (Equation 2.2).²⁴ The remainder of the contiguous cis stereocenters were established via [2,3]-Buchi rearrangement and iodolactonization to



obtain **2.25**, which underwent radical azidation to afford **2.26**.²⁵ It is worth noting that polar azidation substitution reactions resulted in the undesired stereochemistry, indicating the reaction did not proceed through a standard S_N2 mechanism, the details of which are discussed in depth in Dr. Brian Atwood's thesis.²² This was the first route that was able to successfully establish the four stereocenters on the piperidine ring in the correct configuration.

Elaboration of the azide and diaddition of vinyl Grignard to the bridging lactone afforded triene **2.27**, which only required ring-closing metathesis to obtain the seven-membered ring (**2.28**) (Equation 2.3). Unfortunately, all



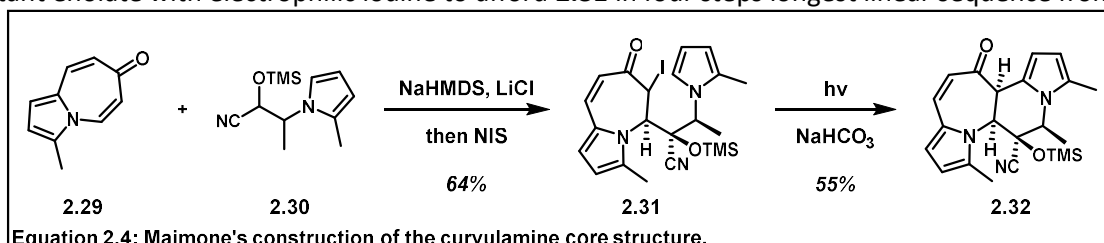
efforts toward alkene metathesis were unsuccessful and the 7,6-bicycle was not afforded.

This synthesis further highlighted the stereochemical challenges the highly congested piperidine ring posed and underscores the utility of intramolecular transfer of stereochemical information to establish the challenging triad of cis stereocenters. The route also made it apparent that formation of

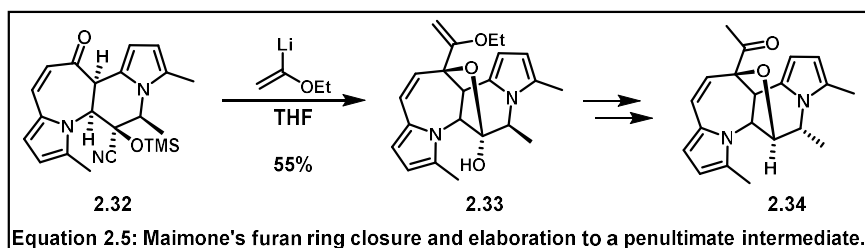
the seven-membered ring would be a synthetic challenge, which had been previously considered an afterthought behind the synthesis of the congested piperidine ring.

2.4.4 Maimone and Coworkers' Total Synthesis

When the Vanderwal lab began this project in 2015, there had been no syntheses of any members of the curvulamine family published in the literature. In 2020, Maimone and coworkers published a total synthesis of curvulamine A (**2.1**).²⁶ The fragment-oriented synthesis conjoined pyrrolo-azapinone **2.29** with electron-rich pyrrole fragment **2.30** via Michael addition and trapping of the resultant enolate with electrophilic iodine to afford **2.31** in four steps longest linear sequence from



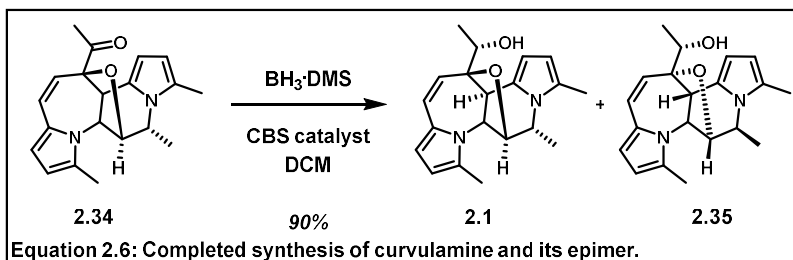
commercially available materials (**Equation 2.4**). Notably, this synthesis affords **2.31** as a mixture of enantiomers, which are resolved later in the synthesis. Capitalizing on the nucleophilicity of the electron-rich pyrrole, irradiation of **2.31** promoted cyclization to afford tetracycle **2.32**. Addition of lithiated ethyl vinyl ether and deprotection of the cyanohydrin formed the central caged ring structure



(**2.33**) (**Equation 2.5**).

Stereocenter epimerization and a two-step procedure to remove the unwanted alcohol was conducted to afford **2.34**.

The final step of the synthesis invoked an enantioselective reduction to resolve the racemates, affording curvulamine (**2.1**) and epimer **2.35** (**Equation 2.6**). Maimone's synthesis of



curvulamine (**2.1**) was concise, affording **2.1** in only 10 steps longest linear sequence.

Maimone and coworkers' successful synthesis of curvulamine was an impressive feat in natural product synthesis, especially when considering that an electron-rich pyrrole was present in every step of the sequence. Maimone credited some poor yielding reactions and the need for intense optimization to undesired pyrrole reactivity. It was for these reasons that, from the outset, the Vanderwal lab had avoided the inclusion of pyrroles in our synthetic considerations.

2.5 Conclusions

The curvulamine family of natural products displays wide array of bioactivities, all of which require further investigation into their mechanisms of actions. Efforts to produce large quantities of material, via synthetic biology, have proven challenging on appreciable scale. The synthetic challenge of these alkaloids is enticing to synthetic chemists, as the highly complex and unprecedented caged structures, as well as the electron-rich pyrroles present opportunity to investigate novel transformations. The structural complexity of these natural products has led to the development of a large breadth of work developed by both the Vanderwal lab and Maimone lab. These natural products have also inspired synthetic efforts that will be discussed in the next two chapters of this thesis, including the pursuit of a synthesis to the core of curvulamine, the synthesis of the curvulamides, and attempts to develop novel pyrrole annulation chemistry.

2.6 References

¹ D'Costa, V. M.; King, C. E.; Kalan, L.; Morar, M.; Sung, W. W. L.; Schwarz, C.; Froese, D.; Zazula, G.; Calmels, F.; Debruyne, R.; Golding, G. B.; Poinar, H. N.; Wright, G. D. "Antibiotic Resistance is Ancient." *Nature* **2011**, *477*, 457–461.

² Rossiter, S. E.; Fletcher, M. H.; Wuest, W. M. "Natural Products as Platforms to Overcome Antibiotic Resistance." *Chem. Rev.* **2017**, *117*, 12415–12474.

³ Smith, P. A.; Romesberg, F. E. "Mechanism of Action of Arylomycin Antibiotics and Effects of Signal Peptidase I Inhibition." *Antimicrob. Agents Chemother.* **2012**, *56*, 5054–5060.

⁴ Szamosvari, D.; Schuhmacher, T.; Hauck, C. R.; Bottcher, T. "A Thiochromenone Antibiotic Derived from the *Pseudomonas* Quinolone Signal Selectively Targets the Gram-Negative Pathogen *Moraxella Catarrhalis*." *Chem. Sci.*, **2019**, *10*, 6624–6628.

⁵ Han, W. B.; Lu, Y. H.; Zhang, A. H.; Zhang, G. F.; Mei, Y. N.; Jiang, N.; Lei, X.; Song, Y. C.; Ng, S. W.; Tan, R. X. "Curvulamine, a New Antibacterial Alkaloid Incorporating Two Undescribed Units from a *Curvularia* Species." *Org. Lett.* **2014**, *16*, 5366–5369.

⁶ a) Wust, J. "Susceptibility of Anaerobic Bacteria to Metronidazole, Ornidazole, and Tinidazole and Routine Susceptibility Testing by Standardized Methods." *Antimicrob. Agents Chemother.* **1977**, *11*, 631–637; b) Manes, G.; Balzano, A. "Tinidazole: From protozoa to *Helicobacter pylori*." *Expert Rev. Anti-Infect. Ther.* **2004**, *2*, 695–705.

⁷ Tan, R. X.; Zhang, G.; Song, Y.; Cui, J.; Wang W. "Method for Preparing Curvularin and Indolizidine Alkaloid and Application." **2011**, CN102329735B, Nanjing University.

⁸ Robles, A. "Pharmacological Treatment of Alzheimer's Disease: Is it Progressing Adequately?" *Open Neurol. J.* **2009**, *3*, 27–44.

⁹ Dai, G. Z.; Han, W. B.; Mei, Y. N.; Xu, K.; Jiao, R. H.; Ge, H. M.; Tan, R. X. "Pyridoxal-5'-Phosphate-Dependent Bifunctional Enzyme Catalyzed Biosynthesis of Indolizidine Alkaloids in Fungi." *Proc. Natl. Acad. Sci. U. S. A.*, **2020**, *117*, 1174–1180.

¹⁰ a) Wei, X.; Liu, C.; An, F.; Liu, Y. "Induced Effect Of Ca²⁺ on Curvulamine Synthesis by Marine-Derived Fungus *Curvularia* Sp. IFB-Z10 Under Submerged Fermentation." *Process Biochemistry* **2019**, *83*, 18–26; b) Yang, J.; Jiao, R. H.; Yao, L. Y.; Han, W. B.; Lu, Y. H.; Tan, R. X. "Control Of Fungal Morphology For Improved Production of a Novel Antimicrobial Alkaloid by Marine-Derived Fungus *Curvularia* Sp. IFB-Z10 Under Submerged Fermentation." *Process Biochemistry* **2015**, *51*, 185–194.

¹¹ Han, W. B.; Zhang, A. H.; Lei, X.; Tan, R. X. "Curindolizine, an Anti-Inflammatory Agent Assembled via Michael Addition of Pyrrole Alkaloids Inside Fungal Cells." *Org. Lett.* **2016**, *18*, 1816–1819.

¹² Abraham, S. M.; Lawrence, T.; Kleiman, A.; Warden, P.; Medghalchi, M.; Tuckermann, J.; Saklatvala, J.; Clark, A. R. "Antiinflammatory Effects of Dexamethasone are Partly Dependent on Induction of Dual Specificity Phosphatase 1." *J. Exp. Med.* **2006**, *203*, 1883–1889.

¹³ Costa, J. F.; Barbosa-Filho, J. M.; Maia, G. L.; Guimarães, E. T.; Meira, C. S.; Ribeiro-dos-Santos, R.; de Carvalho, L. C.; Soares, M. B. "Potent Anti-Inflammatory Activity of Betulinic Acid Treatment in a Model of Lethal Endotoxemia." *Int. Immunopharmacol.* **2014**, *23*, 469–474.

¹⁴ Xuan, J.; Haelsig, K. T.; Scheremt, M.; Machicao, P. A.; Maimone, T. J. "Total Syntheses of Curvulamine and Curindolizine." *J. Am. Chem. Soc.* **2021**, *143*, 7, 2970–2983.

¹⁵ a) Schröder, F.; Franke, S.; Francke, W.; Baumann, H.; Kaib, M.; Pasteels, J. M.; Daloze, D. "A New Family of Tricyclic Alkaloids from *Myrmecaria* Ants." *Tetrahedron*, **1996**, *52*, 13539–13546; b) Ondrus, A. E.; Movassaghi, M. "Total Synthesis and Study of Myrmecarin Alkaloids." *Chem. Commun.* **2009**, 4151–4165;

c) Snyder, S. A.; Elsohly, A. M.; Kontes, F. "Synthetic and Theoretical Investigations of Myrmecarin Biosynthesis." *Angew. Chem., Int. Ed.* **2010**, *49*, 9693–9698.

¹⁶ Tietze, L. F.; Schulz, G. "Investigations into the Biosynthesis of Porphyrins and Corrins—Calculations on 1,3-Allylic Strain and [1,5]-Sigmatropic Rearrangements in Pyrroles, Furans, and Thiophenes." *Chem. Eur. J.* **1997**, *3*, 523–529.

¹⁷ Martin, C. L.; Nakamura, S.; Otte, R.; Overman, L. E. "Total Synthesis of (–)-Condylocarpine." *Org. Lett.* **2011**, *13*, 138–141.

¹⁸ Singh, N.; Singh, S.; Kohli, S.; Singh, A.; Asiki, H.; Rathee, G.; Chandra, R.; Anderson, E. A. *Org. Chem. Front.*, **2021**, *8*, 5550–5573; Banwell, M. G.; Lan, P. "The Total Synthesis of Pyrrole-Containing and Related Marine Natural Products" Thesis Chapter 10, *Guangdong Medical University*, **2020**, 208–226.

¹⁹ a) Schnermann, M. J.; Beaudry, C. M.; Genung, N. E.; Canham, S. M.; Untiedt, N. L.; Karanikolas, B. D. W.; Sutterlin, C.; Overman, L. E. "Divergent Synthesis and Chemical Reactivity of Bicyclic Lactone Fragments of Complex Rearranged Spongian Diterpenes." *J. Am. Chem. Soc.* **2011**, *133*, 17494–17503; b) Korienko, A.; La Clair, J. J. "Covalent modification of biological targets with natural products through Paal-Knorr pyrrole formation." *Nat. Prod. Rep.* **2017**, *34*, 1051–1060.

²⁰ Tan, Y.; Ghandi, K. "Kinetics and Mechanism of Pyrrole Chemical Polymerization." *Synthetic Metals* **2013**, *175*, 183–191.

²¹ Woodward, R. B.; Ayer, W. A.; Beatong, J. M.; Bickelhaupt, F.; Bonnet, R.; Buchshacher, P.; Closs, L. G.; Dutler, H.; Hannah, J.; Hauck, F. P.; Ito, S.; Langemann, A.; Goff, E. L.; Leimgrubber, W.; Lwowski, W.; Sauer, J.; Valenta, Z.; Volz, H. "The Total Synthesis of Chlorophyll *a*." *Tetrahedron* **1990**, *46*, 7599–7659.

²² Atwood, B.; *Unusual Natural Products, Lessons Learned in Pursuit of KS-504D and Curvulamine*; Doctorate Thesis; University of California, Irvine; **2018**.

²³ Fujimoto, R.; Kishi, Y.; Blount, J. F. "Total Synthesis of (–)-Gephyrotoxin." *J. Am. Chem. Soc.* **1980**, *102*, 7154–7156.

²⁴ Rengasamy, R.; Curtis-Long, M. J.; Seo, W. D.; Jeong, S. H.; Jeong, I.-Y.; Park, K. H. "New Building Block for Polyhydroxylated Piperidine." *J. Org. Chem.* **2008**, *73*, 2898–2901.

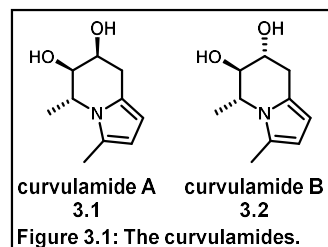
²⁵ a) Büchi, G.; Cushman, M.; Wüest, H. "Conversion of Allylic Alcohols to Homologous Amides by N,N-Dimethylformamide Acetals." *J. Am. Chem. Soc.* **1974**, *96*, 5563–5565; b) Barrero, A. F.; Altarejos, J.; Alvarez-Manzaneda, E. J.; Ramos, J.; Salido, S. "Synthesis of (–)-Ambrox from α -Nerolidol and β -Lonone via Allylic Alcohol [2,3] Sigmatropic Rearrangement." *J. Org. Chem.* **1996**, *61*, 2215–2218.

²⁶ a) Haelsig, K. T.; Xuan, J.; Maimone, T. J. "Total Synthesis of (–)-Curvulamine." *J. Am. Chem. Soc.* **2020**, *142*, 1206–1210; b) Xuan, J.; Haelsig, K. T.; Scheremt, M.; Machicao, P. A.; Maimone, T. J. "Evolution of a Synthetic Strategy for Complex Polypyrrole Alkaloids." *J. Am. Chem. Soc.* **2021**, *143*, 7, 2970–2983.

Chapter 3: Efforts Toward the Synthesis of the Curvulamides and Investigations of Novel Pyrrole Annulation Chemistry

3.1 Introduction

The alkaloids curvulamide A (**3.1**) and curvulamide B (**3.2**) are the smallest members of the curvulamine family of natural products (**Figure 3.1**). These indolizine alkaloids boast high complexity relative to their low molecular weight containing three contiguous stereocenters and an



electron-rich pyrrole moiety, making their syntheses a challenge of its own. The curvulamides also display moderate acetylcholine esterase inhibition (ACEI) activity, drawing interest for their potential pharmaceutical use. With our aim to develop syntheses of all members of the curvulamine family via late-stage pyrrole installation, the piperidine cores of the curvulamides were targeted to test the viability of this strategy. Herein, we report our efforts to synthesize the cores of curvulamides A and B and their use as model systems to gain confidence in our strategy for the syntheses of the curvulamines. Further, our efforts to develop novel methods of pyrrole annulation via C–H activation chemistry are discussed.

3.2 Syntheses of the Curvulamide Piperidine Cores

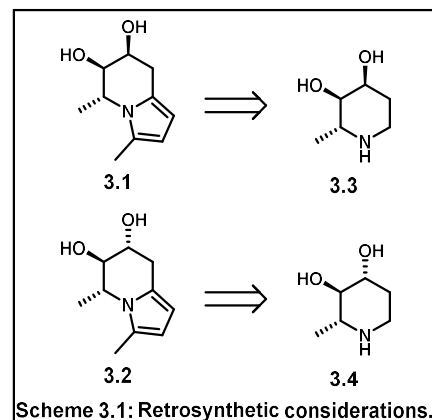
3.2.1 Justification for the Synthesis of the Curvulamides

Our strategies to synthesize all members of the curvulamine family have been based on the synthesis of the nor-pyrrole core structures followed by late-stage installation of the pyrrole heterocycles. Pyrrole installation onto non-activated secondary alkylamines is a relatively unexplored method. Recognizing the risk of relying on chemistry with very limited reported precedent and no published applications in the synthesis of natural products, it was imperative to test the application of pyrrole annulation methodologies on targets with structural similarities to the curvulamine cores. This inspired the Vanderwal lab to pursue the synthesis of piperidines **3.3** and **3.4**, the piperidine cores of

curvulamide A (**3.1**) and curvulamide B (**3.2**) (**Scheme 3.1**). Further, the curvulamides reported biological activity, having shown modest activity as Acetylcholine Esterase Inhibitors (ACEIs), made acquiring these natural products in appreciable amounts for further biotesting a valuable pursuit.¹

3.2.2 Initial Synthetic Efforts from a Previously Synthesized Intermediate

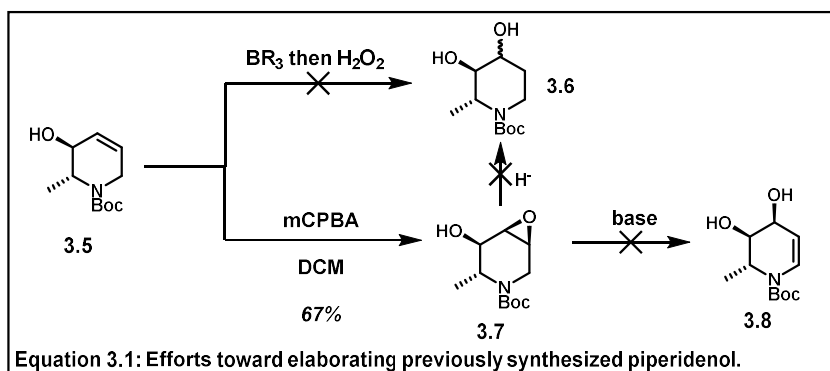
The cores of the curvulamides are previously reported natural products (+)-imino-deoxydigitoxose **3.3** and (-)-6-deoxyfagomine **3.4** (**Scheme 3.1**).^{2,3} Both natural products have been synthesized, though analyses of the reported work led us to conclude that replicating these syntheses would not allow us to obtain enough material needed to test and optimize annulation



conditions, as these syntheses were both long and afforded only milligrams of material. For this reason, we pursued a divergent synthesis we believed to be more concise and scalable, while allowing for diastereoselective syntheses of both piperidine cores.

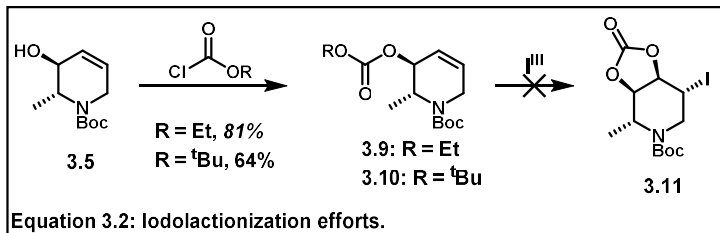
During his investigations of the synthesis of curvulamine, Dr. Brian Atwood developed a robust synthesis to afford **3.5** on multigram scale.^{4,5} Initial efforts targeted curvulamide A, and diol **3.6** was targeted via hydroboration/oxidation of **3.5** (**Equation 3.1**). All conditions generated the undesired 1,3-

diol, which is corroborated by literature precedent.⁶ Epoxide **3.7** was synthesized according to literature procedure.⁷ All efforts to open the epoxide with a



nucleophilic hydride reagent were unproductive or led to decomposition upon use of more forcing conditions. Efforts to open the epoxide via elimination conditions to afford enamine **3.8** resulted in no conversion of the starting material, likely due to poor orbital overlap.

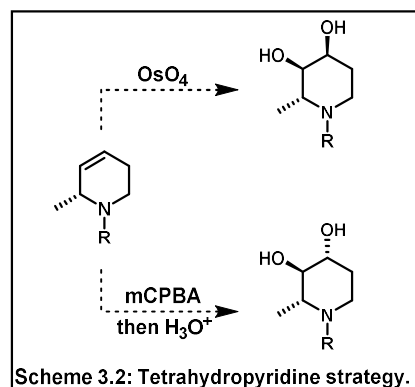
Iodolactonization of carbonates **3.9** and **3.10** was also pursued (Equation 3.2), as the iodide of the resultant carbonate (**3.11**) could be removed via



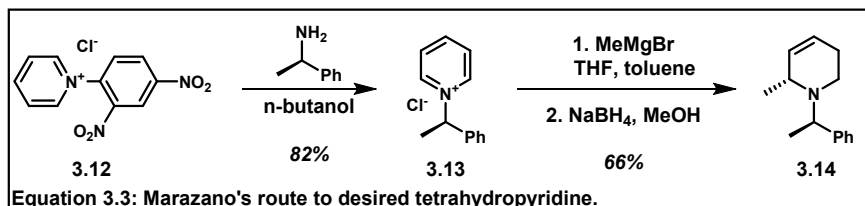
reduction; however, any attempts to generate cyclic carbonate **3.11** were unsuccessful. After elaboration of piperidenol **3.5** proved nonproductive, our synthetic strategy was reconsidered.

3.2.3 Reconsideration of Approach

Retrosynthetic analysis indicated that a methylated tetrahydropyridine could potentially afford both desired piperidine-diols via syn-dihydroxylation or epoxidation and nucleophilic opening with diastereocontrol imparted by the neighboring methyl group (Scheme 3.2). An equivalent tetrahydropyridine, tertiary amine **3.14**, had been synthesized as a



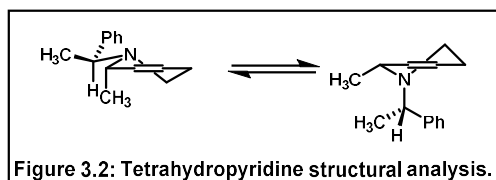
single enantiomer by Marazano and coworkers.⁸ Utilizing Zincke chemistry, pyridinium salt **3.12** was



converted to chiral amine **3.13**.⁹ This pyridinium salt was subjected to methylation

and reduction of the resultant dihydropyridine to afford the enantiopure tetrahydropyridine **3.15** in three steps (Equation 3.3).¹⁰

Molecular modelling indicated that the syn-pentane interaction between the piperidine-bound methyl and the chiral auxiliary may force the methyl into a pseudoaxial configuration, blocking the α -face, (Figure 3.2). Furthermore, the ring-flipped conformation places the chiral auxiliary in a pseudoaxial position, once more blocking the α -face. Both configurations

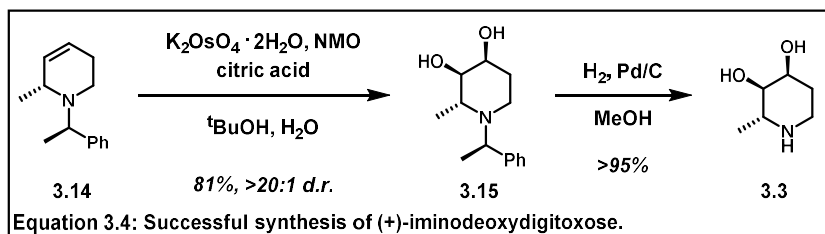


Both configurations

indicated reactivity would likely occur on the β -face as desired, leading to high diastereoselectivity.

3.2.4 Successful Synthesis of The Core of Curvulamide A

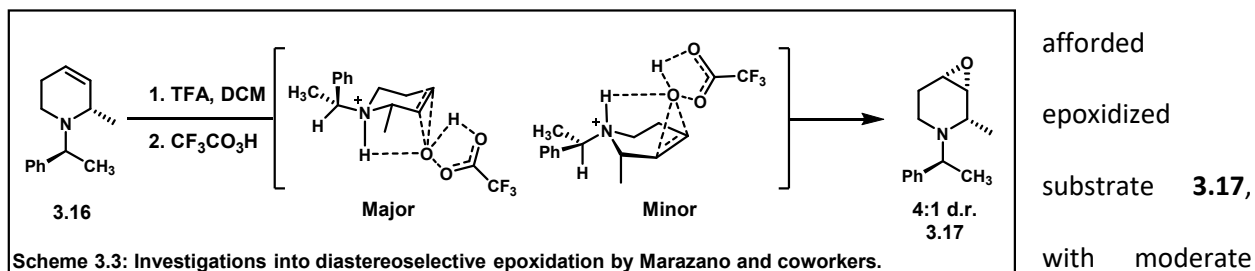
Tetrahydropyridine **3.14** was made on multigram scale via the route reported by Marazano and coworkers. After



screening a series of dihydroxylation conditions, diol **3.15** was obtained via modified Upjohn oxidation conditions in good yields and high diastereoselectivity, corroborating the hypothesis for diastereocontrol developed from modeling studies (**Equation 3.4**). It was noted that the addition of citric acid as a cocatalyst was necessary to afford **3.15** in appreciable yields, as the osmate ester was likely formed and required decomplexation.¹¹ **3.15** was subjected to hydrogenolysis conditions to afford amino-diol **3.3** in quantitative yields. This reaction sequence yielded hundreds of milligrams of (+)-iminodeoxydigitoxose (**3.3**) as a single enantiomer in six steps longest-linear sequence. **3.3** was converted to the hydrochloride salt for comparison to published spectroscopic data; all data is in agreement to that previously reported.²

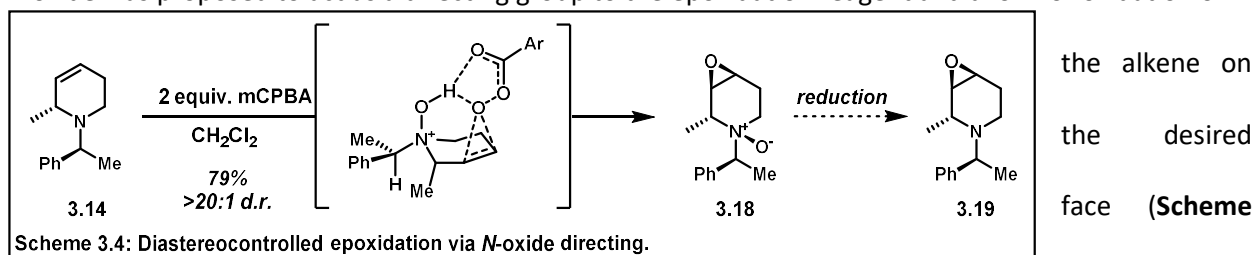
3.2.5 Efforts Toward the Core of Curvulamide B

Epoxidation of the enantiomer of **3.14** (**3.16**) had been investigated by Marazano and coworkers and it was determined that, to avoid oxidation to the *N*-oxide, the amine must first be protonated to form the ammonium salt (**Scheme 3.3**).¹² Since the protonation event is reversible, addition of acid results in the formation of the thermodynamically preferred chair structure and subsequent epoxidation



diastereocontrol driven by intermolecular hydrogen-bonding interactions. Unfortunately, the desired target for our synthesis was the minor diastereomer, and no report had been made on its synthesis.

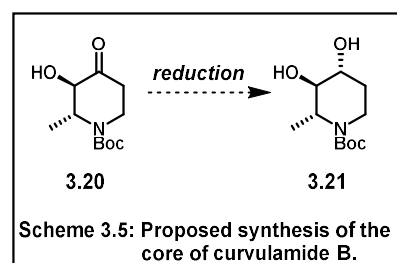
Based on the results published by Marazano, it was believed that the facial selectivity of the irreversible *N*-oxide formation would afford oxidation on the face opposite of the methyl substrate. The *N*-oxide was proposed to act as a directing group to the epoxidation reagent and allow for oxidation of



3.4). Subjecting **3.14** to a single equivalent of oxidant resulted in complete conversion to the *N*-oxide product, indicating that oxidation of the nitrogen was kinetically favored over epoxidation of the alkene. The use of multiple equivalents of oxidant led to the formation of epoxide **3.18** as a single diastereomer, characterized via Nuclear Overhauser Effect (NOE) NMR experiments. Reduction of *N*-oxide **3.18** would afford the desired epoxide (**3.19**) with complete diastereoselectivity, though, to our knowledge, conditions to reduce of *N*-oxides to tertiary amines in the presence of epoxides were not reported in the literature. **3.18** was subjected to a series of reduction conditions but all efforts were unsuccessful. Conditions to afford the more thermodynamical stable diol via hydration were also investigated but resulted in decomposition in all attempts. Without a viable method to reduce the *N*-oxide, this route to curvulamide B was abandoned.

3.2.6 Revised Synthesis to Afford the Piperidine Cores in a Divergent Manner

In an effort to access curvulamide B, we were compelled to reconsider our strategy. Dr. Brian Atwood had previously developed a synthesis of piperidinone **3.20** in his efforts toward curvulamine (discussed in 2.4.3). It was at this time a new route toward

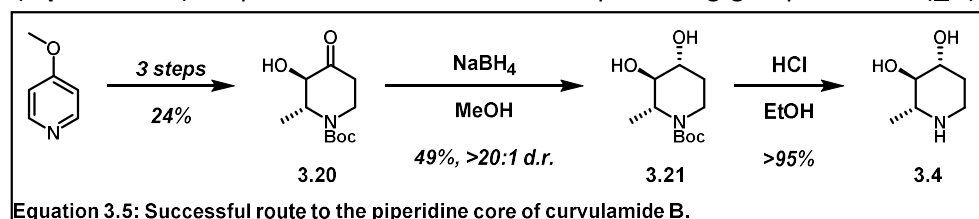


curvulamine was being investigated utilizing intermediate **3.20**. It was proposed that the pseudo-axial

methyl could direct ketone reduction to afford syn-diol **3.21** (Scheme 3.5). It was also proposed that diastereoselective reduction via α -hydroxy directing effects could aid in the diastereoselectivity.¹³

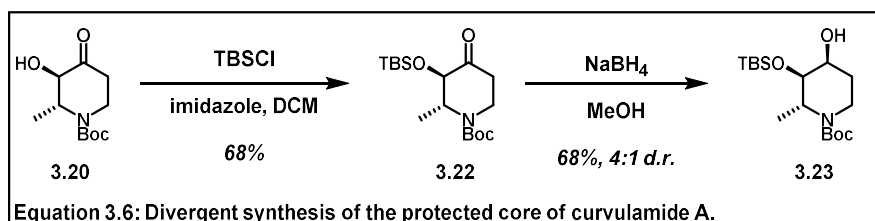
Piperidine **3.20** was afforded as a racemic mixture through an optimized route discussed in 4.3.2. Subjecting **3.20** to sodium borohydride in methanol afforded anti-diol **3.21** in moderate yields as a single diastereomer (Equation 3.5). Deprotection of the carbamate protecting group afforded (–)-6-deoxyfagomine

(**3.4**) in five steps, corroborated by



data reported in the literature.

With the intention of this route being a divergent synthesis to access both curvulamides, methods to obtain the syn-diastereomer were investigated. It was thought that utilizing a large alcohol protecting group would drive reduction to the α -face, not only via steric congestion of the β -face, but also by eliminating potential directing effects the α -hydroxyl group may have provided during reduction.



3.20 was silylated to afford silyl ether **3.22** and was subjected to reduction

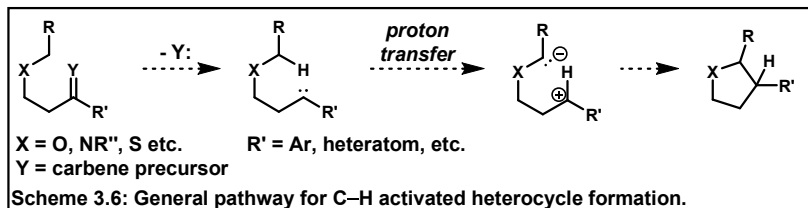
conditions to afford **3.23** in a 4:1 diastereomeric ratio favoring the syn-diol (Equation 3.6). Although the diastereoselectivity of this reaction is modest, further investigations into protecting group strategies and reducing agents could afford the protected forms of both imino-deoxydigitoxose and 6-deoxyfagomine diastereoselectively.

3.3 Efforts Toward the Curvulamides via Pyrrole Annulation

3.3.1 Heterocycle Synthesis via C–H Bond Insertion Reactions

As we developed our strategy to install the pyrrole moieties late in the synthesis, precedent indicated that the most effective way to do so would be via C–H activation and annulation. Annulation

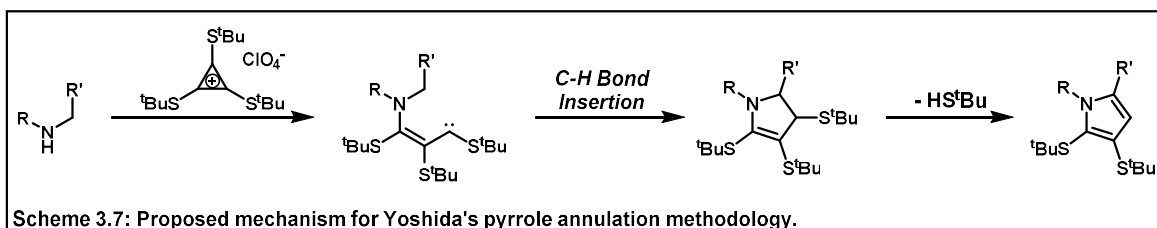
utilizing C–H activation of alkyl heteroatoms is a relatively undeveloped methodology in synthetic chemistry with great potential for building complex heterocycles. Even more rare is the conversion of secondary amines into pyrroles via C–H bond insertion. These reactions generally proceed via carbene formation in strategic positions to allow for intramolecular C–H insertion at activated aliphatic



positions (**Scheme 3.6**).¹⁴ Reported examples commonly rely on neighboring functional groups, usually aromatic moieties or heteroatoms, to stabilize the high energy intermediates. This limits the scope of these reactions, especially for natural product synthesis, as many high-value targets contain no aromatic functionality, and the removal of undesired stabilizing groups can be synthetically challenging and require multiple synthetic steps.

3.3.2 Previously Reported Heterocycle Annulation Methods

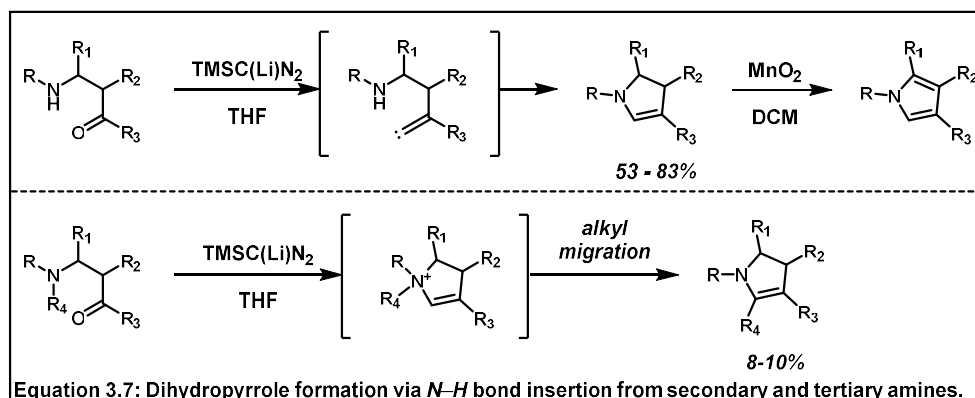
Examples of C–H bond insertion to form heterocycles are limited in scope. Although many methods utilizing carbenes to form heteroarenes are reported, these generally operate via addition to p-systems, which is not applicable to our synthesis.¹⁵ Investigation of the literature informed us of a series



of methods, developed by Yoshida and coworkers, to synthesize nitrogen-containing heterocycles, via the reaction of tris-thiol cyclopropenium salts with amines. These cationic salts were reported to afford thiolated pyridines, benzodiazepenes, and benzimidazoles, the products of which were entirely substrate dependent.¹⁶ Most applicable to our synthesis was the reported synthesis of dithiolated pyrroles, afforded by subjecting secondary amines to tris-thiol cyclopropenium salts in the presence of base.¹⁷ Yoshida's proposed mechanism (**Scheme 3.7**) proceeded via nucleophilic attack of the amine to

the cyclopropenium cation, which underwent ring-opening to afford the allylic carbene. This intermediate would then undergo C–H carbene insertion to afford the dihydropyrrole; enamine-promoted elimination of a thiol afforded the pyrrole. This methodology results in the annulation of pyrroles beginning from secondary amines, which mapped very closely to our proposed pyrrole installation strategy for the curvulamines. Yoshida also demonstrated a method to afford dethiolated pyrroles via hydrogenolysis utilizing Raney nickel.¹⁷ This method had only been applied to afford thiolated 1,2-dialkylated pyrroles, which posed the synthetic challenge of installing the required methyl group; however, the availability of pyrrole annulation chemistry to possibly install pyrroles late in our synthesis was promising.

Another example of heterocycle annulation with possible applications to our system was reported in 1997 by Shirori and coworkers, in which they reported the synthesis of dihydropyrroles utilizing 1,4-amino ketones.¹⁸ 1,4-ketoamines were converted to the alkenyl carbenoid via reaction with lithium trimethylsilyldiazomethane, and subsequent bond insertion into the secondary amine afforded dihydropyrroles, which were converted to the pyrroles under mild oxidation conditions (**Equation 3.7**)

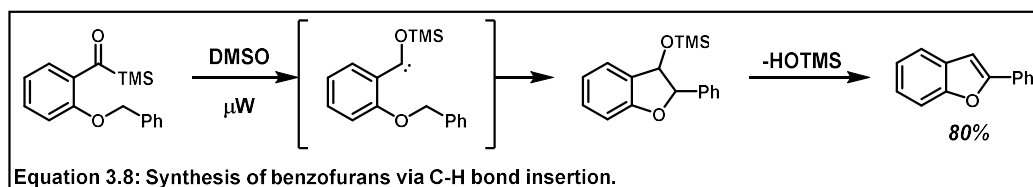


Interestingly, this reactivity was also applied to tertiary amines to afford dihydropyrroles, albeit in very poor

yields. The mechanism proposed by the authors implies the formation of the quaternary ammonium intermediate followed by subsequent alkyl migration. Although the reactivity that matched our envisioned synthesis of curvulamine was low yielding, this precedent indicated feasible pyrrole formation from N–R carbene insertion. It also is one of many examples indicating that pyrroles can be

afforded from less promiscuous dihydropyrroles via mild oxidation, allowing for leniency in the development of an annulation methodology.

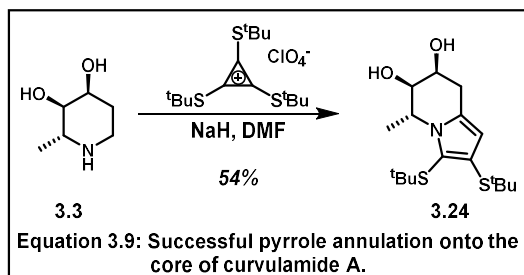
Another example of note in heterocycle formation via C–H carbene insertion was published in 2009 by Dong and coworkers. This strategy utilized acylsilanes as carbene precursors to facilitate the



synthesis of benzofurans (**Equation 3.8**).¹⁹ It was proposed that induction of a Brook rearrangement to form the benzylic carbene facilitates insertion to the neighboring benzylic position. Elimination of the silanol afforded the aromatized products in good yields. Changing the solvent from DMSO to 1,2-dichlorobenzene resulted in C–H bond insertion without elimination of silanol, giving the dihydrobenzofuran products in equivalent yields. Although this method was only applied to the formation of benzofurans, with the aid of stabilizing aromatic groups, investigations into the use of acylsilanes as carbene precursors for pyrrole annulations was of great interest to our group.

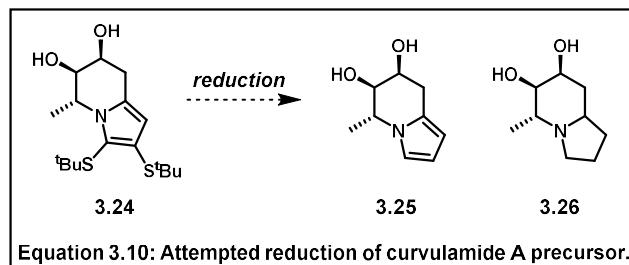
3.3.3 Attempted Applications of Pyrrole Annulation Chemistry to Afford Curvulamide A

Having obtained piperidine **3.3** in appreciable amounts, investigations of pyrrole annulations were undergone. Tris-thiol cyclopropenium was synthesized according to literature precedent and aminodiol **3.3** was subjected to Yoshida's annulation conditions to afford the dithiol-pyrrole **3.24** in yields equivalent to those reported on less complex systems (**Equation 3.9**). The successful pyrrole annulation reaffirmed our confidence in the strategy of a late-stage installation of pyrroles in our synthesis of the



curvulamines. Further, this reaction indicated a previously unreported functional group tolerance of Yoshida's chemistry, proceeding in the presence of the unprotected diol.

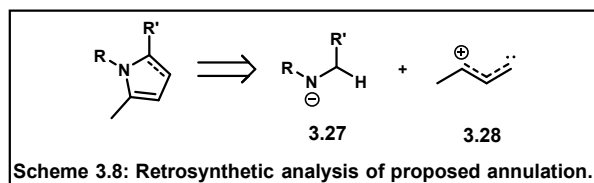
It was recognized that if this methodology was to be employed in our synthesis, dethiolation and pyrrole methylation was necessary for the synthesis of all members



of the curvulamine family. Yoshida and coworkers had published a viable dethiolation method using Raney nickel in ethanol at reflux, which are quite harsh conditions. In an effort to produce **3.25**, **3.24** was subjected to the reported dethiolation conditions, but no reactivity was observed (**Equation 3.10**). A series of reduction conditions were screened and generally gave no reactivity. Utilizing more forcing reduction conditions resulted in complete reduction to the pyrrolidine **3.26**. After extensive screening, no reactions conditions were uncovered that gave dethiolated product **3.25**. The challenging dethiolation and the lack of strategy to install the methyl substitution on the pyrrole in a regioselective manner that might be tolerated by late-stage intermediates led to abandonment of this route. These efforts were considered a success as it proved the feasibility of utilizing pyrrole annulation chemistry in a late-stage intermediate in the synthesis of these natural products.

3.3.4 Strategy for the Development of a Novel Pyrrole Annulation Methodology

When considering previously reported heterocycle annulation chemistry, the synthons **3.27** and **3.28** were considered for the synthesis of

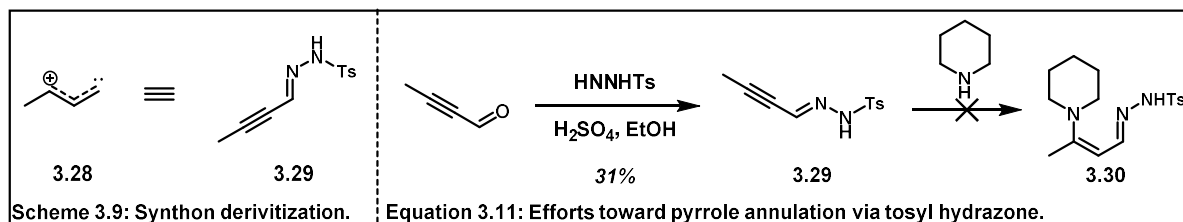


the 2-methylpyrrole necessary for the core of the curvulamine family of natural products (**Scheme 3.8**). Synthon **3.27** was considered equivalent to a secondary amine with an available α -proton, which mapped directly onto the core structure the Vanderwal lab had been targeting. Synthon **3.28** was envisioned as a substrate with an electrophile and a carbene precursor in a 1,3-relationship. This would allow for addition of the amine into the electrophilic site, and C-H insertion after carbene generation.

Derivatization of synthon **3.28** with considerations of previously reported annulation chemistry led to the investigations of many different methods for pyrrole annulation.

3.3.5 Aza-Michael Addition Strategies

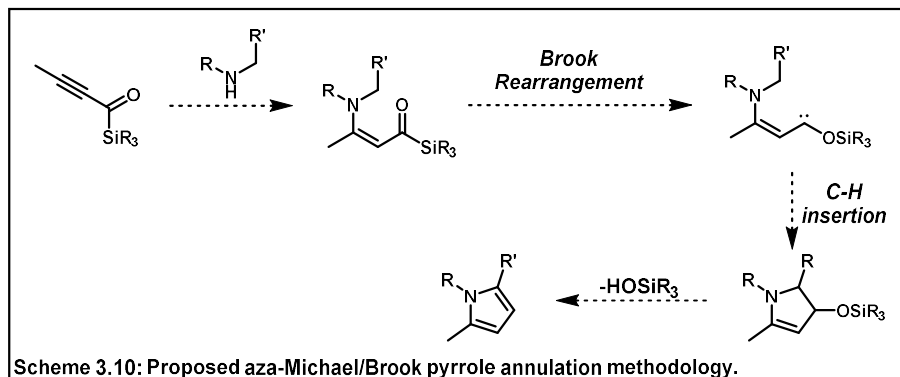
Synthon **3.28** was initially equated to hydrazone **3.29** (Scheme 3.9), which could generate the pyrrole via 1,4-aza-Michael addition followed by decomposition of the tosyl hydrazone to the diazo-species, a well-



precedented carbene precursor.²⁰ Hydrazone **3.29** was synthesized from 2-butynal and was subjected to a series of conditions to induce β -addition to synthesize **3.30**.²¹ Unfortunately, all efforts toward 1,4-addition to the hydrazone substrate were unsuccessful.

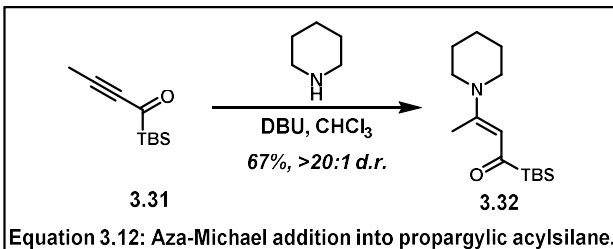
After reconsideration, the C–H bond insertion chemistry developed by Dong and coworkers (section 3.3.2) was used as inspiration for pyrrole annulation methodology (Scheme 3.10). Aza-Michael

addition to propargylic acylsilane would afford the desired carbene precursor, which would be irradiated to induce a



Brook rearrangement of the acylsilane and form the carbene, which would perform C–H insertion to afford the heterocycle. Elimination of silanol, as performed in the seminal work, would then afford the desired pyrrole.

Acylsilane **3.31** was synthesized according to literature procedure, and aza-Michael addition of piperidine occurred to afford **3.32** (Equation 3.12).²² NOE NMR experiments indicated that the



aza-Michael product **3.32** was isolated in the undesired E-conformation. It was presumed that the push-pull system would allow this bond to equilibrate to the desired conformation during irradiation.

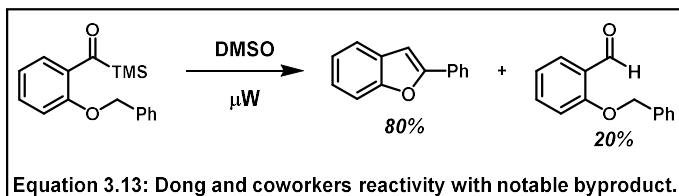
Solvent	Irradiation	Temperature	Result
toluene	oil bath	110 °C	No reaction
DMF	oil bath	153 °C	Decomposition
DMSO	oil bath	189 °C	Decomposition
toluene	microwave	150 °C	Decomposition
DMF	microwave	180 °C	Decomposition
DMSO	microwave	200 °C	Decomposition
benzene	visible light	25 °C	Aldehyde observed
CHCl ₃	visible light	25 °C	Aldehyde observed

Table 3.1: Conditions tested to promote bond insertion.

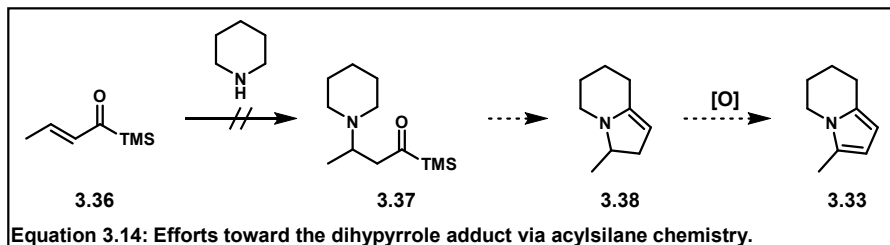
A series of irradiation conditions were screened to promote the rearrangement and bond insertion to afford either pyrrole **3.33** or dihydropyrrole **3.34** (Table 3.1). Heating via standard methods and microwave irradiation of **3.32** resulted in no reaction at modest temperatures and complete decomposition at high temperatures. Irradiation with visible light

afforded a new product, which was characterized as aldehyde **3.35**. No pyrrole or dihydropyrrole was observed. The resultant aldehyde product was circumstantial evidence of the inability of **3.32** to rotate to the desired Z-configuration necessary for C–H bond insertion.

Notably, the aldehyde was reported as the major byproduct of the similar chemistry developed by the Dong lab (Equation 3.13), which seemingly resulted from successful Brook rearrangement but unsuccessful C–H bond insertion, further corroborating the hypothesis that the undesired alkene configuration prevents productive reactivity from occurring.

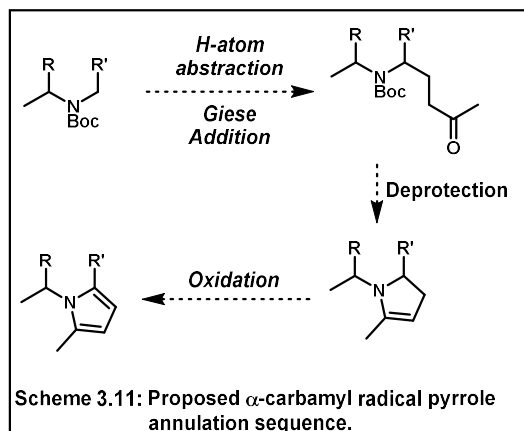


To ensure the steric bulk of the *tert*-butyldimethylsilane was not inhibiting bond rotation, the trimethylacetylsilane and triphenylacetylsilane aza-Michael adducts were synthesized but were also found to decompose to the aldehyde products when exposed to light. To account for the configurational restriction, **3.36** was synthesized according to literature procedure, with the knowledge that the resultant dihydropyrrole (**3.38**) could be readily oxidized to the **3.33** (Equation 3.14). Unfortunately, all efforts to conjoin the fragments via aza-Michael addition proved unsuccessful, and this strategy was abandoned.



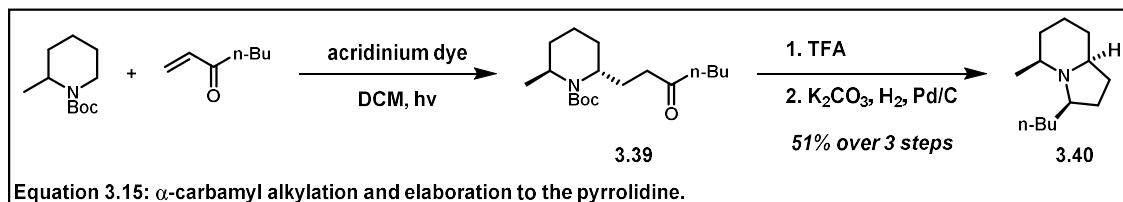
3.3.6 α -Carbamyl Radical Strategy

As our strategies utilizing carbene bond insertion proved fruitless, we turned our attention to alternative methods of activating aliphatic amines. A literature review led us to consider modern methods of C-H activation to afford α -carbamyl radicals via photocatalysis. It was proposed that the Giese addition products generated from α -carbamyl radicals would readily cyclize



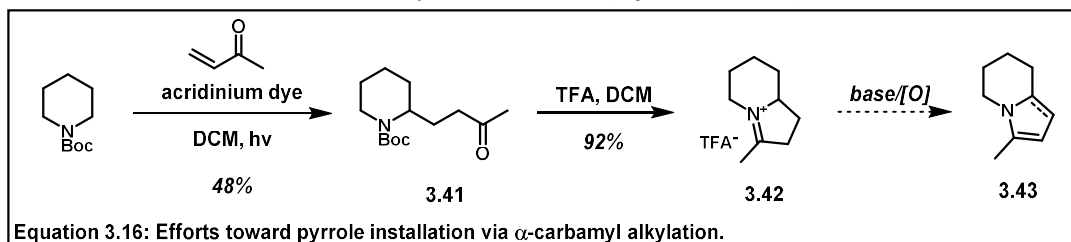
upon deprotection to afford dihydropyrroles (Scheme 3.11). Oxidation utilizing mild conditions would then afford the desired pyrrole. This α -carbamyl radical strategy was promising, as it would allow pyrrole installation to be performed on the carbamate protected core that had been targeted throughout our syntheses. Furthermore, generating α -carbamyl radicals via photocatalysis was particularly compelling, as these methods were mild and functional group tolerant, which would be necessary for reactivity in the late stages of a total synthesis.

Investigation of the literature led us to the chemistry developed by Nicewicz and coworkers, as it was particularly suited to our needs. The conditions were mild and displayed the viability of our proposed method when the reaction was used in the synthesis of pyrrolidine **3.40** from Giese product



3.39 with regioselective preference for the less substituted carbon (**Equation 3.15**).²³ Our pyrrole installation mirrored their synthesis closely, though rather than the reported reduction, the oxidation of the intermediate dihydropyrrole would be performed to afford the desired pyrroles.

Boc-protected piperidine was utilized as a model system and published reaction conditions afforded the desired Giese addition product **3.41** (**Equation 3.16**). Acid-mediated carbamate



deprotection afford iminium salt **3.42** in good yields. All efforts to convert **3.43** to the freebased substrate resulted in ring opening to the ketoamine. Efforts to perform direct oxidation to the pyrrole were also pursued but proved fruitless. Finally, *in situ* freebasing and oxidation was investigated and once more led to decomposition products, so this strategy was abandoned.

3.4 Conclusions

Our efforts to investigate the synthesis of the curvulamides led to the successful total synthesis of enantiopure (+)-imino-deoxydigitoxose, in the most concise route reported to date. A secondary route developed to target both natural products resulted in a divergent synthesis that afforded the natural products (-)-6-deoxyfagomine in five steps and (-)-imino-deoxydigitoxose in six steps from commercially available materials. These substrates were utilized as a model system and successfully

acted as a proof of concept for the late-stage pyrrole installation intended to be applied in the final steps of the synthesis of curvulamine A, while also revealing synthetic challenges that indicated previously reported pyrrole annulation methodologies would not be viable for our strategy. This led to the investigation of novel pyrrole annulation methodologies that have yet to be successful in affording the desired annulation products.

3.5 Distribution of Credit and Contributions

I would like to thank Dr. Brian Atwood for his contribution in the synthesis of many of the intermediates utilized in these strategies, as well as his guidance in the development of these routes. I would also like to thank Bilal Saudi for his aid in the development of pyrrole annulation methodologies.

3.6 Experimental Information

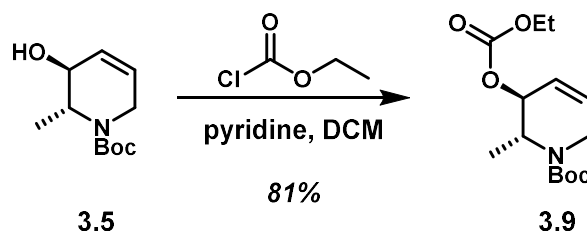
3.6.1 Materials and Methods

All reactions were carried out in oven-dried (140 °C) or flame-dried glassware under an atmosphere of dry argon unless otherwise noted. Dry dichloromethane (CH_2Cl_2), tetrahydrofuran (THF), diethyl ether (Et_2O), acetonitrile (MeCN), toluene (PhMe), and dimethoxyethane (DME) were obtained by percolation through columns packed with neutral alumina and columns packed with Q5 reactant, a supported copper catalyst for scavenging oxygen, under a positive pressure of argon. Solvents used for liquid-liquid extraction and chromatography were: Ethyl acetate, (EtOAc, Sigma-Aldrich, ACS grade) hexanes (Sigma-Aldrich, ACS grade), dichloromethane (CH_2Cl_2 , Fisher, ACS grade), acetone (Sigma-Aldrich, ACS Grade), diethyl ether (Et_2O , Fisher, ACS grade), and pentane (Sigma-Aldrich, ACS grade). Reactions that were performed open to air utilized solvent dispensed from a wash bottle or solvent bottle, and no precautions were taken to exclude water. Column chromatography was performed using EMD Millipore 60 Å (0.040–0.063 mm) mesh silica gel (SiO_2 Analytical thin-layer

chromatography (TLC) was performed on Merck silica gel 60 F254 TLC plates. Visualization was accomplished with UV (210 nm), and potassium permanganate (KMnO_4) or *p*-anisaldehyde staining solutions.

^1H NMR and ^{13}C NMR spectra were recorded at 298 K on Bruker GN500 (500 MHz, ^1H ; 125 MHz, ^{13}C) and Bruker CRYO500 (500 MHz, ^1H ; 125 MHz, ^{13}C) spectrometers. ^1H and ^{13}C spectra were referenced to residual chloroform (7.26 ppm, ^1H ; 77.00 ppm, ^{13}C) or residual methanol (3.31 ppm, ^1H ; 49.00, ppm ^{13}C). Chemical shifts are reported in ppm and multiplicities are indicated by: s (singlet), d (doublet), t (triplet), q (quartet), p (pentet), hept (heptet), m (multiplet), and br s (broad singlet). Coupling constants are reported in Hertz. The raw fid files were processed into the included NMR spectra using MestReNova 11.0, (Mestrelab Research S. L.). Infrared (IR) spectra were recorded on a Varian 640-IR instrument on NaCl plates and peaks are reported in cm^{-1} . Mass spectrometry data was obtained from the University of California, Irvine Mass Spectrometry Facility. High-resolution mass spectra (HRMS) were recorded on a Waters LCT Premier spectrometer using ESI-TOF (electrospray ionization-time of flight) or a Waters GCT Premier Micromass GC-MS (chemical ionization), and data are reported in the form of (*m/z*).

3.6.2 Experimental Procedures



tert*-Butyl(*R*,*3S*)-3-((ethoxycarbonyl)oxy)-2-methyl-3,6-dihydropyridine-*N*-*Boc*-*carboxylate

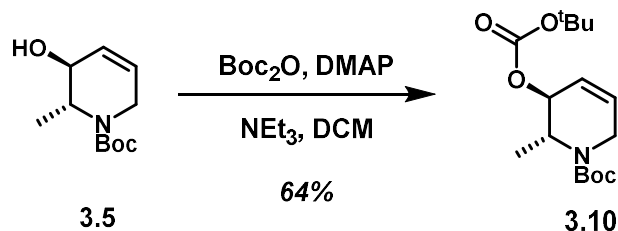
(**3.9**) A 10 mL round bottom flask was charged with alcohol **3.5** (50 mg, 0.23 mmol, 1 equiv), CH_2Cl_2 (0.5 mL), and pyridine (57, 0.70 mmol, 3 equiv). The reaction mixture was cooled to 0

°C. Ethyl chloroformate (67 μ L, 0.70 mmol, 3 equiv) was added dropwise. The reaction mixture was allowed to warm to room temperature and was stirred for 16 h. The reaction mixture was quenched with saturated aqueous ammonium chloride (5 mL) and extracted with EtOAc (3 x 5 mL). The combined organic extracts were dried over MgSO₄ and concentrated *in vacuo*. The residue was purified by chromatography on silica gel, eluting with hexanes/EtOAc 80:20 (v/v), to afford 54 mg (81% yield) **3.9** as a colorless oil.

¹H NMR (500 MHz, CDCl₃): δ 6.04 (s, 1H), 5.85 (s, 1H), 4.79 (s, 1H), 4.55 (s, 1H), 4.41 (s, 1H), 4.17 (q, J = 7.3 Hz, 2H), 3.52 (s, 1H), 1.44 (s, 9H), 1.28 (t, J = 7.3 Hz, 3H), 1.10 (d, J = 8.0 Hz, 3H).

¹³C NMR (125 MHz, CDCl₃): δ 154.9, 131.8, 119.6, 79.9, 72.7, 70.4, 64.0, 28.4, 15.2, 14.3.

HRMS (ES+) *m/z* calc'd for C₁₄H₂₃NO₅ [M+Na]⁺: 308.1474; found: 308.1489.



***tert*-Butyl (*R*,3*S*)-3-((*tert*-butoxycarbonyl)oxy)-2-methyl-3,6-dihydropyridine-4(1*H*)-2-**

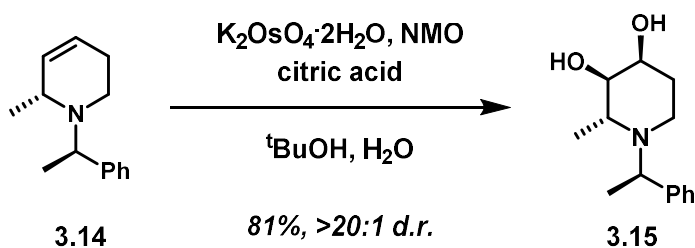
carboxylate (3.10) A 10 mL round bottom flask was charged with alcohol **3.5** (500 mg, 0.23 mmol, 1 equiv), CH₂Cl₂ (5 mL), dimethylaminopyridine (3 mg, 0.023 mmol, 0.1 equiv), triethylamine (0.163 mL, 1.170 mmol, 5 equiv). The reaction mixture was cooled to 0°C then di-*tert*-butyl carbonate (436 mg, 2.344 mmol, 10 equiv) was added portionwise. The reaction mixture was warmed to room temperature and stirred for 4 h. The reaction mixture was quenched with saturated aqueous ammonium chloride (5 mL) and extracted with EtOAc (3 x 5 mL). The combined organic extracts were dried over MgSO₄ and concentrated *in vacuo*. The

residue was purified by chromatography on silica gel, eluting with hexanes/EtOAc 80:20 (v/v), to afford 470 mg (64% yield) **3.10** as a colorless oil.

¹H NMR (500 MHz, CDCl₃): δ 6.02 (s, 1H), 5.84 (s, 1H), 4.76 (s, 1H), 4.55 (s, 1H), 4.36 (s, 1H), 3.51 (d, J = 17.8 Hz, 1H), 1.47 (s, 9H), 1.45 (s, 9H), 1.10 (d, J = 7.0 Hz, 3H).

¹³C NMR (125 MHz, CDCl₃): δ 154.9, 153.3, 131.5, 119.8, 82.2, 79.8, 72.0, 60.6, 28.4, 27.9, 15.3

HRMS (ES+) m/z calc'd for C₁₆H₂₇NO₅ [M+Na]⁺: 336.1787; found: 336.1797.



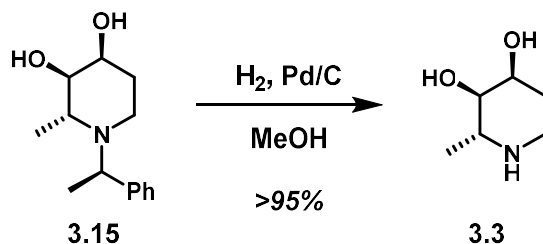
(**2,3R,4S**)-2-Methyl-1-(**R**)-1-phenylethyl)piperidine-3,4-diol (**3.15**)

A 10 mL round bottom flask was charged with tetrahydropyridine **3.14** (410 mg, 2.04 mmol, 1 equiv), *tert*-butanol (9 mL), water (9 mL), *N*-methylmorpholine *N*-oxide (477 mg, 4.08 mmol, 2 equiv), and citric acid (783 mg, 4.08 mmol, 2 equiv). Potassium osmate dihydrate (39 mg, 0.101 mmol, 0.05 equiv) was added. The reaction mixture was stirred for 16 h at room temperature. A saturated aqueous solution sodium bisulfite solution (9 mL) was added and the resulting mixture was stirred for 15 min. The solution was extracted with CH₂Cl₂ (3 x 18 mL). The organic extracts were combined, dried over Na₂SO₄, and concentrated *in vacuo*. The residue was purified by chromatography on silica gel, eluting with CH₂Cl₂/MeOH 90:10 (v/v), to afford 388 mg (81% yield) **3.15** as a colorless oil.

¹H NMR (500 MHz, CDCl₃): δ 7.29 (m, 5H), 3.72 (s, 2H), 3.45 (s, 1H), 2.96 (dq, J = 3.8 Hz, 2H), 2.52 (t, J = 11 Hz, 1H), 1.90 (d, J = 12 Hz, 1H), 1.69 (qd, J = 5 Hz, 1H), 1.38 (d, J = 6.6 Hz, 3H), 0.94, (d, J = 8.0 Hz, 3H).

¹³C NMR (125 MHz, CDCl₃): δ 128.7, 127.3, 72.7, 66.2, 59.6, 55.8, 39.7, 30.1, 22.1.

HRMS (ESI-TOF) m/z calc'd for $C_{14}H_{21}NO_2$ $[M+H]^+$: 258.1470; found: 258.1471.



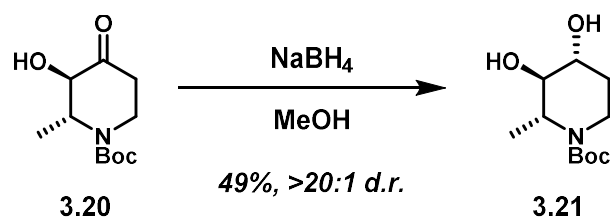
(+)-Iminodeoxydigitoxos (**3.3**) 20 mL scintillation vial was charged with diol **3.15** (154 mg, 0.654 mmol, 1 equiv), methanol (2 mL), and palladium on carbon (139 mg, 0.065 mmol, 0.1 equiv). The air in the reaction vessel was evacuated and replaced with argon, which was then evacuated and replaced with hydrogen gas. The reaction mixture was stirred at room temperature for 24 h. The reaction vessel was evacuated and replaced with argon. The solution was filtered through a pad of celite and washed with methanol (3 x 5 mL). The filtrate was concentrated *in vacuo*. The residue was dissolved in water and washed with hexanes. The aqueous phase was concentrated *in vacuo* to afford 86 mg (>95% yield) of (+)-iminodeoxydigitoxos **3.3** as a white amorphous solid.

1H NMR (500 MHz, $CDCl_3$): δ 3.59 (s, $J = 2.4$ Hz, 1H), 3.04 (dd, $J = 7.4$ Hz, 1H), 2.79 (dt, $J = 6.7$ Hz, 1H), 2.61 (m, 1H), 2.60 (d, $J = 3.7$ Hz, 1H), 1.49 (dq, $J = 4.2$ Hz, 1H), 1.39 (m, 1H), 0.80 (d, $J = 6.0$ Hz, 3H).

^{13}C NMR (125 MHz, $CDCl_3$): δ 71.9, 65.8, 51.1, 38.6, 28.5, 10.1.

HRMS (ESI-TOF) calculated for $C_{13}H_{19}NO_2$ $[M+H]^+$: 132.1024 m/z ; found 132.1029 m/z .

(+)-iminodeoxydigitoxos **3.3** was converted to the HCl salt to compare the structure to previously reported structure. 1H and ^{13}C NMR spectra were consistent with those previously reported.²



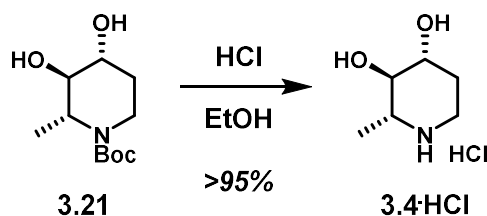
tert-Butyl (R,3R,4R)-3,4-dihydroxy-2-methylpiperidine-1-carboxylate (3.21) A 20 mL

scintillation vial was charged with keto-alcohol **3.20** (37 mg, 0.161 mmol, 1 equiv) and methanol (0.5 mL). The reaction mixture was cooled to 0°C and sodium borohydride (13 mg, 0.322 mmol, 2 equiv) was added portionwise. The solution was allowed to warm to room temperature and was stirred for 2 h. The reaction mixture was quenched with saturated aqueous ammonium chloride (5 mL) and extracted with EtOAc (3 x 10 mL). The organic extracts were combined, dried over Na₂SO₄, and concentrated *in vacuo*. The residue was purified by chromatography on silica gel, eluting with hexanes/EtOAc 70:30 (v/v), to afford 18 mg (49% yield) **3.21** as a white solid.

¹H NMR (500 MHz, CDCl₃): δ 4.18 – 4.13 (m, 1H), 3.92 (s, 1H), 3.79 (d, J = 13.9 Hz, 1H), 3.62 (s, 1H), 3.27 (t, J = 13.1 Hz, 1H), 2.15 – 2.08 (m, 1H), 1.60 (s, 1H), 1.50 (s, 9H), 1.36 (d, J = 6.0 Hz, 3H).

¹³C NMR (125 MHz, CDCl₃): δ 155.9, 79.9, 72.9, 68.9, 53.3, 34.4, 28.5, 28.2, 15.6.

HRMS (ES+) m/z calc'd for C₁₁H₂₁NO₄ [M+H]⁺: 254.1368; found: 254.1374.



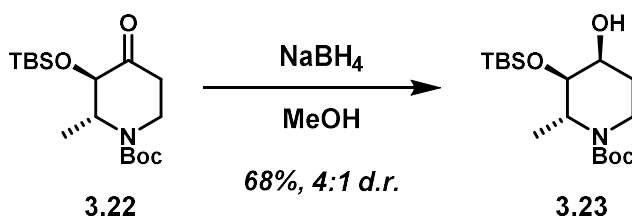
6-Deoxyfagomine (3.4) A 2 dram scintillation vial was charged with diol **3.21** (10 mg, 43.2 μmol, 1 equiv) and EtOH (0.2 mL). The reaction mixture was cooled to 0°C and had 12 M HCl (0.4 mL, 0.44 mmol, 10 equiv) added dropwise. The solution was allowed to warm to room temperature and was

stirred for 16 h. The reaction mixture was diluted with ethanol (1 mL) and filtered through a pad of Celite. The filtrate was concentrated *in vacuo* to afford 7 mg (>95% yield) **3.4** as a white solid.

¹H NMR (600 MHz, CDCl_3): δ 3.66 (s, 1H), 3.39 (J_{CH}, 12.5 Hz, 1H), 3.31 (ν , = 9.6 Hz, 1H), 3.11 – 2.99 (m, 2H), 2.19 (d , = 12.7 Hz, 1H), 1.70 (dd , = 24.9, 10.3 Hz, 1H), 1.38 (d , = 6.4 Hz, 3H).

¹³C NMR (151 MHz, CDCl_3): δ 74.4, 70.3, 55.4, 41.9, 28.9, 14.8.

The product was converted to the free based amine and the ¹H and ¹³C NMR spectra were consistent with those previously reported.³



tert-Butyl (R,3R,4S)-3-(tert-butyldimethylsilyloxy)-4-hydroxy-2-methylpiperidine-1-

carboxylate (3.23) A 20 mL scintillation vial was charged with **3.22** (25 mg, 0.072 mmol, 1

equiv) and methanol (0.15 mL). The reaction mixture was cooled to 0°C and sodium

borohydride (14 mg, 0.360 mmol, 5 equiv) was added portionwise. The solution was allowed to

warm to room temperature and was stirred for 1 h. The reaction mixture was quenched with

saturated aqueous ammonium chloride (1 mL) and extracted with EtOAc (3 x 1 mL). The organic

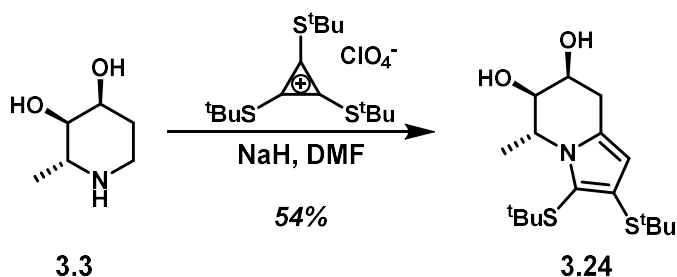
extracts were combined, dried over MgSO_4 , and concentrated *in vacuo*. The residue was purified

by chromatography on silica gel, eluting with hexanes/EtOAc 60:40 (v/v), to afford 17 mg (68% yield) of **3.23** and its diastereomer in a 4:1 ratio, as a tan oil.

¹H NMR (500 MHz, CDCl_3): 4.20 (dd , = 15.2, 7.3 Hz, 1H), 3.91 (d , = 23.8 Hz, 2H), 3.61 (s, 1H), 3.23 (ν , = 13.2 Hz, 1H), 2.15 (ν , = 13.5 Hz, 1H), 1.51 (s, 9H), 1.33 (J_{CH}, 7.5 Hz, 3H), 0.94 (s, 9H), 0.13 (d , = 16.8 Hz, 6H).

¹³C NMR (125 MHz, CDCl₃): δ 72.4, 69.7, 53.0, 35.1, 28.5, 28.5, 27.8, 25.8, 25.7, 15.4, -3.4, -5.0.

HRMS (ES+) m/z calc'd for C₁₇H₃₅NO₄Si [M+Na]⁺:368.2233; found: 368.2233.



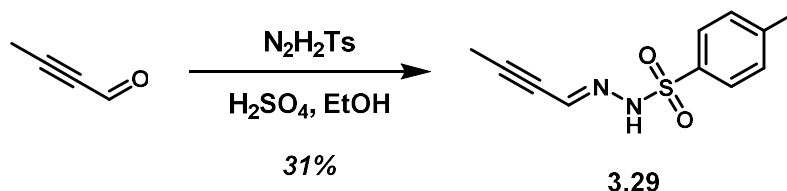
(**6R,7S**)-2,3-Bis(*tert*-butylthio)-5-methyl-5,6,7,8-tetrahydroindolizine-6,7-diol (**3.24**)

A 10 mL round bottom flask was charged with amino-diol (**3.3**) (33 mg, 0.25 mmol, 1 equiv) and dry DMF (5 mL). A solution of tris-thiol cyclopropenium perchlorate (**3.24**) (102 mg, 0.25 mmol, 1 equiv) in dry DMF (2.5 mL) was added and the reaction mixture was stirred at room temperature for 1 h. Sodium hydride (60% in mineral oil) (30 mg, 0.75 mmol, 3 equiv) was added portionwise. The reaction mixture was heated to 80 °C and stirred for 1 h. The reaction mixture was allowed to cool to room temperature and was then quenched with a 1:1 mixture of water and brine (15 mL). The solution was then extracted with EtOAc (3 x 15 mL). The organic layers were combined and washed with water (2 x 10 mL) and brine (10 mL). The organic phase was dried over Na₂SO₄ and concentrated *in vacuo*. The residue was purified by chromatography on silica gel, eluting with hexanes/EtOAc 85:15 (v/v), to afford 46 mg (54% yield) **3.24** as a white amorphous solid.

¹H NMR (500 MHz, CDCl₃): δ 5.71 (s, 1H), 4.37 (s, 1H), 3.87 (s, 1H), 3.29 (m, 2H), 3.03 (td, J = 4.3 Hz, 1H), 2.08 (t, J = 6.6 Hz, 1H), 1.72 (t, J = 9.8 Hz, 1H), 1.48 (rotomers of singlets, J = 22.3, 9H), 1.33 (d, J = 8.0 Hz, 3H), 1.27 (s, 9H)

¹³C NMR (125 MHz, CDCl₃) δ 163.5, 97.8, 81.8, 64.4, 58.6, 49.6, 45.1, 42.3, 35.0, 33.0, 32.0, 31.2, 29.7, 11.0.

HRMS (ESI-TOF) calculated for $C_{11}H_{21}NO_2$ $[M+H]^+$: 344.1718; found 344.1718.

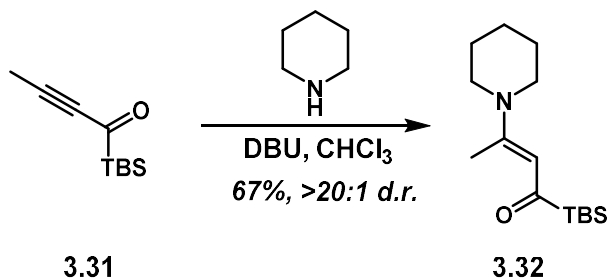


(E)-N'-(But-2-yn-1-ylidene)-4-methylbenzenesulfonohydrazide (3.29) 50 mL round bottom flask was charged with propargylic aldehyde (242 mg, 3.55 mmol, 1 equiv), ethanol (15 mL), and tosyl hydrazine (728 mg, 3.91 mmol, 1.1 equiv). H_2SO_4 (0.210 mL, 3.91 mmol, 1.1 equiv) was added to the reaction mixture dropwise over 1 min. The solution was stirred at room temperature for 16 h. The heterogenous mixture was filtered through a Büchner funnel and the precipitate was washed with ethanol and dried to afford 261 mg (31% yield) of propargylic hydrazon**3.29** as white solid.

$^1\text{H NMR}$ (500 MHz, $CDCl_3$): δ 8.56 (s, 1H), 7.82 (d, $J = 8.4$, 2H), 7.32 (d, $J = 7.9$, 2H), 6.56 (s, 1H), 2.42 (s, 3H), 2.10 (s, 3H).

$^{13}\text{C NMR}$ (125 MHz, $CDCl_3$): δ 144.8, 135.5, 129.7, 127.9, 126.0, 102.2, 69.8, 21.7, 4.8.

HRMS (ESI-TOF) m/z calc'd for $C_{12}H_{12}N_2O_2S$ $[M+Na]^+$: 308.1474; found 308.1489.



(E)-3-(Piperidin-1-yl)-1-(triphenylsilyl)but-2-en-1-one (3.32) mL dram vial was charged with piperidine (139 mg, 1.63 mmol, 1 equiv), CH_2Cl_2 (3 mL), and acyl silan**3.31** (270 mg, 1.63 mmol, 1 equiv). The reaction was stirred at room temperature for 30 min. The reaction mixture was

concentrated *in vacuo*. The residue was purified by chromatography on silica gel, eluting with hexanes/EtOAc 70:30 (v/v), to afford 256 mg (67% yield) **3b** as a yellow oil.

¹H NMR (500 MHz, CDCl₃): δ 5.66 (s, 1H), 3.38 – 3.30 (m, 4H), 2.51 (s, 3H), 1.67 – 1.54 (m, 6H), 0.93 (s, 9H), 0.11 (s, 6H).

¹³C NMR (125 MHz, CDCl₃): δ 224.1, 157.2, 110.6, 103.0, 47.4, 26.9, 25.6, 24.4, 16.6, -6.5.

HRMS (ESI-TOF) m/z calc'd for C₁₄H₂₄NO [M-SiC₆H₁₅+H]⁺: 153.1154; found: 153.1154.

3.7 References

¹ Tan, R. X.; Zhang, G.; Song, Y.; Cui, J.; Wang W. "Method for Preparing Curvularin and Indolizidine Alkaloid and Application." **2011**, CN102329735B, Nanjing University.

² Nishiyama, T.; Kajimoto, T.; Mohile, S. S.; Hayama, N.; Otsuda, T.; Ozeki, M.; Node, M. "The First Enantioselective Synthesis of Imino-Deoxydigitoxose and Protected Imino-Digitoxose by Using L-Threonine Aldolase-Catalyzed Aldol Condensation." *Tetrahedron: Asymmetry* **2009**, *20*, 230–234.

³ Min I. S.; Kim, S. I.; Hong, S.; Kim, I. S.; Jung, Y. H. "Total Synthesis of D-Fagomine and 6-Deoxyfagomine." *Tetrahedron* **2013**, *69*, 3901–3906.

⁴ Rengasamy, R.; Curtis-Long, M. J.; Seo, W. D.; Jeong, S. H.; Jeong, I.-Y.; Park, K. H. "New Building Block for Polyhydroxylated Piperidine." *J. Org. Chem.* **2008**, *73*, 2898–2901.

⁵ Atwood, B. "Unusual Natural Products, Lessons Learned in Pursuit of KS-504D and Curvulamine; Doctorate Thesis." University of California, Irvine; **2018**

⁶ a) Ji, E.; Meng, H.; Zheng, Y.; Ramadoss, V.; Wang, Y. "Copper-Catalyzed Stereospecific Hydroboration of Internal Allylic Alcohols." *Eur. J. Org. Chem.* **2019**, *44*, 7367–7371; b) Gung, B. W.; Ohm, K. W.; Smith, D. T. "Regio- and Diastereofacial Selective Hydroboration of Chiral Allylic Stannanes, Silanes, and Germanes." *Synthetic Communications*, **1994**, *24*, 167–173.

⁷ Cho, J. K.; Rengasamy, R.; Curtis-Long, M. J.; Kim, J. H.; Lee, J. W.; Park, K. H. "Piperidine Azasugars Displaying Competitive A-Rhamnosidase Inhibition and their Kinetic Mechanism." *J. Appl. Biol. Chem.* **2011**, *54*, 881–888.

⁸ a) Genisson, Y., Marizano, C., Mehmandoust, M., Gnecco, D., Das, B. "Zincke's Reaction with Chiral Primary Amines: A Practical Entry to Pyridinium Salts of Interest in Asymmetric Synthesis." *Syn. Lett.* **1992**, *5*, 431–434; b) Guilloteau–Bertin, B., Compere, D., Gil, L., Marizano, C., Das, B. "Stereocontrolled Alkylation of Chiral Pyridinium Salt Toward a Short Enantioselective Access to 2-Alkyl- and 2,6-Dialkyl-1,2,5,6-Tetrahydropyridines." *Eur. J. Org. Chem.* **2000**, *2000*, 1391–1399.

- ⁹ a) Zincke, T. H.; Heuser, G.; Moller, W. "Ueber Dinitrophenylpyridiniumchlorid und dessen Umwandlungsproducte." *Justus Liebig's Annalen der Chemie*. **1904**, *333*, 296–345; b) Zincke, T. H.; Heuser, G.; Moller, W. "Ueber Dinitrophenylpyridiniumchlorid und dessen Umwandlungsproducte." *Justus Liebig's Annalen der Chemie*. **1904**, *330*, 361–374; c) Zincke, T. H.; Weisspfenning, G. "Über Dinitrophenylisochinoliniumchlorid und dessen Umwandlungsprodukte." *Justus Liebig's Annalen der Chemie* **1913**, *396*, 103–131.
- ¹⁰ Guilloteau-Bertin, B.; Compere, D.; Gil, L.; Marizano, C. Das, B. C. "Stereocontrolled Alkylation of Chiral Pyridinium Salt Toward a Short Enantioselective Access to 2-Alkyl- and 2,6-Dialkyl-1,2,5,6-Tetrahydropyridines." *Eur. J. Org. Chem.* **2000**, *8*, 1391–1399.
- ¹¹ Dupaud, P.; Epple, R.; Thomas, A. A.; Fokin, V. V.; Sharpless, K. B. "Osmium-Catalyzed Dihydroxylation of Olefins in Acidic Media: Old Process, New Tricks." *Adv. Synth. and Cat.* **2002**, *421*, 3–4.
- ¹² Gil, L.; Compere, D.; Bertin, B.; Chiaroni, A.; Marazano, C. "An Enantioselective Entry to Substituted 6-Membered Nitrogen Heterocycles from Chiral Pyridinium Salts via Selective Epoxidation of Tetrahydropyridine Intermediates." *Synthesis* **2000**, *2000*, 2117–2126.
- ¹³ a) Nakata, T.; Tanaka, T.; Oishi, T. "Stereoselective Reduction of α -Hydroxy Ketones." *Tetrahedron Lett.* **1983**, *24*, 2653–2656. b) Katzenellenbogen, J. A.; Bowlus, S. B. "Stereoselectivity in the Reduction of Aliphatic α -Ketols with Aluminum Hydride Reagents." *J. Org. Chem.* **1973**, *38*, 627–632.
- ¹⁴ a) Bergstrom, B. D.; Nickerson, L. A.; Shaw, J. T.; Souza, L. W. "Transition Metal Catalyzed Insertion Reactions with Donor/Donor Carbenes." *Angew. Chem.* **2021**, *133*, 6940–6954; b) Goldman, A. S.; Goldberg, K. I. "Activation and Functionalization of C–H Bonds." *ACS Symposium Series*, **2004**, *885*, 1–43.
- ¹⁵ Wang, R.; Xie, X.; Liu, H.; Zhou, Y. "Rh(III)-Catalyzed C–H Bond Activation for the Construction of Heterocycles with sp^3 -Carbon Centers." *Catalysts* **2019**, *9*, 823–852.
- ¹⁶ Yoshida, Z.-I.; Hirai, H.; Miki, S.; Yoneda, S. "Trithiocyclopropenium Ion as a Building Block for Nitrogen Heterocycle Synthesis." *Tetrahedron* **1989**, *45*, 3217–3231.
- ¹⁷ Yoneda, S.; Hirai, H.; Yoshida, Z.-I. "A Novel Synthesis of Pyrroles by the Reactions of Tris(alkylthio)cyclopropenium Salt with Amines." *Heterocycles* **1981**, *15*, 865–869.
- ¹⁸ Yagi, T.; Aoyama, T.; Shioiri, T. "A New Two-Step Preparation of Pyrroles from β -Amino Ketones Utilizing Trimethylsilyldiazomethane." *Synlett* **1997**, *9*, 1063–1064.
- ¹⁹ Shen, Z.; Dong, V. "Benzofurans Prepared by C–H Bond Functionalization with Acylsilanes." *Angew. Chem. Int. Ed.* **2009**, *48*, 784–786.
- ²⁰ a) Randall, S. A.; Hodges, J. A.; McMahon, R. J. "Propynal Equivalents and Diazopropyne: Synthesis of All Mono-¹³C Isotopomers." *Helvetica Chimica Acta*. **2009**, *92*, 1626–1643. b) Abadie, B.; Jardel, D.; Pozzi, G.; Toullec, P.; Vincent, J.-M. "Dual Benzophenone/Copper-Photocatalyzed Giese-Type Alkylation of C(sp³)-H Bonds." *Eur. J. of Chem.* **2019**, *25*, 16120–16127.

²¹ Knezz, S. N.; Waltz, T. A.; Haenni, B. C.; Burrmann, N. J.; McMahon, R. J. "Spectroscopy and Photochemistry of Triplet 1,3-Dimethylpropynylidene." *J. Am. Chem. Soc.* **2016**, *138*, 12596–12604.

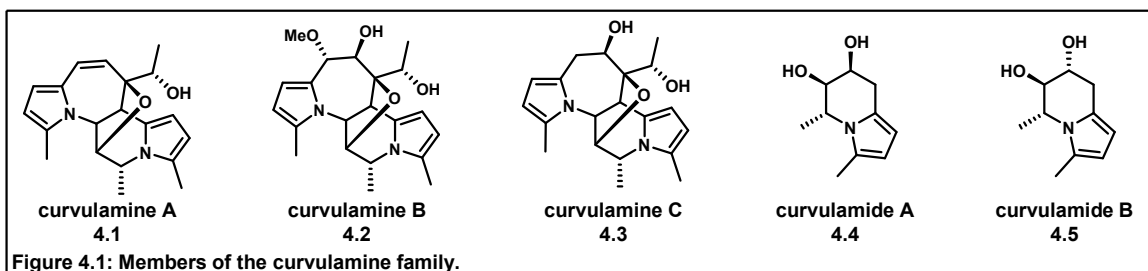
²² Kiriwara, M.; Suzuki, S.; Ishihara, N.; Yamazaki, K.; Akiyama, T.; Ishizuka, Y. "Synthesis of Acylsilanes via Catalytic Dedithioacetalization of 2-Silylated 1,3-Dithianes with 30% Hydrogen Peroxide" *Synthesis* **2017**, *49*, 2009–2014.

²³ McManus, J. B.; Onuska, N. P.; Nicewicz, D. "Generation and Alkylation of α -Carbamyl Radicals via Organic Photoredox Catalysis." *J. Am. Chem. Soc.* **2018**, *140*, 9056–9060.

Chapter 4: Efforts Toward the Total Synthesis of the Curvulamines

4.1 Introduction

Since its discovery in 2014, the curvulamine family of natural products (**Figure 4.1**) has been of great interest to biologists and synthetic chemists.¹ The interesting bioactivities and complex structures

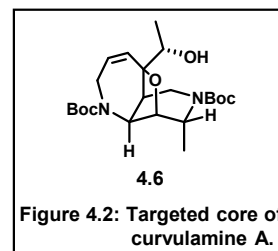


of the five natural alkaloids make them ideal targets for total synthesis. Herein are described our efforts toward the total synthesis of the curvulamines, targeting the nor-pyrrole tricyclic core structures, with the intention of installing the pyrrole rings via a late-stage pyrrole annulation reaction. The attempted routes include a nitrogen-radical initiated polycyclization strategy and an enolate alkenylation strategy. I also describe optimization of a dihydropyridinone synthesis that led to the syntheses of two natural products.

4.2 Radical Bicyclization Route

4.2.1 Synthetic Considerations

Previous efforts by former Vanderwal lab member Dr. Brian Atwood toward the curvulamines gave many insights into the synthesis of their core structure (Discussed in *Chapter 2 Section 4.3* of this manuscript). With the intention of installing the pyrrole rings to afford curvulamine A (**4.1**) late in the



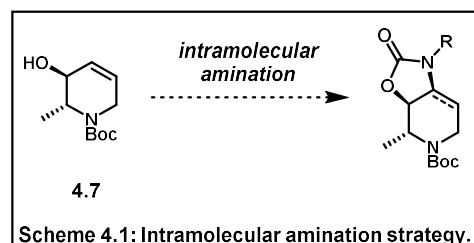
synthesis, the protected tricyclic core **4.6** was chosen as our synthetic target (**Figure 4.2**). One of the most valuable insights inferred by the work of Dr. Atwood was the challenge posed by a stereocontrolled synthesis of the tetrasubstituted piperidine ring.² This ring system contains four of the six stereocenters, three of which are contiguous on the same face of the ring. These three contiguous stereocenters have

been discovered to be extremely challenging to synthesize due to their cis relationship. The orientation of substituents about these stereocenters is further complicated by the allylic strain imposed by the methyl group and any electron-withdrawing amine protecting group, which was deemed necessary to attenuate the reactivity of the piperidine nitrogen.³ The result is three of the four stereocenters on the piperidine ring existing in a pseudoaxial configuration, making the ring system sterically constrained and the diastereoselective synthesis of the piperidine very challenging.

Dr. Atwood's synthetic efforts highlighted the value of intramolecular transfer of stereochemical information in the synthesis of the four contiguous stereocenters. Another valuable insight gained by previous work was the apparent difficulty in the synthesis of the seven-membered ring, as ring-closing metathesis efforts to afford this ring were all unsuccessful, even though rings of this size are generally considered trivial to form via alkene metathesis.⁴ These insights were heavily considered during our second-generation retrosynthetic analysis of the core of the curvulamines. Methods of establishing the contiguous stereocenters of the piperidine ring via intramolecular transfer of functionality was a major focus of our first synthetic attempt.

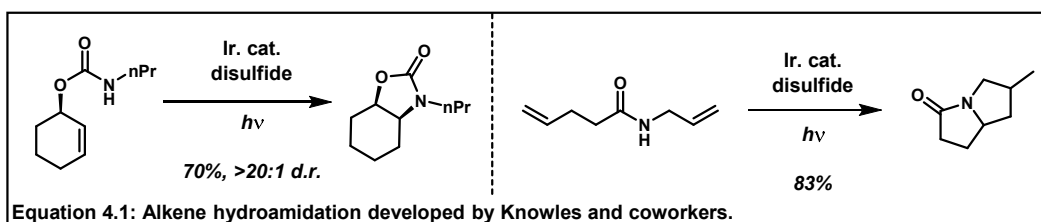
4.2.2 Aza-radical Bicyclization

As we recognized the value of intramolecular reactivity to install cis substituents on the piperidine ring, it seemed reasonable to set the nitrogen-containing stereocenter through intramolecular hydroamination of allylic alcohol **4.7** (Scheme 4.1). Hydroamination of alkenes is well-precedented, particularly in tethered systems or systems with neighboring functionalities that may impart regioselectivity and diastereoselectivity.⁵ Investigating the wide breath of stereoselective aminations of allylic alcohols led us to consider such a carbamate cyclization to set the nitrogen stereocenter with diastereocontrol imparted by the tethered pseudoaxial alcohol. Strategically,



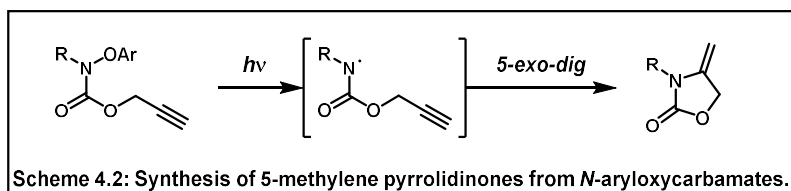
the substituent on the nitrogen would carry the functional group arrangement needed to form the seven-membered ring.

Modern methods of intramolecular alkene hydroamination generally proceed through nitrogen-centered radical intermediates produced via photocatalysis.⁶ Additional investigations led us to consider utilizing the synthetic method developed by Knowles and coworkers in which they utilized photocatalysis to generate radicals on electron-poor nitrogen atoms to perform *5-exo-trig* cyclizations to afford lactams.⁷ Within the scope of their report, Knowles and coworkers highlighted the utility of their chemistry by



subjecting stereodefined carbamates appended to cyclic systems to their photocatalytic conditions, resulting in the formation of *cis*-oxazolidinones in good yields and high diastereoselectivity (**Equation 4.1**).

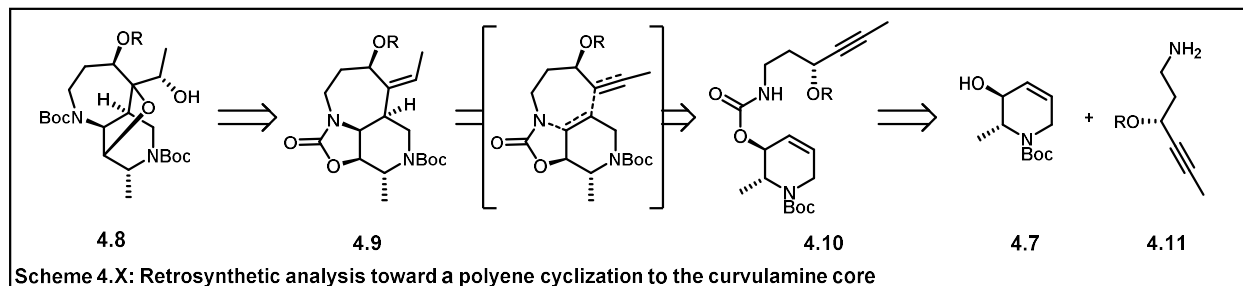
They further expanded the utility of the method by performing radical polyene cyclizations to afford bicyclic systems through a nitrogen-centered-radical-initiated cascade. Similar reactivity developed by the Leonori group utilizes aryloxyamides to generate the nitrogen-centered radical, which combine with



alkynes as to form exocyclic enamine heterocycles (**Scheme 4.2**).⁸ With these precedents in mind, a new route toward the curvulamines was developed.

4.2.3 Retrosynthetic Analysis

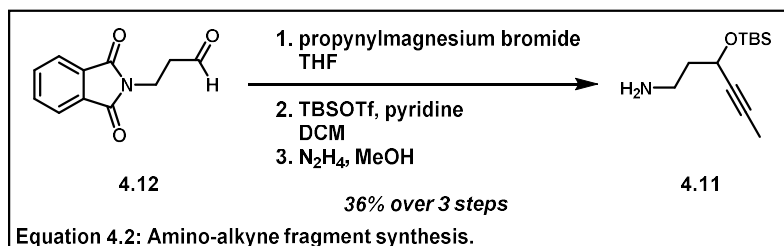
The core of curvulamine C (**4.8**) was the target for this strategy, which was envisioned to be readily converted to the other tetracyclic members of the curvulamine family. The tetrahydrofuran ring of **4.8**



was believed to be accessible via epoxidation of **4.9** and decarbonylation of the oxazolidinone. Dr. Atwood had demonstrated the unprotected alcohol on a similar system readily underwent *5-exo-tet* cyclization, so it was presumed etherification via epoxide opening would generate the caged tricycle. **4.9** was envisioned to be formed utilizing a bicyclization cascade, initiated by the formation of the nitrogen centered radical of the carbamate on **4.10**. The need to form the seven-membered ring via *7-exo-trig/dig* led to our decision to target curvulamine C, as inclusion of π -system present in curvulamine A would undergo the undesired *5-exo-trig* cyclization. The nitrogen-centered radical could be formed through a multitude of pathways; however, most of the precursors were able to be formed through functionalization of the carbamate of **4.10**. This could be accessed by convergence of piperidinol **4.7**, previously synthesized by Dr. Brian Atwood, and amine **4.11**, which was readily afforded via Gabriel synthesis.⁹

4.2.4 Precursor Syntheses

The polyene bicyclization strategy was dependent on the convergence of fragments **4.7** and **4.11**. Piperidine **4.7** had been initially synthesized by Park and coworkers and was made on multigram scale in four steps from commercially available (+)-alaninol using a route developed by Dr. Brian Atwood.⁹ Aminoalkyne fragment **4.11** was synthesized beginning with the precedent synthesis of **4.12**, which was

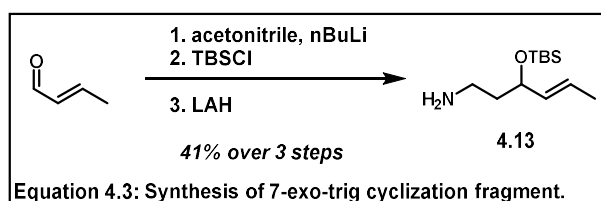


converted to **4.11** via 1,2-addition of 1-propynylmagnesium bromide. Silylation of the resultant alcohol and removal of the amine protecting

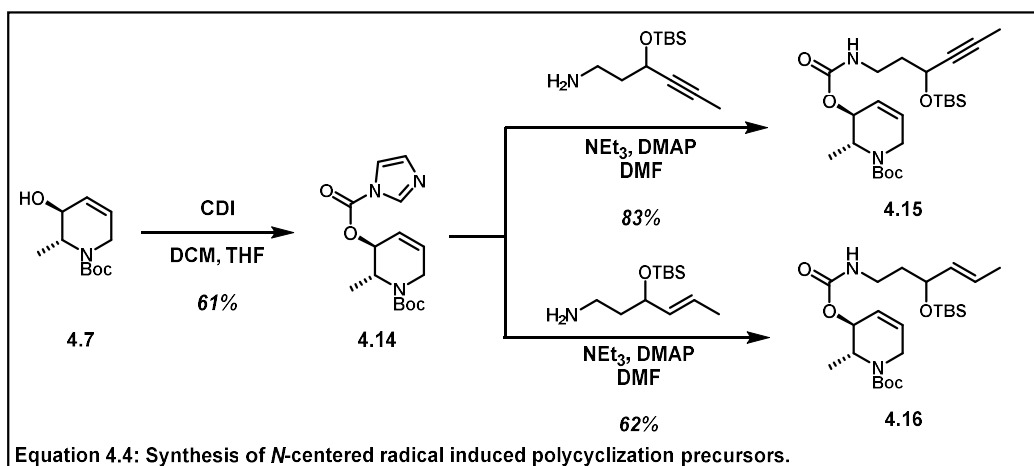
group produced the amine fragment (**4.11**) in four steps from commercial materials (**Equation 4.2**).¹¹

Recognizing the kinetic barrier to radical *7-exo-dig* cyclization, **4.13**, the precursor necessary for *7-exo-trig* cyclization, was also synthesized by modification of a precedent procedure (**Equation 4.3**).¹² Base-

promoted addition of acetonitrile into (*E*)-but-2-enal afforded a secondary alcohol, which was protected as the silyl ether. Reduction of the nitrile

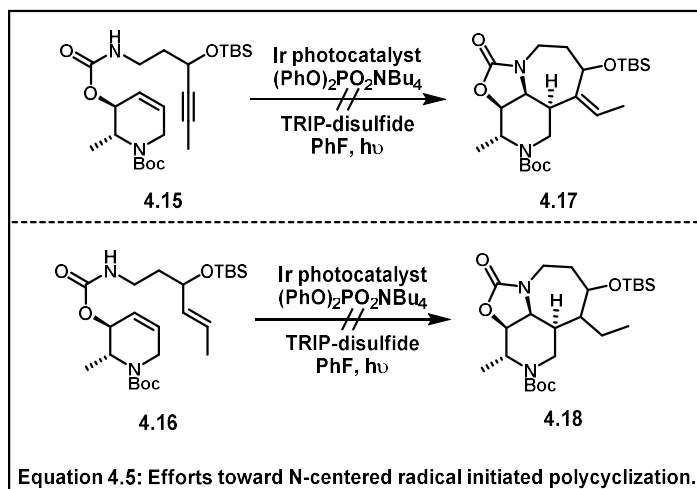


synthesized amine fragment **4.13** in three steps. Alcohol **4.7** was converted to imidazole carbamate **4.8**, which was coupled with amines **4.11** and **4.13** to afford the two radical bicyclization precursors (**4.15**, **4.16**) (**Equation 4.4**).¹³



4.2.5 Efforts Toward Bicyclization

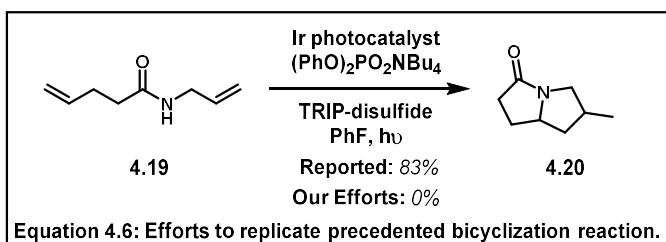
Investigations of the bicyclization began with **4.15** being subjected to the reaction conditions developed by Knowles and coworkers, using reagents donated to our lab by the Knowles group (**Equation**



4.5). Unfortunately, all attempts to form bicyclization product **4.17** did not affect starting material. It was considered that the resultant alkenyl radical intermediate targeted in the synthesis of **4.17** may be too high energy to form, though this was difficult to validate as the monocyclization

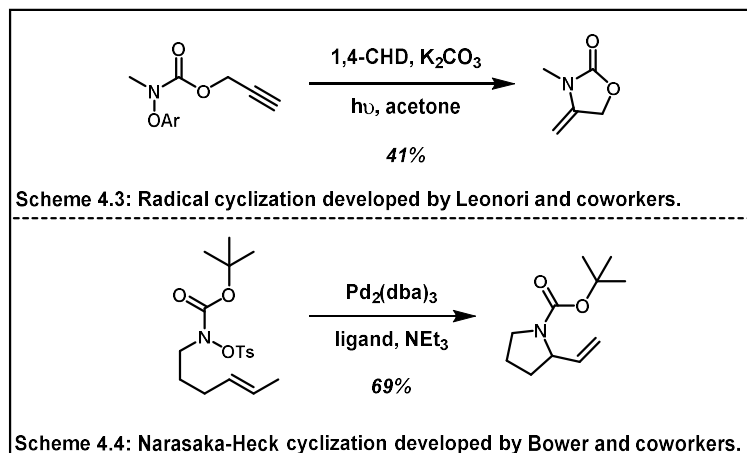
product was also not formed. In order to test the hypothesis that *7-exo-dig* cyclization prevented conversion, **4.16** was subjected to the same reaction conditions. It was noted that **4.18** would be unproductive in our synthesis as the lack of unsaturation would preclude progress toward the target, though the reaction was investigated to probe reactivity. These efforts also resulted only in recovered starting material.

To ensure the reproducibility of the reaction developed by Knowles and coworkers, amide **4.19** was synthesized and subjected to the standard reaction conditions



to produce bicycle **4.20** (**Equation 4.6**). This precedented reaction was irreproducible in our laboratory, even with reagents supplied by the Knowles group. After many helpful discussions with members of the Knowles lab, it was concluded the issue was likely due to differences in our light irradiation apparatuses. Allowing the Knowles group to attempt the reaction with our substrate was considered; however, other methods of nitrogen-centered radical generation were prioritized.

The nitrogen-centered radical was accessible via a series of other methods. The aryloxy carbamate derivative was considered as it gave multiple methods of cyclization. The *N*-centered radical cascade we

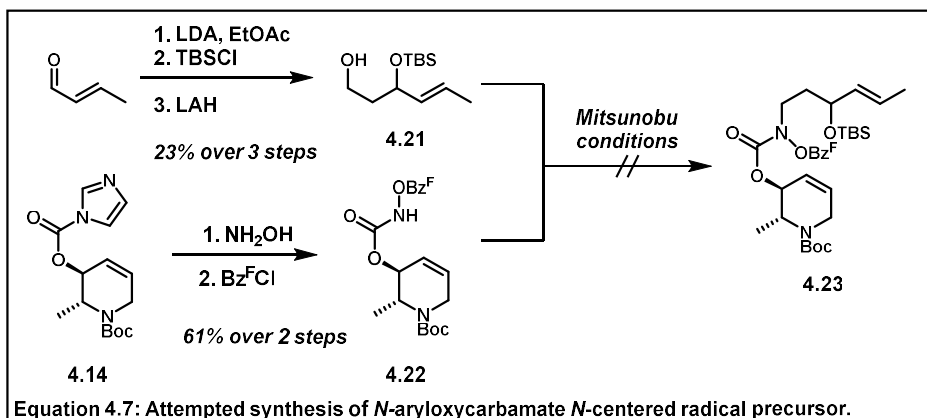


chemistry developed by Bower and coworkers (**Scheme 4.4**).¹⁴

proposed should be feasible through photolytic cleavage of the *N*-O σ bond, as reported by Leonori and coworkers (**Scheme 4.3**).⁸ Further, this same starting material could be elaborated to an oxazolidinone using Narasaka-Heck

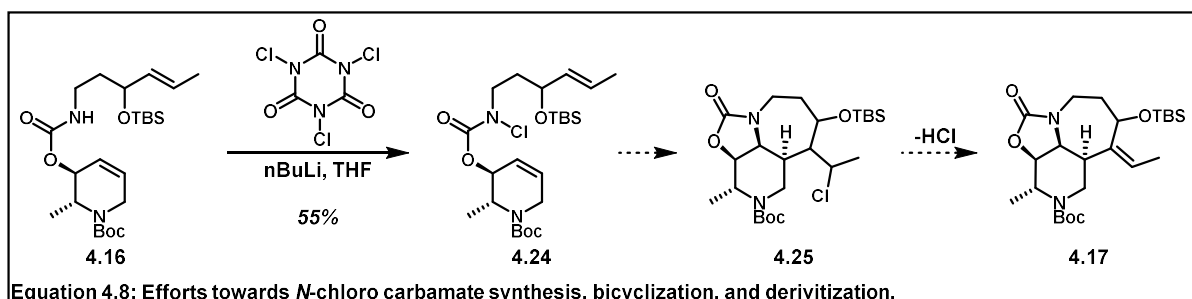
In effort to afford the *N*-aryloxy carbamate precursor (**4.23**), coupling partners **4.21** and **4.22** were synthesized (**Equation 4.7**). Extensive efforts to conjoin the fragments were put forth without success. A

fragment with the hydroxylamine preinstalled was also synthesized; however, any efforts toward addition of an



alkylhydroxylamine into **4.14** proved unsuccessful and this strategy was abandoned.

A more classical approach to nitrogen-centered radical synthesis was then considered, and a strategy utilizing photolytic cleavage of nitrogen–halogen bonds was pursued (**Equation 4.8**). Carbamate



4.16 was readily converted to the *N*-chlorocarbamate **4.24**. Alkene **4.16** was employed in this sequence so as to form alkyl chloride **4.25**. In the absence of a hydrogen atom source, it was hoped that chlorination would propagate the sequence and **4.25** would be readily converted to the previously targeted alkene **4.17** via elimination.

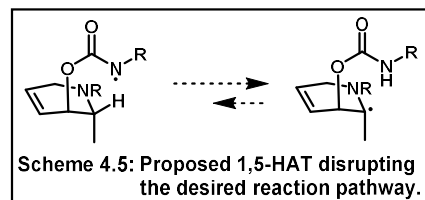
N-chloro carbamate **4.24** was subjected to a series of conditions to effect homolytic cleavage of the *N*–*Cl* bond (**Table 4.1**). The extensive list of conditions included photolysis utilizing different light sources, both with and without addition of

<p>4.24</p>	<p><i>conditions</i></p> <p>-----></p> <p>4.25</p>
PhH, <i>hν</i> MeOH, <i>hν</i> MeOH, <i>hν</i> + heat [Ir(ppy) ₂ dtbby]PF ₆ , ACN, 450 nm, r.t. [Ir(ppy) ₂ dtbby]PF ₆ , DCE, 450 nm, r.t. [Ir(ppy) ₂ dtbby]PF ₆ , DCE, 450 nm, Na ₂ HPO ₄ , r.t. [Ir(ppy) ₂ dtbby]PF ₆ , DCE, 450 nm, Na ₂ HPO ₄ , 40 °C [Ir(ppy) ₂ dtbby]PF ₆ , DCE, mercury lamp, Na ₂ HPO ₄ , r.t.	CuCl, PhH, rt FeSO ₄ H ₂ O, PhH, rt CuCl, DCM, rt FeSO ₄ H ₂ O, DCM, rt FeSO ₄ H ₂ O, PhH, cat. H ₂ SO ₄ , rt PhH, (Bu ₃ Sn) ₂ , AIBN, 80 °C BzOOBz, K ₂ CO ₃ , CF ₃ Ph
<p><i>All reactions resulted in hydrodechlorination at varying rates, or decomposition.</i></p>	
<p>Table 4.1: Efforts toward dehalogenative <i>N</i>-centered radical initiated bicyclization cascade.</p>	

a photocatalyst, transition-metal catalyzed conditions, and conditions commonly used to generate radicals from alkyl halides. None of the tested reaction conditions afforded either monocyclization or bicyclization products. The most commonly observed product arose from protodehalogenation. Conditions with hydrogen atom sources were also tested to see if it was feasible to access any cyclized

product, but also proved unsuccessful. These results indicated that the nitrogen-centered radical was likely being formed but was either unreactive with the alkene or quenched before cyclization occurred.

It was hypothesized that intramolecular hydrogen atom transfer might be occurring, resulting in the stable tertiary α -carbamyl radical (**Scheme 4.5**).¹⁵ Molecular modeling confirmed

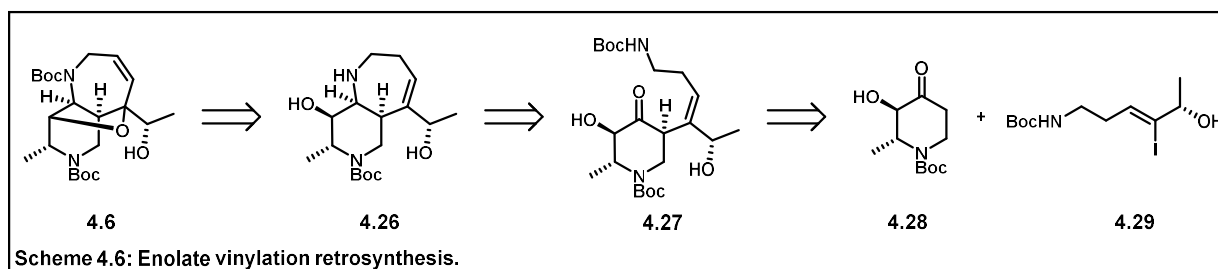


the proximity of the nitrogen and hydrogen atom in question would allow for the proposed 1,5-HAT, though no studies were performed to confirm this hypothesis. After extensive investigations, this synthetic pathway was abandoned.

4.3 Enolate Alkenylation Strategy

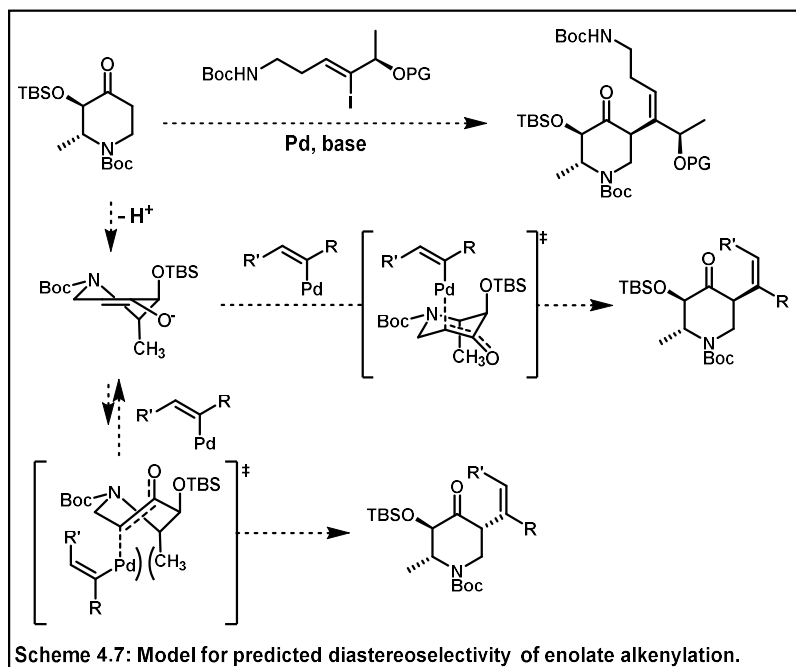
4.3.1 Retrosynthetic Considerations

After considering the shortcomings of previous synthetic attempts, it was postulated that the most synthetically challenging bond to form, both in connectivity and stereochemistry, was the carbon–nitrogen bond connecting the piperidine to the seven-membered ring. A new synthetic strategy was developed centered around that bond being formed early in the synthesis via intramolecular amine condensation, as classical chemistry was thought the most reliable method of forming such a difficult bond (**Scheme 4.6**). The core of curvulamine A (**4.6**) was believed to be accessed from **4.26** via



haloetherification and elimination of the resultant alkyl halide. Disconnection of the seven-membered heterocycle via intramolecular reductive amination draws back to amino–ketone intermediate **4.27**. This condensation was expected to be stereoselective as both neighboring groups are pseudoaxial, blocking

the β -face. The β - γ enone retron was disconnected through enolate alkenylation to afford piperidinone **4.28**, previously synthesized by Dr. Brian Atwood, and alkenyl halide **4.29**. The proposed diastereoselectivity of this reaction was, in part, based on previous indication that the methyl group imposed steric blocking to the α -face of the piperidine ring (**Scheme 4.7**). Molecular modeling also

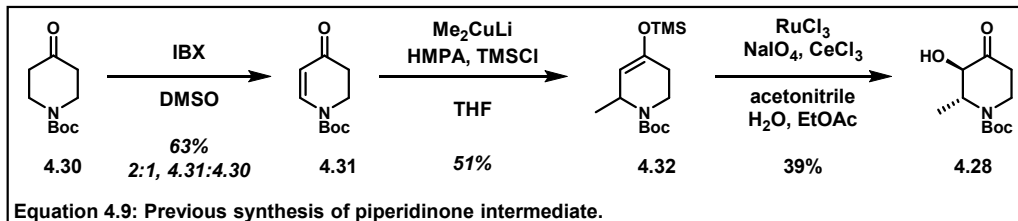


indicated that palladation of the α -face was likely infeasible due to the twist-boat conformation of the intermediate, while the desired α -palladated intermediate was predicted to be much more thermodynamically stable as it existed in a chair conformation.¹⁶ With the stereochemistry

hypothesized to produce the desired substrate, I began to pursue this route.

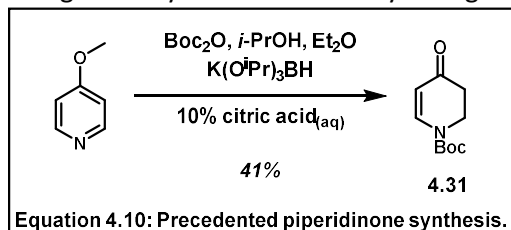
4.3.2 Optimization of Piperidinone Synthesis

Although piperidinone **4.28** had been synthesized by Dr. Brian Atwood, this route had a series of issues that needed to be addressed. The original synthesis began with oxidation of commercially available



piperidinone **4.30** (**Equation 4.9**) but this oxidation generally resulted in only 30–50% conversion to **4.31**, which was inseparable from starting material. This led to reduced yields in the following cuprate addition yielding **4.32**, which was noted to be limited in scale to reactions below 1 gram.

An alternative synthesis to **4.31** from *p*-methoxypyridine (**Equation 4.10**) had been reported, though this synthesis was low yielding and required the use of a glovebox with inert atmosphere to synthesize the non-commercially available reducing agent.¹⁷ This reaction was attempted but resulted in poor yields and modest conversion of starting material on scales larger than

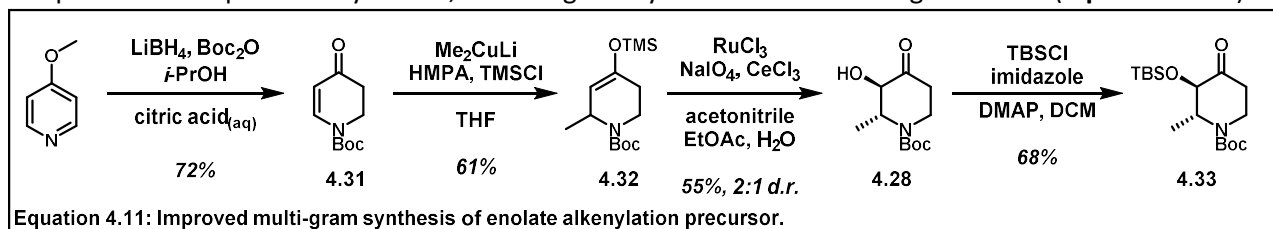


100 mg. Modifications utilizing commercially available reducing agents were investigated (**Table 4.2**). It was discovered that the major issue with this reaction was overreduction to piperidinone **4.30**. It was discovered that lithium borohydride yielded no overreduction product, and after probing the molar ratios of reactants, the reaction yielded full conversion to the desired product. With these optimized conditions in hand, **4.31** was synthesized using commercially available reagents without production of inseparable **4.30**. Testing the limitations of scalability, it was discovered that these conditions were tolerant of 10 gram scale, affording ample amounts of **4.31** in consistent yields.

reducing agent	SM:IRI:Boc ₂ O	Yield
NaBH ₄	1 : 1.1 : 1.1	12%
NaCNBH ₃	1 : 1.1 : 1.1	NR
Na(OAc) ₃ BH	1 : 1.1 : 1.1	NR
LiBH ₄	1 : 1.1 : 1.1	33%
NaBH ₄	1 : 5 : 5	56%
NaBH ₄	1 : 2.5 : 2.5	60%
LiBH ₄	1 : 2.5 : 2.5	74%
LiBH ₄	1 : 1.5 : 2.5	48%

Table 4.2: Optimization of piperidinone synthesis.

With a method to afford **4.31** in large quantities as pure material, the previously developed 1,4-addition conditions were applied and found to have improved yields and improved scalability when compared to the previous synthesis, affording enoxysilane **4.32** on multigram scale (**Equation 4.11**).

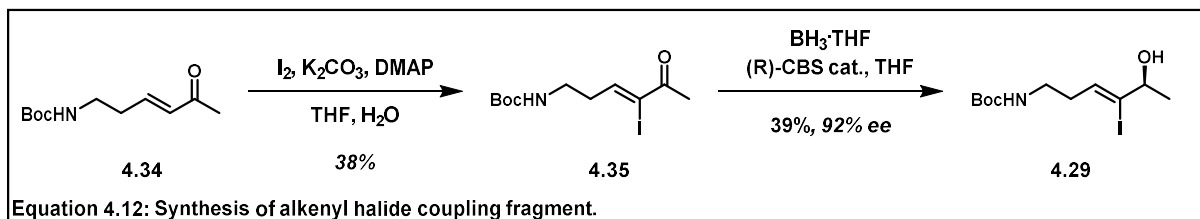


Rubottom oxidation produced keto-alcohol **4.28** in poor diastereoselectivity; however, the diastereomers were easily separated. Protection of the alcohol afforded piperidinone **4.33** on gram scale. This intermediate was also noted to be very similar to the core of the curvulamides. Utilization of this

intermediate to afford the core structures of both curvulamides A and B is discussed in detail in Chapter 3 (Section 3.2.6).

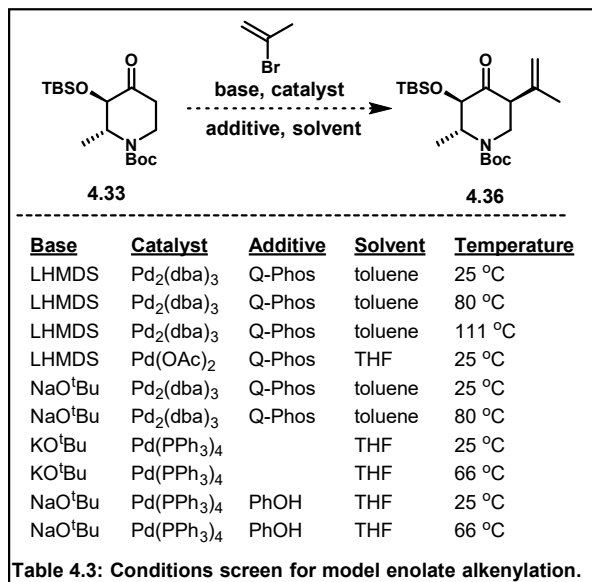
4.3.3 Amine Fragment Synthesis

The alkenyl halide fragment proved to be readily synthesized from known compound **4.34**, which was made in three steps from commercially available materials.¹⁸ α -iodination of the enone gave the



desired alkenyl iodide (**4.35**), which was subjected to enantioselective reduction conditions to afford enantioenriched allylic alcohol **4.29** (Equation 4.12).^{19,20} These reactions were low yielding, though no efforts at optimization were made. As we began considering protecting group strategies for the secondary alcohol, results from model study experiments prevented us from continuing this synthesis.

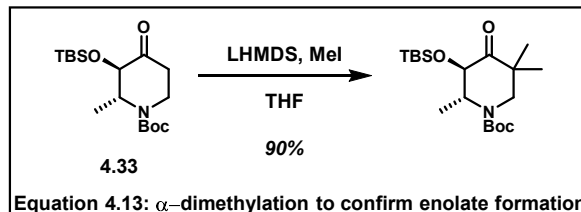
4.3.4 Bimolecular Enolate Vinylation Efforts



To establish optimized enolate alkenylation conditions, piperidinone **4.33** was reacted with a 2-bromopropene as a positive control for enolate alkenylation (Table 4.3). **4.33** was subjected to a series of different palladium sources, ligands and bases according to precedented alkenylation reactions. Solvents and temperatures were also screened. All efforts to generate alkenylated **4.36**

were unsuccessful and ketone **4.33** was recovered in all attempts.²¹

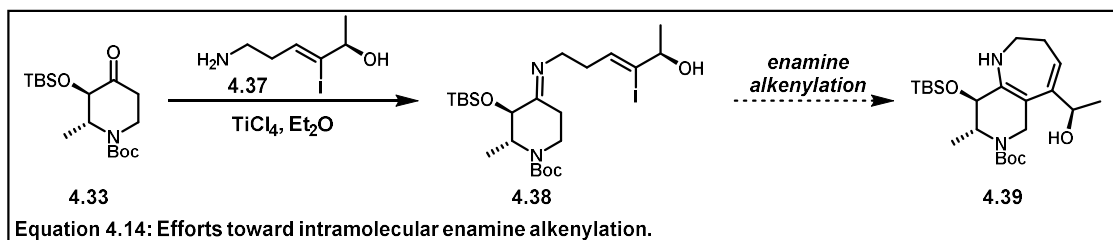
Experiments were performed to better understand the cause of the poor reactivity. Concerns that the enolate was unable to be formed were



investigated and **4.33** was successfully α -dimethylated (**Equation 4.13**), confirming that the enolate was formed. Nickel-catalyzed alkenylation conditions were also tested, though none afforded the desired reactivity.²² Replacing the silane protecting group with a benzyl group, in the belief that the silane may impose too much steric constraint on the system, did not improve the outcome

4.3.5 Imine Condensation Efforts

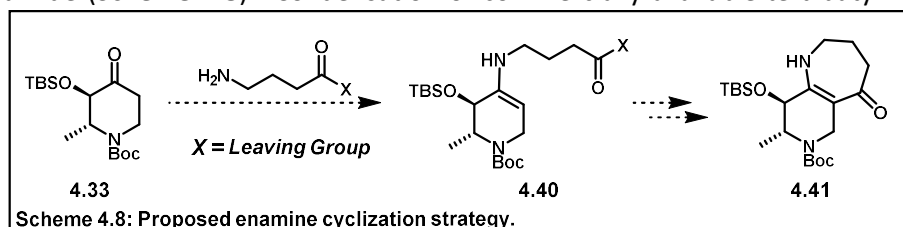
We thought that piperidine **4.33** was too sterically congested to allow formation of the alkylpalladium species. It was considered plausible that the desired bicycle (**4.39**) could be generated through a more facile intramolecular enamine alkenylation (**Equation 4.14**).²³ **4.29** was deprotected to afford amine **4.37** and condensation conditions were screened. Titanium-catalyzed conditions seemingly

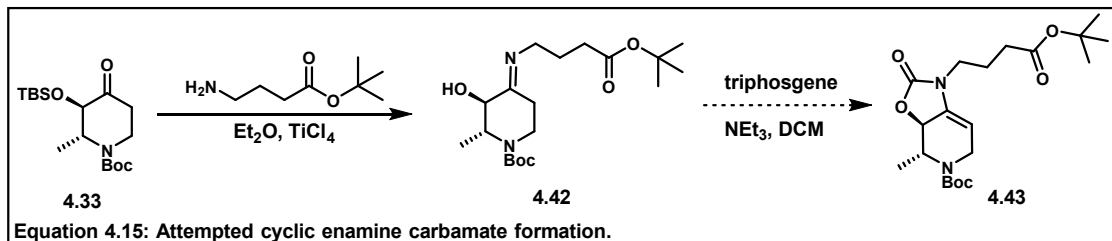


afforded condensation product **4.38** (observed via NMR of crude material) though all efforts to isolate the product were unsuccessful, resulting in decomposition to returned starting materials (**4.33** and **4.37**).²⁴

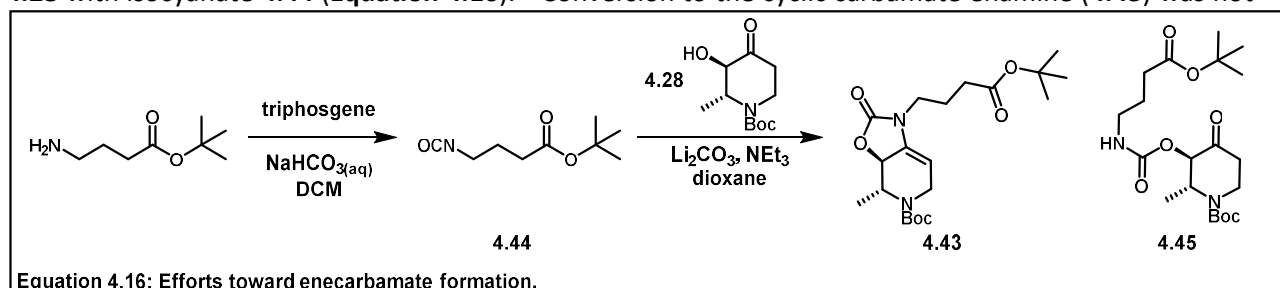
It seemed plausible that condensation of an amine bearing an electrophilic carbonyl could afford the seven-membered ring via nucleophilic enamine addition, which would likely be isolable because it would form the vinylogous amide (**Scheme 4.8**). Condensation of commercially available *tert*-butyl 4-

aminobutanoate with **4.33** was performed and the desired product (**4.42**) was





once again observed via ^1H NMR of crude material (**Equation 4.15**); however, all efforts to isolate **4.42** were unsuccessful, as were all attempts to carry through crude material in hopes of affording a stable intermediate. In an effort to afford the more stable alkenyl oxazolidine, the fragments were subjected to the developed condensation conditions and the reaction mixture was then charged with carbonylating agents to form the stable carbamate *in situ*. Once more, only **4.42** was observed and all efforts to isolate or derivatize this product led to decomposition. The cyclic ene carbamate was targeted through coupling **4.28** with isocyanate **4.44** (**Equation 4.16**).²⁵ Conversion to the cyclic carbamate enamine (**4.43**) was not



observed, but instead the noncyclized carbamate **4.45** was isolated. Due to the apparent instability of all amine condensation products, this route was abandoned.

4.4 Conclusions

It was at the point of considering a new route toward the core of the curvulamines that Maimone and coworkers published their synthesis of curvulamine A. Although we would not be the first to report a total synthesis of the curvulamines, our strategy of the synthesis of pyrrole containing natural products utilizing late-stage pyrrole installation would be a valuable addition to the literature; however, the status of the project at that time discouraged us from pursuing this synthesis any further. My efforts toward the synthesis of the curvulamines investigated both an application of nitrogen-centered radical polycyclization and the utilization of enolate alkenylation chemistry on two complex partners. Although

both strategies proved unsuccessful in their key transformations, both led to deeper understanding of reactivity at the highly congested piperidine ring. Further, our synthetic efforts led to a simple methodology to afford unsaturated piperidinone **4.31** on multigram scale, which was elaborated to afford the protected forms of the natural products imino-deoxydigitoxose and 6-deoxyfagomine in half the synthetic steps previously reported.

4.5 Distribution of Credit and Contributions

I would like to thank Dr. Brian Atwood for his contributions in the development of syntheses to intermediates as well as the characterization of these intermediates.

4.6 Experimental Information

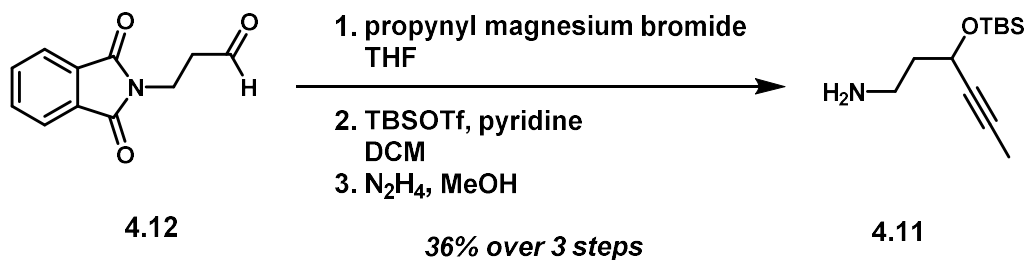
4.6.1 Materials and Methods

All reactions were carried out in oven-dried (140 °C) or flame-dried glassware under an atmosphere of dry argon unless otherwise noted. Dry dichloromethane (CH_2Cl_2), tetrahydrofuran (THF), diethyl ether (Et_2O), acetonitrile (MeCN), toluene (PhMe), and dimethoxyethane (DME) were obtained by percolation through columns packed with neutral alumina and columns packed with Q5 reactant, a supported copper catalyst for scavenging oxygen, under a positive pressure of argon. Solvents used for liquid-liquid extraction and chromatography were: Ethyl acetate, (EtOAc, Sigma-Aldrich, ACS grade) hexanes (Sigma-Aldrich, ACS grade), dichloromethane (CH_2Cl_2 , Fisher, ACS grade), acetone (Sigma-Aldrich, ACS Grade), diethyl ether (Et_2O , Fisher, ACS grade), and pentane (Sigma-Aldrich, ACS grade). Reactions that were performed open to air utilized solvent dispensed from a wash bottle or solvent bottle, and no precautions were taken to exclude water. Column chromatography was performed using EMD Millipore 60 Å (0.040–0.063 mm) mesh silica gel (SiO₂). Analytical thin-layer chromatography (TLC)

was performed on Merck silica gel 60 F254 TLC plates. Visualization was accomplished with UV (210 nm), and potassium permanganate (KMnO₄) or *p*-anisaldehyde staining solutions.

¹H NMR and ¹³C NMR spectra were recorded at 298 K on Bruker GN500 (500 MHz, ¹H; 125 MHz, ¹³C) and Bruker CRYO500 (500 MHz, ¹H; 125 MHz, ¹³C) spectrometers. ¹H and ¹³C spectra were referenced to residual chloroform (7.26 ppm, ¹H; 77.16 ppm, ¹³C) or residual methanol (3.31 ppm, ¹H; 49.00 ppm, ¹³C). Chemical shifts are reported in ppm and multiplicities are indicated by: s (singlet), d (doublet), t (triplet), q (quartet), p (pentet), hept (heptet), m (multiplet), and br s (broad singlet). Coupling constants, *J*, are reported in Hertz. The raw fid files were processed into the included NMR spectra using MestReNova 11.0, (Mestrelab Research S. L.). Infrared (IR) spectra were recorded on a Varian 640-IR instrument on NaCl plates and peaks are reported in cm⁻¹. Mass spectrometry data was obtained from the University of California, Irvine Mass Spectrometry Facility. High-resolution mass spectra (HRMS) were recorded on a Waters LCT Premier spectrometer using ESI-TOF (electrospray ionization-time of flight) or a Waters GCT Premier Micromass GC-MS (chemical ionization), and data are reported in the form of *m/z*.

4.6.2 Experimental Procedures



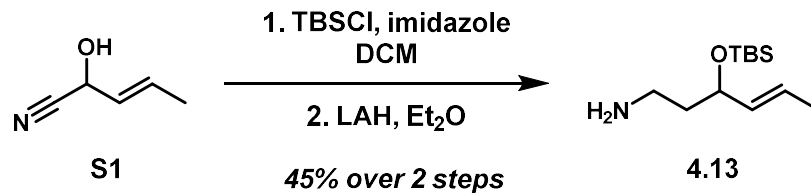
3-(*tert*-Butyldimethylsilyloxy)hex-4-yn-1-amine (4.11) A 10 mL round bottom flask was charged with aldehyde **4.12**¹¹ (100 mg, 0.49 mmol, 1 equiv) and THF (1 mL). The reaction flask was cooled to 0 °C and 0.5 M propynyl magnesium bromide solution (1.0 mL, 0.49 mmol, 1 equiv) was added dropwise over 5

min. The reaction mixture was allowed to warm to room temperature and the solution was stirred for 1 h. Saturated aqueous ammonium chloride solution (3 mL) was added and the solution was extracted with EtOAc (3 x 5 mL). The organic extracts were combined, dried over Na_2SO_4 , and concentrated in vacuo. The residue was dissolved in CH_2Cl_2 (1 mL) and had pyridine (0.12 mL, 1.478 mmol, 3 equiv) added. The reaction mixture was cooled to 0 °C. *Tert*-butyldimethylsilyl trifluoromethylsulfonate (0.22 mL, 0.98 mmol, 2 equiv) was added dropwise to the solution over 1 min. The reaction was warmed to room temperature and allowed to stir overnight. Saturated aqueous ammonium chloride solution was added (3 mL) and the solution was extracted with CH_2Cl_2 three times (3 x 5 mL). The organic extracts were combined, dried over Na_2SO_4 , and concentrated *in vacuo*. The residue was dissolved in methanol (1 mL) and had a 50% solution of hydrazine in water (0.12 mL, 2.46 mmol, 5 equiv) added. The reaction was stirred at room temperature for 1 h. The reaction mixture was diluted with water (5 mL) and extracted with EtOAc (3 x 5 mL). The combined organic layers were dried over Na_2SO_4 , and the filtrate was concentrated *in vacuo*. The residue was purified by chromatography on silica gel, eluting with hexanes/EtOAc/ NEt_3 50:49:1 (v/v), to afford 40 mg (36% yield over 3 steps) **4.11** as a colorless oil.

$^1\text{H NMR}$ (500 MHz, CDCl_3): δ 4.43 (br s, 1H), 2.83 (*J* = 6.6 Hz, 2H), 2.07 (br s, 2H), 1.84 – 1.70 (m, 2H), 1.78 (s, 3H), 0.87 (s, 9H), 0.09 (=d, 2.0 Hz, 6H).

$^{13}\text{C NMR}$ (125 MHz, CDCl_3): δ 80.6, 80.5, 61.6, 42.1, 38.5, 25.8, 18.2, 3.5, -4.5, -5.1.

HRMS (ES+) *m/z* calc'd for $\text{C}_{12}\text{H}_{25}\text{NOSi}$ [M+H] $^+$: 228.1784; found: 228.1775.

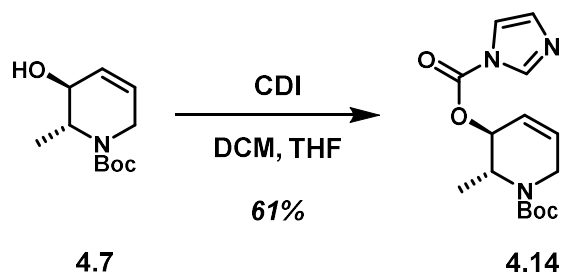


(E)-3-(*tert*-Butyldimethylsilyloxy)hex-4-en-1-amine (4.13) A 250 mL round bottom flask was charged with nitrile **S1**¹² (2.70 g, 25.0 mmol, 1 equiv) and CH₂Cl₂ (100 mL). Imidazole (5.00 g, 75 mmol, 3 equiv) and TBSCl (7.32 g, 50.0 mmol, 2 equiv) were added to the mixture and the reaction was stirred at room temperature for 16 h. The reaction mixture was filtered over celite and washed with CH₂Cl₂ (50 mL). The filtrate was concentrated *in vacuo*. The crude residue was dissolved in Et₂O (100 mL). The reaction flask was cooled to 0°C. Lithium aluminum hydride (1.85 g, 50 mmol, 2 equiv) was added portionwise. The reaction was stirred at 0 °C for 3 h. The reaction mixture was diluted with Et₂O (50 mL) and H₂O (2 mL) was added slowly, followed by 15% NaOH (2 mL), followed by H₂O (6 mL). The solution was warmed to room temperature and stirred 15 min. Na₂SO₄ was added and the reaction was stirred 15 min. The solution was filtered over celite and the filtrate was concentrated *in vacuo*. The residue was purified by chromatography on silica gel, eluting with hexanes/EtOAc/NEt₃ 50:49:1 (v/v), to afford 2.51 g (45% yield over two steps) of **4.13** as a yellow liquid.

¹H NMR (500 MHz, CDCl₃): δ 5.54 (dd, *J* = 15.2, 6.4 Hz, 1H), 5.41 (dd, *J* = 15.4, 6.7 Hz, 1H), 4.15 (dd, *J* = 12.5, 6.5 Hz, 1H), 2.74 (t, *J* = 7.0 Hz, 2H), 1.66 (d, *J* = 6.3 Hz, 3H), 1.65 – 1.56 (m, 4H), 0.86 (s, 9H), 0.10 – 0.02 (d, 6H).

¹³C NMR (125 MHz, CDCl₃): δ 134.7, 125.1, 72.1, 42.2, 38.8, 25.7, 17.6, -2.9.

HRMS (ES+) *m/z* calc'd for C₁₂H₂₇NOSi [M+H]⁺: 230.1940; found: 230.1951.



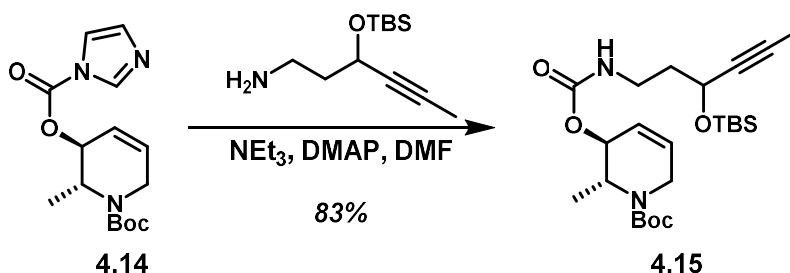
***tert*-Butyl(*R,3S*)-3-(*H*-1-imidazole-1-carbonyloxy)-2-methyl-3,6-dihydropyridine-1(*R*)-**

carboxylate (4.14) A 100 mL round bottom flask was charged with tetrahydropyridine **4.7** (500 mg, 2.34 mmol, 1 equiv) and CH₂Cl₂ (8 mL). A solution of carbonyldiimidazole (762 mg, 4.64 mmol, 2 equiv) in THF (40 mL) was added dropwise to the reaction mixture. The reaction was stirred at room temperature for 16 h. Saturated aqueous ammonium chloride (30 mL) was added to the reaction mixture and the solution was extracted with EtOAc (3 x 30 mL). The organic extracts were combined, dried over Na₂SO₄, and concentrated *in vacuo*. The residue was purified by chromatography on silica gel, eluting with hexanes/EtOAc 80:20 (v/v), to afford 439 mg (61% yield) of **4.14** as a red oil.

¹H NMR (500 MHz, CDCl₃): δ 8.09 (s, 1H), 7.38 (s, 1H), 7.04 (s, 1H), 6.17 (s, 1H), 5.95 (s, 1H), 5.12 (s, 1H), 4.73 (d, *J* = 43.9 Hz, 1H), 4.46 (dd, *J* = 72.4, 15.8 Hz, 1H), 3.61 (s, 1H), 1.41 (m, 9H), 1.18 (t, *J* = 7.1 Hz, 3H).

¹³C NMR (125 MHz, CDCl₃): δ 171.3, 149.7, 148.4, 142.3, 137.2, 117.2, 102.5, 80.4, 73.8, 60.6, 28.4, 21.2, 14.3.

HRMS (ES+) *m/z* calc'd for C₁₅H₂₁N₃O₄ [M+Na]⁺: 330.1430; found: 330.1447.



tert-Butyl- (2S)-3- ((tert-butyl(dimethylsilyloxy)hex-4-yn-1-yl)carbamoyloxy)-2-methyl-

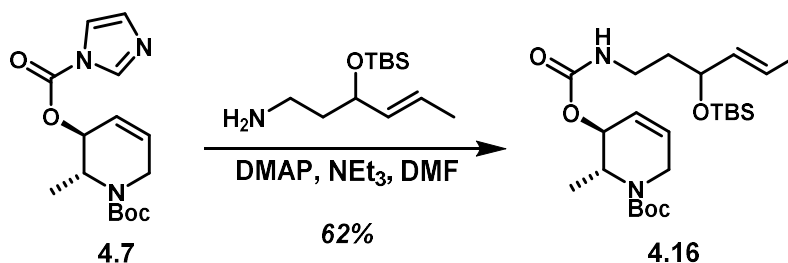
3,6-dihydropyridine-1(2R)-carboxylate (4.15)

A 10 mL round bottom flask was charged with carbamate **4.14** (200 mg, 0.65 mmol, 1 equiv), DMF (1 mL), dimethylaminopyridine (8 mg, 65 μmol , 0.1 equiv), and triethylamine (0.28 mL, 1.95 mmol, 3 equiv). A solution of amine **4.11** (162 mg, 0.72 mmol, 1.1 equiv) in DMF (1 mL) was added to the reaction mixture dropwise. The reaction mixture was heated to 65 $^\circ\text{C}$ and stirred at this temperature for 2 h. The reaction vessel was allowed to cool to room temperature and saturated aqueous ammonium chloride (5 mL) was added to the reaction mixture. The resultant solution was extracted with EtOAc (3 x 5 mL). The organic extracts were combined and washed with water (2 x 10 mL) and brine (10 mL). The organic phase was dried over Na_2SO_4 and the filtrate was concentrated *in vacuo*. The residue was purified by chromatography on silica gel, eluting with hexanes/EtOAc 85:15 (v/v), to afford 251 mg (83% yield) of **4.15** as a yellow oil.

$^1\text{H NMR}$ (500 MHz, CDCl_3): δ 5.96 (s, 1H), 5.81 (s, 1H), 5.15 (s, 1H), 4.82 (s, 1H), 4.44 (d, 2H), 3.50 (s, 1H), 3.33 (s, 1H), 1.86 – 1.75 (m, 4H), 1.43 (s, 8H), 1.237 (t, 3H), 1.06 (d, = 7.0 Hz, 3H), 0.86 (d, = 3.1 Hz, 8H), 0.08 (d, = 16.1 Hz, 5H).

$^{13}\text{C NMR}$ (125 MHz, CDCl_3): δ 156.0, 129.9, 120.9, 81.2, 78.0, 69.5, 65.9, 61.8, 38.0, 31.6, 28.5, 25.8, 22.7, 18.1, 15.3, 3.5, -4.5, -5.1.

HRMS (ES+) m/z calc'd for $\text{C}_{24}\text{H}_{42}\text{N}_2\text{O}_5\text{Si}$ $[\text{M}+\text{Na}]^+$: 489.2761; found: 489.2757.



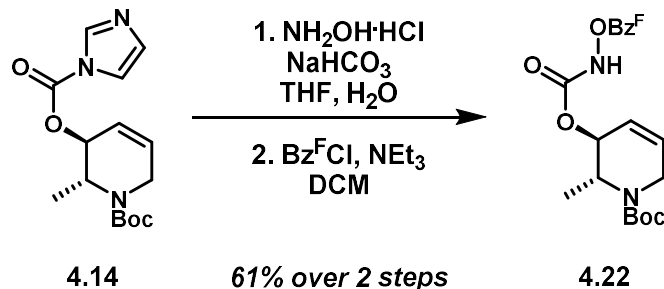
***tert*-Butyl-(*R,S*)-3-(*E*)-3-((*tert*-butyldimethylsilyloxy)hex-4-en-1-yl)carbamoyloxy)-2-methyl-3,6-dihydropyridine-1(*R*)-carboxylate (4.16)**

A 10 mL round bottom flask was charged with carbamate **4.14** (100 mg, 0.33 mmol, 1 equiv), DMF (0.5 mL), dimethylaminopyridine (4 mg, 0.1 equiv), and triethylamine (0.14 mL, 0.99 mmol, 3 equiv). A solution of amine **4.13** (162 mg, 0.66 mmol, 2 equiv) in DMF (0.5 mL) was added to the reaction mixture dropwise. The reaction mixture was heated to 65°C and stirred at this temperature for 16 h. The reaction vessel was allowed to cool to room temperature and saturated aqueous ammonium chloride (5 mL) was added to the reaction mixture. The solution was extracted with EtOAc (3 x 5 mL). The organic extracts were combined then washed with water (2 x 10 mL) and brine (10 mL). The organic phase was dried over Na_2SO_4 , and the filtrate was concentrated *in vacuo*. The residue was purified by chromatography on silica gel, eluting with hexanes/EtOAc 85:15 (v/v), to afford 93 mg (62% yield) of **4.16** as a tan oil.

$^1\text{H NMR}$ (500 MHz, CDCl_3): δ 5.96 (s, 1H), 5.83 (s, 1H), 5.55 (dd, $J = 4.4, 7.2$ Hz, 1H), 5.38 (dd, $J = 15.3, 6.5$ Hz, 1H), 5.04 (s, 1H), 4.84 (s, 1H), 4.47 (s, 1H), 4.32 (s, 1H), 4.15 (dd, $J = 15.1, 4.1$ Hz, 1H), 3.51 (d, $J = 18.5$ Hz, 1H), 3.22 (d, $J = 5.2$ Hz, 2H), 1.65 (d, $J = 6.4$ Hz, 5H), 1.45 (s, 9H), 1.07 (d, $J = 7.1$ Hz, 3H), 0.86 (d, $J = 2.5$ Hz, 9H), 0.07 – -0.05 (m, 6H).

$^{13}\text{C NMR}$ (125 MHz, CDCl_3): δ 156.0, 133.8, 133.7, 130.3, 125.8, 120.9, 79.7, 72.5, 72.3, 69.5, 49.7, 39.2, 37.6, 28.5, 25.9, 25.7, 18.1, 17.6, 15.3, -4.2, -4.8.

HRMS (ES+) m/z calc'd for $\text{C}_{24}\text{H}_{44}\text{N}_2\text{O}_5\text{Si}$ $[\text{M}+\text{Na}]^+$: 491.2917; found: 491.2907.

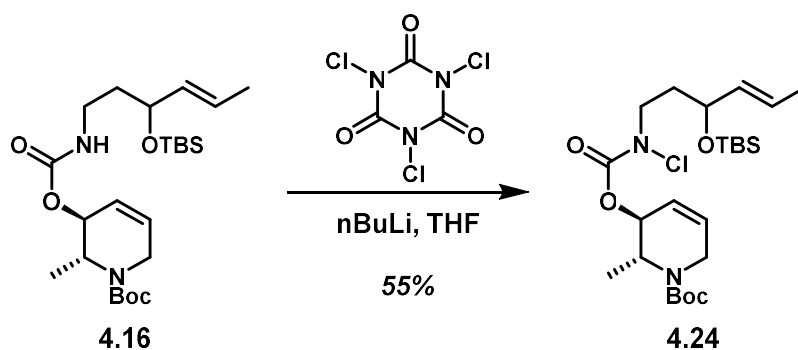


tert-Butyl-(2S)-2-methyl-3-(1(perfluorophenoxy)carbamoyloxy)-3,6-dihydropyridine-4-carboxylate (4.22)

A 10 mL round bottom flask was charge with **4.14** (50 mg, 0.16 mmol, 1 equiv) and THF (0.5 mL). To this solution ammonium hydroxide hydrochloride (23 mg, 0.32 mmol, 2 equiv) was added. A solution of NaHCO₃ (41 mg, 0.48 mmol, 3 equiv) in THF (0.5 mL) was then added. The reaction mixture was stirred at room temperature for 16 h. The mixture was diluted with Et₂O (5 mL) and washed with a saturated aqueous solution of NH₄Cl (5 mL). The organic phase was dried over Na₂SO₄ and concentrated *in vacuo*. The residue was passed through silica gel, eluting with hexanes/EtOAc 50:50 (v/v). The filtrate was concentrated *in vacuo*. The resultant residue was dissolved in CH₂Cl₂ (1 mL). The solution was cooled to 0 °C before triethylamine (23 mL, 0.16 mmol, 1 equiv) and pentafluorobenzoyl chloride (43 mg, 0.16 mmol, 1 equiv) were added. The reaction mixture was warmed to room temperature and stirred for 5 h. The solution was diluted with water (2 mL) and extracted with CH₂Cl₂ (3 x 3 mL). The organic extracts were combined, dried over Na₂SO₄, and concentrated *in vacuo*. The residue was purified by chromatography on silica gel, eluting with hexanes/EtOAc 92:8 (v/v), to afford 46 mg (61% yield over two steps) **4.22** as a brown oil.

¹H NMR (500 MHz, CDCl₃): δ 6.13 (br s, 1H), 5.96 (br s, 1H), 5.23 (br s, 1H), 4.67 (t, 7 Hz, 1H), 4.41 (m, 1H), 3.59 (t, 7.1 Hz, 1H), 1.44 (s, 8H), 1.16 (t, 7.1 Hz, 3H).

¹³C NMR (125 MHz, CDCl₃): δ 171.2, 158.7, 154.6, 80.1, 60.4, 34.7, 31.6, 28.3, 28.1, 22.7, 14.1.



***tert*-Butyl-(*R*,3*S*)-3-((*E*)(3-(*tert*-butyldimethylsilyloxy)hex-4-en-1-yl)chlorocarbonyloxy)-2-**

methyl-3,6-dihydropyridine-1(*R*)-carboxylate (4.24) A 10 mL round bottom flask was charged with

carbamate **4.16** (93 mg, 0.20 mmol, 1 equiv) and dry THF (2 mL). The solution was cooled to -78 °C.

A 2.5 M solution of *n*-butyllithium in hexanes (0.17 mL, 0.42 mmol, 2.1 equiv) was added to the reaction mixture

dropwise over 5 min. The mixture was stirred at -78 °C for 30 min. Trichloroisocyanuric acid (46 mg, 0.199

mmol, 1 equiv) was added as a single portion to the reaction mixture. The reaction mixture was slowly

allowed to warm to room temperature as it was stirred over 24 h. Saturated aqueous ammonium chloride

(5 mL) was added to the reaction mixture. The solution was extracted with EtOAc (3 x 5 mL). The organic

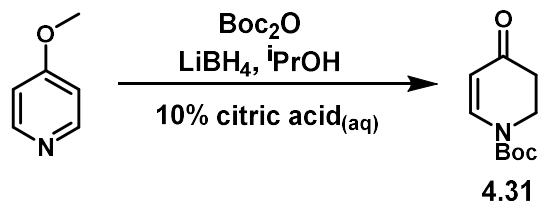
phases were combined, dried over Na₂SO₄, and the filtrate was concentrated *in vacuo*. The residue was

purified by chromatography on silica gel, eluting with hexanes/EtOAc 90:10 (v/v), to afford 55 mg (55%

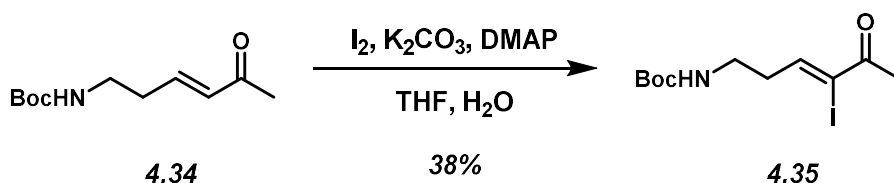
yield) of **4.24** as a tan oil.

¹H NMR (500 MHz, CDCl₃): δ 6.02 (s, 1H), 5.88 – 5.77 (m, 1H), 5.55 (dd, 5.1, 6.7 Hz, 1H), 5.37 (dd, 15.2, 6.8 Hz, 1H), 4.86 (s, 1H), 4.61 – 4.34 (m, 2H), 4.15 – 4.05 (m, 1H), 3.72 – 3.40 (m, 3H), 1.81 (dd, 14.9, 7.3 Hz, 2H), 1.65 (dd, 6.5 Hz, 3H), 1.52 – 1.49 (m, 3H), 1.44 (s, 9H), 1.09 (dd, 7.1 Hz, 3H), 0.85 (s, 10H), -0.00 (dd, 11.8 Hz, 6H).

¹³C NMR (125 MHz, CDCl₃): δ 155.6, 154.7, 133.8, 127.5, 126.7, 125.9, 79.8, 72.5, 70.5, 51.4, 47.9, 35.7, 31.9, 28.4, 25.9, 19.3, 18.2, 13.8, -4.2, -4.9.



tert-Butyl 4-oxo-3,4-dihydropyridine-1(2H)-carboxylate (4.31): A 250 mL round bottom flask was charged with *p*-methoxypyridine (9.00 g, 82.5 mmol, 1 equiv), isopropanol (180 mL), and lithium borohydride (4.49 g, 206.2 mmol, 2.5 equiv). The solution was cooled to 0°C, then di-*tert*-butyl dicarbonate (45.00 g, 206.2 mmol, 2.5 equiv) was added portionwise. The reaction mixture was stirred at 0 °C for 15 min, warmed to room temperature, and stirred at room temperature for 2h. The reaction mixture was quenched with a 10% (w/v) aqueous solution of citric acid (100 mL). The biphasic mixture was stirred rigorously for 20 min. The phases were separated, and the aqueous phase was extracted with CH₂Cl₂ (2 x 50 mL). The combined organic extracts were dried over Na₂SO₄ and concentrated *in vacuo*. The residue was purified by chromatography on silica gel, eluting with hexanes/EtOAc 80:20 (v/v), to afford 11.68 g (72% yield) of **4.31** as a white solid. ¹H and ¹³C NMR spectra were consistent with those previously reported.¹⁷



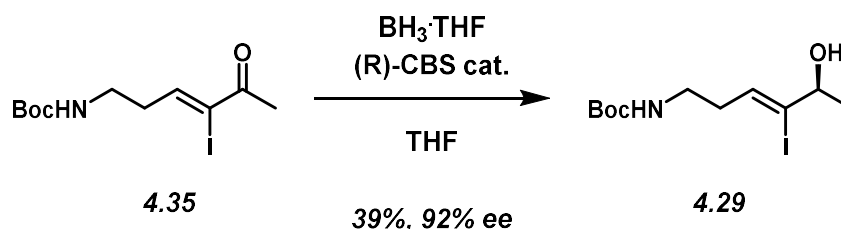
tert-Butyl (Z)-4-iodo-5-oxohex-3-en-1-ylcarbamate (4.35): 100 mL round bottom flask was charged with **4.34** (445 mg, 2.09 mmol, 1 equiv), THF (10 mL), and CH₂Cl₂ (10 mL). K₂CO₃ (356 mg, 2.50 mmol, 1.2 equiv), I₂ (836 mg, 3.14 mmol, 1.5 equiv), and DMAP (83 mg, 0.42 mmol, 0.2 equiv) were then added to this solution. The reaction mixture was stirred at room temperature 4h. The reaction mixture was diluted

with EtOAc (40 mL), washed with a saturated aqueous solution of Na_2O_3 (40 mL), then washed with 0.1 M HCl (aq) (40 mL). The organic phase was dried over Na_2SO_4 and concentrated *in vacuo*. The residue was purified by chromatography on silica gel, eluting with hexanes/EtOAc 85:15 (v/v), to afford 275 mg (38% yield) of **4.35** as a colorless oil.

$^1\text{H NMR}$ (500 MHz, CDCl_3): δ 7.13 (t, J , = 6.1 Hz, 1H), 4.77 (s, 1H), 3.43 (J, = 5.8 Hz, 2H), 2.67 (q, = 6.6 Hz, 2H), 2.55 (s, 3H), 1.48 (s, 9H).

$^{13}\text{C NMR}$ (125 MHz, CDCl_3): δ 192.5, 156.1, 150.3, 114.2, 79.7, 60.4, 39.3, 38.5, 28.4.

HRMS (ES+) m/z calc'd for $\text{C}_{11}\text{H}_{18}\text{NO}_3$ [M+Na] $^+$: 362.0229; found: 362.0226.



tert-Butyl (S,Z)-(5-hydroxy-4-iodohex-3-en-1-yl)carbamate (4.29) 2 dram scintillation vial was charged with THF (0.25 mL), *R*-2-methyl-CBS-oxazaborolidine (1 μ L, 0.68 μ mol, 1 equiv) and $\text{BH}_3\cdot\text{THF}$ (7 μ L, 1.12 μ mol, 2 equiv). The reaction was stirred for 15 min. A solution of **4.35** (23 mg, 0.68 μ mol, 1 equiv) in THF (0.25 mL) was added dropwise. The reaction was stirred at room temperature for 1 h. The reaction mixture was diluted with EtOAc (2 mL) and washed with a saturated aqueous ammonium chloride (2 mL). The organic phase was dried over Na_2SO_4 and concentrated *in vacuo*. The residue was purified by chromatography on silica gel, eluting with hexanes/EtOAc 60:40 (v/v), to afford 9 mg (39% yield) **4.29** as a colorless oil.

$^1\text{H NMR}$ (500 MHz, CDCl_3): δ 6.01 (t, = 6.7 Hz, 1H), 4.65 (s, 1H), 4.04 (J, = 4.5 Hz, 1H), 3.34 – 3.22 (m, 2H), 2.49 – 2.38 (m, 2H), 1.50 (s, 9H), 1.37 (t, = 6.2 Hz, 3H).

¹³C NMR (125 MHz, CDCl₃): 156.0, 131.8, 74.5, 39.1, 36.5, 28.5, 23.7.

HRMS (ES+) *m/z* calc'd for C₁₁H₂₀NO₃I [M+Na]⁺: 364.0386; found: 364.0394.

4.7 References

- ¹ Han, W. B.; Lu, Y. H.; Zhang, A. H.; Zhang, G. F.; Mei, Y. N.; Jiang, N.; Lei, X.; Song, Y. C.; Ng, S. W.; Tan, R. X. "Curvulamine, a New Antibacterial Alkaloid Incorporating Two Undescribed Units from a *Curvularia* Species." *Org. Lett.* **2014**, *16*, 5366–5369.
- ² Atwood, B. "Unusual Natural Products, Lessons Learned in Pursuit of KS-504D and Curvulamine; Doctorate Thesis." **2018**, University of California, Irvine.
- ³ Tietze, L. F.; Schulz, G. "Investigations into the Biosynthesis of Porphyrins and Corrins—Calculations on 1,3-Allylic Strain and [1,5]-Sigmatropic Rearrangements in Pyrroles, Furans, and Thiophenes." *Chem. Eur. J.* **1997**, *3*, 523–529.
- ⁴ Illuminati, G.; Mandolini, L. "Ring Closure Reactions of Bifunctional Chain Molecules." *Acc. Chem. Res.* **1981**, *14*, 95–102.
- ⁵ a) Huo, J.; He, G.; Chen, W.; Hu, X.; Deng, Q.; Chen, D. "A Minireview of Hydroamination Catalysis: Alkene and Alkyne Substrate Selective, Metal Complex Design." *BMC Chem.* **2019**, *13*; b) Muller, T. E.; Hultsch, K. C.; Yus, M.; Foubelo, F.; Tada, M. "Hydroamination: Direct Addition of Amines to Alkenes and Alkynes." *Chem. Rev.* **2008**, *108*, 3795–3892; c) Das, K.; Koushik, S.; Maji, B. "Manganese-Catalyzed Anti-Markovnikov Hydroamination of Allyl Alcohols via Hydrogen-Borrowing Catalysis." *ACS Catal.* **2021**, *112*, 7060–7069.
- ⁶ a) Park, S.; Jeong, J.; Fujita, K.-I.; Yamamoto, A.; Yoshida, H. "Anti-Markovnikov Hydroamination of Alkenes with Aqueous Ammonia by Metal-Loaded Titanium Oxide Photocatalyst." *J. Am. Chem. Soc.* **2020**, *142*, 12709–12714; b) Zhao, D.; Li, J.; Tang, T. "Metal-free Photocatalytic Intermolecular anti-Markovnikov Hydroamination of Unactivated Alkenes." *Eur. J. Org. Chem.* **2021**, *18*, 2650–2654. c) List, B.; Diaz-Oviedo, D. "Making Primary Amine Synthesis Simple: Photocatalytic Olefin Hydroamination." *Synfacts* **2021**, *17*, 564.
- ⁷ Nguyen, S.; Zhu, Q.; Knowles, R. "PCET-Enabled Olefin Hydroamidation Reactions with *N*-Alkyl Amides." *ACS Cat.*, **2019**, *9*, 4502–4507.
- ⁸ Popescu, M. V.; Douglas, J. J.; Sheikh, N. S.; Leonori, D. "Visible-Light-Mediated 5-*exo-dig* Cyclizations of Amidyl Radicals." *Eur. J. Org. Chem.* **2017**, 2108–2111.
- ⁹ S. Gabriel "Ueber eine Darstellungsweise primärer Amine aus den entsprechenden Halogenverbindungen." *Chem. Ber.* **1887**, *20*, 2224–2236.
- ¹⁰ Rengasamy, R.; Curtis-Long, M. J.; Seo, W. D.; Jeong, S. H.; Jeong, I.-Y.; Park, K. H. "New Building Block for Polyhydroxylated Piperidine." *J. Org. Chem.* **2008**, *73*, 2898–2901.

- ¹¹ a) Dailler, D.; Rocaboy, R. Baudoïn, O. "Synthesis of β -Lactams by Palladium(0)-Catalyzed C(3)- β -H Carbamoylation." *Angew. Chem. Int. Ed.* **2017**, *56*, 7218–7222; b) Sen, S. E.; Roach, S. L. "A Convenient Two-Step Procedure for the Synthesis of Substituted Allylic Amines from Allylic Alcohols." *Synthesis*, **1995**, *7*, 756–758.
- ¹² Huang, C.; Li, Z.-Y.; Song, J.; Xu, H.-C. "Catalyst- and Reagent-Free Formal Aza-Wacker Cyclizations Enabled by Continuous-Flow Electrochemistry." *Angew. Chem. Int. Ed.* **2021**, *60*, 11237–11241.
- ¹³ Lanzillotto, M.; Konnert, L.; Lamaty, F.; Martinez, J.; Colacino, E. "Mechanochemical 1,1'-Carbonyldiimidazole-Mediated Synthesis of Carbamates." *ACS Sustainable Chem. Eng.*, **2015**, *3*, 2882–2889.
- ¹⁴ Hazelden, I.; Langer, T.; Munday, R.; Bower, J. "Enantioselective Aza-Heck Cyclizations of *N*-(Tosyloxy)carbamates: Synthesis of Pyrrolidines and Piperidines." *J. Am. Chem. Soc.* **2019**, *141*, 3356–3360.
- ¹⁵ a) Hioe, J.; Zipse, H. "Radical Stability and its Role in Synthesis and Catalysis." *Org. Biomol. Chem.* **2010**, *8*, 3609–3617; b) McManus, J. B.; Onuska, N. P.; Nicewicz, D. "Generation and Alkylation of α -Carbamyl Radicals via Organic Photoredox Catalysis." *J. Am. Chem. Soc.* **2018**, *140*, 9056–9060.
- ¹⁶ Fürst, A.; Plattner, P. A. "Über Steroide und Sexualhormone. 160. Mitteilung. 2 α , 3 α - und 2 β , 3 β -Oxido-cholestane; Konfiguration der 2-Oxy-cholestane." *Helv. Chim. Acta* **1949**, *32*, 275.
- ¹⁷ a) Briner, K.; Burkhardt, J. P.; Burkholder, T. P.; Cunningham, B. E.; Fisher, M. J.; Gritton, W. H.; Jesudason, C. D.; Miller, S. C.; Mullaney, J. T.; Reinhard, M. R.; Rothhaar, R. R.; Stevens, F. C.; Winneroski, L. L.; Xu, Y.; Xu, Y.-C. "Serotonergic Benzofurans." PCT Int. Appl. 2001, 152. WO0109122A2 b) Pizzuti, M. M.; Minnaard, A. J.; Feringa, B. "Copper-free 'click': 1,3-dipolar cycloaddition of azides and arynes." *Org. & Biomol. Chem.* **2008**, *6*, 3463–3466.
- ¹⁸ Kitajima, M.; Murakami, Y.; Takahashi, N.; Wu, Y.; Kogure, N.; Zhang, R.-P.; Takayama, H. "Asymmetric Total Synthesis of Novel Pentacyclic Indole Alkaloid, Kopsiyunnanine E, Isolated from *Kopsia arborea*." *Org. Lett.* **2014**, *16*, 5000–5003.
- ¹⁹ Krafft, M. E.; Cran, J. "A Convenient Protocol for the α -Iodination of α,β -Unsaturated Carbonyl Compounds with I₂ in an Aqueous Medium." *Synlett.* **2005**, *8*, 1263–1266.
- ²⁰ a) Corey, E. J.; Shibata, S.; Bakshi, R. K. "An efficient and catalytically enantioselective route to (S)-(-)-phenyloxirane." *J. Org. Chem.* **1988**, *53*, 2861–2863; b) Corey, E. J.; Link, J. O. "A General, Catalytic, and Enantioselective Synthesis of α -Amino Acids." *J. Am. Chem. Soc.*, **1992**, *114*, 1906–1908.
- ²¹ a) Huang, J.; Bunel, E.; Faul, M. M. "Palladium-Catalyzed α -Vinylolation of Carbonyl Compounds." *Org. Lett.* **2007**, *9*, 4343–4346; b) Chieffi, A.; Kamikawa, K.; Ahmen, J.; Fox, J. M.; Buchwald, S. L. "Catalytic Asymmetric Vinylolation of Ketone Enolates." *Org. Lett.* **2001**, *3*, 1897–1900. c) Ankner, T.; Cosner, C. C.; Helquist, P. "Palladium- and Nickel-Catalyzed Alkenylation of Enolates." *Chem. Eur. J.* **2013**, *19*, 1858–1871.

²² Grigalunas, M.; Ankner, T.; Norrby, P.-O.; Wiest, O.; Helquist, P. "Ni-Catalyzed Alkenylation of Ketone Enolates under Mild Conditions: Catalyst Identification and Optimization." *J. Am. Chem. Soc.* **2015**, *137*, 7019–7022.

²³ Nandi, R. K.; Takeda, N.; Ueda, M.; Miyata, O. "Nucleophilic β -alkenylation of N-alkoxyenamines: an umpolung strategy for the preparation of β,γ -unsaturated ketones." *Tetrahedron Lett.* **2016**, *57*, 2269–2272.

²⁴ Salomo, E.; Gallen, A.; Sciortino, G.; Ujaque, G.; Grabulosa, A.; Lledos, A.; Riera, A.; Verdaguer, X. "Direct Asymmetric Hydrogenation of *N*-Methyl and *N*-Alkyl Imines with an Ir(III)H Catalyst." *J. Am. Chem. Soc.* **2018**, *140*, 16967–16970.

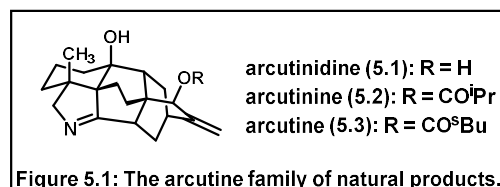
²⁵ Martinez, R.; Jimenez-Vazquez, H. A.; Tamariz, J. "Highly Regioselective C-5 Alkynylation of Imidazoles by One-Pot Sequential Bromination and Sonogashira Cross Coupling." *Tetrahedron Lett.* **2000**, *56*, 3857–3866.

Chapter 5: Progress Toward the Total Synthesis of the Arcutine Family of

Natural Products

5.1 Introduction

The arcutines (**Figure 5.1**) are a subfamily of diterpene alkaloids with four members that differ in the substitution of the allylic oxygen and isopyrroline nitrogen. The natural product arcutinidine (**5.1**) is hypothesized to be the biosynthetic precursor for all members and has been a major target of interest for synthetic chemists as it is readily derivatized to all other



members of the family. Three total syntheses of arcutinidine have been reported, all following the synthetic strategy of linear syntheses to the arcutine skeleton. Herein, I describe our efforts toward a convergent synthesis to the arcutines. Although this synthesis has yet to be completed, the syntheses of both fragments of the molecule have been completed and they have been united in a convergent step. Completion of this synthesis would result in the most concise synthesis of the arcutines to date.

5.2 Discovery, Biological Evaluations, and Previous Syntheses of the Arcutines

5.2.1 Diterpene Alkaloids

The diterpene alkaloids are a large group of tetracyclic, pentacyclic, or hexacyclic natural products with a nitrogen containing heterocycle.¹ There are over 950 members within the diterpene alkaloid family encompassing a series of subfamilies, differentiated by their bond arrangement and bridged cyclic structures.² The range of bioactivity of the entire family is broad, though many diterpene alkaloids exhibit activity as voltage-gated ion channel inhibitors.³ These natural products are generally derived from plant matter, although some members of the family are derived from fungi, sponges, and other natural

sources.⁴ The diterpene alkaloids are common targets for total synthesis, not only for their various potent bioactivities, but also due to the synthetic challenges their highly complex skeletal structures pose.⁵

5.2.2 Discovery of the Arcutines

Aconitum arcuatum Maxim was a plant commonly used in folk medicine to treat patients suffering from rheumatism and radiculitis. Early research on the bioactivity of this plant species indicated that it does have antibacterial properties.⁶ Studies of the aerial portion of *A. arcuatum* led to the isolation of a novel diterpene alkaloid from plant extracts, named arcutin (later referred to as arcutine) by Saidkhodzhaeva and coworkers in 2000.⁷ The structure of the novel natural product was determined via NMR characterization and confirmed via X-ray crystallography. The C10–C20 bridge, characteristic in all previously reported diterpene alkaloids, was replaced with an unprecedented C5–C20 bridge and an azomethane linkage to the C20 carbon, classifying this as a new subfamily of diterpene alkaloid natural products. Further analysis of extracts derived from *A. arcuatum* revealed another member of the subfamily, arcutinine, which was found to differ only by the ester substitution on the C15-hydroxy group.⁸ Saponification of the ester afforded full conversion to arcutinidine, which is presumed to be the biosynthetic precursor to the isolated natural products.

In 2017, another natural product with the same core substructure, aconicarmicharcutinium A (**Figure 5.2**), was discovered by Shi and coworkers; interestingly, this natural product was isolated

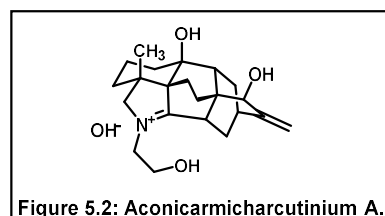


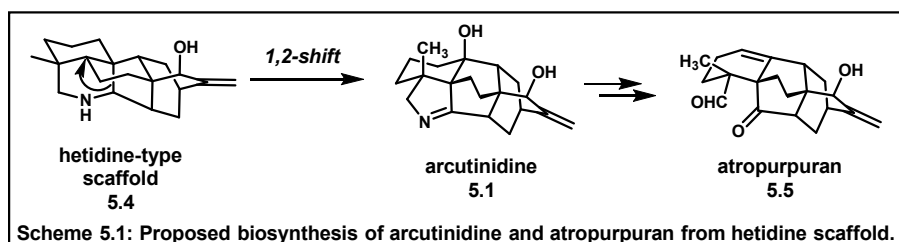
Figure 5.2: Aconicarmicharcutinium A.

from a different species of plant of the same genus, *Aconitum carmichaelii*.⁹ This natural product was isolated as the iminium-hydroxide salt, containing the same structure as arcutinidine only differentiating at the substitution of the isopyrroline nitrogen, bolstering the theory that arcutinidine acts as a biosynthetic precursor to all arcutine natural products as this natural product was derived from the non-esterified core. To our knowledge, no studies have been performed to probe the bioactivity of the arcutine

natural products. The complexity of these natural products and the need of material for potential bioactivity investigations has led multiple groups to initiate efforts toward an efficient total synthesis.

5.2.3 Biosynthesis

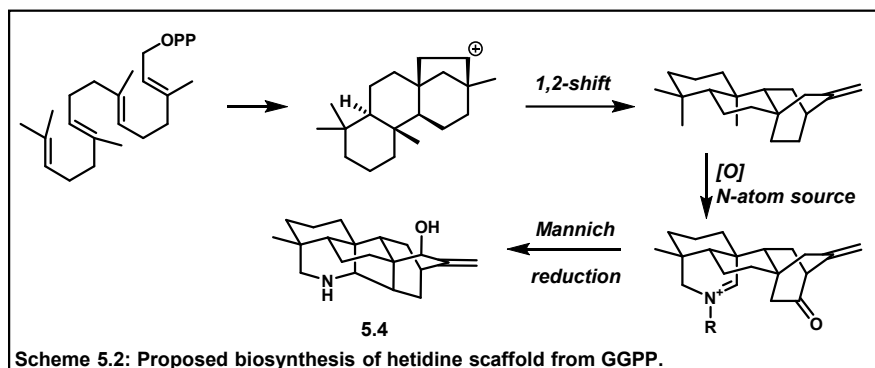
In 2016 the Sarpong group performed computational investigations to probe the biosynthetic pathway for the formation of the arcutines.¹⁰ It was proposed that the arcutines and atropurpuran (**5.5**), a pentacyclic diterpene with relatively similar skeletal structure, are a biosynthetically linked, both being derived from a hetidine-type skeleton (**5.4**) (**Scheme 5.1**).¹¹ Two probable biosynthetic pathways were



proposed and comparative calculations were performed to

investigate energetic differences between key 1,2-shifts to afford the arcutine scaffold and atropurpuran from two key precursors.¹² With this information, they concluded the most energetically favorable and likely pathway was the conversion of the core of hetidine to arcutinidine. Oxidation events followed by hydrolysis leads to the formation of atropurpuran.

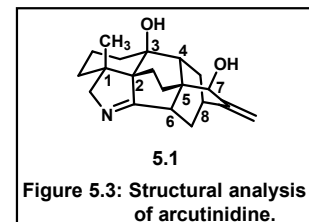
Based on these conclusions, Sarpong and coworkers proposed a complete biosynthetic pathway to the arcutines: beginning with a polyene cyclization of geranylgeranyl pyrophosphate (GGPP), followed by a series of rearrangements, oxidation events, and a Mannich reaction to generate the hetidine core precursor (**Scheme 5.2**).¹³ Rearrangement of the hetidine scaffold affords arcutinidine (**5.1**), which is



further functionalized to afford all other members of the arcutine family.

5.2.4 Structural Analysis

The arcutines contain a high level of complexity relative to their modest size. Many structural features are worth noting when considering arcutinidine (**5.1**) as a synthetic target (**Figure 5.3**). The molecule contains a hexacyclic core with two bridging ring systems, eight stereocenters, seven of



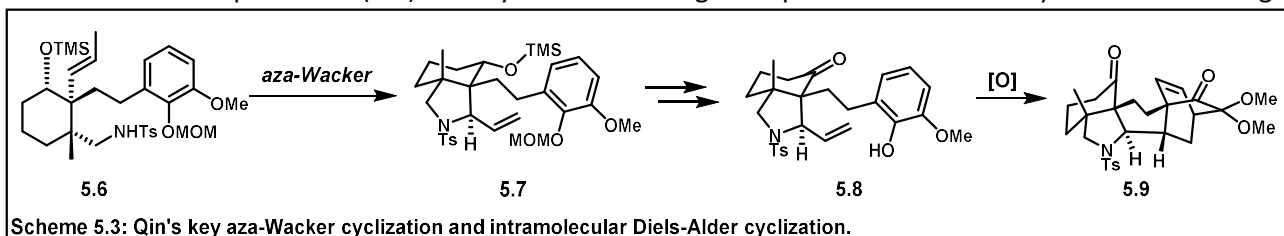
which are contiguous. Furthermore, three of these stereocenters (labelled 1, 2, and 5) are all-carbon quaternary centers, two of which are vicinal to one another. Vicinal quaternary centers are recognized as a synthetic challenge that has sparked a field of interest in their synthesis.¹⁴ Other functionalities of interest include the terminal alkene and allylic alcohol, the tertiary alcohol appended to the central bicyclic ring system, and the isopyrroline heterocycle. These complexities offer a vast challenge that enticed many groups to attempt to synthesize the arcutines.

5.3 Previous Total Syntheses

5.3.1 Qin's Total Synthesis

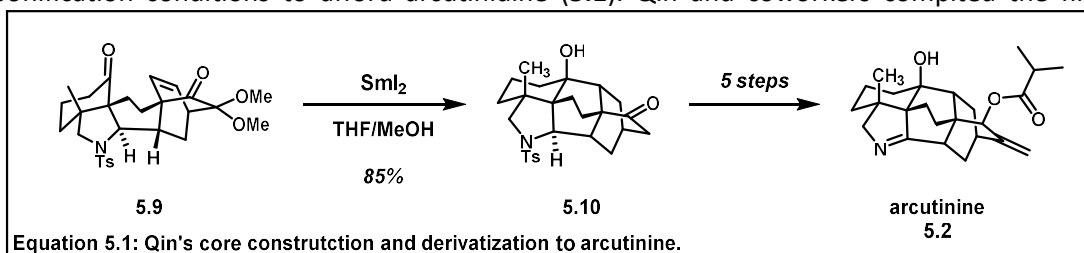
Qin and coworkers published the first total synthesis of arcutinidine in 2019. This publication was succeeded by two more reports on the same topic submitted for review the same month.¹⁵ The group envisioned rapid construction of four rings of the hexacyclic core via an aza-Wacker cyclization, followed by dearomative oxidation and subsequent intramolecular Diels-Alder (IMDA) cycloaddition (**Scheme 5.3**).

The aza-Wacker precursor (**5.6**) was synthesized in eight steps from commercially available starting



materials. The first stereogenic center was established via cyclohexanone β -cyanation to afford a racemic mixture of products. **5.6** was also produced as enantiopure material via an asymmetric 1,4-methyl

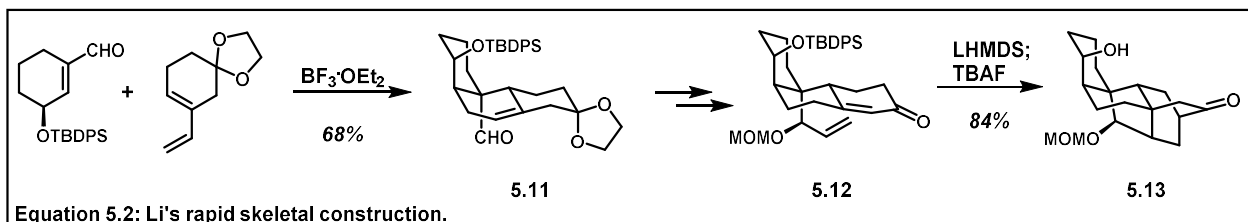
addition, which allowed them to access **5.1** as enantiopure material, albeit in a less efficient manner. **5.6** underwent the key transformation to afford **5.7** and was converted to **5.8** in three steps. Oxidative dearomatization of **5.8** afforded **5.9** via intramolecular Diels-Alder cycloaddition. From **5.9**, the closure of the final ring was performed via ketyl-alkene cyclization (**Equation 5.1**), which was discovered to completely reduce the acetal in tandem, to obtain **5.9**. Conversion of the ketone to the allylic ester, followed by deprotection and oxidation of the pyrrolidine afforded arcutinine (**5.2**), which was subjected to saponification conditions to afford arcutinidine (**5.1**). Qin and coworkers completed the first total



synthesis of two members of the arcutine family in racemic form in 22 steps longest linear sequence and as enantiopure material in 30 steps. The key aza-Wacker/IMDA transformation was a concise method of building complexity, but the synthetic sequence to afford the aza-Wacker precursor and the multiple functional group manipulations required to convert the structural skeleton to the natural product made this synthesis relatively lengthy. The synthesis of the final ring via ketyl-olefin cyclization, was a strategy also utilized in Sarpong's synthesis of **5.1**, as well as in Qin's previously reported synthesis of atropurpuran, proving to be a robust method of forming the central ring.¹⁶

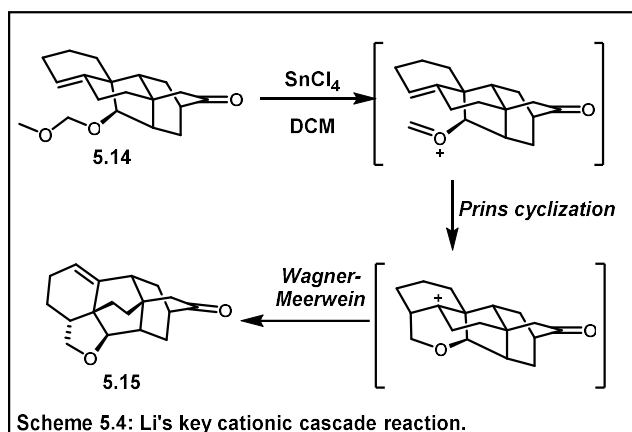
5.3.2 Li's Total Synthesis

The Li group targeted the total synthesis of arcutinidine and published their completed enantioselective synthesis in 2019.¹⁷ Their strategy invoked a bimolecular Diels-Alder to form tricycle **5.11** followed by an intramolecular Diels-Alder cycloaddition to build the bridged bicyclic system **5.13**



(Equation 5.2). The use of IMDA reactions to build the key bridged bicyclic systems is a strategy very commonly employed in syntheses of diterpene alkaloids.¹⁸ To install oxidation in the necessary positions, **5.14** was subjected to Lewis acidic conditions to induce a cationic cascade reaction (Scheme 5.4).

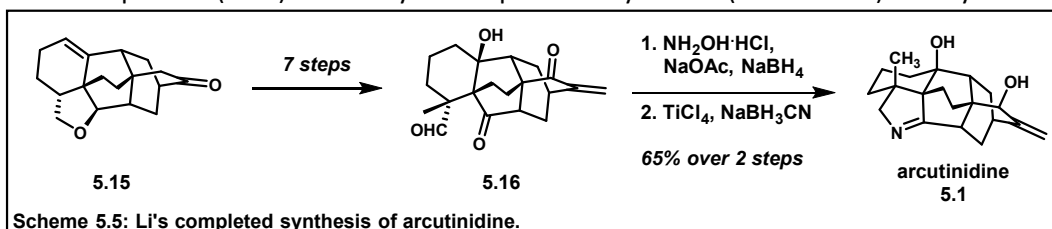
Decomposition of the methoxymethyl protecting group to the oxocarbenium cation induced a Prins



cyclization affording the cationic oxacycle, which underwent a Wagner-Meerwein rearrangement to afford the central [2.2.2]-bridged system. The cation then suffered elimination to afford **5.15** in modest yield. This ring-expansion parallels the biosynthesis proposed by Sarpong and coworkers

and mimics the conversion of the hetidine-type scaffold to the arcutine scaffold (Section 5.2.3).¹⁹

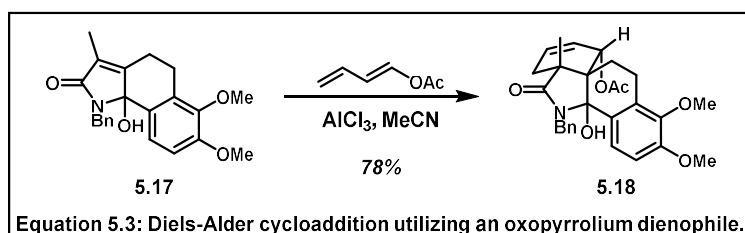
Although the synthesis of the core structure was highly efficient, a seven-step sequence of redox and functional group manipulations were required to afford the skeletal structure of the arcutines with the correct oxidation pattern (**5.16**) necessary to complete the synthesis (Scheme 5.5). The synthetic strategy



by Li mirrors aspects of Sarpong's proposed biosynthesis, connecting the relationship between the oxidation pattern of atropurpuran and the arcutine precursor **5.16**. Forming the imine-heterocycle via reductive condensation of hydroxylamine with **5.16**, in tandem with reduction of the enone carbonyl, afforded arcutinidine (**5.1**) in 19 steps longest linear sequence. The strategy incorporated by Li and coworkers is similar to the other published syntheses of the arcutines, in which concise formation of the skeleton was achieved at the cost of a series of necessary functional group manipulations.

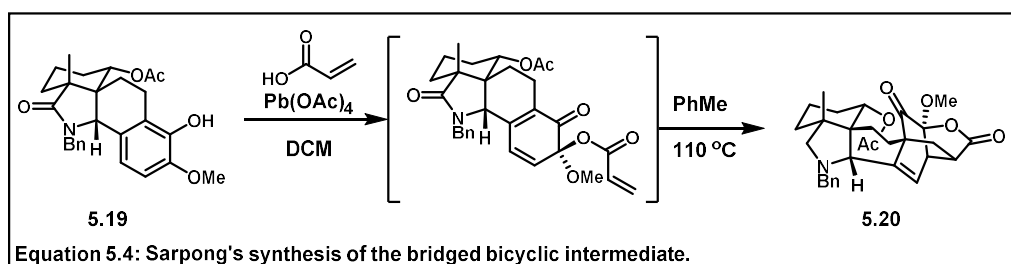
5.3.3 Sarpong's Total Synthesis

In 2019, Sarpong and coworkers published their total synthesis of arcutinidine.²⁰ The group credited their retrosynthetic analysis to Corey's chemical network analysis combined with modern density functional theory (DFT) calculations to determine a synthetically viable route.²¹ A major discovery reported in this publication was the development of an unprecedented Diels-Alder cycloaddition utilizing oxopyrrolium dienophiles (**Equation 5.3**). The Lewis acid catalyzed Diels-Alder cycloaddition was determined to be feasible via a series of DFT calculations. Utilizing masked-oxopyrrolium precursor **5.17**,



Lewis acid activation initiated a completely regioselective Diels-Alder cycloaddition affording key tetracyclic

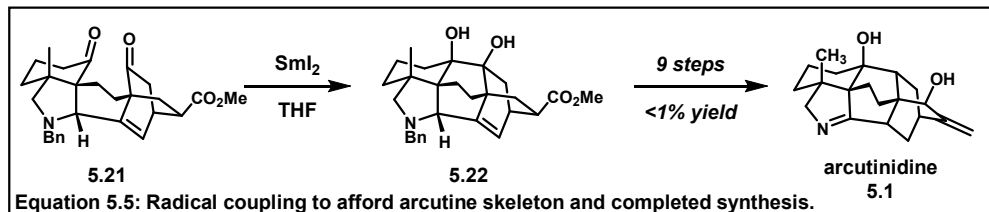
intermediate **5.18** in four steps from commercially available starting materials. Redox manipulations and deprotections afforded tetracycle **5.19**, which was subjected to a two-step dearomative oxidation/IMDA cycloaddition sequence to afford **5.20** in 60% yield over two steps (**Equation 5.4**). **5.20** was subjected to



a three step sequence to produce dione **5.21**, which was

subjected to pinacol coupling conditions, reminiscent of the ketyl-alkene cyclization conditions developed

by Li and coworkers, to afford **5.22** (Equation 5.5). After this concise synthesis of the arcutine core, a nine-step sequence of functional group manipulations was required to afford the natural product (**5.1**), resulting in the total synthesis of arcutinidine in 25

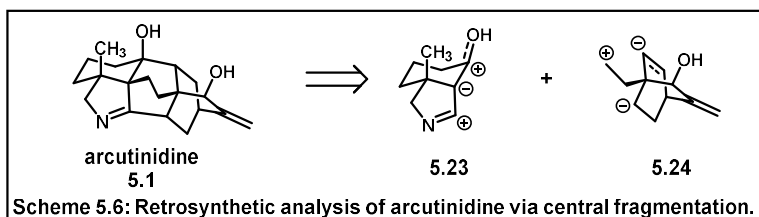


steps from commercially available starting materials. Although the synthesis of the structural skeleton was efficient, the strategy resulted in intermediates lacking necessary functionalization at key positions, which was accounted for late in the synthesis in a lengthy series of low yielding transformations.,

5.4 Efforts Toward the Total Synthesis of the Arcutines

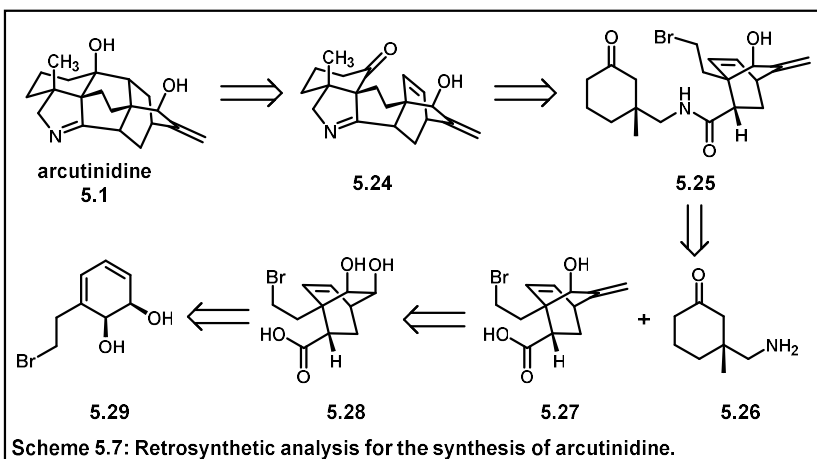
5.4.1 Synthetic Analysis

In our consideration of the previously reported syntheses of the arcutines, it became apparent that all previous efforts utilized a similar strategy: build the skeletal framework efficiently then introduce or adjust functional groups in a lengthy sequence. Our strategy was instead to develop a convergent synthesis by separating the molecule down its central bonds into two halves (synthon **5.23** and **5.24**). We envisioned taking advantage of the consonant relationship of the 1,3-carbonyl system of bicycle **5.23**, as

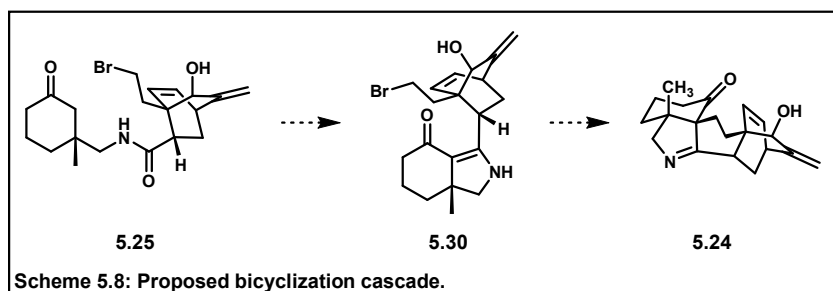


well as a reductive cyclization utilized in many previous syntheses (Scheme 5.6). We believed that targeting the synthesis of the molecule in a convergent manner, rather than the previous, linear efforts, would allow for a more efficient synthesis than any previously reported, as it preinstalled the functionality of the natural product, avoiding the need for late-stage functional group manipulations.

Arcutinidine (**5.1**), having been shown to be derivatized to all other members of the arcutine family, was our retrosynthetic target (**Scheme 5.7**). From the natural product, our initial disconnection mimicked the ketyl



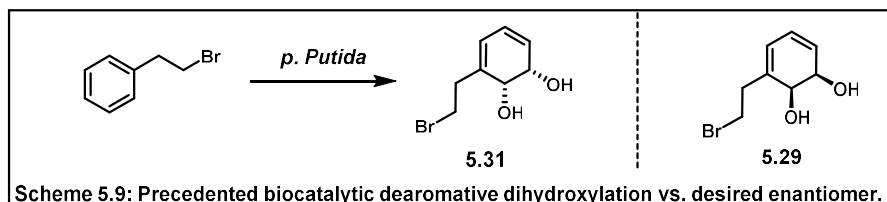
radical cyclization utilized in Qin and Sarpong's syntheses to afford **5.24**.^{16,17,21} We envisioned a Dieckmann condensation followed by alkylation at the α -carbon of the resultant vinylogous amide (**5.30**) to afford the central ring (**Scheme 5.8**).²² **5.25** could be disconnected into amine fragment **5.26** and bridged bicycle



5.27. The [2.2.2]-bridged bicycle **5.27** could be reverted to diol **5.28** through regioselective oxidation (precedented on

similar bicyclic systems) and methylene Wittig transform.²³ Diol **5.28** would be accessed through cycloaddition of oxidative dearomatization product **5.29**; the Diels-Alder reactivity of the cyclic dienes afforded by dihydroxylative dearomatization is well precedented.²⁴ The enantioselective synthesis of amine **5.26** will be discussed in section 5.4.2.

This synthetic pathway could allow for the synthesis of arcutinidine in as few as seven synthetic steps from commercially available (2-bromoethyl benzene) (**Scheme 5.9**). While it was recognized that precedented biocatalyzed dearomatic dihydroxylation

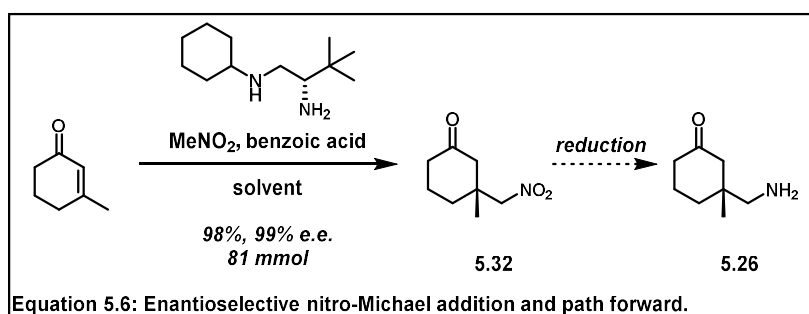


the undesired enantiomer **5.31**, the synthesis of the non-natural enantiomer of arcutinidine was still

considered a valuable pursuit as it could act as a proof of concept toward a highly efficient synthesis. Access to the desired enantiomer could be resolved through collaboration with laboratories specialized in biocatalysis or directed evolution.

5.4.2 Amine Fragment Synthesis

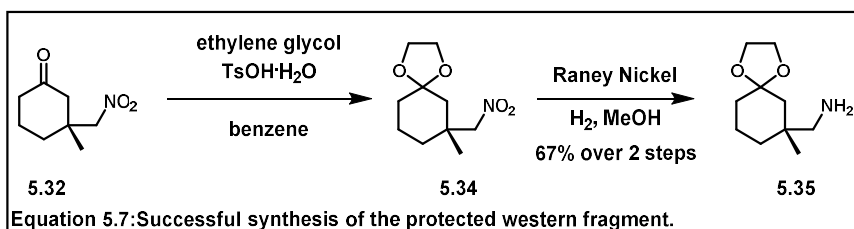
The amino-ketone fragment **5.26** was envisioned to arise from an enantioselective nitro-Michael addition preceded by the work of Dixon and Ye (**Equation 5.6**).²⁵ This reaction produced **5.32** in highly



scalable, high-yielding, and enantioselective manner. **5.32** was subjected to reduction, which resulted in a complex mixture of products, hypothesized to be a

mixture of condensation products and the secondary alcohol. To avoid overreduction and hemiaminal formation, **5.32** was converted to the ketal and the nitro group was reduced using Raney nickel catalyzed

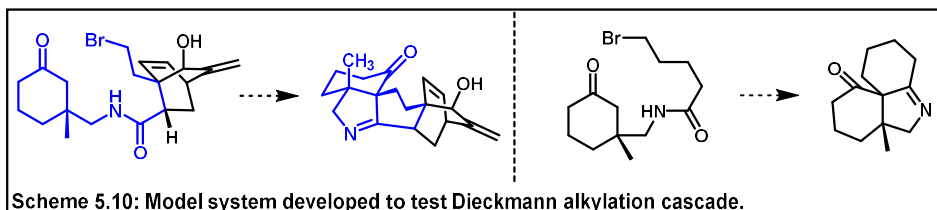
hydrogenation conditions to afford the protected fragment (**5.35**) in three steps (**Equation 5.7**).



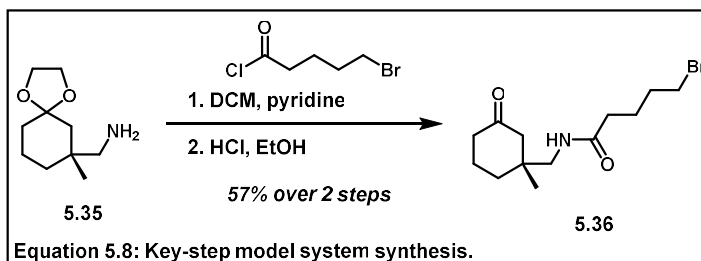
5.4.3 Key Transformation Model System

A model system was devised to test the key Dieckmann condensation/alkylation reaction utilizing **5.35**. The minimum scaffold necessary for testing this reactivity was only the amide and a long chain alkyl

halide, represented in blue (**Scheme 5.10**). The model system



(**5.36**) was made via acylation of amine **5.35** with 5-bromo valeryl chloride followed by conversion of the ketal to the ketone (**Equation 5.8**).



Conditions were explored to induce bicyclization of **5.36** (**Table 5.1**). Heating **5.36** with catalytic quantities of Brønsted-Lowry acid resulted in no reactivity or decomposition. Subjecting **5.36** to

Solvent	Additive	Temperature	Result
Cl-Ph	cat. pTsOH	Reflux	No reaction
Cl-Ph	1 equiv pTsOH	Reflux	Decomposition
DMF	cat. pTsOH	Reflux	Decomposition
DMF	1 equiv pTsOH	Reflux	Decomposition
-	-	130 °C	5.37 isolated
PhCl	cat. pTsOH	μ W, 200° C	No reaction
PhCl	1 equiv pTsOH	μ W, 200° C	Decomposition
PhCl	cat. pTsOH	μ W, 200° C (1Hr)	No reaction
1,2-PhCl ₂	cat. pTsOH	Reflux	No reaction

Table 5.1: Conditions screen to induce the Dieckmann-alkylation transformation.

stoichiometric amounts of Brønsted-Lowry acid and heating resulted in complete decomposition. Heating **5.36** in the absence of solvent resulted in a product tentatively assigned as desired tricycle **5.37**. This product had a near perfect match to the predicted C¹³ NMR spectra. The

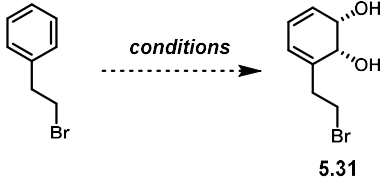
tentatively positive result and the knowledge that the actual system would likely require its own optimization efforts encouraged us to continue our pursuits.

5.4.4 Biocatalytic Dearomative Dihydroxylation

Arene oxidation must overcome the high thermodynamic barrier of dearomatization.²⁶ These reactions generally rely on the use of combinations of strong oxidants and transition metal catalysts or biocatalysis.²⁷ The Hudlicky and Boyd groups have championed the use of *in vivo* enzymatic catalysis to afford such substrates.²⁸ Through correspondence with members of these labs, it was discovered the requirement of specialized bioreactors and the inability to run these reactions on scales greater than a few hundred milligrams were problems that limited our potential access to intermediate **5.31**.

Due to the need for specialized equipment and restricted access to the required strain of bacteria, we chose to collaborate with the Prescher lab at UCI. In collaboration with Dr. Anna Love and Dr. Ryan Kozlowski, multiple attempts at screening dearomative dihydroxylation conditions of the desired substrate were performed utilizing modified strains of *E. coli* (Table 5.2).

We realized that without access to specialized bioreactors, we were unable to generate over 10 milligrams of **5.31**. We had been in contact with multiple groups who are capable of producing appreciable quantities of



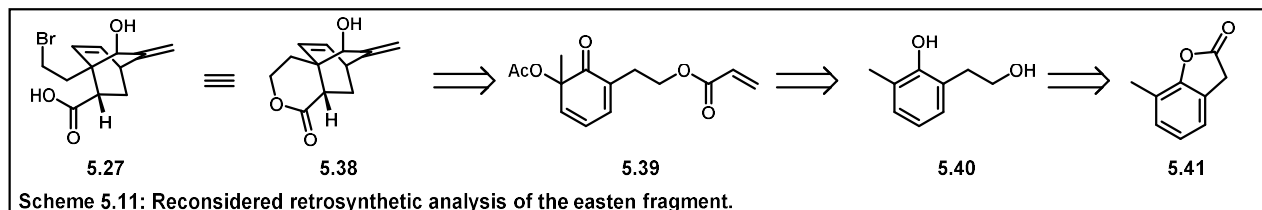
Plasmid	Phenethyl bromide	Toluene	Dodecane	Broth	Result
pAL096	30 μ L	-	+	Luria	-
pAL096	30 μ L	-	-	Luria	-
pAL097	30 μ L	-	+	Luria	-
pAL097	30 μ L	-	-	Luria	-
pAL096	-	46 μ L	+	Luria	-
pAL096	-	46 μ L	-	Luria	-
pAL097	-	46 μ L	+	Luria	-
pAL097	-	46 μ L	-	Luria	-
pAL097	50 μ L	-	-	Mineral	11 mg
pAL097	147 μ L	-	-	Mineral	10 mg

Table 5.2: Efforts toward biocatalytic dearomative dihydroxylation.

5.31, though it was concluded that these labs were unable to ship us substantial amounts due to concerns over the noted thermal decomposition of the product, which risked explosion during transit.

5.4.5 Retrosynthetic Reconsiderations

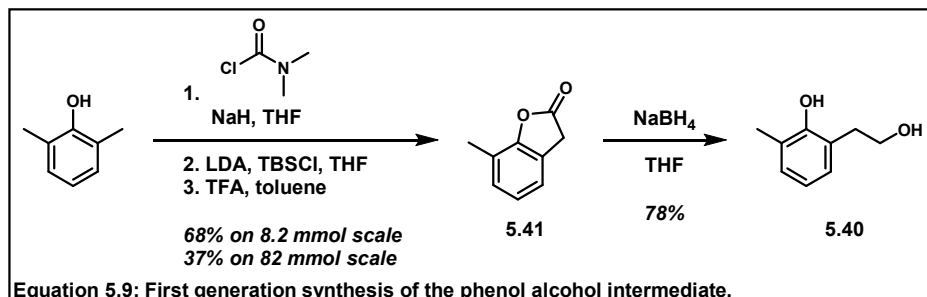
We chose to pursue an alternative synthesis of the bridged bicyclic fragment to act as a proof-of-concept before investing deeply into external collaborations. We thought that bridged bicycle **5.27** was synthetically equivalent to lactone **5.38** (Scheme 5.11). We believed we could synthesize this lactone fragment via intramolecular Diels-Alder cycloaddition of **5.39**. The cyclic dienone was considered a retron



for an oxidative dearomatization transform, leading to phenol **5.40**, the reduction product of literature precedent benzofuranone **5.41**.

5.4.6 Phenol Synthesis

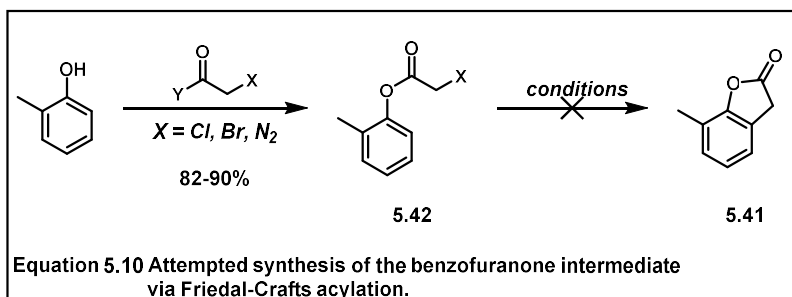
In pursuit of our newly developed synthesis, **5.41** was made in three steps from 2,6-dimethylphenol, which was successfully converted to the **5.40** via reduction (**Equation 5.9**).²⁹ The literature precedented synthesis to the benzofuranone **5.41** was readily replicated on 500 milligram scale



in yields like those reported. On multigram scale, however, the yields were greatly

diminished. The poor scalability was attributed to the quenching of trifluoroacetic acid (TFA) that, on scales requiring hundreds of milliliters of TFA, resulted in exothermic decomposition of the product. All measures taken to prevent this decomposition, such as cooling the reaction mixture prior to quenching and extended quenching, showed little improvement of yields. We believed that a highly scalable synthesis would be necessary to produce the bridged bicyclic fragment, so we began to investigate alternative routes to **5.41**.

Benzofuranone **5.41** was thought to be accessible via intramolecular Friedel-Crafts alkylation (**Equation 5.10**). The synthesis of the parent benzofuranone from phenol through a two-step procedure utilizing intramolecular Friedel-Crafts alkylation was reported to be scalable and high yielding.³⁰



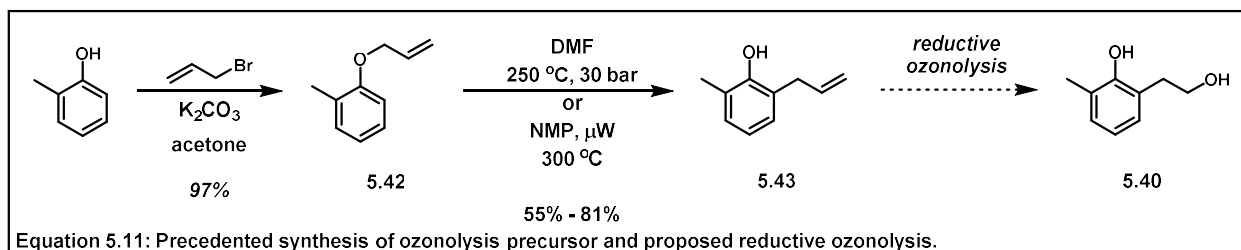
Acylation of ortho-cresol with

chloroacetyl chloride afforded **5.42** ($X=Cl$), which was subjected to the reported conditions but returned only starting material. The bromo and diazo variants also failed to cyclize under reported conditions. Rigorous screening of Lewis and Brønsted-Lowry acid-catalyzed Friedel-Crafts alkylation conditions

resulted in either no reaction or complete decomposition, so this strategy to synthesize **5.41** was abandoned.³¹

5.4.7 Reductive Ozonolysis Strategy

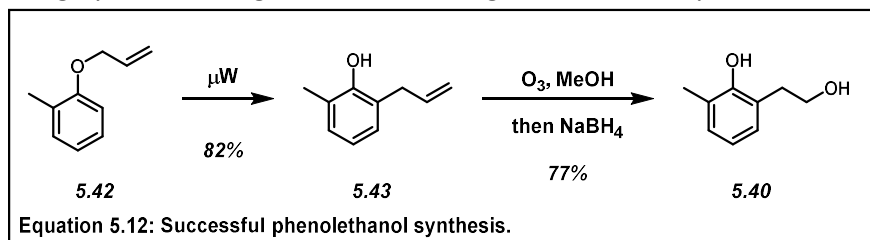
Our focus turned to a direct synthesis of **5.40** via reductive ozonolysis of known allylphenol **5.43** (**Equation 5.11**). Although **5.43** is sold by some commercial vendors it is an expensive starting material, so the precedent two step synthesis of **5.43** from *o*-cresol was pursued. Allyl ether **5.42** was made



Equation 5.11: Precedent synthesis of ozonolysis precursor and proposed reductive ozonolysis.

according to literature precedent.³² A limitation of this route was the need for high temperatures and pressures in a very low concentration to induce the Claisen rearrangement. Our laboratory was not equipped with the appropriate high-pressure reaction vessel required to perform this chemistry on the multigram scale. Synthesis of **5.43** via microwave irradiation at low concentrations would be highly limiting to scale.

Alternative methods to induce the Claisen rearrangement were investigated (**Equation 5.12**) and we discovered that microwave irradiation of **5.42** in the absence of solvent generated **5.43**, affording **5.40** in high yields, on 20 grams scale in a single batch. Ozonolysis of **5.43** in methanol followed by reductive

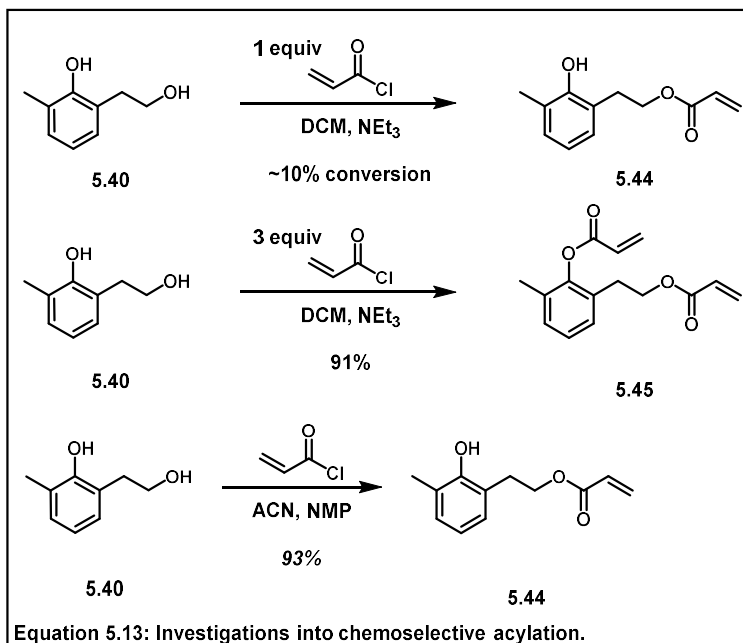


Equation 5.12: Successful phenolethanol synthesis.

quenching of the ozonide yielded over 30 grams of **5.40** in a single reaction.

5.4.8 Chemoselective Acryloylation

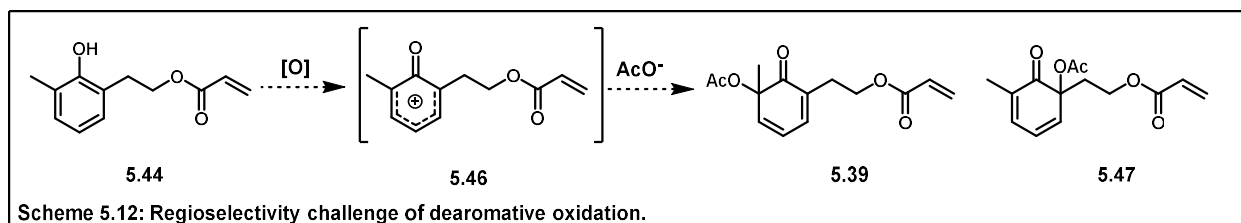
Acryloylation of **5.40** posed a chemoselectivity issue as the phenolic oxygen could potentially be acylated in preference to the primary alcohol (Equation 5.13). Initial studies indicated that attempts at kinetically controlled acylation resulted in poor conversion to **5.44** and increased equivalents of acryloyl chloride resulted in complete



conversion to bis-ester **5.45**. It had been reported that acryloylation of primary alcohols in the presence of phenols could be achieved utilizing a solvent mixture of acetonitrile and *N*-methylpyrrolidine.³³ Subjecting **5.40** to these conditions afforded **5.44** in good yields on 10-gram scale with complete chemoselectivity.

5.4.9 Dearomative Oxidation

Dearomative oxidation of **5.44** posed a challenge of regioselectivity, as the carbocationic intermediate (**5.46**) had two potential sites for acetoxylation with no indication of a steric or electronic



preference for the desired diene **5.39** (Scheme 5.12).

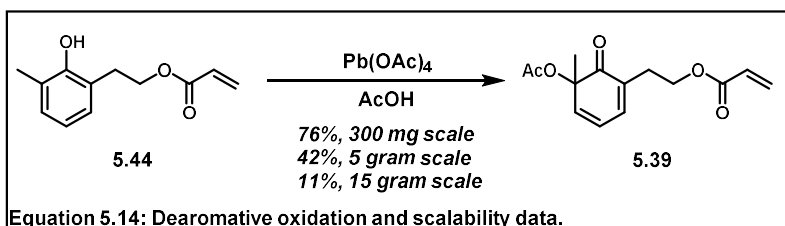
Investigations into well-precedented hypervalent-iodine mediated oxidations resulted in the complete conversion to the undesired

Conditions	Result
PIDA, DCM	5.47
PIFA, HFIP	5.47
IBX, Bu ₄ Ni, DCE, TFA	No reaction
Pb(OAc) ₄ , AcOH	5.39

Table 5.3: Screen of common conditions to induce dearomative oxidation.

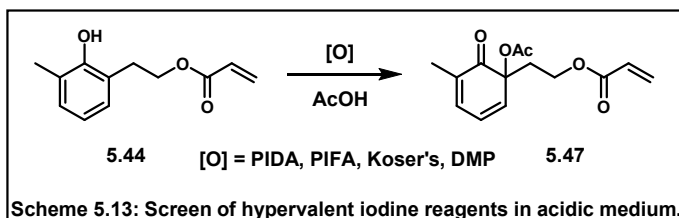
regioisomer **5.47** (Table 5.3). Fortunately, when **5.44** was subjected to lead tetraacetate in acidic media **5.39** was isolated as the sole regioisomer in good yields. When **5.44** was subjected to these conditions on

multigram scale the yields declined (Equation 5.14). It was observed that during the quenching



procedure on larger scales stable emulsions containing large quantities of lead byproduct were formed, potentially leading to loss of product.

Reevaluation of previous results (Table 5.3) led to the hypothesis that preference for the desired regioisomer could be credited to the use of acetic acid as the solvent. **5.44** was subjected to a series of hypervalent-iodine oxidants with acetic acid as the solvent, but all experiments still resulted in formation of the undesired



regioisomer (**5.47**) (Scheme 5.13). These results indicated the possibility that the acetylation event did not occur through a bimolecular reaction, but rather through intramolecular transfer of the acetate group. Based on this hypothesis, we concluded that regioselectivity was likely determined by the characteristics of the oxidant, leading us to abandon all hypervalent iodine oxidants.

We turned our attention back to optimization of the lead tetraacetate-mediated conditions on large scale (Table 5.4). It was hypothesized that thermal decomposition of the product may occur during

Conditions	Result
A - AcOH, Cooled to 0 °C during quench	A - 21%
B - DCM, acetic acid removed	B - 40% conversion
C - DCM, 10 equiv acetic acid	C - 72%

Table 5.4: Optimization of lead acetate-mediated dearomative oxidation.

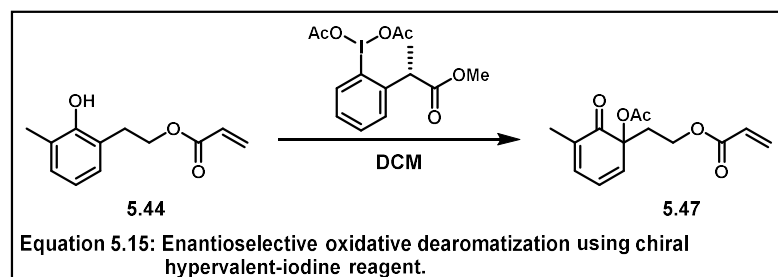
the exothermic quench of the large excess of acetic acid resulting in poor yields at larger scales. Attempts at maintaining temperature while neutralizing the

reaction mixture, led to minimal improvement in yield. The hypervalent iodine reagent screen indicated that the acetic acid solvent is likely inconsequential to regioselectivity. Removing the acetic acid entirely

and running the reaction in dichloromethane led to poor conversion. The use of a moderate excess of acetic acid with dichloromethane as the solvent allowed for complete conversion to **5.39** and no notable decomposition during work up. These conditions also prevented the formation of emulsions during the workup. **5.39** was isolated in consistent yields on scales up to 15 grams.

5.4.10 Preliminary Investigations into Enantioselective Oxidative Dearomatization

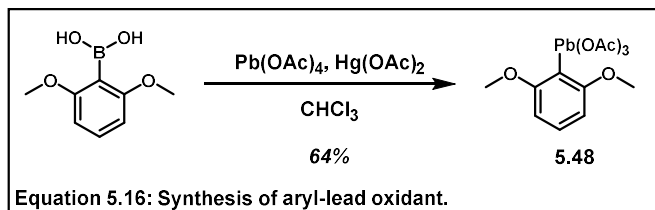
While the oxidative dearomatization afforded **5.39** as a mixture of racemates, it was our goal to synthesize each member of the arcutine family as a single enantiomer. Further, accessing enantiopure **5.39** was imperative to avoid forming a mixture of diastereomers when the fragments were converged. Enantioselective oxidative dearomatization reactions are known and rely on chiral hypervalent iodine reagents.³⁴ **5.44** was subjected to a common chiral hypervalent iodine reagent but that experiment only



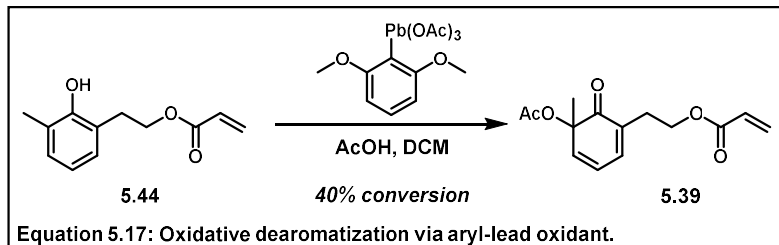
generated undesired regioisomer **5.47** (Equation 5.15). Examination of the literature revealed no reports of chiral lead tetraacetate reagents.

Aryl-lead triacetate reagents have been reported and are commonly used as aryl transfer reagents, though some examples of their use as oxidants have been reported.³⁵ We hypothesized that we could develop a chiral aryl-lead acetate reagent, reminiscent of the chiral hypervalent iodine reagents, and perform oxidative dearomatization to afford enantioenriched regioisomer **5.39**.

It was plausible that the oxidant would perform the dearomatization event, but transfer the aryl group rather than the acetate, so a model system was developed. **5.48** was synthesized from the aryl boronic acid (Equation 5.16).



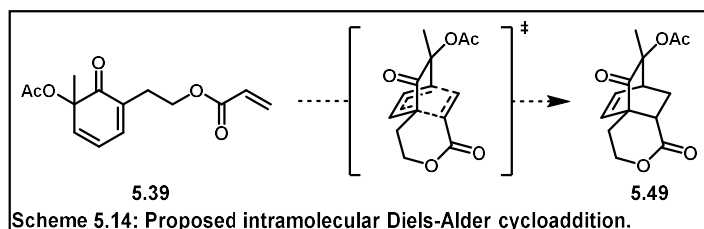
Notably, we included the dimethoxy functionality to replicate the functional handles that would likely be present on a chiral reagent. **5.44**



was subjected to the standard oxidation conditions but replacing lead tetraacetate with aryl-lead reagent **5.48** (Equation 5.17). Gratifyingly, we noted modest conversion to the desired regioisomer (**5.39**) with no noted arylation or undesired regioisomer byproducts. We were satisfied that these results acted a proof-of-concept, calling for future investigations in the use of chiral lead acetate reagents for the synthesis of enantiopure arcutines.

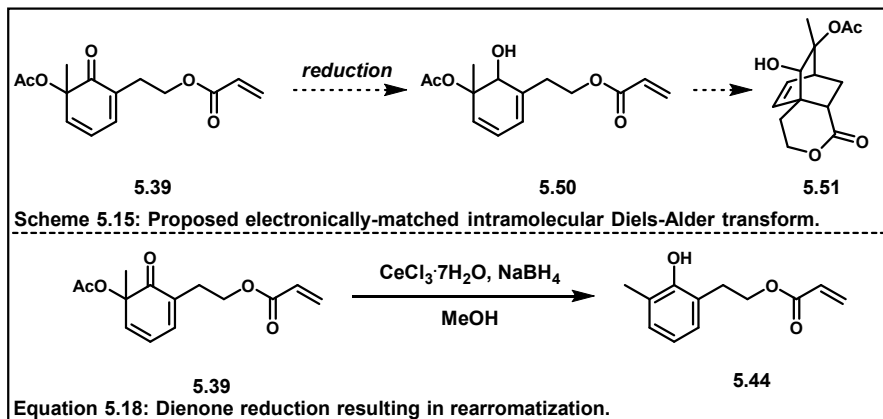
5.4.11 Electronically Mismatched Intramolecular Diels-Alder Cycloaddition

Intramolecular Diels-Alder cycloaddition of **5.39** could afford bridged-bicycle **5.49** (Scheme 5.14). The



diastereoselectivity was predicted to favor the desired **5.49** based on steric blocking of the methyl group versus the acetate group.³⁶ **5.39** in toluene was heated to reflux for multiple days resulting in no conversion. Since both the diene and dienophile of **5.39** were electron deficient, this could potentially preclude the intramolecular Diels-Alder cycloaddition.³⁷ It was predicted that reduction of dienone **5.39**

to the electronically-matched diene-dienophile system (**5.50**) could spontaneously undergo IMDA (Scheme 5.15) to synthesize alcohol **5.51**.



When **5.39** was subjected to Luche reduction conditions, neither allylic alcohol **5.50** nor Diels-Alder product **5.51** were observed. Instead, aromatic intermediate **5.44** was afforded quantitatively (**Equation 5.18**).³⁸ It was suspected that the introduction of an acidic site allowed for facile elimination of the acetate and restored aromaticity.

The mismatched intramolecular Diels-Alder cycloaddition was reinvestigated, as similar reactions reported are performed at temperatures much higher than conditions previously tested.³⁹ A series of condition screens revealed that heating **5.39** in dichlorobenzene at reflux with sub-stoichiometric amounts of butylated hydroxytoluene (BHT) afforded **5.49** as a single diastereomer in high yields (**Equation 5.19**). BHT was included to prohibit side-reactivity with adventitious oxygen.⁴⁰ The structure and stereochemistry were unambiguously confirmed via X-ray crystallographic analysis (**Figure 5.4**).

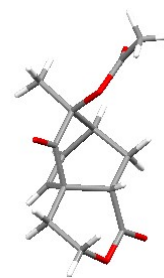
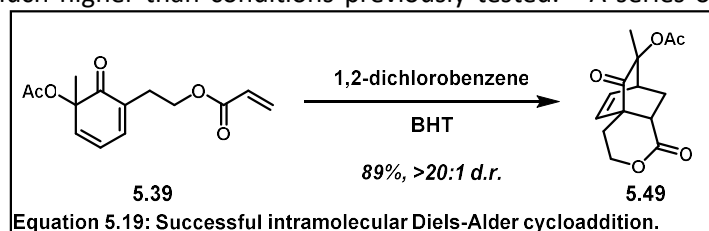
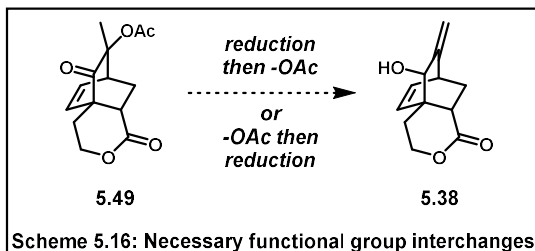


Figure 5.4: Unambiguous structural determination of cycloaddition product via X-ray crystallography.

On multigram scale the yield was notably decreased. Although TLC and NMR analysis of the crude material indicated complete consumption of starting material, large amounts of starting material were isolated via column chromatography. 2D TLC indicated that **5.49** was likely sensitive to pH 5 silica gel and would revert to **5.39** via acid-catalyzed retro Diels-Alder cycloreversion.⁴¹ The decomposition was likely more notable on larger scale reactions due to the increased time required for isolation. Isolation conditions were explored, and it was discovered that column chromatography with neutralized pH 7 silica gel stationary phase afforded **5.49** in yields equivalent to the milligram scale reactions on 15-gram scale.

5.4.12 Optimization of Ketone Reduction

Multiple paths to convert α -acetoxy ketone **5.49** to allylic alcohol **5.38** were feasible (Scheme 5.16). Initial efforts to access the enone intermediate via acetate elimination were unsuccessful, so ketone reduction was



performed. When **5.49** was subjected to sodium borohydride in methanol the produced the α -hydroxy acetate **5.51** and its diastereomer as a 1:1 mixture (Table 5.5). Screening a series of solvents revealed that

Solvent Ratio	d.r.	Yield
MeOH	1:1	47%
THF:MeOH, 1:1	2.5:1	61%
THF:MeOH, 4:1	9:1	78%
THF: <i>i</i> PrOH, 4:1	2:1	41%
THF:MeOH 99:1	>20:1	58%
THF	>20:1	60%

Table 5.5: Ketone reduction solvent screen.

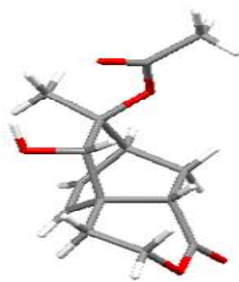


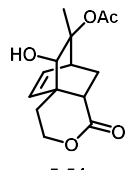
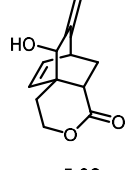
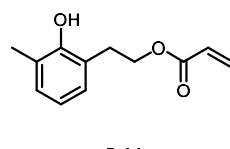
Figure 5.5: Unambiguous structural determination of reduction product via X-ray crystallography.

use of a THF/methanol solvent mixture resulted in improved diastereoselectivity toward a single product, which was unambiguously confirmed to be the desired diastereomer (**5.51**) via X-ray crystallography (Figure 5.5). A consistent trend was observed in the ratio of THF relative to methanol. Running the reaction with THF as the sole solvent resulted in complete diastereoselectivity for the desired product. Multiple minor byproducts were also formed that had not been observed in reactions including methanol. It was decided that the 4:1 solvent mixture condition would be most effective and allowed for the highest recovery **5.51** on gram scale in good yields.

5.4.13 Acetate Pyrolysis

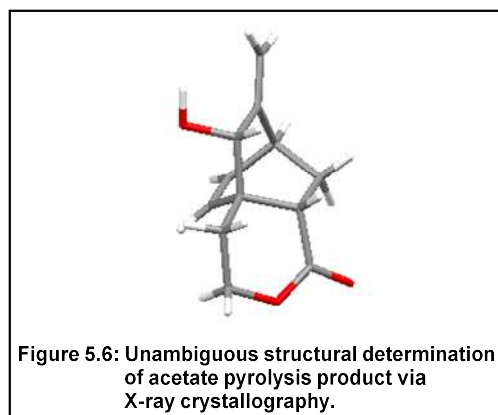
We decided to investigate direct elimination of the acetoxy group to afford terminal alkene **5.38**.

The common two-step route of acetoxy elimination, employing saponification and dehydration, could

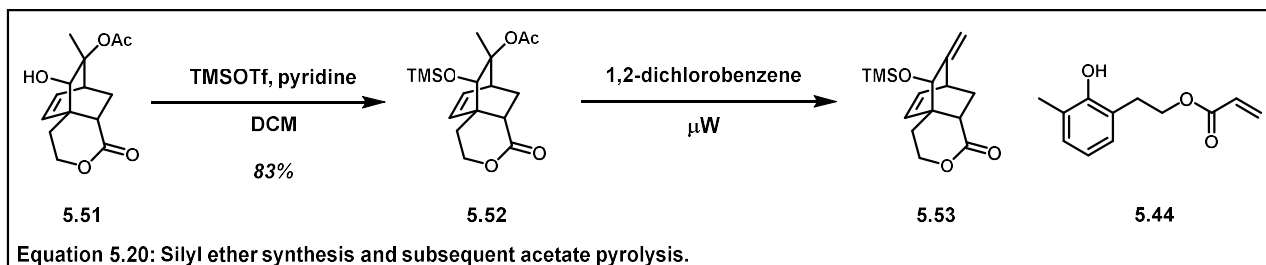
	→ <i>conditions</i>		
5.51		5.38	5.44
<u>Conditions</u>		<u>Result</u>	
NaO ^t Bu, THF		No reaction	
NaO ^t Bu, Sc(OTf) ₃ , THF		Decomposition	
NaO ^t Bu, Sc(OTf) ₃ , DCM		No reaction	
1,2-Cl ₂ Ph, μW, 300° C		1.0:1.1, 5.51: 5.44	
Table 5.6: Conditions screen to induce acetate pyrolysis.			
<u>Time (min)</u>	<u>5.38:5.44:5.51</u>	<u>Yield</u>	
20	1 : 0.5 : 2.5	25%	
80	1 : 0.7 : 0.5	47%	
110	1 : 1.2 : 0.0	45%	
100	1 : 0.9 : 0.0	53%	
Table 5.7: Acetate pyrolysis optimization.			

lead to undesired reactivity if the lactone were opened and the resultant primary alcohol was subjected to dehydration conditions.⁴² A combination of Brønsted-Lowry base and Lewis acid conditions were screened to induce acetate elimination but all were unsuccessful (Table 5.6).⁴³ The classic method of ester

pyrolysis was considered, though these reactions are generally only performed on simple hydrocarbon substrates due to the harsh conditions required to induce *syn*-elimination.⁴⁴ Irradiation of **5.51** in a microwave reactor yielded a mixture of terminal alkene **5.38** and cycloreversion byproduct **5.44**. Once again, the structure was unambiguously assigned via X-ray crystallography (Figure 5.6). Reaction conditions were optimized to decrease the amount of undesired byproduct formed. Irradiation at 250 °C led to the slowest rate of cycloreversion and running the reaction for 100 minutes allowed for full starting material consumption, affording **5.38** in modest yields (Table 5.7).



X-ray crystallographic analysis of **5.51** indicated a hydrogen-bonding interaction between the acetate carbonyl and the proton of the alcohol group. With the knowledge that the allylic alcohol would likely need to be protected in the subsequent steps, we thought that protection of the alcohol before



the acetate pyrolysis could disrupt the hydrogen bonding event and affect cycloreversion. Optimized silylation conditions afforded **5.52**, which was

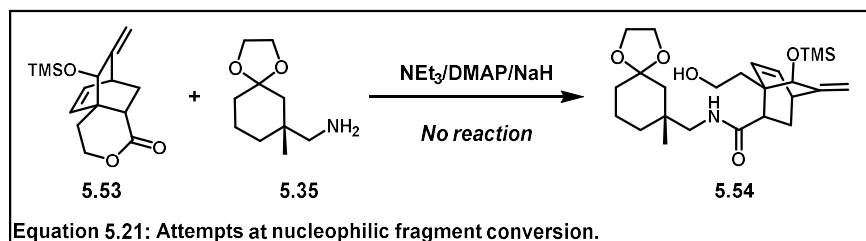
Temperature	Time	5.53 : 5.44 : 5.52	Yield
250° C	30 min	1.00 : 0.00 : 1.63	38%
250° C	45 min	1.00 : 0.11 : 0.72	56%
250° C	60 min	1.00 : 0.31 : 0.00	77%
225° C	60 min	1.00 : 0.00 : 5.07	67%
240° C	60 min	1.00 : 0.28 : 1.42	37%

Table 5.8: Optimization of acetate pyrolysis of silylated substrate.

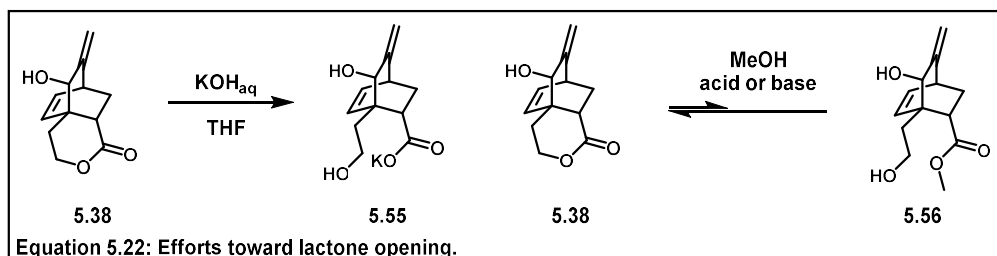
subjected to microwave irradiation (Equation 5.20). We noted that the rate of conversion to **5.53** was increased nearly two-fold when compared to the unprotected substrate (**5.51**), allowing for complete consumption of starting material with reduced byproduct formation (Table 5.8). The optimized conditions for acetate pyrolysis produced **5.53** in good yields, allowing us access to hundreds of milligrams of the protected bridged bicyclic fragment.

5.4.14 Fragment Convergence

Efforts to converge **5.53** and **5.35** via direct addition of the amine into the lactone carbonyl led to no



conversion to amide **5.54** (Equation 5.21). Attempts to saponify **5.38** afforded potassium carboxylate salt **5.55**, but any efforts to isolate the carboxylate salt or the neutralized carboxylic acid resulted in returned **5.38** (Equation 5.22). Attempts to derivatize the primary alcohol **5.55**, including silylation and conversion



to the halide via Appel conditions, afforded only returned **5.38**.

Transesterification efforts resulted in poor conversion to **5.56**, which rapidly reverted to lactone during isolation efforts.

Recognizing the propensity for the lactone of **5.53** and **5.38** to remain cyclized, alternative ring opening methods were investigated. Lewis acid mediated nucleophilic lactone opening aimed to afford

iodoester **5.57** resulted in modest conversion to a new product (tentatively assigned as **5.58**), which

was presumed to be formed via the

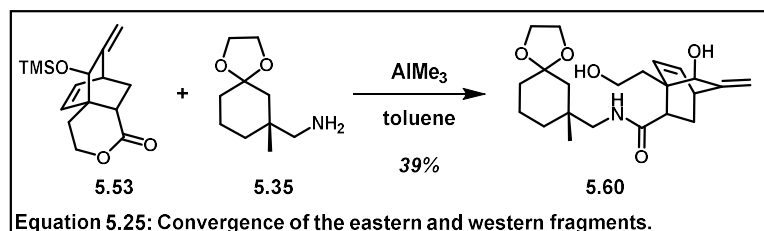
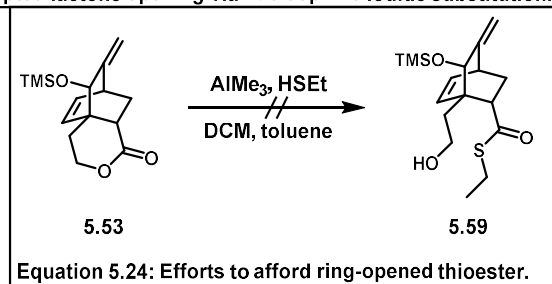
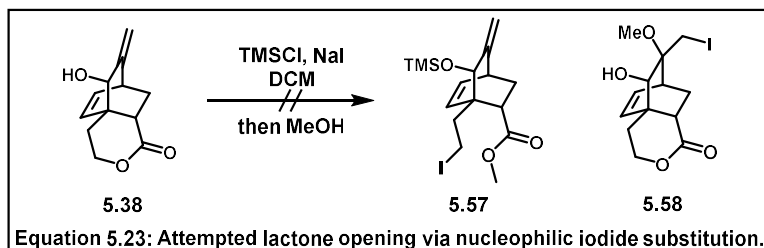
iodonium intermediate (Equation 5.23).⁴⁵ A similar issue had been faced by Qin and coworkers in their synthesis of atropurpuran, which they resolved by

forming the thiol ester, which was seemingly less labile to cyclization.¹⁷ Unfortunately, all attempts to afford thioester **5.59** resulted in either decomposition or returned starting material (Equation 5.24).

Addition of the amine into the lactone was reconsidered as the amide was likely more stable and less prone to relactonization. A series of Lewis acid-catalyzed conditions were screened, and it was discovered the trimethylaluminum-mediated amidation afforded **5.60** in modest yields (Equation 5.25).⁴⁶

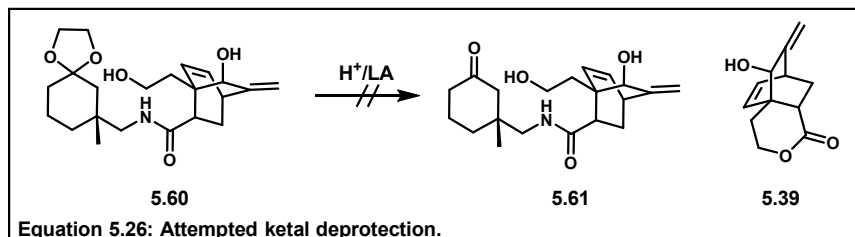
Because the synthesis of **5.53** produced racemic material, the amide coupling reaction afforded **5.60** and its

diastereomer, which were inseparable via chromatography. It was also observed that the trimethylsilyl group was removed during the reaction. Although the yields were modest, optimization efforts were delayed, and the material was carried through to derivatization.



5.4.15 Attempts at Derivatization

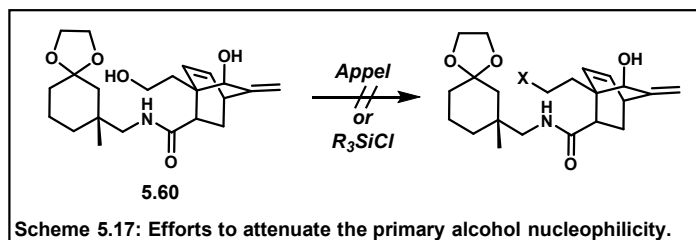
Converged product **5.60** was subjected to a series Brønsted-Lowry and Lewis acids to deprotect the ketal and obtain **5.61**, but all attempts resulted in either no reaction or decomposition via



relactonization to afford **5.38** and a complex mixture of amine products (Equation

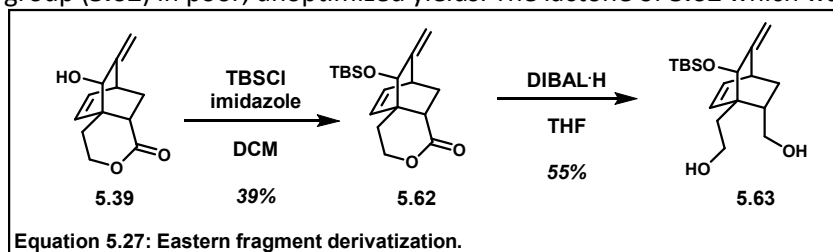
5.26).⁴⁷ Recognizing the need to remove the nucleophilic alcohol to prevent relactonization, **5.60** was subjected to Appel conditions, but once more lactone **5.39** was isolated (Scheme 5.17). Efforts to silylate the primary alcohol also resulted in relactonization. These results indicated that any electrophilic reagent

would act likely as a Lewis acid, activate the amide, and induce lactonization. It became apparent that direct coupling of the fragments would be nonproductive for the synthesis.



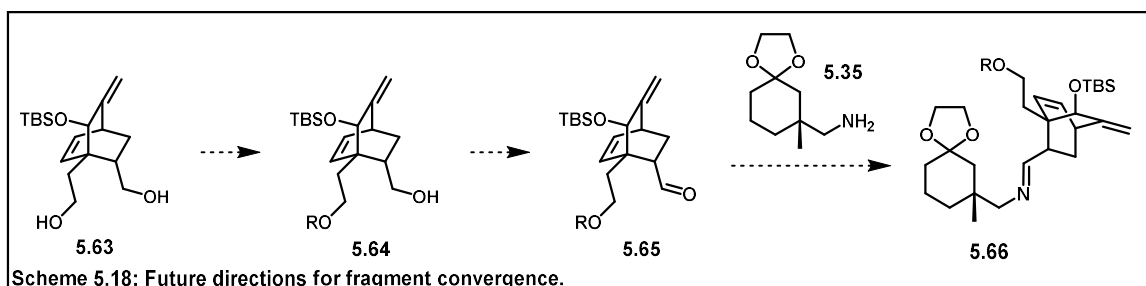
5.4.16 Revised Fragment Convergence and Future Directions

To remove the issue of unproductive lactonization, an alternative route to fragment convergence was devised (Equation 5.27). Lactone **5.39** was silylated with the more robust *tert*-butyldimethylsilyl group (**5.62**) in poor, unoptimized yields. The lactone of **5.62** which was reduced to diol **5.63**. Currently, A



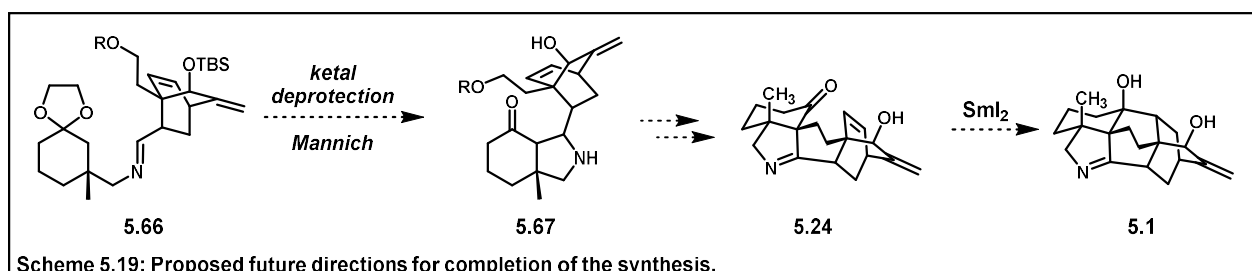
series of protecting group strategies are being investigated to produce monoprotected **5.64**

(Scheme 5.18). Although both alcohols are primary, we believe regioselectivity can be controlled by steric interactions between the bridged bicyclic ring system and a bulky protecting group, such as a trityl group.



5.64 is thought to be readily oxidized to aldehyde **5.65**, which would undergo condensation **5.35** to afford imine **5.66**.

Although imine **5.66** no longer matches the scaffold required for the proposed Dieckmann condensation, it is poised to undergo a formal Mannich reaction to afford **5.67** (Scheme 5.19). Oxidation



of the secondary amine and conversion of the trityl ether to an effective leaving group will allow for the proposed alkylation to afford **5.24**. The diastereoselectivity of the proposed reaction is thought to be controlled via the methylamine stereocenter, though this will require deep investigation. **5.24** which only requires the well-precedented ketyl-alkene cyclization to afford arcutinidine (**5.1**). This route would afford arcutinidine in 18 synthetic steps longest linear sequence, which would constitute the most efficient synthesis reported to date. Other necessary investigations include synthesizing the bridged bicyclic fragment in an enantioselective manner, which either requires development of a novel chiral dearomative oxidation, or separation of enantiomers via chiral resolution.

5.5 Conclusions

With the successful coupling of fragments required for this convergent synthesis, our efforts toward the arcutines are progressing toward the end of the synthesis. The highly scalable synthesis of the bridged bicyclic fragment could lead to the synthesis of a multitude of diterpene alkaloids containing this

motif. Although unforeseen issues have increased the overall step count, completion of this synthesis by future members of the Vanderwal lab would still result in the most concise synthesis of arcutinidine reported. Further, the success of this first-generation route would affirm our strategy and potentially lead to collaborative work that could result in a highly efficient second-generation synthesis.

5.6 Distribution of Credit and Contributions

I would like to thank Dr. Ryan Kozlowski for his contributions in the cocreation of this project. I would also like to recognize his contributions in the collaboration in the synthesis of many intermediates early in the synthesis.

5.7 Experimental Information

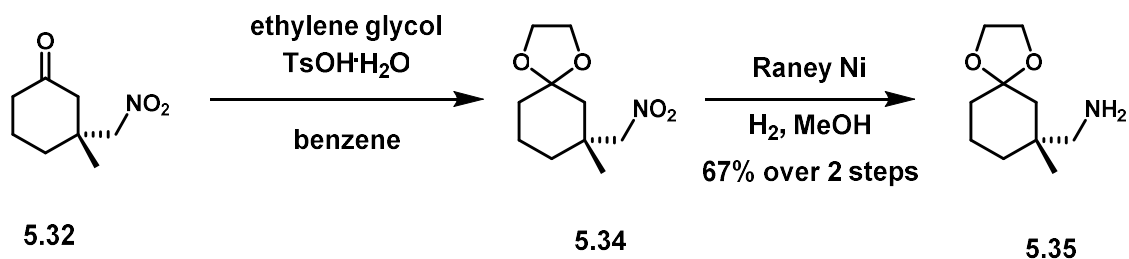
5.7.1 Materials and Methods

All reactions were carried out in oven-dried (140 °C) or flame-dried glassware under an atmosphere of dry argon unless otherwise noted. Dry dichloromethane (CH_2Cl_2), tetrahydrofuran (THF), diethyl ether (Et_2O), acetonitrile (MeCN), toluene (PhMe), and dimethoxyethane (DME) were obtained by percolation through columns packed with neutral alumina and columns packed with Q5 reactant, a supported copper catalyst for scavenging oxygen, under a positive pressure of argon. Solvents used for liquid-liquid extraction and chromatography were: Ethyl acetate, (EtOAc, Sigma-Aldrich, ACS grade) hexanes (Sigma-Aldrich, ACS grade), dichloromethane (CH_2Cl_2 , Fisher, ACS grade), acetone (Sigma-Aldrich, ACS Grade), diethyl ether (Et_2O , Fisher, ACS grade), and pentane (Sigma-Aldrich, ACS grade). Reactions that were performed open to air utilized solvent dispensed from a wash bottle or solvent bottle, and no precautions were taken to exclude water. Column chromatography was performed using EMD Millipore 60 Å (0.040–0.063 mm) mesh silica gel (SiO₂). Analytical thin-layer chromatography (TLC)

was performed on Merck silica gel 60 F254 TLC plates. Visualization was accomplished with UV (210 nm), and potassium permanganate (KMnO₄) or *p*-anisaldehyde staining solutions.

¹H NMR and ¹³C NMR spectra were recorded at 298 K on Bruker GN500 (500 MHz, ¹H; 125 MHz, ¹³C) and Bruker CRYO500 (500 MHz, ¹H; 125 MHz, ¹³C) spectrometers. ¹H and ¹³C spectra were referenced to residual chloroform (7.26 ppm, ¹H; 77.16 ppm, ¹³C) or residual methanol (3.31 ppm, ¹H; 49.00 ppm, ¹³C). Chemical shifts are reported in ppm and multiplicities are indicated by: s (singlet), d (doublet), t (triplet), q (quartet), p (pentet), hept (heptet), m (multiplet), and br s (broad singlet). Coupling constants, *J*, are reported in Hertz. The raw fid files were processed into the included NMR spectra using MestReNova 11.0, (Mestrelab Research S. L.). Infrared (IR) spectra were recorded on a Varian 640-IR instrument on NaCl plates and peaks are reported in cm⁻¹. Mass spectrometry data was obtained from the University of California, Irvine Mass Spectrometry Facility. High-resolution mass spectra (HRMS) were recorded on a Waters LCT Premier spectrometer using ESI-TOF (electrospray ionization-time of flight) or a Waters GCT Premier Micromass GC-MS (chemical ionization), and data are reported in the form of *m/z*.

5.7.2 Experimental Procedures



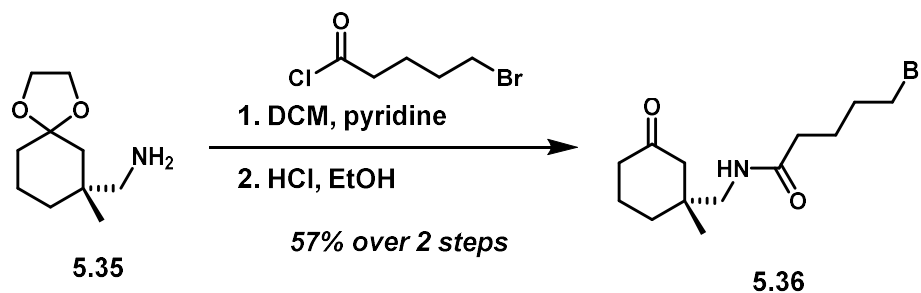
(R)-(7-Methyl-1,4-dioxaspiro[4.5]decan-7-yl)methanamine (5.35): 25 mL round bottom flask was charged with ketone **5.32**²⁵ (342 mg, 2.01 mmol, 1 equiv), benzene (4 mL), ethylene glycol (496 mg, 8.04 mmol, 4 equiv), and *p*-toluenesulfonic acid (19 mg, 0.10 mmol, 0.05 equiv). The reaction mixture was heated to 100 °C and stirred at this temperature for 4 h. The solution was

cooled and diluted with water (10 mL). The phases were separated and the aqueous phase was extracted with Et₂O (3 x 5 mL). The combined organic extracts were passed through a plug of silica gel which was washed with Et₂O (15 mL). The filtrate was concentrated *in vacuo*. The residue was dissolved in MeOH (3 mL). Raney Nickel (15 mg, 0.10 mmol, 0.05 equiv) was added to the reaction mixture. The atmosphere of the reaction vessel was evacuated and refilled with argon gas three times, then evacuated and filled with hydrogen gas three times. The solution was stirred at room temperature for 16 h. The atmosphere was evacuated and filled with argon. The solution was filtered over celite and washed with methanol (10 mL). The filtrate was concentrated *in vacuo*. The residue was purified by chromatography on silica gel, eluting with DCM/MeOH 95:5 (v/v), to afford 248 mg (67% yield over two steps) **5.35** as a clear colorless oil.

¹H NMR (500 MHz, CDCl₃): δ 3.86 – 3.82 (m, 4H), 2.54 (d, 13.0 Hz, 1H), 2.39 (d, = 13.1 Hz, 1H), 1.86 (s, 2H), 1.51 (ddd, 22.9, 14.3, 9.5 Hz, 5H), 1.31 (d, = 13.8 Hz, 1H), 1.23 – 1.14 (m, 2H), 0.87 (s, 3H).

¹³C NMR (126 MHz, CDCl₃): δ 109.3, 64.1, 64.0, 52.3, 42.5, 36.2, 34.8, 34.5, 24.4, 19.6.

HRMS (ES+) *m/z* calc'd for C₁₀H₁₉NO₂ [M+H]⁺: 186.1494; found: 186.1487.



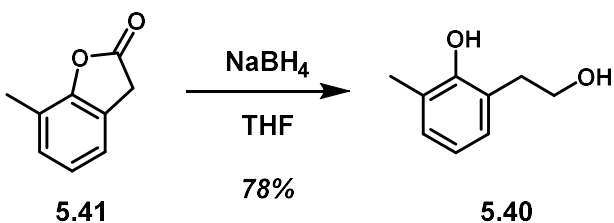
(R)-5-Bromo-N-((1-methyl-3-oxocyclohexyl)methyl)pentanamide (5.36) 10 mL round bottom flask was charged with amine **5.35** (100 mg, 0.54 mmol, 1 equiv), CH₂Cl₂ (1.6 mL), and pyridine (90 mg, 1.08 mmol, 2 equiv). The reaction mixture was cooled to 0 °C and 5-bromovaleryl chloride (215 mg, 1.08 mmol, 2 equiv) was added dropwise. The reaction was warmed to room temperature and stirred for 1 h.

Saturated aqueous ammonium chloride (5 mL) was added and the solution was extracted with CH_2Cl_2 (3 x 5 mL). The combined organic extracts were dried over Na_2SO_4 and concentrated *in vacuo*. The residue was dissolved in ethanol (1.5 mL) and had 6M HCl_{aq} (0.15 mL, 1.62 mmol, 3 equiv) added dropwise. The reaction was stirred at room temperature for 4 h. The solution was neutralized with 1M NaOH (1 mL). The solution was extracted with EtOAc (3 x 5 mL) and the combined organic extracts were washed with water (5 mL). The organic phase was dried over Na_2SO_4 and concentrated *in vacuo*. The residue was purified by chromatography on silica gel, eluting with DCM/MeOH 99:1 (v/v), to afford 78 mg (57% yield over 2 steps) of **5.36** as a colorless oil.

$^1\text{H NMR}$ (500 MHz, CDCl_3): δ 6.28 (s, 1H), 3.42 (J t, 6.6 Hz, 2H), 3.20 (dd, = 13.6, 6.8 Hz, 1H), 3.10 (dd, = 13.7, 6.3 Hz, 1H), 2.32 – 2.22 (m, 5H), 2.08 (J d, 13.7 Hz, 1H), 2.03 – 1.94 (m, 1H), 1.88 (dd, = 14.2, 6.6 Hz, 2H), 1.82 – 1.76 (m, 2H), 1.71 – 1.50 (m, 3H), 0.91 (s, 3H).

$^{13}\text{C NMR}$ (126 MHz, CDCl_3): δ 211.9, 173.0, 51.1, 48.9, 41.0, 40.4, 35.5, 33.8, 33.4, 32.1, 24.3, 23.0, 21.9.

HRMS (Cl^-)/z calc'd for $\text{C}_{13}\text{H}_{22}\text{BrNO}_2$ [M+H] $^+$: 304.0912; found: 304.0915.



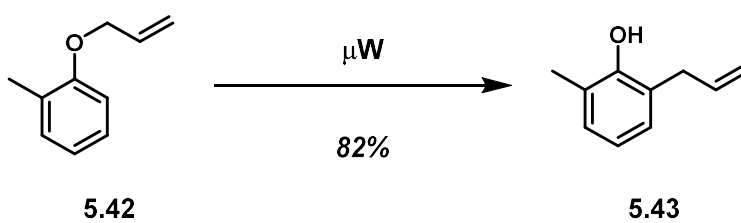
2-(2-Hydroxyethyl)-6-methylphenol (5.40) 20 mL scintillation vial was charged with **5.41**²⁹ (100 mg, 0.68 mmol, 1 equiv) and THF (2 mL) and was cooled to 0°C. Sodium borohydride (51 mg, 1.35 mmol, 2 equiv) was added portionwise. The reaction was stirred for 16 h, slowly warming to room temperature. 1M HCl (2 mL) was added to the reaction mixture dropwise over 10 min then stirred 15 min. The solution was extracted with EtOAc (3 x 3 mL). The organic phases were combined, washed with a saturated

aqueous solution of NaHCO₃ (5 mL) and brine (5 mL). The organic phase was dried over Na₂SO₄ and concentrated *in vacuo* to afford 80 mg (78% yield) of **5.40** as a clear, colorless oil. The product was used in the subsequent step without any further purification.

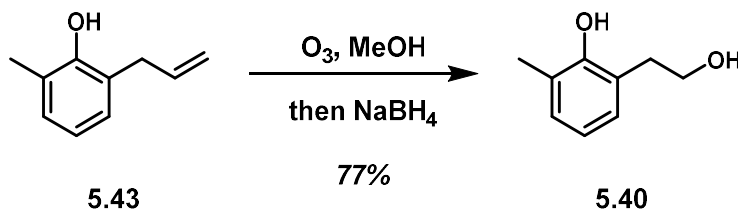
¹H NMR (500 MHz, CDCl₃): δ 7.10 (*d*, = 7.4 Hz, 1H), 6.97 (*d*, = 7.4 Hz, 1H), 6.83 (*t*, = 7.4 Hz, 1H), 4.00 (*d*, *J* = 5.0 Hz, 2H), 2.94 (*d*, = 5.1 Hz, 2H), 2.33 (*s*, 3H).

¹³C NMR (126 MHz, CDCl₃): δ 153.6, 129.7, 128.6, 126.5, 125.9, 120.1, 64.8, 34.8, 16.4.

HRMS (*Cl*+) *m/z* calc'd for C₁₀H₁₉NO₂ [M]⁺: 152.0837; found: 152.0837.

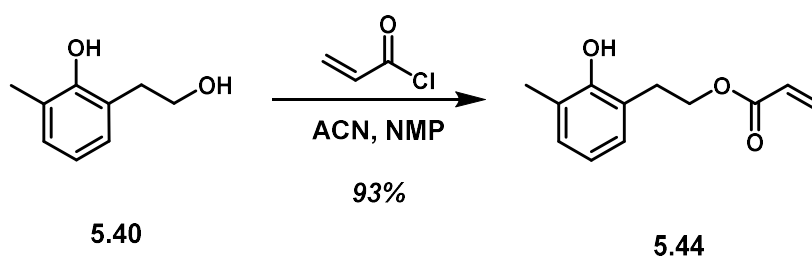


2-Allyl-6-methylphenol (5.43) A G30 glass microwave vial was charged with allylated phenol **5.42** (24.0 g, 0.162 mol, 1 equiv). The reaction was irradiated in a microwave reactor at 250 °C for 30 minutes. The residue was purified by chromatography on silica gel, eluting with hexanes/EtOAc 90:10 (*v/v*), to afford 19.6 g (82% yield) of **5.43** as a colorless oil. ¹H and ¹³C NMR spectra were consistent with those previously reported.³²



2-(2-Hydroxyethyl)-6-methylphenol (5.40) 500 mL round bottom flask was charged with allyl phenol **5.43** (10.0 g, 67.1 mmol, 1 equiv), and methanol (200 mL). The solution was cooled to -78 °C and ozone

was bubbled through the solution for 3 h. NaBH₄ (7.7 g, 0.202 mol, 3 equiv) was added portionwise. The solution was allowed to warm to room temperature and stirred for 16 h. The solution had saturated aqueous ammonium chloride (100 mL) added. The solution was extracted with Et₂O (3 x 100 mL). The organic extracts were combined, dried over Na₂SO₄ and concentrated *in vacuo* to afford 7.9 g (77% yield) of **5.43** as a colorless oil. ¹H and ¹³C NMR spectra were consistent with those previously reported.

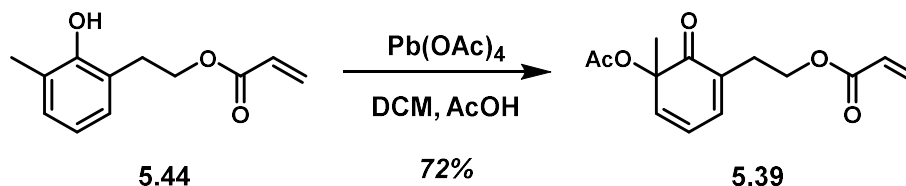


2-Hydroxy-3-methylphenethyl acrylate (5.44) A 250 mL round bottom flask was charged with phenol **5.40** (10.8 g, 71.2 mmol, 1 equiv), acetonitrile (120 mL), and n-methylpyrrolidone (60 mL). The solution was cooled to 0 °C and acryloyl chloride (8.6 mL, 142.4 mmol, 1.5 equiv) was added dropwise over 5 min. The reaction mixture was slowly warmed to room temperature as it was stirred over 16 h. 1M HCl_(aq) (100 mL) was added to the reaction mixture and the solution was extracted with CH₂Cl₂ (3 x 100 mL). The organic extracts were combined and washed with saturated aqueous ammonium chloride solution (3 x 50 mL) and twice with brine (50 mL). The organic phase was dried over Na₂SO₄ and concentrated *in vacuo*. The residue was dissolved in CH₂Cl₂ and filtered through a short plug of silica gel. The filtrate was concentrated *in vacuo* to afford 13.7 g (93% yield) of **5.44** as a colorless oil.

¹H NMR (500 MHz, CDCl₃): δ 7.04 (*d*, = 7.4 Hz, 1H), 6.98 (*d*, = 7.5 Hz, 1H), 6.78 (*t*, = 7.5 Hz, 1H), 6.45 (*d*, = 17.3 Hz, 1H), 6.15 (*dd*, = 17.3, 10.5 Hz, 1H), 5.92 (*s*, 1H), 5.87 (*dd*, = 10.5 Hz, 1H), 4.36 (*t*, = 7.2 Hz, 2H), 3.00 (*t*, = 7.2 Hz, 2H), 2.27 (*s*, 3H).

¹³C NMR (126 MHz, CDCl₃): δ 166.8, 152.9, 131.5, 129.8, 128.6, 128.2, 124.3, 122.9, 120.2, 64.7, 30.3, 16.1.

HRMS (ES+) m/z calc'd for C₁₂H₁₄O₃ [M+Na]⁺: 229.0841; found: 229.0846.

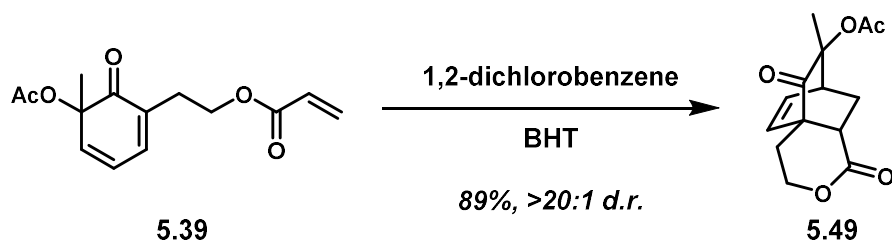


2-(5-Acetoxy-5-methyl-6-oxocyclohexa-1,3-dien-1-yl)ethyl acrylate (5.39) 250 mL round bottom flask was charge with phenol **5.44** (15.0 g, 57.3 mmol, 1 equiv), CH₂Cl₂ (150 mL), acetic acid (44 mL, 570.1 mmol, 10 equiv), and lead tetraacetate (48.4 g, 86.5 mmol, 1.5 equiv). The reaction mixture was stirred at room temperature for 30 min. The solution was slowly poured into a mixture of saturated aqueous sodium bicarbonate (400 mL) and ice. The mixture was extracted with CH₂Cl₂ (3 x 100 mL). The combined organic extracts were washed with brine (100 mL). The organic phase was dried over Na₂SO₄ and concentrated *in vacuo*. The residue was purified by chromatography on silica gel, eluting with hexanes/EtOAc 75:25 (v/v), to afford 15.1 g (72% yield) of **5.39** as a brown oil.

¹H NMR (500 MHz, CDCl₃): δ 6.88 (d, J = 5.5 Hz, 1H), 6.43 (d, J = 17.4 Hz, 1H), 6.24 (dd, J = 9.3, 3.6 Hz, 2H), 5.87 (dd, J = 15.8, 5.4 Hz, 1H), 4.40 – 4.28 (m, 2H), 2.89 – 2.80 (m, 1H), 2.73 – 2.64 (m, 1H), 2.13 (s, 3H), 1.44 (s, 3H).

¹³C NMR (126 MHz, CDCl₃): δ 198.2, 169.5, 166.0, 140.9, 137.9, 130.8, 128.5, 123.6, 121.6, 79.05, 62.8, 28.7, 23.7, 20.5.

HRMS (ES+) m/z calc'd for C₁₂H₁₄O₃ [M+Na]⁺: 229.0841; found: 229.0846.



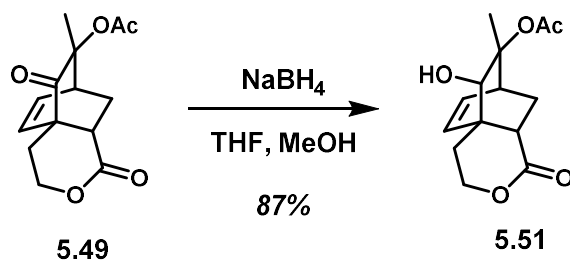
(**4S,7S,9S**)-9-Methyl-1,10-dioxo-1,3,4,7,8,8a-hexahydro-7,4a-ethanoisochromen-9-yl acetate

(**5.49**) A 1 liter round bottom flask was charged with **5.39** (11.5 g, 42.9 mmol, 1 equiv), dichlorobenzene (430 mL) and butylated hydroxytoluene (0.1 g, 4.3 mmol, 0.1 equiv). The reaction flask was equipped with a reflux condenser, heated to reflux (~175°C), and stirred at this temperature for 16 h. The reaction mixture was allowed to cool to room temperature and the solvent was removed *in vacuo*. The residue was purified by chromatography on pH 7 silica gel, eluting with hexanes/EtOAc 75:25 (v/v), to afford 10.2 g (89% yield) **5.49** as a white solid.

¹H NMR (500 MHz, CDCl₃): δ 6.61 (t, *J* = 7.5 Hz, 1H), 5.79 (d, *J* = 8.0 Hz, 1H), 4.56 – 4.44 (m, 1H), 4.37 (td, *J* = 11.3, 4.2 Hz, 1H), 3.80 (d, *J* = 5.7 Hz, 1H), 3.11 – 2.96 (m, 2H), 2.25 – 2.18 (m, 1H), 2.12 (s, 3H), 2.10 – 2.00 (m, 2H), 1.60 (s, 3H).

¹³C NMR (126 MHz, CDCl₃): δ 201.6, 172.4, 169.7, 138.8, 131.1, 79.2, 65.2, 49.9, 40.5, 38.6, 26.22, 23.1, 22.3, 21.6.

HRMS (Cl⁺) *m/z* calc'd for C₁₄H₁₆O₅ [M]⁺: 229.0841; found: 229.0846.



(*4S,7S,8aS,9S,10S*)-10-Hydroxy-9-methyl-1-oxo-1,3,4,7,8,8a-hexahydro-4a,7-

ethanoisochromen-9-yl acetate (5.51) A 100 mL round bottom flask was charged with ketone

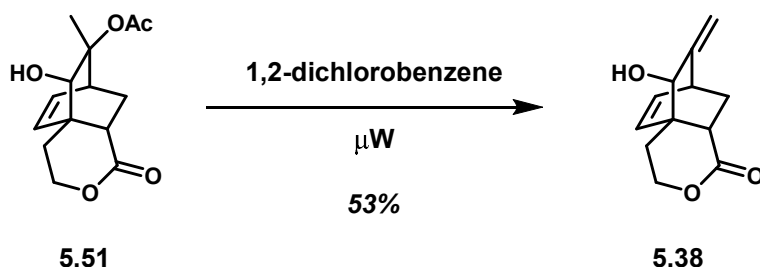
5.49 (1.98 g, 7.51 mmol, 1 equiv), THF (30 mL), and methanol (7.5 mL). The reaction flask was cooled to 0 °C and sodium borohydride (311 mg, 8.23 mmol, 1.1 equiv) was added portionwise.

The reaction flask was warmed to room temperature and stirred for 4 h. The reaction mixture was quenched with a saturated aqueous solution of ammonium chloride (40 mL). The phases were separated, and the aqueous phase was extracted with EtOAc (3 x 40 mL). The organic extracts were combined and washed with brine (30 mL). The organic phase was dried over Na_2SO_4 and concentrated *in vacuo*. The residue was purified by chromatography on silica gel, eluting with hexanes/EtOAc 70:30 (v/v), to afford 1.74 g (87% yield) 5.51 as a white solid.

$^1\text{H NMR}$ (500 MHz, CDCl_3): δ 6.34 (t, $J = 7.2$ Hz, 1H), 5.88 (d, $J = 7.9$ Hz, 1H), 4.39 (t, $J = 5.8$ Hz, 2H), 3.70 (s, 1H), 2.88 (s, 1H), 2.78 (s, 1H), 2.44 (s, 1H), 2.30 – 2.13 (m, 3H), 2.03 (d, $J = 13.2$ Hz, 3H), 1.80 (d, $J = 12.8$ Hz, 1H), 1.29 (s, 3H).

$^{13}\text{C NMR}$ (126 MHz, CDCl_3): δ 173.4, 172.1, 134.6, 131.8, 87.4, 80.5, 66.0, 42.1, 41.9, 41.7, 29.2, 22.2, 22.1, 20.2.

HRMS (ESI- m/z) calc'd for $\text{C}_{14}\text{H}_{18}\text{O}_5$ $[\text{M}+\text{Na}]^+$: 289.1052; found: 289.1045.



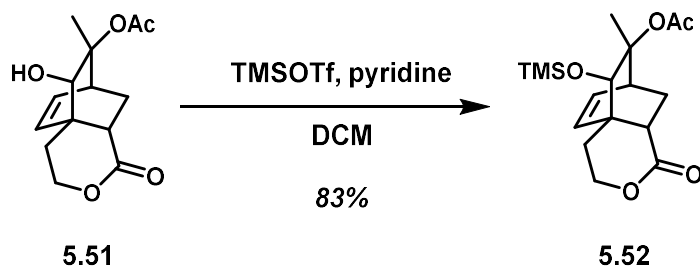
(*4S,7S,10R*)-10-Hydroxy-9-methylene-3,4,8,8a-tetrahydro-4a,7-ethanoisochromen-1(1*H*)-one

5.51) A G30 glass microwave vial was charged with bridged bicycle **5.38** (400 mg, 1.502 mmol, 1 equiv) and dichlorobenzene (15 mL). The solution was degassed with argon for 15 minutes. The reaction mixture was irradiated in a microwave reactor at 250 °C for 100 min. The solvent was removed *in vacuo* and the residue was purified by chromatography on pH 7 silica gel, eluting with hexanes/EtOAc 30:70 (v/v), to afford 164 mg (53% yield) **5.51** as a white solid.

$^1\text{H NMR}$ (500 MHz, CDCl_3): δ 6.61 – 6.54 (t, 1H), 5.76 (d, 8.1 Hz, 1H), 5.12 (d, = 10.6 Hz, 2H), 4.43 – 4.39 (t, 2H), 3.96 (s, 1H), 3.20 – 3.15 (m, 1H), 2.38 (d, 6.3 Hz, 1H), 2.32 (d, = 14.7, 5.6 Hz, 1H), 2.27 – 2.20 (m, 1H), 1.93 (dd, 12.8, 6.3, 2.5 Hz, 1H), 1.87 (ddd, = 12.8, 9.6, 3.0 Hz, 1H).

$^{13}\text{C NMR}$ (126 MHz, CDCl_3): δ 173.7, 152.4, 137.7, 130.9, 111.2, 75.5, 65.9, 43.6, 40.3, 40.1, 29.9, 29.3.

HRMS (CI+) m/z calc'd for $\text{C}_{12}\text{H}_{14}\text{O}_3$ [M] $^+$: 206.0943; found: 206.0953.



(*4S,7S,9S,10S*)-9-Methyl-1-oxo-10-(trimethylsilyloxy)-1,3,4,7,8,8a-hexahydro-4a,7-

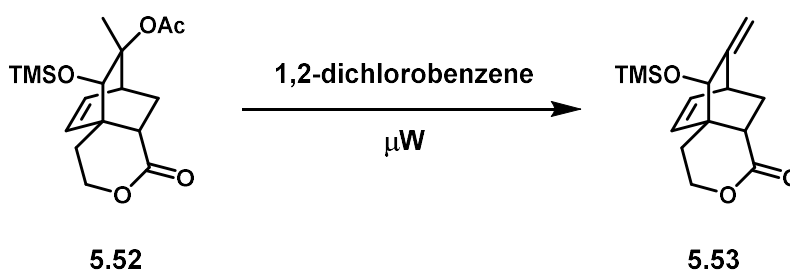
ethanoisochromen-9-yl acetate (**5.52**) A 25 mL round bottom flask was charged with alcohol **5.51** (685

mg, 2.57 mmol, 1 equiv), CH₂Cl₂ (10 mL), and pyridine (0.42 mL, 5.15 mmol, 2 equiv). The solution was cooled to -78 °C and had trimethylsilyl triflate (0.52 mL, 2.83 mmol, 1.1 equiv) added dropwise. The reaction mixture was allowed to warm to room temperature slowly as it was stirred for 16 h. The reaction was quenched with saturated aqueous sodium bicarbonate (10 mL). The phases were separated, and the aqueous phase was extracted with CH₂Cl₂ (3 x 10 mL). The organic extracts were combined, dried over Na₂SO₄ and concentrated *in vacuo*. The residue was triturated in hexanes to afford 717 mg (83% yield) of **5.52** as a white solid.

¹H NMR (500 MHz, CDCl₃): δ 6.37 (t, = 7.6 Hz, 1H), 5.84 (d, = 8.1 Hz, 1H), 4.51 – 4.37 (m, 2H), 3.69 (d, = 15.3 Hz, 1H), 3.24 – 3.16 (m, 1H), 2.42 (dd, = 9.8, 6.4 Hz, 1H), 2.16 (dd, = 9.9, 3.1 Hz, 2H), 2.03 (s, 3H), 1.97 – 1.89 (m, 1H), 1.66 (dd, = 13.4, 6.3, 2.4 Hz, 1H), 1.32 (s, 3H), 0.16 (s, 9H).

¹³C NMR (126 MHz, CDCl₃): δ 173.4, 170.1, 134.7, 131.4, 88.5, 83.1, 66.2, 42.8, 41.0, 40.7, 29.8, 24.6, 22.3, 21.2, 0.4.

HRMS (Cl+) m/z calc'd for C₁₇H₂₆O₅Si [M]⁺: 338.1549; found: 338.1559.



(*4S,7S,10R*)-9-Methylene-10-((trimethylsilyl)oxy)-3,4,8,8a-tetrahydro-4a,7-

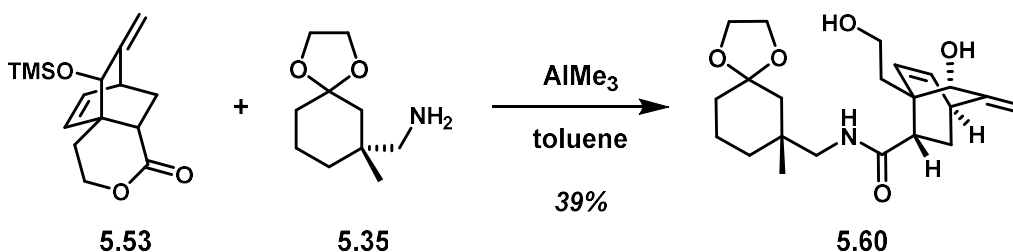
ethanoisochromen-1(*H*)-one (**5.53**) A G30 glass microwave vial was charged with **5.52** (400 mg, 1.44 mmol, 1 equiv) and dichlorobenzene (12 mL). The solution was degassed with argon for 15 minutes. The reaction mixture was irradiated in a microwave reactor at 250 °C for 60 min. The

solvent was removed *in vacuo* and the residue was purified by chromatography on pH 7 silica gel, eluting with hexanes/EtOAc 90:10 (v/v), to afford 253 mg (77% yield) **5.53** as a white solid.

¹H NMR (500 MHz, CDCl₃): δ 6.55 (t, *J* = 7.4 Hz, 1H), 5.84 (d, *J* = 8.2 Hz, 1H), 5.09 (s, 1H), 4.95 (s, 1H), 4.48 – 4.44 (m, 2H), 4.05 (s, 1H), 3.17 (t, *J* = 2.9 Hz, 1H), 2.35 (t, *J* = 7.9 Hz, 1H), 2.22 – 2.16 (m, 1H), 2.03 (dt, *J* = 7.0, 3.4 Hz, 1H), 1.93 (dt, *J* = 8.8, 2.3 Hz, 2H), 0.17 (s, 8H).

¹³C NMR (126 MHz, CDCl₃): δ 173.5, 151.7, 136.2, 130.3, 110.4, 76.6, 66.3, 43.4, 41.2, 40.7, 30.1, 29.9, 1.0.

HRMS (Cl⁺) *m/z* calc'd for C₁₅H₂₂O₃Si [M]⁺: 278.1338; found: 278.1346.



(*R*,*2S*,*4S*,*7S*)-7-hydroxy-1-(2-hydroxyethyl)-*N*-(*R*)-7-methyl-1,4-dioxaspiro[4.5]decan-7-yl)methyl)-8-methylenebicyclo[2.2.2]oct-5-ene-2-carboxamide (**5.60**):

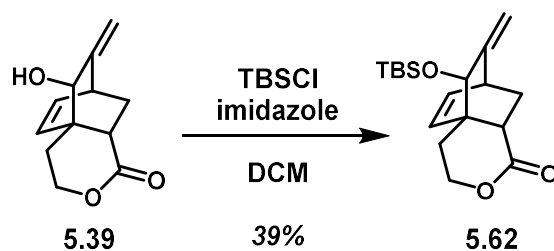
A flame-dried 2 dram scintillation vial was charged with amine **5.35** (28 mg, 0.14 mmol, 2 equiv) and toluene (0.10 mL) and was cooled to 0 °C. A solution of trimethylaluminum (0.014 mL, 0.14 mmol, 2 equiv) in toluene (0.12 mL) was added dropwise. The reaction was stirred at 0 °C for 30 min. A solution of lactone **5.53** (20 mg, 0.07 mmol, 1 equiv) in toluene (0.12 mL) was added dropwise. The reaction mixture was heated to 110 °C and stirred at this temperature for 16 h. The solution was cooled to room temperature, had saturated aqueous Rochelle's salt (1 mL) added dropwise. The resultant solution was stirred vigorously for 30 min. The solution was extracted with EtOAc (3 x 1 mL). The organic phases were combined, dried over Na₂SO₄ and concentrated *in vacuo*. The residue was

purified by chromatography on pH 7 silica gel, eluting with hexanes/EtOAc 90:10 (v/v), to afford 11 mg (39% yield) of an inseparable mixture of **5.60** and its diastereomer as a yellow oil.

¹H NMR (500 MHz, CDCl₃): δ 6.63 (s, 1H), 5.93 (J d, 7.7 Hz, 1H), 5.88 (s, 1H), 5.14 (J d, 19.3 Hz, 2H), 4.23 (s, 1H), 3.97 (s, 6H), 3.38 (J dd, 5.1, 7.9 Hz, 2H), 3.23 (s, 1H), 3.11 – 3.04 (m, 1H), 2.68 (d, = 7.5 Hz, 1H), 2.23 (d, = 14.7 Hz, 2H), 2.08 – 1.99 (m, 3H), 1.54 (s, 2H), 1.46 (d, = 13.6 Hz, 2H), 1.31 (s, 5H), 0.98 (J t, 4.4 Hz, 3H).

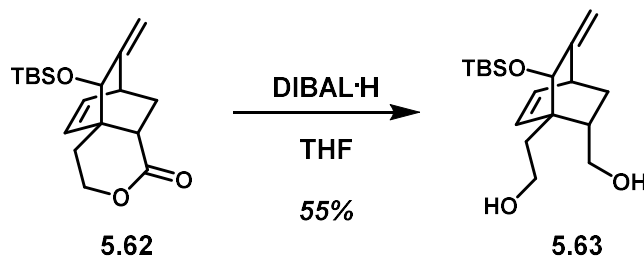
¹³C NMR (126 MHz, CDCl₃): δ 175.0, 174.9, 152.6, 152.5, 134.6, 134.5, 133.2, 133.2, 109.9, 109.8, 109.1, 109.0, 73.4, 73.3, 64.3, 64.2, 64.1, 64.1, 59.0, 48.1, 47.9, 46.4, 46.3, 43.4, 40.4, 40.4, 36.1, 34.8, 34.7, 34.5, 34.4, 34.4, 34.1, 34.0, 31.7, 29.7, 26.0, 19.6.

HRMS (Cl⁺)/z calc'd for C₁₅H₂₂O₃Si [M]⁺: 278.1338; found: 278.1346.



(~~4S,7S,10R~~)-10-(~~tert~~-Butyldimethylsilyloxy)-9-methylene-3,4,8,8a-tetrahydro-4a,7-

ethanoisochromen-1(~~H~~)-one (**5.39**) A 10 mL round bottom flask was charged with **5.39** (140 mg, 0.68 mmol, 1 equiv) and CH₂Cl₂ (2.8 mL). To this solution TBSCl (196 mg, 1.36 mmol, 2 equiv) and imidazole (140 mg, 2.04 mmol, 3 equiv) were added. The reaction was stirred at room temperature for 16 h. To the solution saturated aqueous ammonium chloride (4 mL) was added and the resultant solution was extracted with CH₂Cl₂ (3 x 5 mL). The combined organic extracts were dried over Na₂SO₄ and concentrated *in vacuo*. The residue was purified by chromatography on silica gel, eluting with hexanes/EtOAc 90:10 (v/v), to afford 87 mg (39% yield) **5.62** as a white solid.



2-((1S,4S,6R,7S)-6-((tert-butyldimethylsilyl)oxy)-7-(hydroxymethyl)-5-methylenebicyclo[2.2.2]oct-2-en-1-yl)ethan-1-ol (5.63)

A 10 mL round bottom flask was charged with **5.62** (20 mg, 62.4 μmol, 1 equiv) and THF (0.5 mL). The solution was cooled to -78°C and DIBAL-H (48 μL, 0.25 mmol, 4 equiv) was added dropwise. The reaction was slowly warmed to room temperature as the reaction stirred for 16 h. The solution was cooled to 0 °C and diluted with Et₂O (2 mL). To this solution was added H₂O (0.1 mL), 15% NaOH(aq) (0.1 mL), and H₂O (0.2 mL). The reaction was warmed to room temperature and stirred for 15 minutes. The solution was dried over Na₂SO₄ and concentrated *in vacuo*. The residue was purified by chromatography on silica gel, eluting with hexanes/EtOAc 60:40 (v/v), to afford 11 mg (55% yield) of **5.63** as a white solid.

5.8 References

¹ Pelletier, S. W.; Keith, L. H. "The Alkaloids: Chemistry and Physiology." *Elsevier, Sciences and Technology* **1970**, *12*, 15-17.

² a) Wang, F.-P.; Chen, Q.-H.; Liang, X.-T.; Cordell, G. A. "The C18-Diterpenoid Alkaloids, In the Alkaloids: Chemistry and Biology." Ed.; *Academic Press: San Diego*, **2009**, *67*, 1–78. b) Wang, F.-P.; Liang, X.-T.; Cordell, G. A. "The C19-Diterpenoid Alkaloids, In The Alkaloids: Chemistry and Biology." *Academic Press: San Diego*, **2002**, *59*, 1–280.

³ a) Ameri, A. "The Effects of Aconitum Alkaloids on the Central Nervous System." *Prog. Neurobiol.* **1998**, *56*, 211–235; b) Wang, F. P.; Liang, X. T. *Alkaloids* **2002**, *59*, 1–280.

⁴ (a) Xu, L.-L.; Hai, P.; Zhang, S.-B.; Xiao, J.-F.; Gao, Y.; Ma, B.-J.; Fu, H.-Y.; Chen, Y. M.; Yang, X. L. "Prenylated Indole Diterpene Alkaloids from a Mine-Soil-Derived *Tolypocladium* sp." *J. Nat. Prod.* **2019**, *82*, 221–231; (b) Hong, L.-L.; Sun, J.-B.; Yang, F.; Liu, M.; Tang, J.; Sun, F.; Jiao, W.-H.; Wang, S.-P.; Zhang, W.; Lin, H.-W. "New Diterpene Alkaloids from the Marine Sponge *Agelas mauritiana*." *RSC Adv.*, **2017**, *7*, 23970–23976.

- ⁵ Dank, C.; Sanichar, R.; Choo, K.-L.; Olsen, M.; Lautens, M. "Recent Advances Towards Syntheses of Diterpenoid Alkaloids." *Synthesis* **2019**, *51*, 3915–3946.
- ⁶ Fedorov, A. A. "Flowering Plants, Their Chemical Composition, and Use." *Plant Resources of the USSR* **1985**, *37*. Nauka, Moscow.
- ⁷ Tashkhodzhaev, B.; Saidkhodzhaeva, Sh. A.; Bessonova, I. A.; Antipin, M. Y. "Arcutin — A New Type of Diterpene Alkaloids." *Chem. Nat. Compd.* **2000**, *36*, 79–83.
- ⁸ Saidkhodzhaeva, Sh. A.; Bessonova, I. A.; Abdullaev, N. D. "Arcutinine, A New Alkaloid from Aconitum Arcuatum." *Chem. Nat. Compd.* **2001**, *37*, 466–469.
- ⁹ Meng, X.-H.; Jiang, Z.-B.; Guo, Q.-L.; Shi, J.-G. "A Minor Arcutine-Type C₂₀-Diterpenoid Alkaloid Iminium Constituent of 'Fu Zi'." *Chin. Chem. Lett.* **2017**, *28*, 588–592.
- ¹⁰ Weber, M.; Owens, K.; Sarpong, R. "Atropurpuran—Missing Biosynthetic Link Leading to the Hetidine and Arcutine C₂₀-Diterpenoid Alkaloids or an Oxidative Degradation Product?" *Tetrahedron Letters*, **2015**, *56*, 3600–3603.
- ¹¹ Xie, S.; Chen, G.; Yan, H.; Hou, J.; He, Y.; Zhao, T.; Xu, J. "13-Step Total Synthesis of Atropurpuran." *J. Am. Chem. Soc.* **2019**, *141*, 3435–3439.
- ¹² a) Ditchfield, R.; Hehre, W. J.; Pople, J. A. "Self-Consistent Molecular-Orbital Methods. IX. An Extended Gaussian-Type Basis for Molecular-Orbital Studies of Organic Molecules." *J. Chem. Phys.* **1971**, *54*, 724–729 b) Hehre, W. J.; Ditchfield, R.; Pople, J. A. "Self-Consistent Molecular Orbital Methods. XIV. An Extended Gaussian-Type Basis for Molecular Orbital Studies of Organic Molecules. Inclusion of Second Row Elements." *J. Chem. Phys.* **1972**, *56*, 2257–2262.
- ¹³ Wang, F.-P.; Wang, Q.-H.; Chen, Q.-H. "In *The Alkaloids: Chemistry and Biology*; Cordell, G. A., Ed." *Academic Press*, **2010**, *69*, 1–577.
- ¹⁴ (a) Zheng, H.; Wang, Y.; Xu, C.; Xu, X.; Lin, L.; Liu, X.; Feng, X. "Stereodivergent Synthesis of Vicinal Quaternary-Quaternary Stereocenters and Bioactive Hyperolactones." *Nat. Commun.* **2018**, *9*, 1968–1975; (b) Long, R.; Huang, J.; Gong, J.; Yang, Z. "Direct Construction of Vicinal All-Carbon Quaternary Stereocenters in Natural Product Synthesis." *Nat. Prod. Rep.* **2015**, *32*, 1584–1601; (c) Quasdorf, K. W.; Overman, L. E. "Catalytic Enantioselective Synthesis of Quaternary Carbon Stereocentres." *Nature* **2014**, *516*, 181–191; (d) Büschleb, M.; Dorich, S.; Hanessian, S.; Tao, D.; Schenthal, K. B.; Overman, L. E. "Synthetic Strategies toward Natural Products Containing Contiguous Stereogenic Quaternary Carbon Atoms." *Angew. Chem., Int. Ed.* **2016**, *55*, 4156–4186.
- ¹⁵ Nie, W.; Gong, J.; Chen, Z.; Lui, J.; Tian, J. L.; Song, H.; Liu, X.-Y.; Qin, Y. "Enantioselective Total Synthesis of (–)-Arcutinine." *J. Am. Chem. Soc.* **2019**, *141*, 9712–9718.
- ¹⁶ Gong, J.; Chen, H.; Liu, X.-Y.; Wang, Z.-X.; Nie, W.; Qin, Y. "Total Synthesis of Atropurpuran." *Nat. Commun.* **2016**, *7*, 12183–12188.
- ¹⁷ Zhou, K.; Xia, X.; Leng, X.; Li, A. "Asymmetric Total Synthesis of Arcutinidine, Arcutinine, and Arcutine." *J. Am. Chem. Soc.* **2019**, *141*, 13718–13723.

18 (a) Chen, R.; Zhang, F.; Hua, Y.; Dong, S.; Lei, X.; Xiao, H.; Wang, Y.; Ding, S.; Shen, Y.; Zhang, Y. "Total Synthesis of Stemarene and Betaerene Diterpenoids: Divergent Ring-Formation Strategy and Late-Stage C–H Functionalization." *CCS Chem.* **2022**, *4*, 987-995; (b) Masamune, S. "Total Syntheses of Diterpenes and Diterpene Alkaloids. V. Atisine." *J. Am. Chem. Soc.* **1964**, *86*, 290–291.

¹⁹ (a) Andrez, J.-C.; Giroux, M.-A.; Lucien, J.; Canesi, S. "Rapid Formation of Hindered Cores Using an Oxidative Prins Process." *Org. Lett.* **2010**, *12*, 4368-4371; (b) Reddy, B. V. S.; Muralikrishna, K.; Yadav, J. S.; Babu, N. J.; Sirisha, K.; Sarma, A. V. S. "Tandem Prins/Wagner/Ritter Process for the Stereoselective Synthesis of (3-oxabicyclo[4.2.0]octanyl)amide and (1-(5-aryltetrahydrofuran-3-yl)cyclobutyl)amide Derivatives." *Org. Biomol. Chem.* **2015**, *13*, 5532-5536.

²⁰ Owens, K. R.; McCowen, S. V.; Blackford, K. A.; Ueno, S.; Hirooka, Y.; Weber, M.; Sarpong, R. "Total Synthesis of the Diterpenoid Alkaloid Arcutinidine Using a Strategy Inspired by Chemical Network Analysis." *J. Am. Chem. Soc.* **2019**, *149*, 13713–13717.

²¹ Corey, E. J.; Howe, W. J.; Orf, H. W.; Pensak, D. A.; Petersson, G. "General methods of synthetic analysis. Strategic Bond Disconnections for Bridged Polycyclic Structures." *J. Am. Chem. Soc.* **1975**, *97*, 6116–6124.

²² a) Liu, Y.-P.; Zhu, C.-J.; Yu, C.-C.; Wang, A.-E.; Huang, P.-Q. "Tf₂O-Mediated Intermolecular Coupling of Secondary Amides with Enamines or Ketones: A Versatile and Direct Access to β -Enaminones." *Eur. J. Org. Chem.* **2019**, *42*, 7169–7174; b) Huang, P.-Q.; Fan, T. "Intramolecular Keto Lactam Condensation: A Convenient and Straightforward Approach to Bicyclic Vinylogous Lactams." *Eur. J. Org. Chem.* **2017**, 6369–6374; c) Demir, A. S.; Enders, D. "Regioselective Alkylations of Cyclic 1,3-Diketones *via* Metalated Dimethylhydrazones." *J. Prakt. Chem.* **1997**, *339*, 553–563.

²³ a) Schwartz, B. D.; Matousva, E.; White, R.; Banwell, M. G.; Willis, A. C. "A Chemoenzymatic Total Synthesis of the Protoilludane Aryl Ester (+)-Armillarivin." *Org. Lett.* **2013**, *15*, 1934–1937; b) Banwell, M. G.; Hockless, D. C. R.; Holman, J. W.; Longmore, R. W.; McRae, K. J.; Pham, H. T. T. "Chemoenzymatic and Enantiodivergent Routes to Highly Functionalised Steroidal Nuclei." *Synlett* **1999**, *9*, 1491–1494.

²⁴ a) Banwell, M. G.; Edwards, A. J.; Harfoot, G. J.; Joliffe, K. A. "A Chemoenzymatic Synthesis of the Linear Triquinane (-)-Hirsutene and Identification of Possible Precursors to the Naturally Occurring (+)-Enantiomer." *Tetrahedron* **2004**, *60*, 535–547; b) Boyd, D. R.; Sharma, N. D.; Coen, G. P.; Gray, P. J.; Malone, J. F.; Gawronski, J. "Enzyme-Catalysed Synthesis and Absolute Configuration Assignments of *cis*-Dihydrodiol Metabolites from 1,4-Disubstituted Benzenes." *Chem. Eur. J.* **2007**, *13*, 5804–5811. c) Lan, P.; Ye, S.; Banwell, M. G. "The Application of Dioxygenase-Based Chemoenzymatic Processes to the Total Synthesis of Natural Products." *Chem. Asian J.* **2019**, *14*, 4001–4012; d) Hudlicky, T.; Boros, C. T.; Boros, E. E. "A Model Study Directed Towards a Practical Enantioselective Total Synthesis of (-)-Morphine." *Synthesis* **1992**, 174–178.

²⁵ a) Gu, X.; Dai, Y.; Guo, T.; Franchino, A.; Dixon, D. J.; Ye, J. "A General, Scalable, Organocatalytic Nitro-Michael Addition to Enones: Enantioselective Access to All-Carbon Quaternary Stereocenters." *Org. Lett.* **2015**, *17*, 1505–1508; b) Wei, Y.; Liu, Z.; Wu, X.; Fei, J.; Gu, X.; Yuan, X.; Ye, J. "Remote Construction of Chiral Vicinal Tertiary and Quaternary Centers by Catalytic Asymmetric 1,6-Conjugate Addition of Prochiral Carbon Nucleophiles to Cyclic Dienones." *Chem. Eur. J.* **2015**, *21*, 18921–18924.

- ²⁶ Southgate, E. H.; Pospech, J.; Fu, J.; Holycross, J. F.; Sarlah, D. "Dearomative Dihydroxylation with Arenophiles." *Nat. Chem.* **2016**, *8*, 922–929.
- ²⁷ Werjes, W. C.; Southgate, E. H.; Sarlah, D. "Recent Advances in Chemical Dearomatization of Nonactivated Arenes." *Chem. Soc. Rev.* **2018**, *47*, 7996–8017.
- ²⁸ a) Stabile, M. R.; Hudlicky, T.; Meisels, M. L. "New chiral synthon from bromoethylbenzene: Absolute stereochemistry of a biooxidation metabolite." *Tetrahedron: Asymmetry* **1995**, *6*, 537–542; b) Boyd, D. R.; Sharma, N. D.; Stevenson, P. J.; Hoering, P.; Allen, C. C. R.; Dansette, P. M. "**Monooxygenase- and Dioxygenase-Catalyzed Oxidative Dearomatization of Thiophenes by Sulfoxidation, *cis*-Dihydroxylation and Epoxidation.**" *Int. J. Mol. Sci.* **2022**, *23*, 909–941.
- ²⁹ Kalinin A. V.; Miah, M. A. J.; Chattopadhyay, S.; Tsukazaki, M.; Wicki, M.; Nguen, T.; Coelho, A. L.; Kerr, M.; Snieckus M. V. "Anionic Homologous Fries Rearrangement of *o*-(2-methylaryl)carbamates. A Regiospecific Route to Benzo[*b*]furan-2(1*H*)-ones including an Unnamed Metabolite from *Helenium* Species." *Synlett*, **1997**, *7*, 839–841.
- ³⁰ Meng, Q.; Song, B.; Tang, X.; Zhao, J. "Bisphenol Polymer Structural Units and Method of Making the Same." *Faming Zhuanli Shenqing* **2020**, CN110790734A.
- ³¹ Reuping, M.; Nachtsheim, B. J. "A Review of New Developments in the Friedel–Crafts Alkylation – From Green Chemistry to Asymmetric Catalysis." *Bellstein J. Org. Chem.* **2010**, *6*, 1–24.
- ³² Triandafillidi, I. Sideri, I.; Tzaras, D.; Spiliopoulou, N.; Kokotos, C. "Green Organocatalytic Synthesis of Dihydrobenzofurans by Oxidation–Cyclization of Allylphenols." *Synthesis* **2017**, *49*, 4254–4260.
- ³³ Tsuchiya, K.; Endo, T. *Jpn. Kokai Tokkyo Koho* **2014**, JP2014055212A
- ³⁴ Dohi, T.; Takenaga, N.; Nakae, T.; Toyoda, Y.; Yamasaki, M.; Shiro, M.; Fujioka, H.; Maruyama, A.; Kita, Y. "Asymmetric Dearomatizing Spirolactonization of Naphthols Catalyzed by Spirobiindane-Based Chiral Hypervalent Iodine Species." *J. Am. Chem. Soc.* **2013**, *135*, 4558–4566.
- ³⁵ a) Kovtonyuk, V. N.; Kobrina, L. S. "Selective *Ortho*-Arylation of Polyfluorinated Hydroxyaromatic Compounds with Lead Aryl Acetates." *J. Fluor. Chem.* **1993**, *63*, 243–251; b) Donnelly, D. M. X.; Finel, J.–P.; Rattigan, B. A. "Organolead-Mediated Arylation of Allyl β -Ketoesters: A Selective Synthesis of Isoflavanones and Isoflavones." *J. Chem. Soc., Perkin Trans.* **1993**, *1*, 1729–1735.
- ³⁶ a) Muller, P. "Glossary of Terms Used in Physical Organic Chemistry (IUPAC Recommendations 1994)." *Pure Appl. Chem.* **1994**, *66*, 1077–1184; b) Anderson, J. E. *Fortschritte der Chemischen Forschung* **1974**, *45*, 139.
- ³⁷ Carey, Francis A.; Sundberg, Richard J. *Advanced Organic Chemistry: Part B: Reactions and Synthesis* **2007**, *5*, 836–850, New York: Springer. ISBN:978–0387683546.
- ³⁸ a) Luche, J.-L. "Lanthanides in Organic Chemistry. Selective 1,2 Reductions of Conjugated Ketones." *J. Am. Chem. Soc.* **1978**, *100*, 2226–2227; b) Luche, J.-L.; Rodriguez-Hahn, L.; Crabbe, P. "Reduction of Natural Enones in the Presence of Cerium Trichloride." *J. Chem. Soc. Chem. Commun.* **1978**, *14*, 601–602.

- ³⁹ Liu, Q.; Cheng, L.-J.; Wang, K. "A Theoretical Study of an Electronically Mismatched Diels–Alder Cycloaddition." *RSC Advances* **2017**, *7*, 30618–30625.
- ⁴⁰ Burton, G. W.; Ingold, K. U. "Autoxidation of Biological Molecules. 1. Antioxidant Activity of Vitamin E and Related Chain-Breaking Phenolic Antioxidants *In Vitro*." *J. Am. Chem. Soc.* **1981**, *103*, 6472–6477.
- ⁴¹ a) Gocan, S. "Two-Dimensional Thin-Layer Chromatography." *J. Liq. Chromatogr. Relat. Technol.* **2004**, *27*, 1105–1113; b) Gassman, R. G.; Singleton, D. A. "Acid-Catalyzed Intramolecular "Diels-Alder" Reactions. The Cycloaddition of Allyl Cations to 1,3-Dienes." *J. Am. Chem. Soc.* **1994**, *106*, 6085–6086.
- ⁴² a) Ernst, V.; Caravatti, G.; Franck, P.; Aristoff, P.; Moody, C.; Becker, A.-M.; Felix, D.; Eschenmoser, A. "On the Stereochemistry of E'- and E'-Reactions." *J. Chem. Lett.* **1987**, *16*, 219–222; b) Nogi, K.; Fujihara, T.; Terao, J.; Tsuji, Y. "Cobalt-Catalyzed Carboxylation of Propargyl Acetates with Carbon Dioxide." *Chem. Comm.* **2014**, *50*, 13052–13055.
- ⁴³ Liebesking, L. S.; Fengl, R. W.; Welker, M. E. "A Practical Synthesis of α,β -Unsaturated Iron Acyls. Chiral Enolate Synthesis." *Tetrahedron Letters* **1985**, *26*, 3075–3078.
- ⁴⁴ a) Williamson, K. J.; Keller, R. T.; Fonken, G. S.; Szmuszkovicz, J.; Johnson, W. S. "A Procedure for Acetate Pyrolysis. The Preparation of 2-Cyclohexenone." *J. Org. Chem.* **1962**, *27*, 1612–1615; b) Ratchford, W. P.; Cope, A. C.; Armstrong, W. R.; Ryan, J. J. *Organic Synthesis* **1955**, *3*, 30; c) Ratchford, W. P.; Cope, A. C.; Armstrong, W. R.; Ryan, J. J. *Organic Synthesis* **1949**, *29*, 2.
- ⁴⁵ Kolb, M.; Barth, J. "A Convenient Preparation of Iodoalkyl Esters from Lactones." *Synth. Comm.* **1981**, *11*, 763–767.
- ⁴⁶ a) Gustafsson, T.; Ponten, F.; Seeberger, P. H. "Trimethylaluminium Mediated Amide Bond Formation in a Continuous Flow Microreactor as Key to the Synthesis of Rimonabant and Efaproxiral." *Chem. Comm.* **2008**, *9*, 1100–1102; b) Nemeth, B.; Guegan, J.-P.; Veszpremi, T.; Guillemin, J.-C. "Trimethylaluminum and Borane Complexes of Primary Amines." *Inorg. Chem.* **2013**, *52*, 346–354; c) Chung, S.; Uccello, D. P.; Choi, H.; Montgomery, J. I.; Chen, J. "Trimethylaluminium-Facilitated Direct Amidation of Carboxylic Acids." *Synlett* **2011**, *14*, 2072–2074.
- ⁴⁷ Gregg, B. T.; Golden, K. C.; Quinn, J. F. "Indium(III) Trifluoromethanesulfonate as an Efficient Catalyst for the Deprotection of Acetals and Ketals." *J. Org. Chem.* **2007**, *72*, 5890–5893.

Chapter 6: Investigations into Alkene Metathesis in the Presence of Iron-Tricarbonyl Complexed Diene Systems

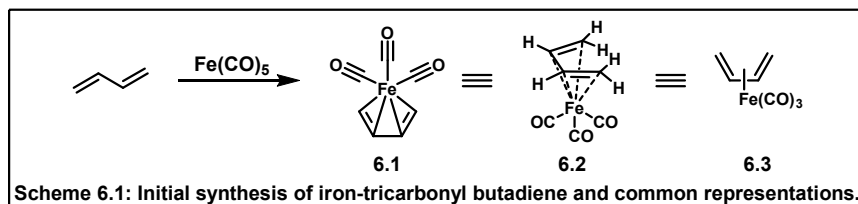
6.1 Introduction

Iron tricarbonyl diene complexes are an understudied area of organometallic chemistry. These metal- π interactions have been incorporated as diene protecting groups to attenuate diene reactivity over multiple reactive steps that would otherwise face chemoselectivity issues. No studies have been published in the literature investigating the utilization of iron-protected dienes in the presence of any alkene cross metathesis reaction conditions. Successful alkene metathesis in the presence of iron-tricarbonyl complexed dienes would allow for the rapid synthesis of Diels-Alder precursors. Notably, these could allow for facile synthesis of fused and bridged bicyclic systems obtained from transannular Diels-Alder (TADA) cycloadditions. The syntheses of the diene-dienophile precursors are generally difficult, due to chemoselectivity issues involving competing reactivity of multiple π -systems. Herein are described studies toward the utilization of alkene metathesis reactions in the presence of iron-diene complexes.

6.2 Previous Work on Iron-Tricarbonyl Complexed Dienes

6.2.1 History of Diene-Iron Tricarbonyl Complexes

The complexation of dienes with iron tricarbonyl was first reported in 1930 by Rheilen, Gruhl, Hessling, and Pfrenge in their synthesis of iron-tricarbonyl butadiene (**6.1**) (Scheme 6.1).¹ The group

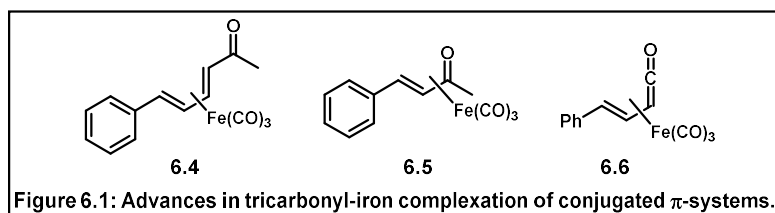


proposed a chelation of the iron to the diene. These products are most accurately

represented in a three-dimensional sense as **6.2** but are generally represented as **6.3**. The proposed

chelation was considered unlikely due to their high thermal stability, but this complexation was further corroborated by Pauson and Hallam through spectroscopic and reactivity studies.² Lillya and coworkers further advanced iron-tricarbonyl complexation with other conjugated π -systems by developing the first iron-dienone complex (**6.4**) and demonstrating its utility in NMR spectroscopic analysis (**Figure 6.1**).³

Lewis and coworkers took a similar interest in unsaturated carbonyl systems and discovered diiron

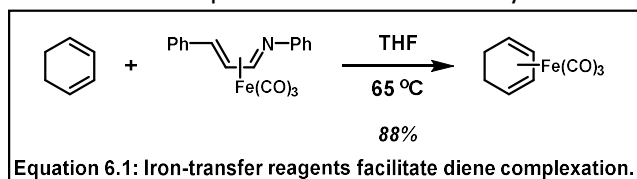


nonacarbonyl was capable of protecting α,β -unsaturated ketones (**6.5**) through the conjugated π -

system. It was later demonstrated α,β -unsaturated imines could be protected in the same manner.⁴ The efficacy of this method of diene stabilization was proven as Saberi and coworkers demonstrated the ability to trap α,β -unsaturated ketenes (**6.6**) as isolable intermediates.⁵

6.2.2 Methods of Iron-Diene Complexation

Iron tricarbonyl diene complexation was initially performed thermally in nonpolar solvents using iron nonacarbonyl.¹ Although this is still a common method of synthesis, most rely on the more stable and less hazardous diiron nonacarbonyl, as it is solid, less pyrophoric, and poses a lesser health hazard if one were to come into contact with it.⁶ As a means of performing mild complexation reactions, modern methods of iron-diene syntheses involve the use of an iron transfer catalyst.⁷ The use of aromatic α,β -unsaturated compounds as iron-tricarbonyl transfer reagents, first developed by Lewis and coworkers,



utilize enones and α,β unsaturated imines as catalysts for the facile synthesis of iron-diene

complexes at modest temperatures (**Equation 6.1**).⁸ Enantioselective methods of iron tricarbonyl transfer have been developed utilizing this catalytic method, though the enantiopurity of the products formed by reactions with these catalysts are poor to modest.⁹ Another modern method of iron

tricarbonyl complexation is through the use of sonication, a convenient and mild method that shows good selectivity for diene complexation in the presence of other π -systems and functional groups.¹⁰

6.2.3 Decomplexation Methodologies

Decomplexation of diene-iron tricarbonyls has also been an area of research worth noting as the methods employed have varying functional group tolerance. Oxidative decomplexation via ceric ammonium nitrate (CAN), developed by Lewis and coworkers in 1973 is the earliest reported and most commonly used method.¹¹ Alternatives were sought as CAN is a harsh oxidant, leading Shvo and Hazum to develop a mild decomplexation method utilizing trimethylamine *N*-oxide.¹² A third method reported for oxidative decomplexation is the employment of iron trichloride in aqueous methanol, a mild method developed by Saberi and coworkers in the 1990s.⁸ Harsh oxidants are non-compatible with iron-diene complexes as they often result in decomplexation and further reactivity with the diene to afford complex mixtures of products.¹³ A single example of decomplexation of a cyclic diene complex utilizing mCPBA has been reported by Schuhmann and coworkers; however, the reaction afforded a mixture of decomplexed product and aromatized product, which may call for investigation of mCPBA decomplexation on acyclic iron-diene systems.¹⁴

6.2.4 Iron-Tricarbonyl Diene Complex Reactivity

Fischer and Fischer reported the first synthetic use of diene-iron tricarbonyl complexes through hydride abstraction to form the η^5 -iron salt, exhibiting the ability of the iron-complex to stabilize neighboring cations.¹⁵ In 1963 Petit and coworkers performed acidic cleavage of alcohol groups neighboring the iron-diene to form the η^5 -iron cation salt; they further demonstrated the synthetic utility of the resultant carbocation via reduction to afford the formal dehydroxylated iron-diene product.¹⁶ Lillya demonstrated the ability of iron-butadiene to perform Friedel-Crafts acylation to synthesize iron-dienone complexes regioselectively.¹⁷ Investigations of the utility of iron-diene

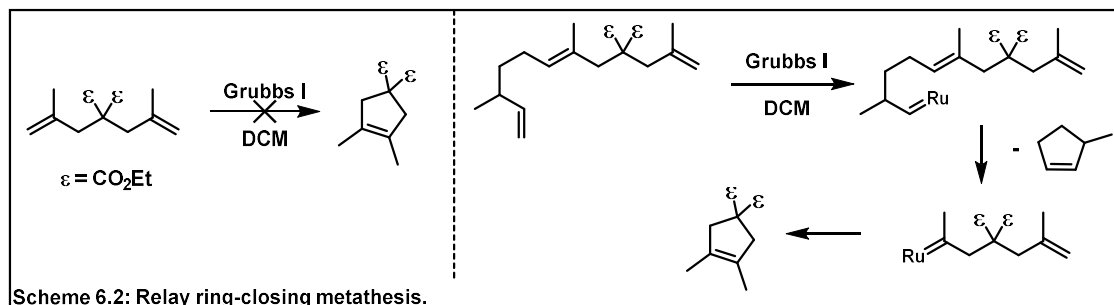
complexes were performed by Birch and coworkers in the 1960s. Birch displayed the synthetic utility of iron pentacarbonyl when subjected to 1,4-dienes, generally produced via aromatic reductions, to afford isomerized, conjugated dienes.¹⁸ Pearson continued the work Birch had developed by demonstrating nucleophilic addition to the cyclic η^5 -iron cation salts with an array of nucleophiles including cyanide, 1,3-dicarbonyl systems and alkyl anions.¹⁹ Pearson reported a highly regioselective method of forming quaternary γ -substituted enones in high yields.²⁰

6.2.5 Stability of Iron–Diene Complexes

Iron-tricarbonyl diene complexes are generally utilized for their high level of stability in the presence of reagents that would otherwise react with the diene system.¹ Pearson and coworkers demonstrated the tolerance of iron-diene complexes to a series of reagents.^{19,20} They reported the use of reductive conditions by subjecting a moderately complex iron-diene intermediate to a series of hydride reducing agents (NaBH_4 , DIBAL-H, LAH). Interestingly, although oxidation is the common method of decomplexation, they also demonstrated a series of oxidative conditions that left the iron-diene complex intact. These conditions include epoxidation of distal π -systems and oxidations of alcohols. They further demonstrated the stability of iron dienes in a series both acid and base mediated reactions, as well as their tolerance to both nucleophiles and electrophiles. The stability of these systems has been displayed in multiple total syntheses in which iron-diene complexes were introduced and carried through a series of reactivity prior to decomplexation.²¹

6.3 Alkene Metathesis in the Presence of Iron-Diene Systems

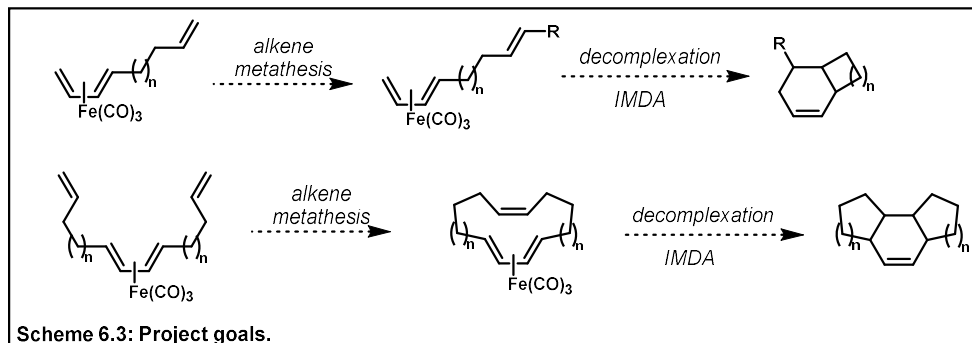
6.3.1 Alkene Metathesis Off-site Reactivity and Relay



Investigations into alkene metathesis have proven that a major limitation is the formation of undesired byproducts when reactants with multiple π -systems are subjected to metathesis conditions.²² The formation of these byproducts are a result off-target reactions with undesired π -systems, either caused by the inherent reactivity of the π -systems or the intramolecular transfer of the catalyst to a less accessible π -system through the process of catalyst relay. Hoye and coworkers capitalized on catalytic relay to promote alkene metatheses of inaccessible π -systems by incorporating easily accessible alkene fragments to perform intramolecular transfer of the metathesis catalyst, a strategy was named Relay Ring Closing Metathesis (RRCM) **Scheme 6.2**).²³ This method has proven invaluable for the syntheses of previously inaccessible carbocycles, though it highlights the major limitation of ring-closing metathesis to afford TADA precursors. The kinetically challenging metathesis macrocyclization required to form the dienophile of a TADA substrate in the presence of a diene would likely result in catalytic relay to the diene and molecular fragmentation. The incorporation of iron tricarbonyl complexed dienes would allow for chemoselective metathesis of unprotected alkenes to afford dienophiles and prevent fragmentation through catalyst relay.

6.3.2 Project Considerations

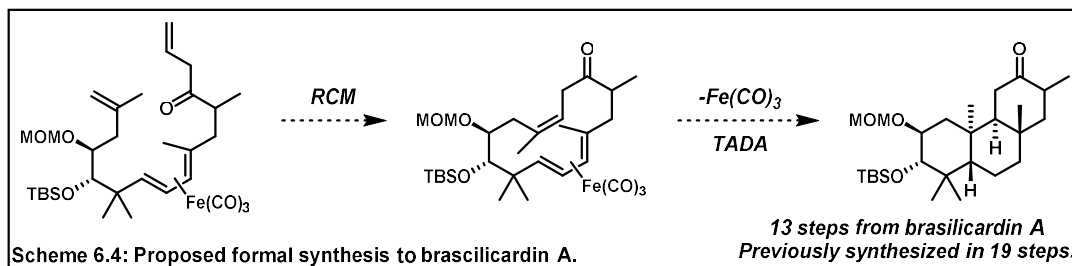
In our investigations into previously reported reactivity of iron-diene complexes, we noted that there had been no evidence of alkene cross metathesis reactions in the presence of iron-diene complexes. Incorporating iron-protected dienes in the presence of an alkene metathesis substrate would allow for the synthesis of selectively substituted olefins that could be utilized in intramolecular



Diels-Alder (IMDA)
cycloadditions
(Scheme 6.3). We
also envisioned this
strategy to be

applicable to macrocyclizations to afford iron tricarbonyl protected transannular Diels-Alder (TADA) cycloaddition precursors.

This strategy would allow for rapid access to complex multicyclic systems and could be extended to facile total syntheses of natural products that have been proven accessible through TADA cycloadditions. Considering plausible applications of this strategy, we believed it could be utilized to intercept a previously reported synthesis of brasilicardin A, in a fraction of the step count, from a

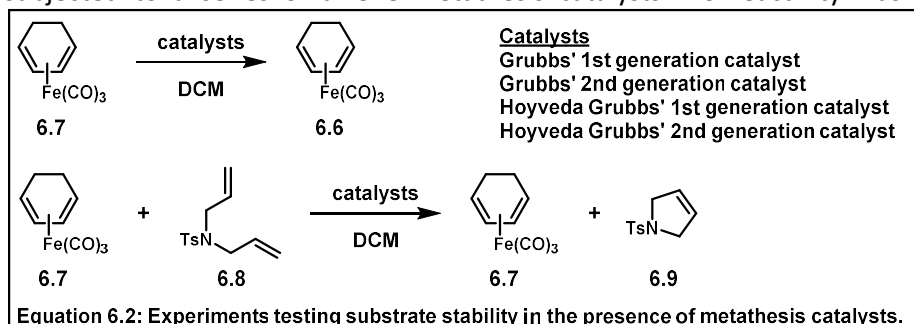


relatively simple intermediate (Scheme 6.4).²⁴ It was decided to investigate the utilization of alkene metathesis on systems that would be very labile to diene decomposition due to catalyst relay, while hoping to extend this project to the synthesis of transannular Diels-Alder precursors. Development of

this strategy would allow for previously inviable alkene metatheses and for improvement in synthetic strategy toward Diels-Alder precursors.

6.3.3 Model Studies

A series of model systems were developed to ensure the stability of iron-diene complexes in the presence of alkene metathesis catalysts. **6.7**, synthesized according to literature precedent, was subjected to a series of alkene metathesis catalysts. No reactivity was observed, and the starting

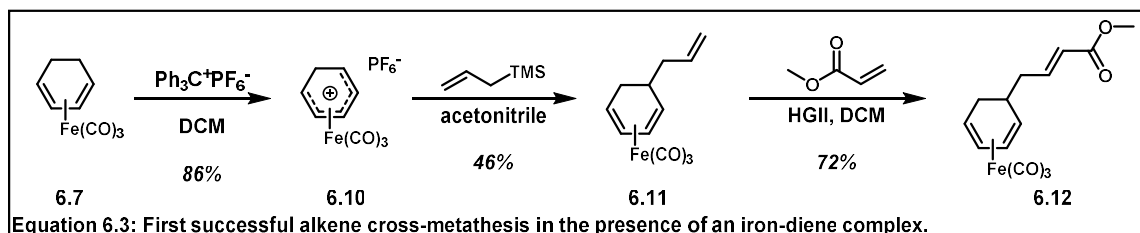


material was fully recovered (**Equation 6.2**). This confirmed the stability of iron-diene

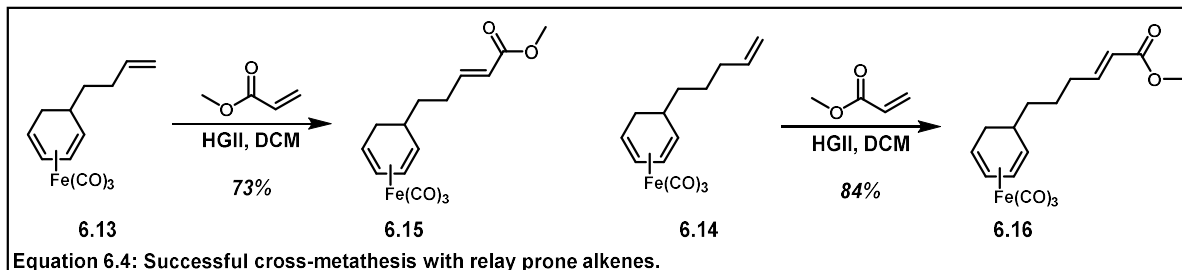
complexes in the presence of alkene metathesis catalysts. It was also found that after subjecting **6.8** to standard alkene metathesis conditions in the presence of an equimolar ration of iron-diene complex **6.7**, full conversion to **6.9** was observed, while **6.7** was again fully recovered. This indicated that iron-diene complexes do not impede the reactivity of alkene metathesis catalysts. The results of these experiment indicated that iron-diene complexes were inert when subjected to alkene metathesis conditions.

6.3.4 Cross-Metathesis Studies

With confidence that iron-diene systems were stable to alkene metathesis conditions, compounds containing iron-diene complexes and unprotected alkenes were synthesized for investigation. Alkene **6.11** was synthesized via allyl addition to the iron-stabilized η^5 -salt **6.10**. **6.11** was subjected to standard cross metathesis conditions, and **6.12** was isolated in good yields with no noted



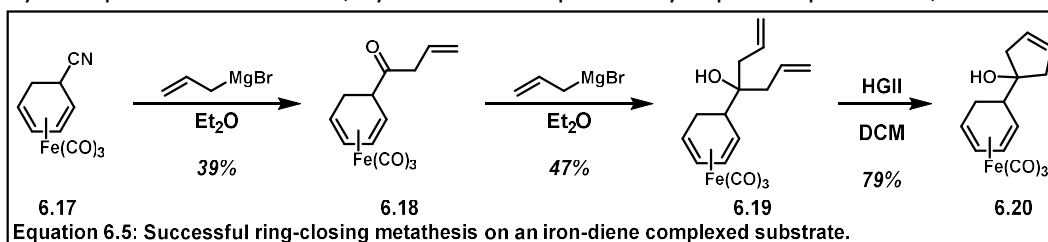
iron-diene decomposition products (**Equation 6.3**). Although this was considered an important step in our investigations, as it was the first example of alkene metathesis performed on a substrate containing both a reactive alkene and an iron tricarbonyl complexed diene, it was not entirely conclusive to the



effectiveness of this strategy, as relay of the catalyst on this system would require the formation of a four-membered ring transition state, potentially making cross-metathesis the more kinetically favored product than catalyst relay. For this reason, **6.13** and **6.14** were both synthesized and subjected to alkene cross-metathesis conditions (**Equation 6.4**). Both reactions afforded the desired cross-metathesis products (**6.15**, **6.16**) in good yields, indicating that the iron-diene complex prevented catalyst relay, and was, therefore, an effective diene protecting group for alkene metathesis.

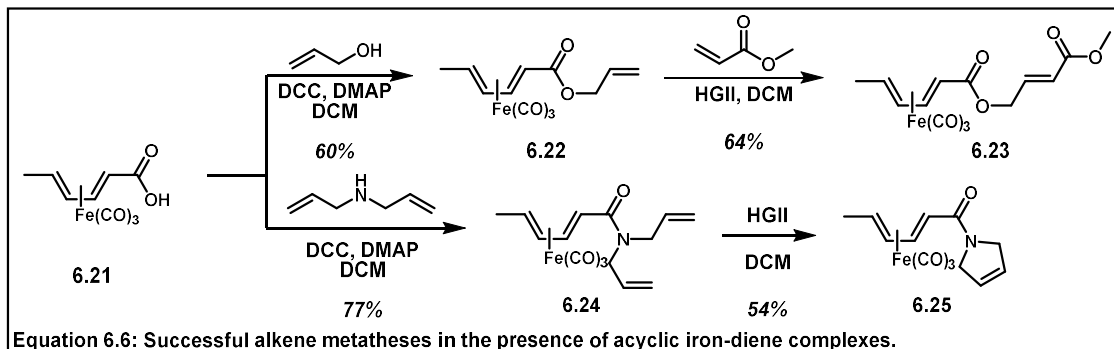
6.3.5 Expansion of Scope

To further our confidence in this strategy, we investigated a series of cyclic and acyclic iron tricarbonyl complexed dienes. **6.17**, synthesized via previously reported procedure, was subjected to



allylation conditions to afford ketone **6.18** (**Equation 6.5**). Subsequent allyl Grignard addition produced **6.19**, which was subjected to ring-closing metathesis conditions to afford carbocycle **6.20** in good yields.

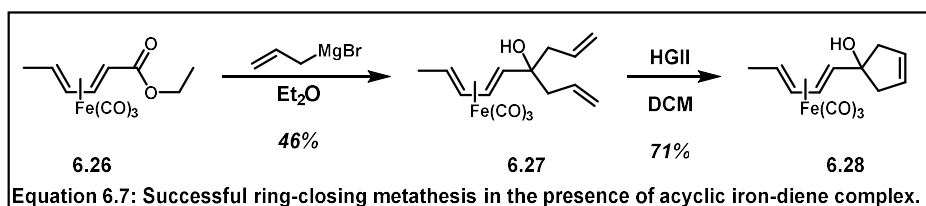
Synthesis of **6.21** was performed according to literature procedure and was converted to allyl ester **6.22**, which underwent cross-metathesis to afford **6.23** (Equation 6.6).²⁵ Amide **6.24** was



synthesized via amide coupling conditions and was found to undergo ring-closing metathesis producing

6.25 in modest yields. Ester **6.26** was also subjected to diallylation to afford tertiary alcohol **6.27**, which

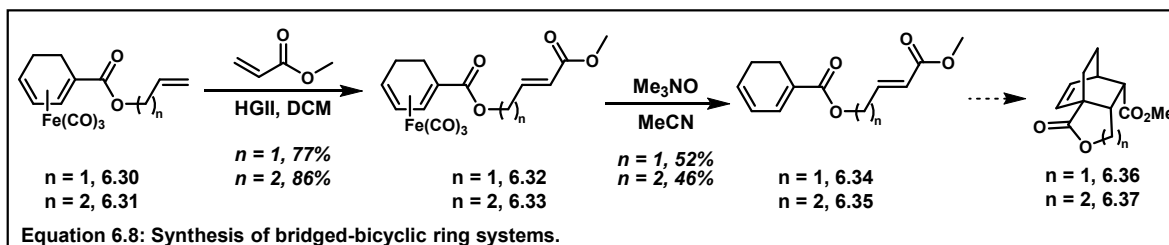
was then subjected to ring-closing metathesis to produce **6.28** in good



yields (Equation 6.7).

6.3.6 Synthesis of Bridged Bicyclic Systems

In an effort to highlight the synthetic utility of this strategy, substrates that could afford more complex products were targeted. **6.29** was made according to literature precedent and subsequently



esterified to afford **6.30** and **6.31** (Equation 6.8). Both compounds were subjected to cross-metathesis

to afford **6.32** and **6.33**, which were decomplexed to synthesize **6.34** and **6.35** was performed. Current

investigations are being undergone to afford the IMDA products **6.36** and **6.37**. It is recognized that

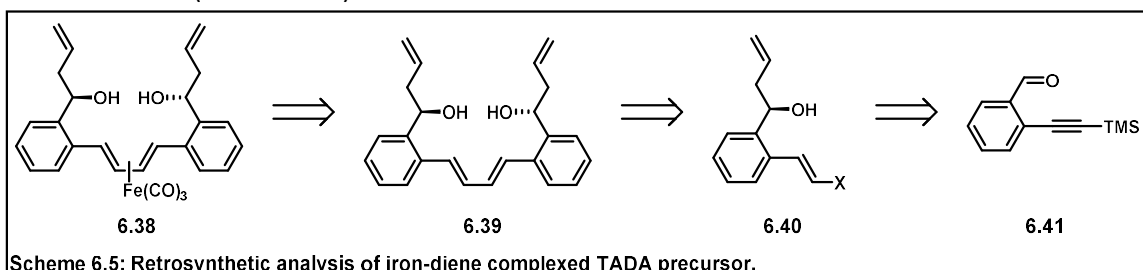
these compounds could be afforded by esterification utilizing alcohols with preinstalled

functionalization; these products were synthesized in this manner as a proof of concept for the strategy.

6.4 Applications of this Strategy Toward Transannular Diels-Alder Adducts

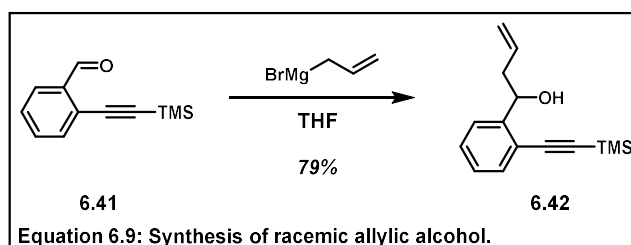
6.4.1 Substrate Synthesis

In the pursuit of a TADA substrate containing an iron-diene complex, we developed a synthetic route toward **6.38** (Scheme 6.5). It was believed that **6.38** could be accessed via dimerization of cross-

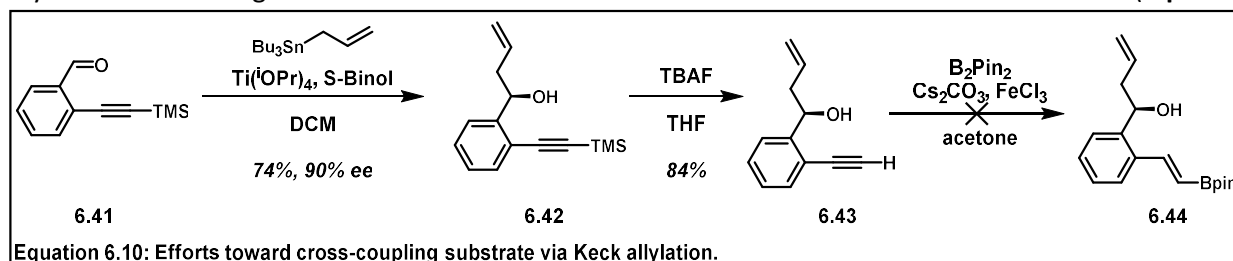


coupling fragments **6.40** and subsequent iron-tricarbonyl complexation of **6.39**. **6.40** was thought to be readily accessed from literature precedent **6.41** via allylation and alkyne hydrofunctionalization.

6.41 was synthesized according to literature procedure and was subjected to allylmagnesium bromide to obtain **6.42** as a racemic mixture (Equation 6.9). We noted that carrying through

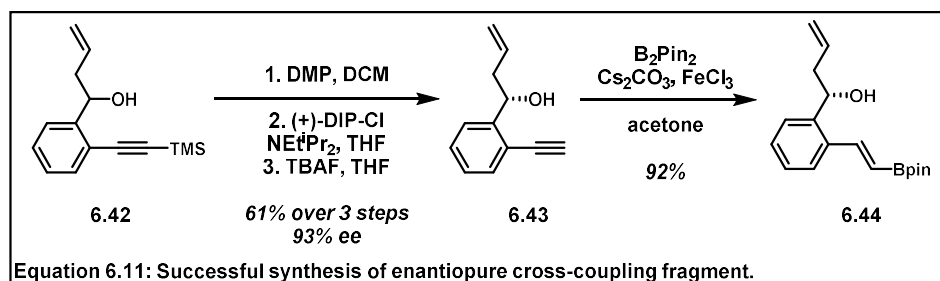


this synthesis with the racemic alcohol may be problematic, as the subsequent iron-protection would result in a mixture of diastereomers that would make characterization difficult. For this reason, Keck allylation was investigated and showed to afford the alcohol **6.42** in 90% enantiomeric excess (Equation



6.10). Unfortunately, the resulting product was contaminated with an inseparable tin byproduct. Desilylation was performed in good yields to afford **6.43**, though the tin byproduct was still inseparable from the product. All efforts toward hydroborylation of **6.44** were unsuccessful.

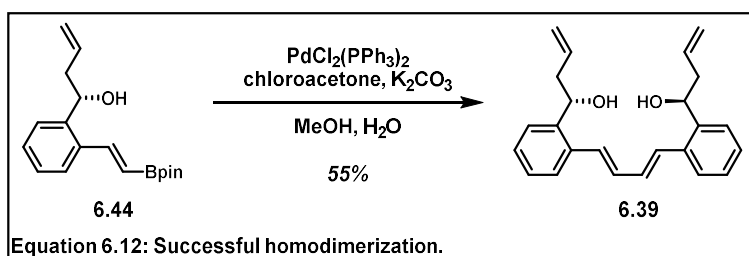
We observed that hydroborylation of racemic **6.43** afforded alkenyl borane **6.44**. It was believed that the inseparable tin byproduct was preventing hydroborylation from occurring. We pursued an



alternative route to enantiopure **6.42**. Oxidation of racemic **6.42** and reduction of

the ketone via transfer hydrogenation with (+)-DIP-Cl to produce **6.42** in high enantiomeric excess (Equation 6.11).²⁶ Desilylation and borylation was performed to generate Suzuki coupling fragment **6.44**

in good yields. Subjecting vinyl boronic ester **6.44** to Suzuki coupling conditions afforded homodimerized **6.39** in modest yields (Equation 6.12).



Complexation of **6.39** with iron tricarbonyl to synthesize **6.38** was investigated (Table 6.1). Initial efforts utilized ultrasound sonication, a method that had shown to obtain iron-diene complexes in the

Solvent	Temp.	Modification	
benzene	25 °C	Sonicated	A
benzene	40 °C	Sonicated	
toluene	110 °C	-	
DME	60 °C	cat. A added	
toluene	110 °C	cat. A added	
toluene	110 °C	B added	

Structure	Label
	A
	B

Table 6.1: Efforts toward iron-diene complexation.

presence of allylic alcohols.¹¹ A mixture of products were formed, though all isolated products contained unreacted diene. It is possible the neighboring alcohol was extruded, due to the ability of iron tricarbonyl complexes to stabilize the resultant carbocation, resulting in a stable cationic system.²⁷ Thermal conditions were investigated but had no effect on the starting material. Methods utilizing iron-transfer reagents were also explored, but once more did not react with **6.39**. It is hypothesized that the

aromatic character of the conjugated diene increased the diene stability, resulting in undesired side reactivity with the allylic alcohols.

Due to the difficulties encountered in complexing the diaryl-diene system, a new approach toward a TADA substrate was developed. Known iron diene complex **6.45** was known to be accessed in three steps from commercial materials.²⁸ With the iron-diene preinstalled, elaboration to RCM precursor **6.46** was imagined to be accomplished via diallylation.

All efforts to allylate **6.45** via nucleophilic displacement of allylbromide were unsuccessful (**Table 6.2**). Isolation of the η^5 -cationic system was investigated but was also

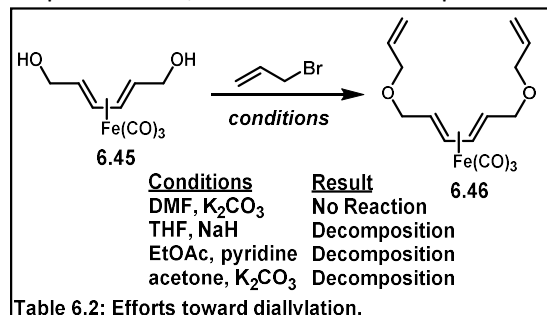
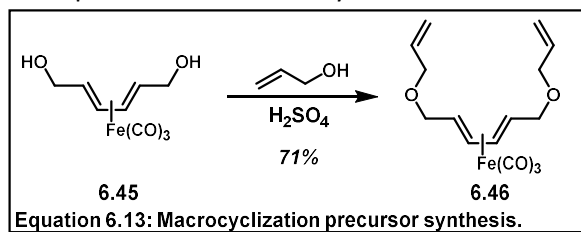


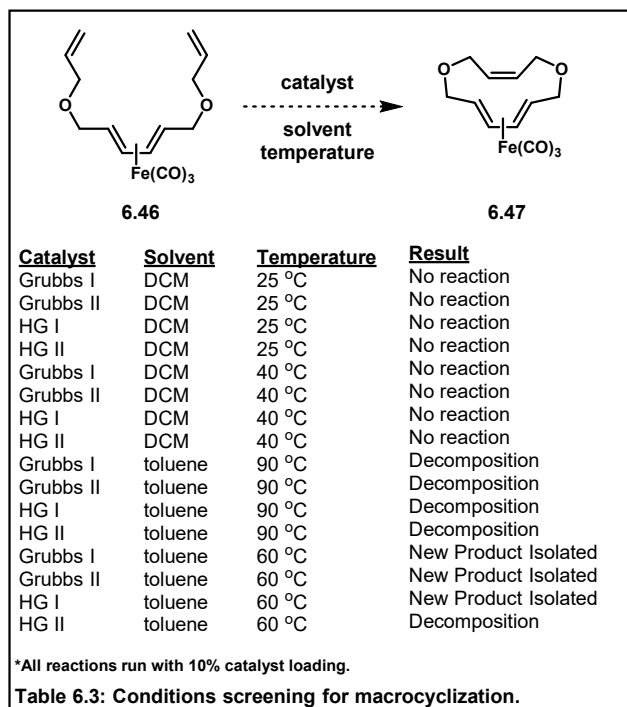
Table 6.2: Efforts toward diallylation.

unsuccessful, seemingly producing polymerization products. Investigations into the cation stabilizing nature of iron-dienes revealed that in-situ generation of the η^5 -cationic system, under catalytic quantities of Brønsted-Lowry acid, and trapping with nucleophilic solvent led to synthesis of **6.46**. This constitutes a novel method for the synthesis of diene systems (**Equation 6.13**), which calls for deeper studies of the scope of nucleophilic partners.

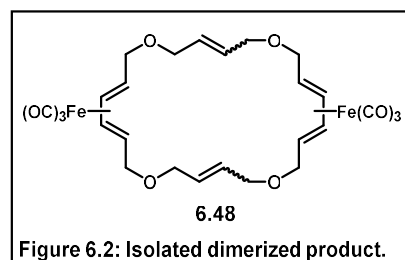


6.4.2 Investigation of Macrocyclization

6.46 was utilized for reactive screening, as dodecane macrocycles are known to exhibit very low thermodynamic ring strain. **6.46** was subjected to a series of alkene metathesis conditions, with varying metathesis catalyst, solvent, and temperature (**Table 6.3**). Screening indicated that moderately elevated temperatures afforded full conversion to a new product, tentatively assigned as **6.47**

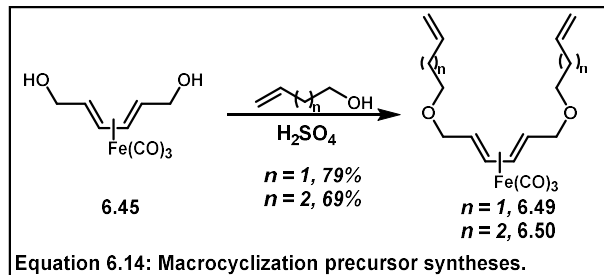


Decomplexation of **6.47** was performed and a new product was isolated that contained both decomplexed diene and dienophile, though no IMDA product was observed. It was believed IMDA cycloaddition would occur spontaneously, as the IMDA precursor had been previously synthesized but was reported to be only isolated as the cycloaddition product.²⁹ The product was subjected to heating up to 110 °C but was unreactive. The inability of the substrate to undergo IMDA cycloaddition coupled with high-resolution mass spectrometry analysis indicated that the undesired dimer **6.48** was formed in the macrocyclization reaction (**Figure 6.2**). It was presumed that the rigidity of the iron–diene complex does not grant the orbital overlap required for the reaction

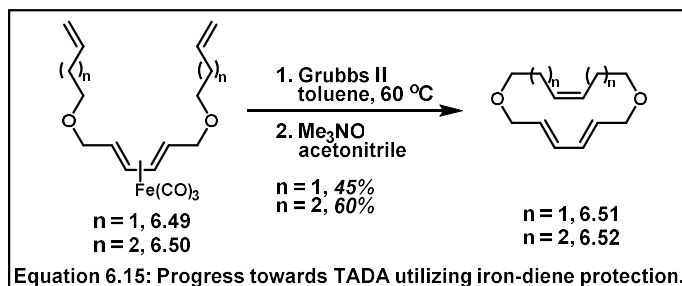


to occur as desired, instead resulting in intermolecular dimerization to the 24-membered macrocycle **6.48**. The rigidity of the diene system is reminiscent of previous attempts to synthesize paracyclophanes via ring-closing metathesis, which have been found to be non-productive in the formation of carbocycles smaller than 14-membered rings, though the iron–diene systems likely exhibit lesser constraints when compared to cyclophanes.³⁰

Due to the restrictions of ring size allowable in the macrocyclization of iron-diene complexes, larger ring systems were pursued. Utilizing the previously developed reaction with



but-3-en-1-ol and pent-4-en-1-ol, **6.49** and **6.50** were made. **6.49** was a major target of interest as the [6,6,6]-tricycle is more commonly found in natural products and would prove the synthetic utility of this strategy. These compounds were subjected to ring-closing metathesis conditions and decomplexation



to afford new products tentatively assigned as TADA precursors **6.51** and **6.52** (Equation **6.15**). Currently, we are screening conditions to induce IMDA cycloaddition with both

fragments while working in collaboration with our mass spectrometry facility to confirm the structure of both products.

6.5 Conclusions

Having proven the viability of iron-tricarbonyl complexes for protection with respect to alkene metathesis, we believe this strategy can be exploited to allow for facile synthesis of diene-dienophile pairs for Diels-Alder cycloadditions. Herein, we have shown the capability of these π -metal complexes to inhibit kinetically favored catalyst relay reactivity, allowing for selective alkene metatheses. The metatheses shown to be feasible include cross metathesis, ring-closing metathesis and macrocyclization reactions. We have utilized this chemistry to synthesize selectively substituted bridged bicyclic systems, motifs found in many natural products. Further, this strategy has been used to synthesize transannular Diels-Alder products in a facile manner. With the conclusions drawn from this research the Vanderwal lab is currently considering total syntheses of natural products utilizing this strategy.

6.6 Distribution of Credit and Contributions

I would like to thank Samantha Nguyen for her contributions in the synthesis of intermediates and performance of reactions.

6.7 Experimental Information

6.7.1 Materials and Methods

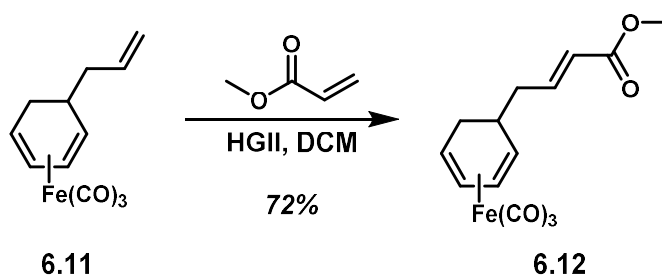
All reactions were carried out in oven-dried (140 °C) or flame-dried glassware under an atmosphere of dry argon unless otherwise noted. Dry dichloromethane (CH_2Cl_2), tetrahydrofuran (THF), diethyl ether (Et_2O), acetonitrile (MeCN), toluene (PhMe), and dimethoxyethane (DME) were obtained by percolation through columns packed with neutral alumina and columns packed with Q5 reactant, a supported copper catalyst for scavenging oxygen, under a positive pressure of argon. Solvents used for liquid-liquid extraction and chromatography were: Ethyl acetate, (EtOAc, Sigma-Aldrich, ACS grade) hexanes (Sigma-Aldrich, ACS grade), dichloromethane (CH_2Cl_2 , Fisher, ACS grade), acetone (Sigma-Aldrich, ACS Grade), diethyl ether (Et_2O , Fisher, ACS grade), and pentane (Sigma-Aldrich, ACS grade). Reactions that were performed open to air utilized solvent dispensed from a wash bottle or solvent bottle, and no precautions were taken to exclude water. Column chromatography was performed using EMD Millipore 60 Å (0.040–0.063 mm) mesh silica gel (SiO_2). Analytical thin-layer chromatography (TLC) was performed on Merck silica gel 60 F254 TLC plates. Visualization was accomplished with UV (210 nm), and potassium permanganate (KMnO_4) or *p*-anisaldehyde staining solutions.

^1H NMR and ^{13}C NMR spectra were recorded at 298 K on Bruker GN500 (500 MHz, ^1H ; 125 MHz, ^{13}C) and Bruker CRYO500 (500 MHz, ^1H ; 125 MHz, ^{13}C) spectrometers. ^1H and ^{13}C spectra were referenced to residual chloroform (7.26 ppm, ^1H ; 77.00 ppm, ^{13}C) or

residual methanol (3.31 ppm¹H; 49.00, ppm ¹³C). Chemical shifts are reported in ppm and multiplicities are indicated by: s (singlet), d (doublet), t (triplet), q (quartet), p (pentet), hept (heptet), m (multiplet), and br s (broad singlet). Coupling constants are reported in Hertz. The raw fid files were processed into the included NMR spectra using MestReNova 11.0, (Mestrelab Research S. L.). Infrared (IR) spectra were recorded on a Varian 640-IR instrument on NaCl plates and peaks are reported in cm⁻¹. Mass spectrometry data was obtained from the University of California, Irvine Mass Spectrometry Facility. High-resolution mass spectra (HRMS) were recorded on a Waters LCT Premier spectrometer using ESI-TOF (electrospray ionization-time of flight) or a Waters GCT Premier Micromass GC-MS (chemical ionization), and data are reported in the form of (*m/z*).

Note: Tricarbonyl-iron diene complexes are unstable when subjected to mass spectrometry ionization. No High-Resolution Mass Spectrometry Data was obtained for any iron-tricarbonyl complexed compounds.

6.7.2 Experimental Procedures

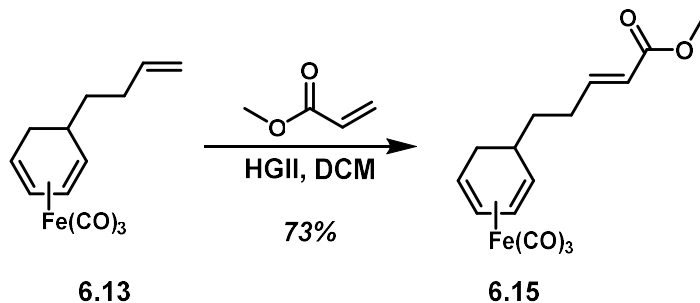


General Procedure A – Alkene cross metathesis to afford α,β -unsaturated esters: **Methyl (*E*)-4-iron-tricarbonyl[(1,2,3,4)-cyclohexa-2,4-dien-1-yl]but-2-enoate (6.12)** An oven-dried 2 dram scintillation vial was equipped with a magnetic stir bar and charged with **6.11** (4.0 mg, 15.4 μ mol, 1 equiv) and dry CH₂Cl₂ (0.1 mL). Methyl acrylate (3.8 mg, 46.2 μ mol, 3 equiv) and Hoyveda–Grubbs 2nd Generation

Catalyst (0.9 mg, 1.5 μ mol, 0.1 equiv) were added to the reaction mixture. The solution was sparged with argon gas for 5 minutes. The reaction mixture was stirred at room temperature for 16 h. The solvent was removed *in vacuo*. The residue was purified by chromatography on silica gel, eluting with hexanes/EtOAc 97:3 (v/v), to afford 3.5 mg (72% yield) **6.12** as a yellow oil.

$^1\text{H NMR}$ (600 MHz, CDCl_3) δ 6.88 – 6.76 (m, 1H), 5.77 (J_d, 15.7 Hz, 1H), 5.38 (s, 1H), 5.30 (s, 1H), 3.73 (s, 3H), 3.05 (J_d, 13.8 Hz, 2H), 2.27 (s, 1H), 2.18 – 2.05 (m, 2H), 2.02 (J_d, 9.2 Hz, 1H), 0.92 (m, 1H).

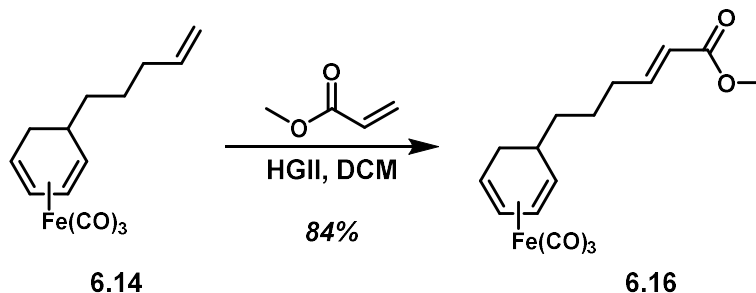
$^{13}\text{C NMR}$ (151 MHz, CDCl_3) δ 211.9, 166.9, 147.4, 122.3, 85.9, 84.5, 65.5, 59.6, 51.5, 42.2, 37.3, 30.3.



Methyl (E)-5-iron-tricarbonyl[(1,2,3,4-cyclohexa-2,4-dien-1-yl)]pent-2-enoate (6.15) Alkene **6.13** (13 mg, 47.4 μ mol) was subjected to *General Procedure A* to give ester **6.15** (11 mg, 73% yield) as a yellow oil.

$^1\text{H NMR}$ (500 MHz, CDCl_3) δ 6.96 – 6.83 (m, 1H), 5.78 (J_d, 15.6 Hz, 1H), 5.41 – 5.33 (m, 1H), 5.33 – 5.23 (m, 1H), 3.72 (s, 3H), 3.15 – 2.98 (m, 2H), 2.13 – 2.06 (m, 2H), 2.10 – 2.05 (m, 1H), 2.01 (dd, 14.4, 10.5, 3.8 Hz, 1H), 1.39 (dt, = 5.7, 4.8 Hz, 1H), 1.33 – 1.26 (m, 1H).

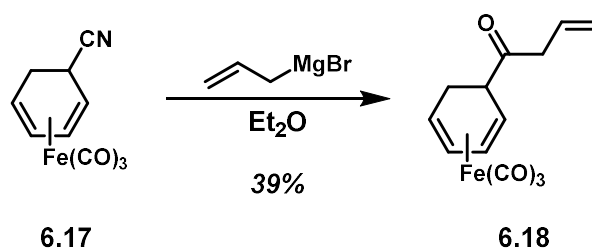
$^{13}\text{C NMR}$ (126 MHz, CDCl_3) δ 212.1, 167.1, 149.0, 121.0, 85.7, 84.5, 66.0, 59.7, 51.5, 38.2, 37.7, 31.0, 30.8



Methyl (E)-6-iron-tricarbonyl[(1,2,3,4)-cyclohexa-2,4-dien-1-yl]hex-2-enoate (6.16) Alkene **6.14** (16 mg, 55.5 μmol) was subjected to *General Procedure A* to give ester **6.16** (16 mg, 84% yield) as a yellow oil.

$^1\text{H NMR}$ (499 MHz, CDCl_3) δ 6.98 – 6.83 (m, 1H), 5.79 (*J* = 15.7 Hz, 1H), 5.35 (*d*, = 4.7 Hz, 1H), 5.27 (*d*, *J* = 5.2 Hz, 1H), 3.72 (s, 3H), 3.06 (*J* = 33.5 Hz, 2H), 2.14 (*q*, = 7.1 Hz, 2H), 2.09 – 1.92 (m, 2H), 1.39 (s, 2H), 1.28 – 1.16 (m, 3H).

$^{13}\text{C NMR}$ (151 MHz, CDCl_3) δ 212.2, 167.1, 149.2, 121.1, 85.6, 84.6, 66.7, 59.9, 51.5, 39.5, 38.1, 32.3, 30.7, 26.7.

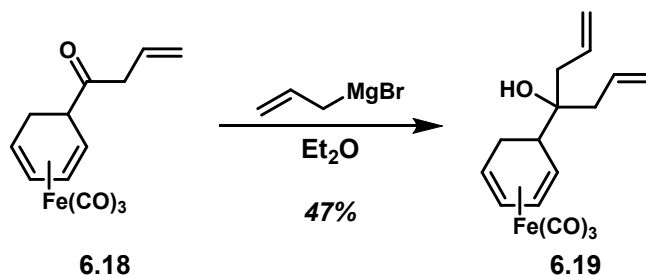


1-Iron-tricarbonyl[(1,2,3,4)-cyclohexa-2,4-dien-1-yl]but-3-en-1-one (6.18) A 10 mL round bottom flask was charged with **6.17** (138 mg, 0.56 mmol, 1 equiv) and diethyl ether (1.7 mL). The reaction flask was cooled to 0 °C. A 1.0 M solution of allyl magnesium bromide in diethyl ether (0.85 mL, 0.84 mmol, 1.5 equiv) was added to the reaction mixture dropwise. The reaction was allowed to warm to room temperature and stirred for 4 hours. 1.0 M $\text{HCl}_{(\text{aq})}$ (3 mL) was added and the resulting mixture was

stirred for 30 minutes. The phases were separated, and the aqueous phase was extracted with diethyl ether (2 x 3 mL). The organic phases were combined, dried over Na_2SO_4 , and concentrated *in vacuo*. The residue was purified by chromatography on silica gel, eluting with hexanes/EtOAc 95:5 (v/v), to afford 63 mg (39 % yield) of **6.18** as a yellow oil.

$^1\text{H NMR}$ (500 MHz, CDCl_3) δ 5.87 (ddt, = 17.1, 10.2, 6.9 Hz, 1H), 5.44 – 5.39 (m, 2H), 5.22 – 5.15 (m, 1H), 5.12 (dq, = 17.1, 1.5 Hz, 1H), 3.24 – 3.12 (m, 3H), 3.07 (dt, 10.8, 3.5 Hz, 1H), 3.04 – 3.00 (m, 1H), 2.00 (ddd, = 14.6, 10.8, 3.5 Hz, 1H), 1.86 (dt, = 15.2, 2.4 Hz, 1H).

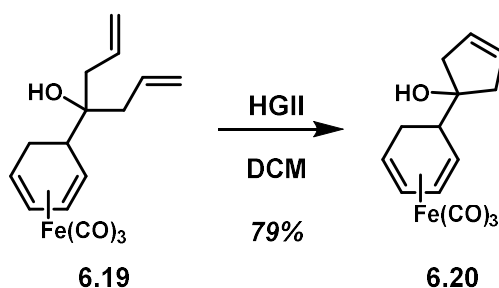
$^{13}\text{C NMR}$ (126 MHz, CDCl_3) δ 211.3, 208.4, 130.5, 118.9, 86.9, 84.2, 60.8, 58.4, 49.8, 46.0, 27.8.



4-Iron-tricarbonyl[(1,2,3,4)-cyclohexa-2,4-dien-1-yl]hepta-1,6-dien-4-ol (6.19): A 10 mL round bottom flask was charged with **6.18** (30 mg, 0.10 mmol, 1 equiv) and diethyl ether (0.3 mL). The reaction flask was cooled to 0 °C. A 1.0 M solution of allyl magnesium bromide in diethyl ether (0.12 mL, 0.12 mmol, 1.2 equiv) was added to the reaction mixture dropwise. The reaction was allowed to warm to room temperature and stirred for 2 hours. Saturated aqueous ammonium chloride (0.5 mL) was added. The phases were separated, and the aqueous phase was extracted with diethyl ether (2 x 1 mL). The organic phases were combined, dried over Na_2SO_4 , and concentrated *in vacuo*. The residue was purified by chromatography on silica gel, eluting with hexanes/EtOAc 95:5 (v/v), to afford 16 mg (47 % yield) of **6.19** as a yellow oil.

$^1\text{H NMR}$ (500 MHz, CDCl_3) δ 5.94 – 5.79 (m, 2H), 5.54 – 5.47 (m, 1H), 5.47 – 5.39 (m, 1H), 5.24 – 5.12 (m, 4H), 3.12 (dd, = 5.2, 2.7 Hz, 2H), 2.40 (dt, = 10.8, 3.7 Hz, 1H), 2.35 – 2.24 (m, 2H), 2.20 (dd, = 14.0, 7.4 Hz, 1H), 2.11 (dd, = 14.0, 7.7 Hz, 1H), 1.95 (ddd, = 14.9, 11.0, 3.9 Hz, 1H), 1.58 (d, = 15.5 Hz, 1H), 1.53 (s, 1H).

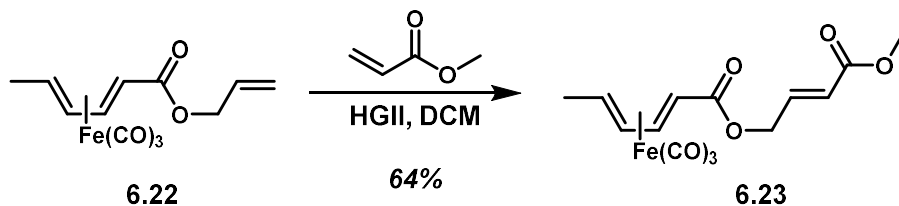
$^{13}\text{C NMR}$ (126 MHz, CDCl_3) δ 212.0, 133.5, 133.5, 119.1, 119.0, 86.0, 85.2, 75.7, 60.5, 59.9, 46.3, 42.3, 41.6, 25.8.



General Procedure B – Alkene ring-closing metathesis to afford carbocycles: **1-Iron-tricarbonyl[(1,2,3,4- η)-cyclohexa-2,4-dien-1-yl]cyclopent-3-en-1-ol (6.20)**: An oven-dried 2 dram scintillation vial was equipped with a magnetic stir bar and charged with **6.19** (16 mg, 48.5 μmol , 1 equiv) and dry CH_2Cl_2 (1.0 mL). Hoyveda-Grubbs 2nd Generation Catalyst (3 mg, 4.9 μmol , 0.1 equiv) was added to the reaction mixture. The solution was sparged with argon gas for 5 minutes. The reaction mixture was stirred at room temperature for 16 h. The solvent was removed *in vacuo*. The residue was purified by chromatography on silica gel, eluting with hexanes/EtOAc 95:5 (v/v), to afford 11 mg (79% yield) **6.20** as a yellow oil.

$^1\text{H NMR}$ (600 MHz, CDCl_3) δ 5.66 (s, 2H), 5.46 – 5.38 (m, 2H), 3.07 (dd, = 8.0, 4.0, 2.0 Hz, 2H), 2.46 (d, = 17.1 Hz, 1H), 2.40 – 2.32 (m, 2H), 2.26 (dd, = 16.3 Hz, 1H), 2.16 (d, = 16.6 Hz, 1H), 1.95 (ddd, = 14.9, 10.8, 4.0 Hz, 1H), 0.93 – 0.78 (m, 2H).

¹³C NMR (126 MHz, CDCl₃) δ 212.0, 128.8, 128.5, 85.9, 85.3, 83.2, 61.4, 60.1, 48.2, 46.5, 45.8, 29.8, 26.9.

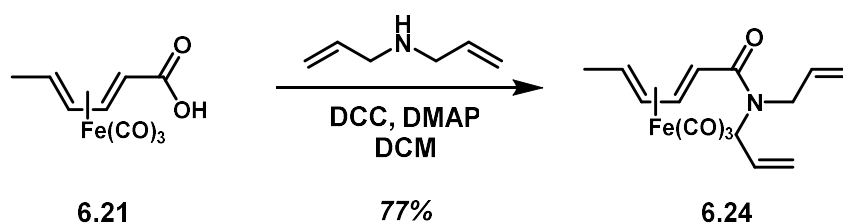


(E)-4-Methoxy-4-oxobut-2-en-1-yl-iron-tricarbonyl[(1,2,3,4)-(2E,4E)-hexa-2,4-dienoate] (6.23): ~~6.22~~

(21 mg, 71.9 μmol) was subjected to *General Procedure A* to afford ester **6.23** (16 mg, 64% yield) as a yellow oil.

¹H NMR (500 MHz, CDCl₃) δ 6.94 (dt, = 15.8, 4.5 Hz, 1H), 6.03 (dt, = 15.7, 1.8 Hz, 1H), 5.79 (dd, = 8.0, 5.0 Hz, 1H), 5.26 – 5.20 (m, 1H), 4.77 (ddd, = 16.2, 4.5, 1.9 Hz, 1H), 4.67 (ddd, = 16.2, 4.5, 1.9 Hz, 1H), 3.75 (s, 3H), 1.48 (s, 3H), 1.00 (s, 1 Hz, 1H), 0.87 (d, = 6.9 Hz, 1H).

¹³C NMR (126 MHz, CDCl₃) δ 171.7, 166.3, 141.7, 121.6, 88.6, 82.7, 62.5, 59.5, 51.8, 44.8, 19.2.



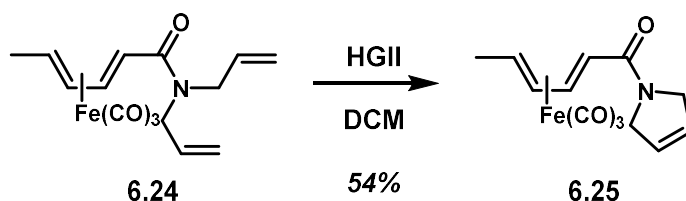
(E)-N,N-Diallylhexa-iron-tricarbonyl[(1,2,3,4)-2,4-dienamide] (6.24): A 2 dram scintillation vial

was charged with carboxylic acid **6.21** (30 mg, 0.10 mmol, 1 equiv) and CH₂Cl₂ (0.5 mL). To this solution was added diallylamine (13 mg, 0.11 mmol, 1.1 equiv), DCC (28 mg, 0.11 mmol, 1.1 equiv) and DMAP (2 mg, 0.01 mmol, 0.1 equiv). The reaction mixture was stirred at room temperature for 12 h. Saturated aqueous ammonium chloride (1 mL) was added. The phases were separated and the aqueous phase was

extracted with CH₂Cl₂ (1 mL). The combined organic extracts were dried over Na₂SO₄ and concentrated *in vacuo*. The residue was purified by chromatography on silica gel, eluting with hexanes/EtOAc 90:10 (v/v), to afford 30 mg (77% yield) **6.24** as a clear yellow oil.

¹H NMR (500 MHz, CDCl₃) δ 6.01 – 5.94 (m, 1H), 5.83 – 5.65 (m, 2H), 5.25 (J = 8.7, 5.2 Hz, 1H), 5.21 – 5.04 (m, 4H), 4.35 – 4.24 (m, 1H), 4.08 (J = 7.4 Hz, 1H), 3.77 (d, = 17.6 Hz, 1H), 3.61 (dd, = 15.3, 6.3 Hz, 1H), 1.45 (d, = 6.2 Hz, 3H), 1.01 (d, = 7.7 Hz, 2H).

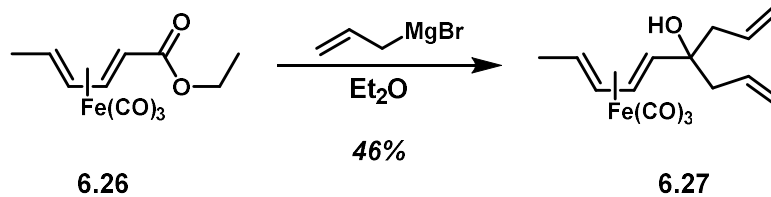
¹³C NMR (126 MHz, CDCl₃) δ 171.0, 133.3, 133.3, 116.9, 116.6, 88.6, 83.5, 58.9, 49.1, 48.4, 46.1, 19.2.



(*E*,*E*)-1-(2,5-Dihydro-1H-pyrrol-1-yl)hexa-iron-tricarbonyl[(1,2,3,4-*E*-2,4-dien]-1-one (**6.25**):Amide **6.24** (30 mg, 90 μmol) was subjected to *General Procedure B* to afford **6.25** (15 mg, 54% yield) as a yellow oil.

¹H NMR (600 MHz, CDCl₃) δ 6.01 (dd, = 7.2, 5.6 Hz, 1H), 5.94 (d, = 6.2 Hz, 1H), 5.87 (d, = 6.3 Hz, 1H), 5.32 (dd, = 8.6, 5.1 Hz, 1H), 4.40 – 4.21 (m, 4H), 1.53 (J = 6.1 Hz, 3H), 1.47 – 1.41 (m, 1H), 1.02 (J = 7.8 Hz, 1H).

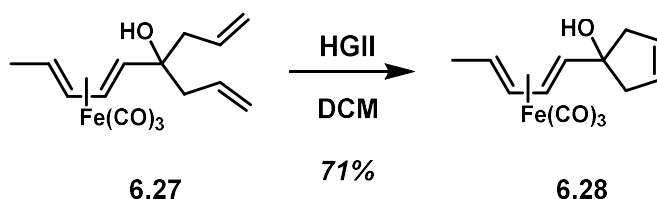
¹³C NMR (151 MHz, CDCl₃) δ 169.0, 126.5, 124.8, 88.3, 82.6, 58.8, 53.3, 52.9, 47.1, 19.2.



1-((E,3E)-Penta-iron-tricarbonyl[(1,2,3,4)-1,3-dien]-1-yl)-6,8-dien-5-ol (6.27) A 10 mL round bottom flask was charged with **6.26** (50 mg, 0.17 mmol, 1 equiv) and diethyl ether (1.0 mL). The reaction flask was cooled to 0 °C. A 1.0 M solution of allyl magnesium bromide in diethyl ether (0.45 mL, 0.43 mmol, 2.5 equiv) was added to the reaction mixture dropwise. The reaction was allowed to warm to room temperature and stirred for 2 hours. Saturated aqueous ammonium chloride (1 mL) was added. The extracts were separated, and the aqueous phase was extracted two times with diethyl ether (2 x 1 mL). The organic phases were combined, dried over Na₂SO₄, and concentrated *in vacuo*. The residue was purified by chromatography on silica gel, eluting with hexanes/EtOAc 95:5 (v/v), to afford 26 mg (46% yield) of **6.27** as a yellow oil.

¹H NMR (499 MHz, CDCl₃) δ 5.94 – 5.78 (m, 2H), 5.28 (dd, 8.8, 5.0 Hz, 1H), 5.23 – 5.13 (m, 3H), 5.11 – 5.00 (m, 2H), 2.42 – 2.14 (m, 4H), 1.41 (t, 6.2 Hz, 3H), 1.05 – 0.99 (m, 2H).

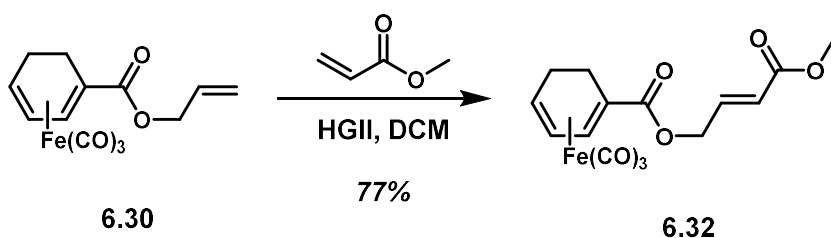
¹³C NMR (126 MHz, CDCl₃) δ 133.4, 132.9, 119.9, 119.4, 83.9, 79.9, 73.4, 72.0, 56.8, 48.4, 46.8, 19.1.



1-((E,3E)-Penta-iron-tricarbonyl[(1,2,3,4)-1,3-dien]-1-yl)cyclopent-3-en-1-ol (6.28) Alcohol **6.27** (26 mg, 81.3 μmol) was subjected to *General Procedure B* to afford **6.28** (17 mg, 71% yield) as a yellow oil.

¹H NMR (499 MHz, CDCl₃) δ 5.69 (s, 2H), 5.40 (dt, 8.8, 5.2 Hz, 1H), 5.05 (dd, = 8.7, 5.1 Hz, 1H), 2.52 (ddd, = 54.8, 50.1, 17.7 Hz, 4H), 1.41 (d, = 6.2 Hz, 3H), 1.21 (d, = 8.8 Hz, 1H), 1.05 (dq, = 12.8, 6.4 Hz, 1H).

¹³C NMR (126 MHz, CDCl₃) δ 129.3, 128.7, 84.3, 81.2, 79.8, 71.7, 57.0, 51.0, 50.4, 19.2.

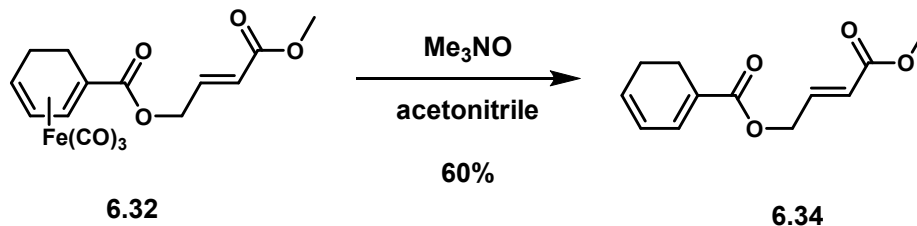


(E)-4-Methoxy-4-oxobut-2-en-1-yl-iron-tricarbonyl[(1,2,3,4)-cyclohexa-1,3-diene]-1-carboxylate

(**6.32**) Ester **6.30** (92 mg, 0.31 mmol) was subjected to *General Procedure A* to afford **6.32** (83 mg, 77% yield) as a yellow oil.

¹H NMR (500 MHz, CDCl₃) δ 6.97 (dt, = 15.8, 4.5 Hz, 1H), 6.11 – 6.00 (m, 2H), 5.44 – 5.32 (m, 1H), 4.85 (ddd, = 16.1, 4.4, 1.7 Hz, 1H), 4.69 (ddd, = 16.2, 4.4, 1.8 Hz, 1H), 3.75 (s, 3H), 3.44 – 3.37 (m, 1H), 2.23 – 2.15 (m, 1H), 1.98 – 1.90 (m, 1H), 1.76 – 1.68 (m, 1H), 1.46 (J = 14.6, 8.5, 3.4 Hz, 1H).

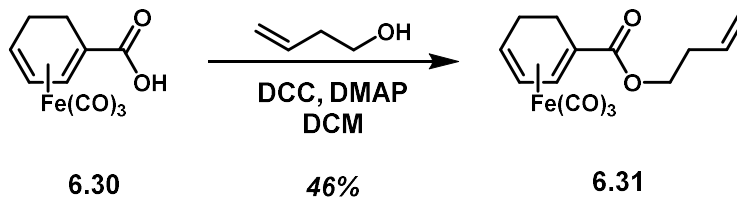
¹³C NMR (126 MHz, CDCl₃) δ 210.2, 171.6, 166.3, 141.7, 121.7, 88.5, 85.5, 63.9, 63.5, 62.7, 51.8, 25.2, 22.9.



(E)-4-Methoxy-4-oxobut-2-en-1-yl cyclohexa-1,3-diene-1-carboxylate (6.34) A 2 dram scintillation vial was charged with **6.32** (32 mg, 88 μmol , 1 equiv) and acetonitrile (0.5 mL). The reaction flask was cooled to 0 °C before adding trimethylamine *N*-oxide (66 mg, 0.88 mmol, 10 equiv). The reaction mixture was warmed to room temperature and stirred for 4 h. The reaction mixture was diluted with CH_2Cl_2 (1 mL) and washed with water (2 x 1 mL). The organic phase was dried over Na_2SO_4 and concentrated *in vacuo*. The residue was purified by chromatography on silica gel, eluting with hexanes/EtOAc 95:5 (v/v), to afford 12 mg (60% yield) of **6.34** as a clear colorless oil.

$^1\text{H NMR}$ (500 MHz, CDCl_3) δ 7.07 (*d*, $J = 5.5$ Hz, 1H), 7.00 (*dt*, $J = 15.7, 4.4$ Hz, 1H), 6.17 (*dd*, $J = 9.3, 4.7$ Hz, 1H), 6.07 (*dd*, $J = 15.5, 10.8$ Hz, 2H), 4.83 (*dd*, $J = 4.2, 1.6$ Hz, 2H), 3.75 (*s*, 3H), 2.47 (*t*, $J = 9.6$ Hz, 2H), 2.29 (*dd*, $J = 5.8, 3.9$ Hz, 2H).

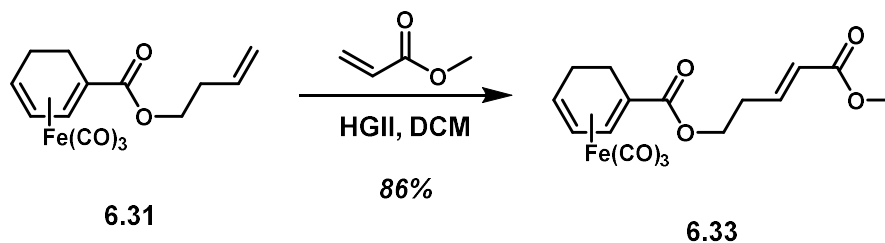
$^{13}\text{C NMR}$ (126 MHz, CDCl_3) δ 166.6, 166.4, 142.0, 134.2, 134.2, 129.8, 128.6, 123.9, 121.5, 62.5, 51.8, 22.9, 20.7.



But-3-en-1-yl iron-tricarbonyl[(1,2,3,4)-cyclohexa-1,3-diene]-1-carboxylate (6.31) A 10 mL round bottom flask was charged with carboxylic acid **6.30** (100 mg, 0.38 mmol, 1 equiv), CH_2Cl_2 (2 mL), and 1-buten-3-ol (30 mg, 0.42 mmol, 1.1 equiv). To this solution was added DCC (86 mg, 0.42 mmol, 1.1 equiv) and DMAP (5 mg, 0.04 mmol, 0.1 equiv). The reaction was stirred at room temperature for 16 h. Saturated aqueous ammonium chloride (3 mL) was added, and the resultant solution was extracted with CH_2Cl_2 (3 x 3 mL). The combined organic extracts were dried over Na_2SO_4 and concentrated *in vacuo*. The residue was purified by chromatography on silica gel, eluting with hexanes/EtOAc 95:5 (v/v), to afford 55 mg (46% yield) **6.31** as a clear colorless oil.

$^1\text{H NMR}$ (600 MHz, CDCl_3) δ 6.03 (d, $J = 3.8$ Hz, 1H), 5.80 (dd, $J = 17.0, 10.1$ Hz, 1H), 5.39 – 5.32 (m, 1H), 5.10 (dd, $J = 26.3, 13.6$ Hz, 2H), 4.24 (dt, $J = 11.0, 6.8$ Hz, 1H), 4.11 – 4.03 (m, 1H), 2.40 (dd, $J = 13.2, 6.5$ Hz, 2H), 2.16 (dd, $J = 19.4, 7.2$ Hz, 1H), 1.92 (dd, $J = 11.6, 7.8$ Hz, 2H), 1.56 (d, $J = 12.5$ Hz, 1H), 1.46 – 1.38 (m, 1H).

$^{13}\text{C NMR}$ (151 MHz, CDCl_3) δ 210.3, 172.1, 134.2, 117.2, 88.5, 88.4, 85.2, 85.1, 64.9, 63.6, 63.2, 35.0, 33.1, 25.5, 25.2, 22.9.

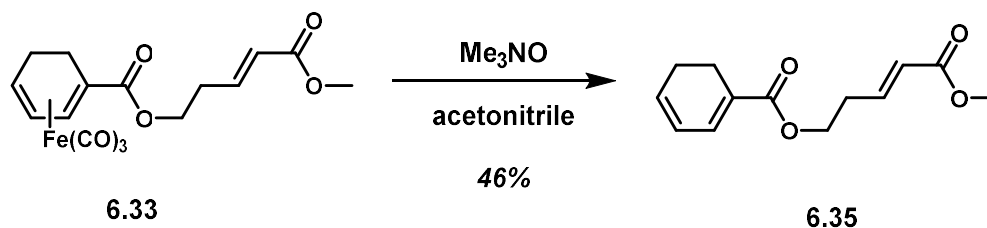


(E)-5-Methoxy-5-oxopent-3-en-1-yl-iron-tricarbonyl[(1,2,3,4)-cyclohexa-1,3-diene]-1-carboxylate

6.33 Ester **6.31** (55 mg, 0.17 mmol) was subjected to *General Procedure A* to afford **6.33** (56 mg, 86% yield) as a yellow oil.

¹H NMR (500 MHz, CDCl₃) δ 6.94 (dt, = 15.6, 6.9 Hz, 1H), 6.01 (d, = 4.2 Hz, 1H), 5.92 (d, = 15.7 Hz, 1H), 5.40 – 5.29 (m, 1H), 4.29 (dt, = 11.1, 6.5 Hz, 1H), 4.19 – 4.09 (m, 1H), 3.73 (J, = 7.3 Hz, 3H), 3.38 (dd, = 3.7, 2.7 Hz, 1H), 2.62 – 2.49 (m, 2H), 2.14 (ddd, = 15.0, 11.9, 3.2 Hz, 1H), 1.91 (ddt, = 15.4, 11.8, 3.6 Hz, 1H), 1.72 – 1.63 (m, 1H), 1.41 (ddd, = 14.8, 8.4, 3.5 Hz, 1H).

¹³C NMR (126 MHz, CDCl₃) δ 210.2, 172.0, 166.7, 144.6, 123.2, 88.5, 85.3, 64.4, 63.4, 62.4, 51.6, 31.5, 25.2, 22.9.



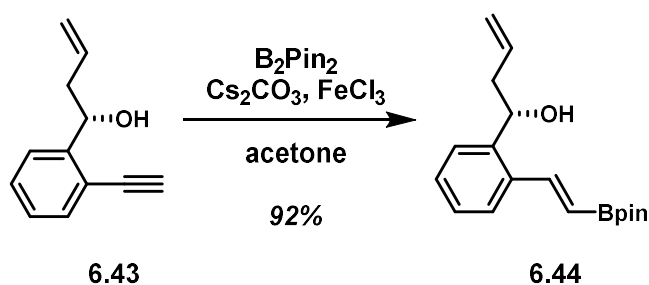
(E)-5-Methoxy-5-oxopent-3-en-1-yl cyclohexa-1,3-diene-1-carboxylate (6.35)

A 2 dram scintillation vial was charged with **6.33** (44 mg, 0.12 mmol, 1 equiv) and acetonitrile (0.5 mL). The reaction flask was cooled to 0 °C before adding trimethylamine *N*-oxide (85 mg, 1.2 mmol, 10 equiv). The reaction mixture was warmed to room temperature and stirred for 4 h. The reaction mixture was diluted with CH₂Cl₂ (1 mL) and washed with water (2 x 1 mL). The organic phase was dried over Na₂SO₄ and concentrated *in vacuo*.

vacuo. The residue was purified by chromatography on silica gel, eluting with hexanes/EtOAc 95:5 (v/v), to afford 12 mg (46% yield) **6.35** as a clear colorless oil.

¹H NMR (600 MHz, CDCl₃) δ 7.00 – 6.97 (m, 1H), 6.96 – 6.91 (m, 1H), 6.14 (J = 15.7 Hz, 1H), 6.08 – 6.04 (m, 1H), 5.93 (J = 15.7 Hz, 1H), 4.27 (t, J = 6.4 Hz, 2H), 3.74 (s, 3H), 2.59 (J = 6.5 Hz, 2H), 2.43 (t, J = 10.0 Hz, 2H), 2.27 (dd, J = 10.4, 2.9 Hz, 2H).

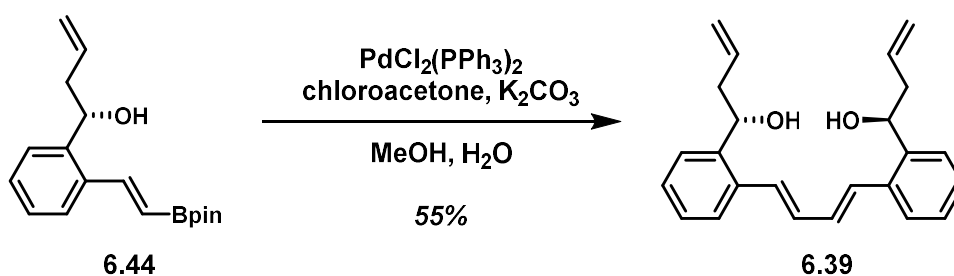
¹³C NMR (151 MHz, CDCl₃) δ 167.3, 166.7, 144.7, 133.8, 133.6, 128.5, 124.0, 123.1, 62.2, 51.6, 31.6, 22.9, 20.7.



(S,E)-1-(2-(2-(4,4,5,5-Tetramethyl-1,3,2-dioxaborolan-2-yl)vinyl)phenyl)but-3-en-1-ol (**6.44**) dram scintillation vial was charged with alkyne **6.43** (50 mg, 0.29 mmol, 1 equiv) and acetone (2 mL). To the solution was added bis(pinacolato)diboron (110 mg, 0.44 mmol, 1.5 equiv), cesium carbonate (189 mg, 0.58 mmol, 2 equiv), and iron trichloride (5 mg, 0.03 mmol, 0.1 equiv). The reaction mixture was heated to 60 °C and was stirred at this temperature for 16 h. The reaction mixture was diluted with EtOAc (5 mL) and was filtered through a pad of celite. The solids were washed with EtOAc (5 mL). The organic phases were combined and washed with water (5 mL). The organic phase was dried over Na_2SO_4 and concentrated *in vacuo*. The residue was purified by chromatography on silica gel, eluting with hexanes/EtOAc 96:4 (v/v), to afford 80 mg (92% yield) **6.44** as a clear colorless oil.

$^1\text{H NMR}$ (600 MHz, CDCl_3) δ 7.71 (d , J = 18.0 Hz, 1H), 7.53 (d , J = 6.9 Hz, 2H), 7.32 (dd , J = 24.7, 17.3 Hz, 2H), 6.05 (d , J = 18.1 Hz, 1H), 5.86 (dq , J = 10.0, 7.3 Hz, 1H), 5.21 – 5.13 (m , 3H), 2.57 – 2.40 (m , 2H), 1.31 (s , 12H).

$^{13}\text{C NMR}$ (151 MHz, CDCl_3) δ 146.3, 141.5, 135.7, 134.6, 131.0, 128.9, 127.6, 126.5, 125.4, 118.5, 83.4, 69.2, 43.2, 25.1, 24.9, 24.8.

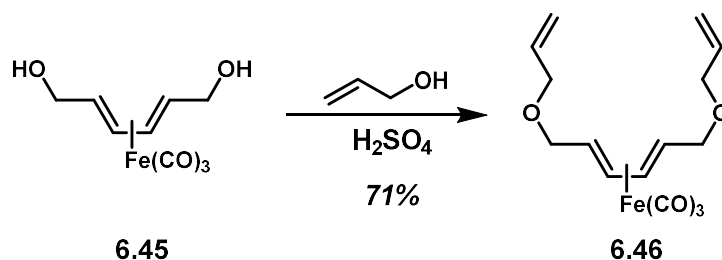


(*S,S'*)-1,1'-(*E,E'*-1,3-butadiene-1,4-diyl)bis(2,1-phenylene)bis(but-3-en-1-ol) (**6.39**)
 A scintillation vial was charged with boronic ester **6.44** (80 mg, 0.27 mmol, 1 equiv) and methanol (2.5 mL). To the solution was added chloroacetone (245 mg, 2.7 mmol, 10 equiv), bis(triphenylphosphine)palladium(II) dichloride (19 mg, 0.03 mmol, 0.1 equiv), and K_2CO_3 (110 mg, 0.81 mmol, 3 equiv) in H_2O (0.5 mL) was added dropwise. The reaction mixture was stirred at room temperature for 16 h. The reaction mixture was quenched with a saturated aqueous solution of ammonium chloride (3 mL) and the solution was extracted three times with CH_2Cl_2 (3 x 3 mL). The organic extracts were combined, dried over Na_2SO_4 and concentrated *in vacuo*. The residue was purified by chromatography on silica gel, eluting with hexanes/EtOAc 90:10 (v/v), to afford 50 mg (55% yield) of **6.39** as a clear colorless oil.

¹H NMR (500 MHz, CDCl₃) δ 7.66 – 7.62 (m, 2H), 7.60 – 7.56 (m, 2H), 7.39 – 7.33 (m, 4H), 7.06 (t, =dd, 12.0, 9.6 Hz, 2H), 7.00 – 6.91 (m, 2H), 5.94 (d, 10.0, 7.6 Hz, 2H), 5.25 (t, = 13.7 Hz, 4H), 5.18 (dd, = 8.3, 4.2 Hz, 2H), 2.66 – 2.50 (m, 4H).

¹³C NMR (126 MHz, CDCl₃) δ 140.95, 134.76, 134.62, 131.69, 129.66, 127.95, 127.63, 125.89, 125.81, 118.54, 69.86, 43.02.

HRMS (ES+) m/z calc'd for C₂₆H₂₆O₂ [M+Na]⁺: 369.1830; found: 369.1824.

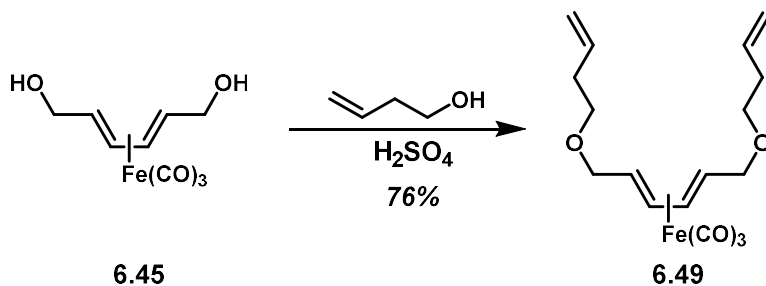


General Procedure C – Etherification to afford iron-hexa-2,4-diene diethers: (**(E,E)**-1,6-

Bis(allyloxy)hexa-iron-tricarbonyl[(E,E)-1,3,5-hexatriene (6.46) A 2 dram scintillation vial was charged with **6.45** (50 mg, 0.19 mmol, 1 equiv) and allyl alcohol (0.35 mL, 0.56 mmol, 30 equiv). A drop of conc. H₂SO₄ (2 mg) was added to the reaction mixture. The solution was stirred for 4 h. The solution was quenched with a saturated aqueous solution of sodium bicarbonate (1 mL) and was stirred for 5 min. The mixture was extracted with CH₂Cl₂ (3 x 1 mL). The organic extracts were combined, dried over Na₂SO₄, and concentrated *in vacuo*. The residue was purified by chromatography on silica gel, eluting with hexanes/EtOAc 100:0–94:6 (v/v), to afford 46 mg (71% yield) **6.46** as a yellow oil.

¹H NMR (600 MHz, CDCl₃) δ 5.90 (s, 1H), 5.28 (t, = 17.2 Hz, 1H), 5.20 (dd, = 20.9, 7.5 Hz, 2H), 3.97 (d, = 22.3 Hz, 2H), 3.60 (s, 1H), 3.39 (s, 1H), 1.22 (s, 1H).

¹³C NMR (151 MHz, CDCl₃) δ 134.6, 117.2, 84.3, 71.6, 71.5, 57.9.

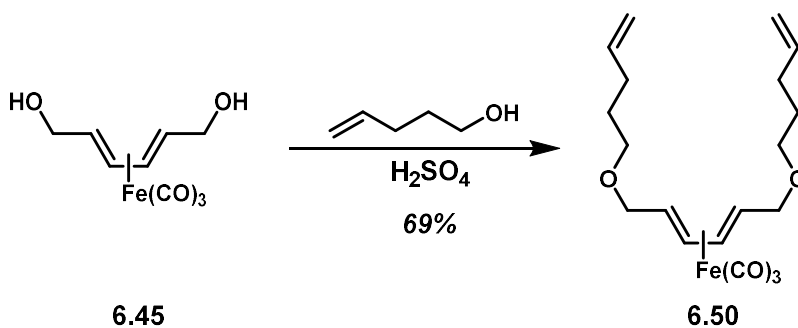


(*E*)-1,6-Bis(3-buten-1-yloxy)hexa-iron-tricarbonyl[(1*E*,2*Z*)-1,4-diene] (6.49) General Procedure

C was performed using **6.45** (51 mg, 0.19 mmol) and 3-butenol to afford **6.49** (54 mg, 76% yield) as a yellow oil.

$^1\text{H NMR}$ (500 MHz, CDCl_3) δ 5.82 (dd t , $J = 17.0, 10.2, 6.7$ Hz, 1H), 5.22 – 5.18 (m, 1H), 5.14 – 4.95 (m, 2H), 3.60 (dd t , $J = 11.1, 4.8$ Hz, 1H), 3.51 (dt, $J = 9.1, 6.7$ Hz, 1H), 3.45 – 3.40 (m, 1H), 3.38 (dd t , $J = 11.1, 7.6$ Hz, 1H), 2.36 – 2.29 (m, 2H), 1.22 – 1.17 (m, 1H).

$^{13}\text{C NMR}$ (126 MHz, CDCl_3) δ 135.2, 116.5, 84.2, 72.2, 70.0, 58.0, 34.3.



(*E*)-1,6-Bis(4-penten-1-yloxy)hexa-iron-tricarbonyl[(1*E*,2*Z*)-1,4-diene] (6.50) General Procedure

C was performed using **6.45** (110 mg, 0.41 mmol) and 4-pentenol to afford **6.50** (116 mg, 69% yield) as a yellow oil.

¹H NMR (499 MHz, CDCl₃) δ 5.80 (dd_t, = 16.9, 10.2, 6.6 Hz, 1H), 5.20 (q, = 4.2 Hz, 1H), 5.01 (d, = 17.1 Hz, 1H), 4.95 (d, = 10.1 Hz, 1H), 3.57 (dd, = 11.1, 4.9 Hz, 1H), 3.48 – 3.43 (m, 1H), 3.39 – 3.35 (m, 2H), 2.12 (dd, = 14.4, 7.1 Hz, 2H), 1.65 (dt, = 13.9, 6.8 Hz, 2H), 1.19 (dd, = 12.0, 6.9 Hz, 1H).

¹³C NMR (125 MHz, CDCl₃) δ 138.3, 114.8, 84.1, 72.2, 70.0, 58.3, 30.3, 28.9.

6.8 References

¹ Rheilen, H.; Gruhl, A.; Hessling, G. V.; Pfrengle, O. "Über Carbonyle und Nitrosyle." *Annalen* **1930**, *482*, 161.

² Hallam, C. F.; Pauson, P. L. "Metal Derivatives of Conjugated Dienes. Part I. Butadiene and Cyclohexadiene Iron Tricarbonyls." *J. Chem. Soc. London* **1958**, 642–645.

³ Lillya, C. P.; Sahatjian, R.A. "Protonated ketones as NMR models for organotransition metal cations." *J. Organometal. Chem.* **1971**, *32*, 371.

⁴ a) Howell, J. A. S.; Johnson, B. F. G.; Josty, P. L.; Lewis, J. "Synthesis and Reactions of Tetracarbonyl- and Tricarbonyliron Complexes of A,B-Unsaturated Ketones." *J. Organomet. Chem.* **1972**, *39*, 329–330; b) Evans, G.; Johnson, B. F. G.; Lewis, J. "Synthetic Studies Relating to Acetylgosterol- (Tricarbonyl)iron." *J. Organomet. Chem.* **1975**, *102*, 507–510; c) Knölker, H.-J.; Gonser, P. "Tricarbonyl(η^1 -aza-1,3-butadiene) iron Complexes as Iron Tricarbonyl Transfer Reagents: 1-Aza-1,3-butadiene-Catalyzed Transfer of the Iron Tricarbonyl Fragment and Complexation of 1,3-Dienes by Polymer-Supported Iron Tricarbonyl." *Synlett* **1992**, *6*, 517–520.

⁵ Saberi, S. P.; Salter, M. M.; Slawin, A. M.; Thomas, S. E.; Williams, D. J. "Iron(III)Chloride Oxidation of Tricarbonyl(Vinylketene)iron(0)-Alkyne Adducts." *Chem. Soc. Perkin Trans. 1* **1994**, *2*, 167–171.

⁶ a) Bretherick, L. *Handbook of Reactive Chemical Hazards* **1979**, *2*, 670–674; b) Bretherick, L. *Hazards in the Chemical Laboratory* **1981**, *3*, 421.

⁷ Knolker, H.-J.; Baum, E.; Gonser, P.; Rhode, G.; Rottele, H. "1,4-Diaryl-1-azabuta-1,3-diene-Catalyzed Complexation of Cyclohexa-1,3-diene by the Tricarbonyliron Fragment: Development of Highly Efficient Catalysts, Optimization of Reaction Conditions, and Proposed Mechanism." *Organometallics*, **1998**, *17*, 3916–3925.

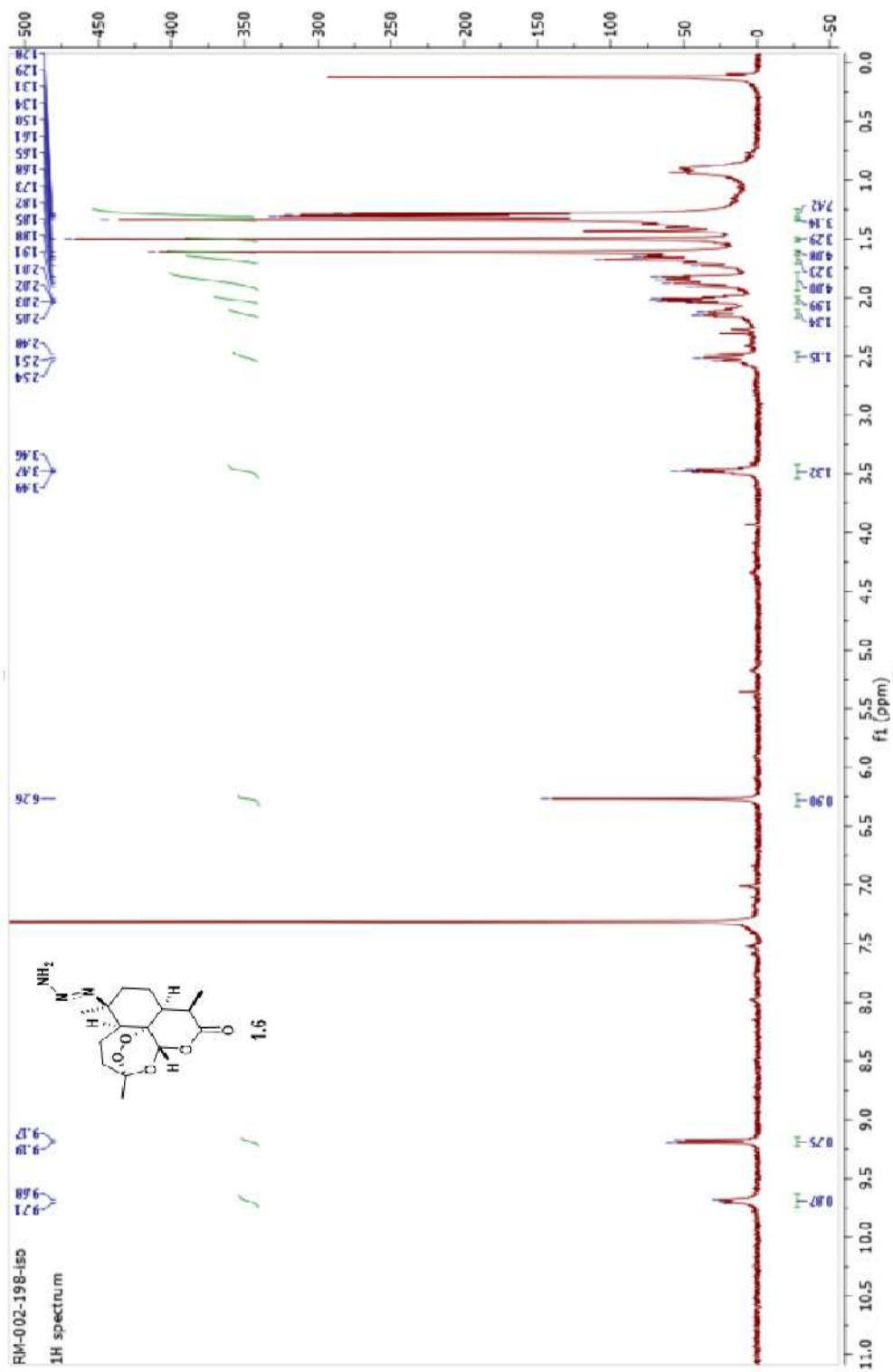
⁸ Knoelker, H.-J.; Baum, G.; Foitzik, N.; Goesmann, H.; Gonser, P.; Jones, P. G.; Rottele, H. "Synthesis, Molecular Structure, Fluxional Behavior, and Tricarbonyliron Transfer Reactions of (η^1 -Azabuta-1,3-diene)tricarbonyliron Complexes." *Eur. J. Inorg. Chem.* **1998**, *7*, 993–1007.

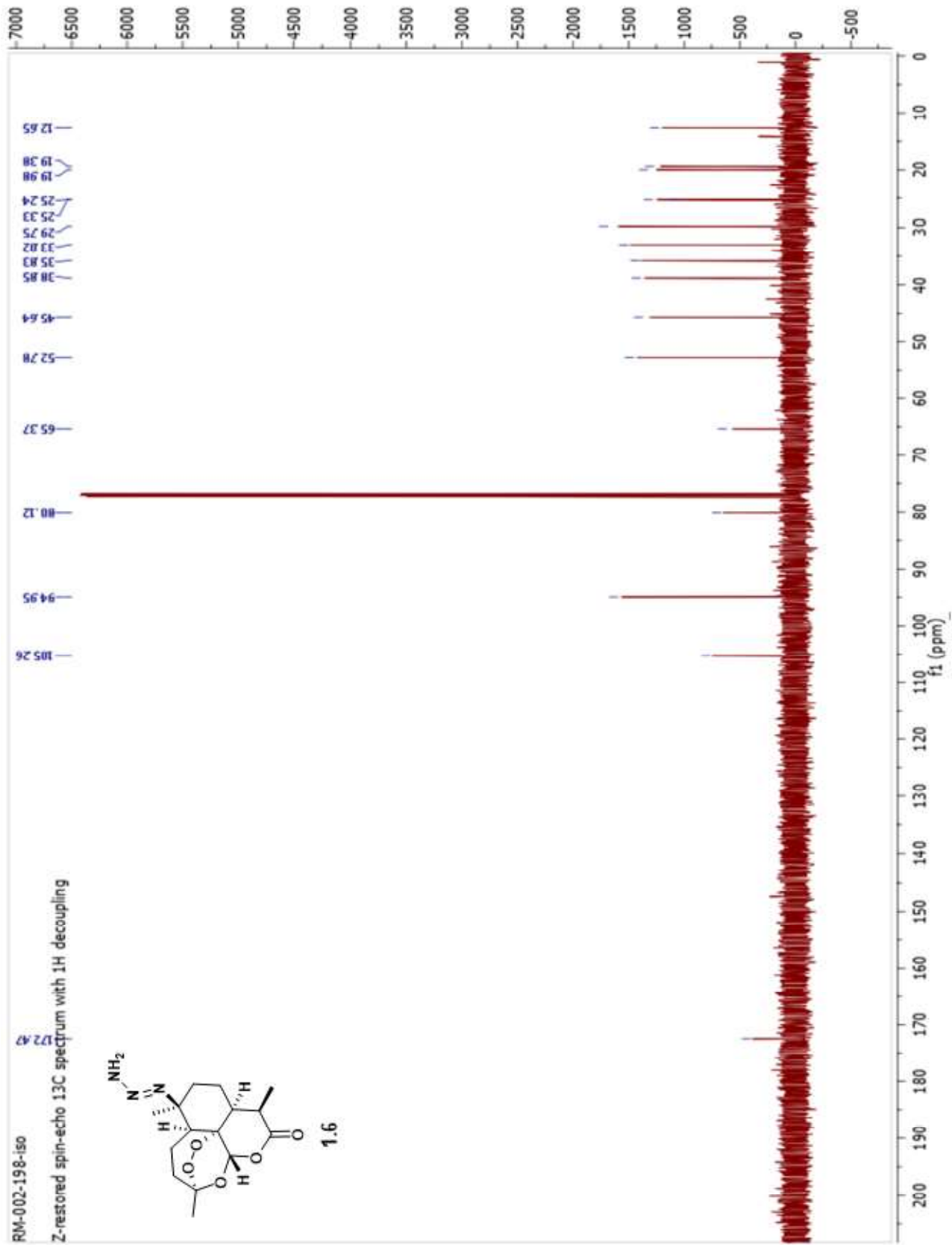
⁹ Maywald, F.; Eilbracht, P. "A Chiral 1-Aza-1,3-butadiene Tricarbonyliron Complex as Fe(CQ)Transfer Reagent for the Enantioselective Complexation of 1,3-Dienes." *Synlett* **1996**, *4*, 380–382.

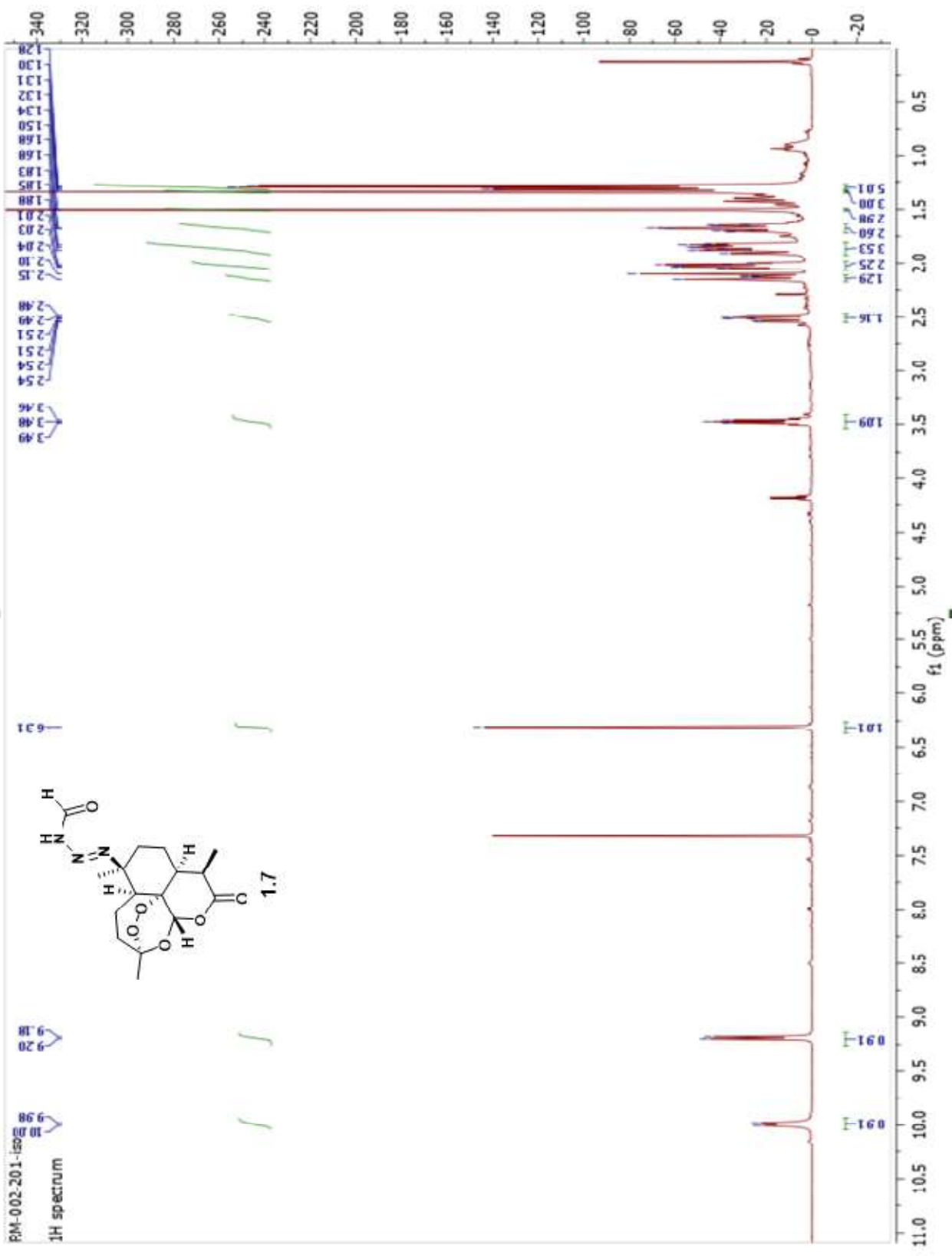
- ¹⁰ Ley, S. V.; Low, C. M. R.; White, A. D. "Application of Ultrasound to the Preparation of Tricarbonyliron Diene Complexes." *J. Organomet. Chem.* **1986**, *302*, 13–16.
- ¹¹ Banthorpe, D. V.; Fitton, H.; Lewis, J. "Isomerisation and Addition Reactions of Some Monoterpene–Tricarbonyliron Complexes." *J. Chem. Soc., Perkin Trans. 1* **1973**, 2051–2057.
- ¹² Y. Shvo, Y.; Hazum, E. "A Simple Method for the Disengagement of Organic Ligands from Iron Complexes." *J. Chem. Soc., Chem. Commun.*, **1974**, 336–337.
- ¹³ Adam, W.; Schuhmann, R. M. "Iron Tricarbonyl Complexes in Oxidation Chemistry: Regio- and Stereoselective Oxyfunctionalization of Trienes by Singlet Oxygen and Dimethyldioxirane." *J. Org. Chem.* **1996**, *61*, 874–878.
- ¹⁴ Adam, W.; Schuhmann, R. M. "Selective Oxyfunctionalization of (Tricarbonylcyclohexadiene)iron-Substituted Furans with Singlet Oxygen and Dimethyldioxirane." *Liebigs Annalen* **1996**, *4*, 635–640.
- ¹⁵ Fischer, E. O.; Fischer, R. D. "Ein Cyclohexadienyl-eisen-tricarbonyl-Kation." *Angew. Chem.*, **1960** *72*, 919–920.
- ¹⁶ Mahler, J. E.; Pettit, R. "Organo-Iron Complexes. II. π -Pentadienyl- and π -1,5-Dimethylpentadienyliron Tricarbonyl Cations." *J. Am. Chem. Soc.* **1963**, *85*, 3955–3959.
- ¹⁷ a) Graf, R. E.; Lillya, C. P. "Reactivity of Tricarbonyl(diene)iron Compounds Toward Electrophiles and Charge Distribution In Tricarbonyl(π -Allyl)Iron Cations." *J. Am. Chem. Soc.* **1972**, *94*, 8282–8283; b) Graf, R. E.; Lillya, C. P. "Speed Liquid Chromatographic Analysis of Organo-iron Compounds." *J. Organometal. Chem.* **1973**, *47*, 413–416.
- ¹⁸ Birch, A. J.; Cross, P. E.; Lewis, J.; White, D. A.; Wild, S. B. "The Chemistry of Co-Ordinated Ligands. Part II. Iron Tricarbonyl Complexes of Some Cyclohexadienes." *J. Chem. Soc.* **1968**, 332–340.
- ¹⁹ Pearson, A. J. "Tricarbonyl(diene)iron Complexes: Synthetically Useful Properties." *Acc. Chem. Res.* **1980**, *13*, 463–469.
- ²⁰ Pearson, A. J.; Raithby, P. R. "Organoiron Complexes in Organic Synthesis. Part 4. Direct Ring Connection Between Highly Substituted Centres. A Potential Approach to Trichothecane Synthesis." *J. Chem. Soc., Perkin Trans 1* **1980**, 395–399.
- ²¹ a) Donaldson, W. A.; Chaudhury, S. "Recent Applications of Acyclic (Diene)iron Complexes and (Dienyl)iron Cations in Organic Synthesis." *J. Org. Chem.* **2009**, *23*, 3831–3843; b) Knolker, H.-J.; Braier, A.; Brocher, D. J.; Cammerer, S.; Frohner, W.; Gonser, P.; Hermann, H.; Herzberg, D.; Reddy, K. R.; Rohde, G. "Recent Applications of Tricarbonyliron-diene Complexes to Organic Synthesis" *Pure Appl. Chem.* **2001**, *73*, 1075–1086; c) Palframan, M. J.; Kociok-Kohn, G.; Lewis, S. E. "Total Synthesis of (+)-Grandifloracin by Iron Complexation of a Microbial Arene Oxidation Product." *Org. Lett.* **2011**, *13*, 3150–3153; d) Roush, W. R.; Wada, C. K. "Application of h-4-Diene Iron Tricarbonyl Complexes in Acyclic Stereocontrol: Asymmetric Synthesis of the as-Indacene Unit of Ikarugamycin (A Formal Total Synthesis)" *J. Am. Chem. Soc.* **1994**, *116*, 2151–2152.

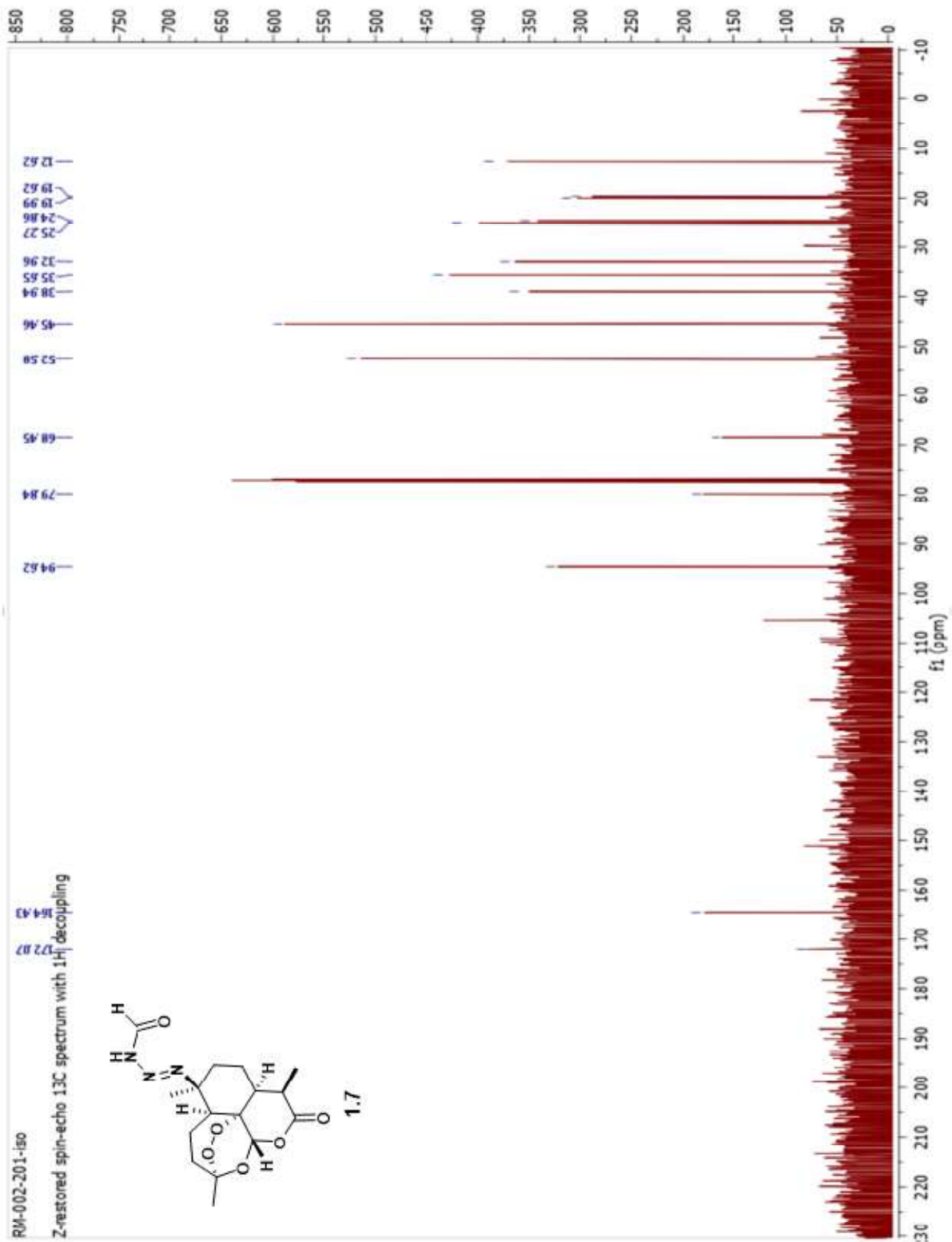
- ²² Chatterjee, A. K.; Choi, T.-L.; Sanders, D. P.; Grubbs, R. H. "A General Model for Selectivity in Olefin Cross Metathesis." *J. Am. Chem. Soc.* **2003**, *125*, 11360–11370.
- ²³ Hoye, T. R.; Jeffrey, C. S.; Tennakoon, M. A.; Wang, J.; Zhao, H. "Relay Ring-Closing Metathesis (RRCM): A Strategy for Directing Metal Movement Throughout Olefin Metathesis Sequences." *J. Am. Chem. Soc.* **2004**, *126*, 10210–10211.
- ²⁴ Anada, M.; Hanari, T.; Kakita, K.; Kurosaki, Y.; Katsuse, K.; Sunadoi, Y.; Jinushi, Y.; Takeda, K.; Matsunaga, S.; Hashimoto, S. "Total Synthesis of Brascilicardins A and C." *Org. Lett.* **2017**, *19*, 5581–5584.
- ²⁵ a) Pearson, A. J.; Alimardanov, A. "Studies on Intramolecular Coupling of Tricarbonyl(diene)iron Systems with Pendant Olefinic Groups: Configurational Requirements for Reactions of Acyclic Diene Complexes and Mechanistic Implications." *Organometallics* **1998**, *17*, 3739–3746; b) Cais, M.; Maoz, N. "Organometallic studies: XVI. Iron π -Complexes Of β -Ionone and Other Model Compounds for Vitamin A." *J. Organomet. Chem.* **1966**, *5*, 370–383.
- ²⁶ Liang, J.; Lalonde, J.; Borup, B.; Mitchell, V.; Mundorff, E.; Trinh, N.; Kochrekar, D. A.; Cherat, R. N.; Pai, G. G. "Development of a Biocatalytic Process as an Alternative to the (-)-DIP-Cl-Mediated Asymmetric Reduction of a Key Intermediate of Montelukast." *Org. Process Res. Dev.* **2010**, *14*, 193–198.
- ²⁷ Franck-Neumann, M.; Kastler, A. "Diquinanes, Eight-membered Carbocycles and new Di-bridged Bis- π -allyl Complexes by Intramolecular Reactions of Unsaturated Tricarbonyl [Trimethylenemethane] iron Complexes. Non Destructive Ozonolysis of Trimethylenemethane Complexes." *Synlett* **1995**, *1*, 61–63.
- ²⁸ Howell, J. A. S.; Palin, M. G.; Hafa, H. E.; Top, S.; Jaouen. "Biochemical Resolution and Generation of Planar Chirality in Formyl Substituted (Diene)Fe(σ)Complexes." *Tetrahedron Asymmetry* **1992**, *3*, 1355–1356.
- ²⁹ Iafe, R. G.; Kuo, J. L.; Hochstatter, D. G.; Saga, T.; Turner, J. W.; Merlic, C. A. "Increasing the Efficiency of the Transannular Diels-Alder Strategy via Palladium(II)-Catalyzed Macrocyclizations." *Org. Lett.* **2013**, *15*, 582–585.
- ³⁰ a) Tae, J.; Yang, Y.-K. "Efficient Synthesis of Macrocyclic Paracyclophanes by Ring-Closing Metathesis Dimerization and Trimerization Reactions." *Org. Lett* **2003**, *5*, 741–744; b) Yang, L.; Song, L.; Huang, C.; Huang, M.; Liu, B. "Exploiting *Ortho*-Substitution Effect on Formation of Oxygen-Containing [10]Paracyclophane Through Ring-Closing Metathesis." *Org. Chem. Front.* **2016**, *3*, 319–323.

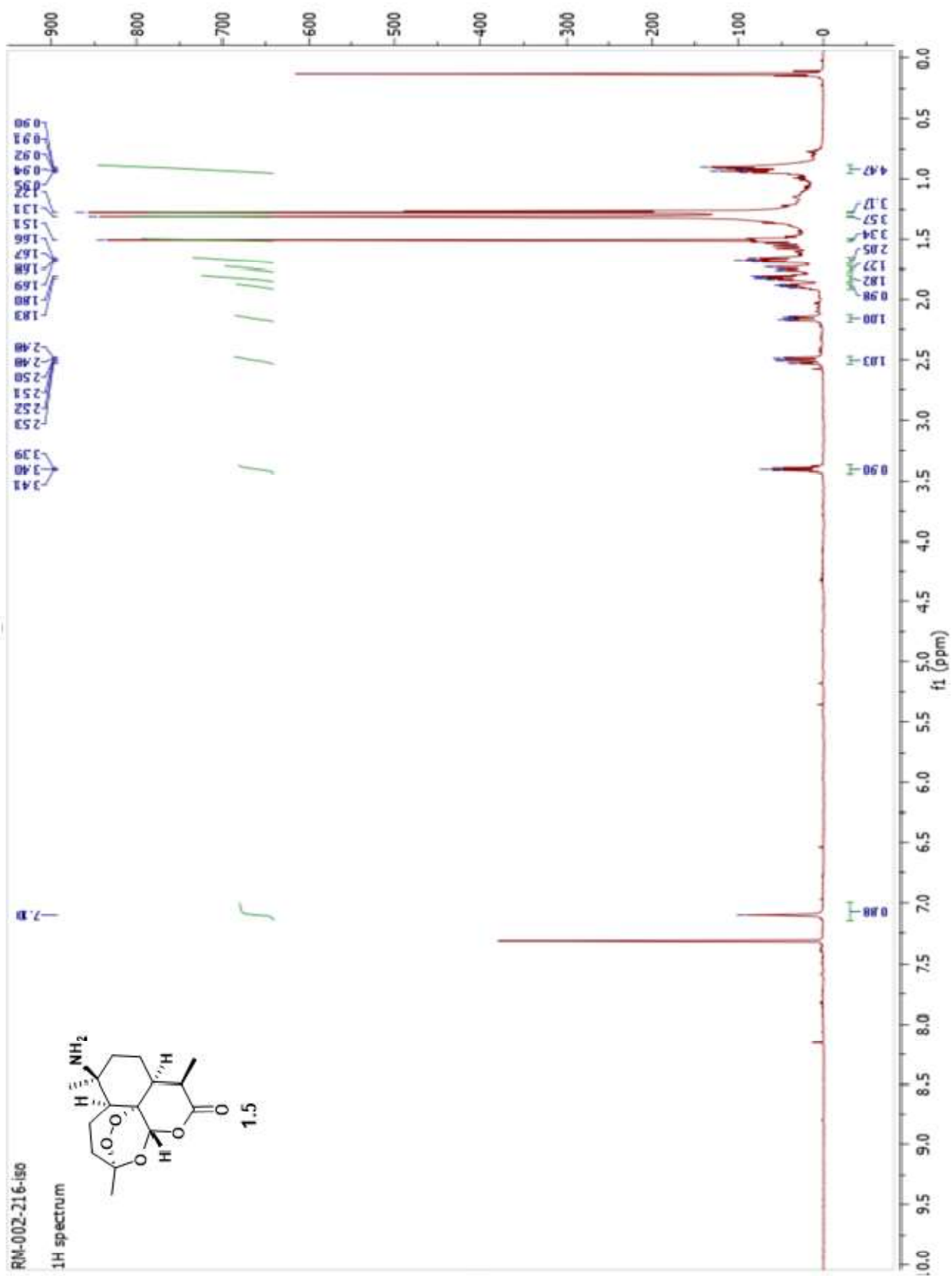
APPENDIX A: NMR SPECTRA

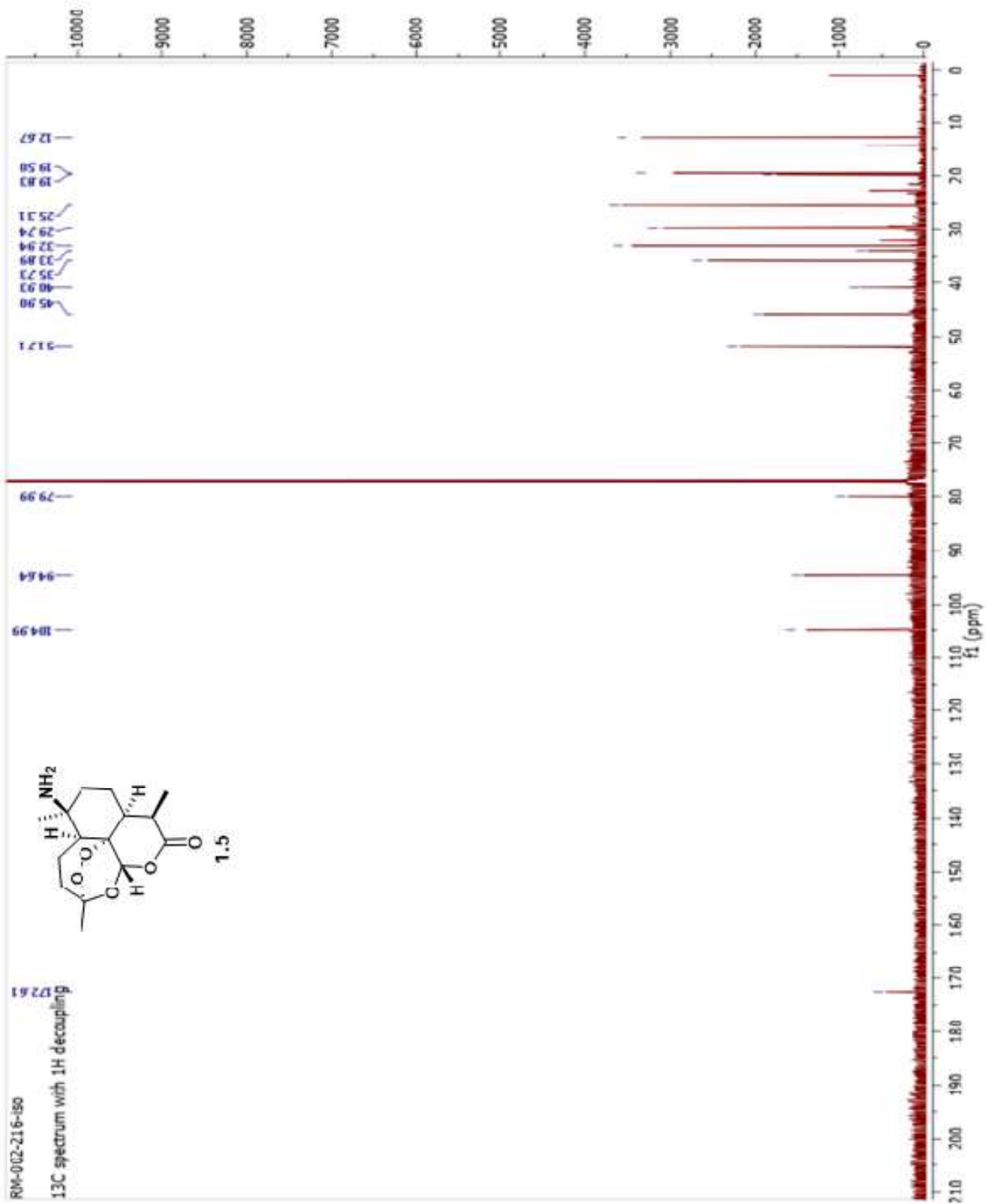


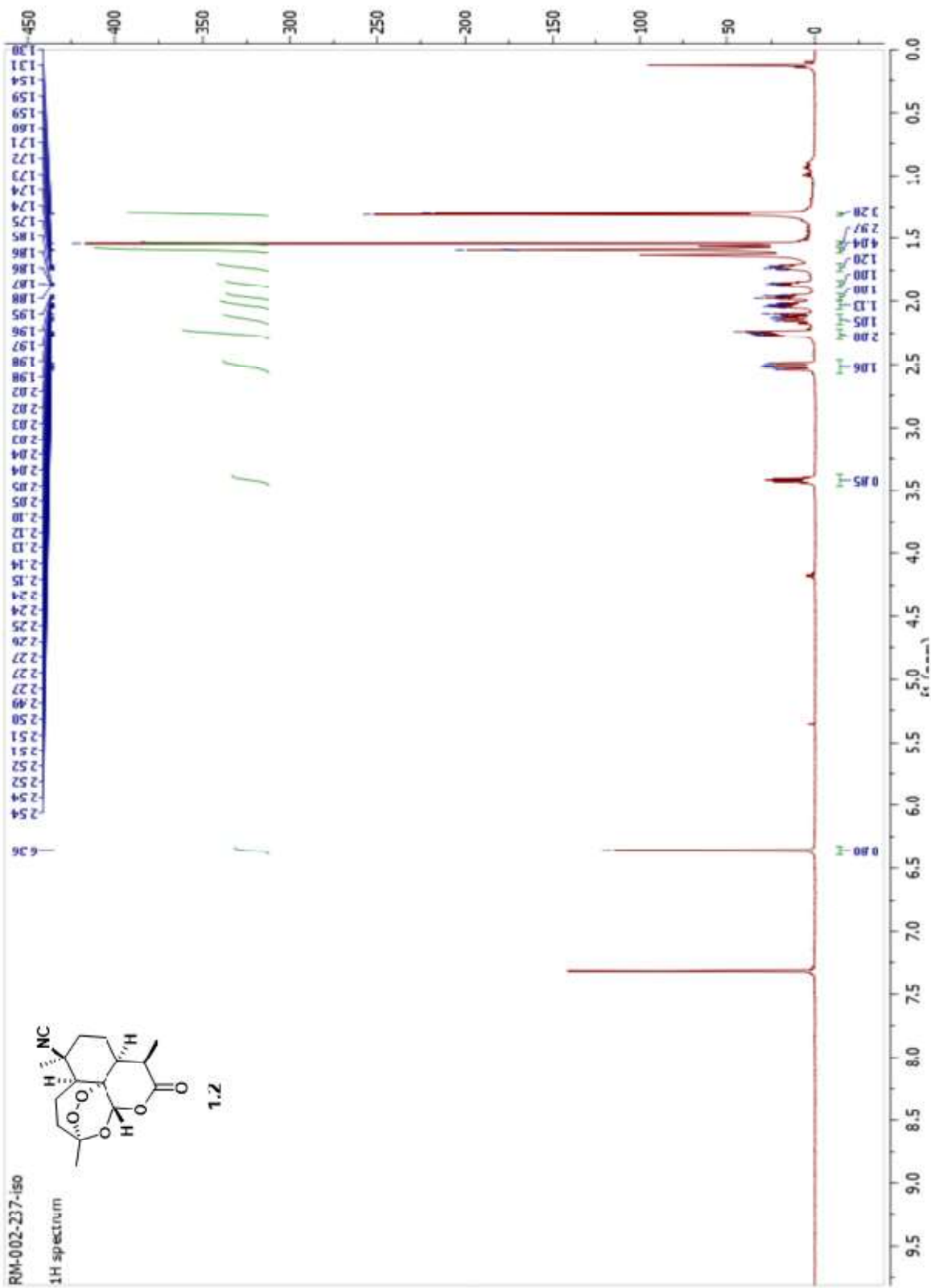


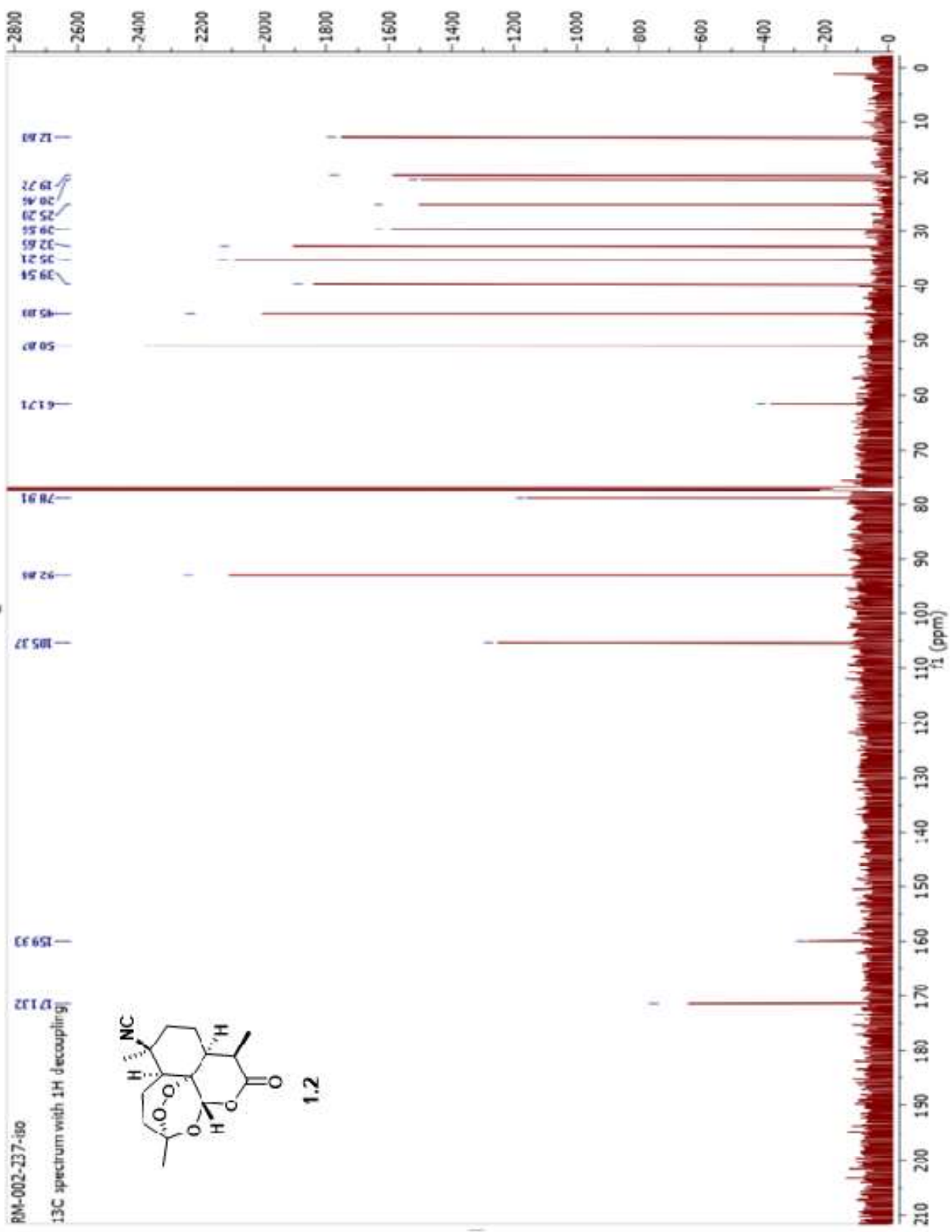


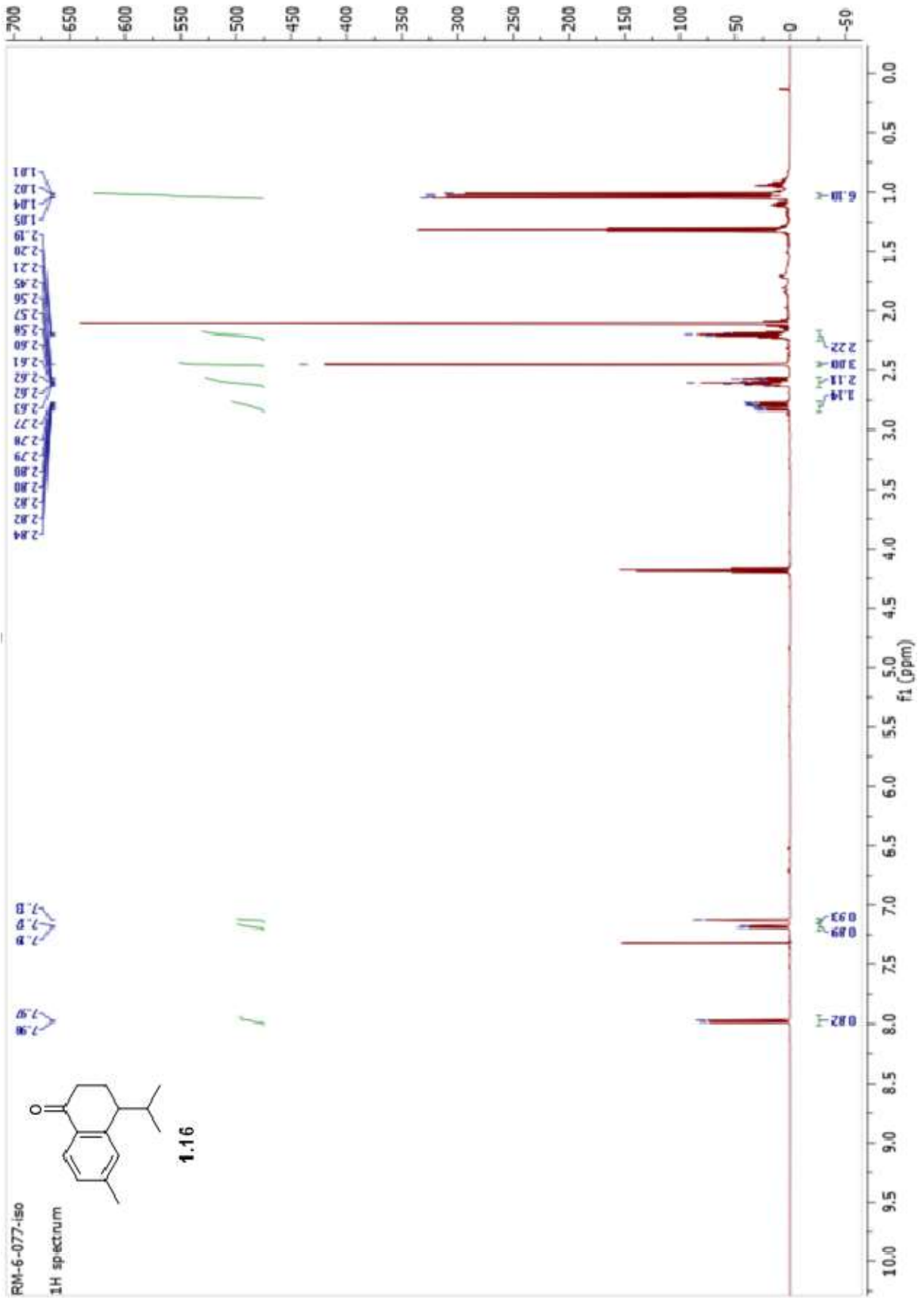


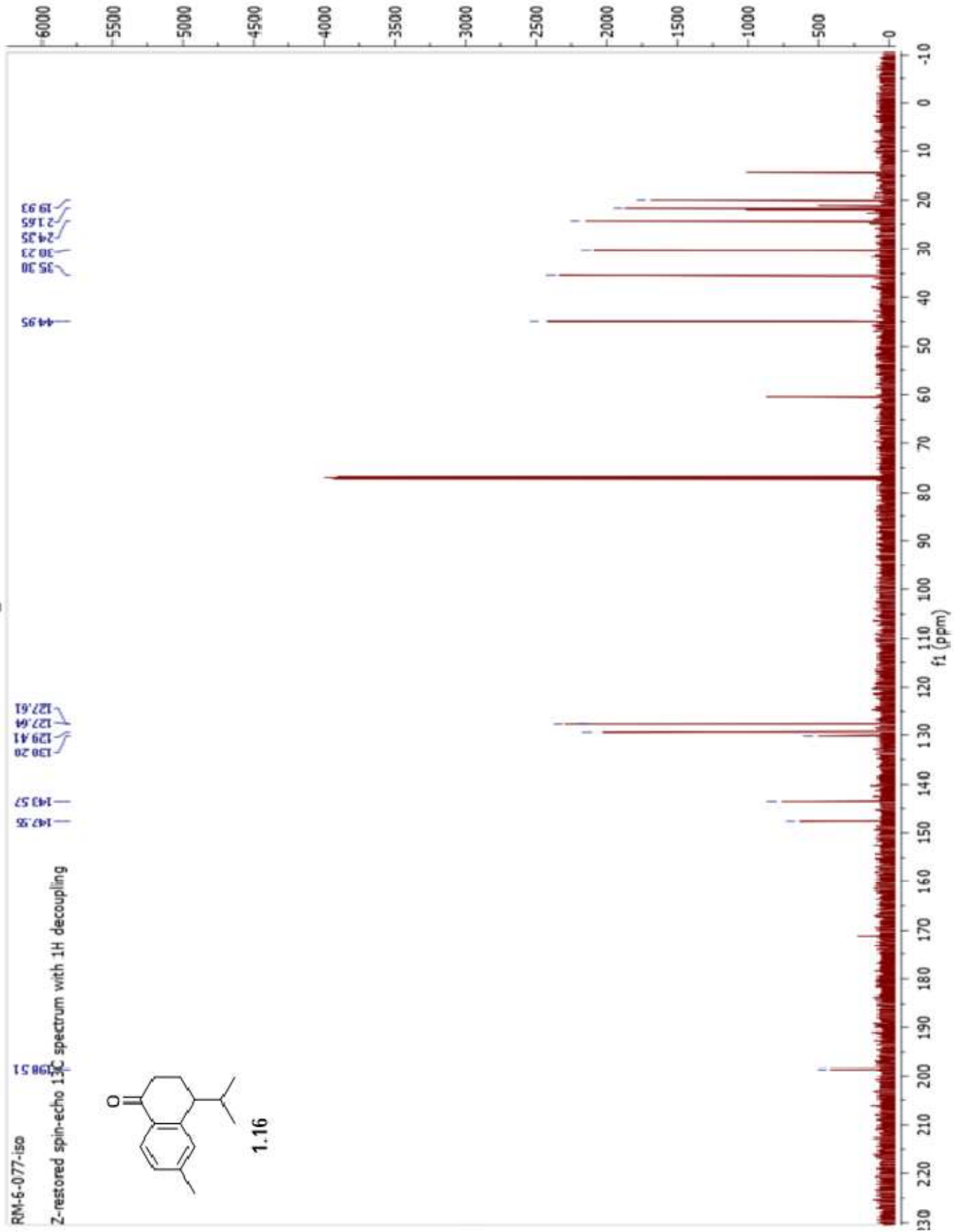


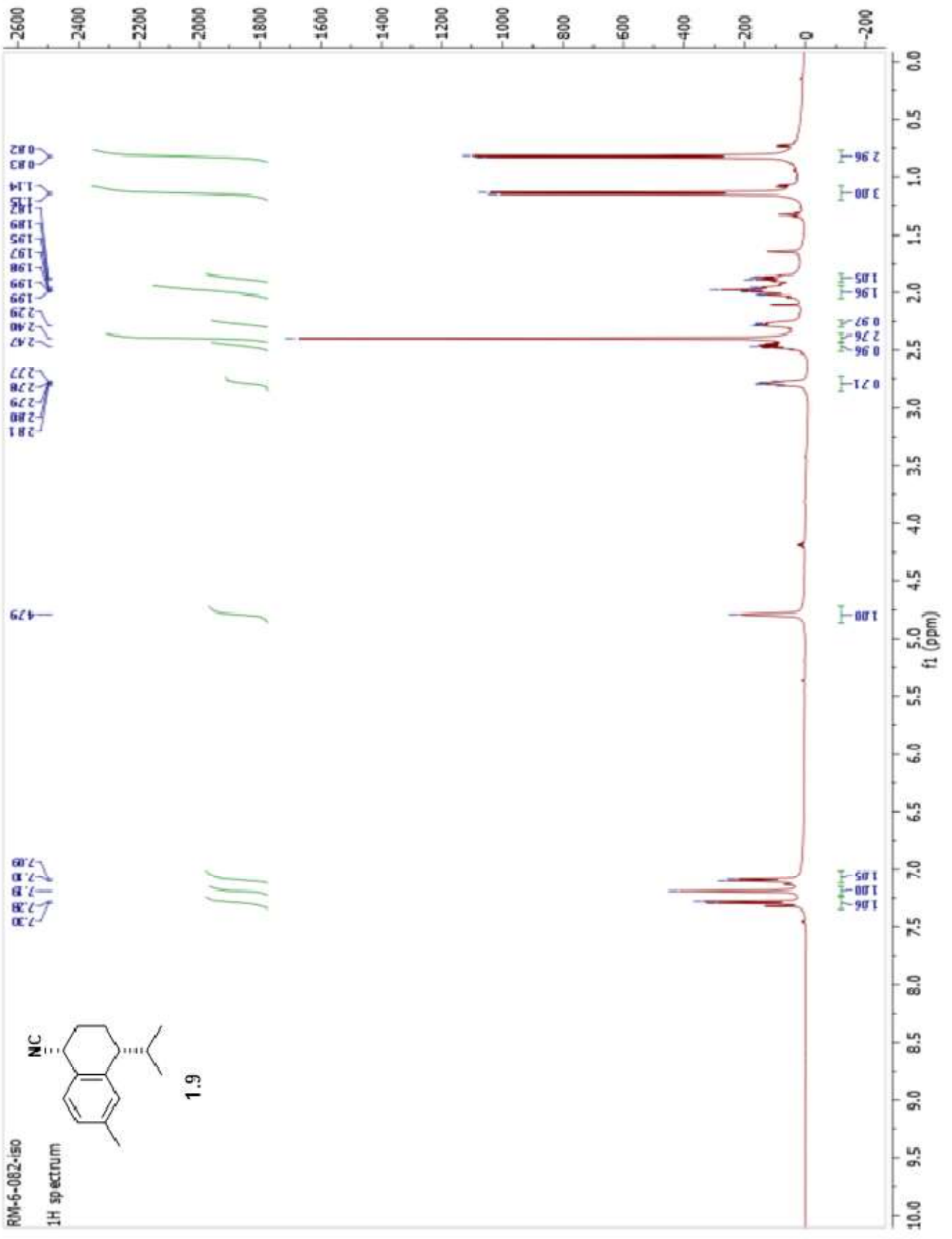


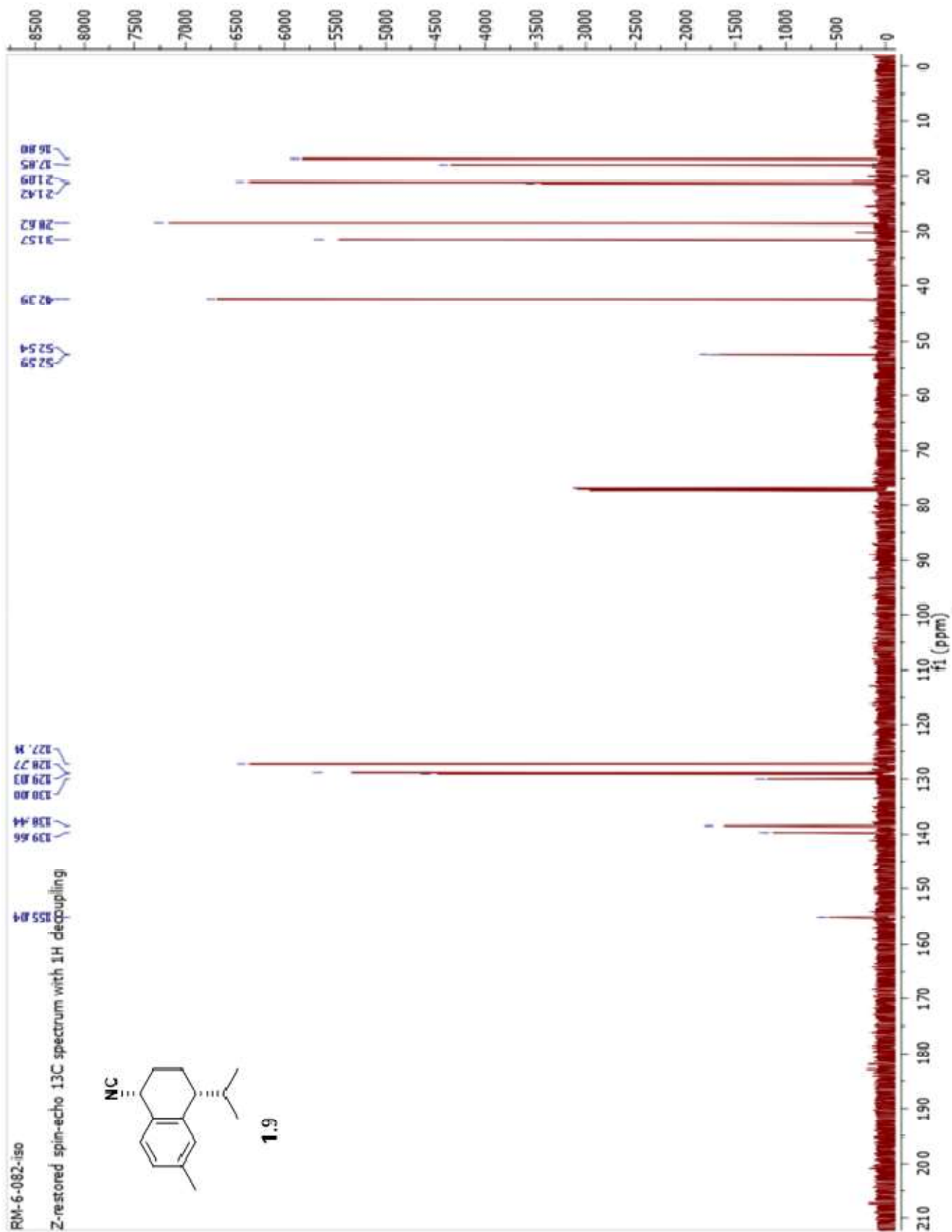


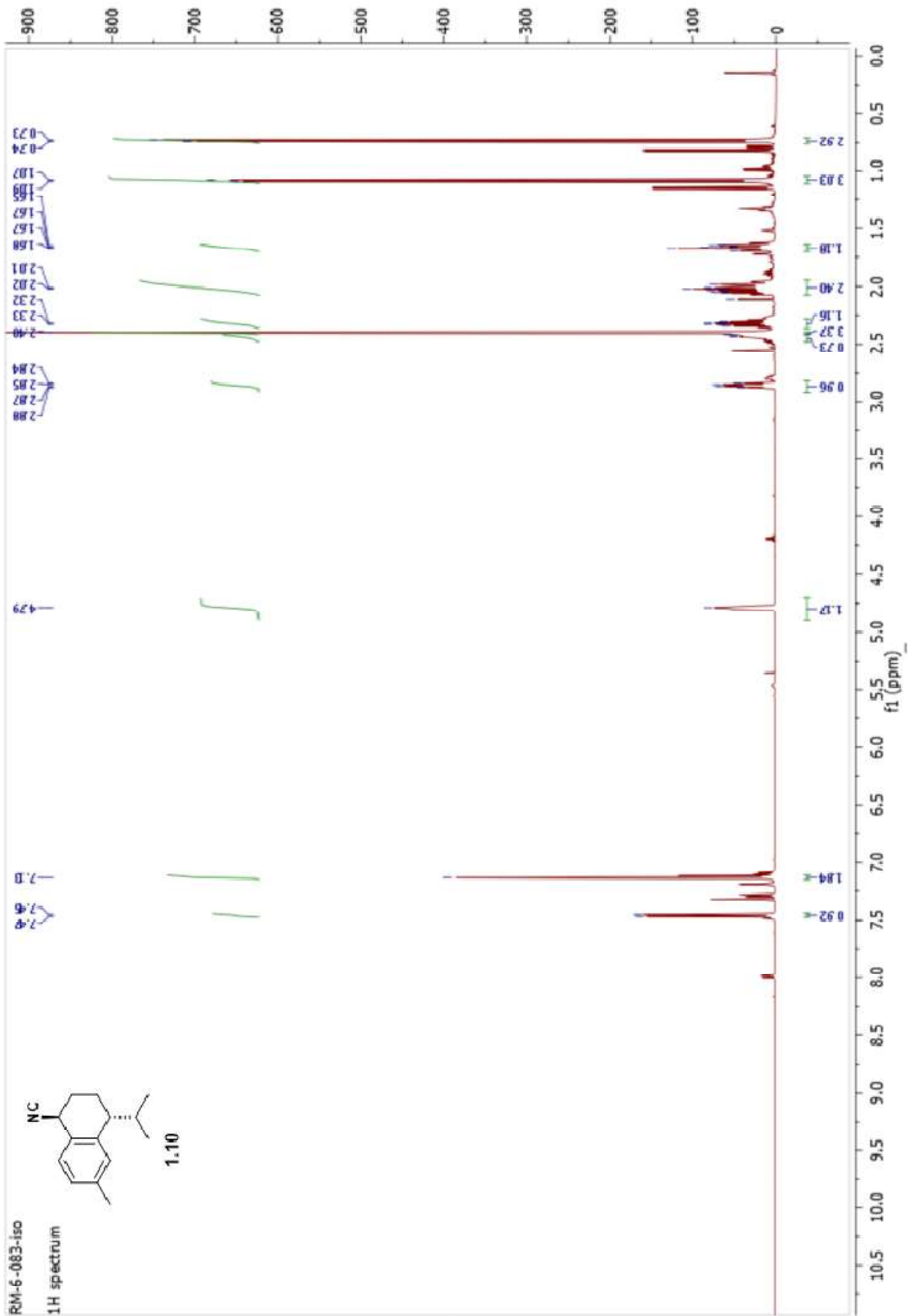


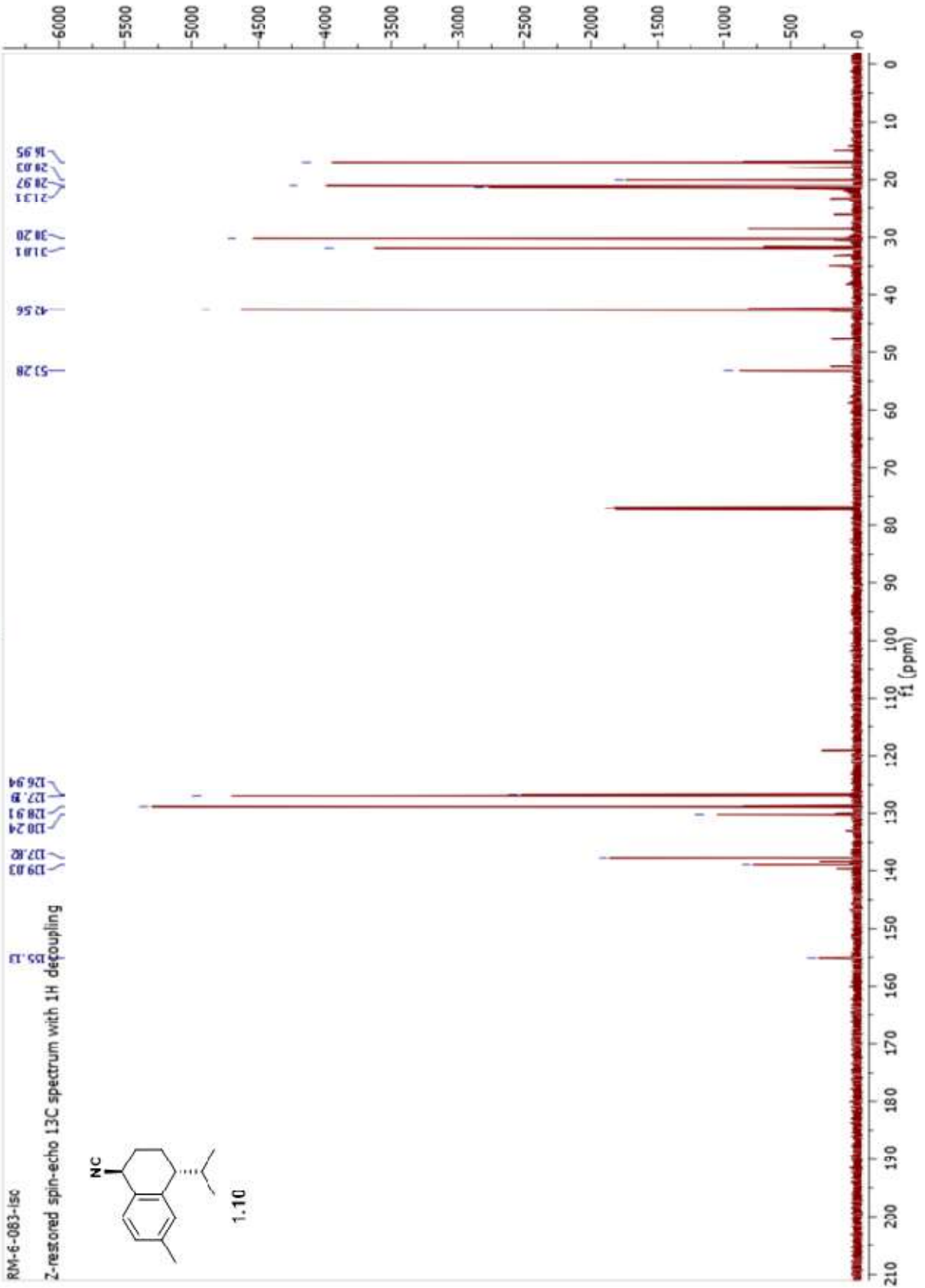


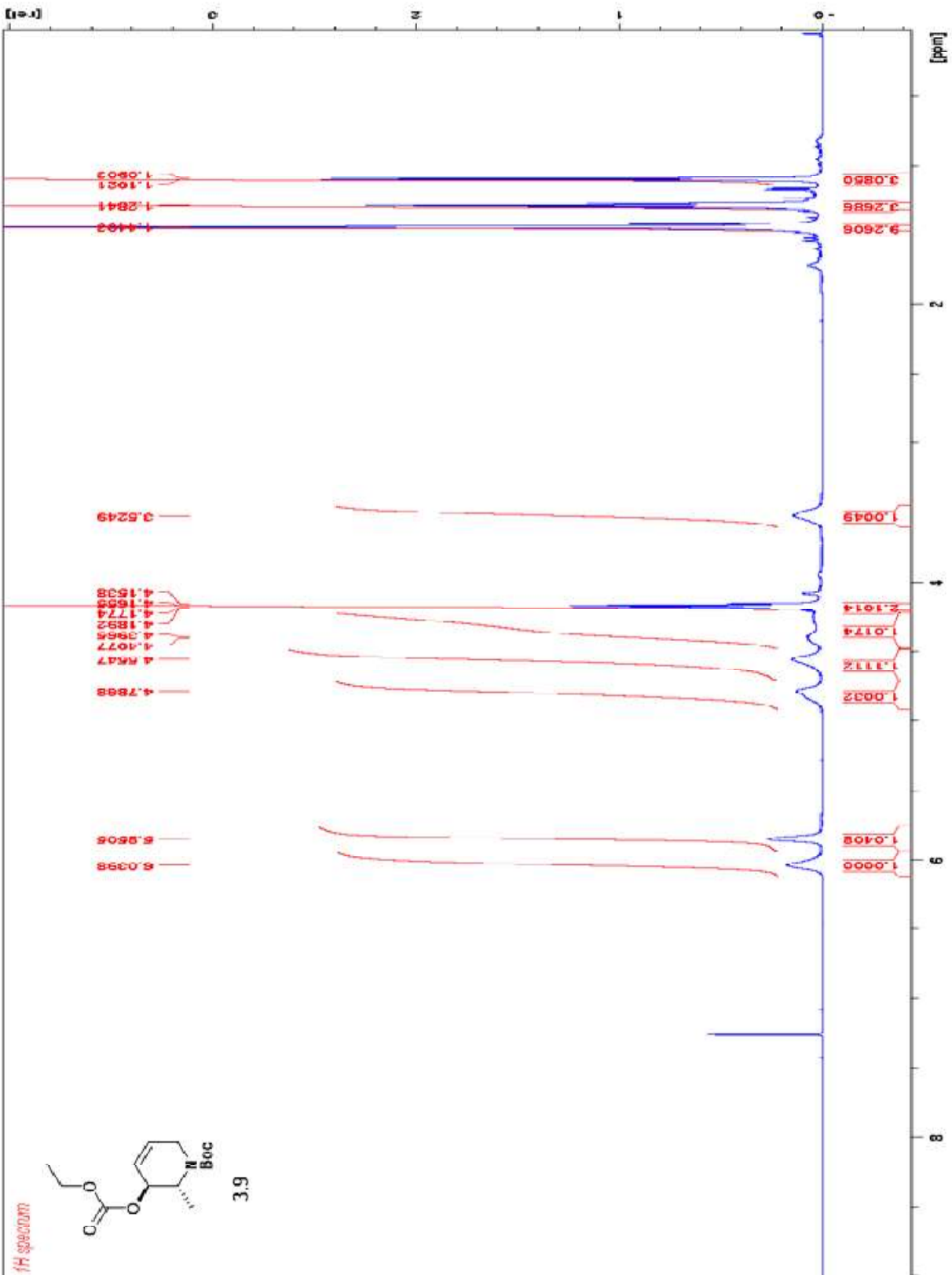


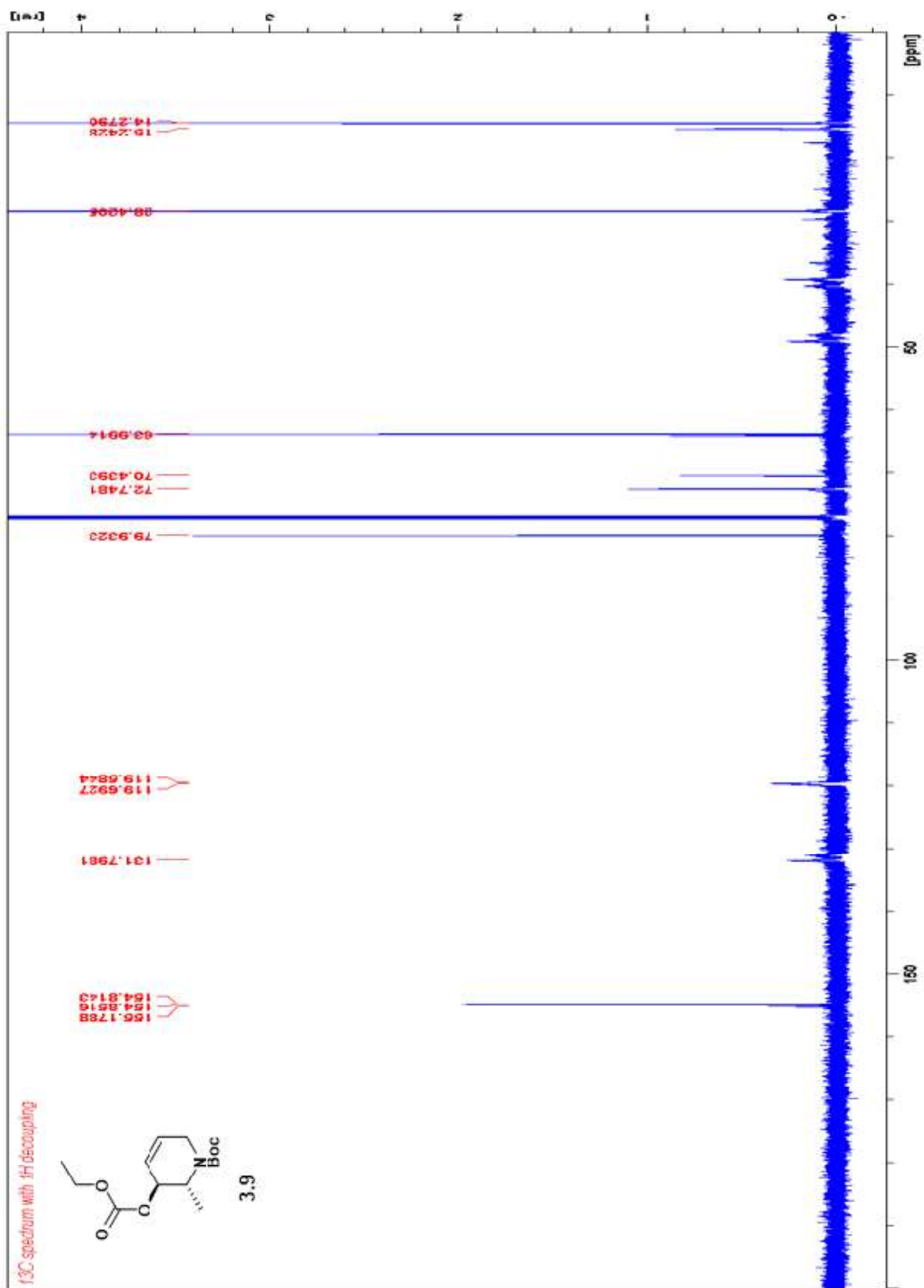


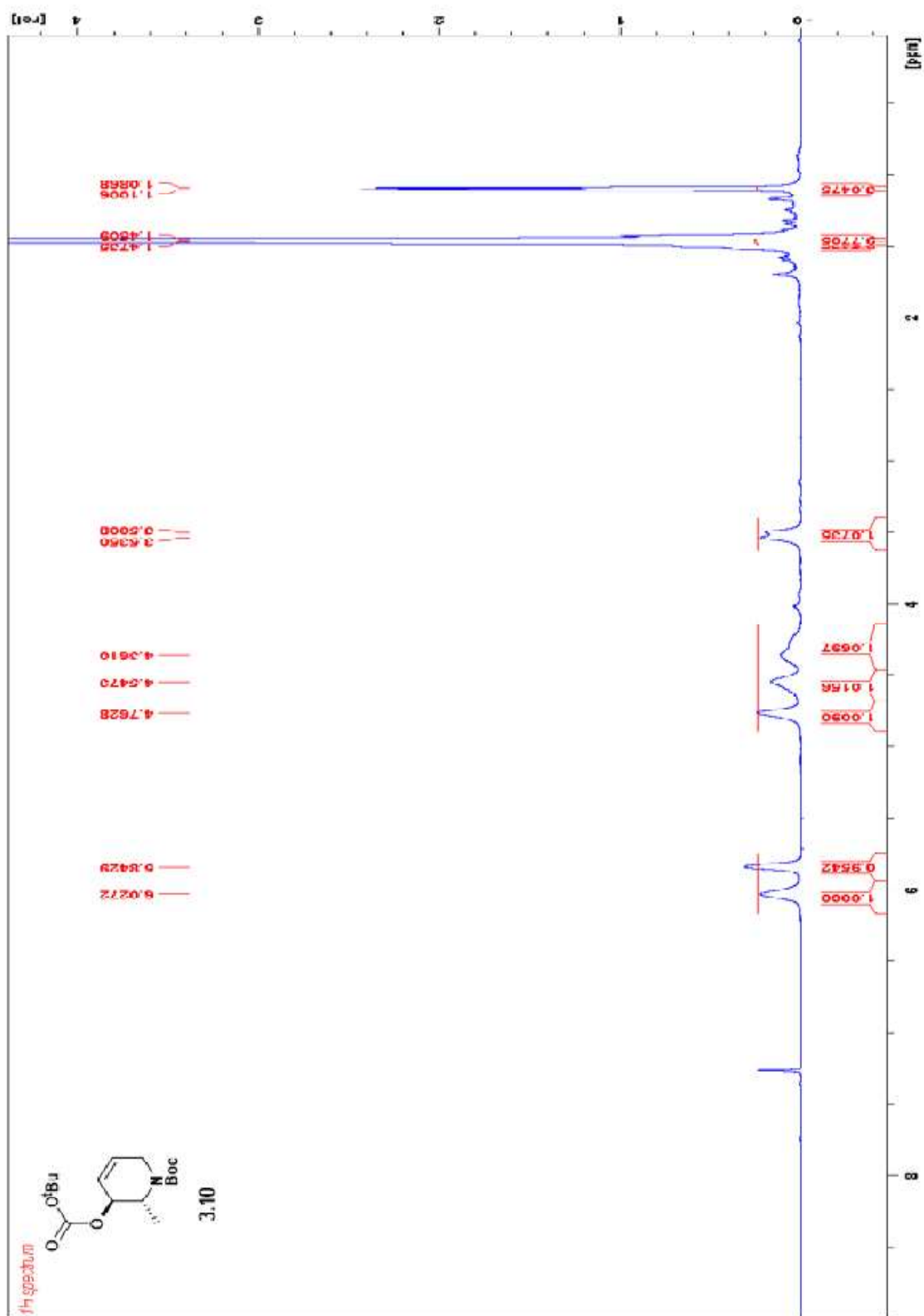


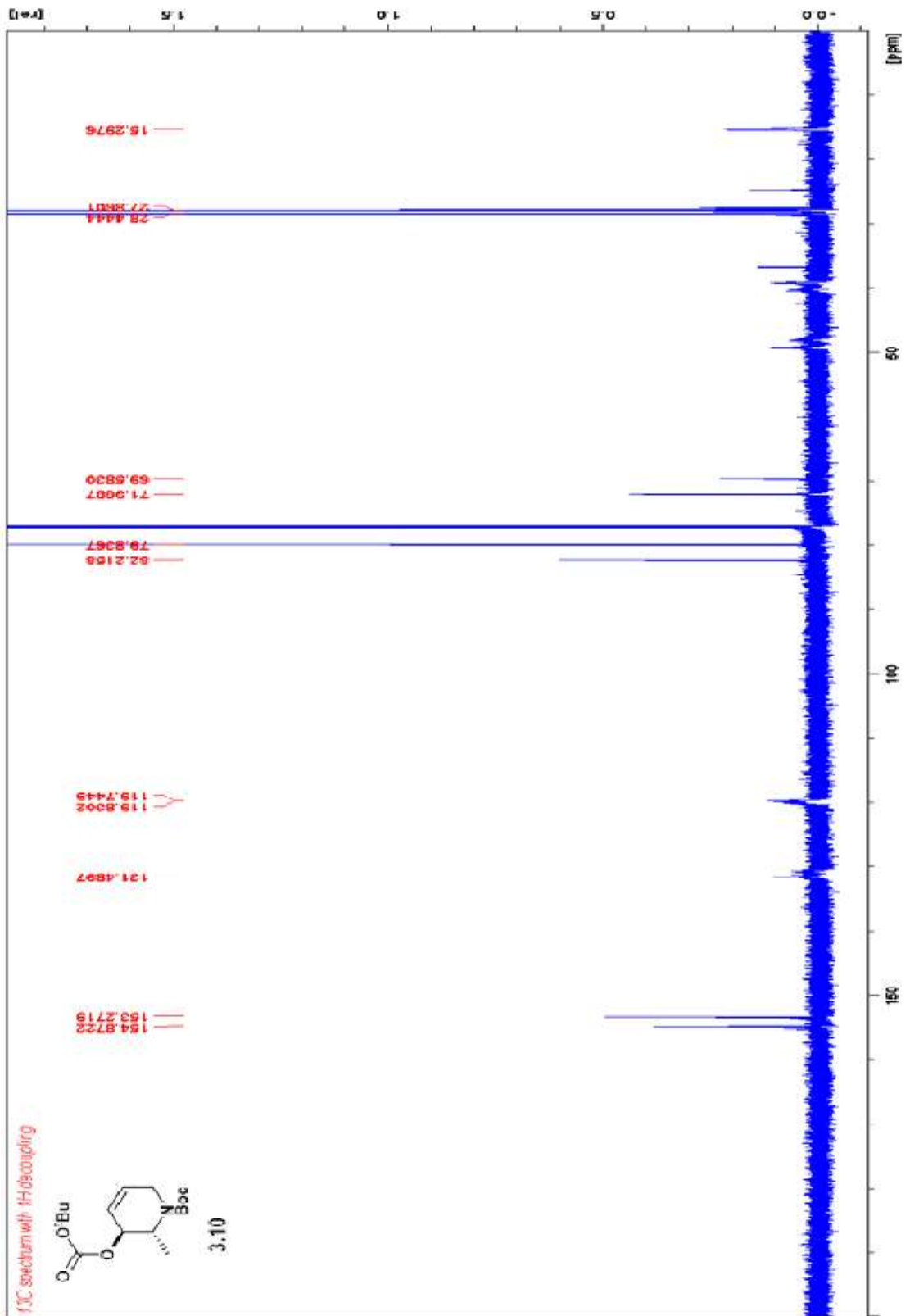


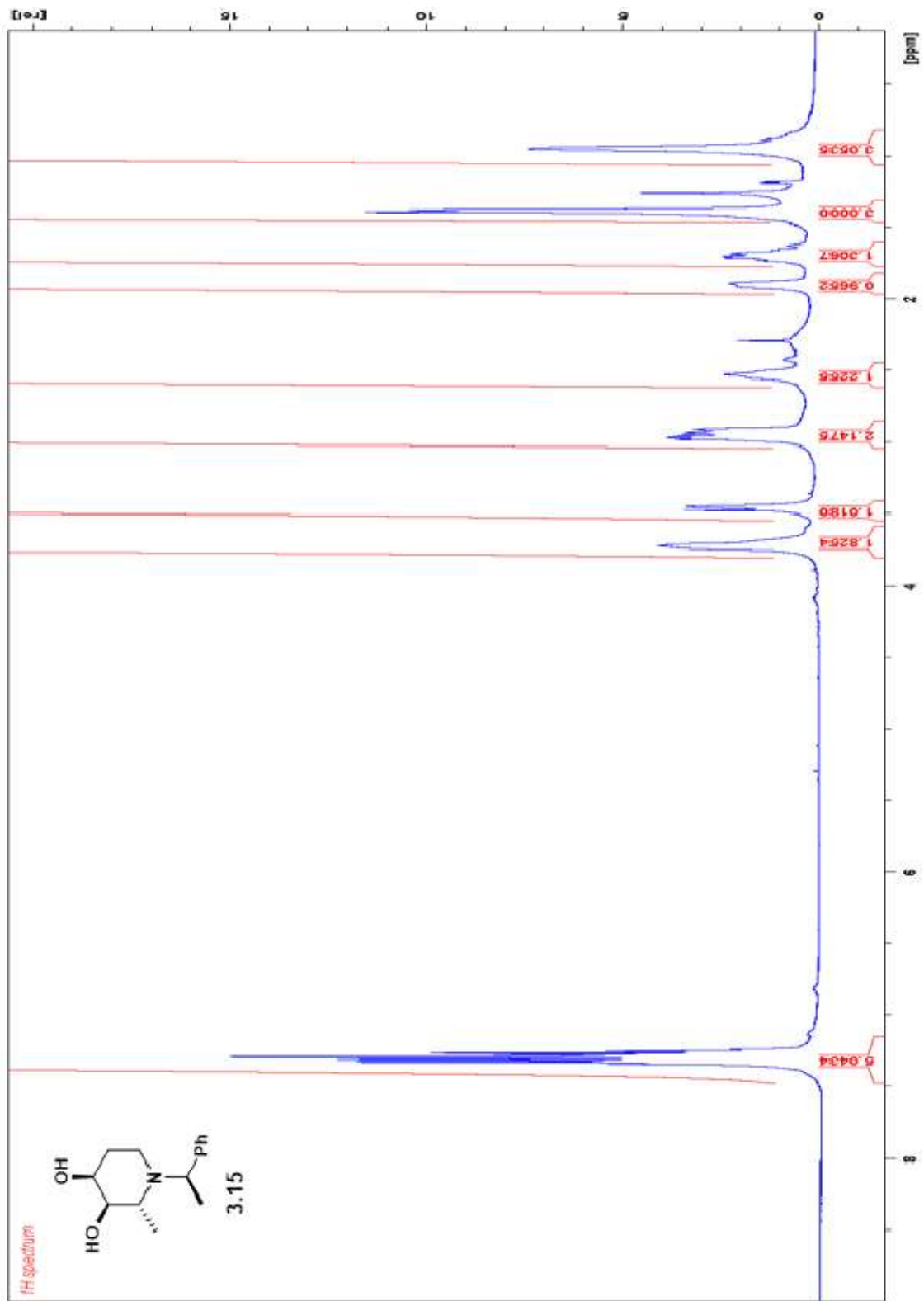


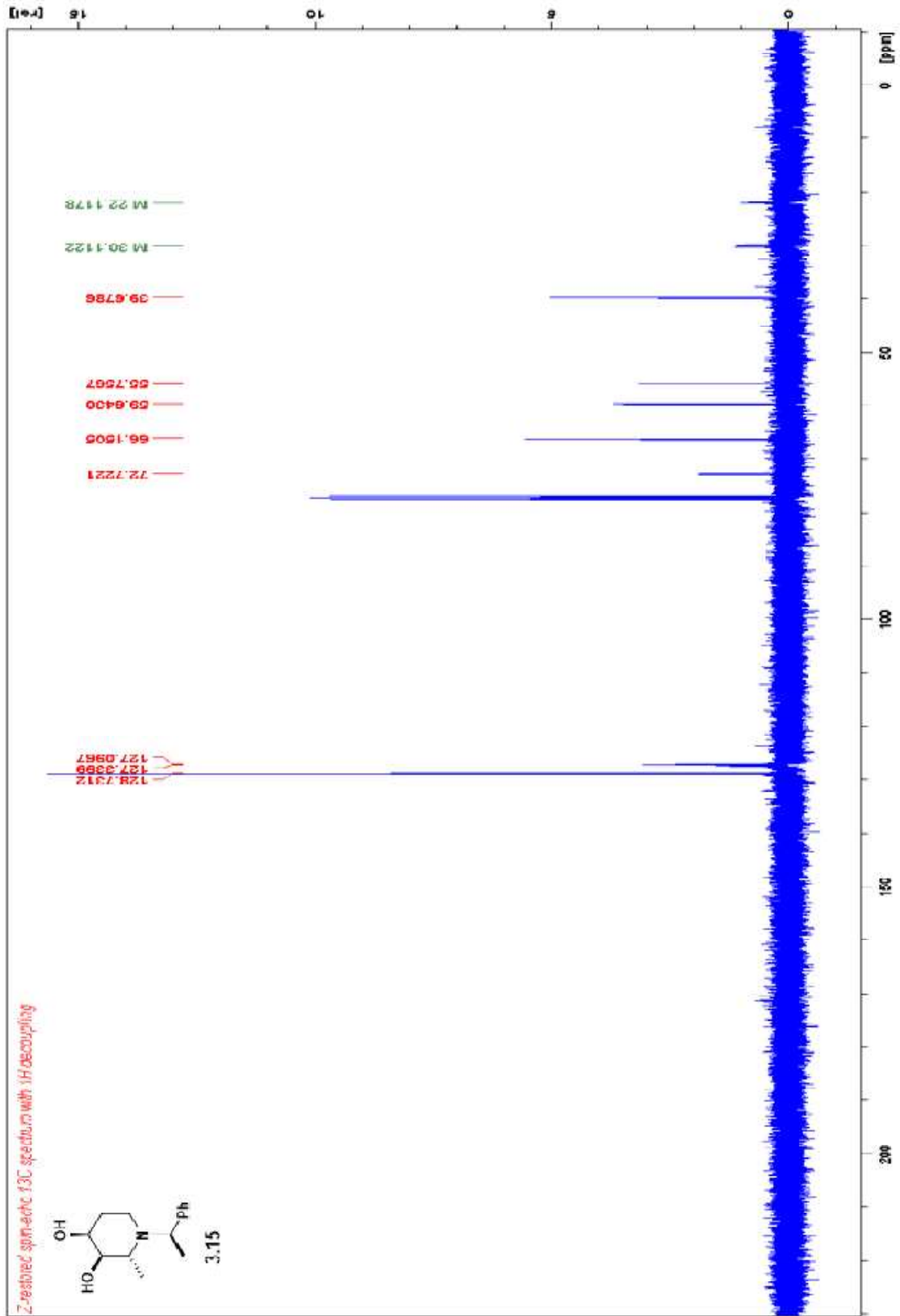


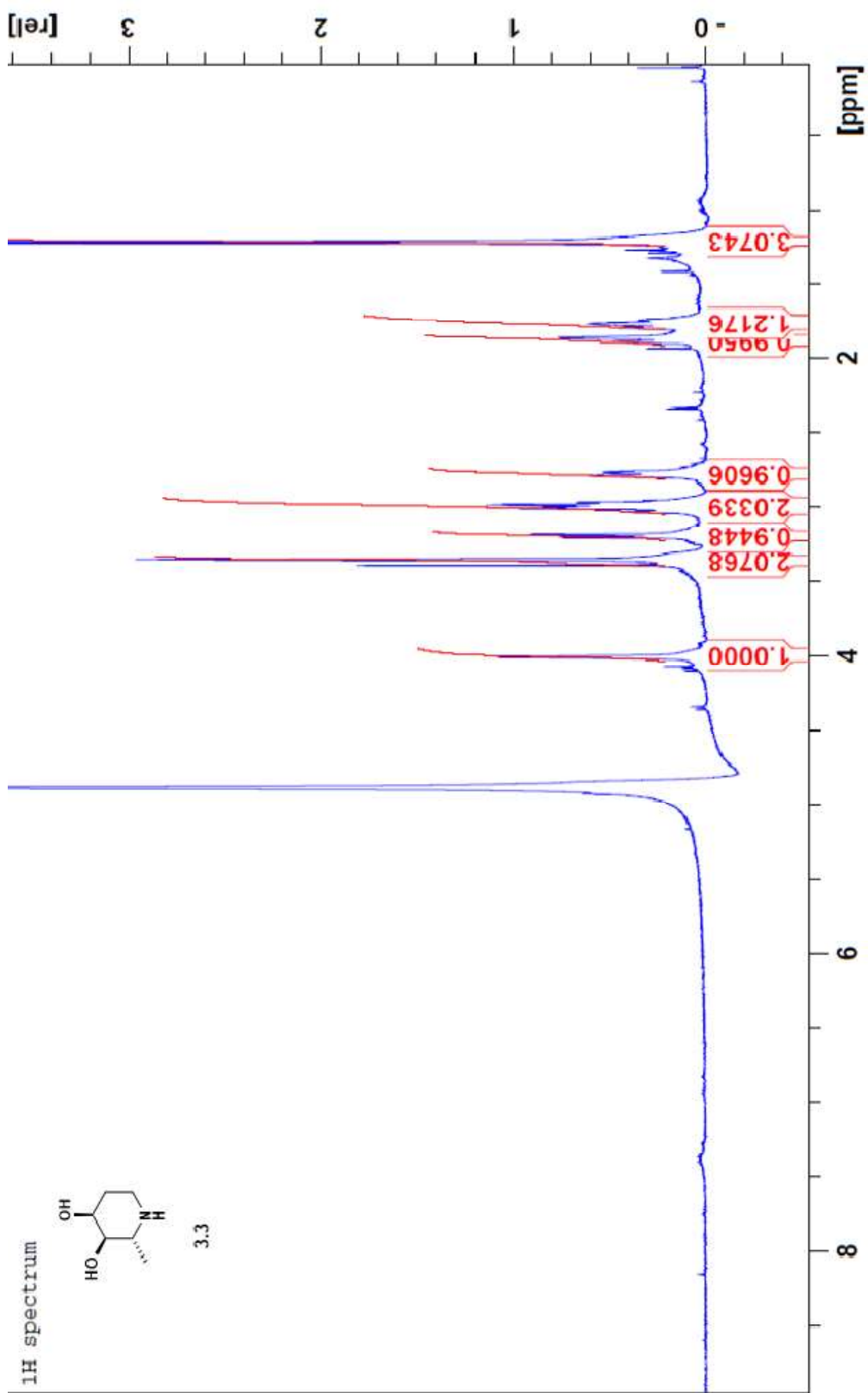


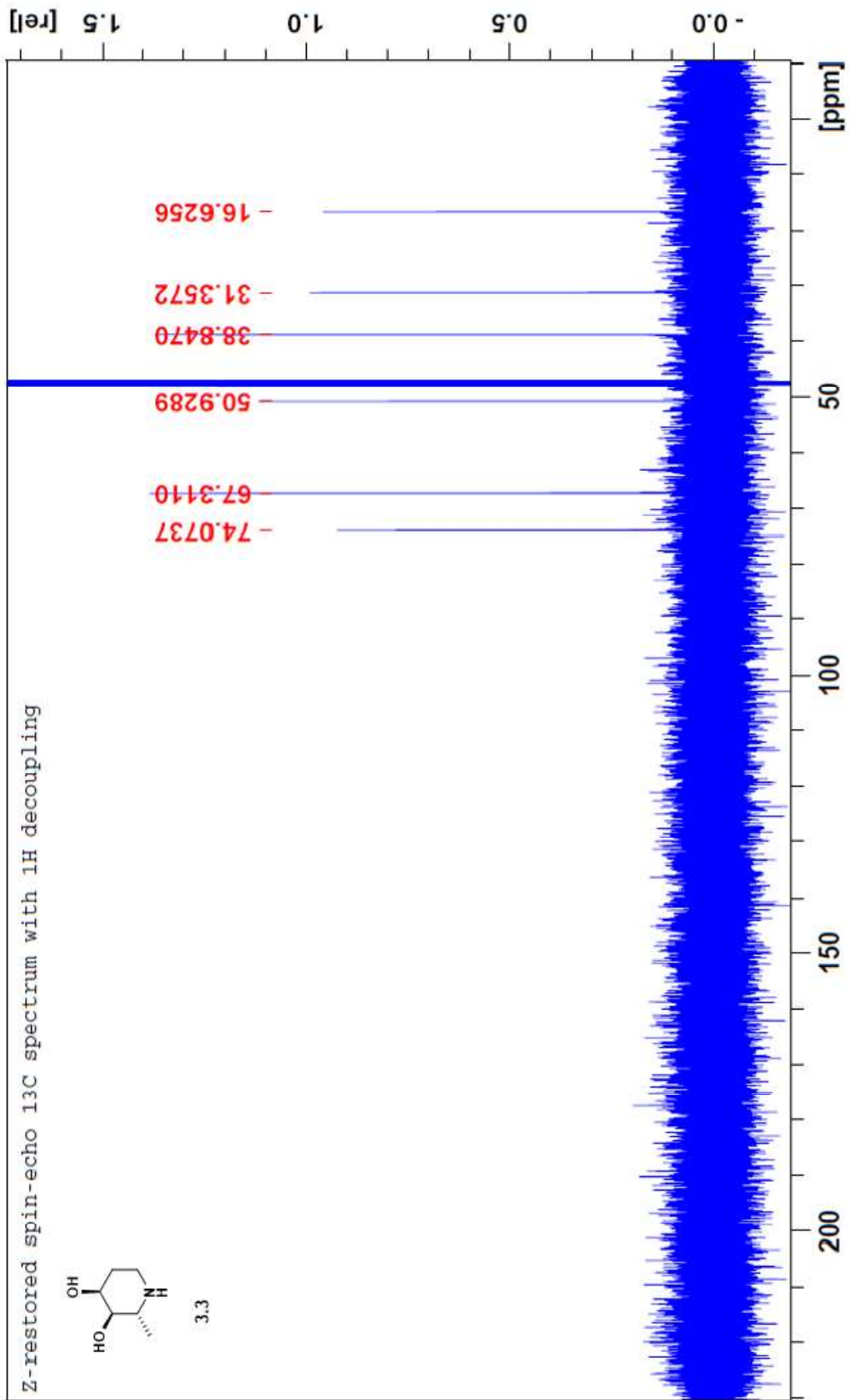


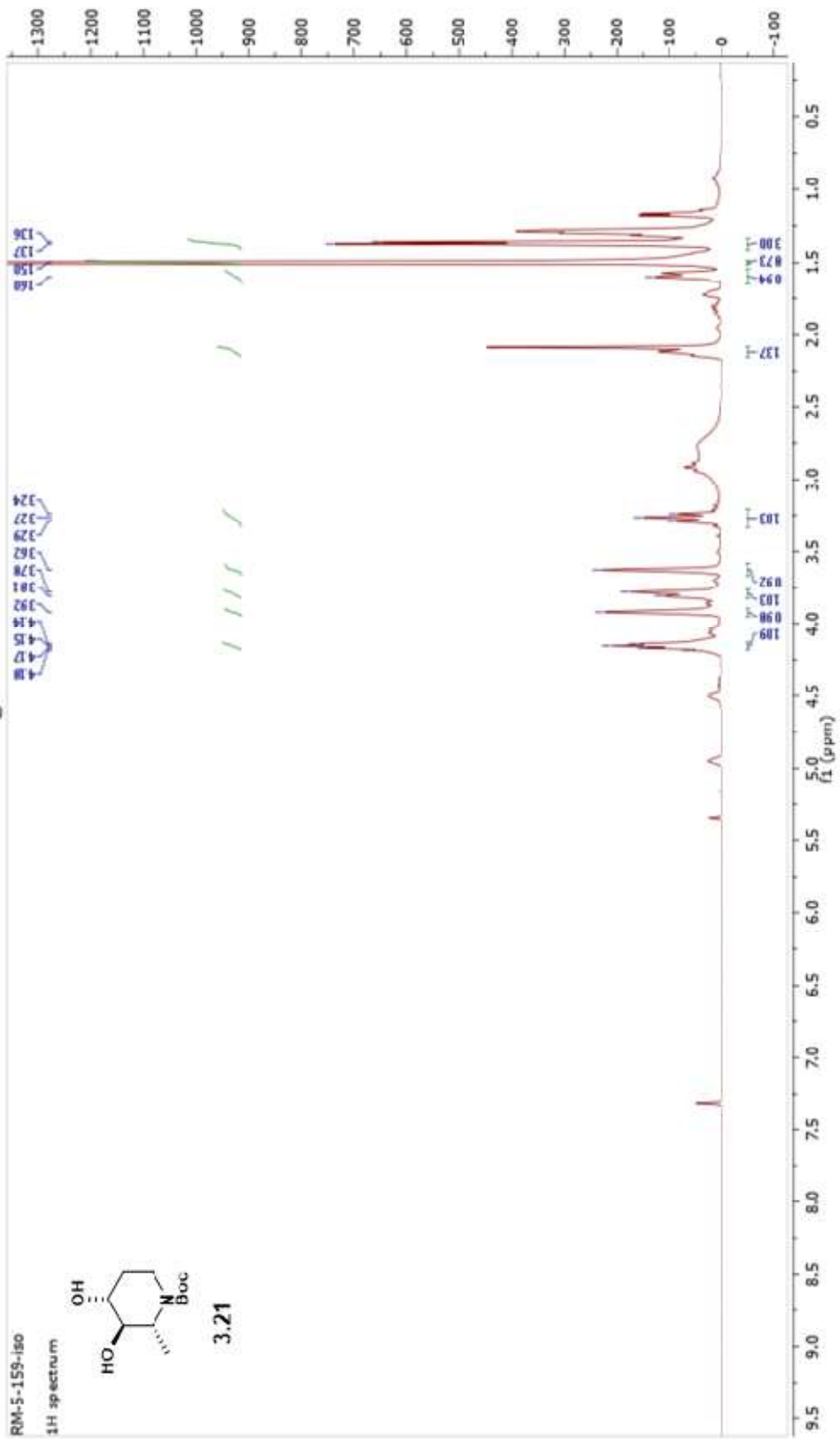


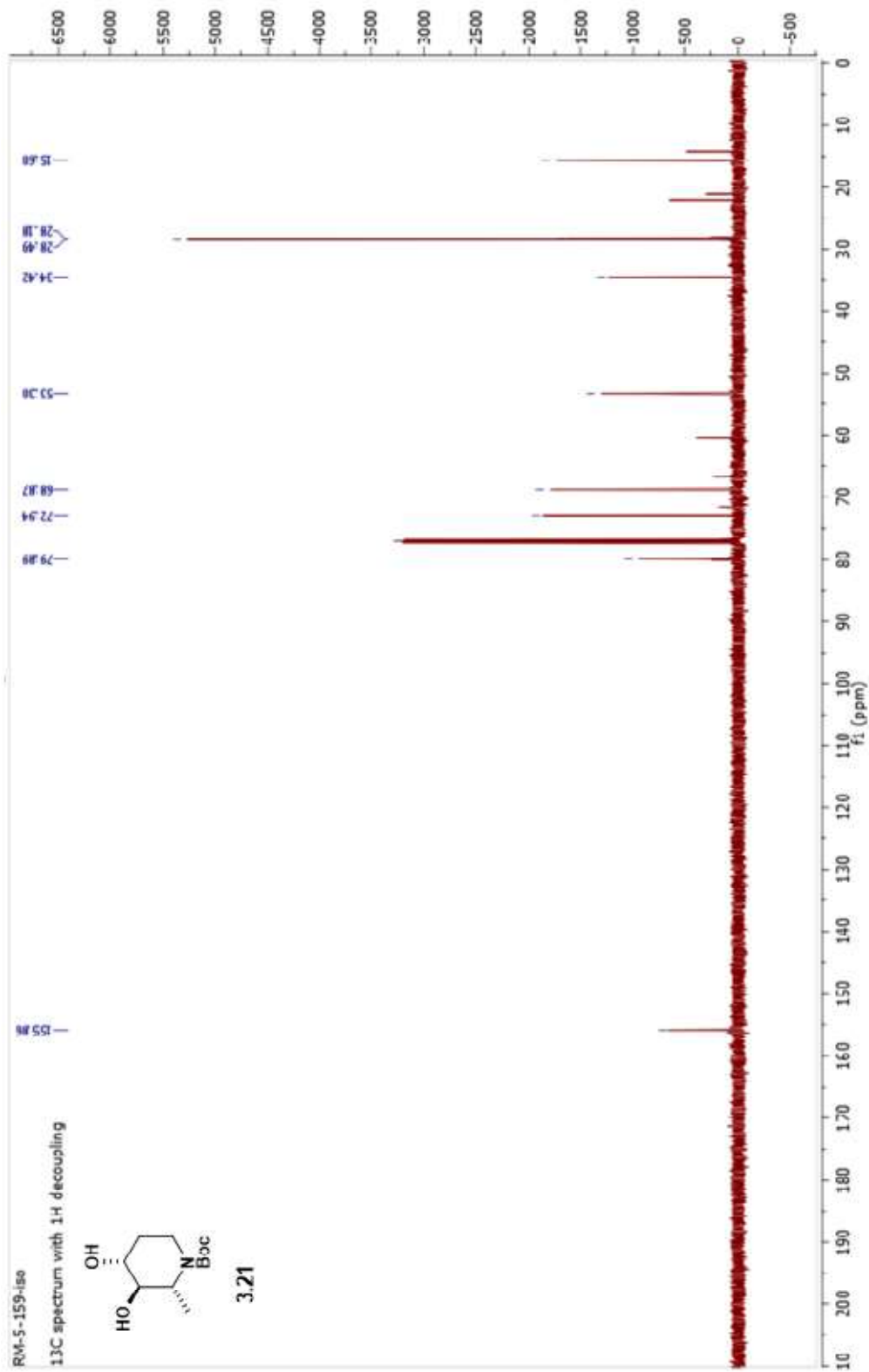


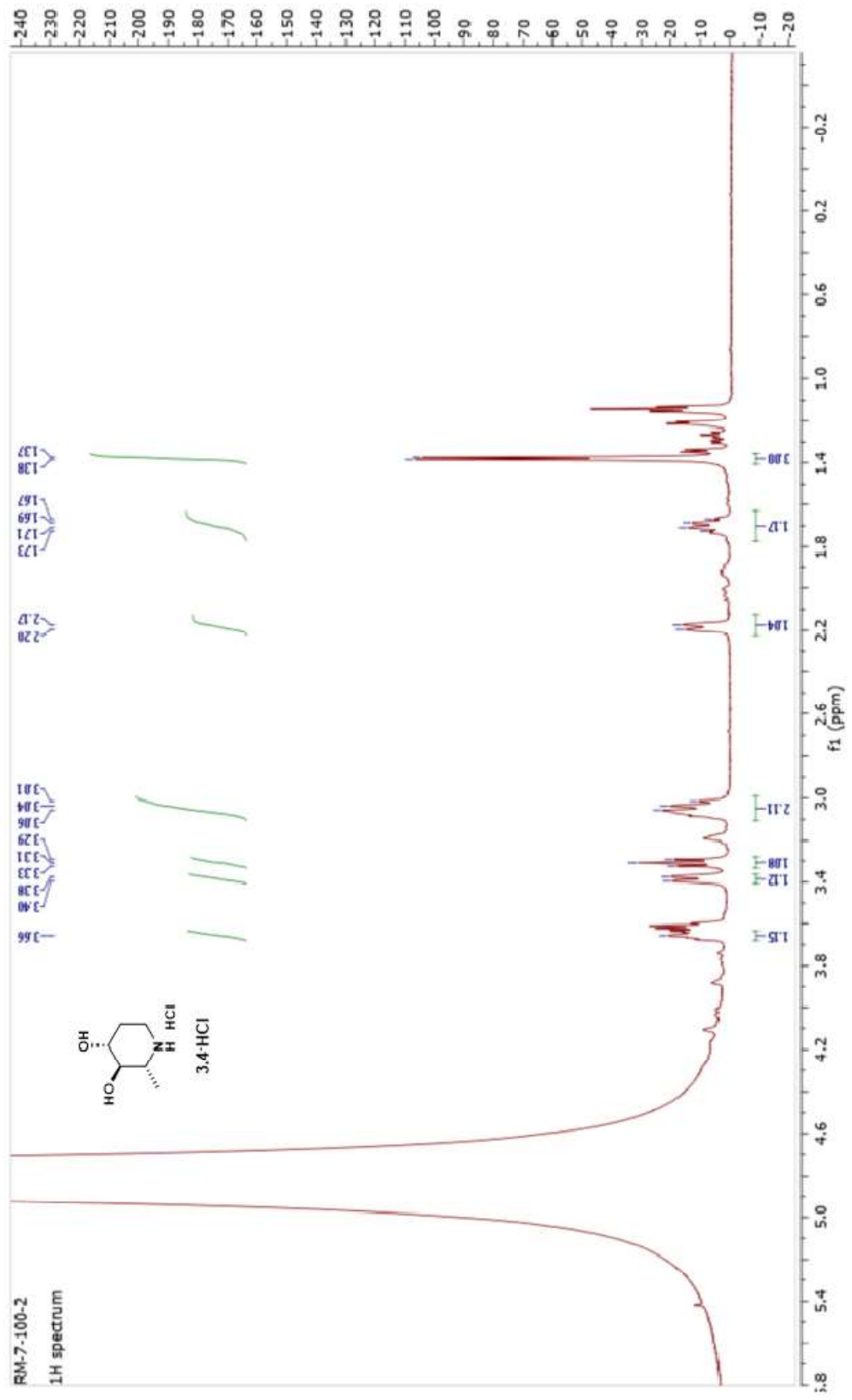


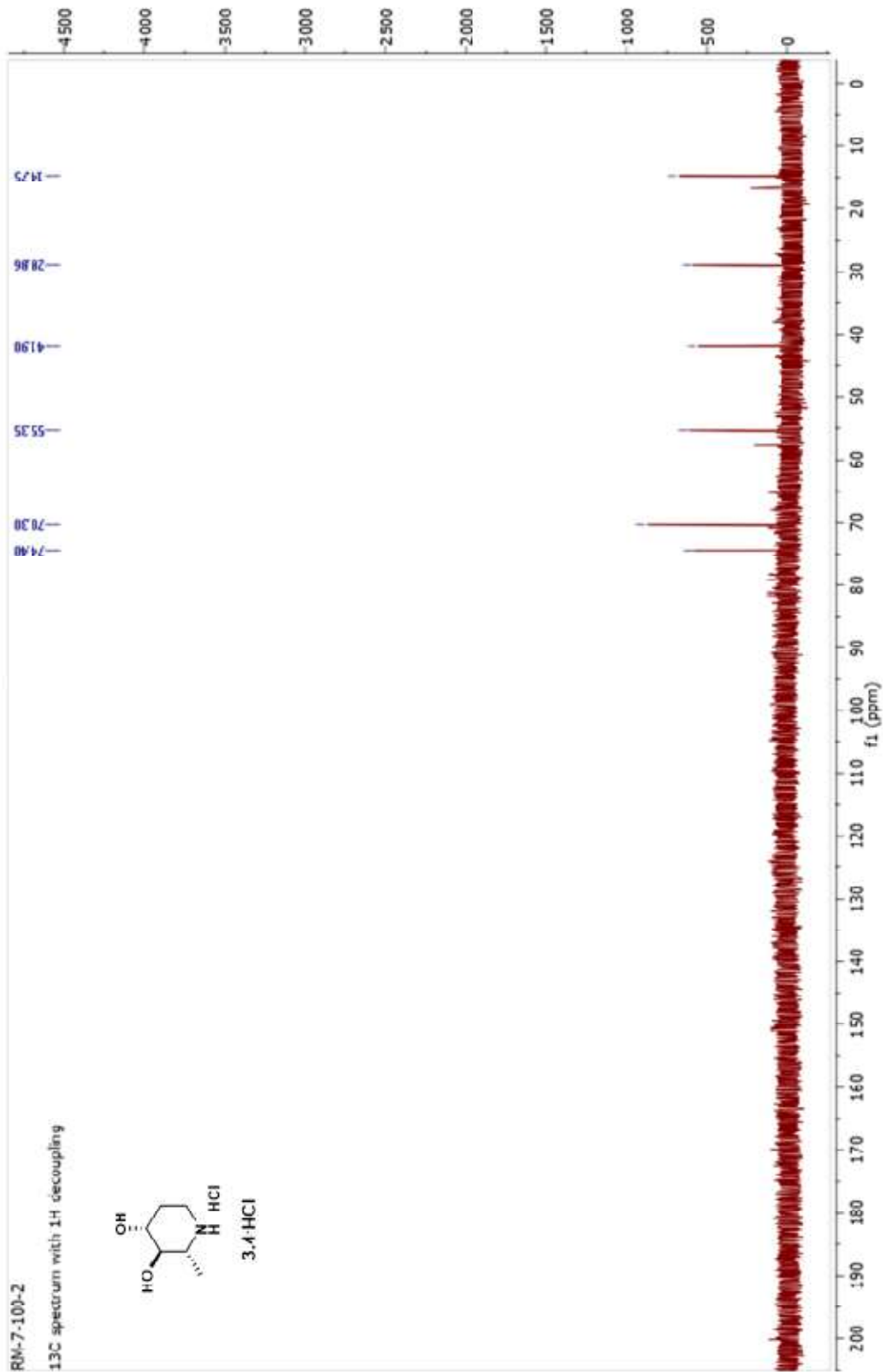


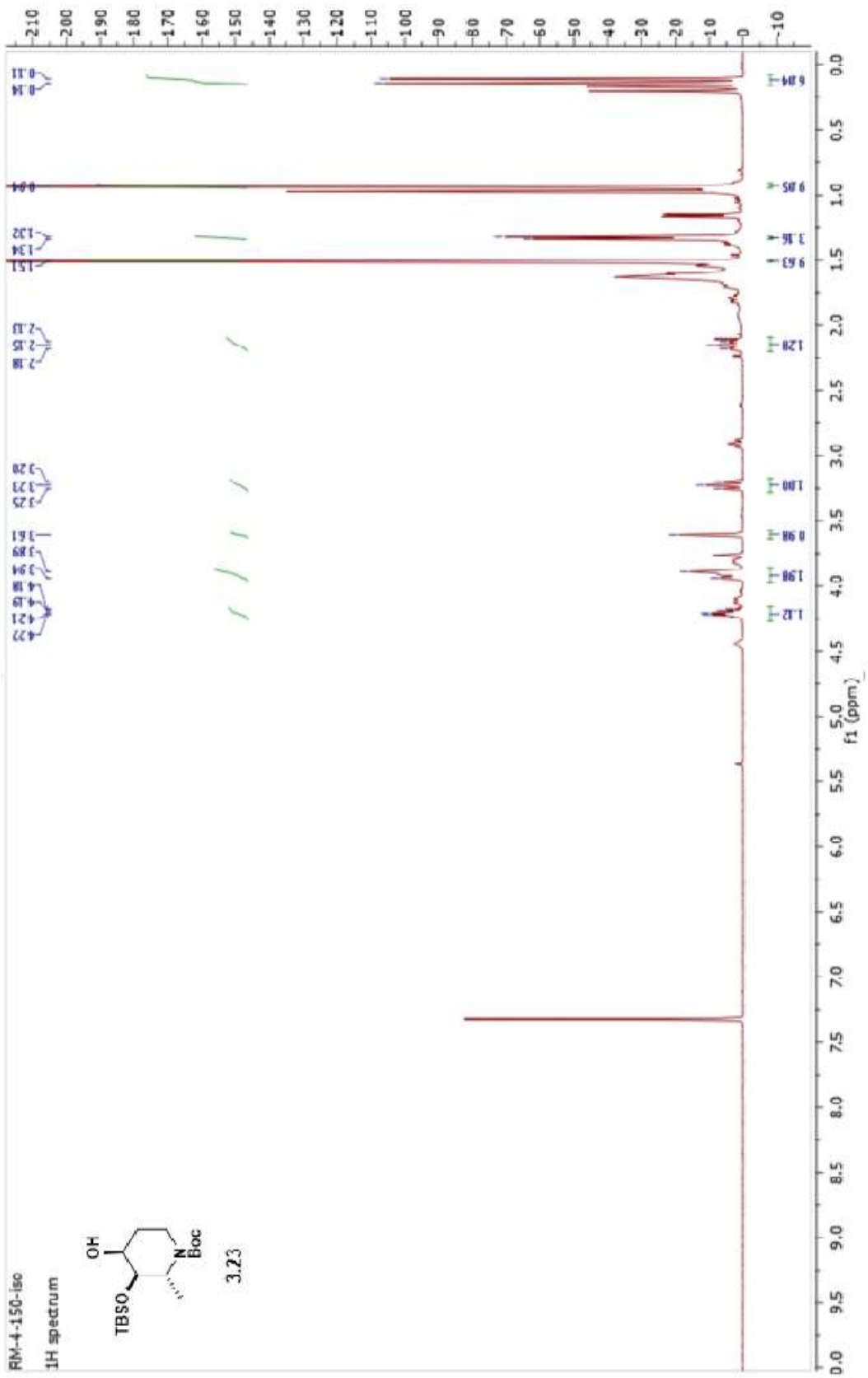


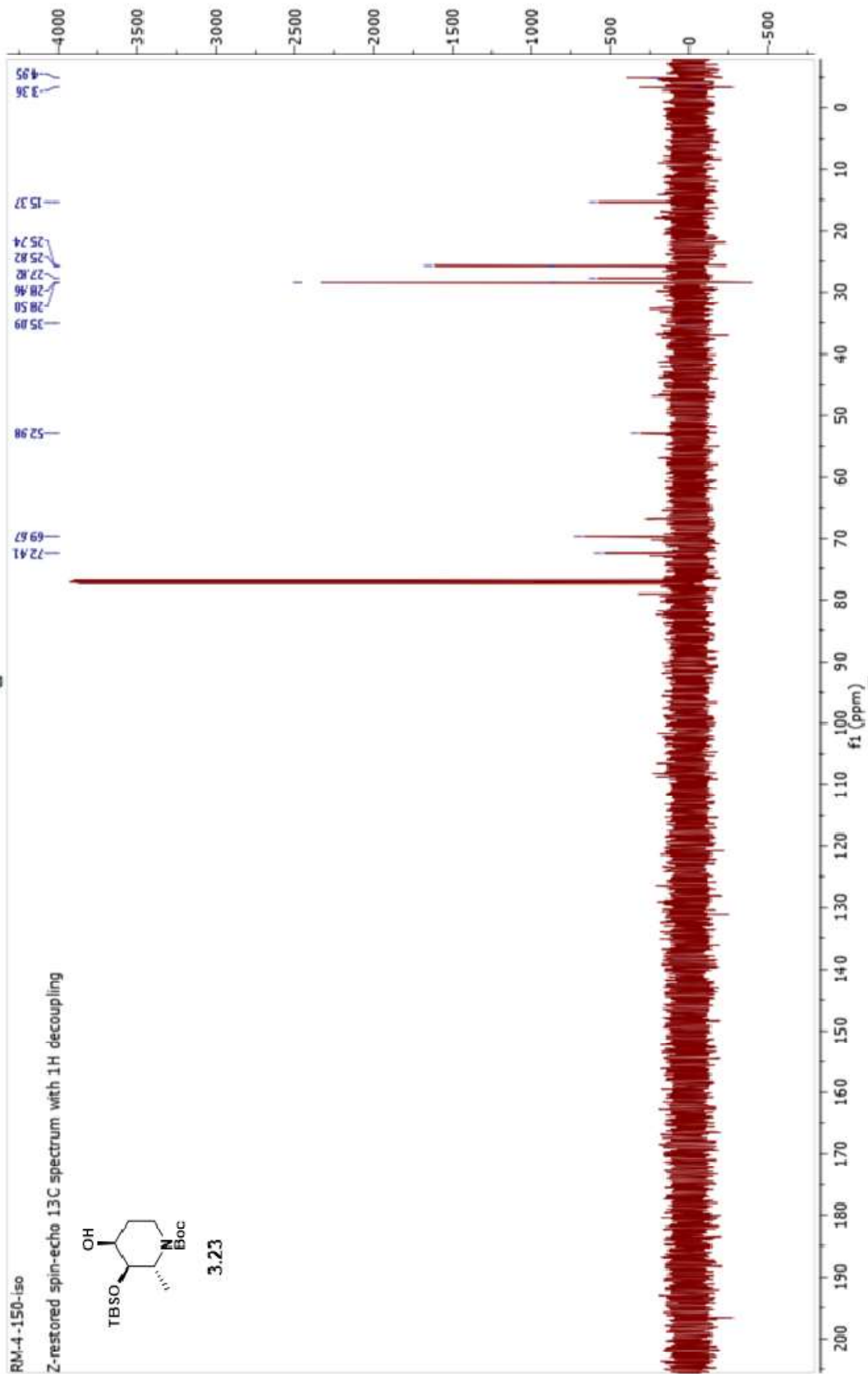


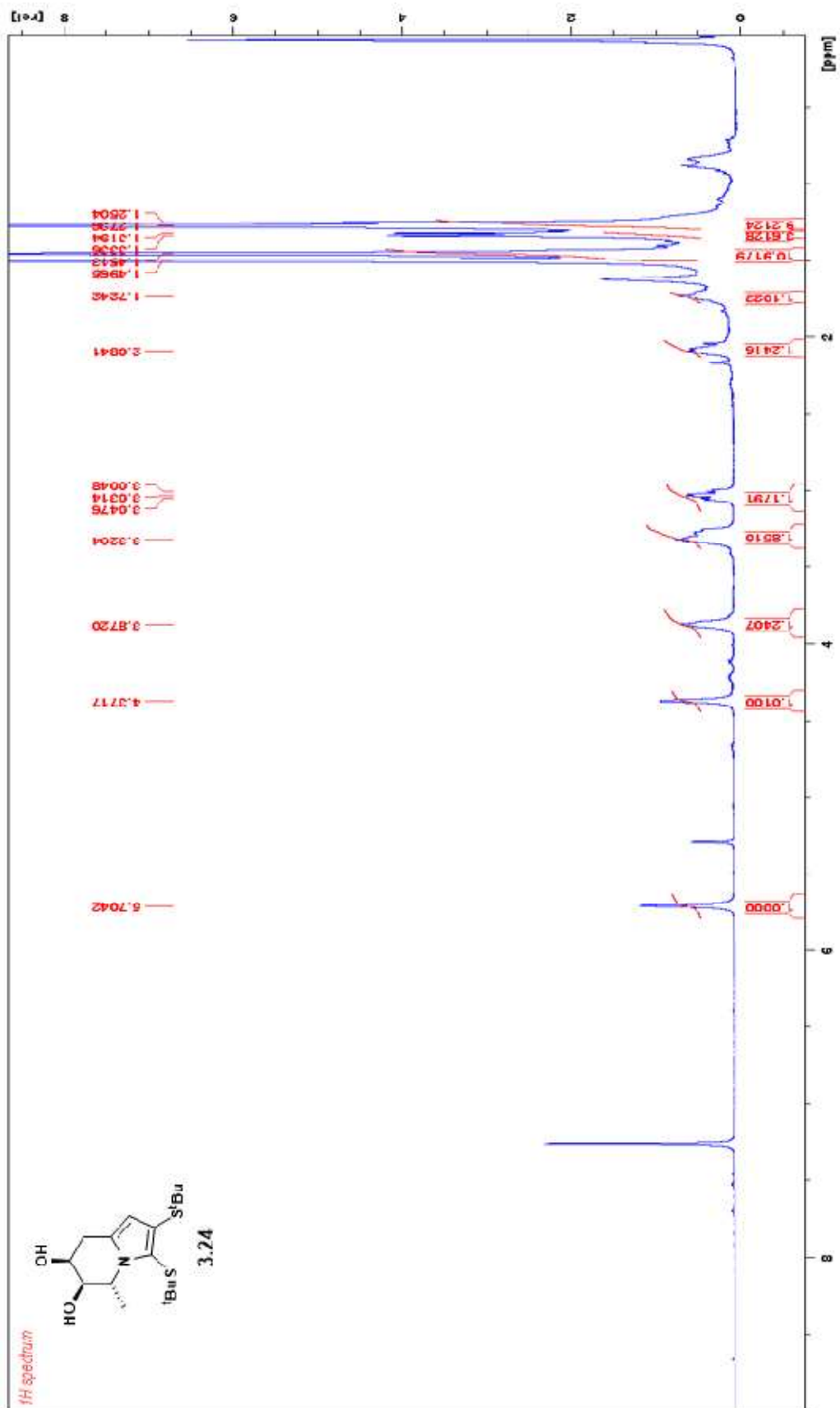


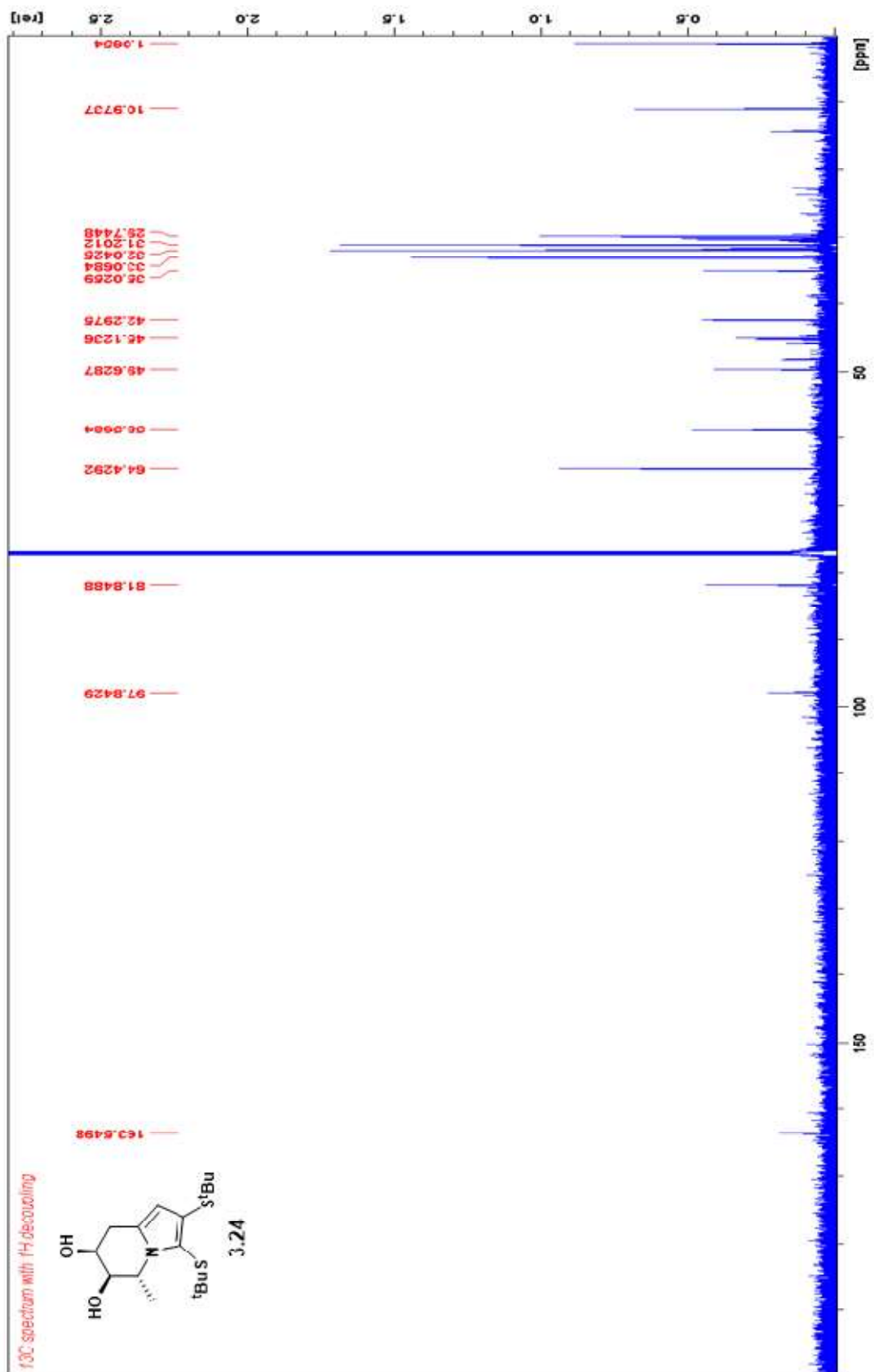


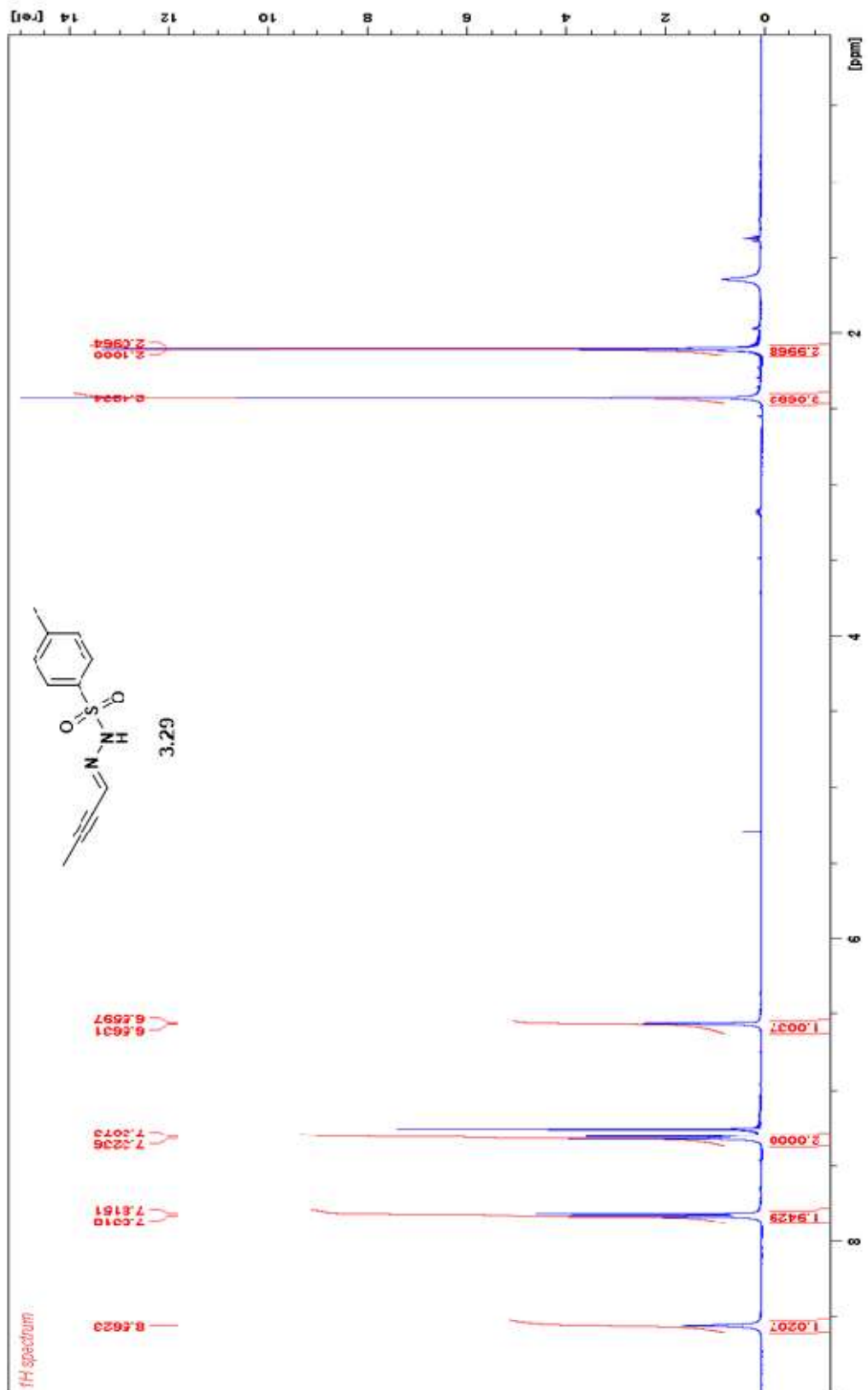


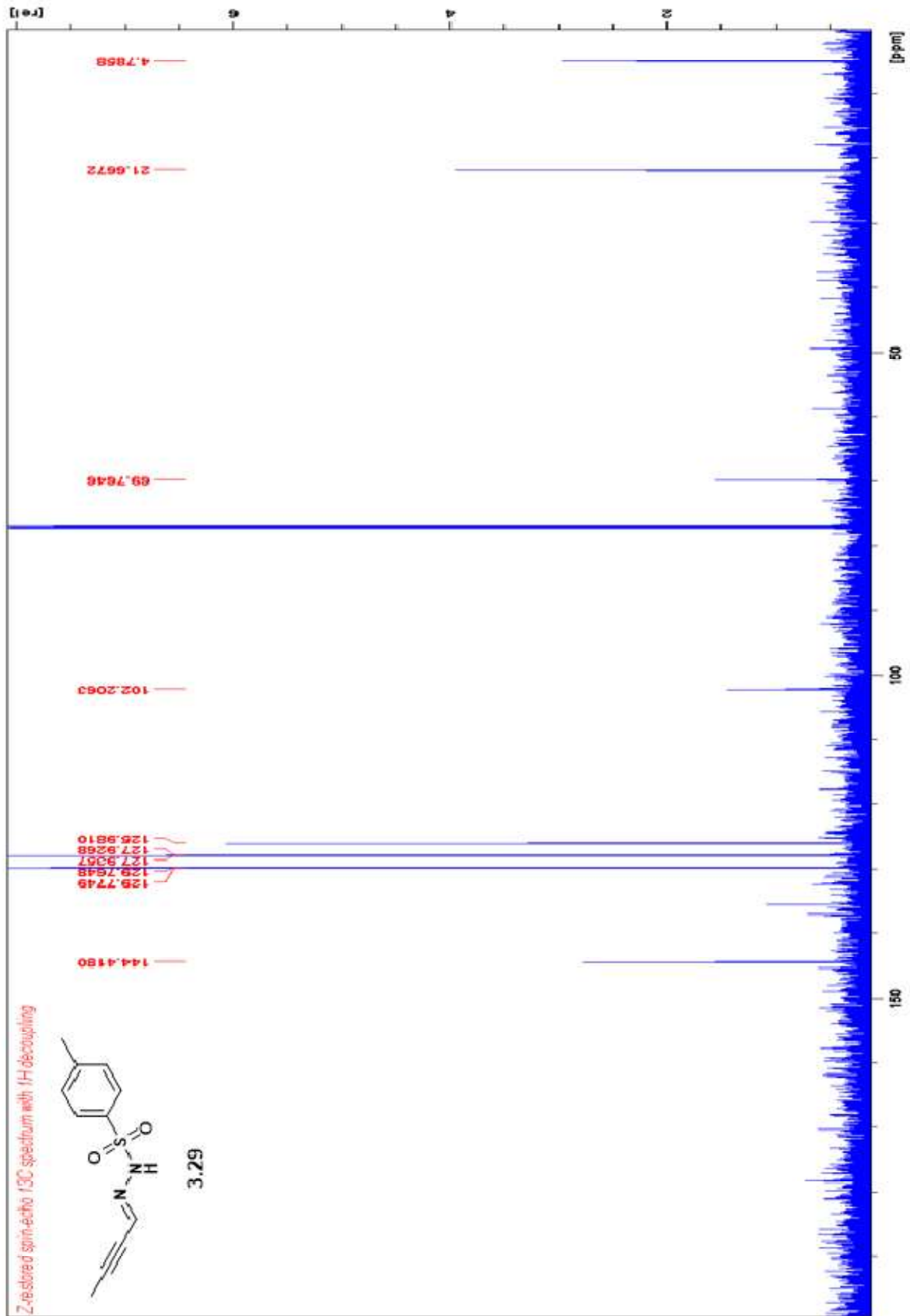


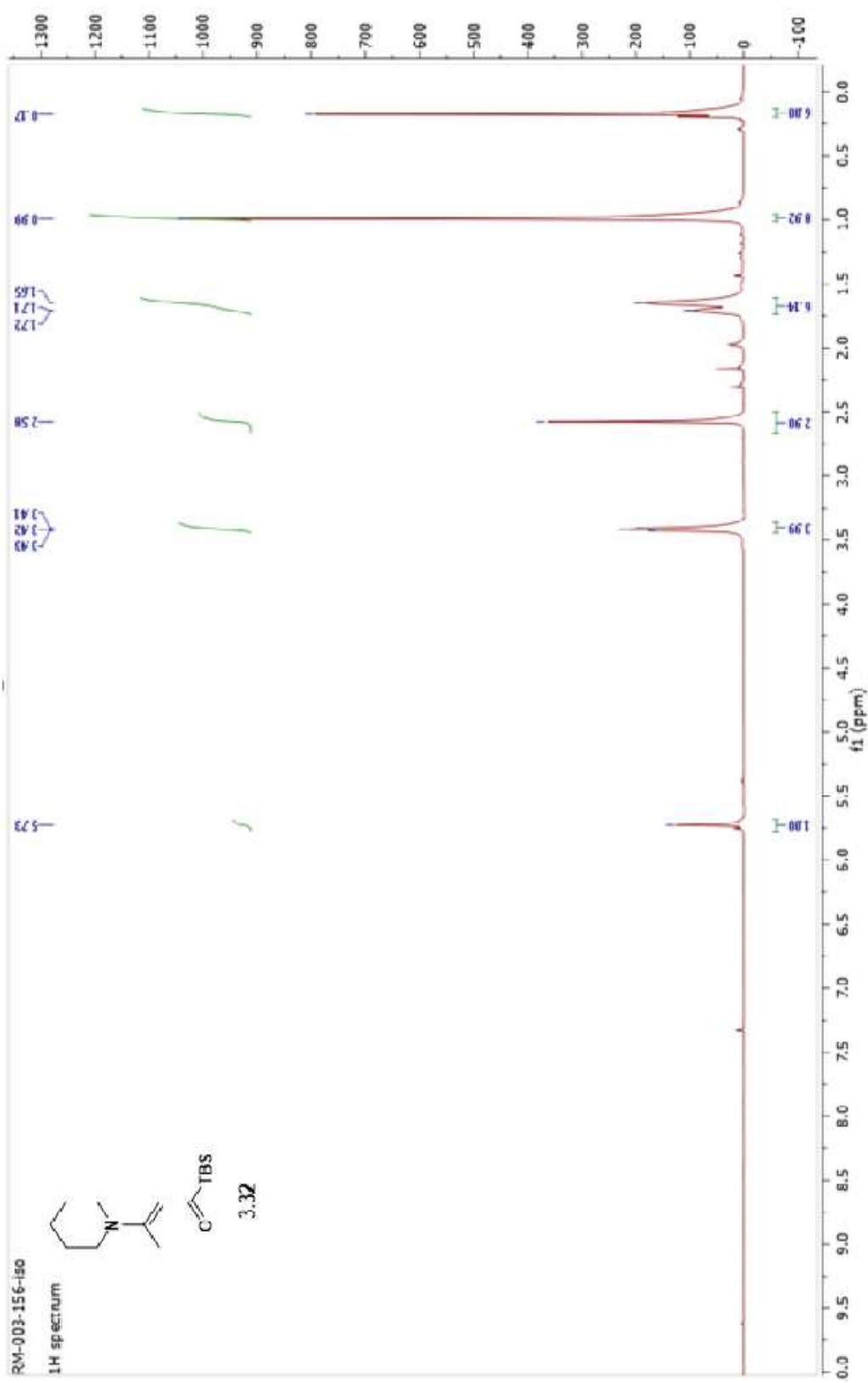


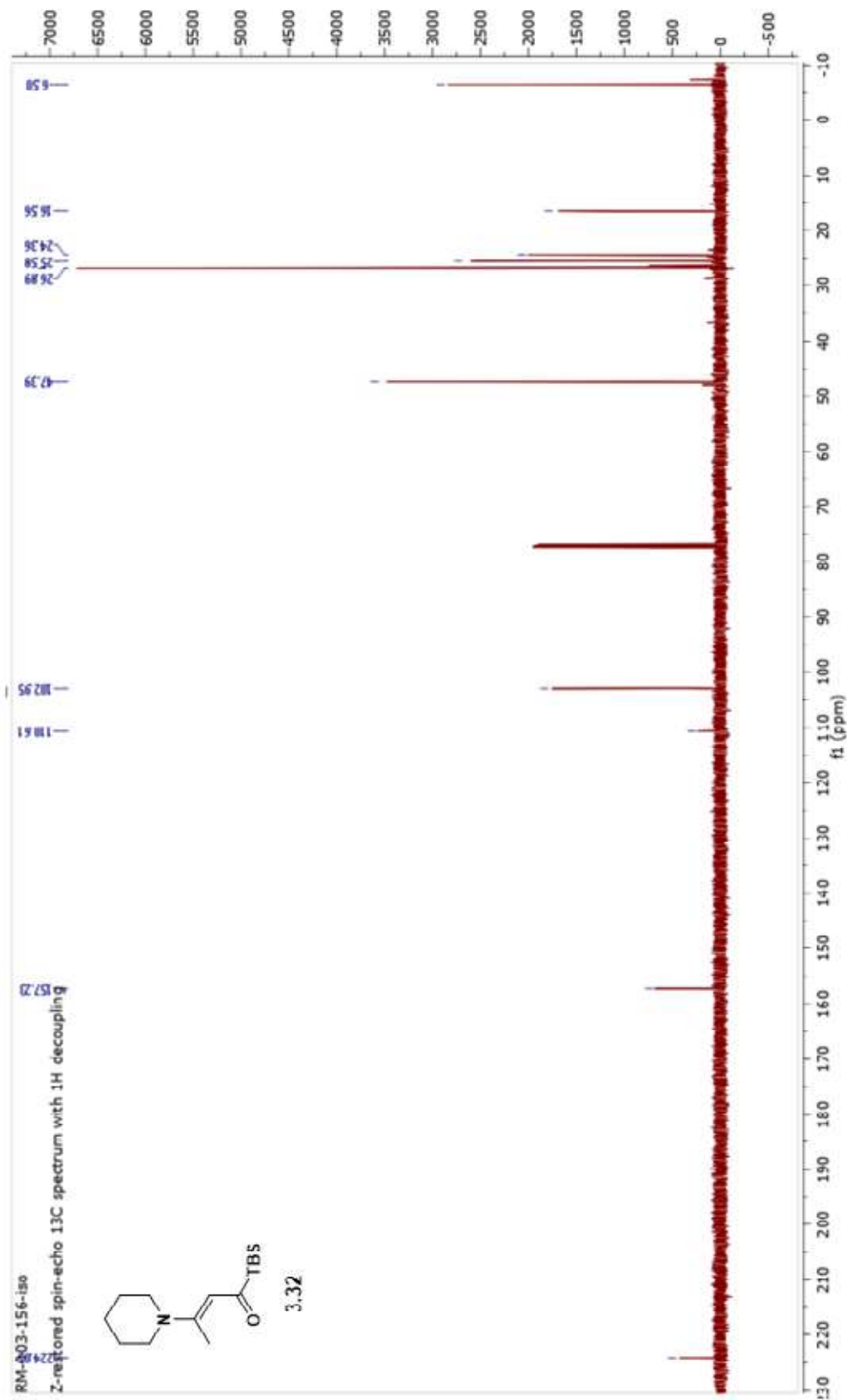


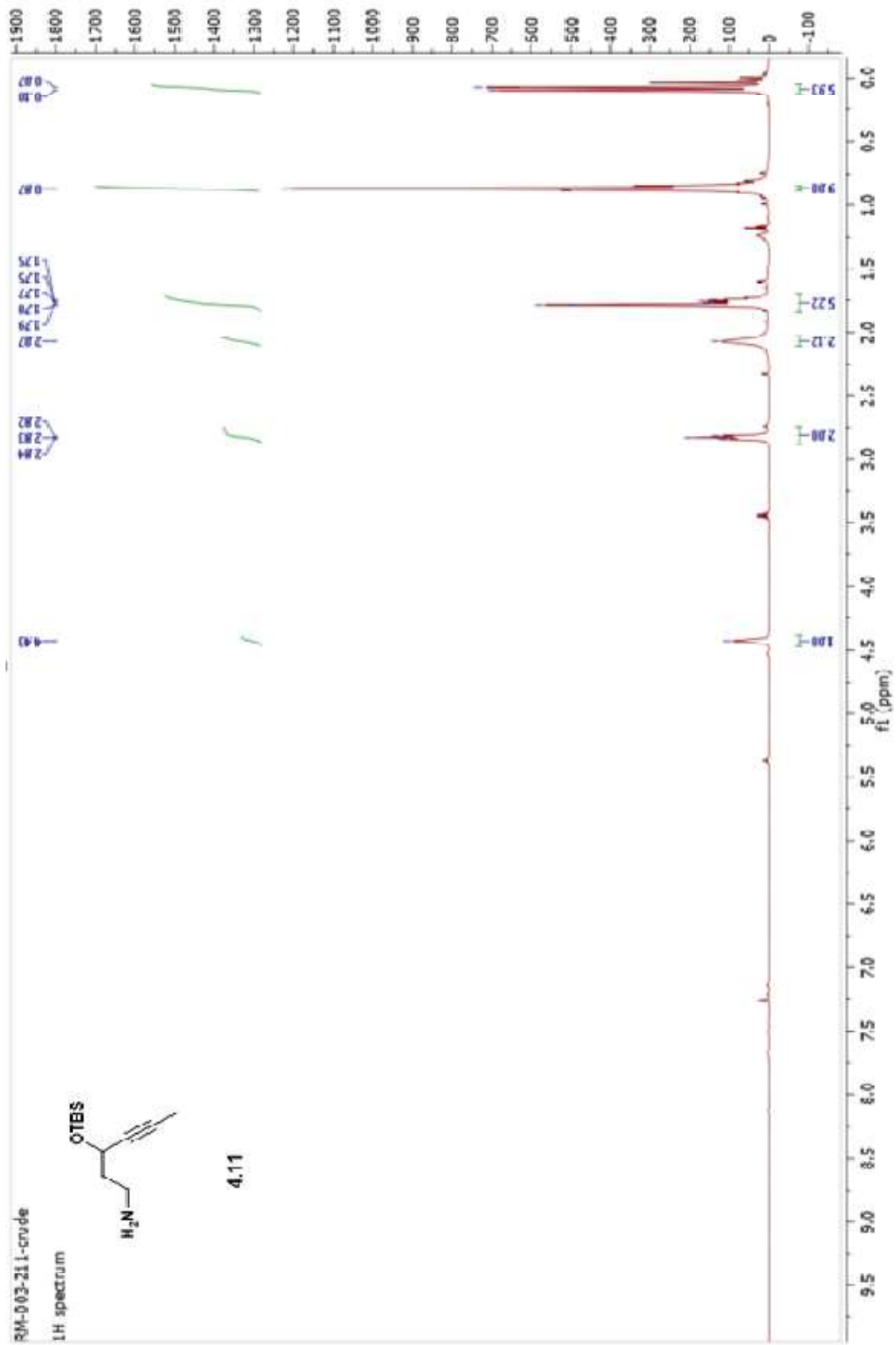


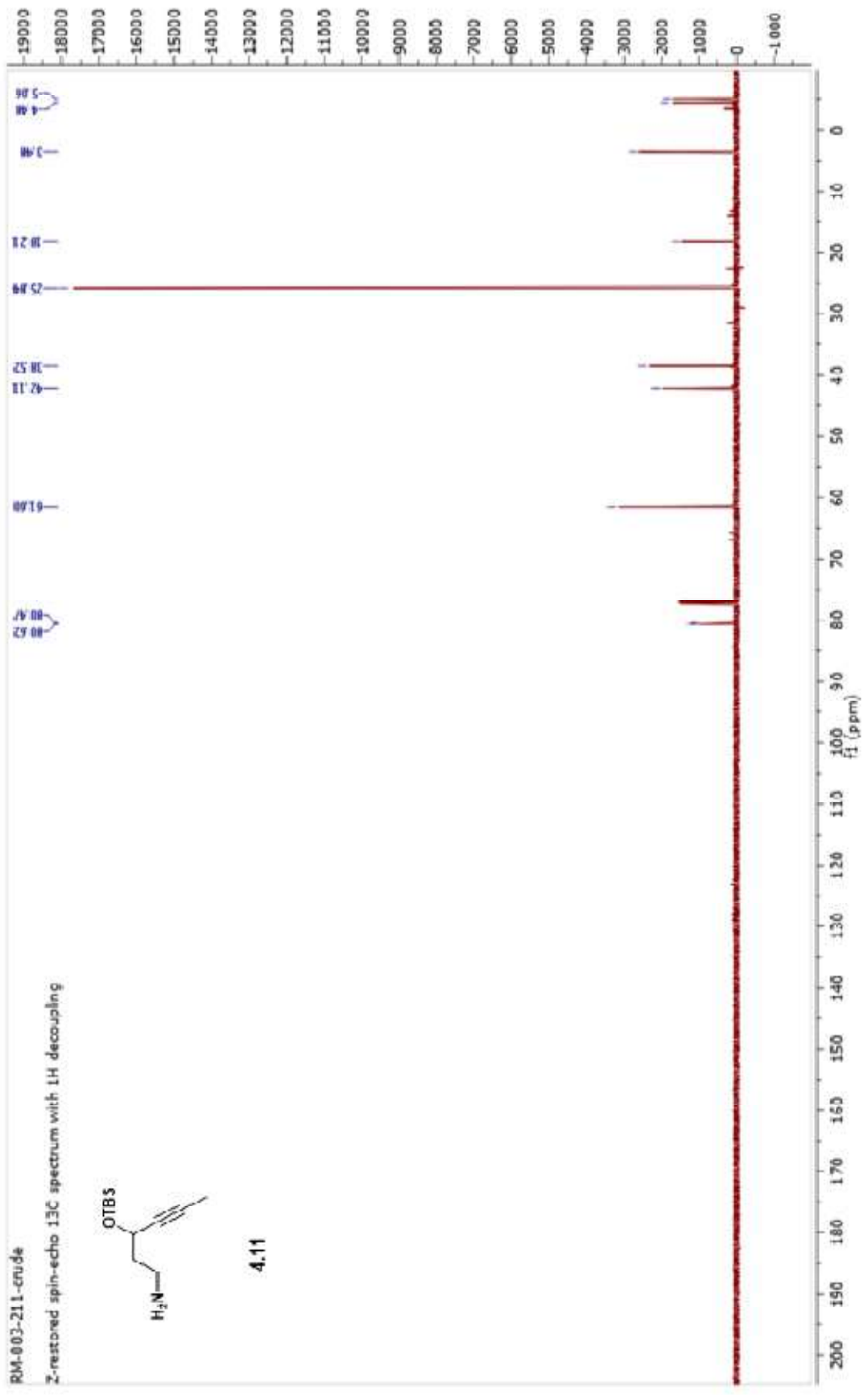


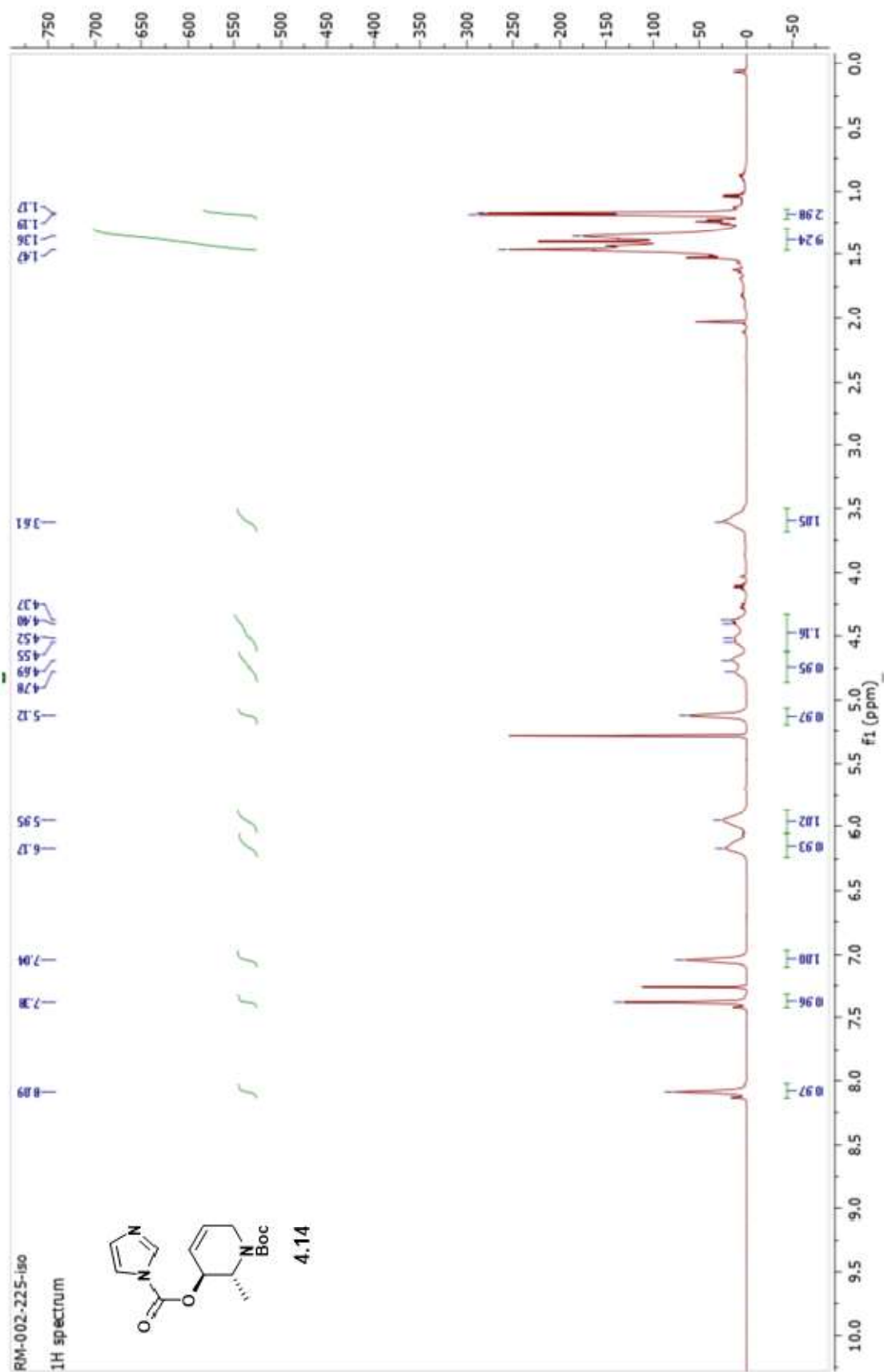


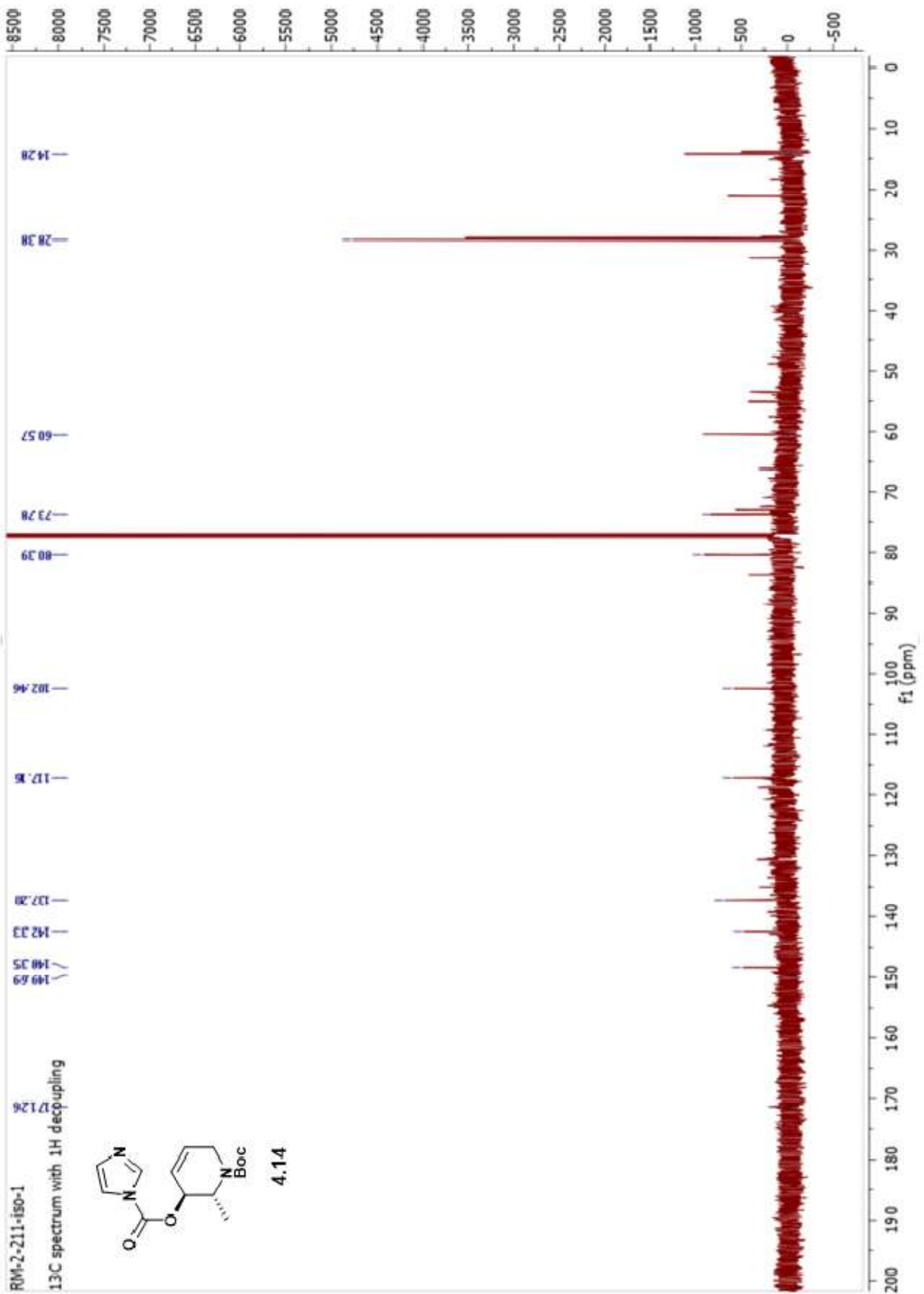


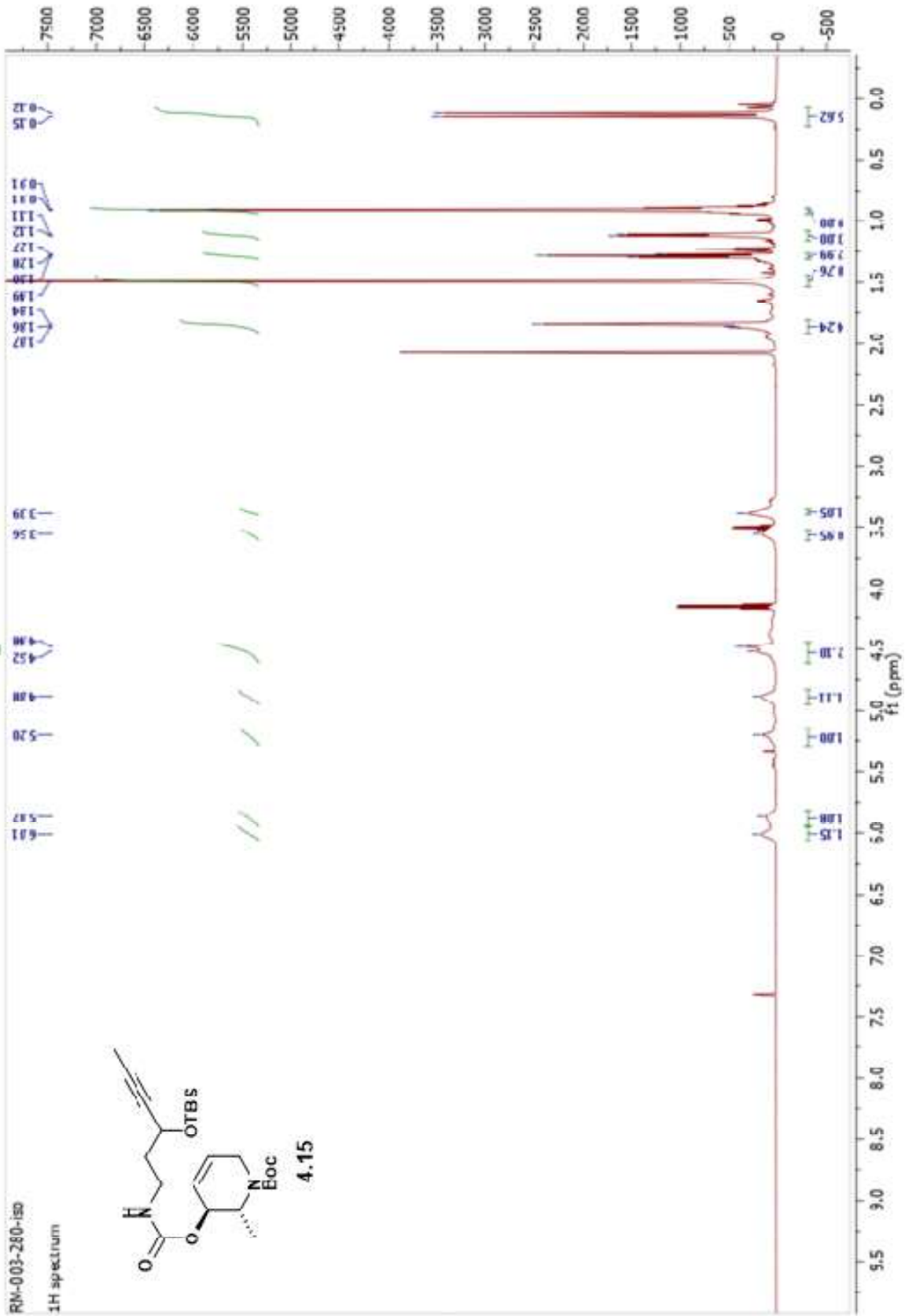


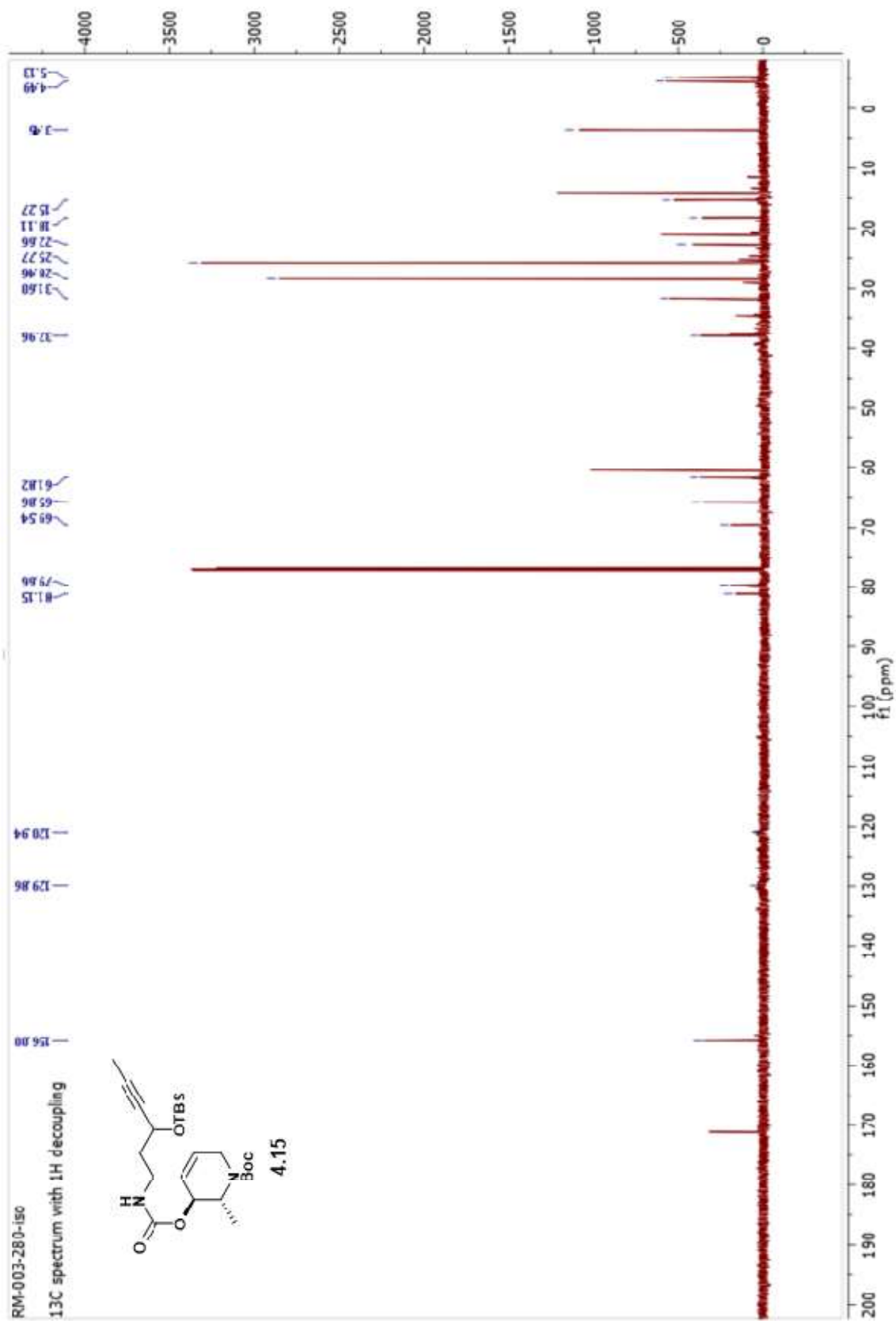


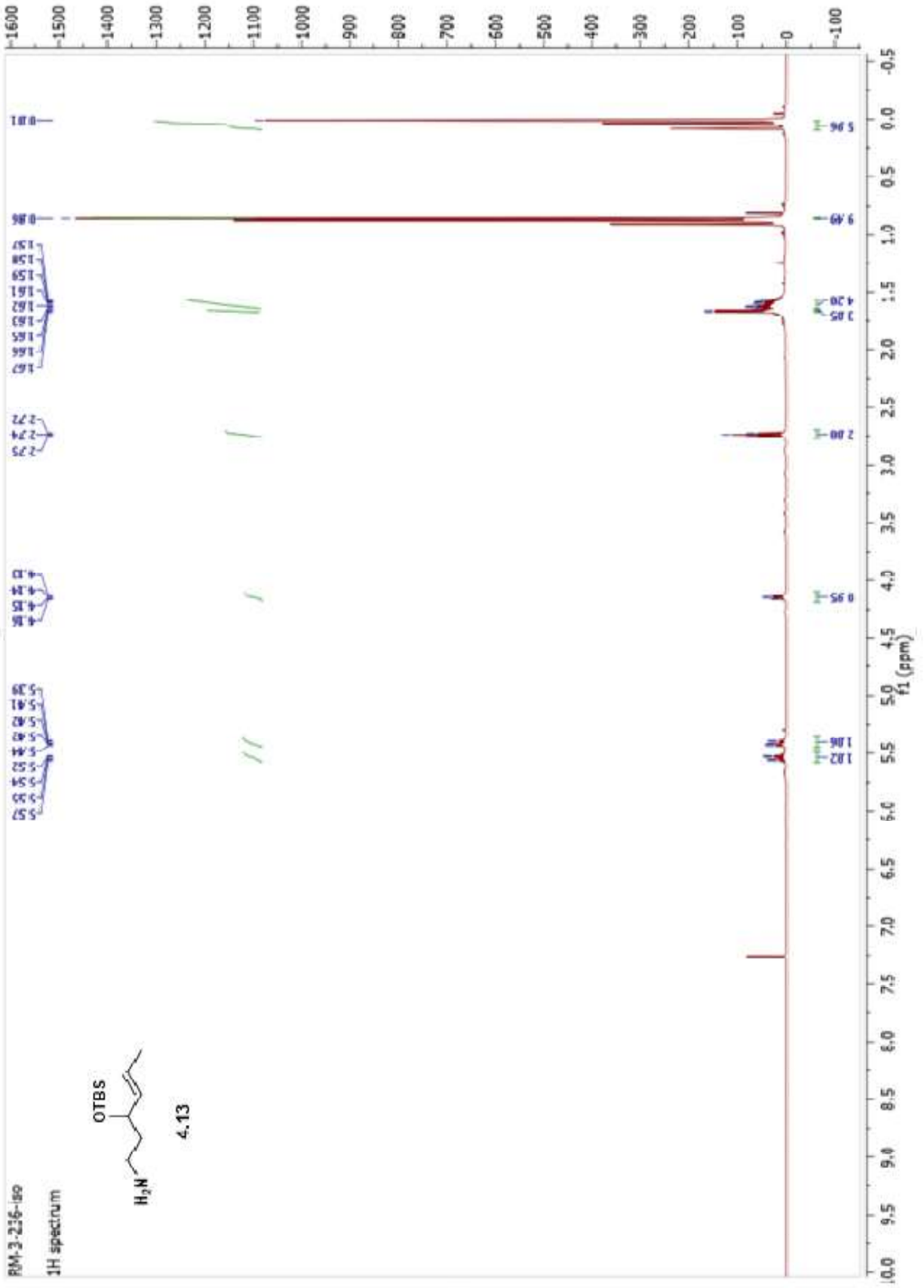


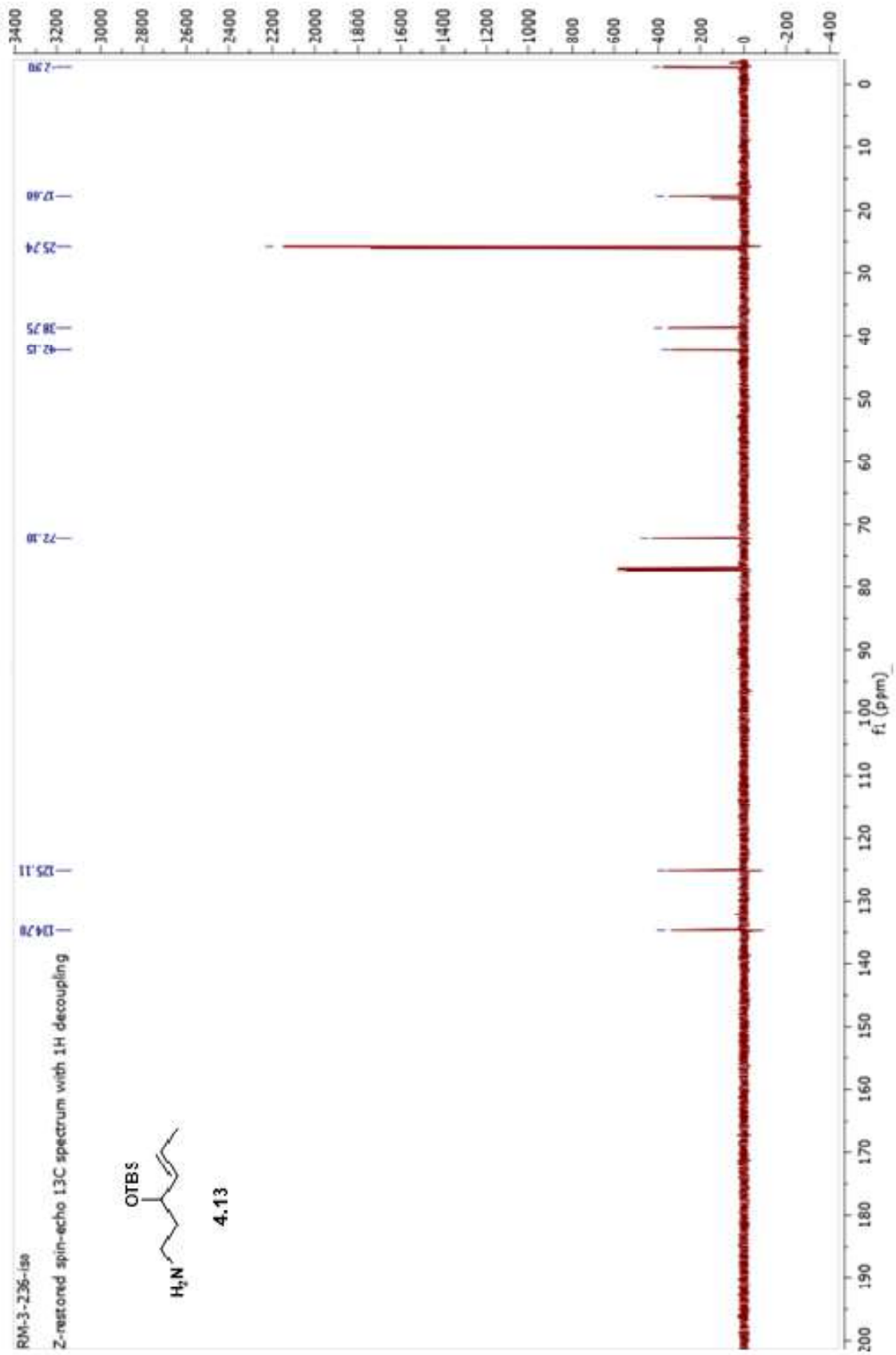


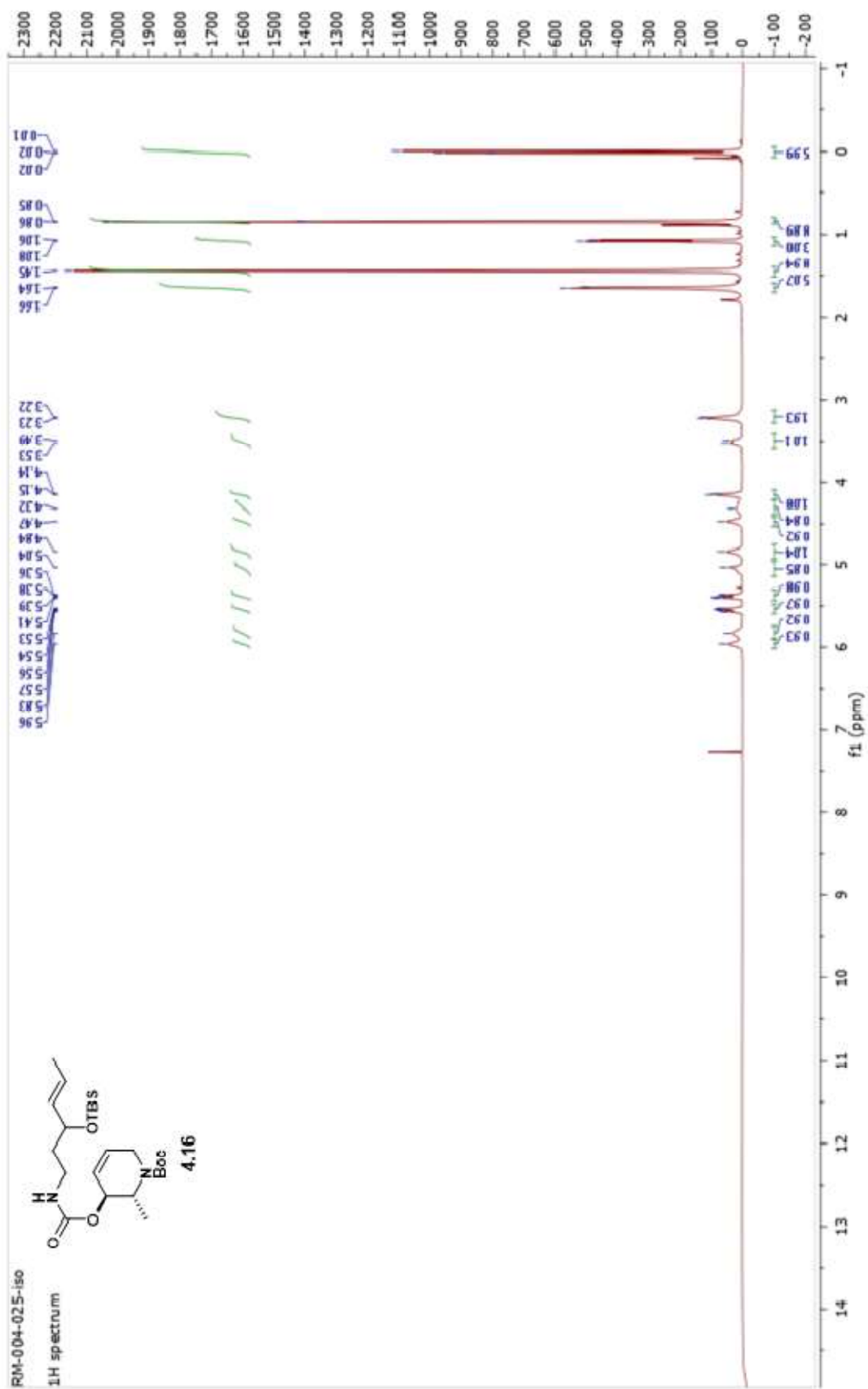


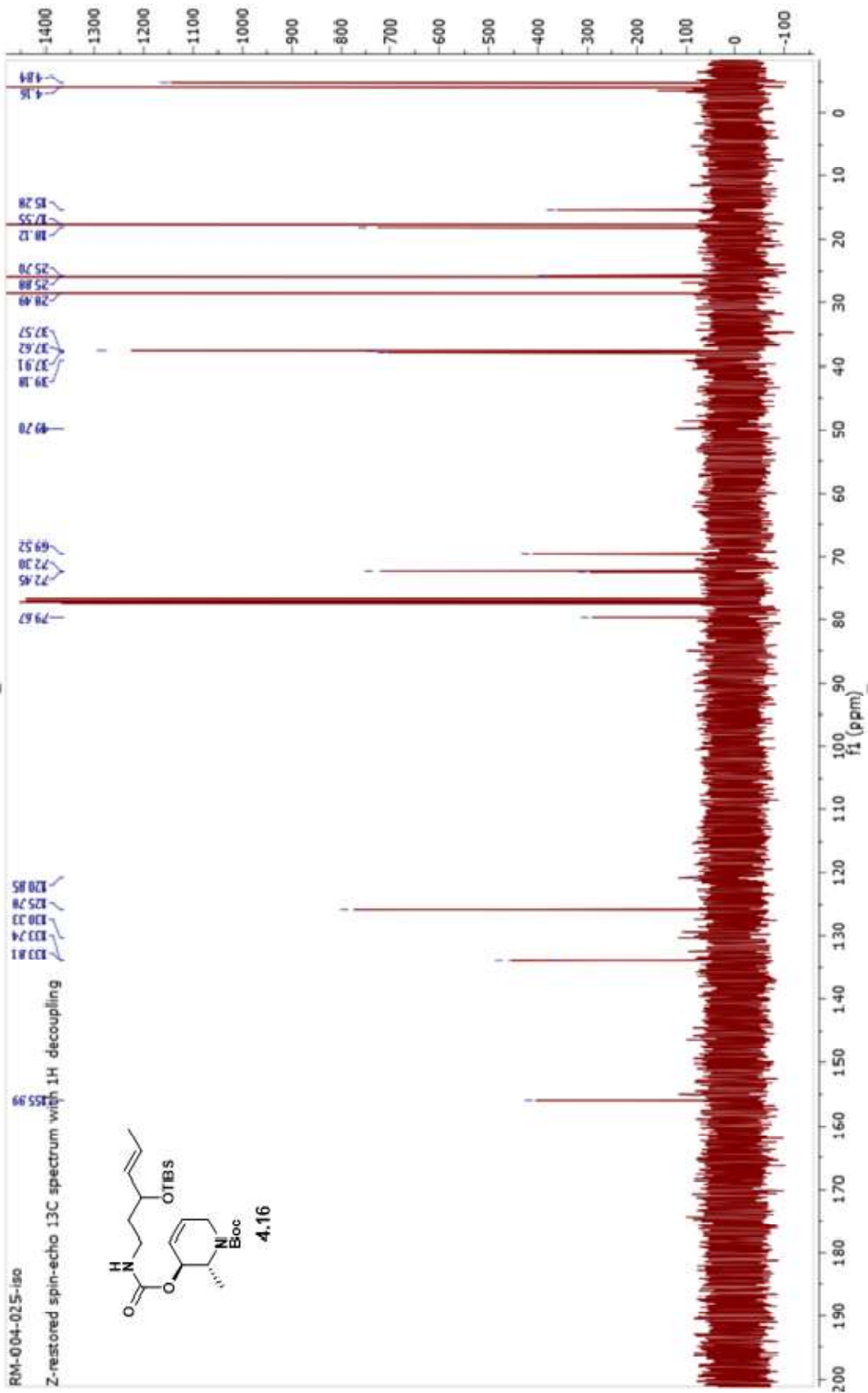


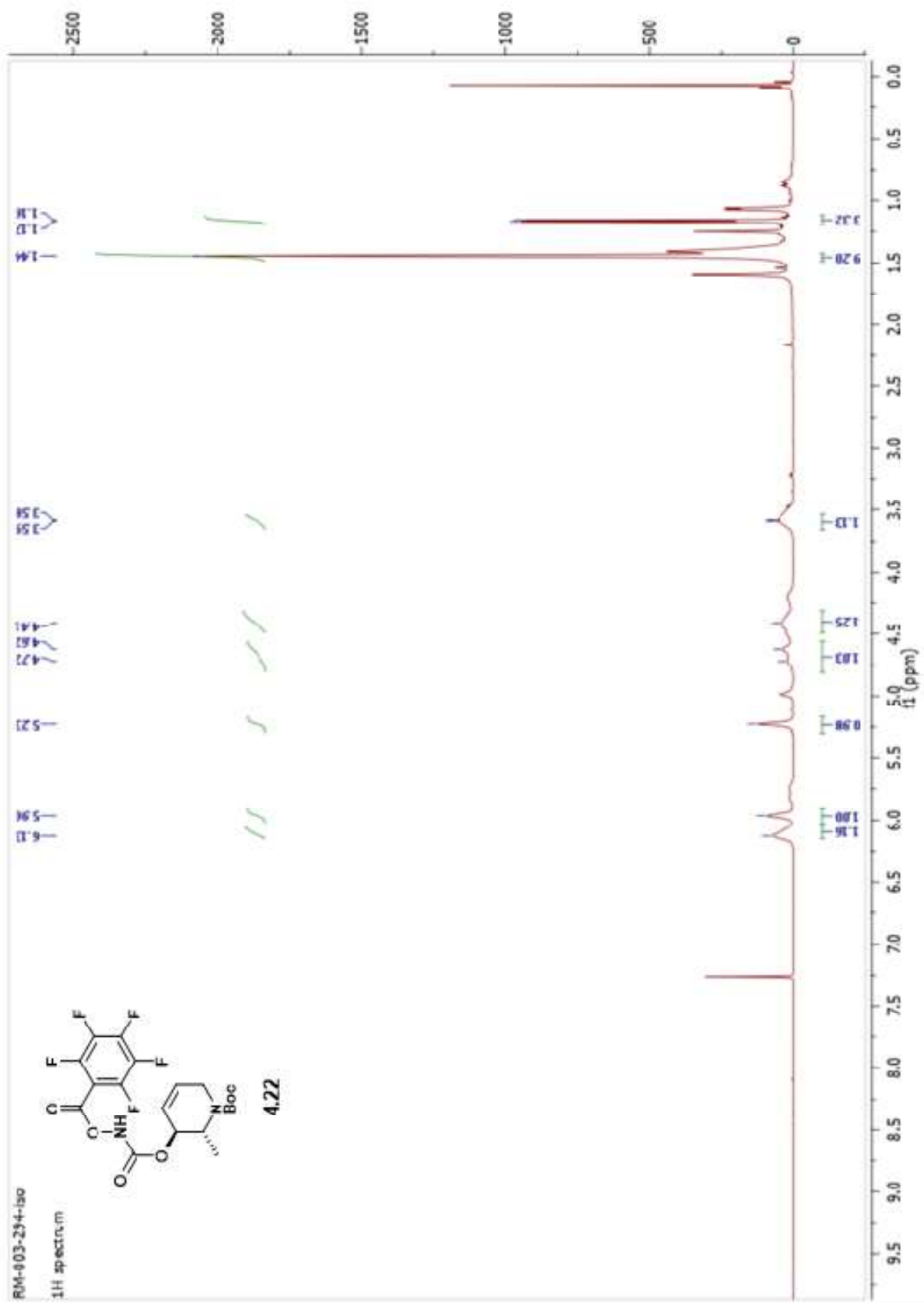


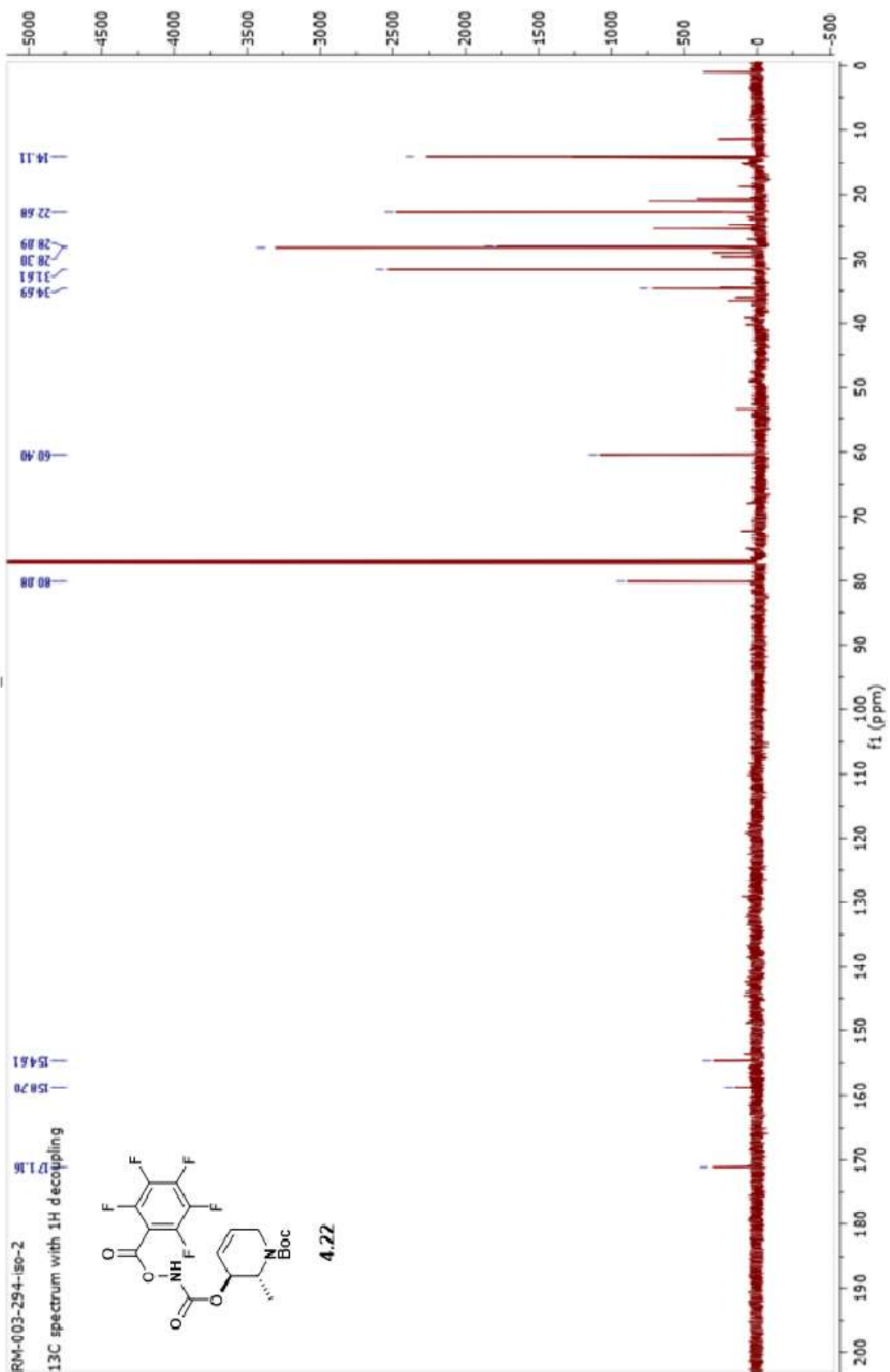


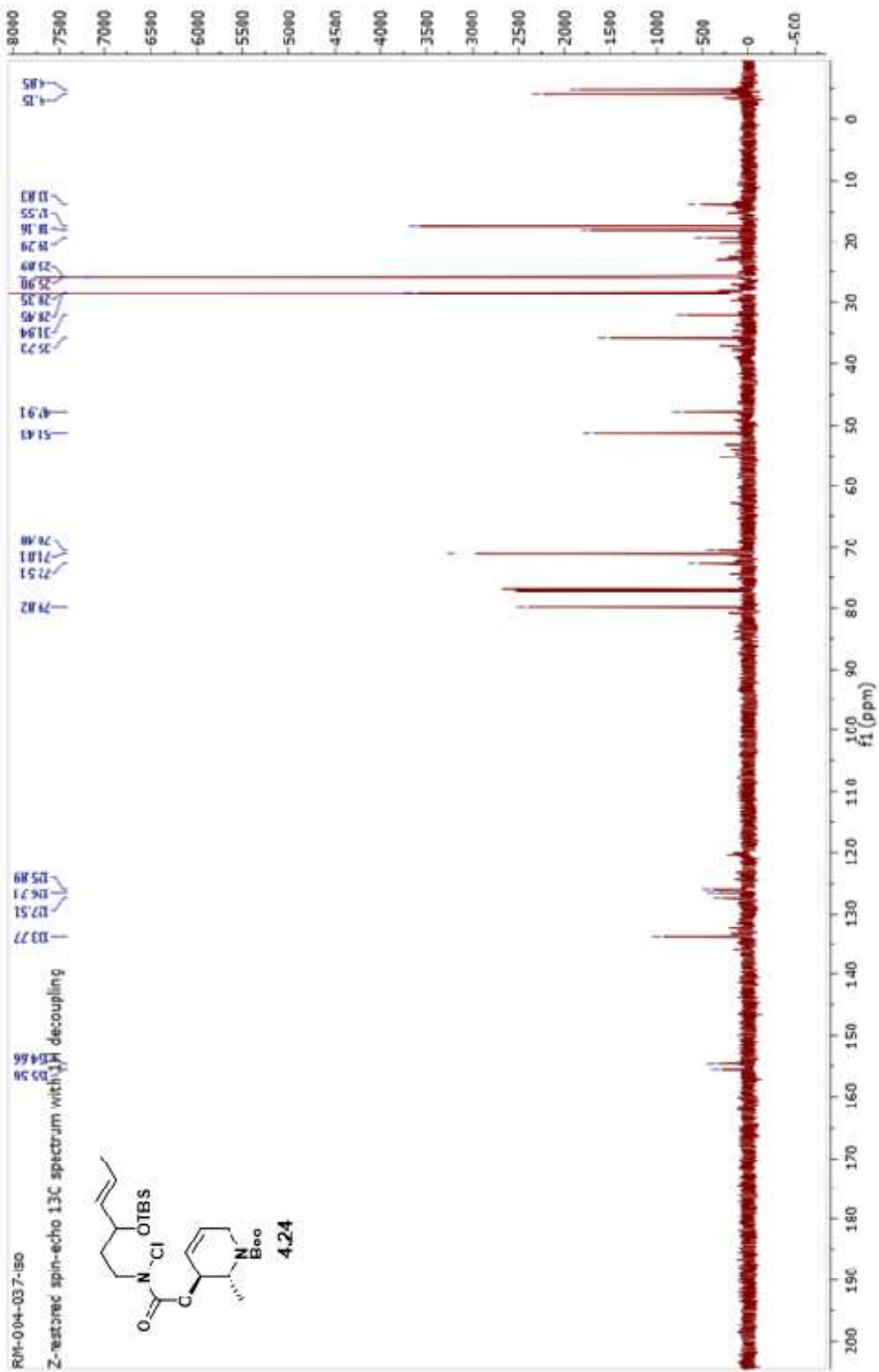


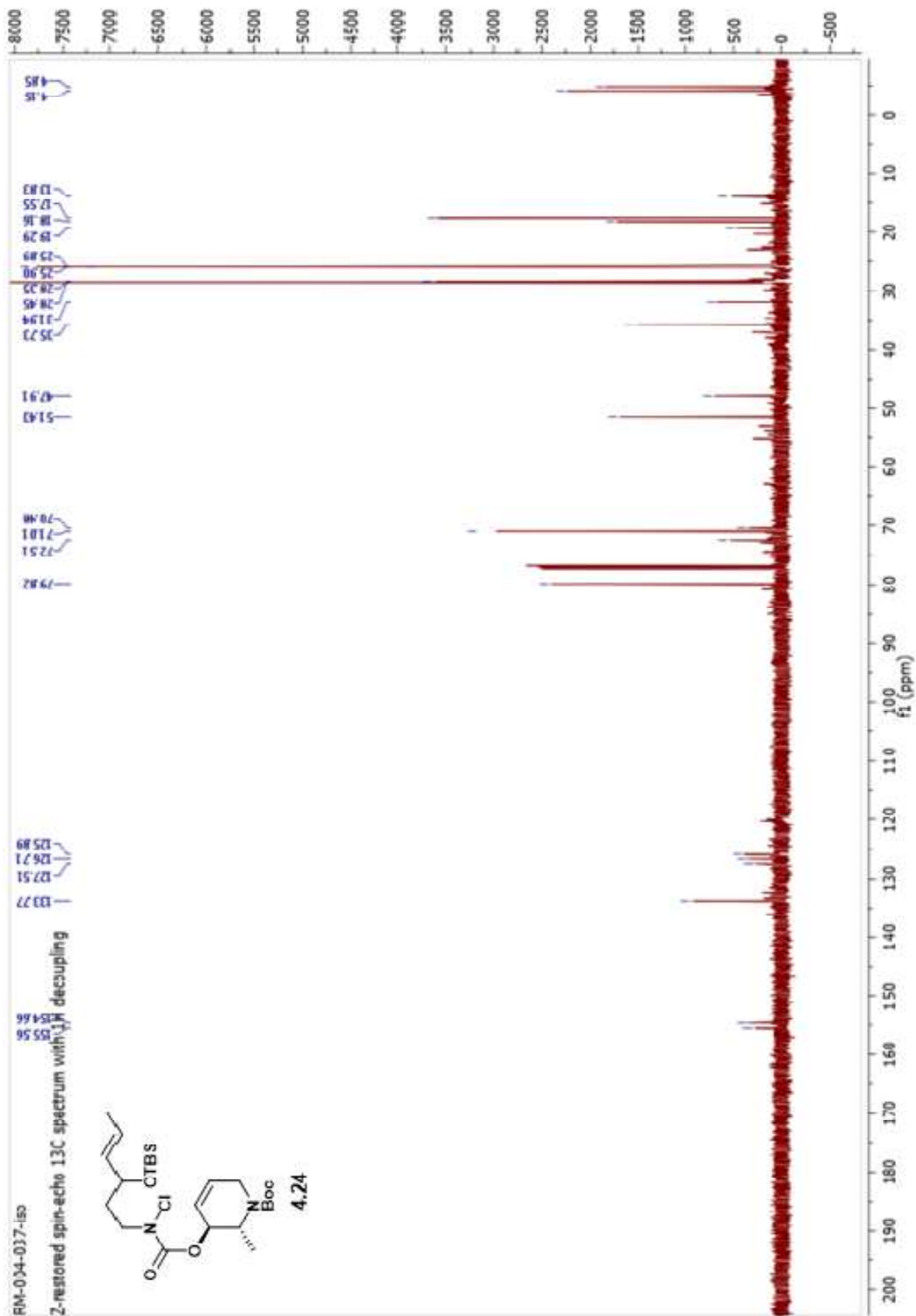


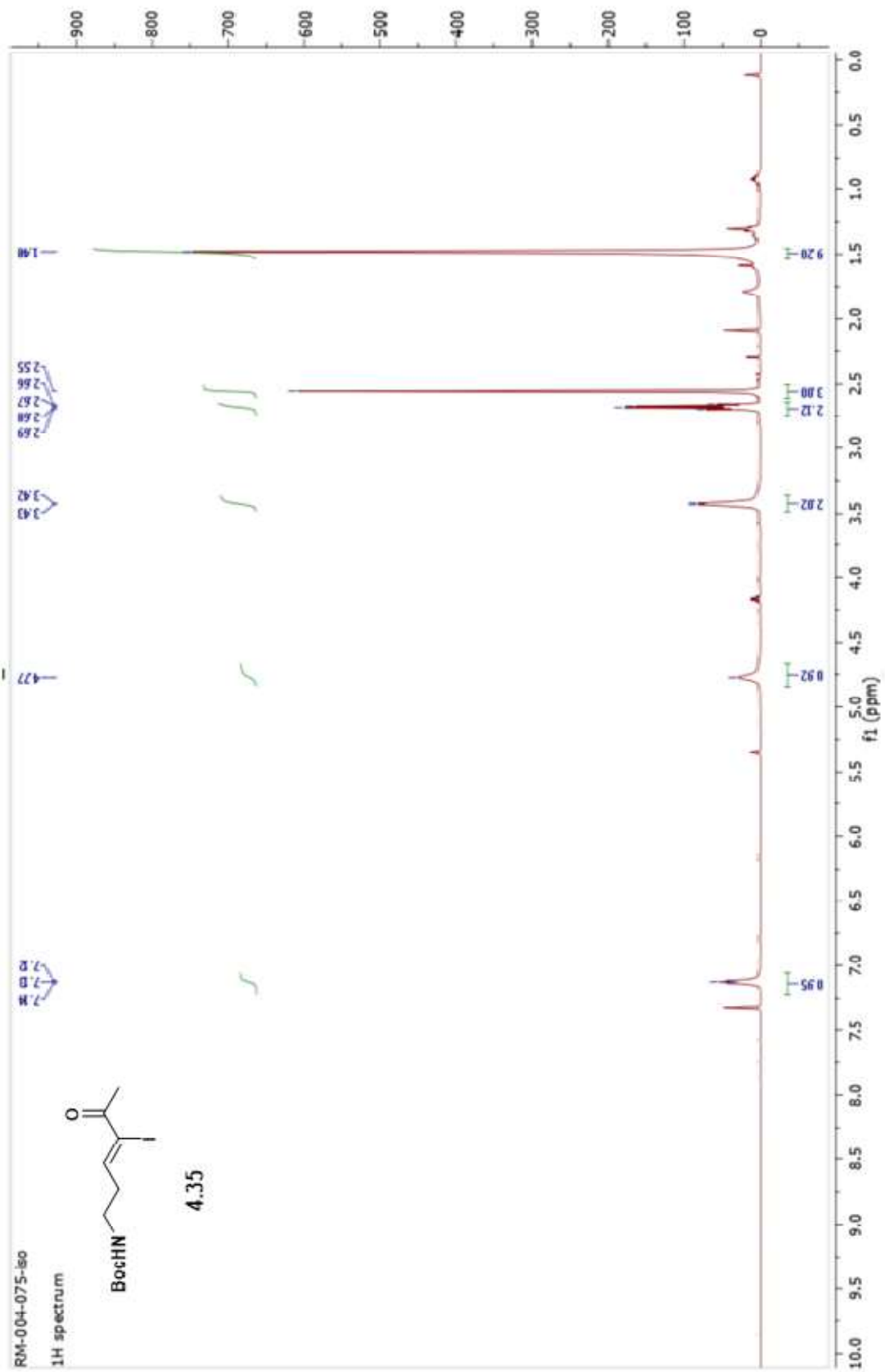


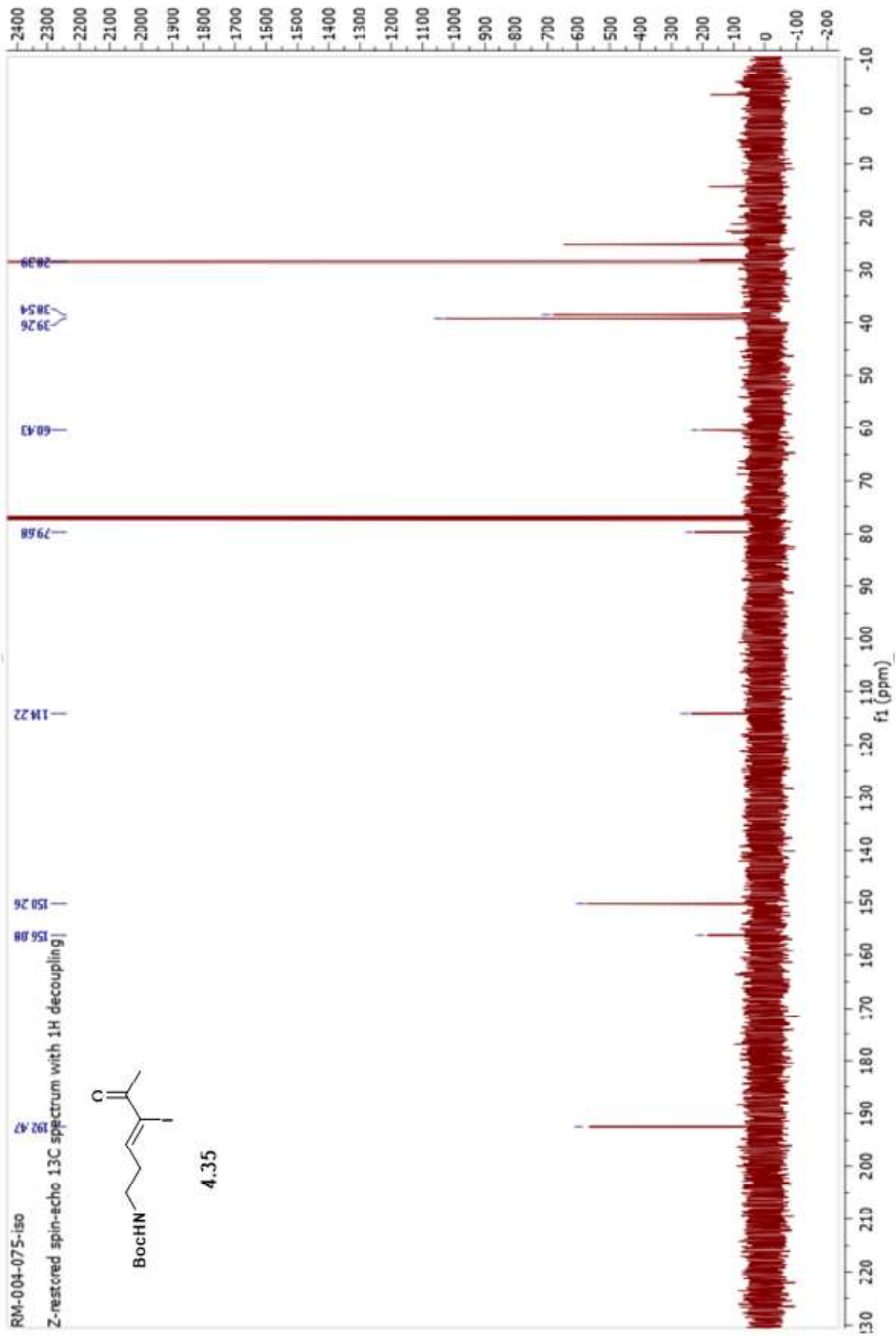


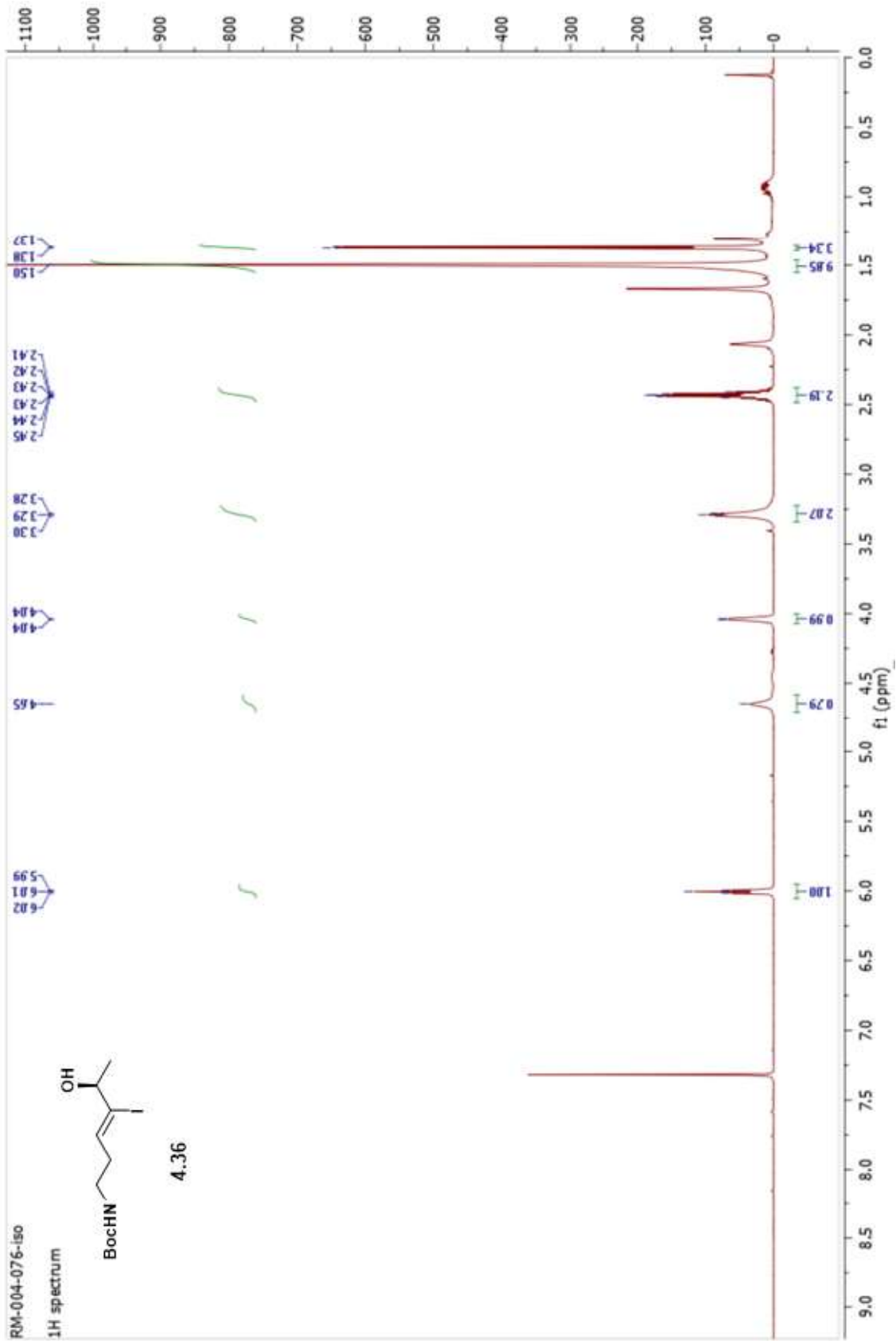


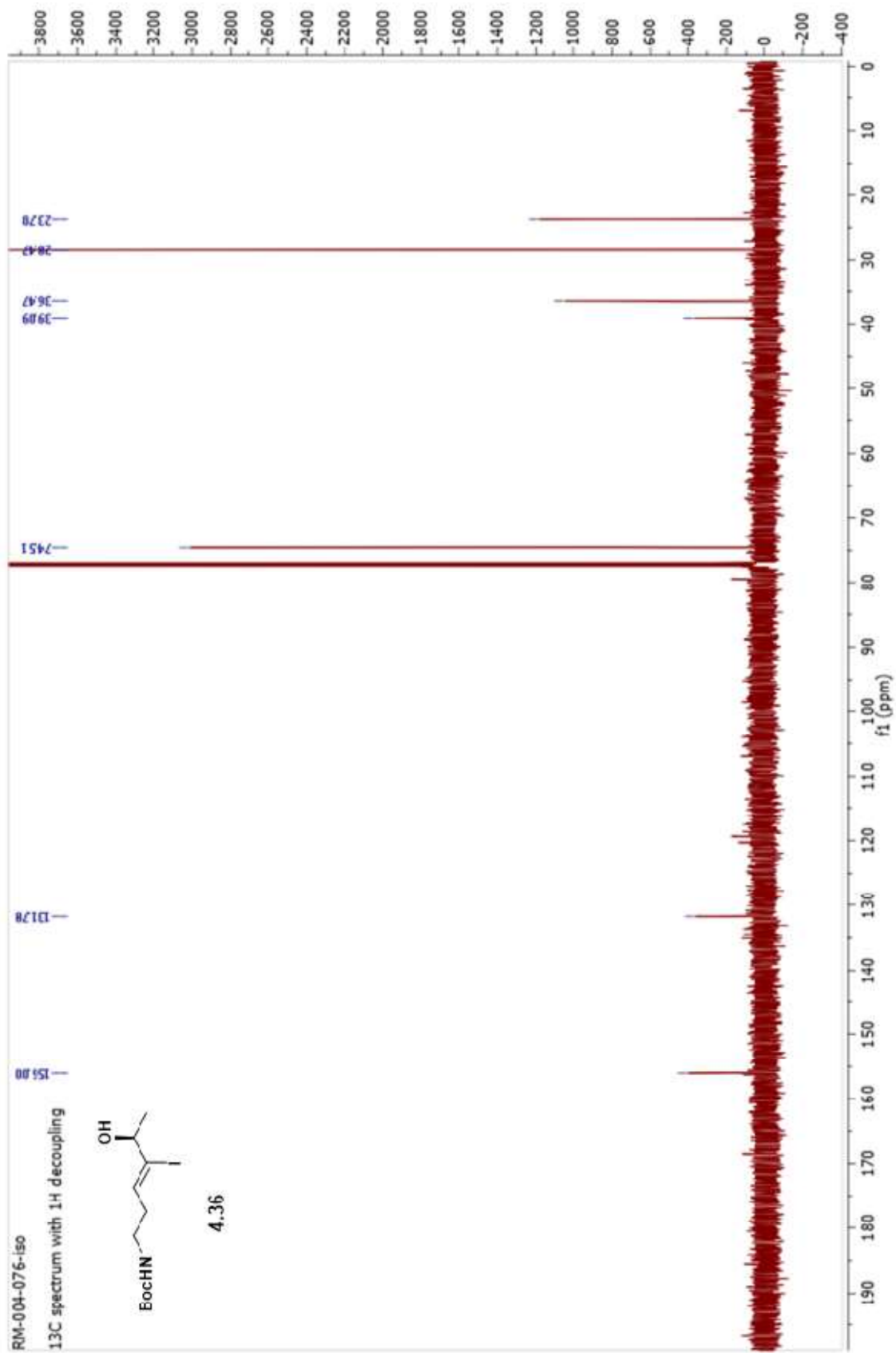


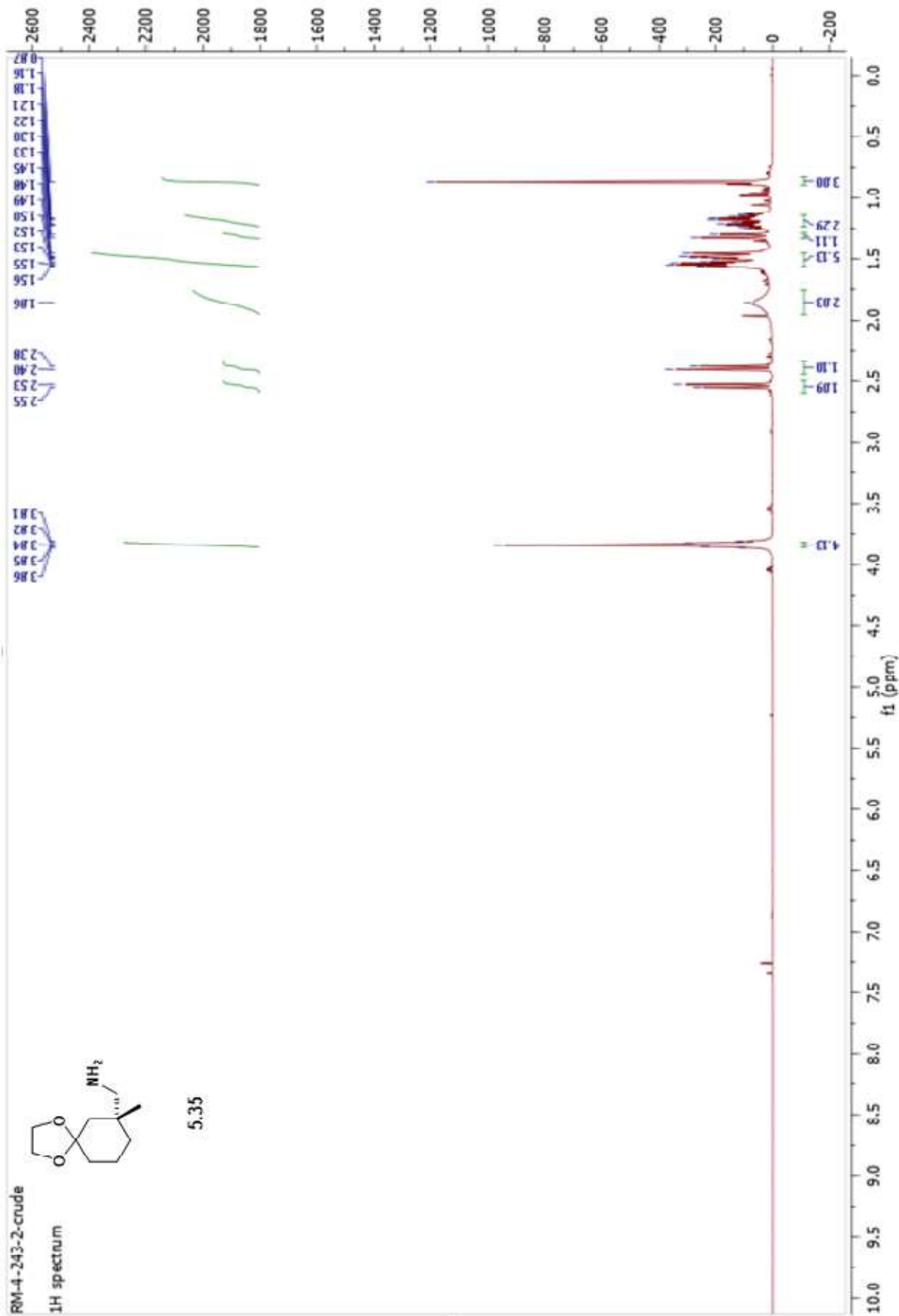


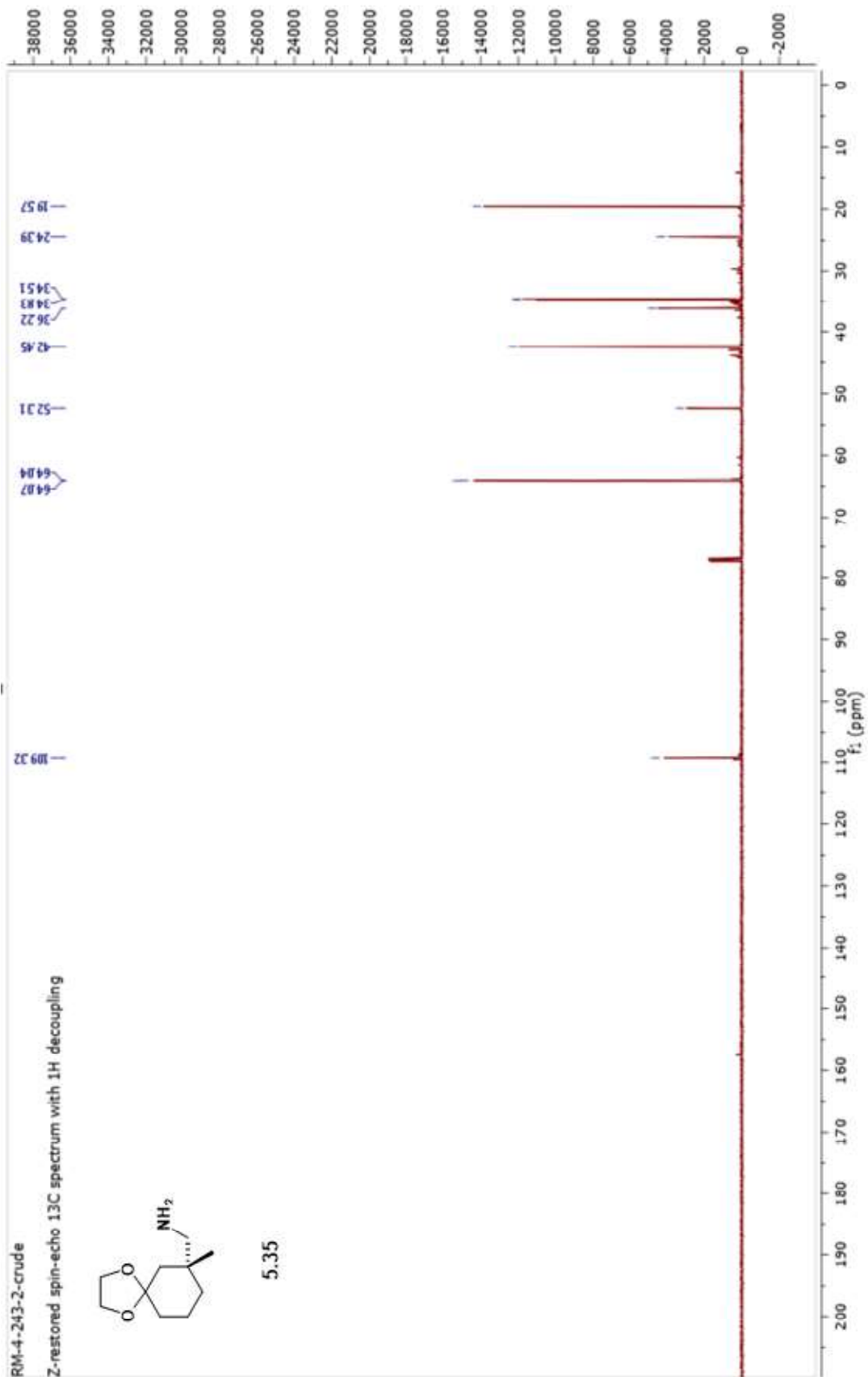


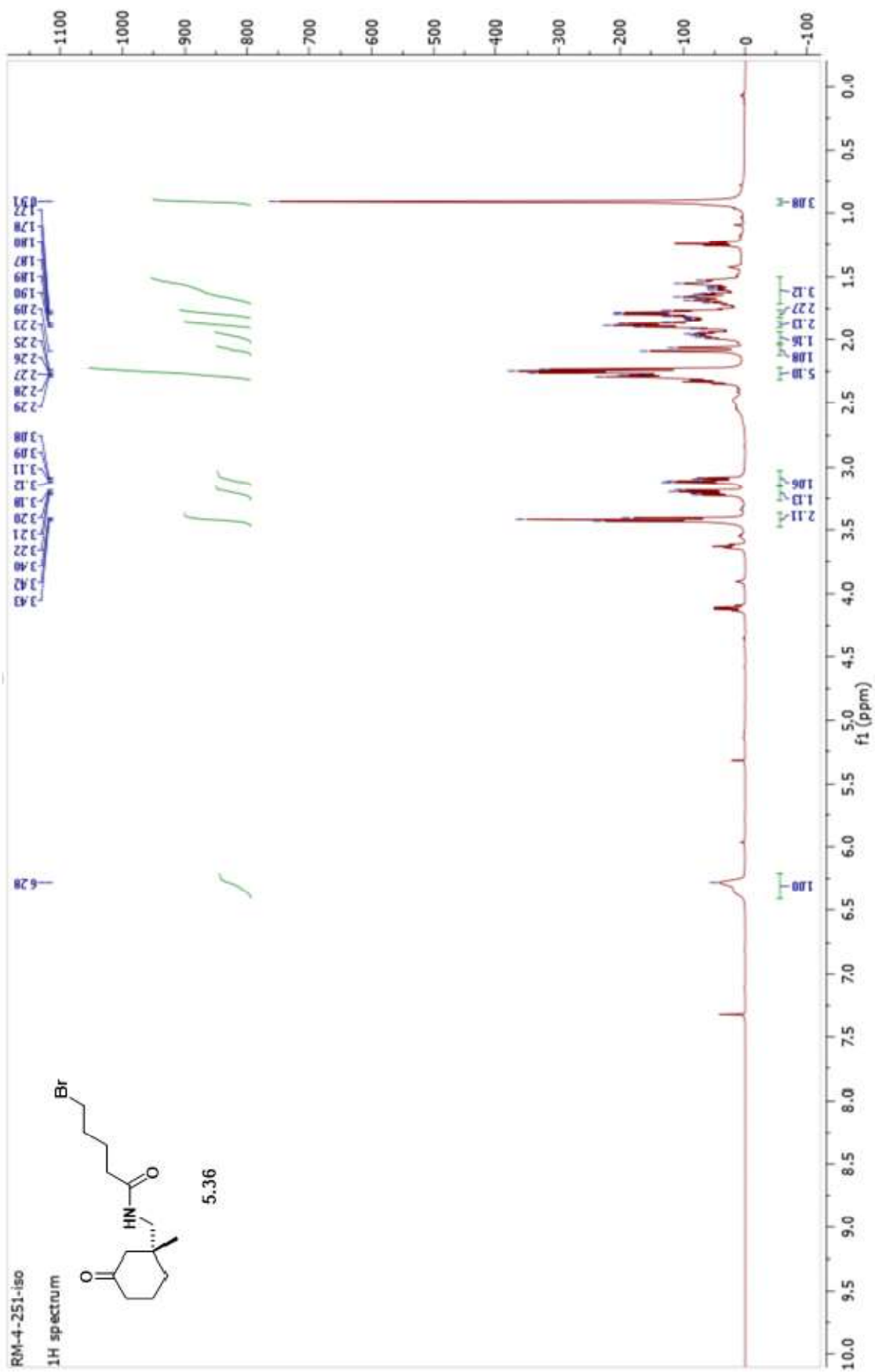


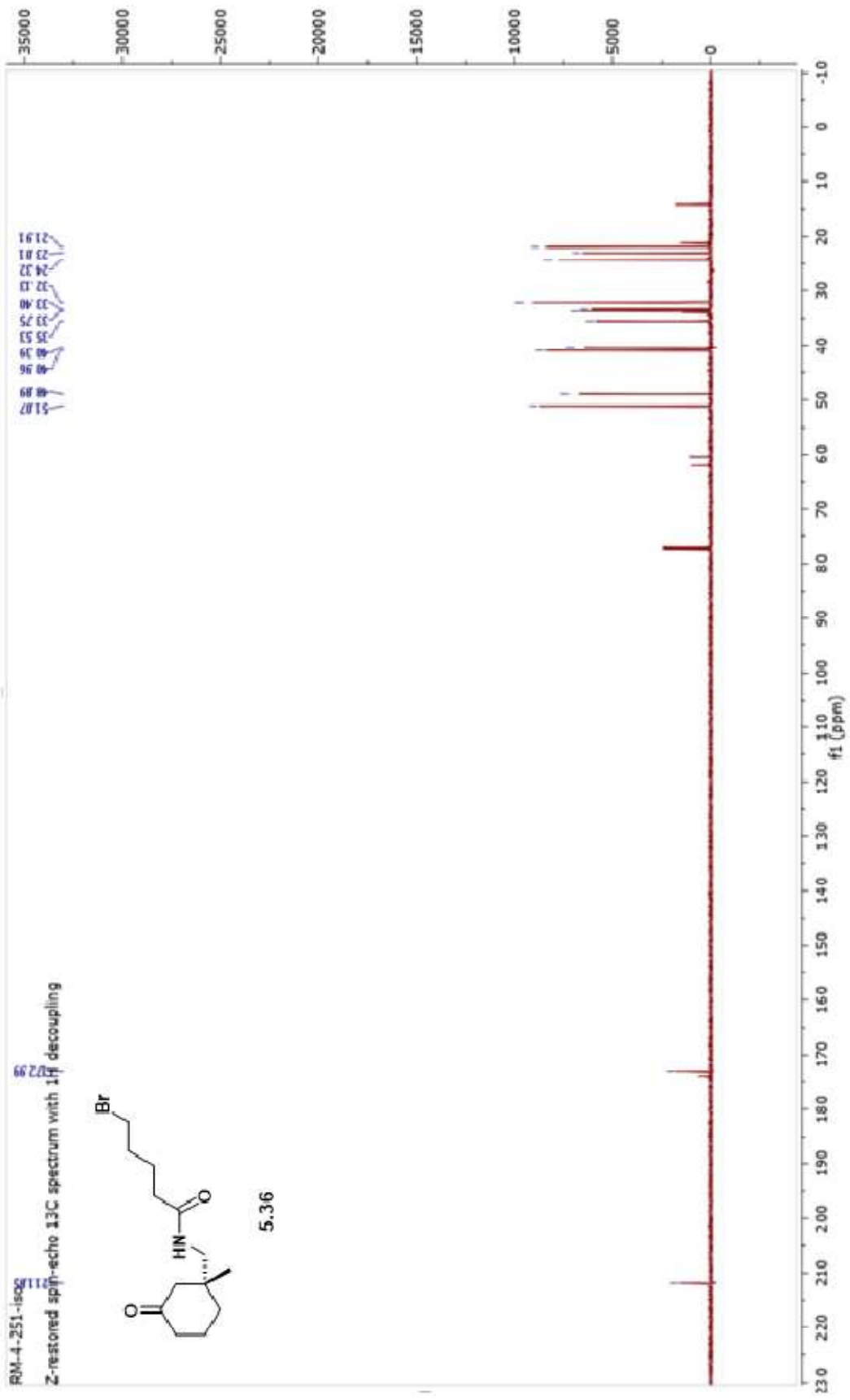


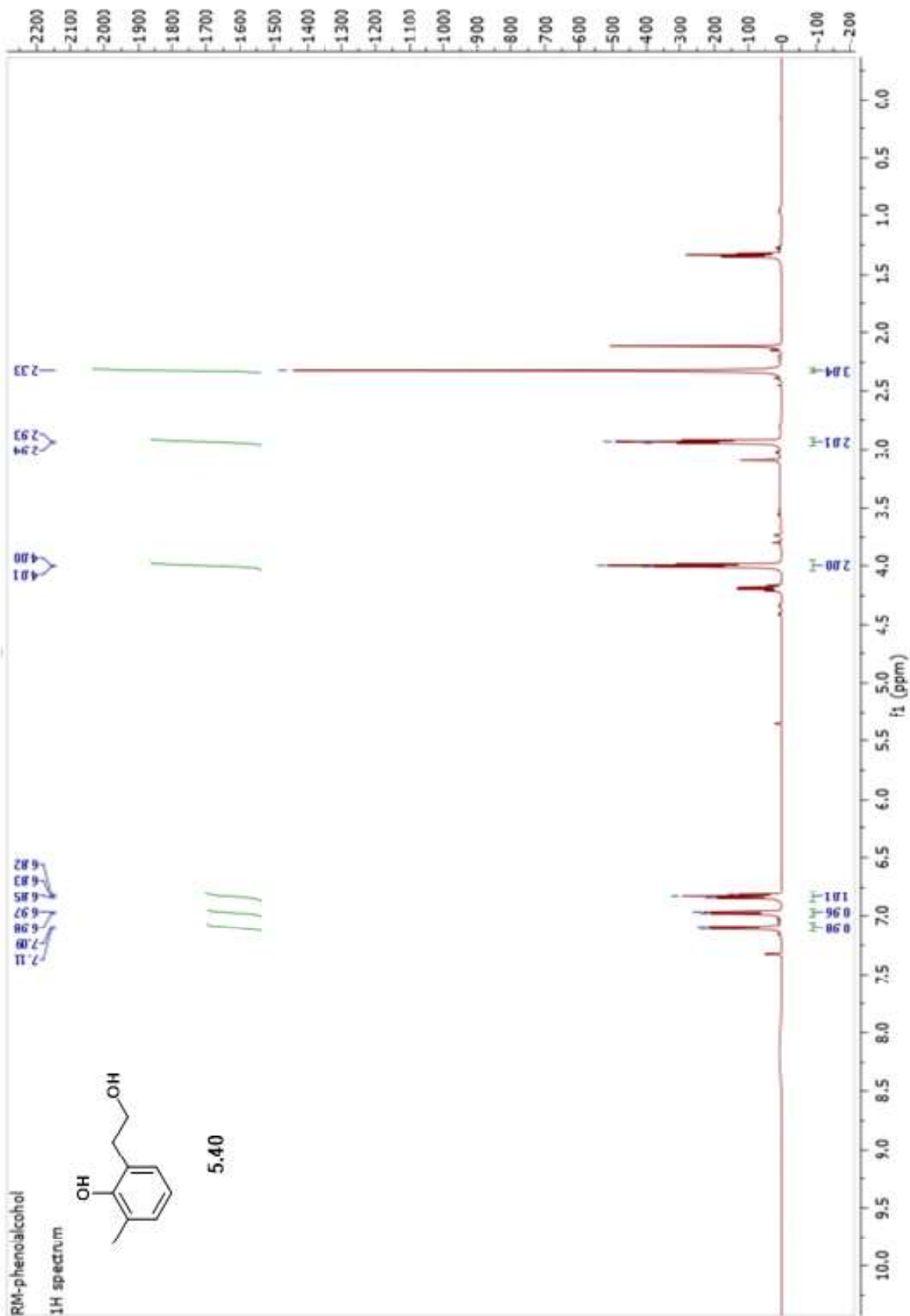


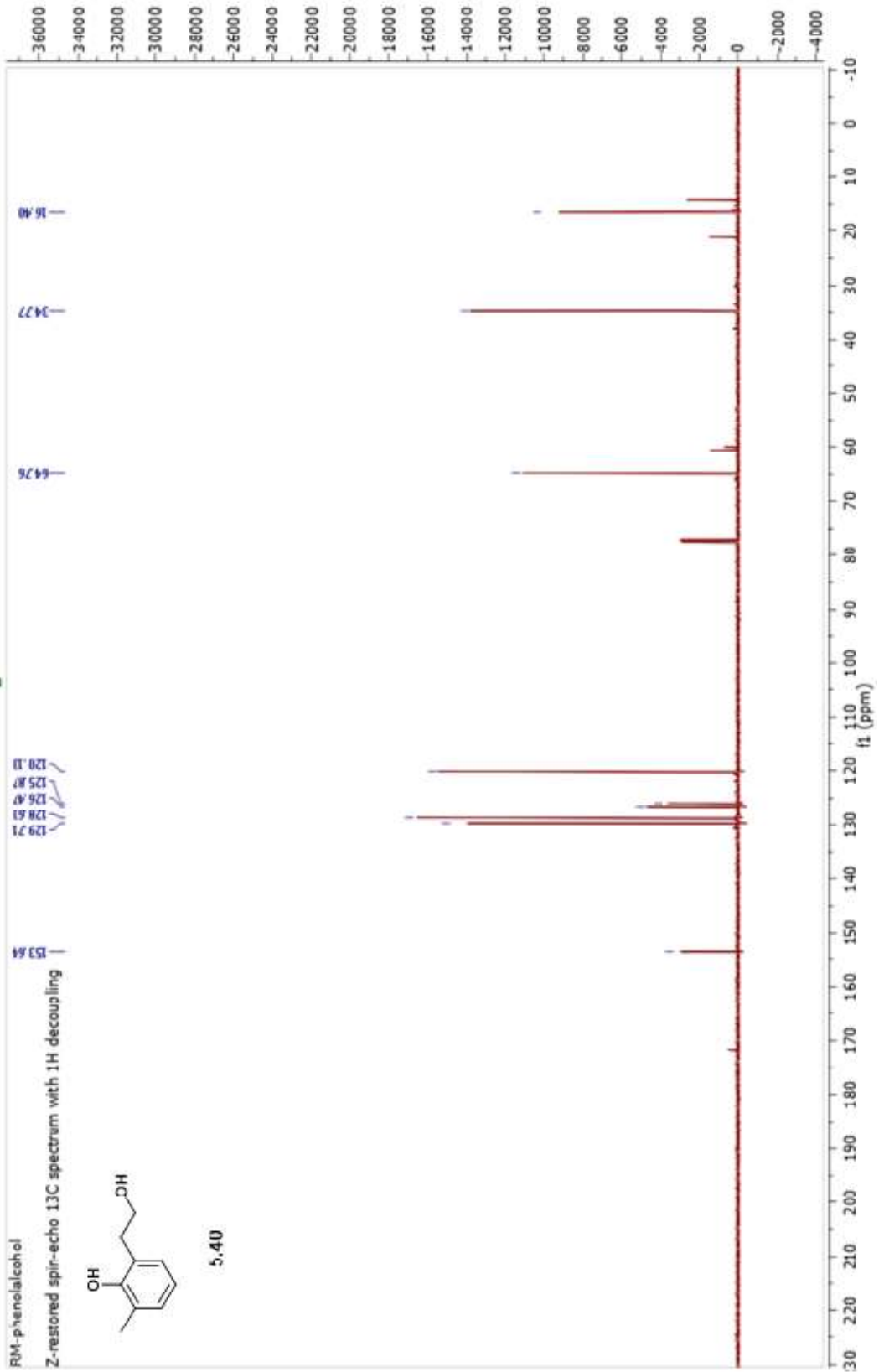


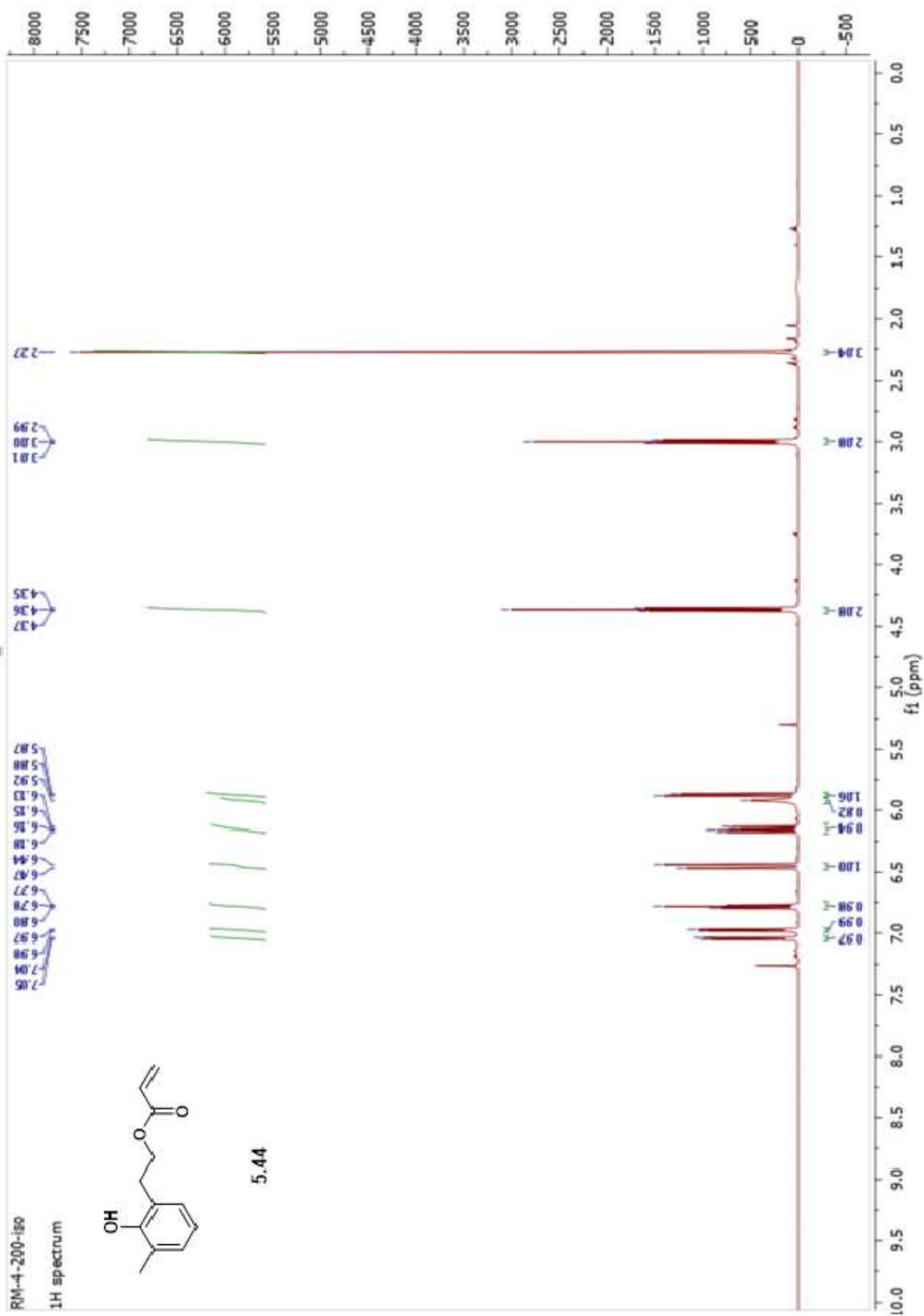


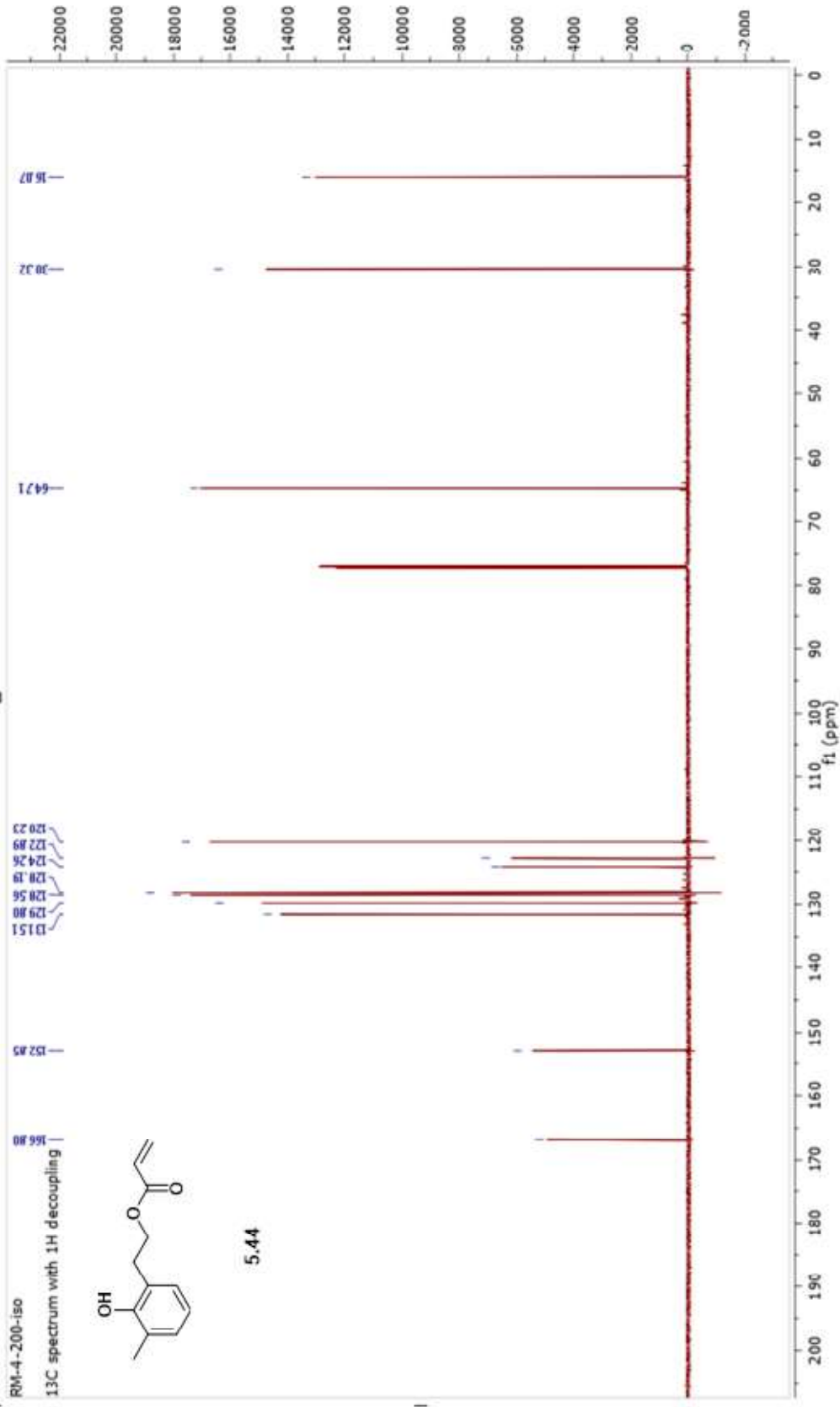


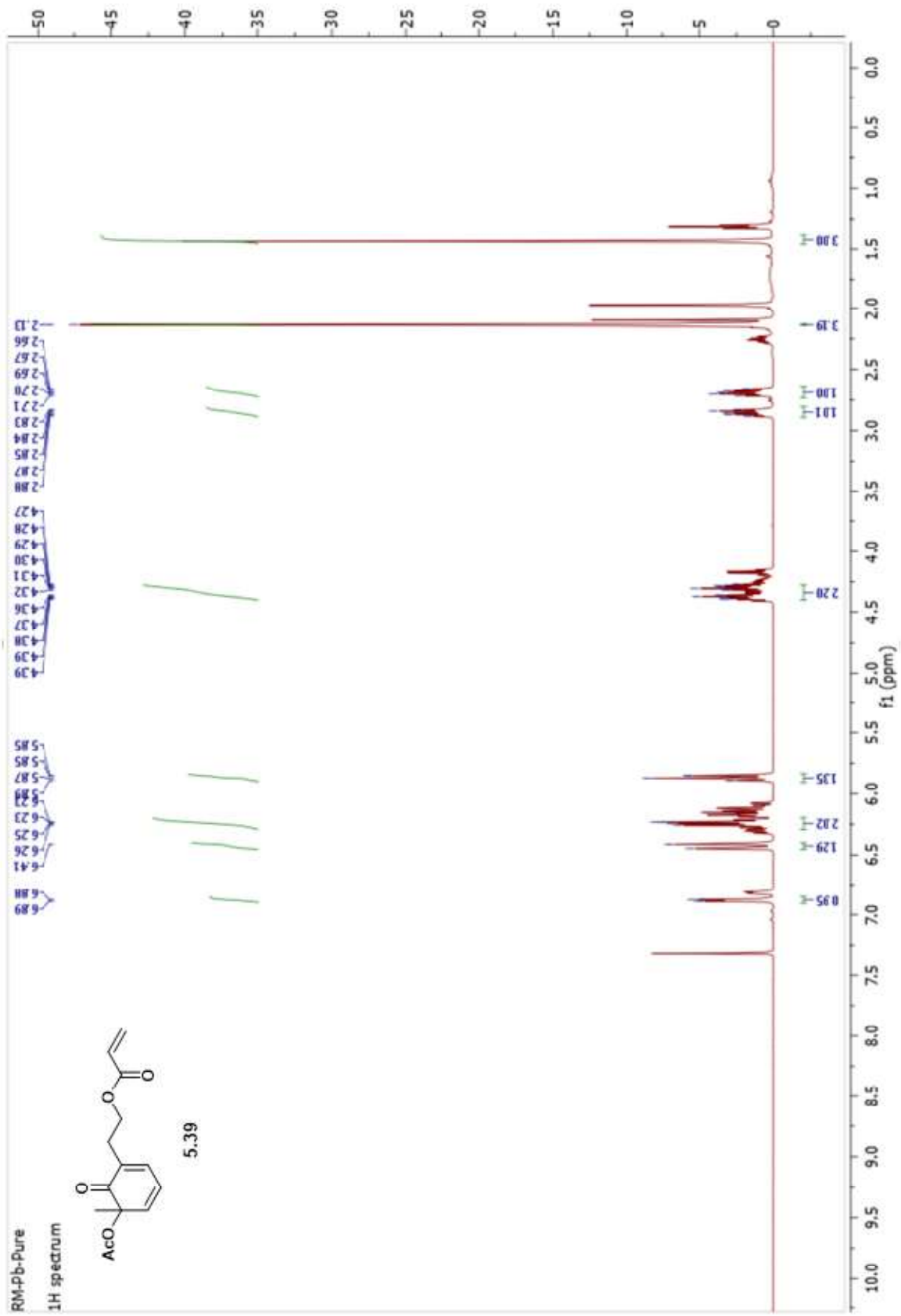


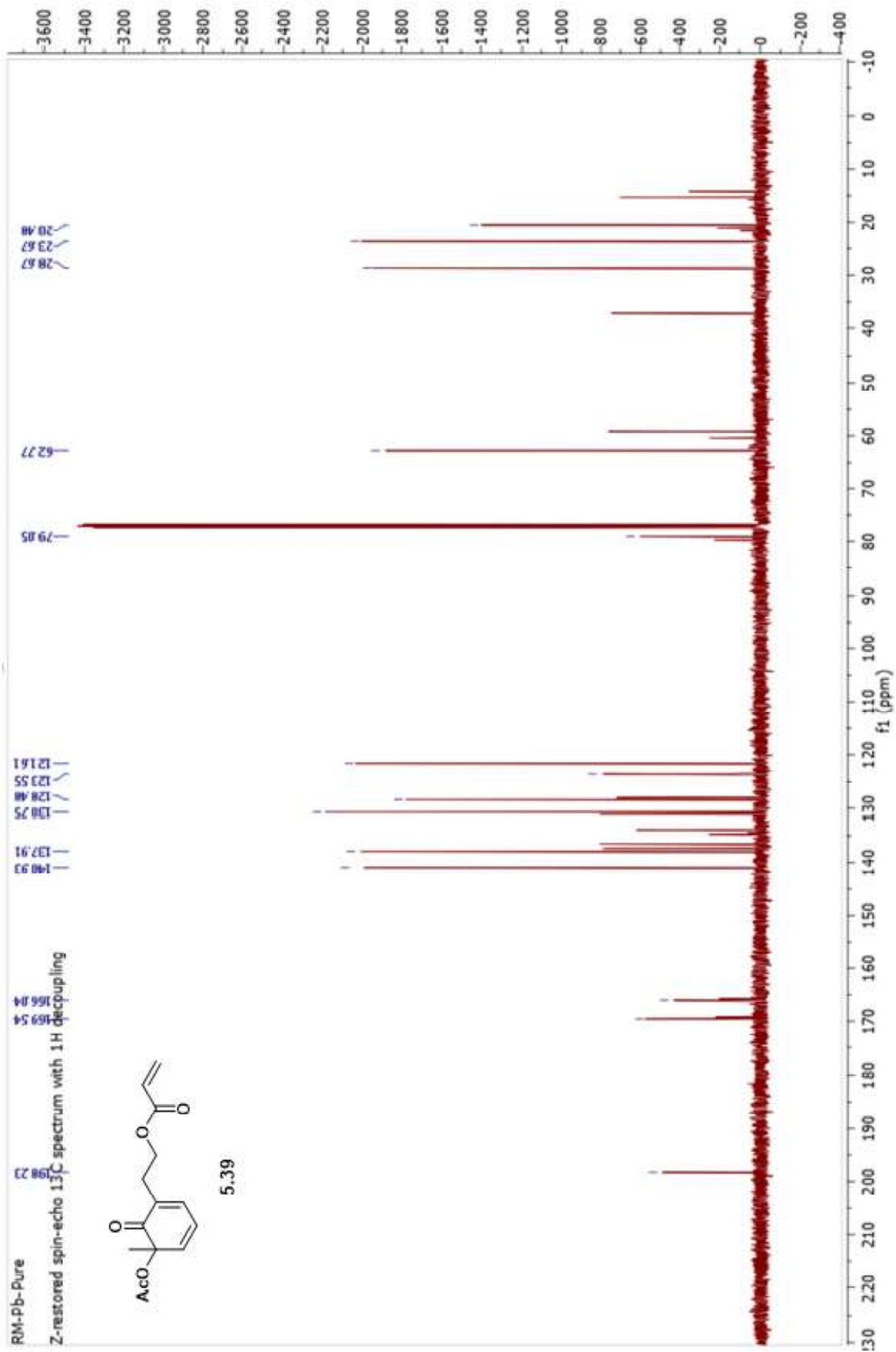


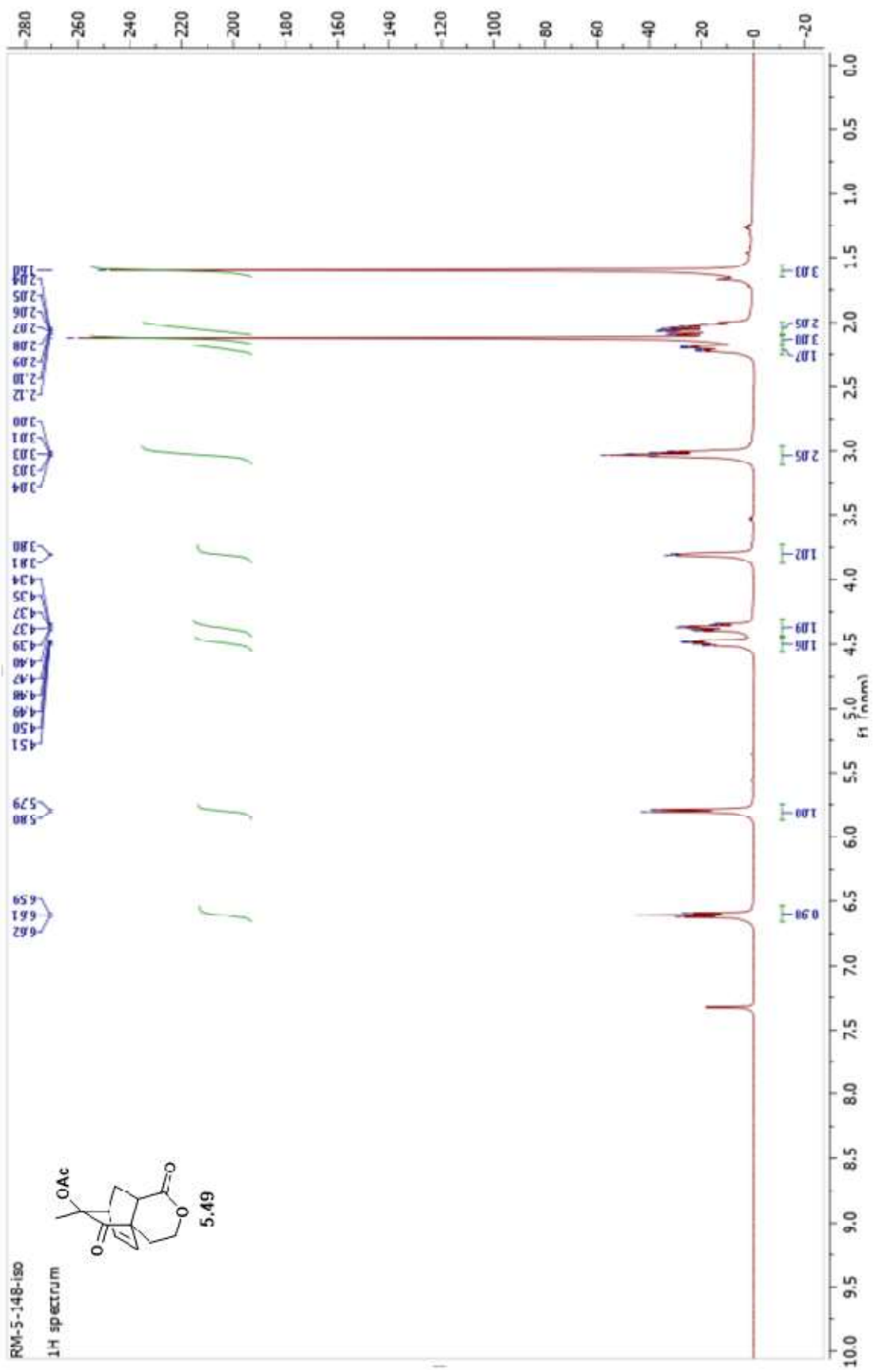


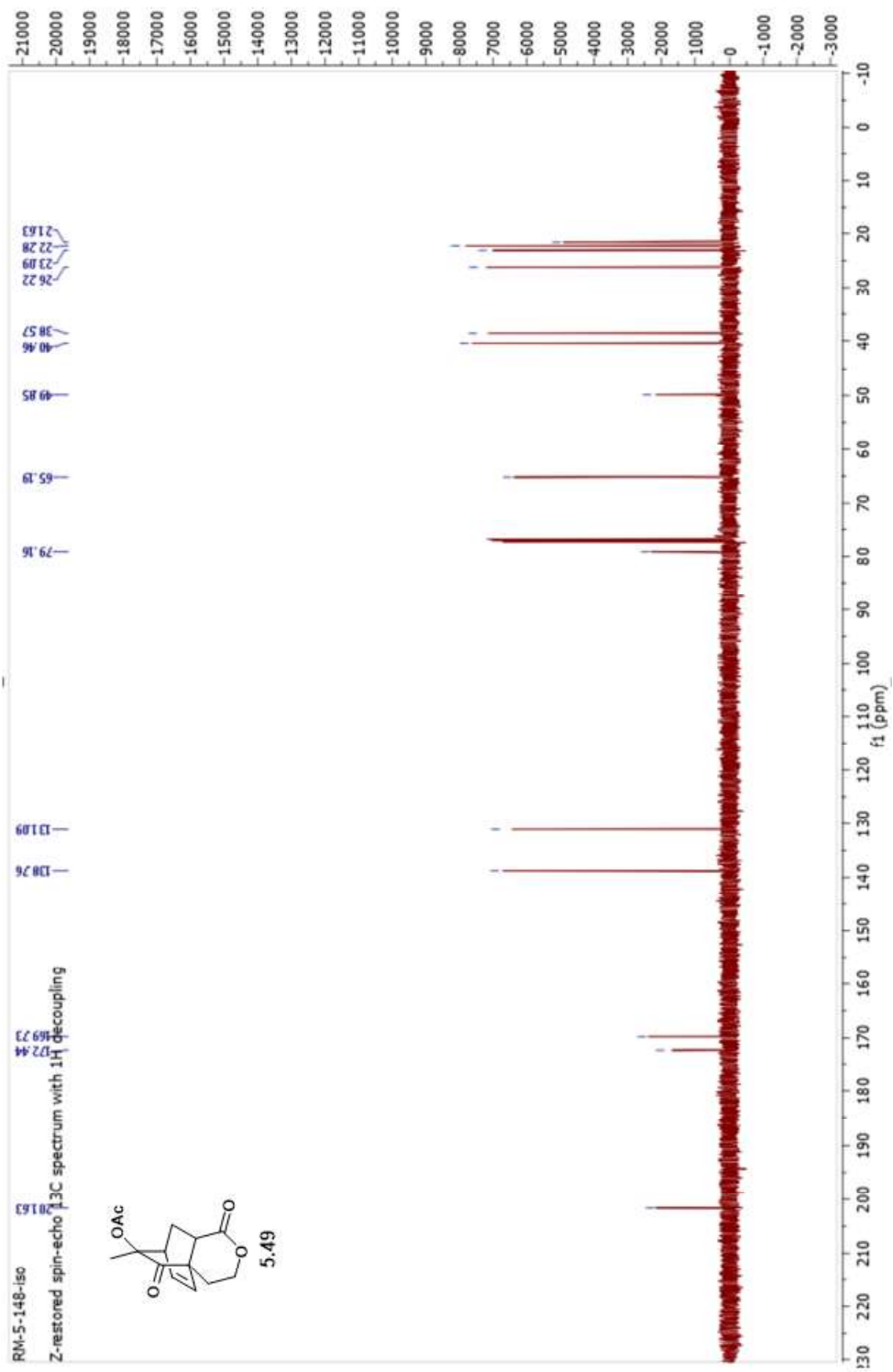


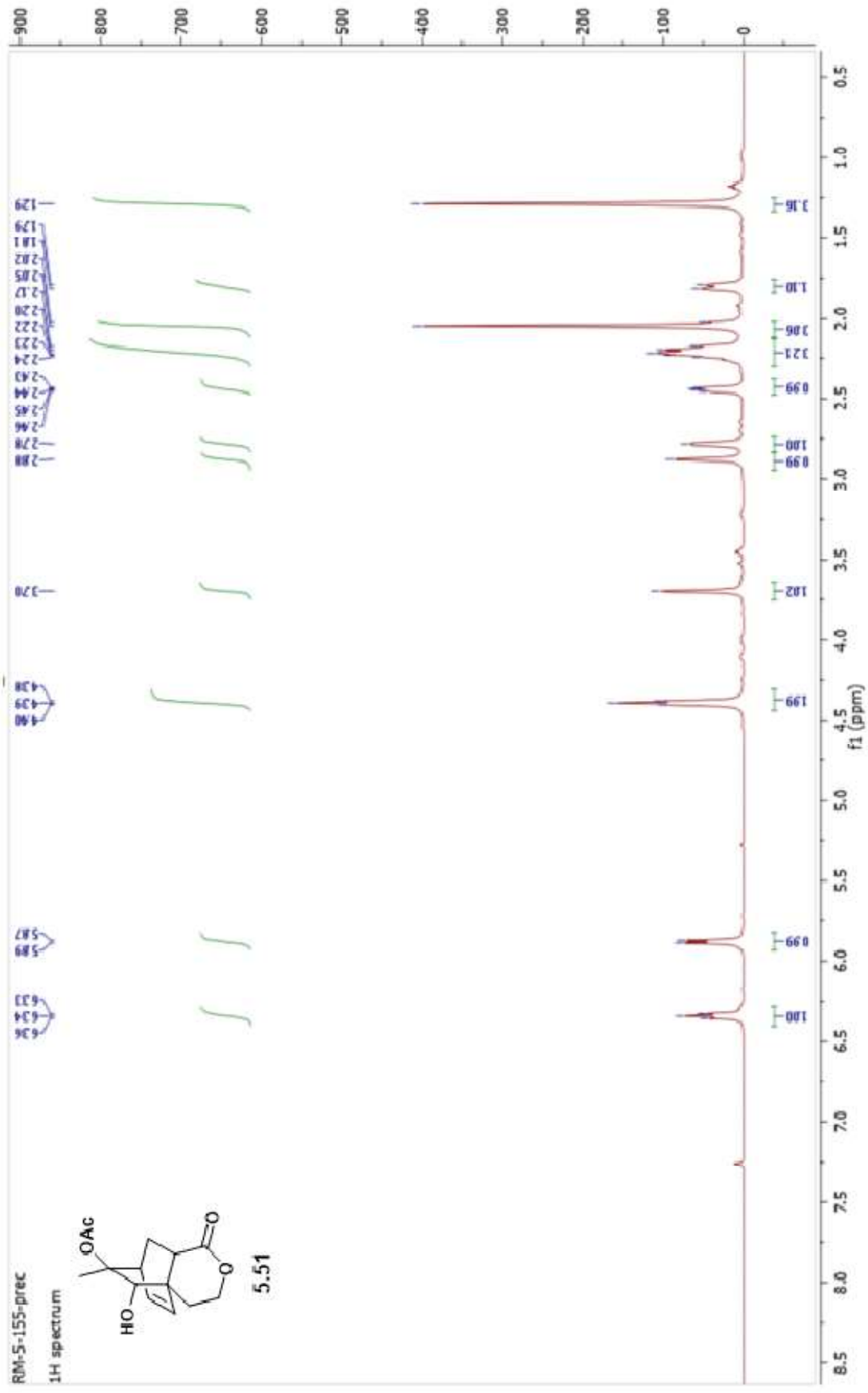


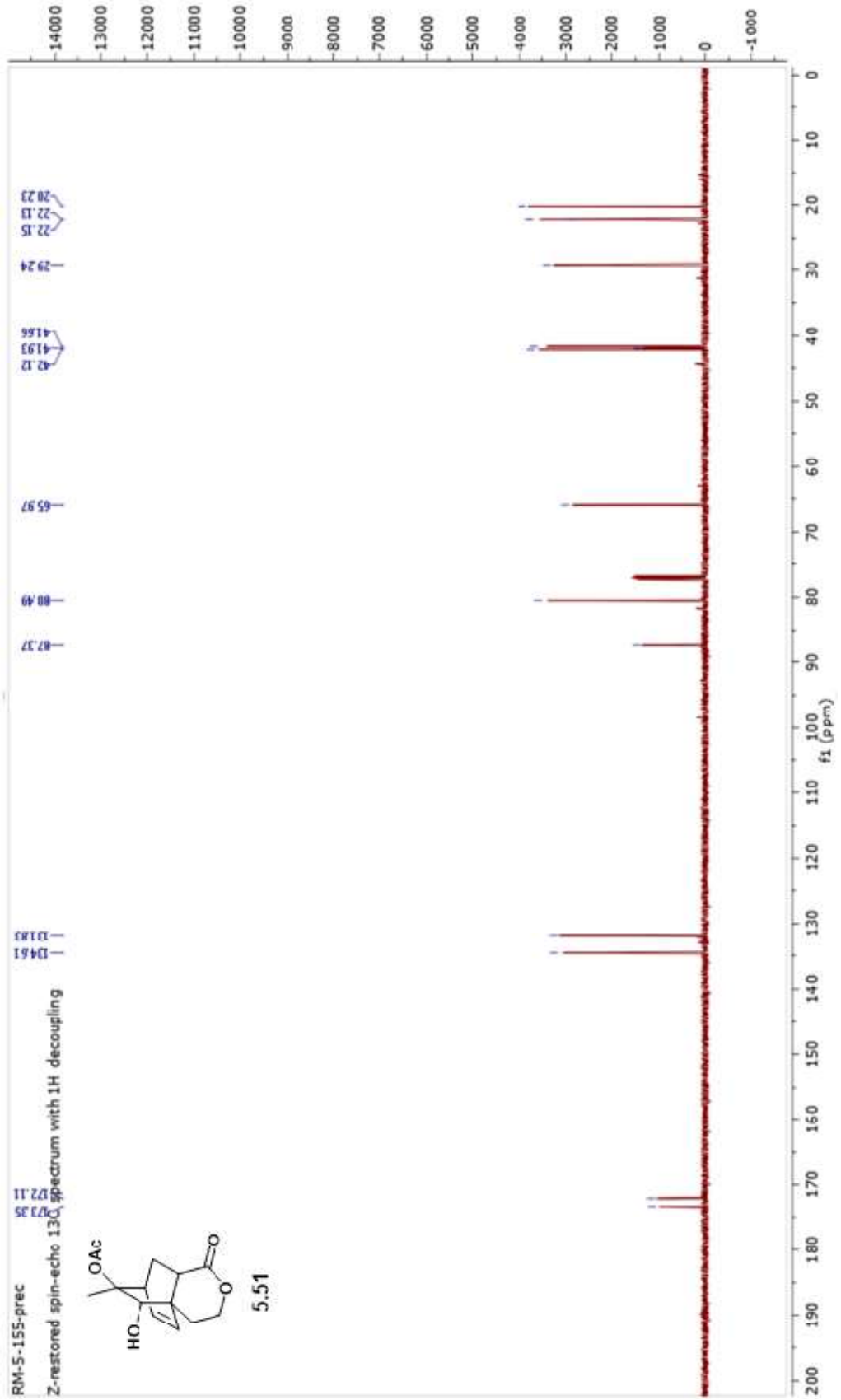


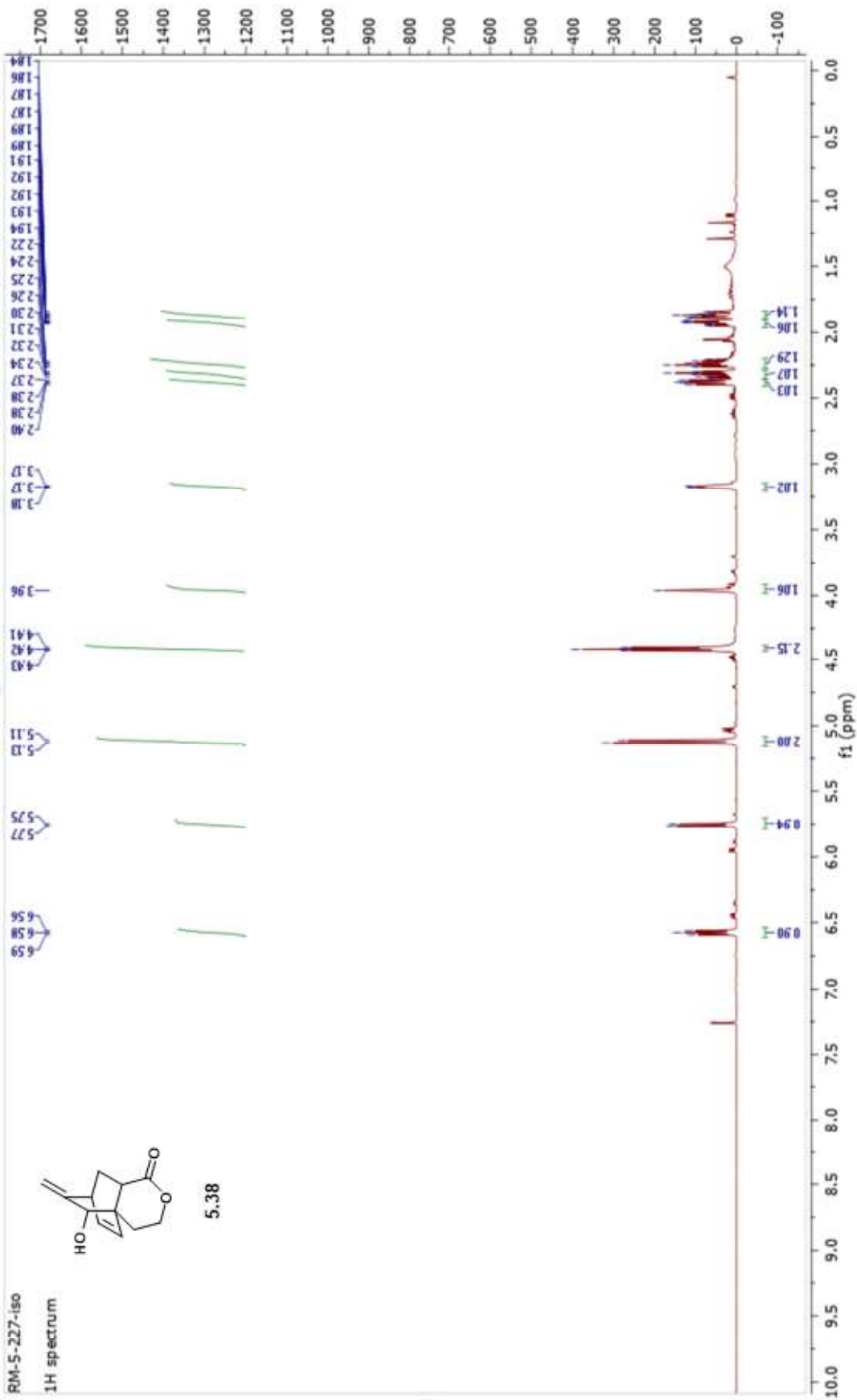


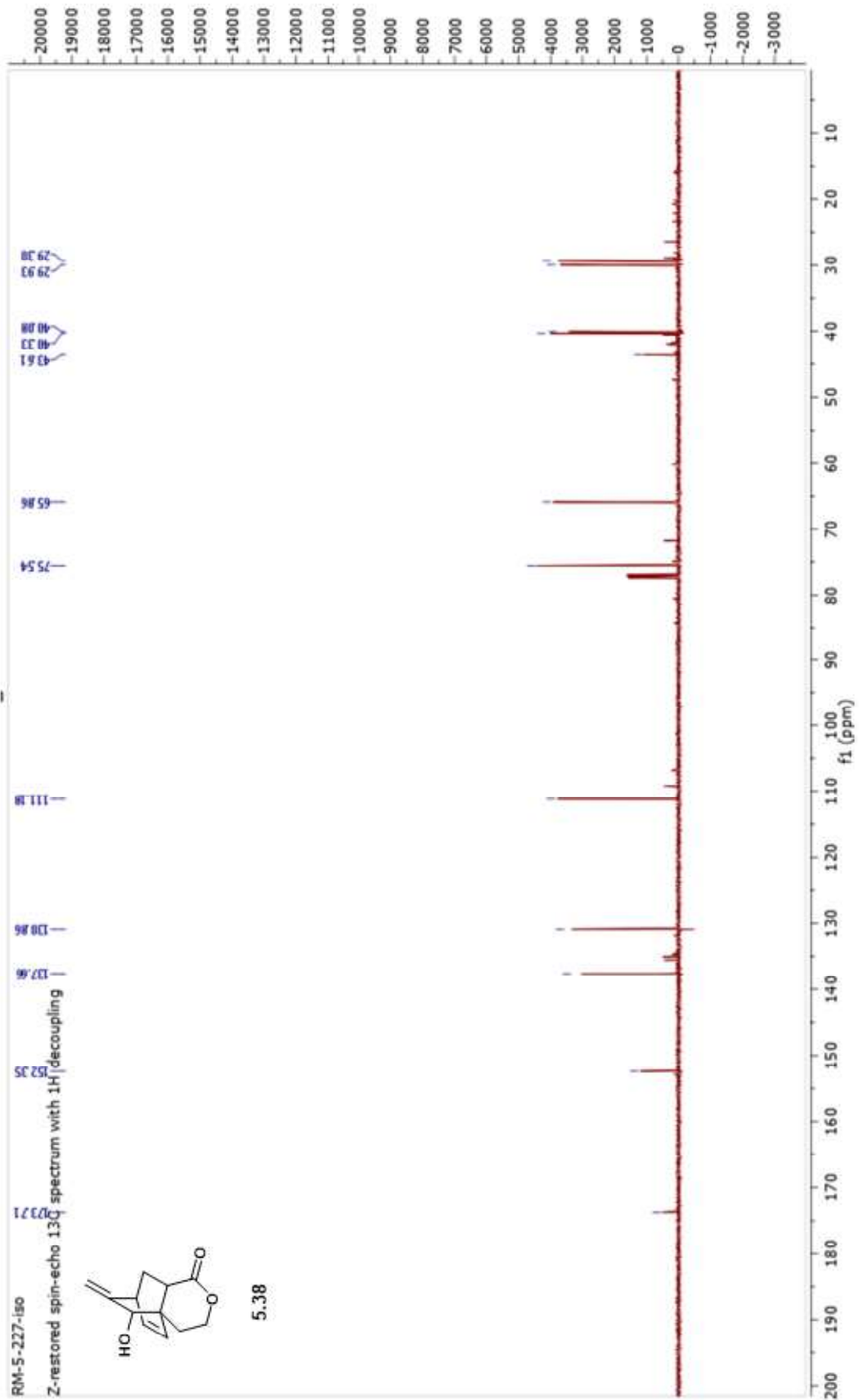


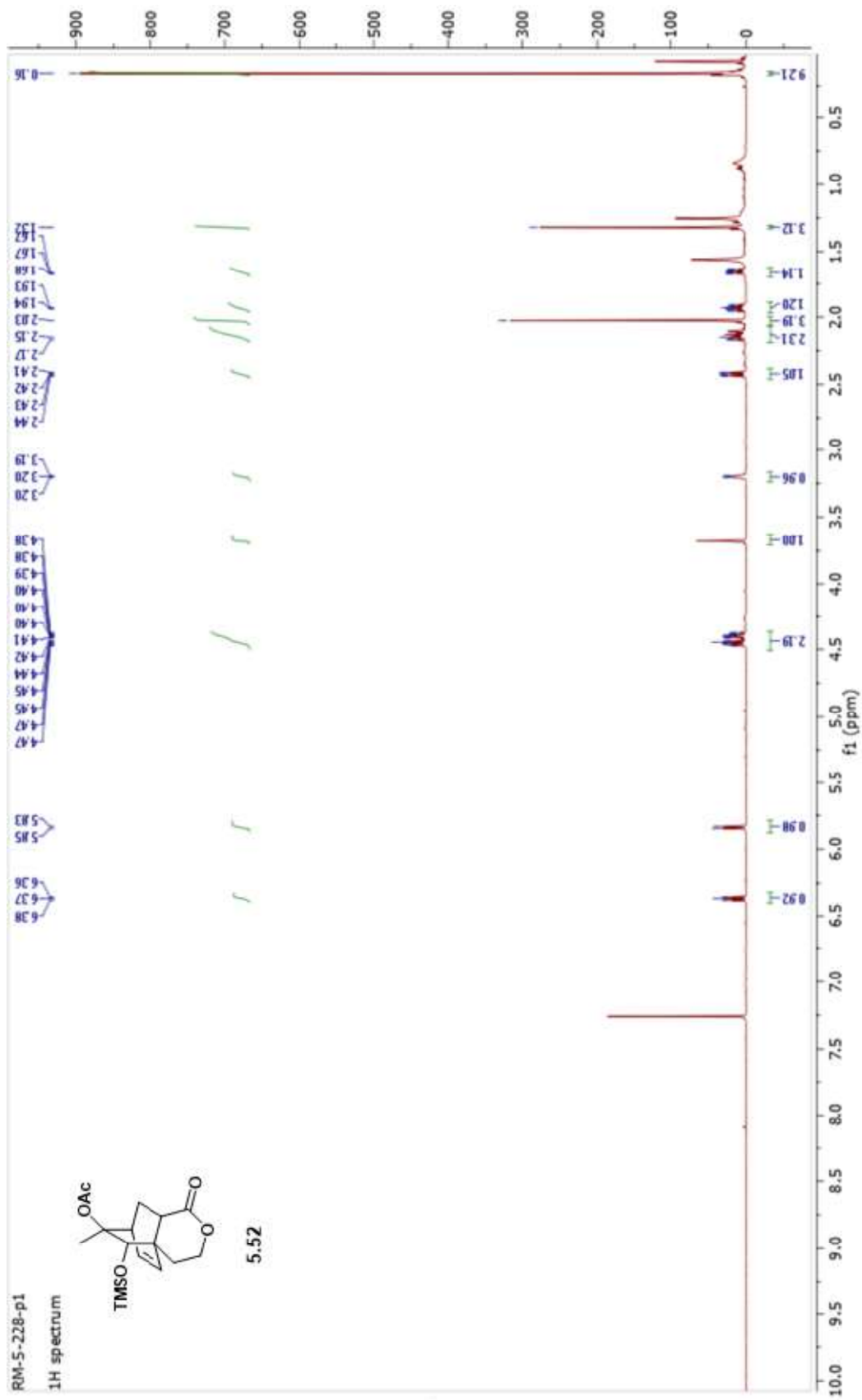


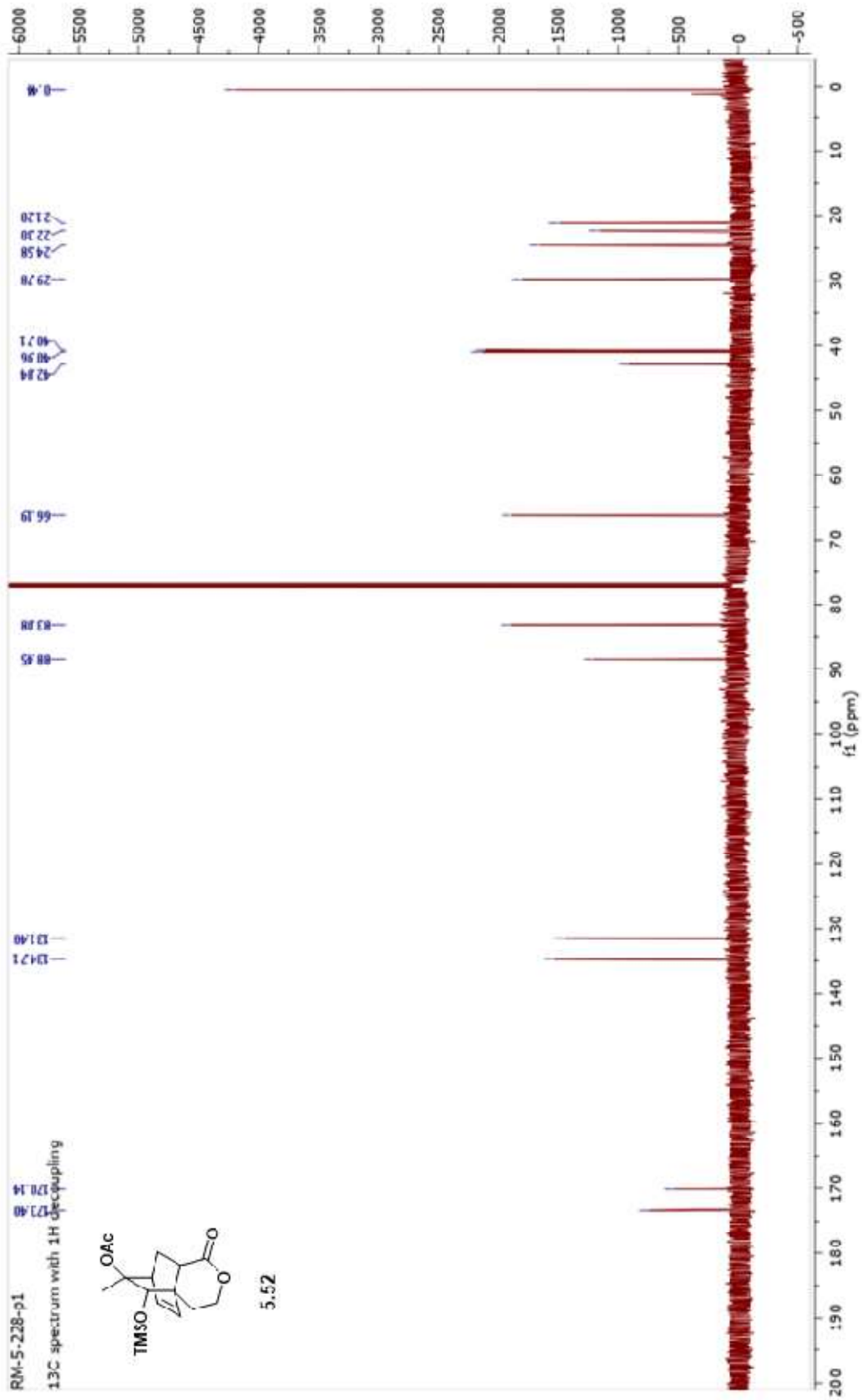


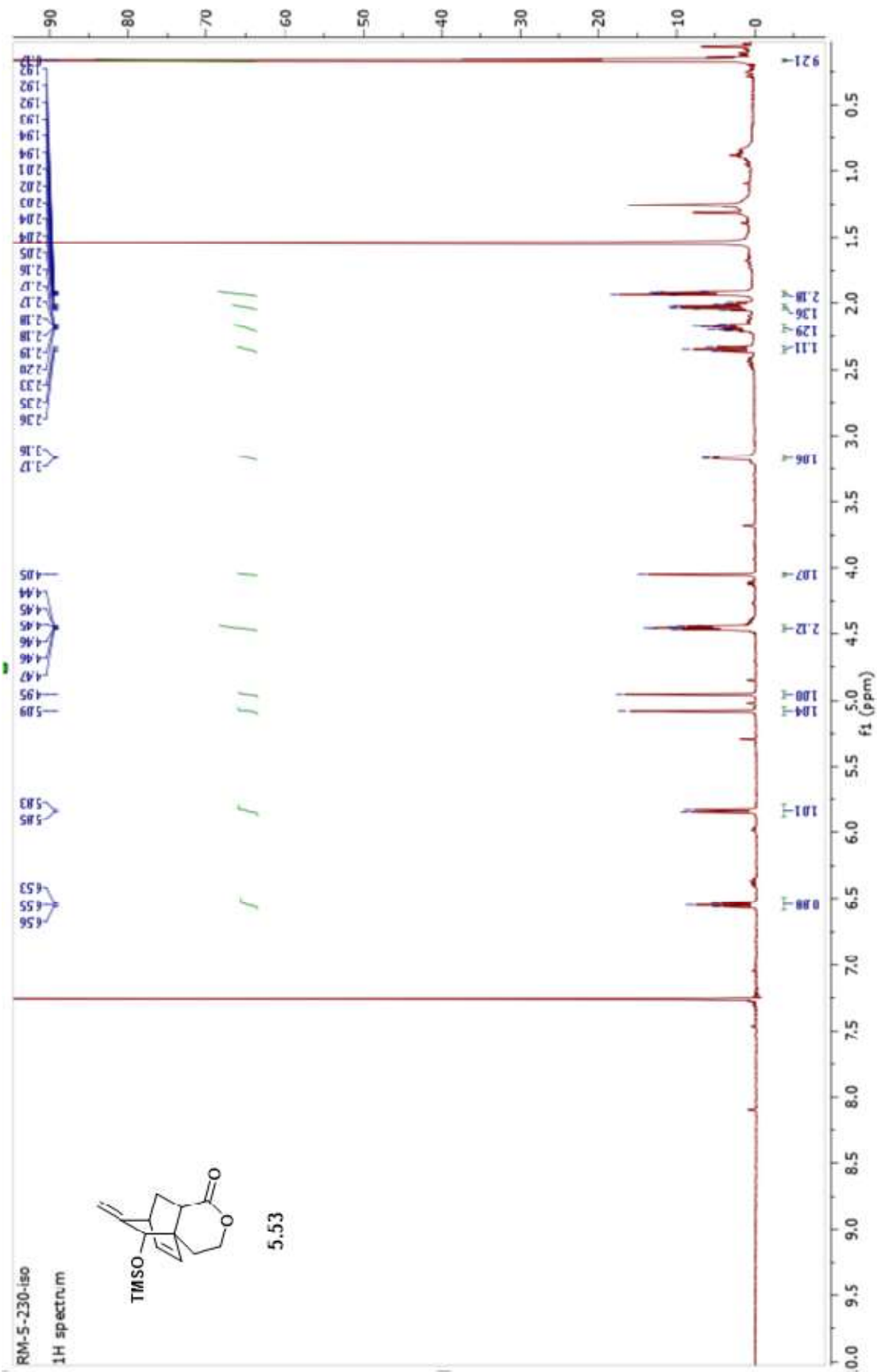


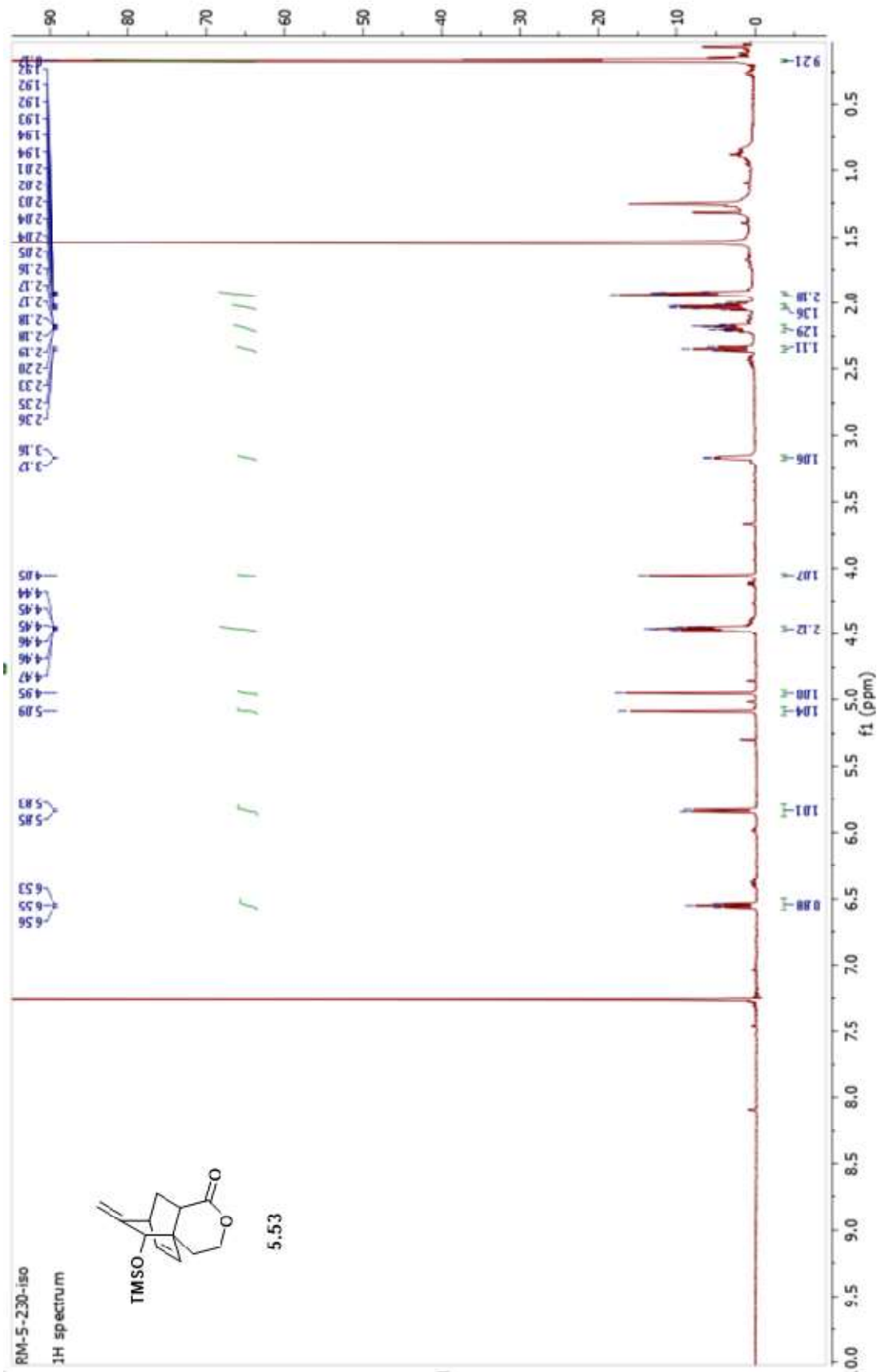


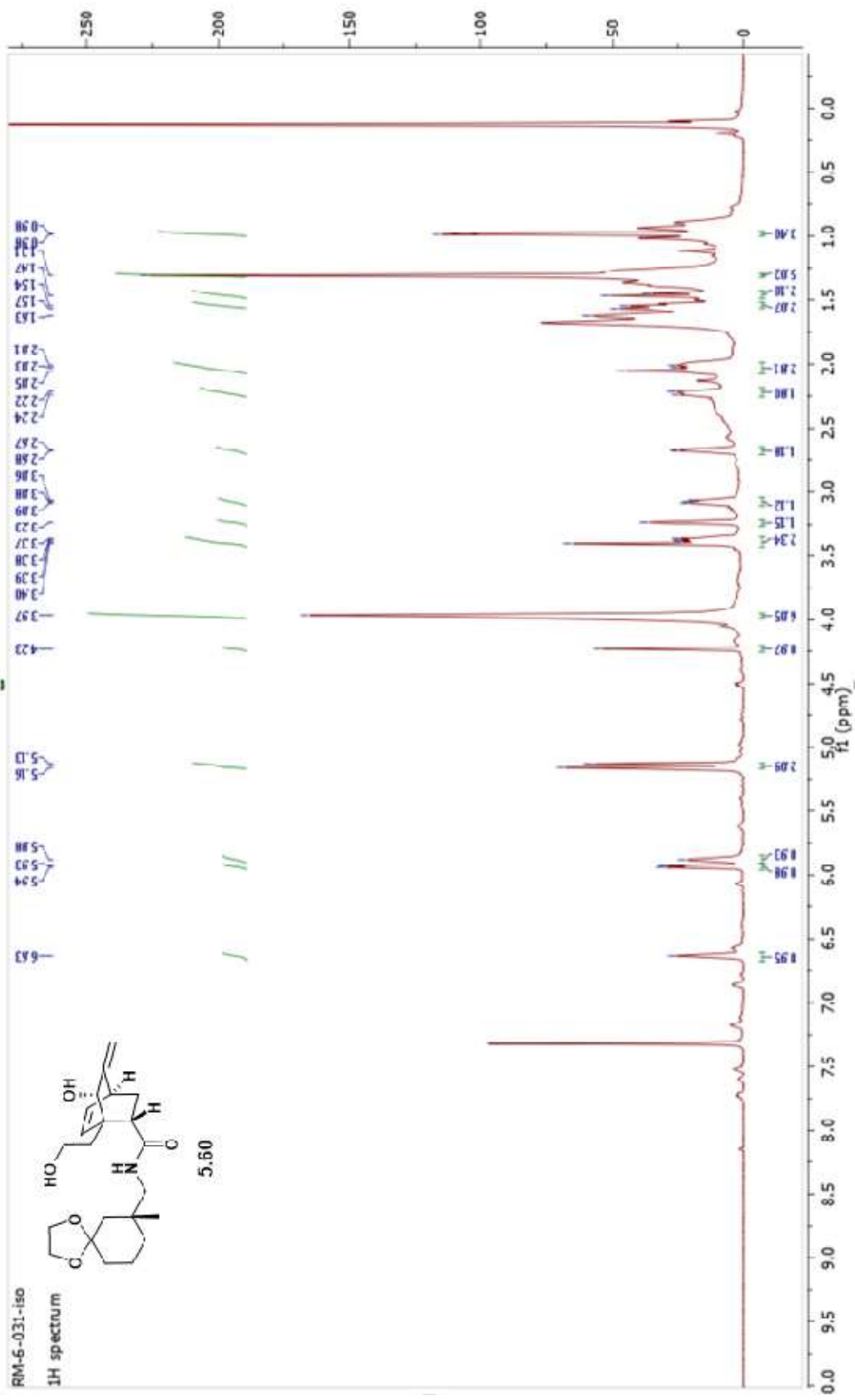


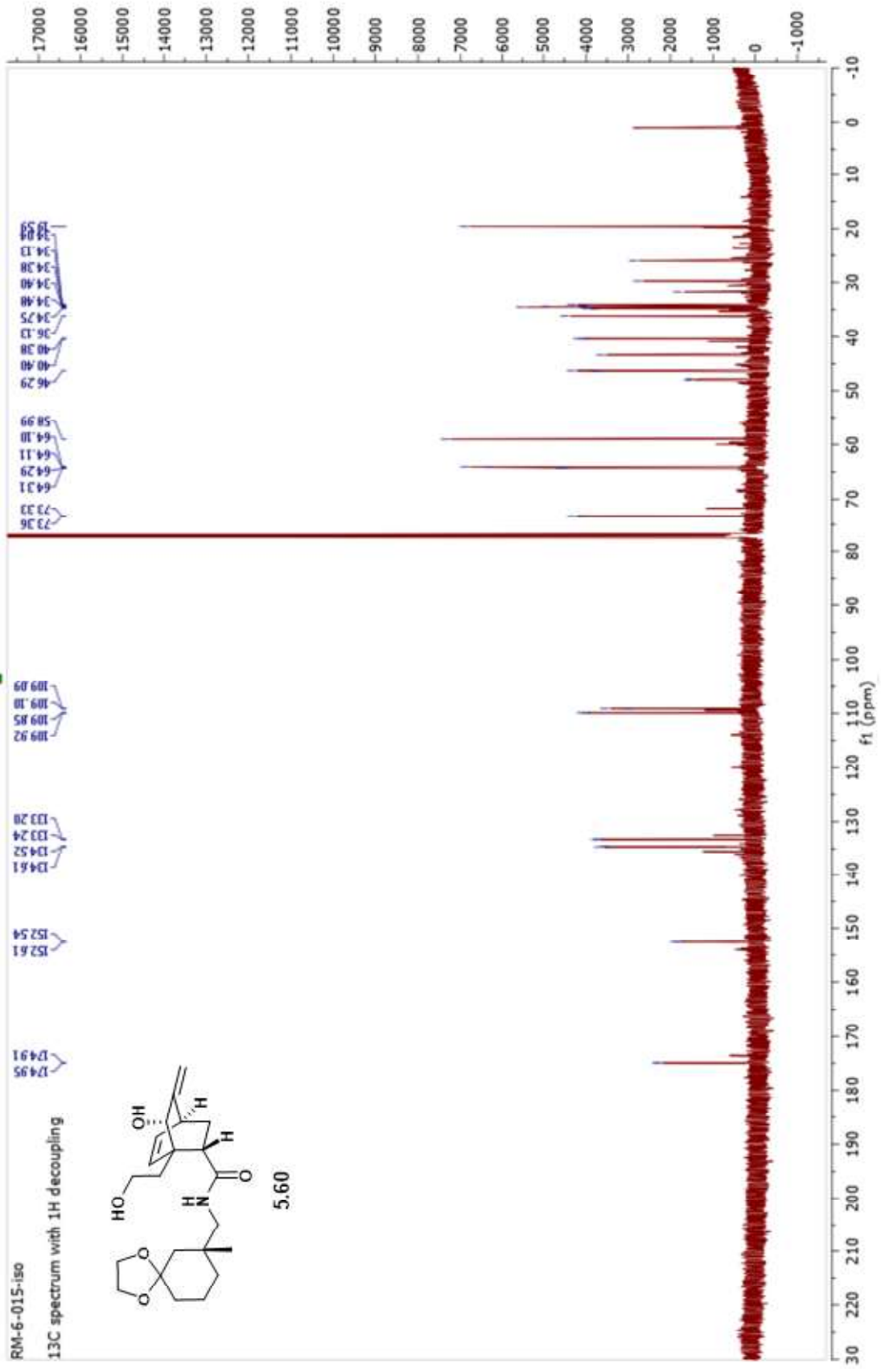


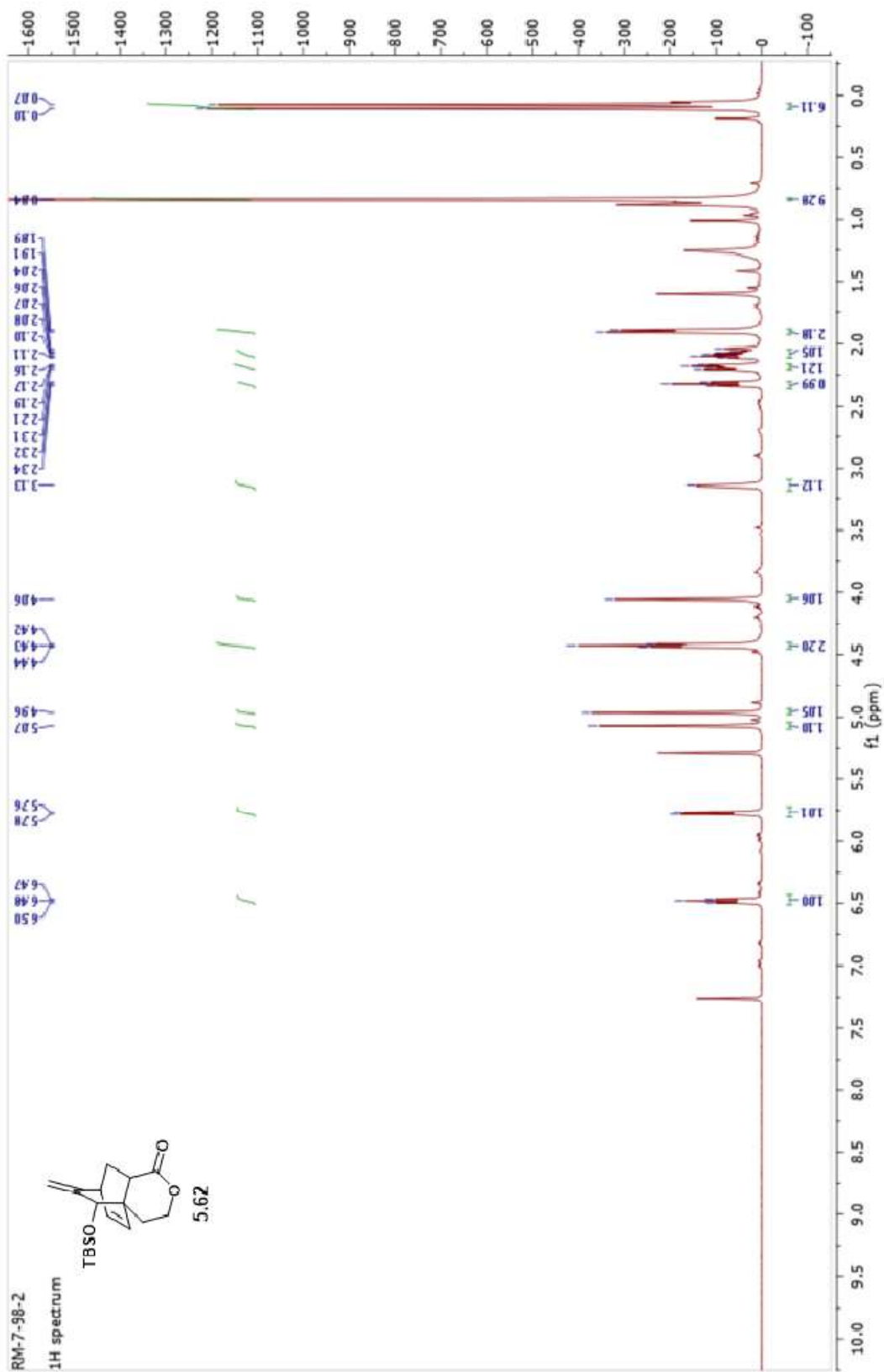


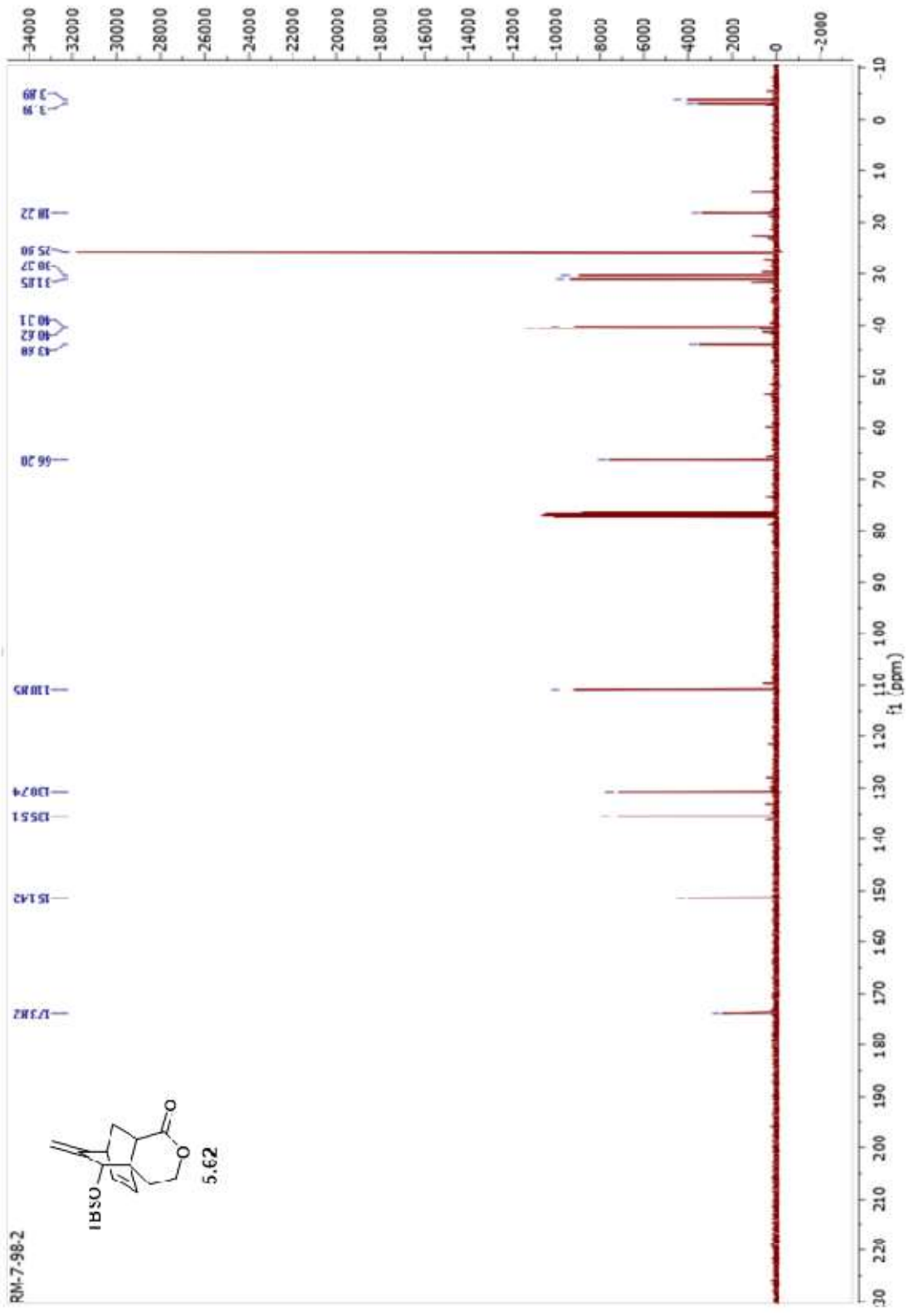


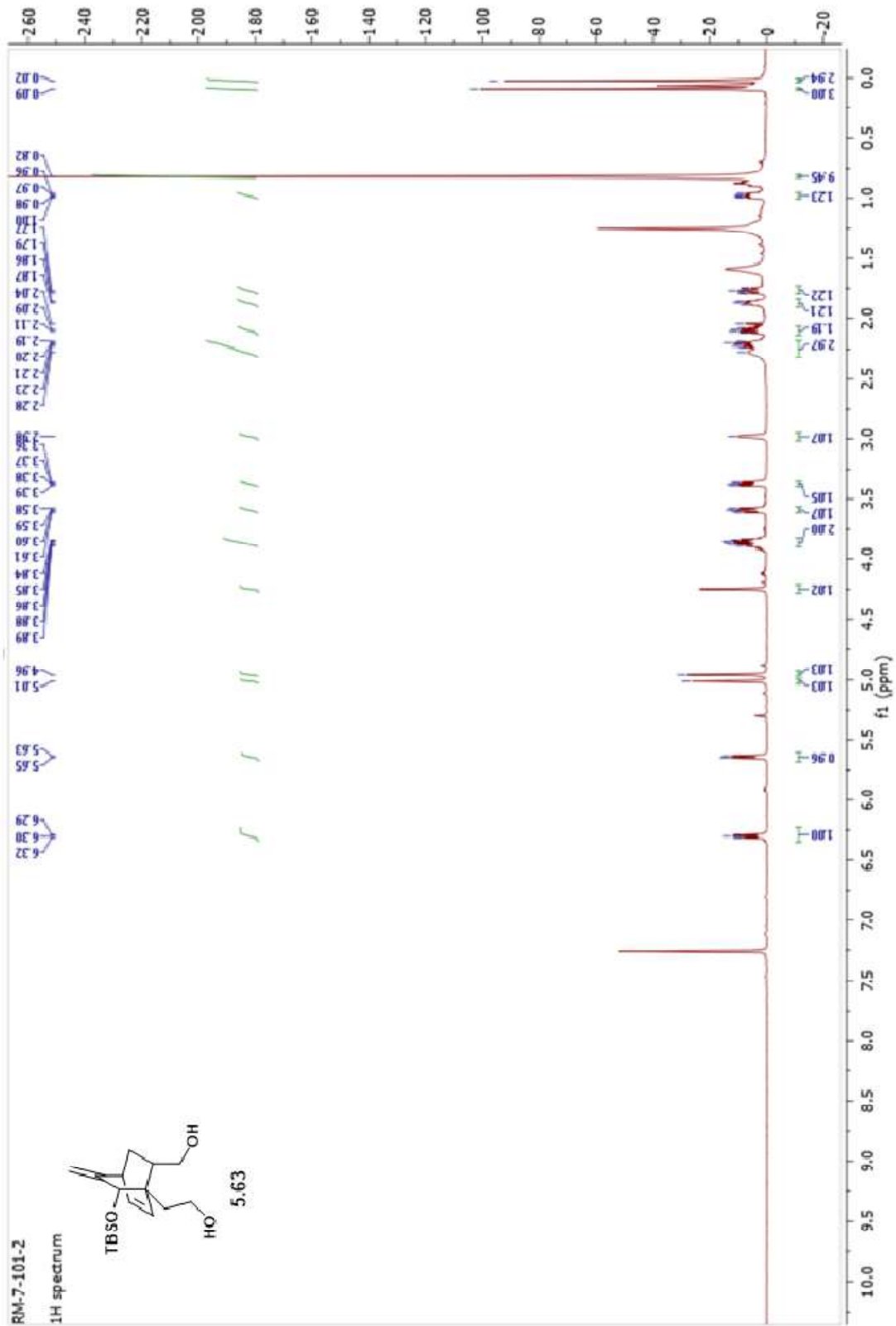


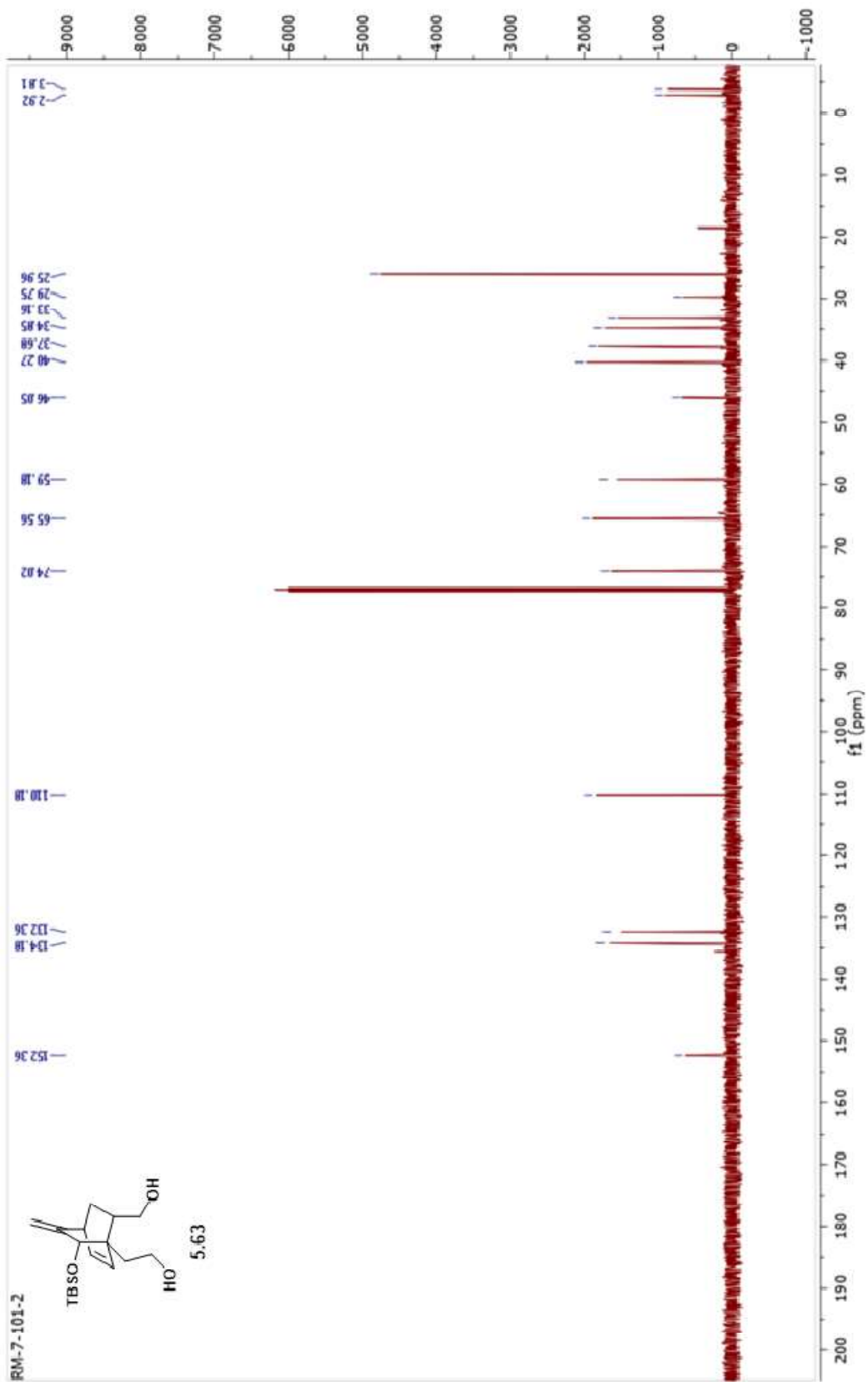


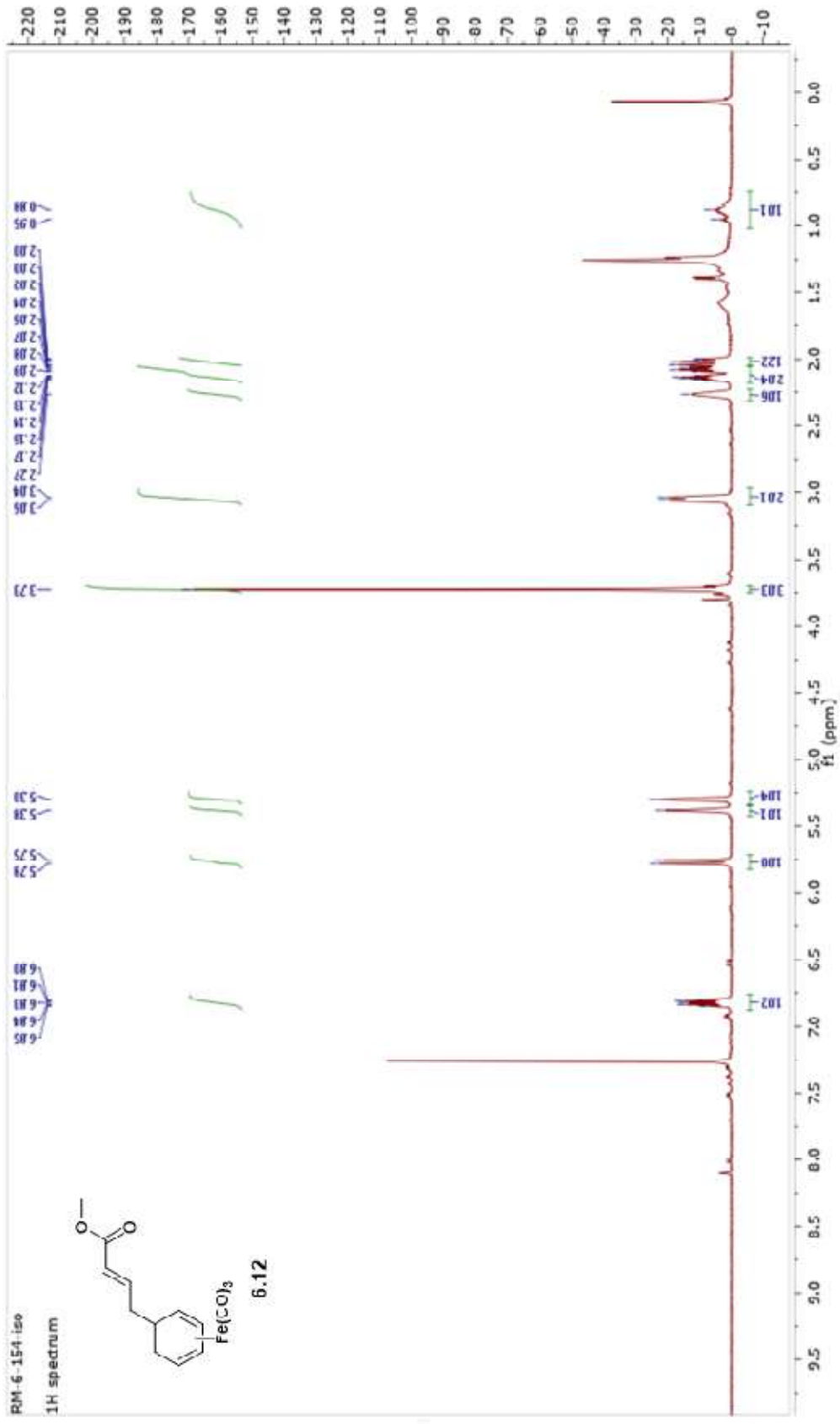


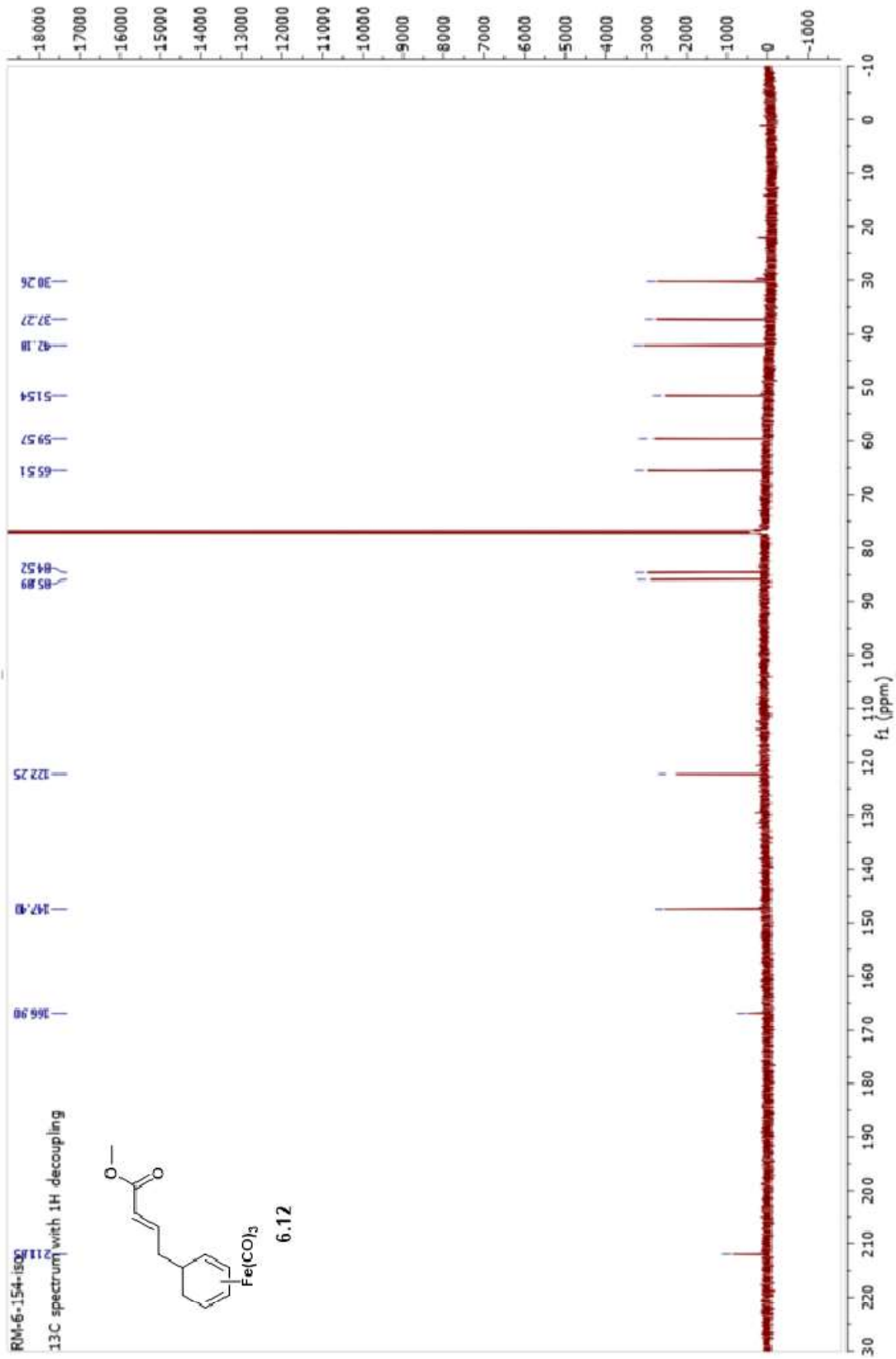


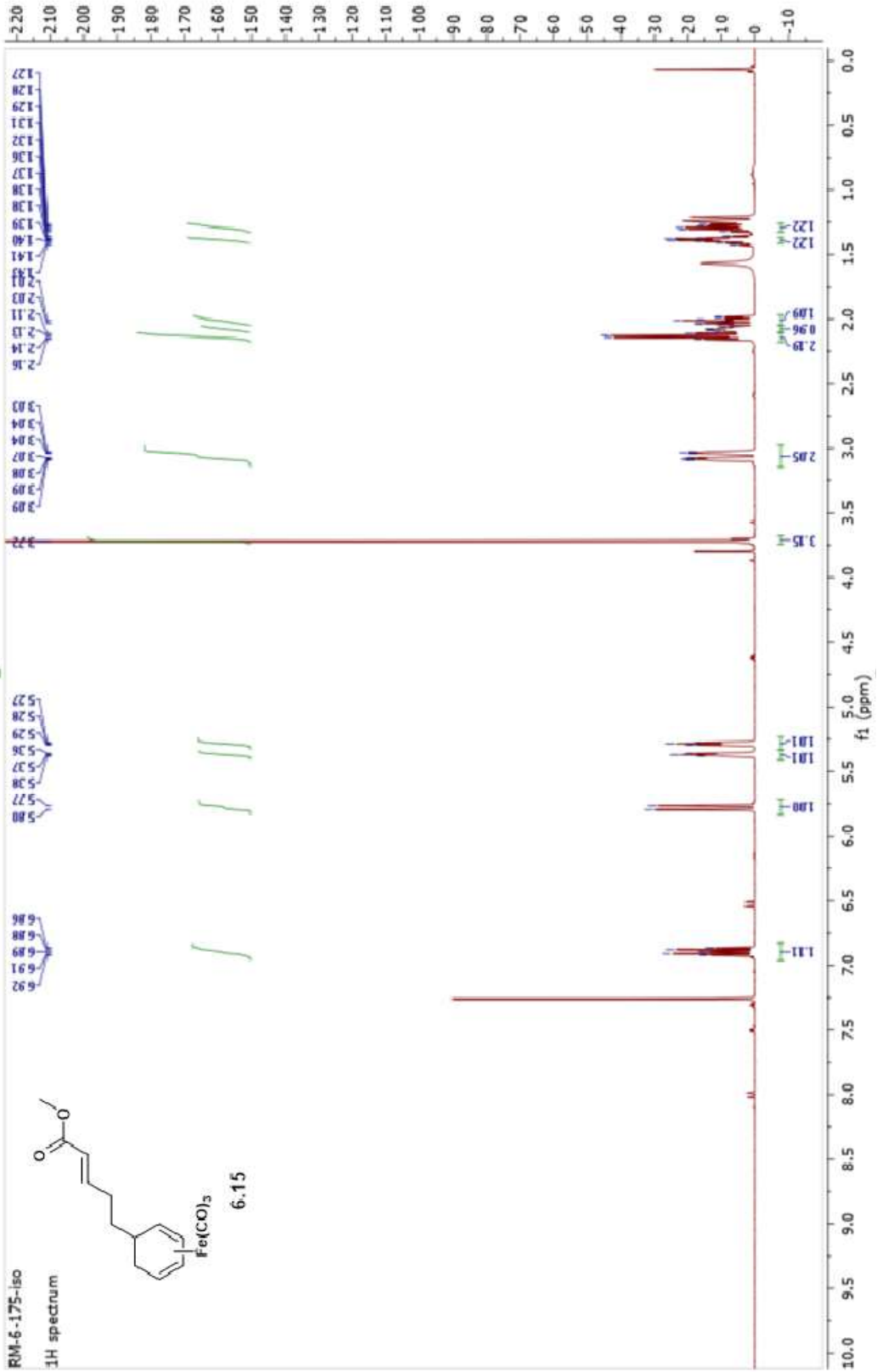


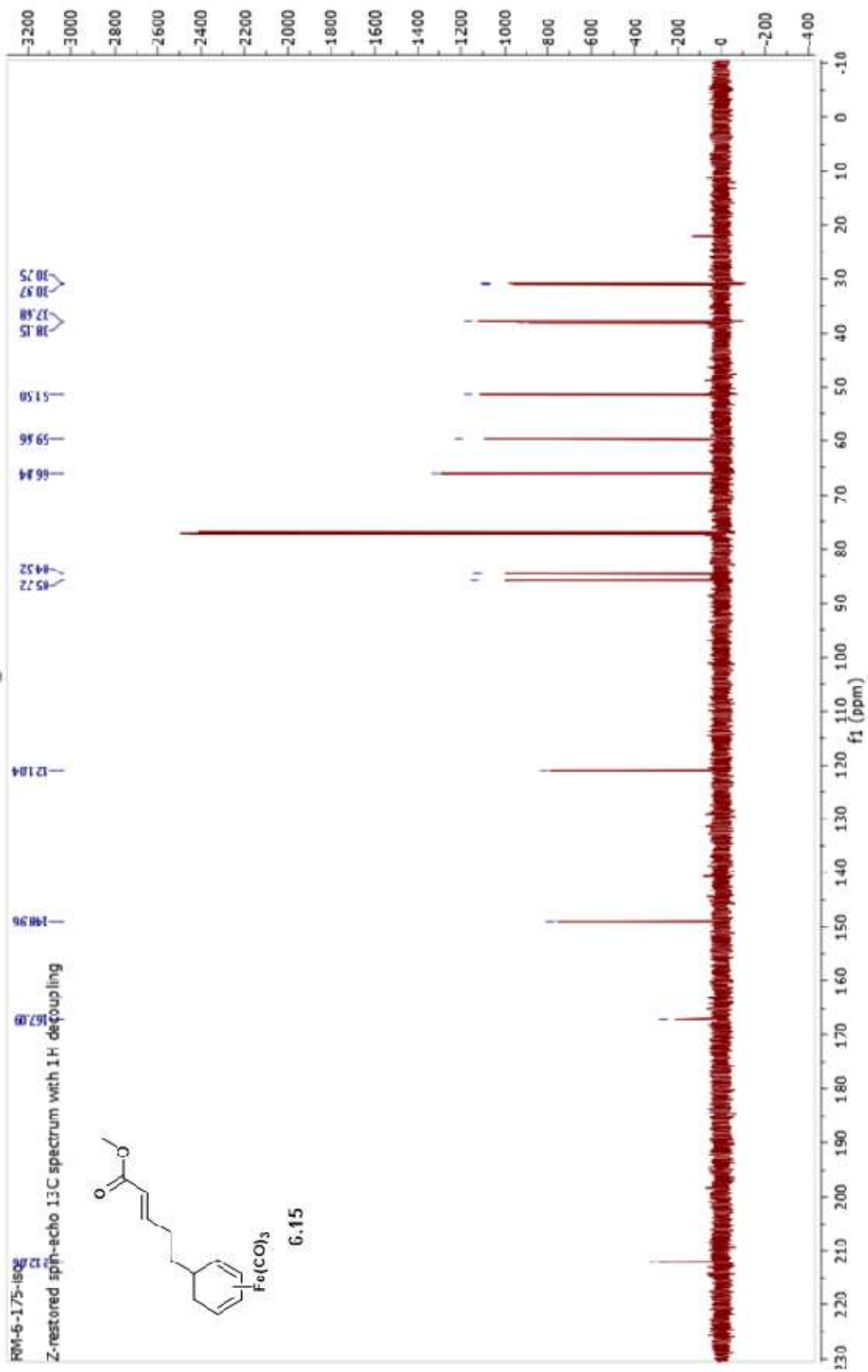


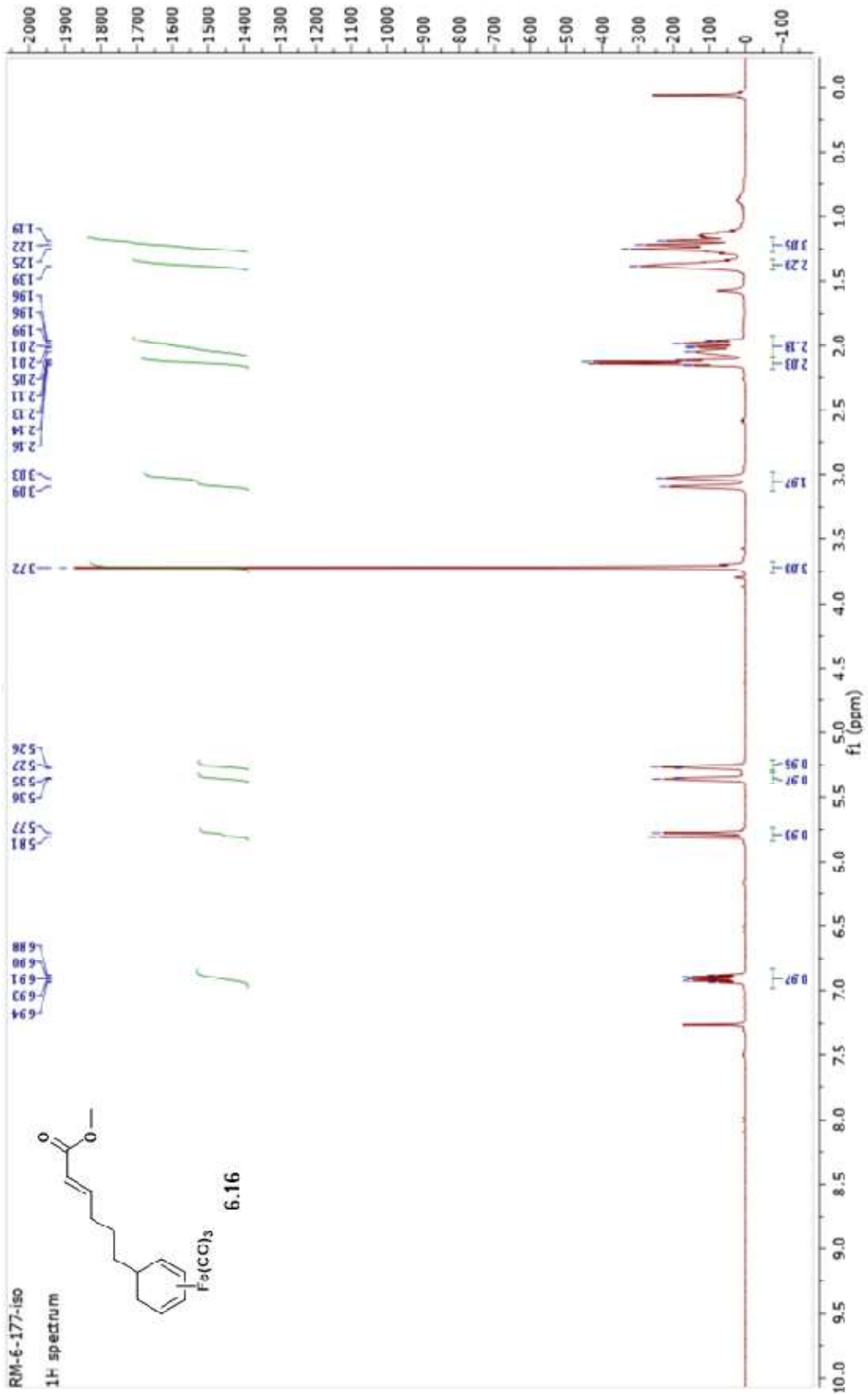


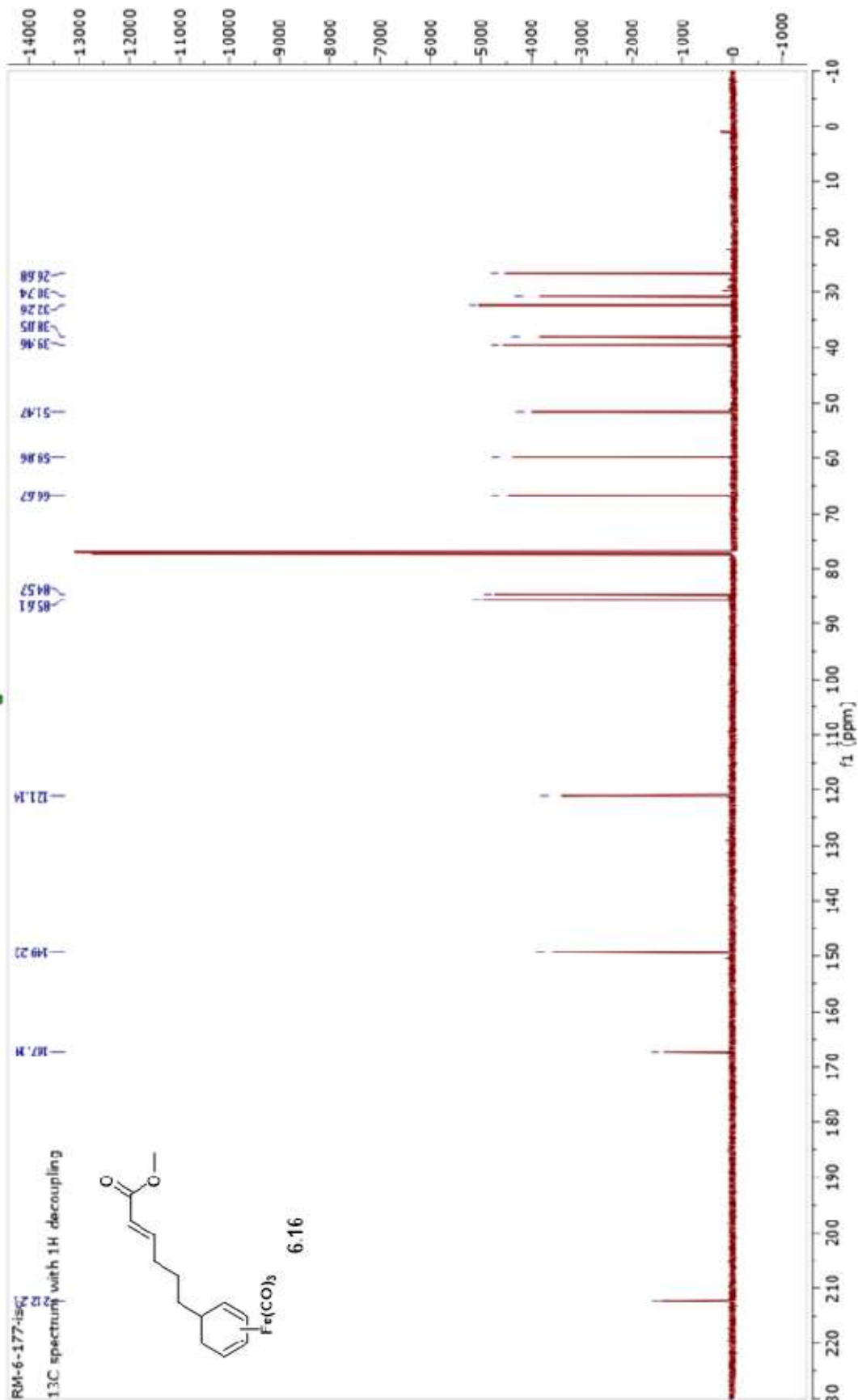


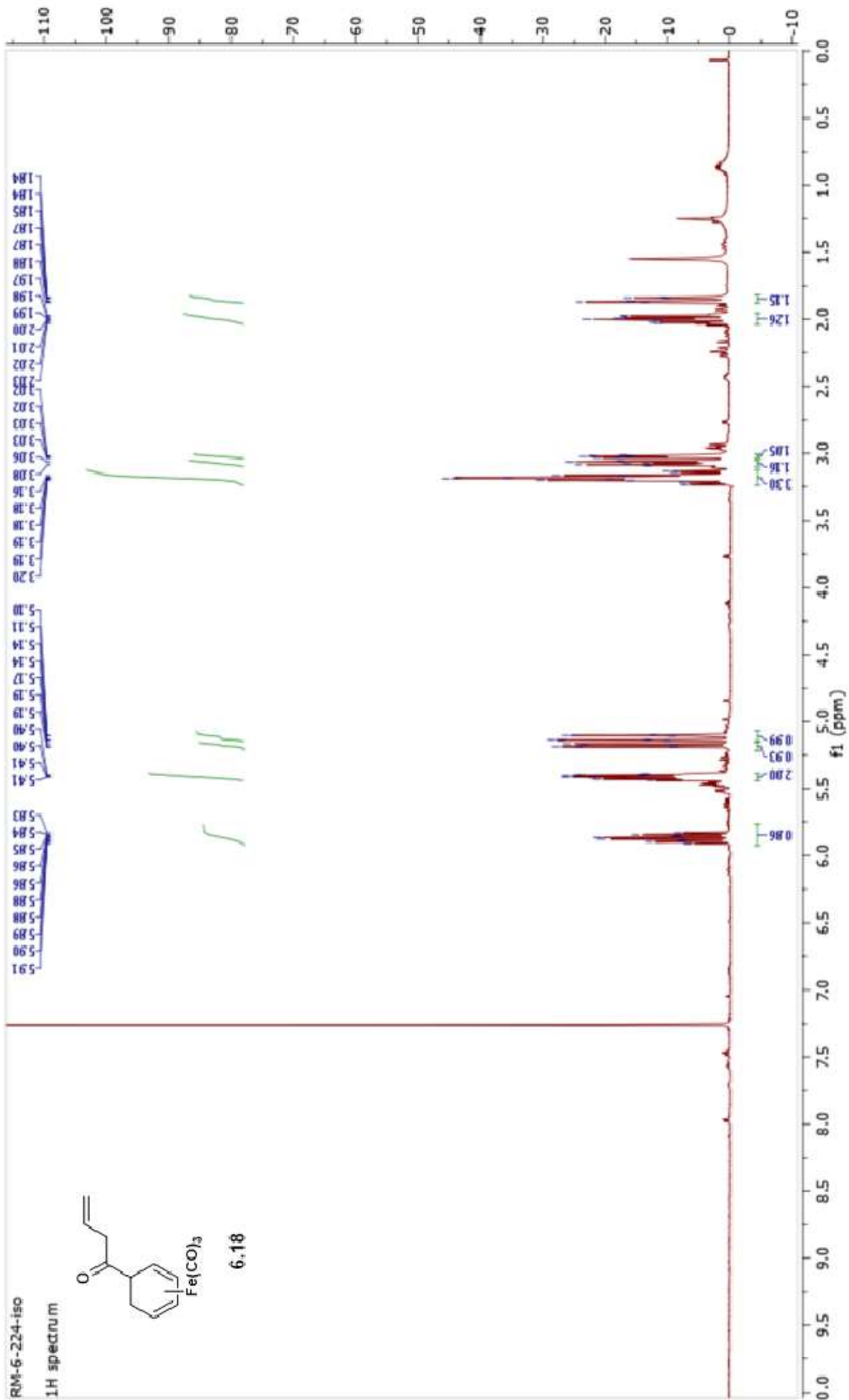


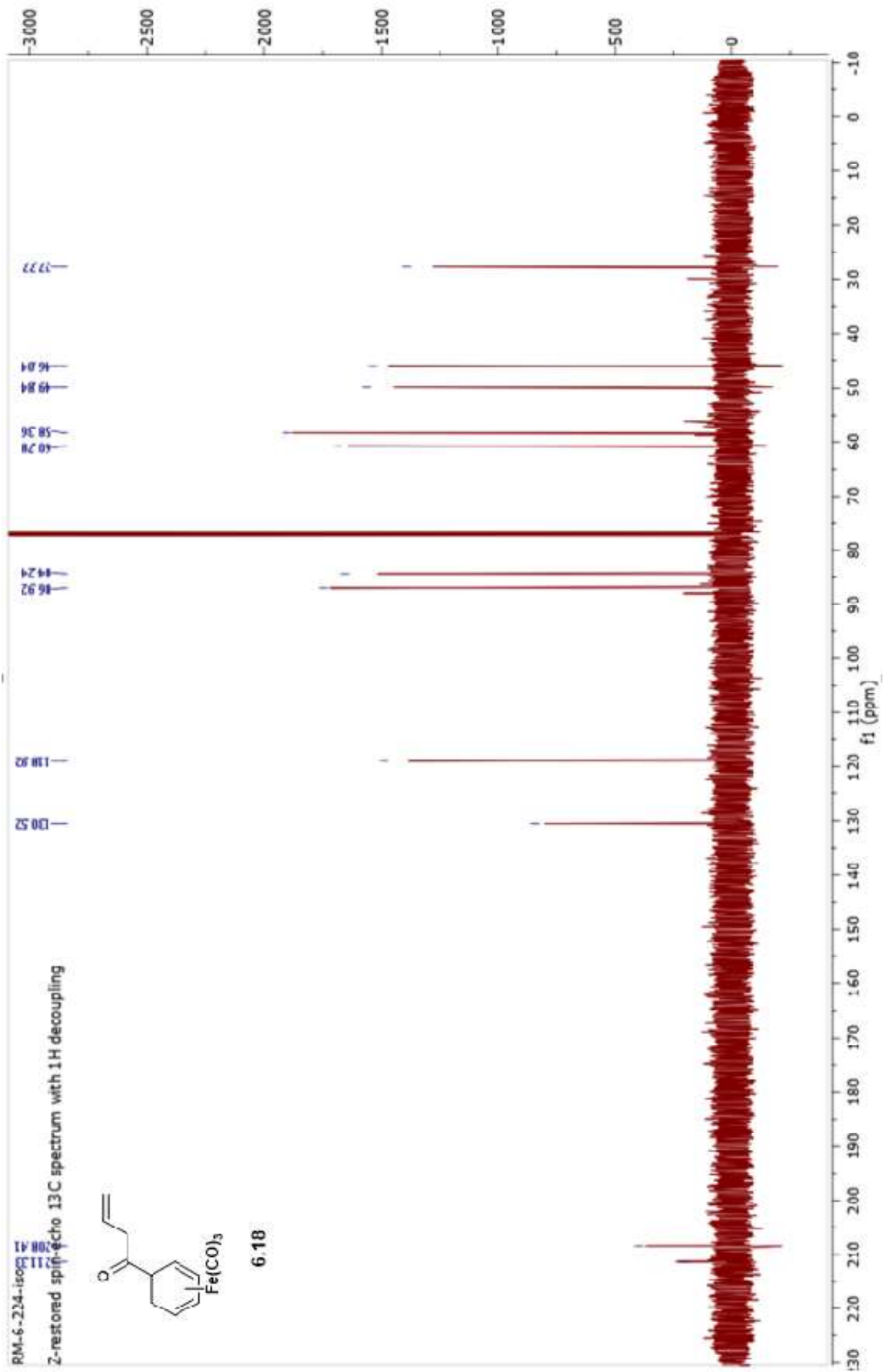


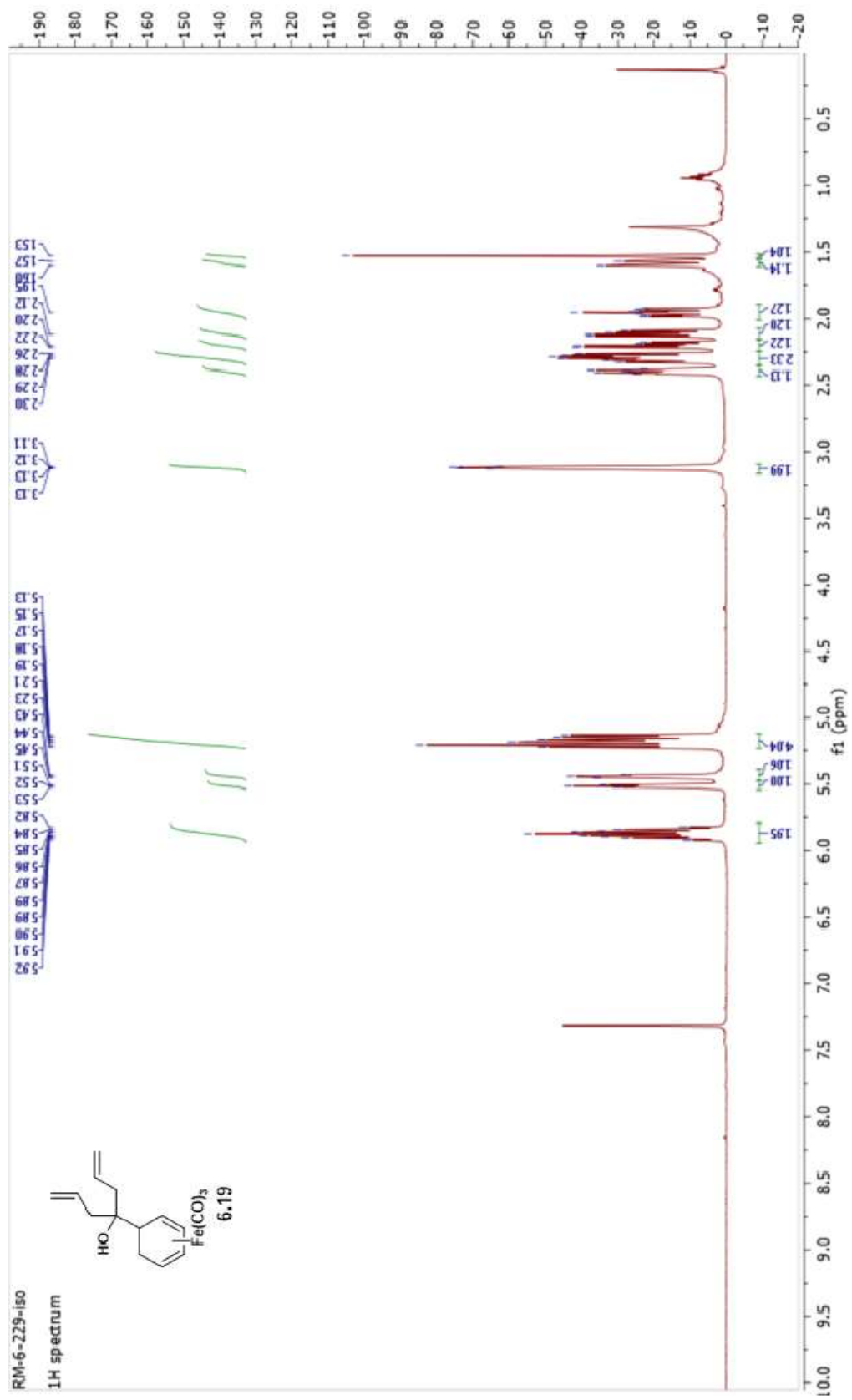


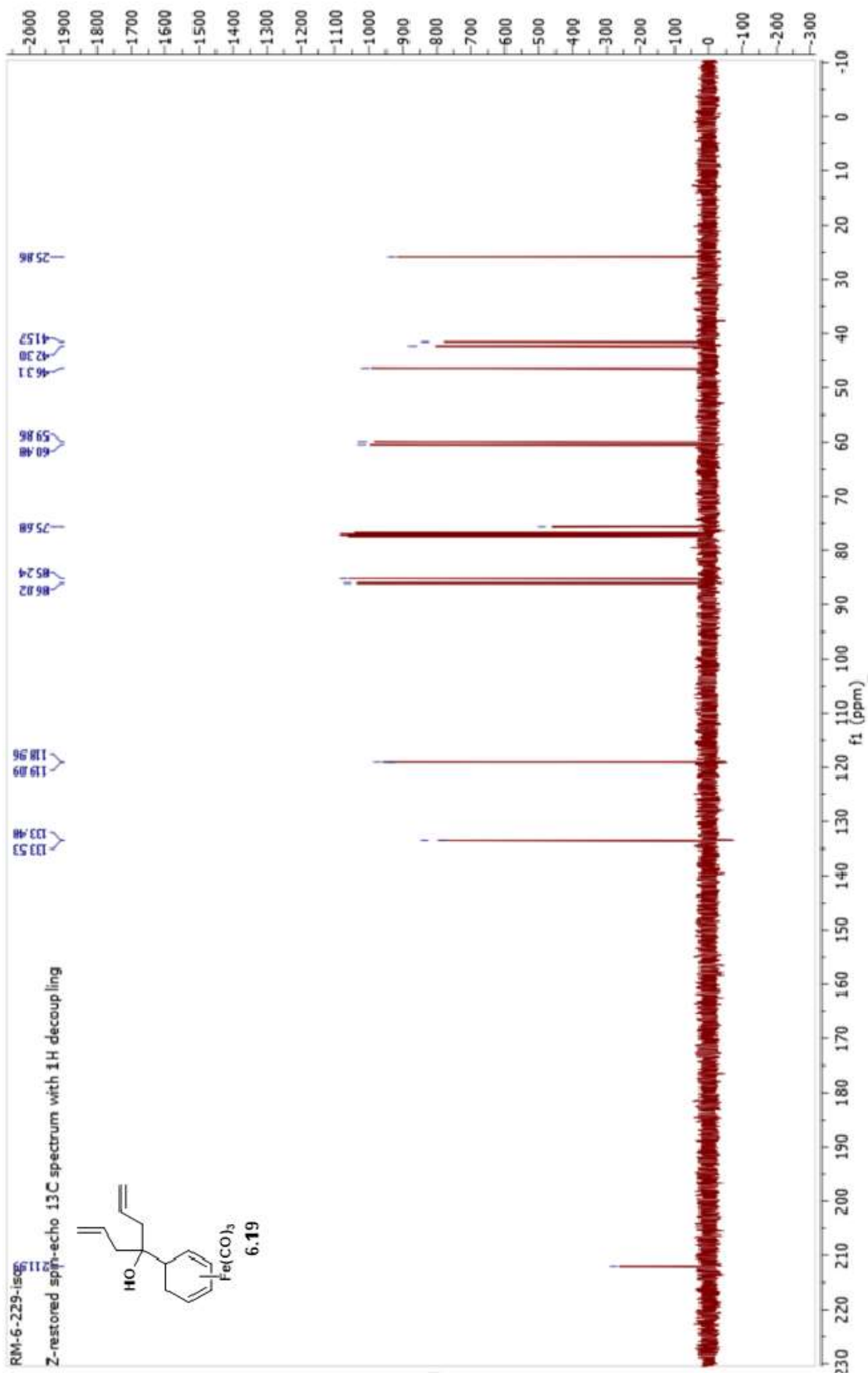


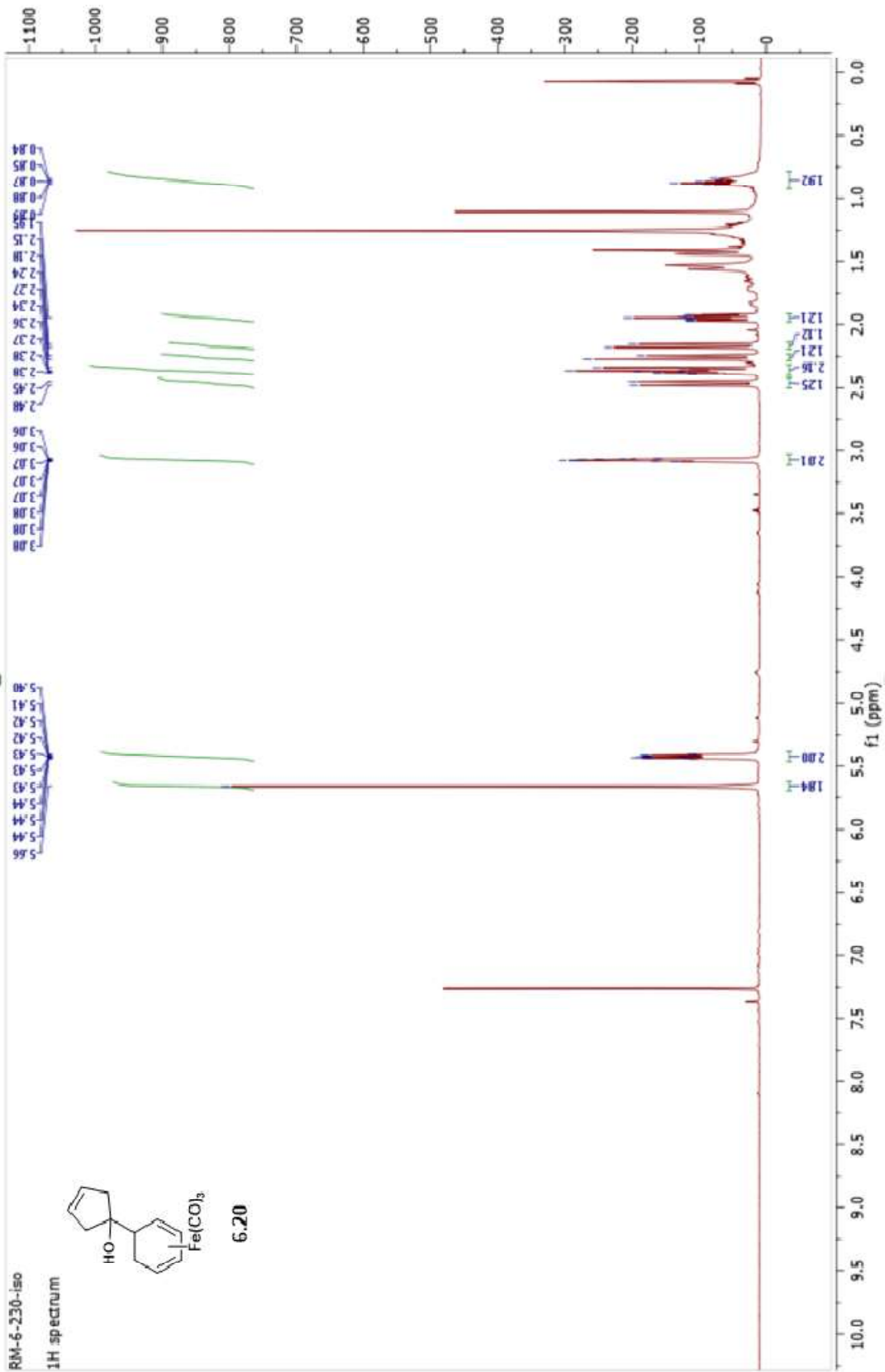


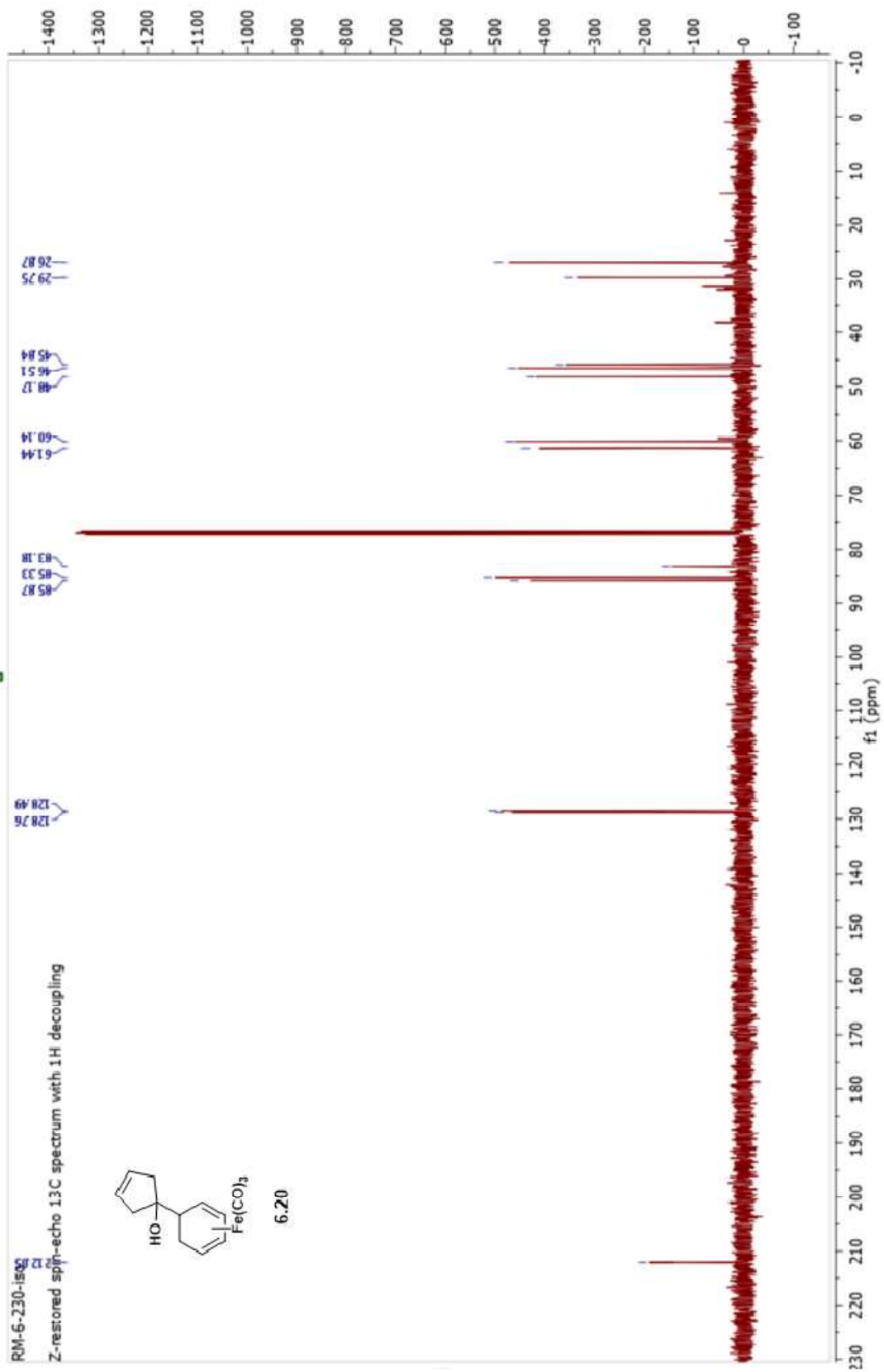


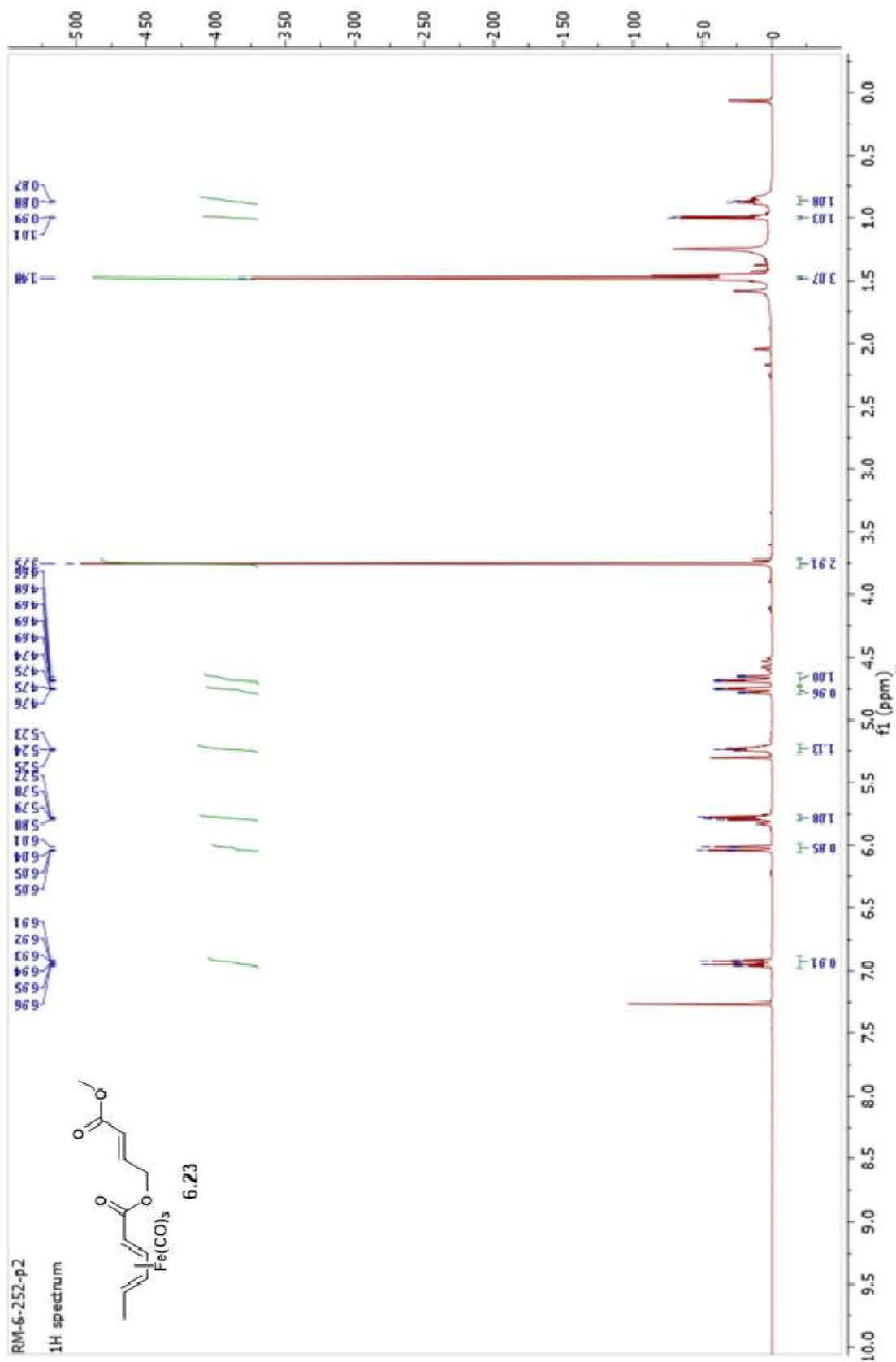


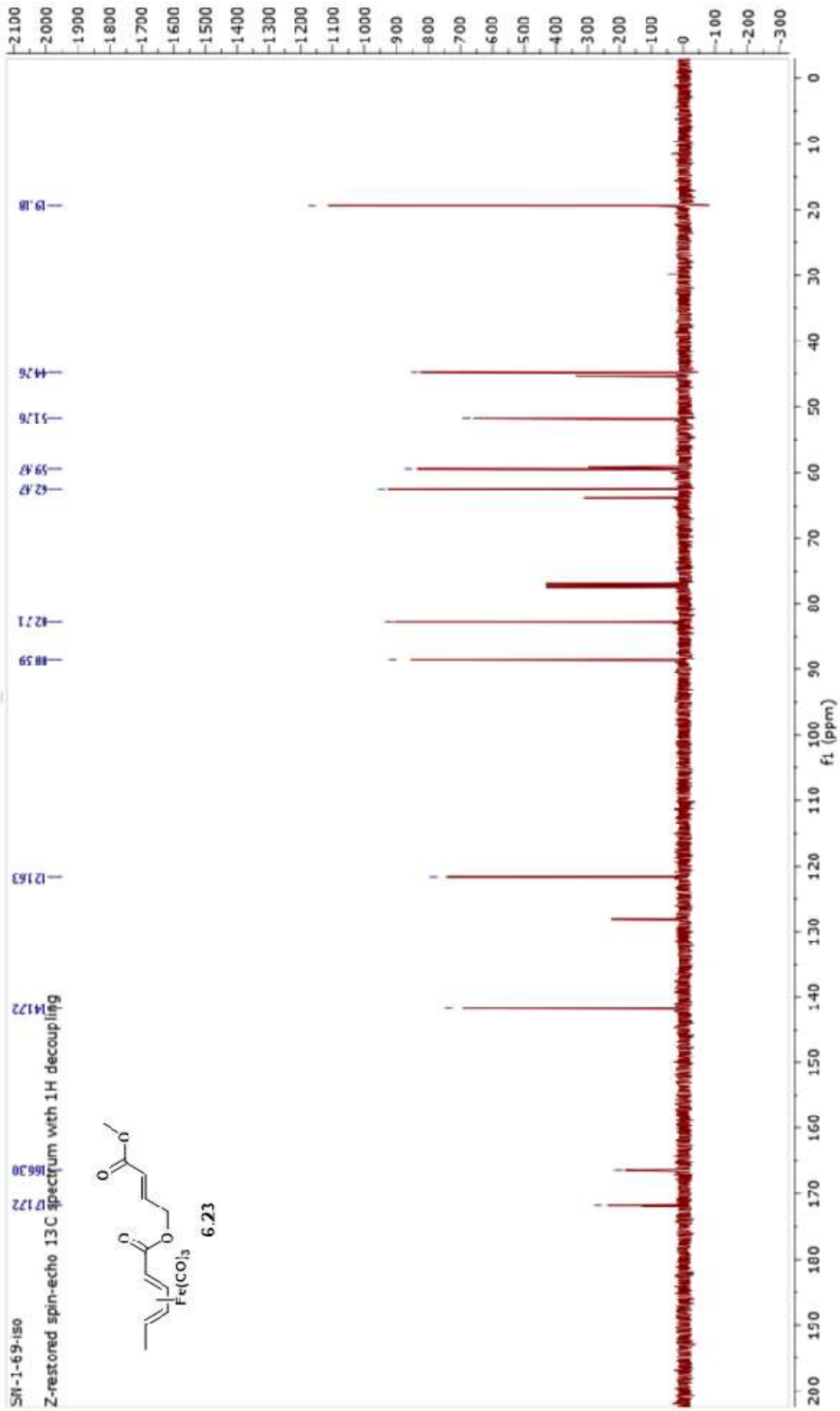


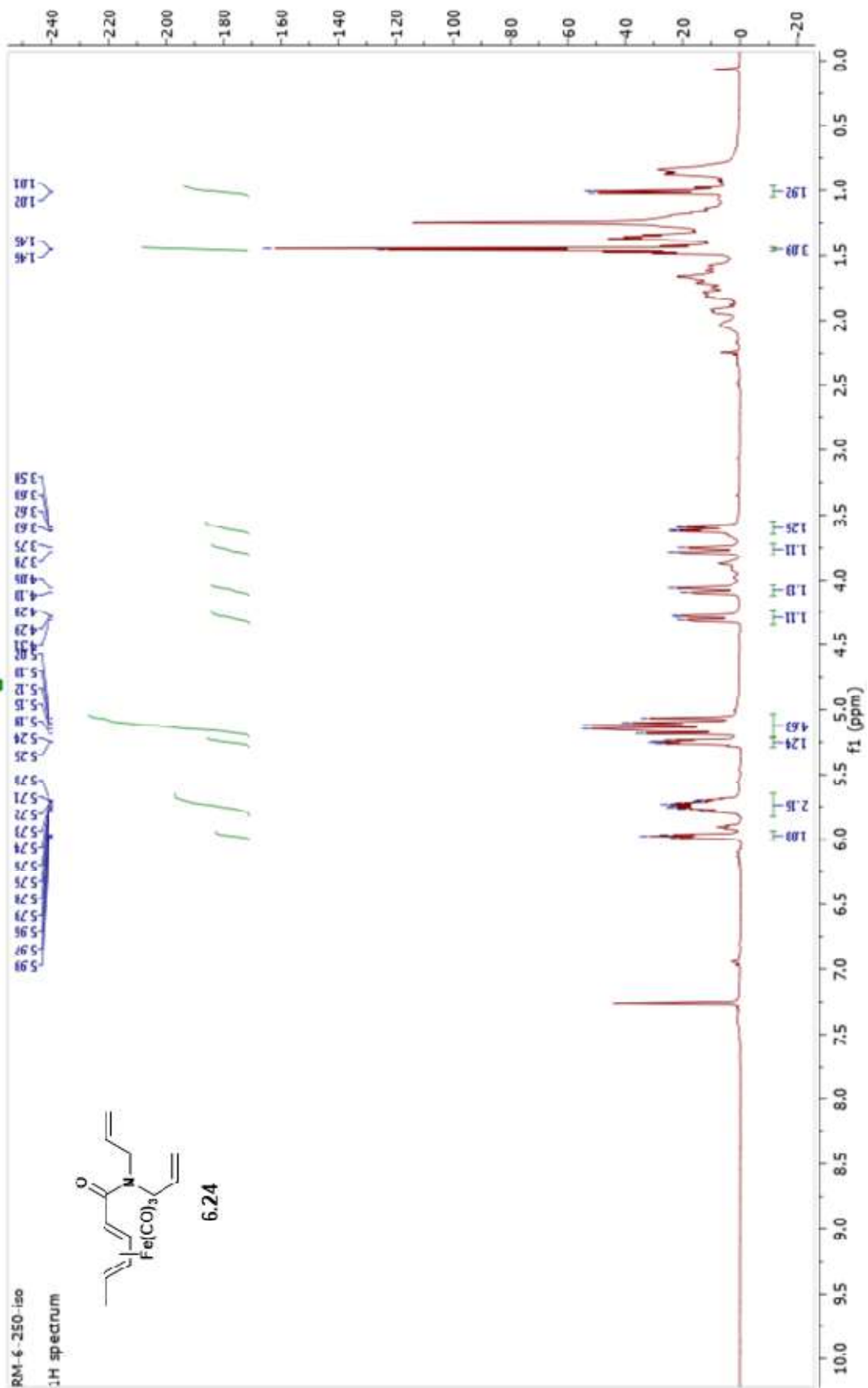


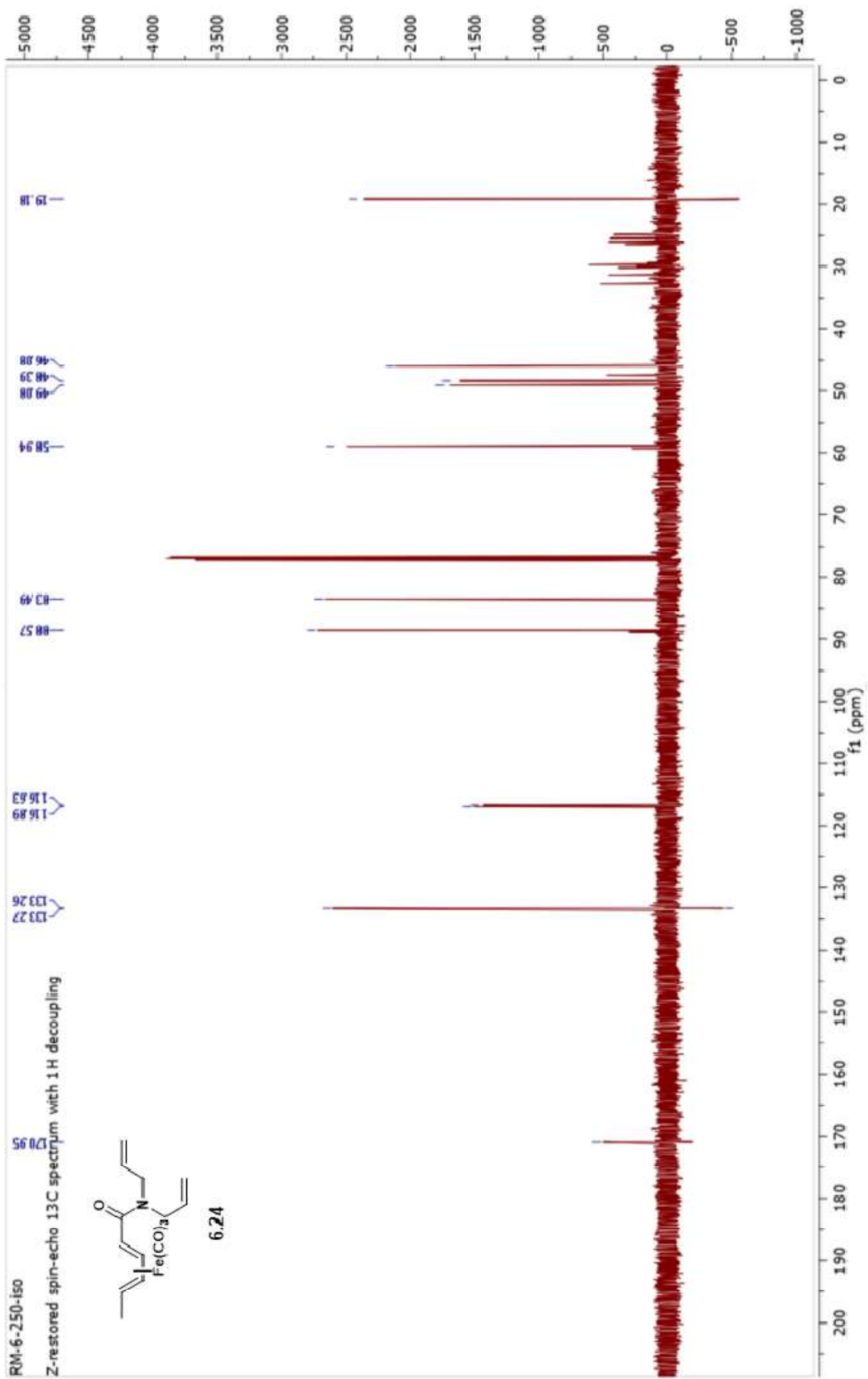


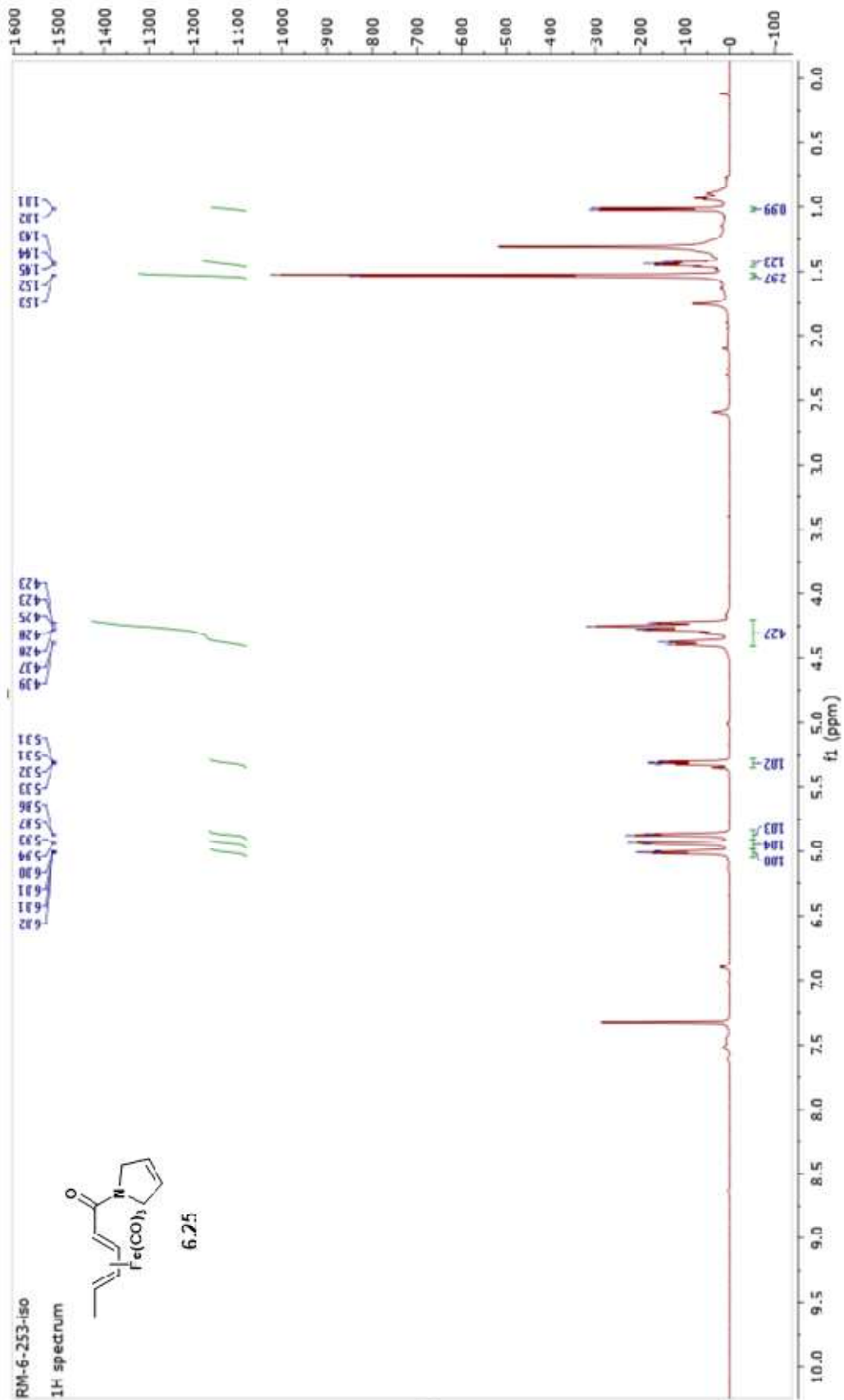


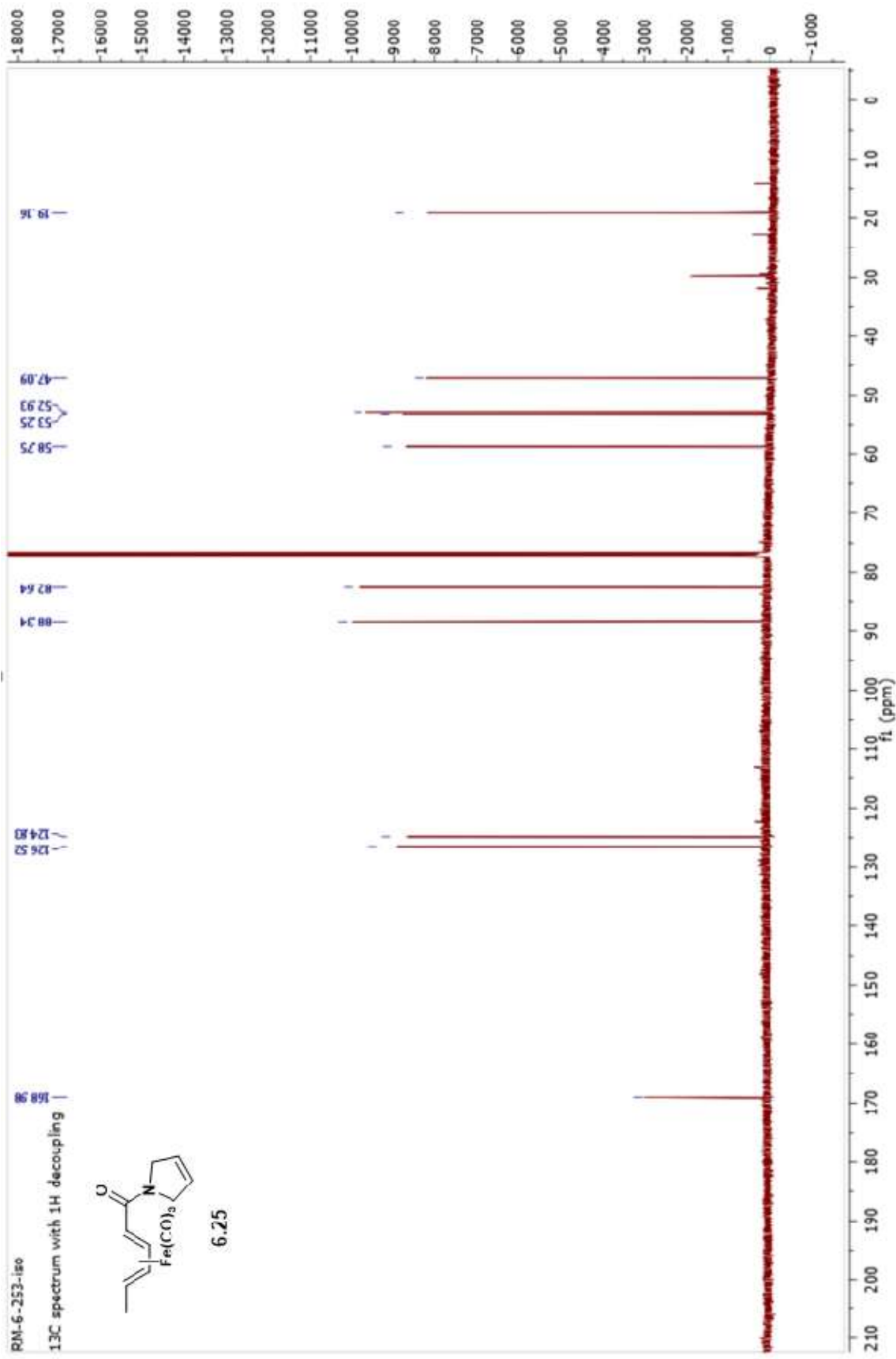


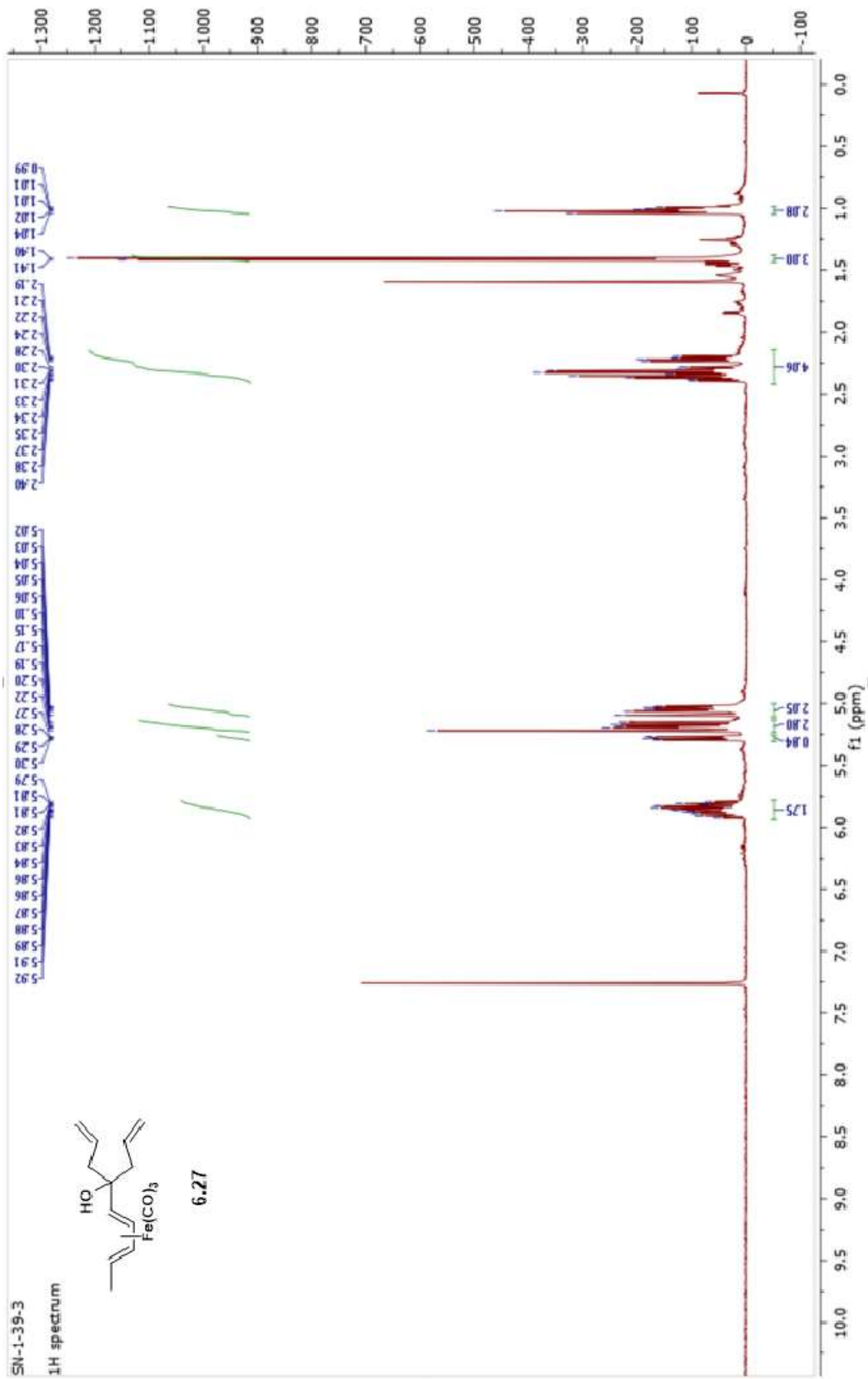


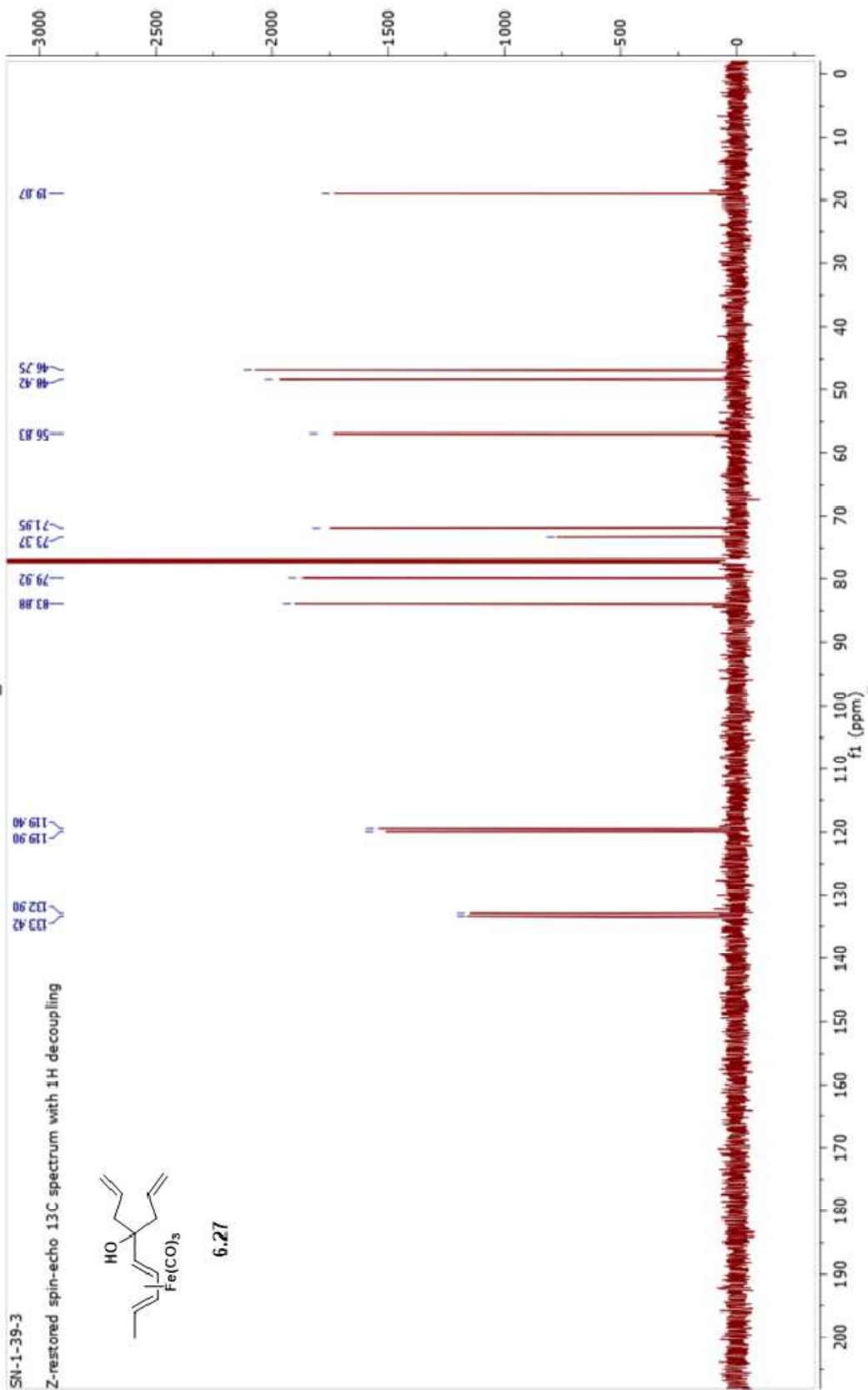


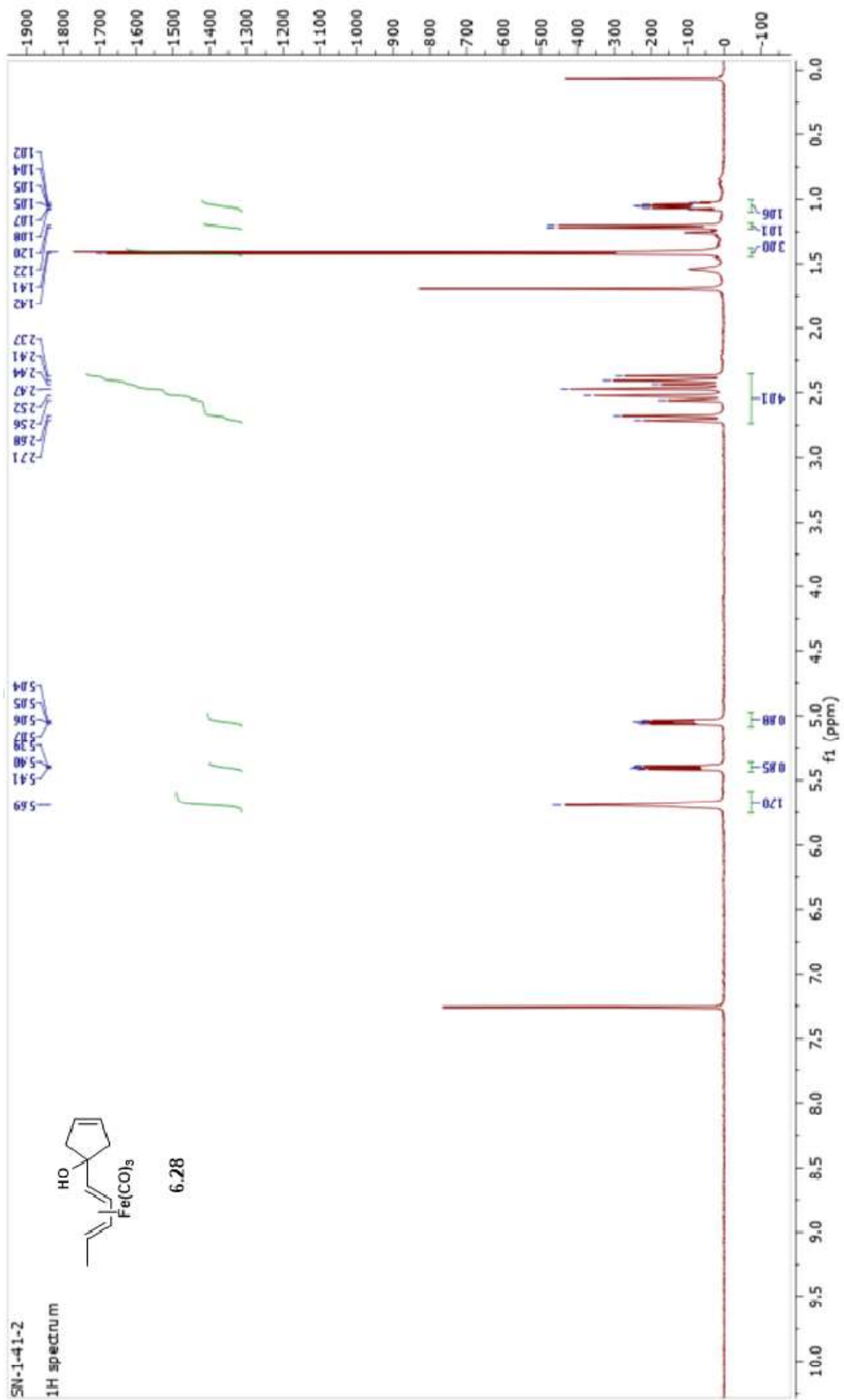


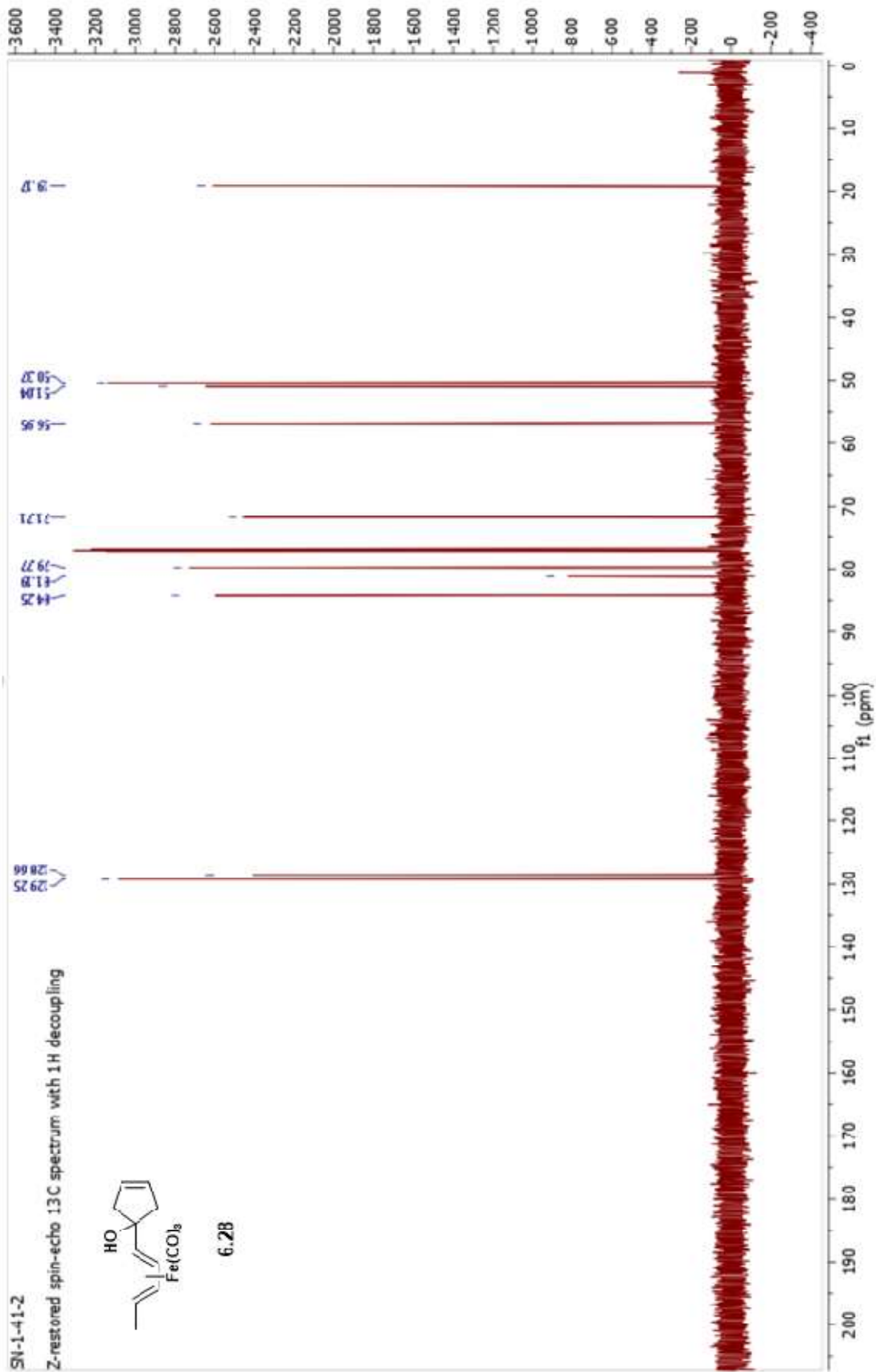


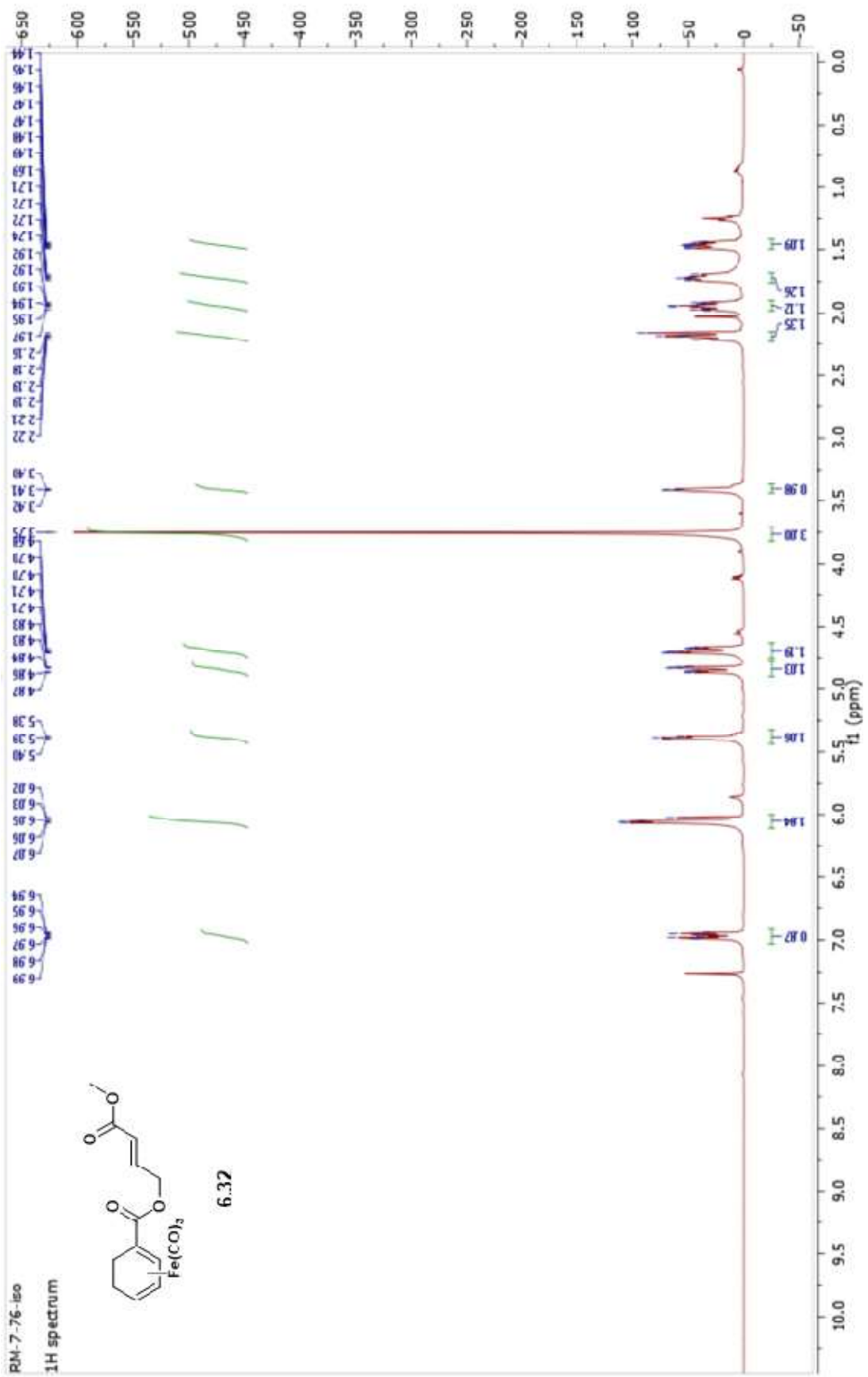


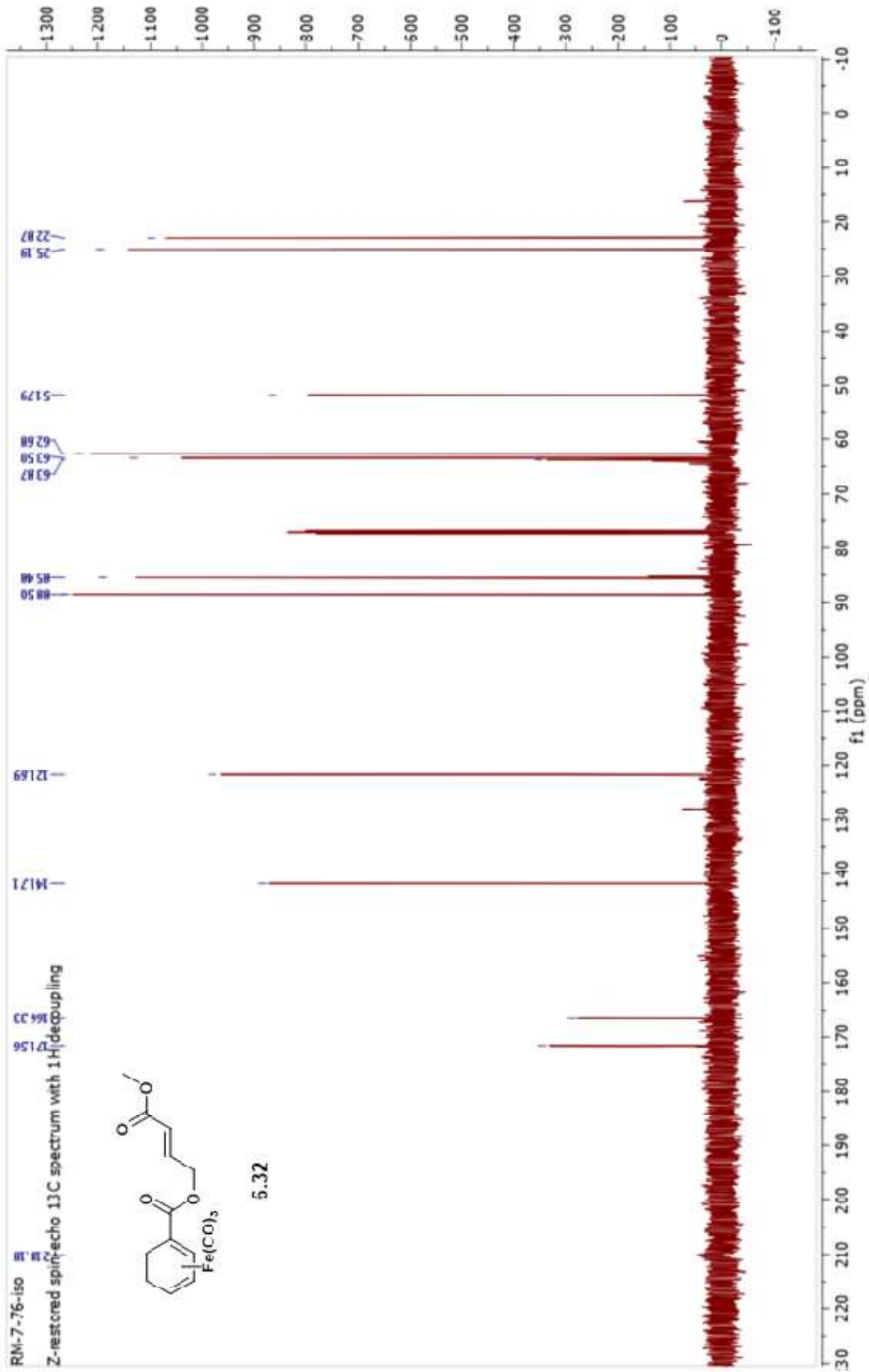


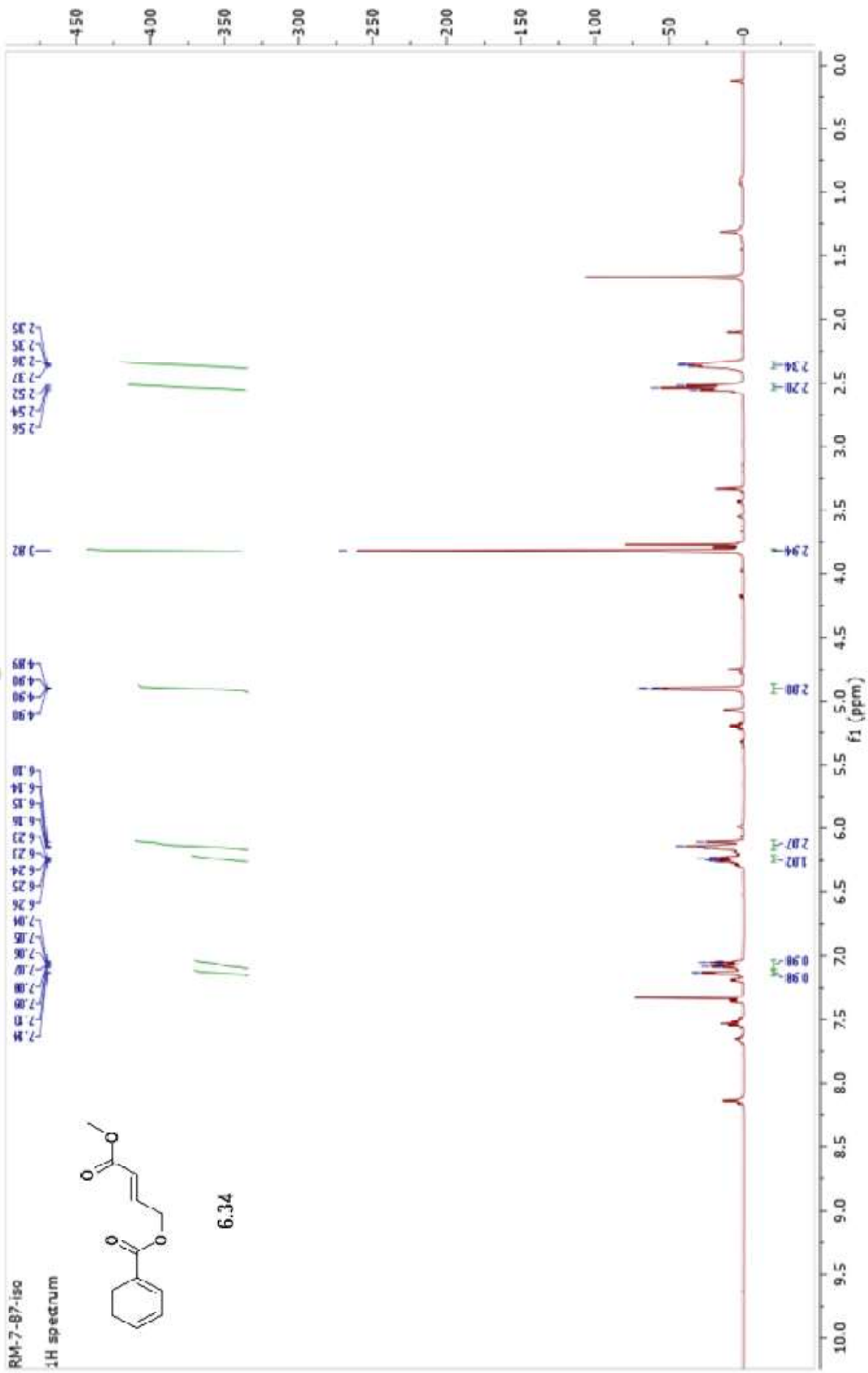


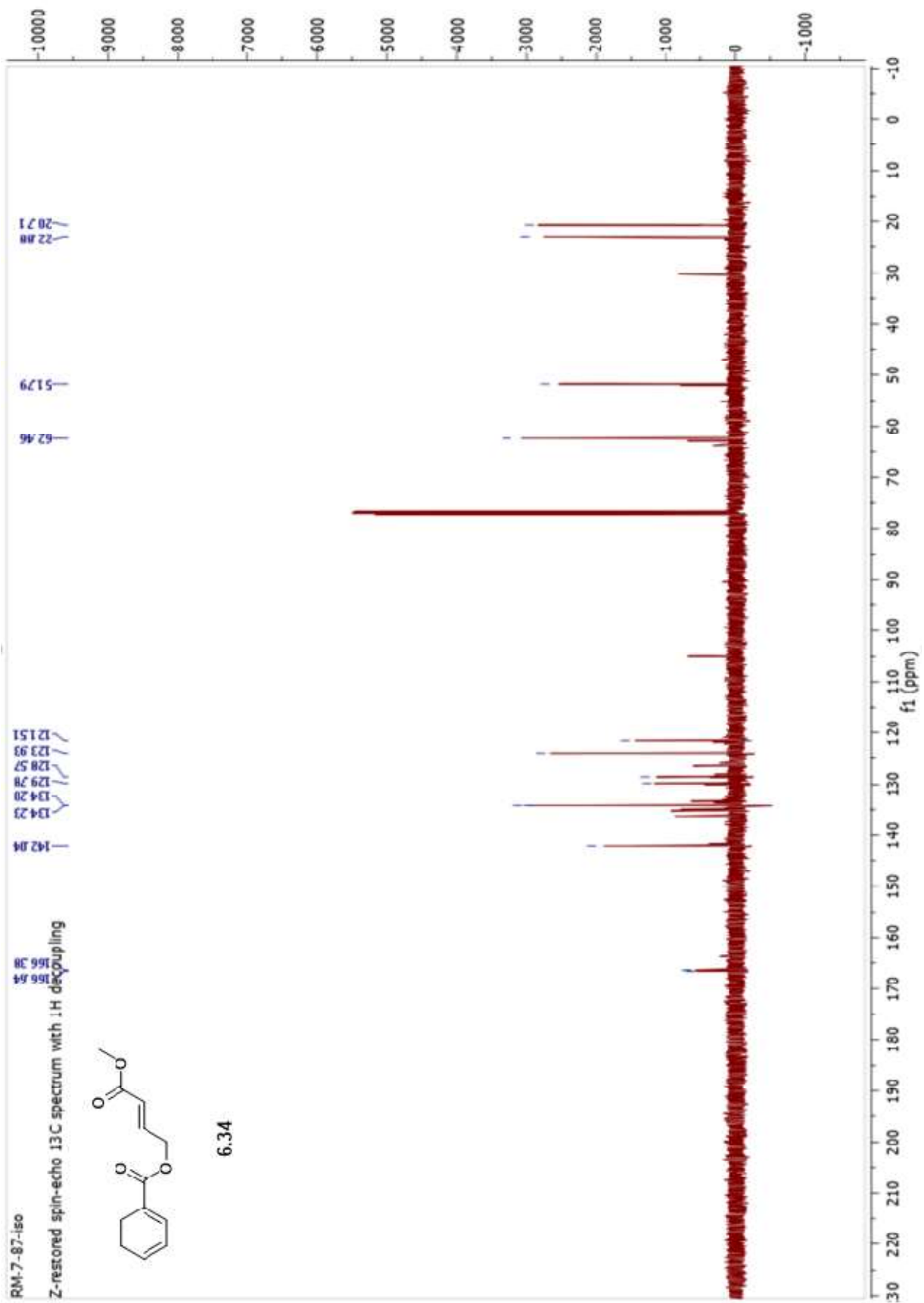


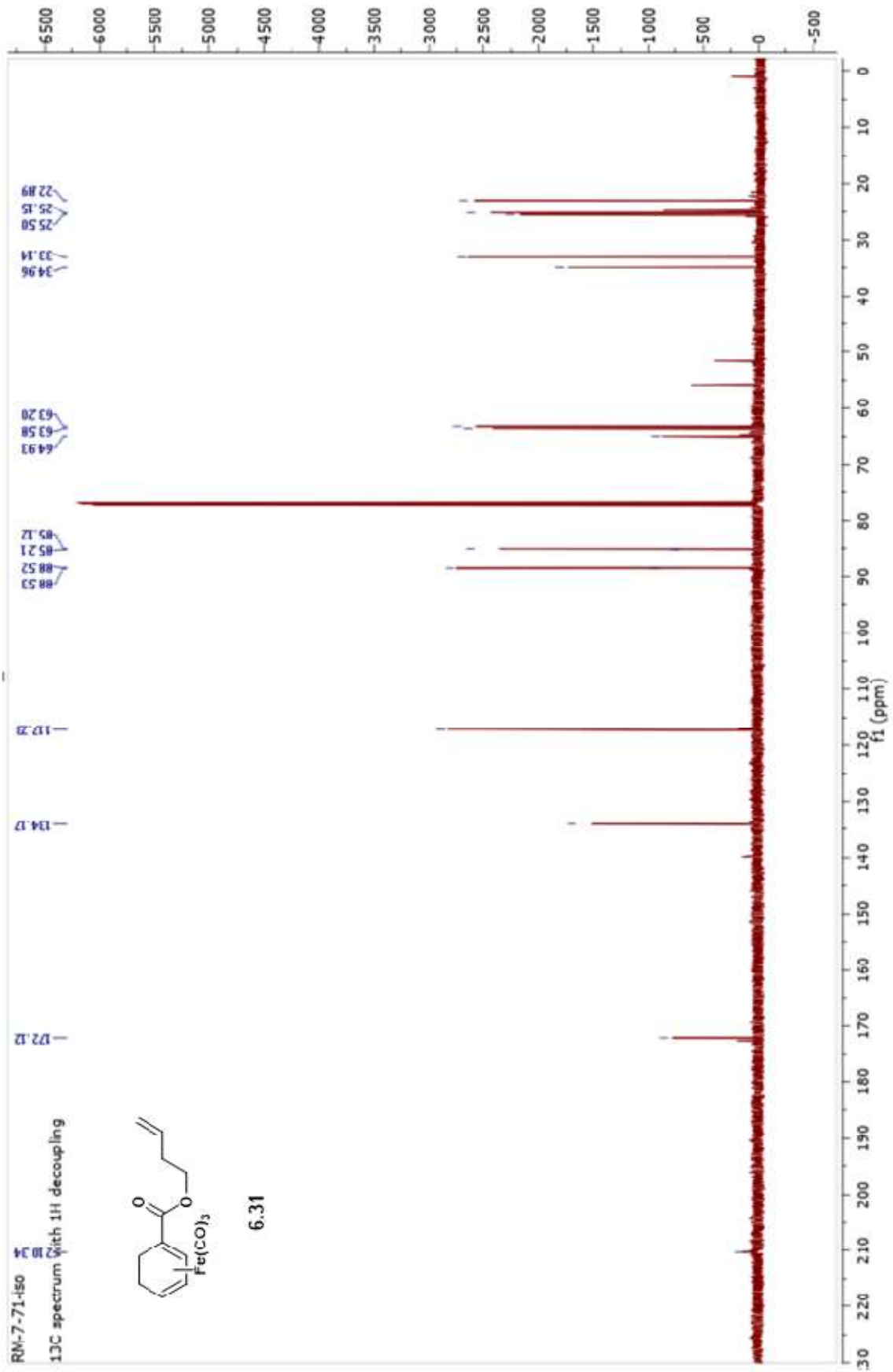


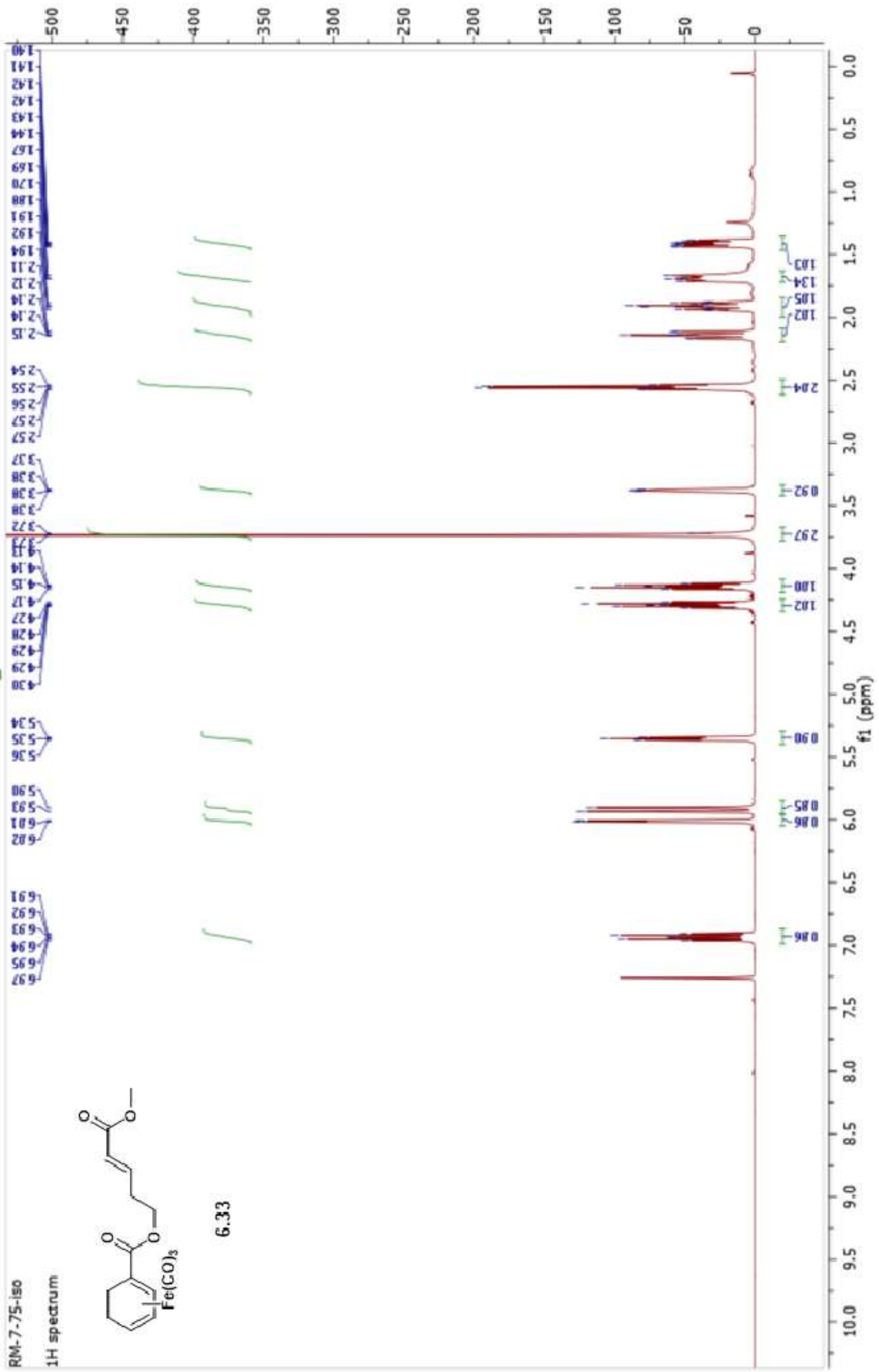


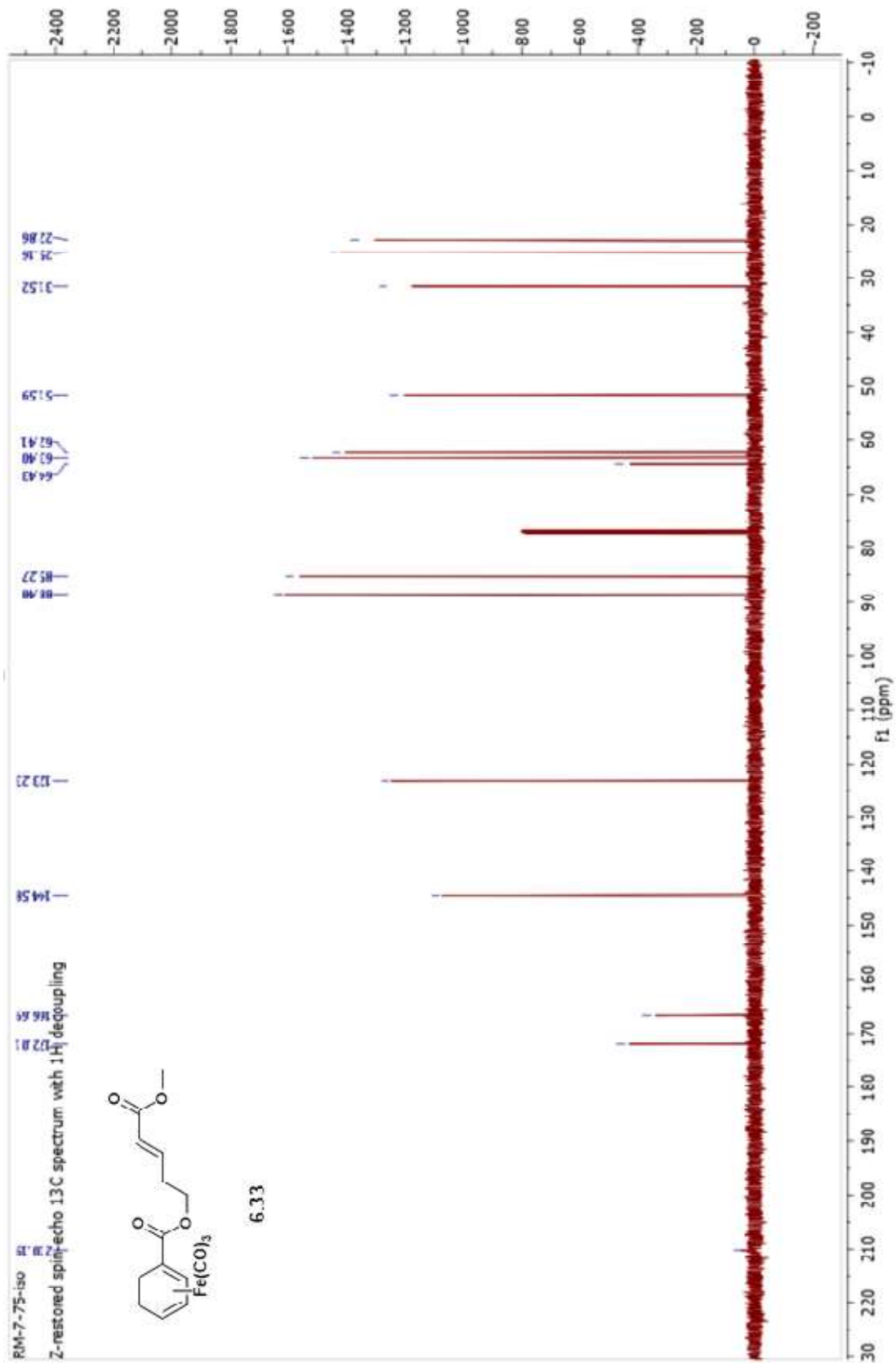


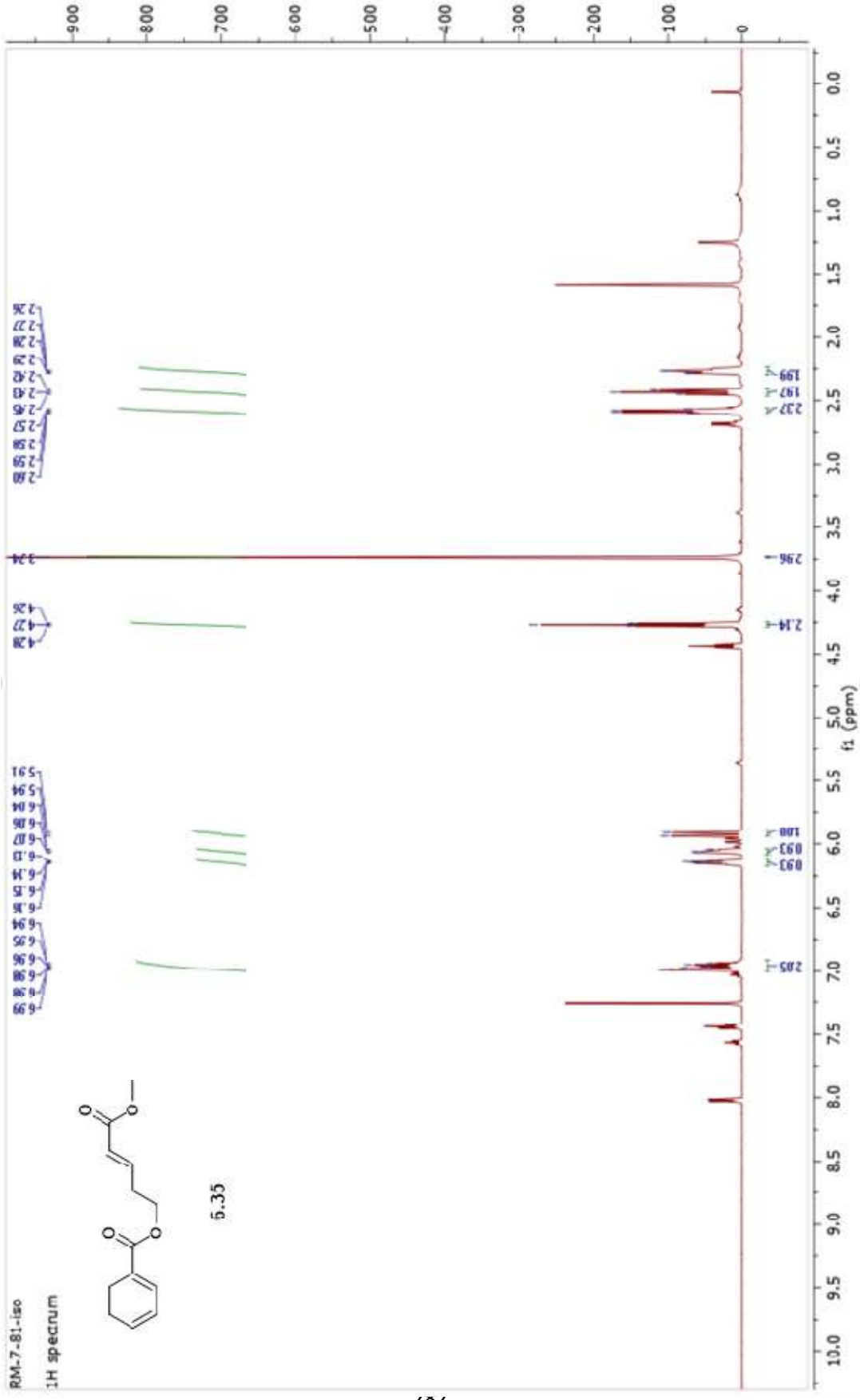


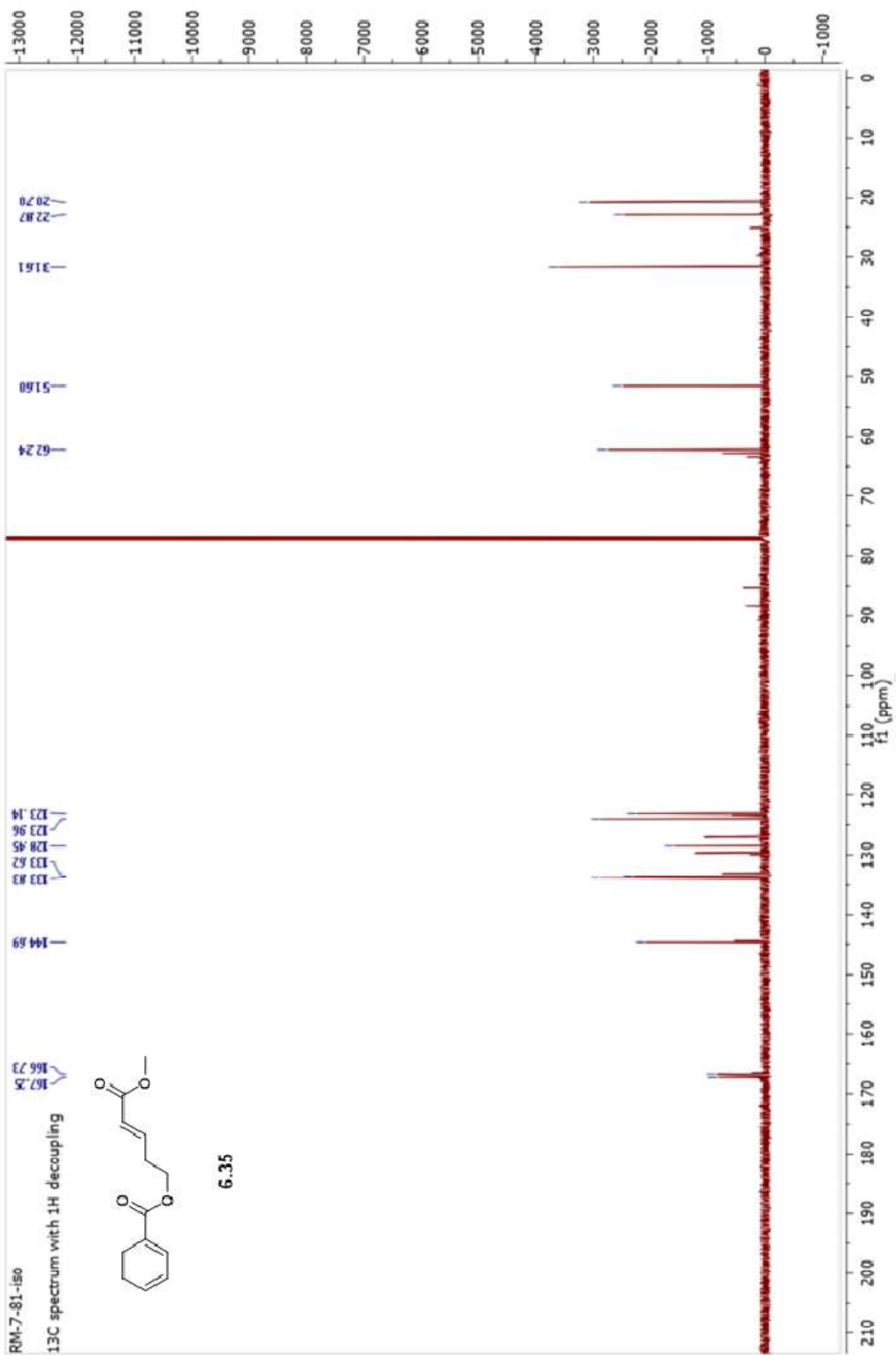


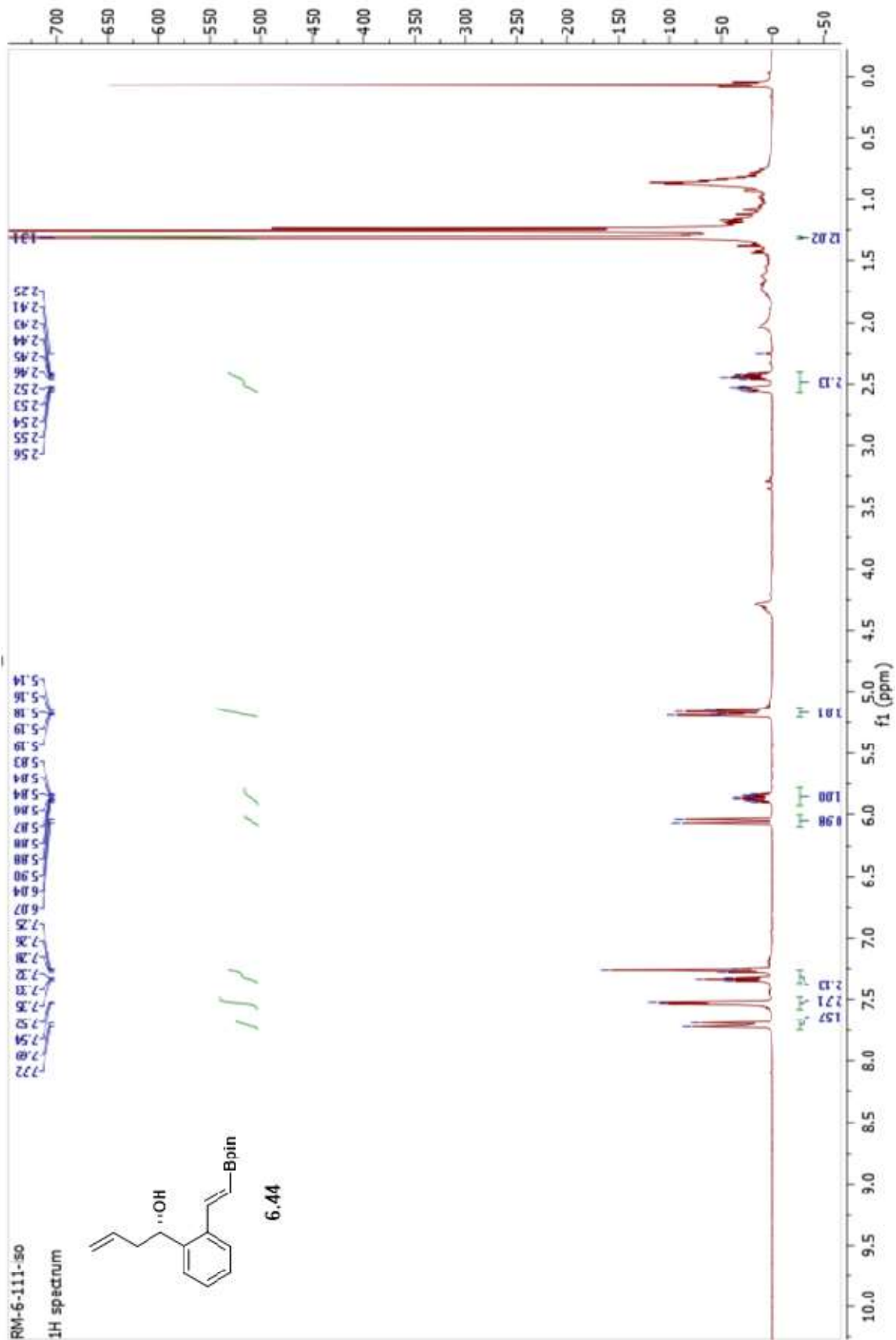


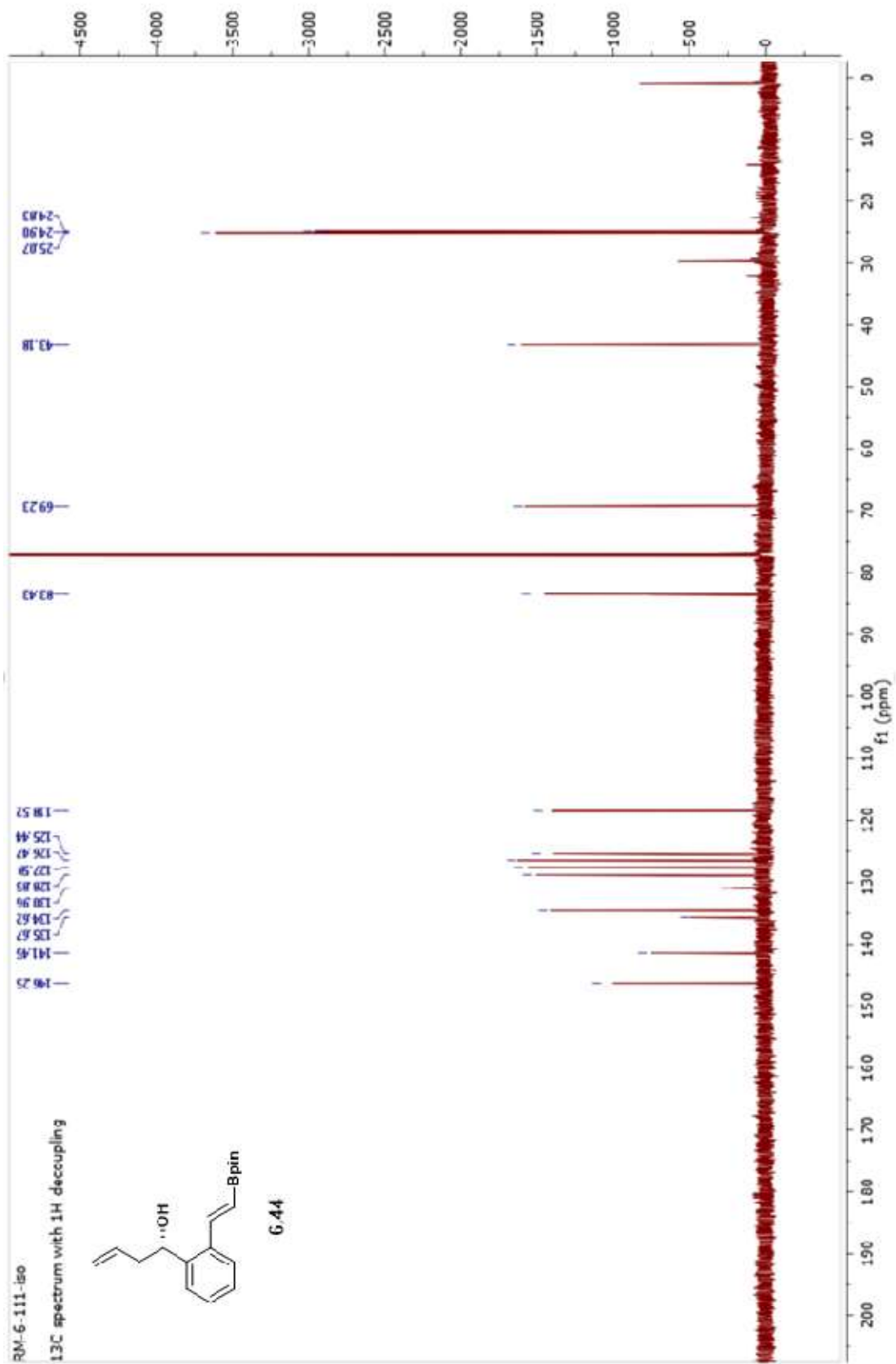


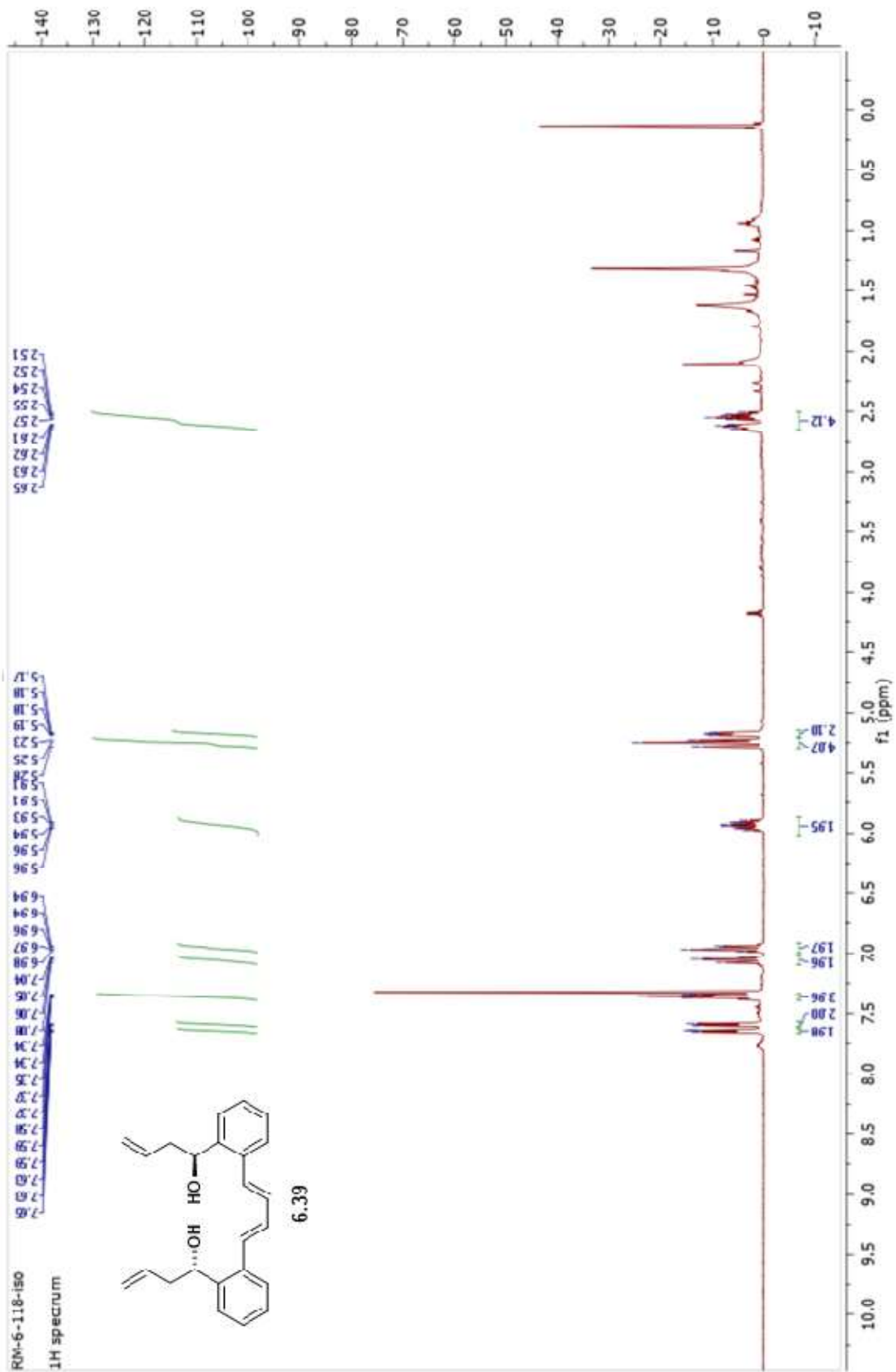


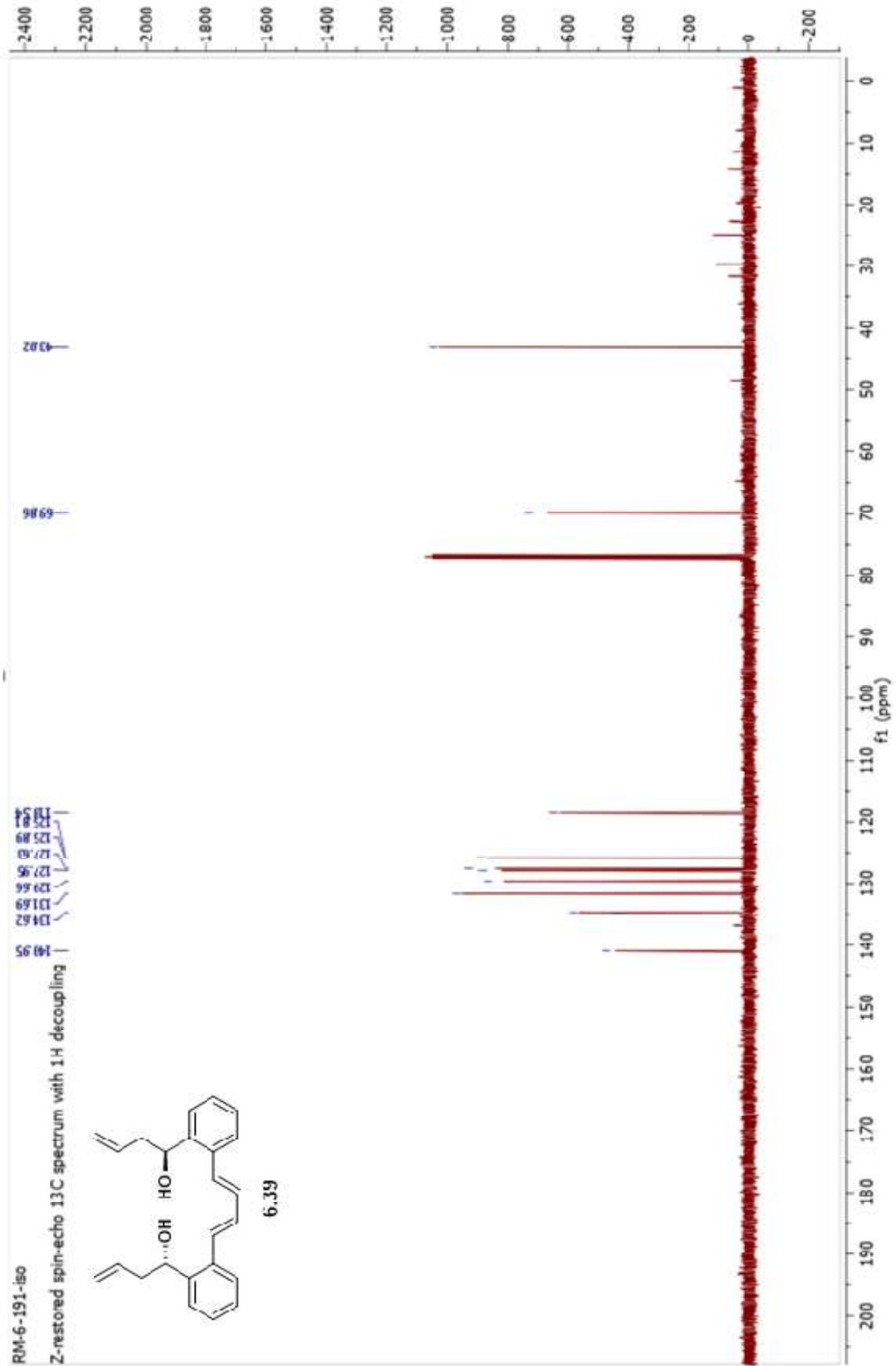


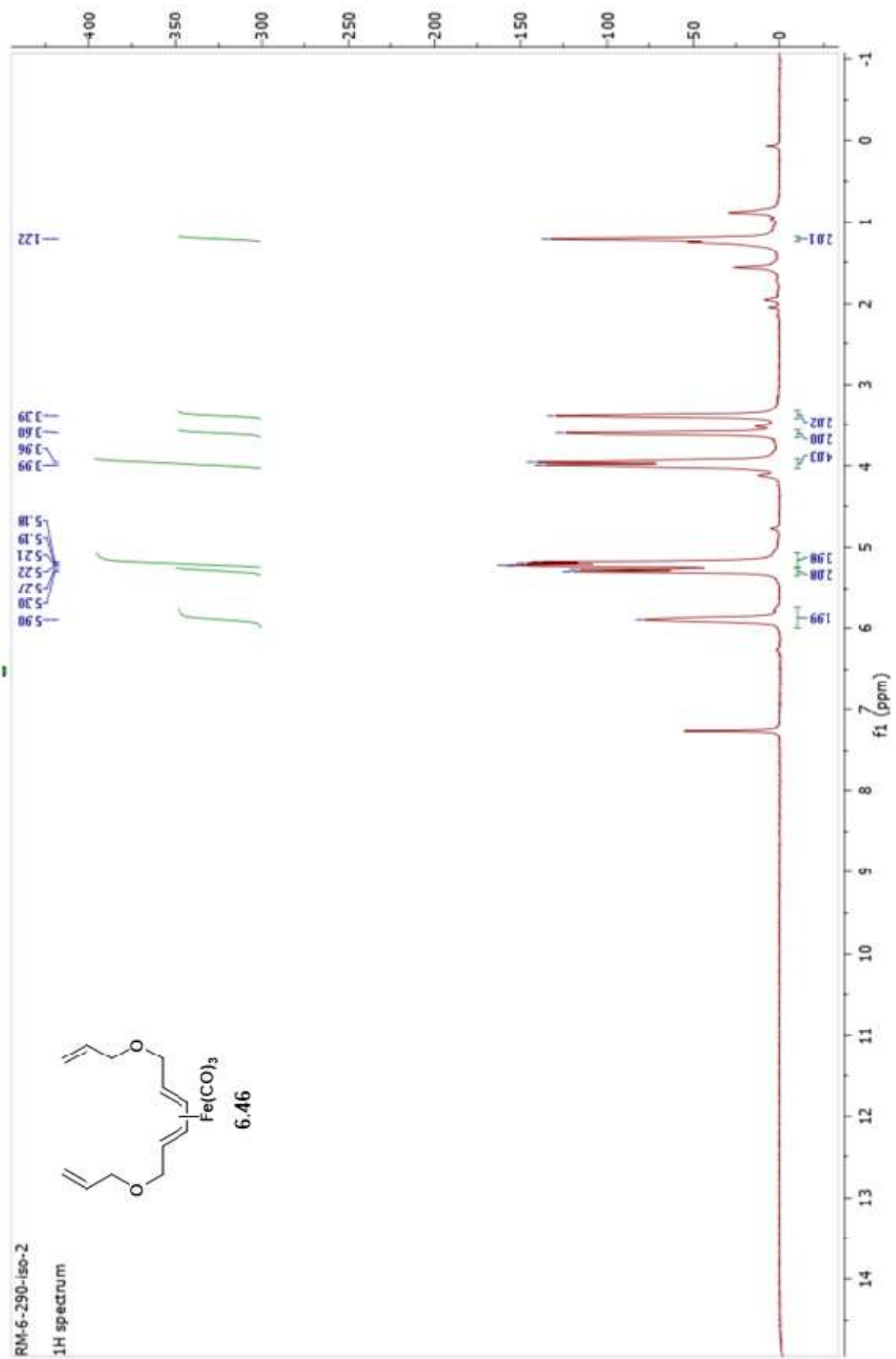


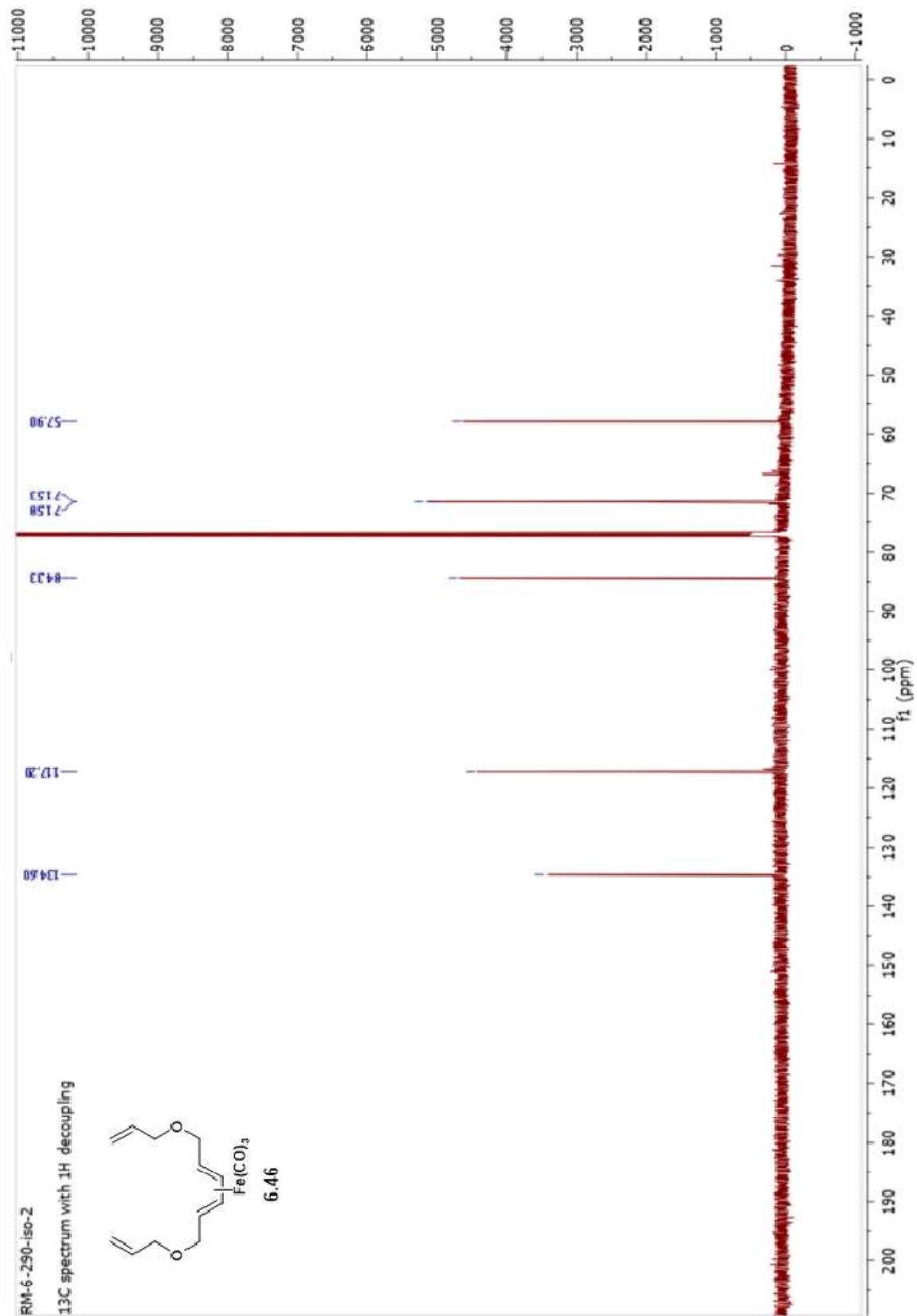


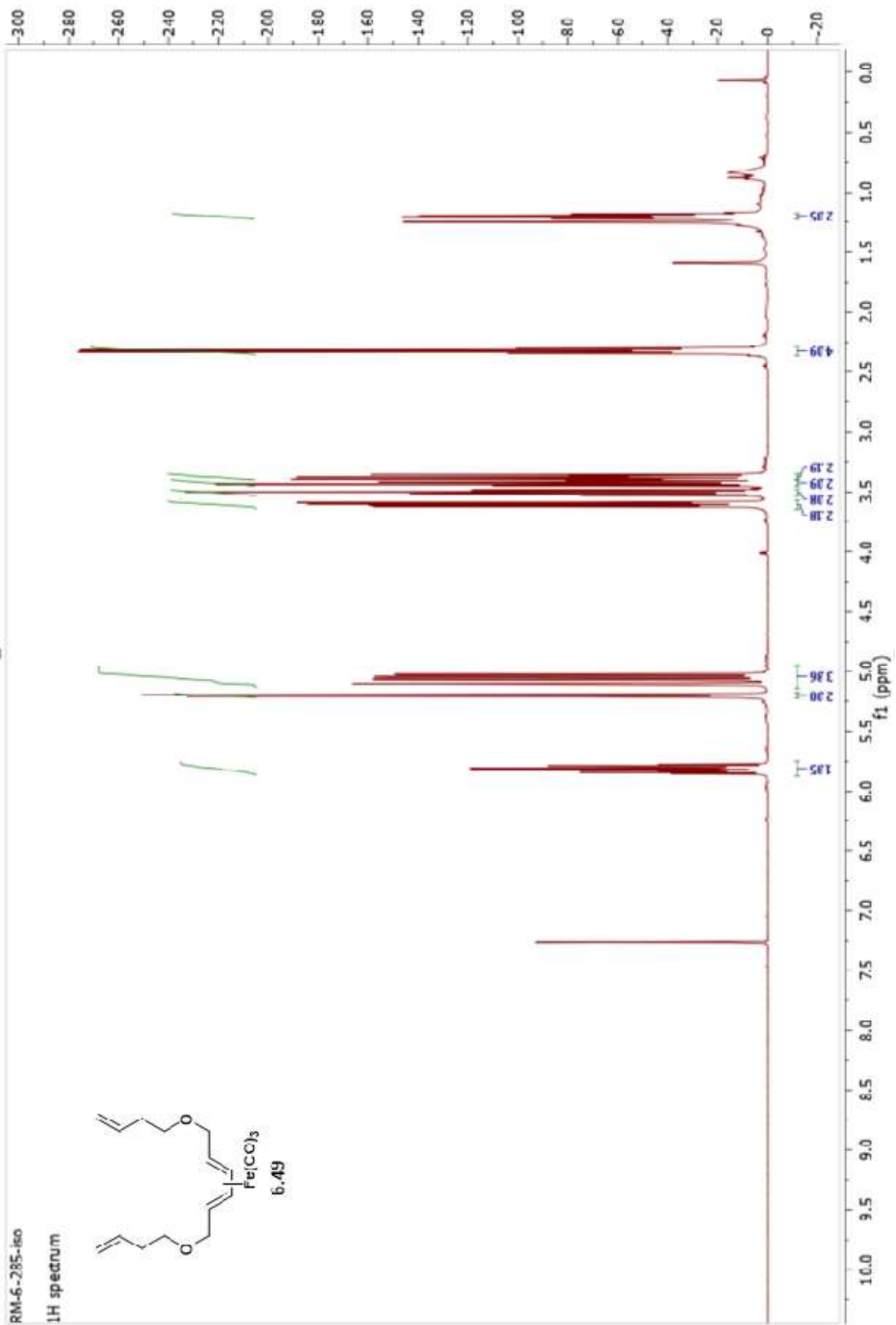


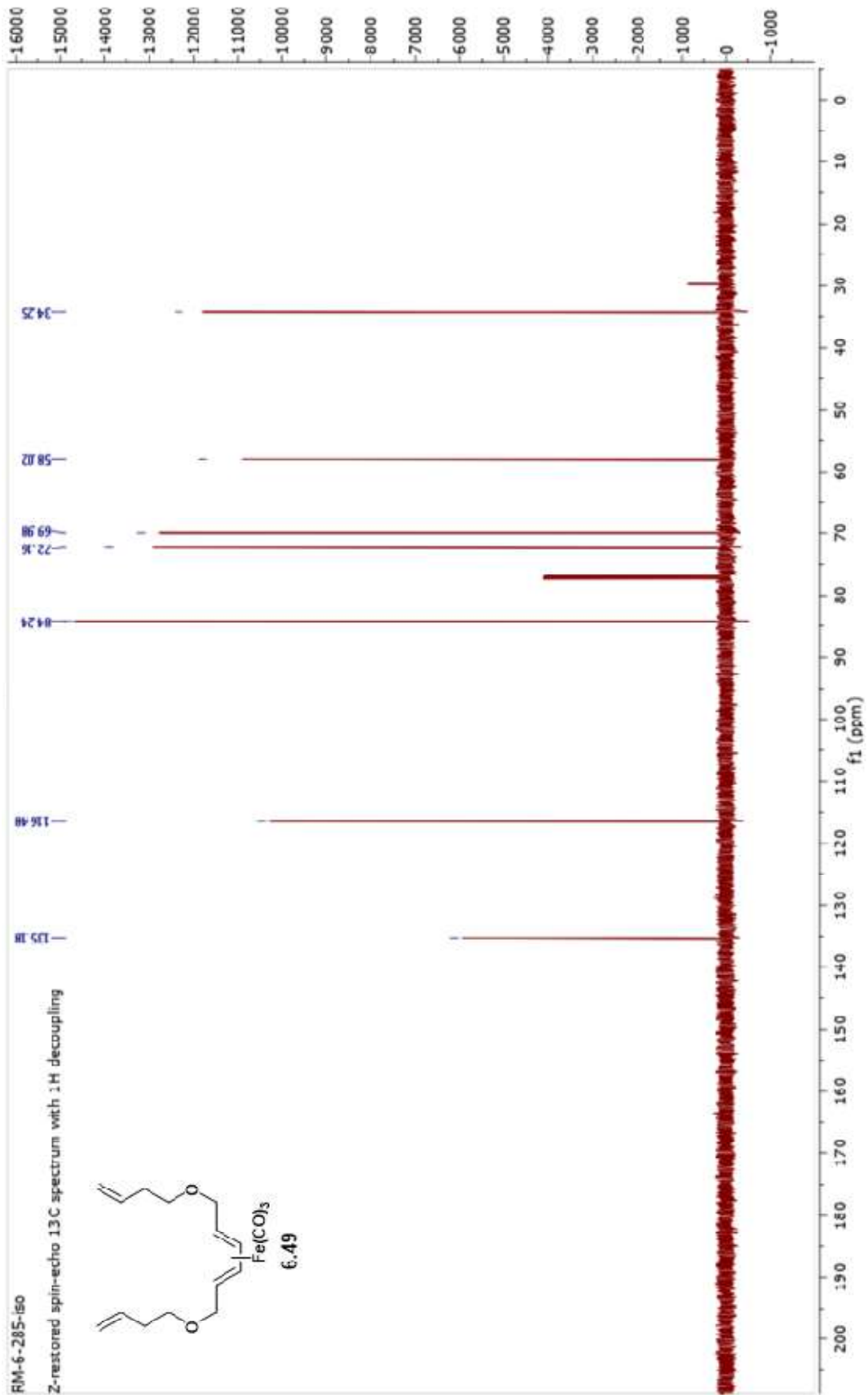


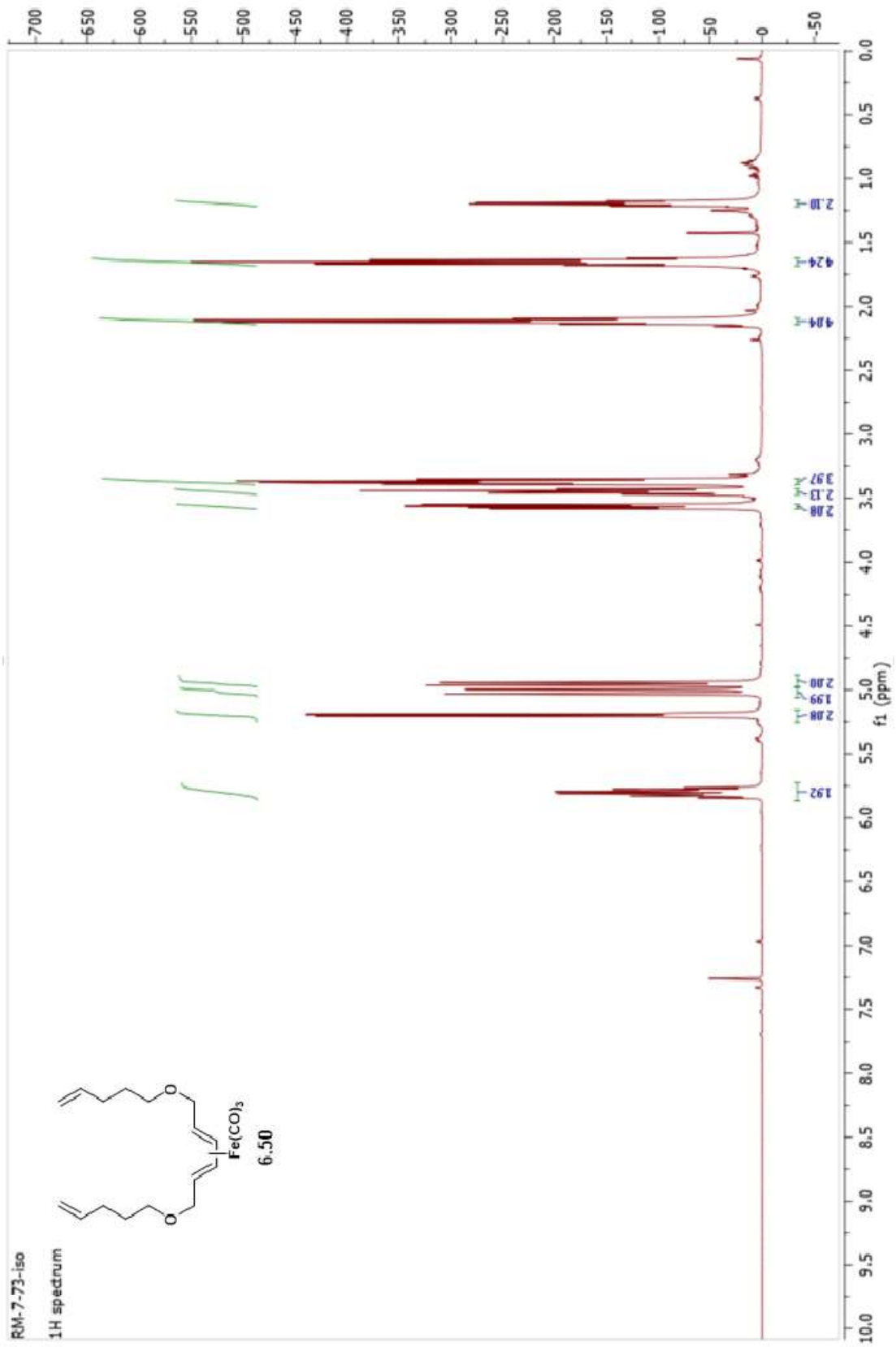


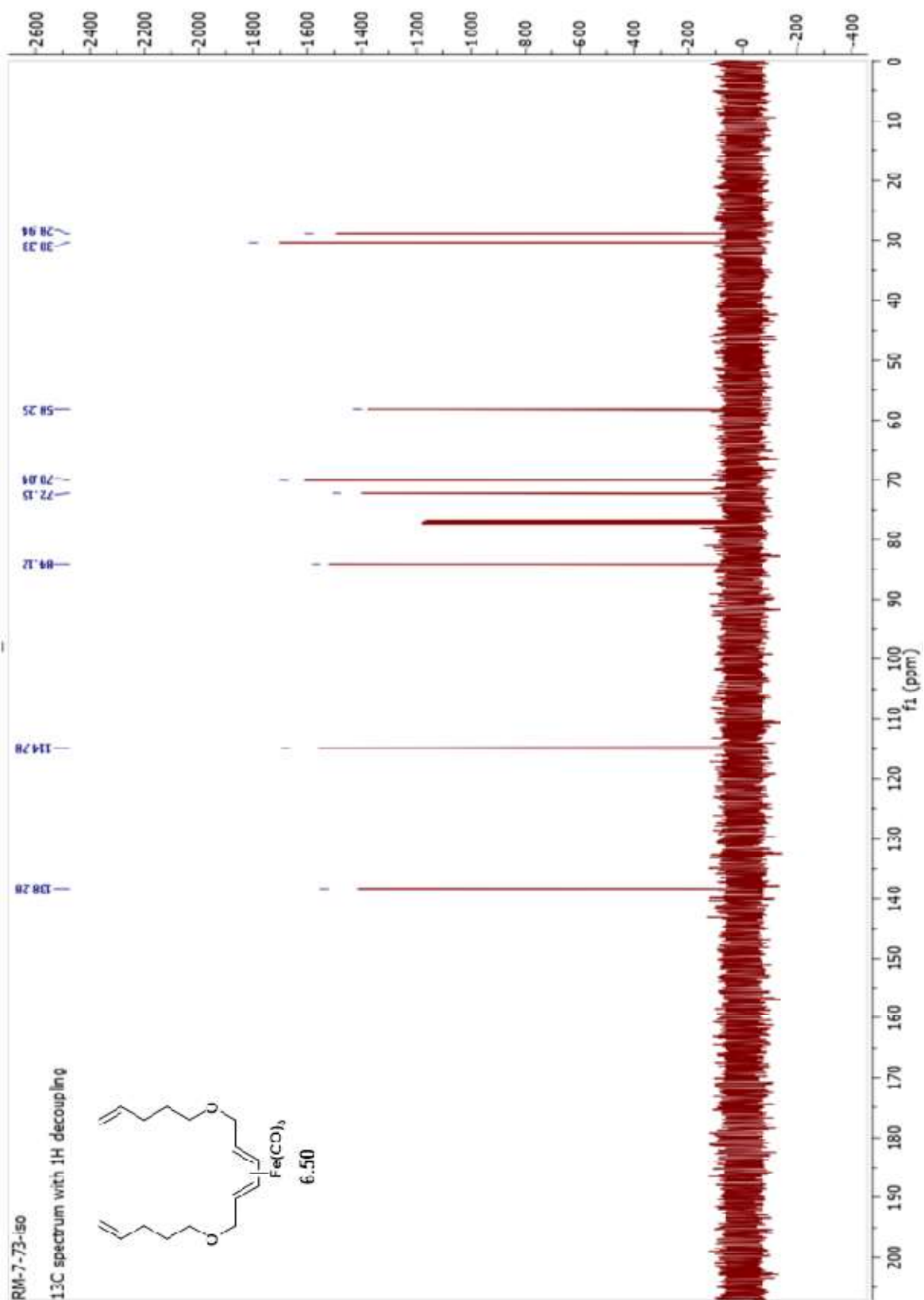












APPENDIX B: X-RAY CRYSTALLOGRAPHIC DATA

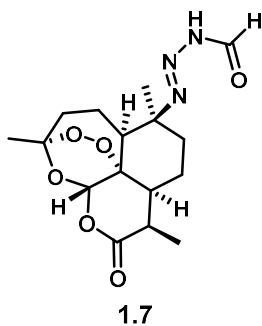


Table 1. Crystal data and structure refinement for cdv54.

Identification code	cdv54 (Riley Mills)	
Empirical formula	C ₁₆ H ₂₃ N ₃ O ₆	
Formula weight	353.37	
Temperature	88(2) K	
Wavelength	0.71073 Å	
Crystal system	Monoclinic	
Space group	P2 ₁	
Unit cell dimensions	a = 6.5920(6) Å	α = 90°.
	b = 10.9394(10) Å	β = 91.1366(12)°.
	c = 11.3239(11) Å	γ = 90°.
Volume	816.43(13) Å ³	
Z	2	
Density (calculated)	1.437 Mg/m ³	
Absorption coefficient	0.111 mm ⁻¹	
F(000)	376	
Crystal color	colorless	
Crystal size	0.376 x 0.238 x 0.098 mm ³	
Theta range for data collection	1.799 to 27.099°	
Index ranges	-8 ≤ h ≤ 8, -13 ≤ k ≤ 13, -14 ≤ l ≤ 14	

Reflections collected	8783
Independent reflections	3587 [R(int) = 0.0171]
Completeness to theta = 25.500°	99.7 %
Absorption correction	Semi-empirical from equivalents
Max. and min. transmission	0.8621 and 0.7409
Refinement method	Full-matrix least-squares on F ²
Data / restraints / parameters	3587 / 1 / 318
Goodness-of-fit on F ²	1.060
Final R indices [I > 2sigma(I) = 3417 data]	R1 = 0.0275, wR2 = 0.0633
R indices (all data, 0.78 Å)	R1 = 0.0303, wR2 = 0.0647
Largest diff. peak and hole	0.237 and -0.178 e.Å ⁻³

Table 2. Atomic coordinates ($\times 10^4$) and equivalent isotropic displacement parameters ($\text{\AA}^2 \times 10^3$)

for cdv54. $U(\text{eq})$ is defined as one third of the trace of the orthogonalized U tensor.

	x	y	z	$U(\text{eq})$
O(1)	5972(2)	-2780(2)	8423(1)	25(1)
O(2)	5627(2)	-1119(1)	7345(1)	16(1)
O(3)	5096(2)	628(1)	6274(1)	15(1)
O(4)	6719(2)	-606(1)	4935(1)	18(1)
O(5)	8754(2)	-489(1)	5490(1)	16(1)
O(6)	4019(2)	4808(2)	10036(1)	28(1)
N(1)	8327(2)	2182(2)	8461(1)	16(1)
N(2)	7790(2)	3265(2)	8532(2)	16(1)
N(3)	6114(3)	3395(2)	9234(2)	17(1)
C(1)	10174(3)	1988(2)	7739(2)	16(1)
C(2)	11489(3)	1092(2)	8465(2)	17(1)
C(3)	10474(3)	-151(2)	8639(2)	17(1)
C(4)	9987(3)	-754(2)	7447(2)	15(1)
C(5)	9029(3)	-2036(2)	7530(2)	16(1)
C(6)	6800(3)	-2005(2)	7849(2)	17(1)
C(7)	6452(3)	86(2)	7086(2)	13(1)
C(8)	5715(3)	530(2)	5063(2)	17(1)
C(9)	7073(3)	1614(2)	4732(2)	18(1)
C(10)	8162(3)	2219(2)	5785(2)	17(1)
C(11)	9520(3)	1376(2)	6544(2)	15(1)
C(12)	8644(3)	62(2)	6664(2)	14(1)
C(13)	11366(3)	3165(2)	7513(2)	21(1)

C(14)	5411(3)	4558(2)	9398(2)	20(1)
C(15)	10239(3)	-2924(2)	8310(2)	21(1)
C(16)	3804(3)	427(2)	4302(2)	22(1)

Table 3. Bond lengths [Å] and angles [°] for cdv54.

O(1)-C(6)	1.206(3)
O(2)-C(6)	1.358(2)
O(2)-C(7)	1.457(2)
O(3)-C(7)	1.401(2)
O(3)-C(8)	1.443(2)
O(4)-C(8)	1.417(2)
O(4)-O(5)	1.4752(18)
O(5)-C(12)	1.463(2)
O(6)-C(14)	1.210(2)
N(1)-N(2)	1.239(2)
N(1)-C(1)	1.495(2)
N(2)-N(3)	1.381(2)
N(3)-C(14)	1.368(3)
C(1)-C(13)	1.533(3)
C(1)-C(2)	1.536(3)
C(1)-C(11)	1.562(3)
C(2)-C(3)	1.530(3)
C(3)-C(4)	1.531(3)
C(4)-C(12)	1.529(3)
C(4)-C(5)	1.541(3)
C(5)-C(6)	1.520(3)
C(5)-C(15)	1.527(3)
C(7)-C(12)	1.531(3)
C(8)-C(16)	1.516(3)
C(8)-C(9)	1.537(3)

C(9)-C(10)	1.531(3)
C(10)-C(11)	1.536(3)
C(11)-C(12)	1.556(3)
C(6)-O(2)-C(7)	121.22(14)
C(7)-O(3)-C(8)	113.76(14)
C(8)-O(4)-O(5)	107.62(13)
C(12)-O(5)-O(4)	111.19(12)
N(2)-N(1)-C(1)	114.13(16)
N(1)-N(2)-N(3)	111.67(16)
C(14)-N(3)-N(2)	116.86(17)
N(1)-C(1)-C(13)	113.38(17)
N(1)-C(1)-C(2)	104.80(15)
C(13)-C(1)-C(2)	109.88(16)
N(1)-C(1)-C(11)	108.70(15)
C(13)-C(1)-C(11)	110.42(16)
C(2)-C(1)-C(11)	109.47(16)
C(3)-C(2)-C(1)	113.10(17)
C(2)-C(3)-C(4)	110.72(16)
C(12)-C(4)-C(3)	111.63(16)
C(12)-C(4)-C(5)	109.50(16)
C(3)-C(4)-C(5)	114.63(16)
C(6)-C(5)-C(15)	111.95(17)
C(6)-C(5)-C(4)	113.18(16)
C(15)-C(5)-C(4)	113.83(17)
O(1)-C(6)-O(2)	117.96(17)
O(1)-C(6)-C(5)	124.18(18)

O(2)-C(6)-C(5)	117.44(17)
O(3)-C(7)-O(2)	106.20(15)
O(3)-C(7)-C(12)	113.33(15)
O(2)-C(7)-C(12)	113.93(15)
O(4)-C(8)-O(3)	107.68(15)
O(4)-C(8)-C(16)	105.17(17)
O(3)-C(8)-C(16)	107.33(16)
O(4)-C(8)-C(9)	112.15(16)
O(3)-C(8)-C(9)	110.58(16)
C(16)-C(8)-C(9)	113.58(18)
C(10)-C(9)-C(8)	114.21(16)
C(9)-C(10)-C(11)	115.80(18)
C(10)-C(11)-C(12)	112.96(16)
C(10)-C(11)-C(1)	112.01(16)
C(12)-C(11)-C(1)	114.65(16)
O(5)-C(12)-C(4)	104.35(15)
O(5)-C(12)-C(7)	110.80(15)
C(4)-C(12)-C(7)	111.58(15)
O(5)-C(12)-C(11)	106.04(15)
C(4)-C(12)-C(11)	112.23(16)
C(7)-C(12)-C(11)	111.47(15)
O(6)-C(14)-N(3)	123.7(2)

Table 4. Anisotropic displacement parameters ($\text{\AA}^2 \times 10^3$) for cdv54. The anisotropic displacement factor exponent takes the form: $-2\pi^2 [h^2 a^{*2} U^{11} + \dots + 2 h k a^* b^* U^{12}]$

	U ¹¹	U ²²	U ³³	U ²³	U ¹³	U ¹²
O(1)	22(1)	16(1)	37(1)	7(1)	7(1)	-1(1)
O(2)	13(1)	14(1)	22(1)	1(1)	0(1)	-1(1)
O(3)	11(1)	18(1)	14(1)	2(1)	1(1)	2(1)
O(4)	15(1)	20(1)	18(1)	-3(1)	-2(1)	2(1)
O(5)	13(1)	22(1)	14(1)	-4(1)	1(1)	2(1)
O(6)	23(1)	34(1)	26(1)	-3(1)	5(1)	10(1)
N(1)	13(1)	17(1)	17(1)	-2(1)	3(1)	0(1)
N(2)	13(1)	18(1)	17(1)	-1(1)	2(1)	-1(1)
N(3)	15(1)	19(1)	17(1)	0(1)	3(1)	-1(1)
C(1)	12(1)	17(1)	18(1)	-2(1)	5(1)	-1(1)
C(2)	12(1)	21(1)	19(1)	-2(1)	1(1)	0(1)
C(3)	14(1)	19(1)	18(1)	1(1)	1(1)	2(1)
C(4)	11(1)	16(1)	17(1)	0(1)	3(1)	2(1)
C(5)	16(1)	15(1)	17(1)	0(1)	2(1)	2(1)
C(6)	17(1)	14(1)	20(1)	-3(1)	0(1)	0(1)
C(7)	12(1)	13(1)	15(1)	0(1)	2(1)	0(1)
C(8)	19(1)	19(1)	14(1)	0(1)	1(1)	3(1)
C(9)	18(1)	22(1)	15(1)	4(1)	2(1)	2(1)
C(10)	16(1)	16(1)	19(1)	4(1)	3(1)	-2(1)
C(11)	13(1)	16(1)	16(1)	0(1)	5(1)	0(1)
C(12)	12(1)	16(1)	12(1)	-1(1)	2(1)	1(1)
C(13)	17(1)	21(1)	24(1)	-1(1)	4(1)	-5(1)

C(14)	20(1)	21(1)	18(1)	-1(1)	-1(1)	4(1)
C(15)	21(1)	19(1)	24(1)	4(1)	0(1)	4(1)
C(16)	21(1)	24(1)	20(1)	-1(1)	-2(1)	0(1)

Table 5. Hydrogen coordinates (\AA) and isotropic displacement parameters ($\text{\AA}^2 \times 10^3$)

for cdv54.

	x	y	z	U (eq)
H(2A)	12680(40)	970(20)	8080(20)	17(6)
H(2B)	11850(40)	1460(20)	9230(20)	19(6)
H(3)	5670(40)	2770(30)	9650(20)	31(7)
H(3A)	9290(40)	-90(20)	9100(20)	18(6)
H(3B)	11460(40)	-670(20)	9070(20)	19(6)
H(4A)	11230(40)	-870(20)	7060(20)	14(5)
H(5A)	8990(30)	-2350(20)	6720(20)	13(5)
H(7A)	6400(30)	510(20)	7791(19)	9(5)
H(9A)	7990(40)	1310(20)	4130(20)	21(6)
H(9B)	6250(30)	2170(20)	4366(19)	13(5)
H(10A)	7100(30)	2580(20)	6280(20)	17(6)
H(10B)	8930(30)	2880(20)	5480(20)	15(5)
H(11A)	10770(40)	1250(20)	6190(20)	12(5)
H(13A)	11690(40)	3520(20)	8290(20)	18(6)
H(13B)	10570(40)	3760(30)	7090(20)	26(7)
H(13C)	12610(40)	2940(20)	7110(20)	24(6)
H(14)	6170(40)	5180(30)	8940(20)	22(6)
H(15A)	9710(40)	-3780(30)	8170(20)	29(7)
H(15B)	10120(40)	-2740(30)	9130(20)	25(6)
H(15C)	11660(40)	-2870(30)	8110(20)	29(7)
H(16A)	3120(40)	-290(30)	4510(20)	21(6)

H(16B)	4150(40)	400(20)	3480(20)	20(6)
H(16C)	2970(40)	1180(20)	4460(20)	18(6)

Table 6. Torsion angles [°] for cdv54.

C(8)-O(4)-O(5)-C(12)	47.96(18)
C(1)-N(1)-N(2)-N(3)	-178.33(15)
N(1)-N(2)-N(3)-C(14)	178.56(18)
N(2)-N(1)-C(1)-C(13)	15.7(2)
N(2)-N(1)-C(1)-C(2)	135.52(17)
N(2)-N(1)-C(1)-C(11)	-107.52(18)
N(1)-C(1)-C(2)-C(3)	62.7(2)
C(13)-C(1)-C(2)-C(3)	-175.11(16)
C(11)-C(1)-C(2)-C(3)	-53.7(2)
C(1)-C(2)-C(3)-C(4)	59.1(2)
C(2)-C(3)-C(4)-C(12)	-56.9(2)
C(2)-C(3)-C(4)-C(5)	177.86(16)
C(12)-C(4)-C(5)-C(6)	-49.9(2)
C(3)-C(4)-C(5)-C(6)	76.4(2)
C(12)-C(4)-C(5)-C(15)	-179.21(16)
C(3)-C(4)-C(5)-C(15)	-52.9(2)
C(7)-O(2)-C(6)-O(1)	153.52(18)
C(7)-O(2)-C(6)-C(5)	-33.5(2)
C(15)-C(5)-C(6)-O(1)	-17.4(3)
C(4)-C(5)-C(6)-O(1)	-147.6(2)
C(15)-C(5)-C(6)-O(2)	170.17(17)
C(4)-C(5)-C(6)-O(2)	39.9(2)
C(8)-O(3)-C(7)-O(2)	-98.18(17)
C(8)-O(3)-C(7)-C(12)	27.7(2)
C(6)-O(2)-C(7)-O(3)	162.55(16)

C(6)-O(2)-C(7)-C(12)	37.1(2)
O(5)-O(4)-C(8)-O(3)	-75.28(16)
O(5)-O(4)-C(8)-C(16)	170.50(14)
O(5)-O(4)-C(8)-C(9)	46.60(19)
C(7)-O(3)-C(8)-O(4)	34.3(2)
C(7)-O(3)-C(8)-C(16)	147.07(17)
C(7)-O(3)-C(8)-C(9)	-88.5(2)
O(4)-C(8)-C(9)-C(10)	-96.2(2)
O(3)-C(8)-C(9)-C(10)	24.0(2)
C(16)-C(8)-C(9)-C(10)	144.73(18)
C(8)-C(9)-C(10)-C(11)	57.4(2)
C(9)-C(10)-C(11)-C(12)	-36.0(2)
C(9)-C(10)-C(11)-C(1)	-167.27(15)
N(1)-C(1)-C(11)-C(10)	64.9(2)
C(13)-C(1)-C(11)-C(10)	-60.0(2)
C(2)-C(1)-C(11)-C(10)	178.88(15)
N(1)-C(1)-C(11)-C(12)	-65.5(2)
C(13)-C(1)-C(11)-C(12)	169.57(16)
C(2)-C(1)-C(11)-C(12)	48.5(2)
O(4)-O(5)-C(12)-C(4)	133.13(14)
O(4)-O(5)-C(12)-C(7)	12.9(2)
O(4)-O(5)-C(12)-C(11)	-108.19(15)
C(3)-C(4)-C(12)-O(5)	166.14(15)
C(5)-C(4)-C(12)-O(5)	-65.84(18)
C(3)-C(4)-C(12)-C(7)	-74.2(2)
C(5)-C(4)-C(12)-C(7)	53.9(2)
C(3)-C(4)-C(12)-C(11)	51.8(2)

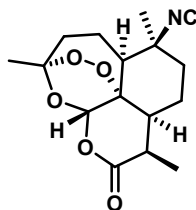
C(5)-C(4)-C(12)-C(11)	179.79(15)
O(3)-C(7)-C(12)-O(5)	-52.7(2)
O(2)-C(7)-C(12)-O(5)	68.84(19)
O(3)-C(7)-C(12)-C(4)	-168.56(16)
O(2)-C(7)-C(12)-C(4)	-47.0(2)
O(3)-C(7)-C(12)-C(11)	65.1(2)
O(2)-C(7)-C(12)-C(11)	-173.31(15)
C(10)-C(11)-C(12)-O(5)	68.13(19)
C(1)-C(11)-C(12)-O(5)	-161.93(14)
C(10)-C(11)-C(12)-C(4)	-178.54(15)
C(1)-C(11)-C(12)-C(4)	-48.6(2)
C(10)-C(11)-C(12)-C(7)	-52.5(2)
C(1)-C(11)-C(12)-C(7)	77.4(2)
N(2)-N(3)-C(14)-O(6)	-176.4(2)

Table 7. Hydrogen bonds for cdv54 [\AA and $^\circ$].

D-H...A	d(D-H)	d(H...A)	d(D...A)	\angle (DHA)
N(3)-H(3)...O(1)#1	0.88(3)	2.53(3)	3.276(2)	143(2)

Symmetry transformations used to generate equivalent atoms:

#1 -x+1,y+1/2,-z+2



1.2

Table 1. Crystal data and structure refinement for cdv57.

Identification code	cdv57 (Riley Mills)	
Empirical formula	$\text{C}_{16} \text{H}_{21} \text{N O}_5$	
Formula weight	307.34	
Temperature	88(2) K	
Wavelength	0.71073 \AA	
Crystal system	Orthorhombic	
Space group	$P2_12_12_1$	
Unit cell dimensions	a = 6.3932(2) \AA	$\alpha = 90^\circ$.
	b = 9.8514(3) \AA	$\beta = 90^\circ$.
	c = 23.6881(8) \AA	$\gamma = 90^\circ$.
Volume	1491.92(8) \AA^3	
Z	4	

Density (calculated)	1.368 Mg/ħ
Absorption coefficient	0.102 mm ⁻¹
F(000)	656
Crystal color	colorless
Crystal size	0.368 x 0.107 x 0.091 mm ³
Theta range for data collection	1.719 to 29.172°
Index ranges	-8 ≤ h ≤ 8, -13 ≤ k ≤ 13, -32 ≤ l ≤ 32
Reflections collected	18742
Independent reflections	3827 [R(int) = 0.0253]
Completeness to theta = 25.500°	100.0 %
Absorption correction	Semi-empirical from equivalents
Max. and min. transmission	0.8622 and 0.8361
Refinement method	Full-matrix least-squares on F ²
Data / restraints / parameters	3827 / 0 / 283
Goodness-of-fit on F ²	1.036
Final R indices [I > 2σ(I) = 3532 data]	R1 = 0.0313, wR2 = 0.0750
R indices (all data, 0.73 Å)	R1 = 0.0360, wR2 = 0.0779
Largest diff. peak and hole	0.285 and -0.165 e.Å ⁻³

Table 2. Atomic coordinates ($\times 10^4$) and equivalent isotropic displacement parameters ($\text{\AA}^2 \times 10^3$)

for cdv57. $U(\text{eq})$ is defined as one third of the trace of the orthogonalized U tensor.

	x	y	z	$U(\text{eq})$
O(1)	168(2)	1050(1)	9154(1)	26(1)
O(2)	320(2)	3023(1)	8730(1)	19(1)
O(3)	249(2)	4930(1)	8188(1)	18(1)
O(4)	1989(2)	3422(1)	7606(1)	20(1)
O(5)	3970(2)	3445(1)	7927(1)	18(1)
N(1)	3513(2)	6732(1)	9258(1)	19(1)
C(1)	5401(3)	6183(2)	8994(1)	17(1)
C(2)	6341(3)	5154(2)	9408(1)	19(1)
C(3)	5038(3)	3864(2)	9468(1)	18(1)
C(4)	4777(2)	3169(2)	8894(1)	15(1)
C(5)	3633(2)	1797(2)	8912(1)	17(1)
C(6)	1273(3)	1918(2)	8961(1)	18(1)
C(7)	1399(2)	4285(2)	8612(1)	15(1)
C(8)	1112(3)	4739(2)	7628(1)	18(1)
C(9)	2718(3)	5849(2)	7498(1)	21(1)
C(10)	3704(3)	6490(2)	8024(1)	19(1)
C(11)	4836(2)	5503(2)	8420(1)	16(1)
C(12)	3709(2)	4114(2)	8472(1)	14(1)
C(13)	2083(3)	7166(2)	9496(1)	27(1)
C(14)	6917(3)	7370(2)	8904(1)	22(1)
C(15)	4517(3)	812(2)	9348(1)	24(1)
C(16)	-732(3)	4714(2)	7226(1)	25(1)

Table 3. Bond lengths [Å] and angles [°] for cdv57.

O(1)-C(6)	1.199(2)
O(2)-C(6)	1.362(2)
O(2)-C(7)	1.4489(19)
O(3)-C(7)	1.3968(19)
O(3)-C(8)	1.4492(19)
O(4)-C(8)	1.415(2)
O(4)-O(5)	1.4767(16)
O(5)-C(12)	1.4588(18)
N(1)-C(13)	1.157(2)
N(1)-C(1)	1.462(2)
C(1)-C(2)	1.533(2)
C(1)-C(14)	1.533(2)
C(1)-C(11)	1.559(2)
C(2)-C(3)	1.526(2)
C(3)-C(4)	1.531(2)
C(4)-C(12)	1.528(2)
C(4)-C(5)	1.537(2)
C(5)-C(6)	1.518(2)
C(5)-C(15)	1.527(2)
C(7)-C(12)	1.523(2)
C(8)-C(16)	1.516(2)
C(8)-C(9)	1.531(2)
C(9)-C(10)	1.532(2)
C(10)-C(11)	1.533(2)
C(11)-C(12)	1.551(2)

C(6)-O(2)-C(7)	123.41(12)
C(7)-O(3)-C(8)	113.48(12)
C(8)-O(4)-O(5)	107.85(11)
C(12)-O(5)-O(4)	111.34(11)
C(13)-N(1)-C(1)	176.02(16)
N(1)-C(1)-C(2)	107.13(13)
N(1)-C(1)-C(14)	107.41(13)
C(2)-C(1)-C(14)	110.23(14)
N(1)-C(1)-C(11)	109.92(13)
C(2)-C(1)-C(11)	111.37(13)
C(14)-C(1)-C(11)	110.65(13)
C(3)-C(2)-C(1)	113.35(13)
C(2)-C(3)-C(4)	110.44(13)
C(12)-C(4)-C(3)	110.96(13)
C(12)-C(4)-C(5)	109.94(12)
C(3)-C(4)-C(5)	114.88(13)
C(6)-C(5)-C(15)	111.42(14)
C(6)-C(5)-C(4)	113.98(13)
C(15)-C(5)-C(4)	113.68(13)
O(1)-C(6)-O(2)	117.38(15)
O(1)-C(6)-C(5)	123.97(15)
O(2)-C(6)-C(5)	118.41(14)
O(3)-C(7)-O(2)	106.20(12)
O(3)-C(7)-C(12)	113.84(13)
O(2)-C(7)-C(12)	114.18(13)
O(4)-C(8)-O(3)	107.62(12)

O(4)-C(8)-C(16)	105.66(14)
O(3)-C(8)-C(16)	106.32(14)
O(4)-C(8)-C(9)	112.47(14)
O(3)-C(8)-C(9)	110.30(13)
C(16)-C(8)-C(9)	114.05(14)
C(8)-C(9)-C(10)	114.03(13)
C(9)-C(10)-C(11)	115.49(14)
C(10)-C(11)-C(12)	112.86(13)
C(10)-C(11)-C(1)	111.79(13)
C(12)-C(11)-C(1)	114.70(12)
O(5)-C(12)-C(7)	110.68(12)
O(5)-C(12)-C(4)	104.67(12)
C(7)-C(12)-C(4)	110.96(12)
O(5)-C(12)-C(11)	106.00(12)
C(7)-C(12)-C(11)	111.75(13)
C(4)-C(12)-C(11)	112.43(12)

Table 4. Anisotropic displacement parameters ($\text{\AA}^2 \times 10^3$) for cdv57. The anisotropic displacement factor exponent takes the form: $-2\pi^2 [h^2 a^{*2} U^{11} + \dots + 2 h k a^* b^* U^{12}]$

	U ¹¹	U ²²	U ³³	U ²³	U ¹³	U ¹²
O(1)	22(1)	28(1)	26(1)	6(1)	1(1)	-7(1)
O(2)	13(1)	22(1)	23(1)	2(1)	1(1)	-2(1)
O(3)	14(1)	21(1)	17(1)	1(1)	-1(1)	3(1)
O(4)	19(1)	23(1)	17(1)	-3(1)	-5(1)	1(1)
O(5)	14(1)	25(1)	14(1)	-3(1)	-1(1)	2(1)
N(1)	18(1)	20(1)	19(1)	-2(1)	-2(1)	1(1)
C(1)	14(1)	20(1)	19(1)	-2(1)	1(1)	1(1)
C(2)	16(1)	22(1)	19(1)	-2(1)	-3(1)	1(1)
C(3)	17(1)	21(1)	16(1)	0(1)	-1(1)	1(1)
C(4)	13(1)	17(1)	15(1)	0(1)	1(1)	1(1)
C(5)	15(1)	18(1)	17(1)	-1(1)	1(1)	0(1)
C(6)	17(1)	22(1)	14(1)	0(1)	0(1)	-2(1)
C(7)	12(1)	18(1)	16(1)	0(1)	1(1)	0(1)
C(8)	19(1)	21(1)	16(1)	0(1)	-2(1)	1(1)
C(9)	23(1)	24(1)	16(1)	3(1)	-1(1)	0(1)
C(10)	19(1)	19(1)	18(1)	3(1)	-1(1)	-2(1)
C(11)	13(1)	18(1)	16(1)	1(1)	2(1)	-1(1)
C(12)	13(1)	17(1)	12(1)	-2(1)	2(1)	0(1)
C(13)	23(1)	31(1)	27(1)	-8(1)	-2(1)	3(1)
C(14)	19(1)	21(1)	27(1)	-2(1)	-1(1)	-3(1)
C(15)	21(1)	21(1)	32(1)	6(1)	-1(1)	0(1)
C(16)	26(1)	28(1)	21(1)	0(1)	-8(1)	1(1)

Table 5. Hydrogen coordinates (\AA) and isotropic displacement parameters ($\text{\AA}^2 \times 10^3$)

for cdv57.

	x	y	z	U (eq)
H(2A)	7670(40)	4900(20)	9265(9)	28(5)
H(2B)	6490(30)	5600(20)	9767(9)	22(5)
H(3A)	3700(40)	4030(20)	9638(9)	22(5)
H(3B)	5730(40)	3210(20)	9723(9)	29(6)
H(4A)	6270(40)	3011(19)	8746(9)	19(5)
H(5A)	3800(30)	1440(20)	8536(8)	16(5)
H(7A)	1270(30)	4848(18)	8947(8)	9(4)
H(9A)	2000(30)	6550(20)	7285(9)	24(5)
H(9B)	3840(40)	5420(20)	7255(9)	26(5)
H(10A)	2640(30)	6940(20)	8237(9)	22(5)
H(10B)	4680(40)	7200(20)	7888(9)	29(5)
H(11A)	6200(30)	5268(19)	8257(8)	13(4)
H(14A)	7350(40)	7730(20)	9261(10)	29(6)
H(14B)	6280(40)	8100(20)	8691(10)	31(6)
H(14C)	8160(40)	7020(20)	8694(11)	40(7)
H(15A)	3870(40)	-30(20)	9286(9)	27(5)
H(15B)	4150(40)	1110(20)	9748(10)	28(6)
H(15C)	6000(40)	760(30)	9297(10)	37(6)
H(16A)	-1640(40)	3950(30)	7307(10)	42(7)
H(16B)	-200(40)	4630(20)	6845(10)	29(6)
H(16C)	-1470(40)	5570(20)	7272(10)	30(6)

Table 6. Torsion angles [°] for cdv57.

C(8)-O(4)-O(5)-C(12)	47.12(15)
N(1)-C(1)-C(2)-C(3)	70.05(17)
C(14)-C(1)-C(2)-C(3)	-173.38(14)
C(11)-C(1)-C(2)-C(3)	-50.17(18)
C(1)-C(2)-C(3)-C(4)	58.24(18)
C(2)-C(3)-C(4)-C(12)	-59.11(17)
C(2)-C(3)-C(4)-C(5)	175.42(13)
C(12)-C(4)-C(5)-C(6)	-47.53(17)
C(3)-C(4)-C(5)-C(6)	78.47(17)
C(12)-C(4)-C(5)-C(15)	-176.69(13)
C(3)-C(4)-C(5)-C(15)	-50.69(18)
C(7)-O(2)-C(6)-O(1)	163.97(15)
C(7)-O(2)-C(6)-C(5)	-21.4(2)
C(15)-C(5)-C(6)-O(1)	-25.3(2)
C(4)-C(5)-C(6)-O(1)	-155.59(15)
C(15)-C(5)-C(6)-O(2)	160.48(14)
C(4)-C(5)-C(6)-O(2)	30.2(2)
C(8)-O(3)-C(7)-O(2)	-98.94(14)
C(8)-O(3)-C(7)-C(12)	27.55(18)
C(6)-O(2)-C(7)-O(3)	156.24(13)
C(6)-O(2)-C(7)-C(12)	29.96(19)
O(5)-O(4)-C(8)-O(3)	-74.74(14)
O(5)-O(4)-C(8)-C(16)	171.98(12)
O(5)-O(4)-C(8)-C(9)	46.95(15)
C(7)-O(3)-C(8)-O(4)	34.50(17)

C(7)-O(3)-C(8)-C(16)	147.34(14)
C(7)-O(3)-C(8)-C(9)	-88.53(16)
O(4)-C(8)-C(9)-C(10)	-96.07(17)
O(3)-C(8)-C(9)-C(10)	24.08(19)
C(16)-C(8)-C(9)-C(10)	143.63(16)
C(8)-C(9)-C(10)-C(11)	58.2(2)
C(9)-C(10)-C(11)-C(12)	-37.71(19)
C(9)-C(10)-C(11)-C(1)	-168.77(14)
N(1)-C(1)-C(11)-C(10)	55.98(17)
C(2)-C(1)-C(11)-C(10)	174.55(14)
C(14)-C(1)-C(11)-C(10)	-62.49(18)
N(1)-C(1)-C(11)-C(12)	-74.13(17)
C(2)-C(1)-C(11)-C(12)	44.43(18)
C(14)-C(1)-C(11)-C(12)	167.40(13)
O(4)-O(5)-C(12)-C(7)	13.69(16)
O(4)-O(5)-C(12)-C(4)	133.30(12)
O(4)-O(5)-C(12)-C(11)	-107.66(13)
O(3)-C(7)-C(12)-O(5)	-53.20(17)
O(2)-C(7)-C(12)-O(5)	68.98(17)
O(3)-C(7)-C(12)-C(4)	-168.96(12)
O(2)-C(7)-C(12)-C(4)	-46.77(17)
O(3)-C(7)-C(12)-C(11)	64.69(16)
O(2)-C(7)-C(12)-C(11)	-173.13(12)
C(3)-C(4)-C(12)-O(5)	168.26(13)
C(5)-C(4)-C(12)-O(5)	-63.55(14)
C(3)-C(4)-C(12)-C(7)	-72.32(16)
C(5)-C(4)-C(12)-C(7)	55.88(16)

C(3)-C(4)-C(12)-C(11)	53.66(16)
C(5)-C(4)-C(12)-C(11)	-178.15(12)
C(10)-C(11)-C(12)-O(5)	69.62(16)
C(1)-C(11)-C(12)-O(5)	-160.79(13)
C(10)-C(11)-C(12)-C(7)	-51.04(17)
C(1)-C(11)-C(12)-C(7)	78.54(16)
C(10)-C(11)-C(12)-C(4)	-176.59(12)
C(1)-C(11)-C(12)-C(4)	-47.00(17)

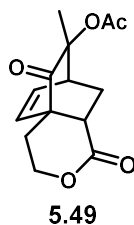


Table 1. Crystal data and structure refinement for cdv68

CCDC number

Empirical formula $C_{14}H_{16}O_5$

Formula weight 264.27

Temperature [K] 93()

Crystal system monoclinic

Space group (number) $P2_1/n$ (14)

a [Å] 6.2135(2)

b [Å]	17.6076(4)
c [Å]	11.0819(4)
α [°]	90
β [°]	95.3222(6)
γ [°]	90
Volume [Å ³]	1207.19(7)
Z	4
ρ_{calc} [gcm ⁻³]	1.454
μ [mm ⁻¹]	0.110
$F(000)$	560
Crystal size [mm ³]	0.356×0.318×0.248
Crystal colour	colorless
Crystal shape	prism
Radiation	MoK α ($\lambda=0.71073$ Å)
2θ range [°]	4.36 to 62.88 ($\theta=0.6$ Å)
Index ranges	$-9 \leq h \leq 9$ $-25 \leq k \leq 24$ $-16 \leq l \leq 16$
Reflections collected	30286

Independent reflections	3781
	$R_{\text{int}} = 0.0258$
	$R_{\text{sigma}} = 0.0175$
Completeness to $\theta = 25.242^\circ$	100.0 %
Data / Restraints / Parameters	3781/0/174
Goodness-of-fit on F^2	1.042
Final R indexes [$\geq 2\sigma(I)$]	$R_1 = 0.0374$ $wR_2 = 0.0920$
Final R indexes [all data]	$R_1 = 0.0454$ $wR_2 = 0.0980$
Largest peak/hole [$\text{e}\text{\AA}^{-3}$]	0.44/-0.35

Table 2. Atomic coordinates and U_{eq} [\AA^2] for cdv68

Atom	x	y	z	U_{eq}
O1	0.45312(14)	0.72572(4)	0.71988(8)	0.02070(17)
O2	0.64886(11)	1.03357(4)	0.76712(6)	0.01158(14)
O3	0.41467(13)	0.75587(4)	0.52555(7)	0.01652(16)
O4	0.75134(12)	1.00865(4)	0.52733(6)	0.01374(15)
O5	0.75623(14)	1.04019(5)	0.96831(7)	0.02270(18)
C1	0.46231(15)	0.77411(6)	0.64338(9)	0.01341(18)
C2	0.52623(14)	0.85643(5)	0.66826(8)	0.01035(17)

H9	0.398371	0.889255	0.643496	0.012
C3	0.59695(15)	0.87167(6)	0.80276(8)	0.01188(17)
H11	0.597794	0.823485	0.848827	0.014
H10	0.493370	0.906750	0.836503	0.014
C4	0.82547(15)	0.90709(5)	0.81557(8)	0.01123(17)
H12	0.877135	0.916137	0.902541	0.013
C5	0.82306(14)	0.98150(5)	0.74156(8)	0.01004(17)
C6	0.64528(16)	1.06262(6)	0.88071(9)	0.01343(18)
C7	0.48742(18)	1.12681(6)	0.88222(10)	0.0183(2)
H1	0.387672	1.117093	0.943977	0.027
H2	0.405548	1.131065	0.802563	0.027
H16	0.565729	1.174285	0.901125	0.027
C8	0.42377(17)	0.81783(6)	0.43860(9)	0.01501(19)
H4	0.310095	0.855572	0.451602	0.018
H3	0.395710	0.797674	0.355234	0.018
C9	0.64369(16)	0.85620(6)	0.45262(9)	0.01348(18)
H8	0.638605	0.902970	0.402849	0.016
H5	0.752805	0.821797	0.422496	0.016
C10	0.71136(15)	0.87659(5)	0.58525(8)	0.01013(17)
C11	0.75842(14)	0.96134(5)	0.60654(8)	0.00990(17)
C12	0.91670(15)	0.83803(5)	0.64006(9)	0.01278(18)
H7	0.998826	0.805048	0.594331	0.015
C13	0.97408(15)	0.85350(6)	0.75643(9)	0.01328(18)
H6	1.099553	0.832326	0.799153	0.016
C14	1.03732(15)	1.02389(6)	0.75513(9)	0.01413(18)
H15	1.021173	1.072726	0.712833	0.021
H13	1.148084	0.993529	0.720033	0.021
H14	1.080716	1.032729	0.841271	0.021

U_{eq} is defined as 1/3 of the trace of the orthogonalized U_{ij} tensor.

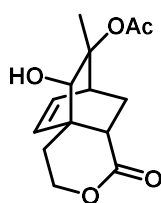
Table 3. Bond lengths and angles for cdv68

Atom–Atom	Length [Å]
O1–C1	1.2070(13)
O2–C6	1.3609(12)
O2–C5	1.4661(11)
O3–C1	1.3507(12)
O3–C8	1.4601(12)
O4–C11	1.2081(12)
O5–C6	1.2040(12)
C1–C2	1.5213(13)
C2–C3	1.5379(13)
C2–C10	1.5785(13)
C3–C4	1.5452(13)
C4–C13	1.5115(13)
C4–C5	1.5451(13)
C5–C14	1.5215(13)
C5–C11	1.5538(13)
C6–C7	1.4976(14)
C8–C9	1.5193(14)
C9–C10	1.5333(13)
C10–C12	1.5212(13)
C10–C11	1.5346(13)
C12–C13	1.3339(14)

Atom–Atom–Atom	Angle [°]
C6–O2–C5	119.31(7)
C1–O3–C8	116.22(8)

O1-C1-O3	119.38(9)
O1-C1-C2	125.03(9)
O3-C1-C2	115.59(8)
C1-C2-C3	112.84(8)
C1-C2-C10	107.50(8)
C3-C2-C10	111.56(7)
C2-C3-C4	109.69(7)
C13-C4-C5	105.98(8)
C13-C4-C3	107.54(8)
C5-C4-C3	109.26(7)
O2-C5-C14	109.21(7)
O2-C5-C4	113.50(7)
C14-C5-C4	113.47(8)
O2-C5-C11	101.50(7)
C14-C5-C11	110.67(8)
C4-C5-C11	107.84(7)
O5-C6-O2	124.41(9)
O5-C6-C7	124.42(9)
O2-C6-C7	111.16(8)
O3-C8-C9	110.75(8)
C8-C9-C10	111.48(8)
C12-C10-C9	115.06(8)
C12-C10-C11	103.40(7)
C9-C10-C11	113.98(8)
C12-C10-C2	107.25(7)
C9-C10-C2	110.86(8)

C11–C10–C2	105.53(7)
O4–C11–C10	124.41(9)
O4–C11–C5	122.07(8)
C10–C11–C5	113.50(8)
C13–C12–C10	115.72(8)
C12–C13–C4	115.30(8)



5.51

Table 1. Crystal data and structure refinement for cdv70.

Identification code	cdv70 (Riley Mills)	
Empirical formula	C ₁₄ H ₁₈ O ₅	
Formula weight	266.28	
Temperature	93(2) K	
Wavelength	0.71073 Å	
Crystal system	Triclinic	
Space group	$P\bar{1}$	
Unit cell dimensions	a = 6.8889(12) Å	$\alpha = 82.560(3)^\circ$.
	b = 9.0969(15) Å	$\beta = 80.589(3)^\circ$.
	c = 10.4736(17) Å	$\gamma = 77.843(3)^\circ$.
Volume	629.92(18) Å ³	
Z	2	

Density (calculated)	1.404 Mg/Å ³
Absorption coefficient	0.106 mm ⁻¹
F(000)	284
Crystal color	colorless
Crystal size	0.349 x 0.268 x 0.229 mm ³
Theta range for data collection	1.981 to 30.587°
Index ranges	-9 ≤ h ≤ 9, -12 ≤ k ≤ 13, -14 ≤ l ≤ 14
Reflections collected	14984
Independent reflections	3771 [R(int) = 0.0314]
Completeness to theta = 25.242°	100.0 %
Absorption correction	Semi-empirical from equivalents
Max. and min. transmission	0.8622 and 0.8326
Refinement method	Full-matrix least-squares on F ²
Data / restraints / parameters	3771 / 0 / 244
Goodness-of-fit on F ²	1.026
Final R indices [I>2sigma(I) = 3182 data]	R1 = 0.0410, wR2 = 0.0946
R indices (all data, 0.70 Å)	R1 = 0.0504, wR2 = 0.1013
Largest diff. peak and hole	0.413 and -0.236 e.Å ⁻³

Table 2. Atomic coordinates ($\times 10^4$) and equivalent isotropic displacement parameters ($\text{\AA}^2 \times 10^3$)

for cdv70. U(eq) is defined as one third of the trace of the orthogonalized U tensor.

	x	y	z	U(eq)
O(1)	7384(1)	7283(1)	146(1)	15(1)
O(2)	6678(1)	2589(1)	3211(1)	15(1)
O(3)	7970(1)	3003(1)	4893(1)	17(1)
O(4)	5608(1)	8952(1)	3122(1)	12(1)
O(5)	4001(1)	9969(1)	1411(1)	16(1)
C(1)	6744(2)	7060(1)	1500(1)	10(1)
C(2)	7379(2)	8184(1)	2300(1)	10(1)
C(3)	8697(2)	7269(1)	3304(1)	11(1)
C(4)	10434(2)	6266(1)	2573(1)	13(1)
C(5)	9909(2)	5300(1)	1903(1)	12(1)
C(6)	7671(2)	5414(1)	1970(1)	10(1)
C(7)	7128(2)	4248(1)	1210(1)	13(1)
C(8)	5768(2)	3293(1)	2064(1)	15(1)
C(9)	7214(2)	3532(1)	3932(1)	12(1)
C(10)	6763(2)	5193(1)	3444(1)	10(1)
C(11)	7501(2)	6216(1)	4245(1)	12(1)
C(12)	8459(2)	9360(1)	1475(1)	15(1)
C(13)	4075(2)	9819(1)	2573(1)	12(1)
C(14)	2492(2)	10554(1)	3583(1)	18(1)

Table 3. Bond lengths [Å] and angles [°] for cdv70.

O(1)-C(1)	1.4167(13)
O(1)-H(1)	0.85(2)
O(2)-C(9)	1.3550(14)
O(2)-C(8)	1.4567(14)
O(3)-C(9)	1.2073(14)
O(4)-C(13)	1.3415(13)
O(4)-C(2)	1.4735(13)
O(5)-C(13)	1.2158(14)
C(1)-C(6)	1.5501(15)
C(1)-C(2)	1.5704(15)
C(1)-H(1A)	1.004(14)
C(2)-C(12)	1.5262(15)
C(2)-C(3)	1.5460(15)
C(3)-C(4)	1.5075(15)
C(3)-C(11)	1.5463(15)
C(3)-H(3A)	0.962(15)
C(4)-C(5)	1.3310(16)
C(4)-H(4A)	0.967(15)
C(5)-C(6)	1.5134(15)
C(5)-H(5A)	0.971(16)
C(6)-C(7)	1.5435(15)
C(6)-C(10)	1.5724(14)
C(7)-C(8)	1.5165(16)

C(7)-H(7A)	0.990(16)
C(7)-H(7B)	0.990(16)
C(8)-H(8A)	0.973(16)
C(8)-H(8B)	0.985(16)
C(9)-C(10)	1.5143(15)
C(10)-C(11)	1.5392(15)
C(10)-H(10A)	0.990(15)
C(11)-H(11A)	0.976(15)
C(11)-H(11B)	0.972(15)
C(12)-H(12A)	0.975(17)
C(12)-H(12B)	0.972(17)
C(12)-H(12C)	0.988(16)
C(13)-C(14)	1.5016(16)
C(14)-H(14A)	0.95(2)
C(14)-H(14B)	0.96(2)
C(14)-H(14C)	0.97(2)
C(1)-O(1)-H(1)	111.6(13)
C(9)-O(2)-C(8)	116.22(9)
C(13)-O(4)-C(2)	119.97(8)
O(1)-C(1)-C(6)	107.39(8)
O(1)-C(1)-C(2)	113.34(9)
C(6)-C(1)-C(2)	109.56(8)
O(1)-C(1)-H(1A)	109.3(8)
C(6)-C(1)-H(1A)	108.7(8)

C(2)-C(1)-H(1A)	108.4(8)
O(4)-C(2)-C(12)	109.52(9)
O(4)-C(2)-C(3)	103.05(8)
C(12)-C(2)-C(3)	110.07(9)
O(4)-C(2)-C(1)	109.93(8)
C(12)-C(2)-C(1)	114.56(9)
C(3)-C(2)-C(1)	109.09(8)
C(4)-C(3)-C(2)	107.66(8)
C(4)-C(3)-C(11)	106.84(9)
C(2)-C(3)-C(11)	109.93(9)
C(4)-C(3)-H(3A)	112.7(9)
C(2)-C(3)-H(3A)	109.6(9)
C(11)-C(3)-H(3A)	110.0(9)
C(5)-C(4)-C(3)	114.51(10)
C(5)-C(4)-H(4A)	124.3(9)
C(3)-C(4)-H(4A)	121.2(9)
C(4)-C(5)-C(6)	114.95(10)
C(4)-C(5)-H(5A)	125.4(9)
C(6)-C(5)-H(5A)	119.6(9)
C(5)-C(6)-C(7)	113.28(9)
C(5)-C(6)-C(1)	108.08(9)
C(7)-C(6)-C(1)	112.27(9)
C(5)-C(6)-C(10)	107.78(8)
C(7)-C(6)-C(10)	110.02(9)
C(1)-C(6)-C(10)	104.98(8)

C(8)-C(7)-C(6)	111.84(9)
C(8)-C(7)-H(7A)	109.1(9)
C(6)-C(7)-H(7A)	110.8(9)
C(8)-C(7)-H(7B)	109.3(9)
C(6)-C(7)-H(7B)	108.9(9)
H(7A)-C(7)-H(7B)	106.7(13)
O(2)-C(8)-C(7)	109.97(9)
O(2)-C(8)-H(8A)	108.2(9)
C(7)-C(8)-H(8A)	113.9(9)
O(2)-C(8)-H(8B)	105.0(9)
C(7)-C(8)-H(8B)	111.1(9)
H(8A)-C(8)-H(8B)	108.3(13)
O(3)-C(9)-O(2)	118.74(10)
O(3)-C(9)-C(10)	125.87(10)
O(2)-C(9)-C(10)	115.39(9)
C(9)-C(10)-C(11)	113.76(9)
C(9)-C(10)-C(6)	109.48(8)
C(11)-C(10)-C(6)	110.62(9)
C(9)-C(10)-H(10A)	104.6(9)
C(11)-C(10)-H(10A)	110.0(9)
C(6)-C(10)-H(10A)	108.1(9)
C(10)-C(11)-C(3)	108.72(8)
C(10)-C(11)-H(11A)	110.4(9)
C(3)-C(11)-H(11A)	109.5(9)
C(10)-C(11)-H(11B)	110.7(9)

C(3)-C(11)-H(11B)	109.9(9)
H(11A)-C(11)-H(11B)	107.7(12)
C(2)-C(12)-H(12A)	109.7(10)
C(2)-C(12)-H(12B)	108.9(10)
H(12A)-C(12)-H(12B)	108.2(14)
C(2)-C(12)-H(12C)	113.5(10)
H(12A)-C(12)-H(12C)	108.4(13)
H(12B)-C(12)-H(12C)	108.0(13)
O(5)-C(13)-O(4)	123.65(10)
O(5)-C(13)-C(14)	125.42(11)
O(4)-C(13)-C(14)	110.93(10)
C(13)-C(14)-H(14A)	110.1(13)
C(13)-C(14)-H(14B)	109.5(12)
H(14A)-C(14)-H(14B)	105.5(17)
C(13)-C(14)-H(14C)	110.4(12)
H(14A)-C(14)-H(14C)	112.0(17)
H(14B)-C(14)-H(14C)	109.2(17)

Table 4. Anisotropic displacement parameters ($\text{\AA}^2 \times 10^3$) for cdv70. The anisotropic

displacement factor exponent takes the form: $-2\pi^2 [h^2 a^{*2} U^{11} + \dots + 2 h k a^* b^* U^{12}]$

	U^{11}	U^{22}	U^{33}	U^{23}	U^{13}	U^{12}
O(1)	24(1)	10(1)	8(1)	0(1)	-2(1)	0(1)
O(2)	23(1)	10(1)	14(1)	0(1)	-4(1)	-5(1)
O(3)	20(1)	15(1)	16(1)	3(1)	-5(1)	-2(1)
O(4)	12(1)	10(1)	11(1)	-3(1)	-1(1)	1(1)
O(5)	20(1)	13(1)	15(1)	1(1)	-4(1)	0(1)
C(1)	12(1)	9(1)	9(1)	-1(1)	-2(1)	-1(1)
C(2)	10(1)	9(1)	10(1)	-2(1)	1(1)	-1(1)
C(3)	11(1)	12(1)	11(1)	-3(1)	-2(1)	-2(1)
C(4)	10(1)	14(1)	13(1)	0(1)	-2(1)	-1(1)
C(5)	11(1)	12(1)	11(1)	0(1)	0(1)	0(1)
C(6)	12(1)	9(1)	8(1)	-1(1)	-2(1)	-1(1)
C(7)	17(1)	10(1)	12(1)	-2(1)	-4(1)	-2(1)
C(8)	17(1)	13(1)	16(1)	-2(1)	-5(1)	-4(1)
C(9)	11(1)	12(1)	12(1)	-1(1)	1(1)	-2(1)
C(10)	10(1)	10(1)	9(1)	-1(1)	-1(1)	-1(1)
C(11)	13(1)	13(1)	9(1)	-1(1)	-2(1)	-3(1)
C(12)	16(1)	12(1)	16(1)	0(1)	0(1)	-5(1)
C(13)	13(1)	7(1)	16(1)	-1(1)	-1(1)	-2(1)
C(14)	16(1)	16(1)	21(1)	-6(1)	2(1)	2(1)

Table 5. Hydrogen coordinates ($\times 10^3$) and isotropic displacement parameters ($\text{\AA}^2 \times 10^3$)

for cdv70.

	x	y	z	U(eq)
H(1)	6880(30)	8160(20)	-172(19)	38(5)
H(1A)	5240(20)	7187(16)	1662(13)	8(3)
H(3A)	9120(20)	7950(16)	3783(14)	12(3)
H(4A)	11800(20)	6340(17)	2606(14)	14(3)
H(5A)	10830(20)	4552(18)	1402(15)	18(4)
H(7A)	6470(20)	4755(18)	456(15)	18(4)
H(7B)	8380(20)	3583(18)	856(15)	20(4)
H(8A)	4440(20)	3855(17)	2353(15)	16(4)
H(8B)	5620(20)	2444(18)	1616(15)	18(4)
H(10A)	5280(20)	5451(17)	3505(14)	14(3)
H(11A)	8360(20)	5608(17)	4849(15)	17(4)
H(11B)	6380(20)	6816(17)	4754(14)	13(3)
H(12A)	9750(30)	8861(19)	1045(16)	24(4)
H(12B)	8710(30)	10046(19)	2041(16)	25(4)
H(12C)	7690(20)	9967(18)	805(16)	21(4)
H(14A)	3080(30)	11050(20)	4120(20)	45(6)
H(14B)	1920(30)	9790(20)	4156(19)	43(5)
H(14C)	1440(30)	11240(20)	3170(20)	45(6)

Table 6. Torsion angles [°] for cdv70.

C(13)-O(4)-C(2)-C(12)	65.50(12)
C(13)-O(4)-C(2)-C(3)	-177.38(9)
C(13)-O(4)-C(2)-C(1)	-61.20(11)
O(1)-C(1)-C(2)-O(4)	127.02(9)
C(6)-C(1)-C(2)-O(4)	-113.05(9)
O(1)-C(1)-C(2)-C(12)	3.20(13)
C(6)-C(1)-C(2)-C(12)	123.13(10)
O(1)-C(1)-C(2)-C(3)	-120.67(9)
C(6)-C(1)-C(2)-C(3)	-0.74(11)
O(4)-C(2)-C(3)-C(4)	172.40(8)
C(12)-C(2)-C(3)-C(4)	-70.86(11)
C(1)-C(2)-C(3)-C(4)	55.63(11)
O(4)-C(2)-C(3)-C(11)	56.37(10)
C(12)-C(2)-C(3)-C(11)	173.11(9)
C(1)-C(2)-C(3)-C(11)	-60.40(11)
C(2)-C(3)-C(4)-C(5)	-59.37(12)
C(11)-C(3)-C(4)-C(5)	58.67(12)
C(3)-C(4)-C(5)-C(6)	1.50(14)
C(4)-C(5)-C(6)-C(7)	-178.53(9)
C(4)-C(5)-C(6)-C(1)	56.41(12)
C(4)-C(5)-C(6)-C(10)	-56.57(12)
O(1)-C(1)-C(6)-C(5)	69.91(11)
C(2)-C(1)-C(6)-C(5)	-53.59(11)

O(1)-C(1)-C(6)-C(7)	-55.75(11)
C(2)-C(1)-C(6)-C(7)	-179.25(9)
O(1)-C(1)-C(6)-C(10)	-175.26(8)
C(2)-C(1)-C(6)-C(10)	61.23(10)
C(5)-C(6)-C(7)-C(8)	124.52(10)
C(1)-C(6)-C(7)-C(8)	-112.71(10)
C(10)-C(6)-C(7)-C(8)	3.82(12)
C(9)-O(2)-C(8)-C(7)	54.34(13)
C(6)-C(7)-C(8)-O(2)	-54.47(12)
C(8)-O(2)-C(9)-O(3)	179.86(10)
C(8)-O(2)-C(9)-C(10)	0.70(13)
O(3)-C(9)-C(10)-C(11)	4.14(16)
O(2)-C(9)-C(10)-C(11)	-176.77(9)
O(3)-C(9)-C(10)-C(6)	128.47(12)
O(2)-C(9)-C(10)-C(6)	-52.44(12)
C(5)-C(6)-C(10)-C(9)	-76.88(11)
C(7)-C(6)-C(10)-C(9)	47.07(11)
C(1)-C(6)-C(10)-C(9)	168.07(9)
C(5)-C(6)-C(10)-C(11)	49.26(11)
C(7)-C(6)-C(10)-C(11)	173.21(9)
C(1)-C(6)-C(10)-C(11)	-65.79(10)
C(9)-C(10)-C(11)-C(3)	130.43(9)
C(6)-C(10)-C(11)-C(3)	6.72(12)
C(4)-C(3)-C(11)-C(10)	-59.94(11)
C(2)-C(3)-C(11)-C(10)	56.61(11)

C(2)-O(4)-C(13)-O(5)

3.42(16)

C(2)-O(4)-C(13)-C(14)

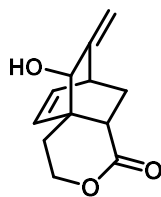
-176.88(9)

Table 7. Hydrogen bonds for cdv70 [Å and °].

D-H...A	d(D-H)	d(H...A)	d(D...A)	<(DHA)
O(1)-H(1)...O(5)#1	0.85(2)	2.05(2)	2.8751(12)	164.3(18)

Symmetry transformations used to generate equivalent atoms:

#1 -x+1,-y+2,-z



5.38

Table 1. Crystal data and structure refinement for cdv71.

Identification code	cdv71 (Riley Mills)	
Empirical formula	C ₁₂ H ₁₄ O ₃	
Formula weight	206.23	
Temperature	133(2) K	
Wavelength	0.71073 Å	
Crystal system	Triclinic	
Space group	$P\bar{1}$	
Unit cell dimensions	a = 6.9370(4) Å	$\alpha = 86.1495(10)^\circ$.
	b = 7.3589(4) Å	$\beta = 89.5224(10)^\circ$.
	c = 10.4415(6) Å	$\gamma = 71.0584(9)^\circ$.
Volume	502.97(5) Å ³	

Z	2
Density (calculated)	1.362 Mg/Å ³
Absorption coefficient	0.097 mm ⁻¹
F(000)	220
Crystal color	colorless
Crystal size	0.337 x 0.332 x 0.136 mm ³
Theta range for data collection	1.955 to 30.968°
Index ranges	-9 ≤ h ≤ 9, -10 ≤ k ≤ 10, -14 ≤ l ≤ 15
Reflections collected	12555
Independent reflections	2986 [R(int) = 0.0287]
Completeness to theta = 25.242°	100.0 %
Absorption correction	Semi-empirical from equivalents
Max. and min. transmission	0.8622 and 0.8098
Refinement method	Full-matrix least-squares on F ²
Data / restraints / parameters	2986 / 0 / 192
Goodness-of-fit on F ²	1.030
Final R indices [I>2sigma(I) = 2544 data]	R1 = 0.0470, wR2 = 0.1260
R indices (all data, 0.69 Å)	R1 = 0.0557, wR2 = 0.1334
Largest diff. peak and hole	0.451 and -0.216 e.Å ⁻³

Table 2. Atomic coordinates ($\times 10^3$) and equivalent isotropic displacement parameters ($\text{\AA}^2 \times 10^3$)

for cdv71. $U(\text{eq})$ is defined as one third of the trace of the orthogonalized U tensor.

	x	y	z	$U(\text{eq})$
O(1)	3768(1)	4475(1)	6710(1)	26(1)
O(2)	6001(1)	4243(1)	8215(1)	33(1)
O(3)	-1267(1)	11278(1)	6917(1)	27(1)
C(1)	432(2)	7140(2)	6633(1)	24(1)
C(2)	1879(2)	5449(2)	5994(1)	28(1)
C(3)	4402(2)	5205(2)	7694(1)	22(1)
C(4)	3139(2)	7120(2)	8169(1)	18(1)
C(5)	4505(2)	8217(2)	8676(1)	24(1)
C(6)	3798(2)	10270(2)	8031(1)	20(1)
C(7)	1576(2)	11193(2)	8337(1)	17(1)
C(8)	227(2)	10123(2)	7820(1)	18(1)
C(9)	1604(2)	8376(2)	7142(1)	16(1)
C(10)	2779(2)	9134(2)	6138(1)	21(1)
C(11)	3912(2)	10107(2)	6594(1)	24(1)
C(12)	869(2)	12764(2)	8986(1)	23(1)

Table 3. Bond lengths [Å] and angles [°] for cdv71.

O(1)-C(3)	1.3319(14)
O(1)-C(2)	1.4575(15)
O(2)-C(3)	1.2143(14)
O(3)-C(8)	1.4222(13)
O(3)-H(3)	0.93(2)
C(1)-C(2)	1.5132(17)
C(1)-C(9)	1.5246(15)
C(1)-H(1A)	0.978(17)
C(1)-H(1B)	0.972(18)
C(2)-H(2A)	0.974(18)
C(2)-H(2B)	0.902(16)
C(3)-C(4)	1.5108(15)
C(4)-C(9)	1.5440(14)
C(4)-C(5)	1.5468(16)
C(4)-H(4A)	0.932(15)
C(5)-C(6)	1.5379(17)
C(5)-H(5A)	0.957(16)
C(5)-H(5B)	0.980(18)
C(6)-C(7)	1.5107(15)
C(6)-C(11)	1.5120(15)
C(6)-H(6A)	0.961(16)
C(7)-C(12)	1.3297(15)
C(7)-C(8)	1.5266(15)

C(8)-C(9)	1.5425(14)
C(8)-H(8A)	0.967(16)
C(9)-C(10)	1.5093(15)
C(10)-C(11)	1.3323(17)
C(10)-H(10A)	0.970(17)
C(11)-H(11A)	0.936(17)
C(12)-H(12A)	0.940(18)
C(12)-H(12C)	0.954(17)
C(3)-O(1)-C(2)	123.70(9)
C(8)-O(3)-H(3)	106.9(11)
C(2)-C(1)-C(9)	109.97(10)
C(2)-C(1)-H(1A)	109.7(10)
C(9)-C(1)-H(1A)	110.2(10)
C(2)-C(1)-H(1B)	107.3(10)
C(9)-C(1)-H(1B)	113.1(11)
H(1A)-C(1)-H(1B)	106.5(14)
O(1)-C(2)-C(1)	114.50(10)
O(1)-C(2)-H(2A)	103.3(10)
C(1)-C(2)-H(2A)	112.8(10)
O(1)-C(2)-H(2B)	103.5(10)
C(1)-C(2)-H(2B)	111.1(10)
H(2A)-C(2)-H(2B)	111.0(14)
O(2)-C(3)-O(1)	117.24(10)
O(2)-C(3)-C(4)	121.67(11)

O(1)-C(3)-C(4)	121.06(10)
C(3)-C(4)-C(9)	112.38(9)
C(3)-C(4)-C(5)	111.34(9)
C(9)-C(4)-C(5)	111.19(9)
C(3)-C(4)-H(4A)	105.5(9)
C(9)-C(4)-H(4A)	108.4(9)
C(5)-C(4)-H(4A)	107.6(9)
C(6)-C(5)-C(4)	108.22(9)
C(6)-C(5)-H(5A)	110.3(10)
C(4)-C(5)-H(5A)	110.9(10)
C(6)-C(5)-H(5B)	110.6(11)
C(4)-C(5)-H(5B)	109.4(10)
H(5A)-C(5)-H(5B)	107.4(14)
C(7)-C(6)-C(11)	106.73(9)
C(7)-C(6)-C(5)	107.83(9)
C(11)-C(6)-C(5)	107.73(9)
C(7)-C(6)-H(6A)	112.4(9)
C(11)-C(6)-H(6A)	111.9(9)
C(5)-C(6)-H(6A)	110.0(9)
C(12)-C(7)-C(6)	123.80(10)
C(12)-C(7)-C(8)	123.63(10)
C(6)-C(7)-C(8)	112.57(8)
O(3)-C(8)-C(7)	112.97(9)
O(3)-C(8)-C(9)	108.05(8)
C(7)-C(8)-C(9)	108.11(8)

O(3)-C(8)-H(8A)	108.0(9)
C(7)-C(8)-H(8A)	111.1(9)
C(9)-C(8)-H(8A)	108.4(10)
C(10)-C(9)-C(1)	114.44(9)
C(10)-C(9)-C(8)	107.17(9)
C(1)-C(9)-C(8)	112.94(9)
C(10)-C(9)-C(4)	108.02(9)
C(1)-C(9)-C(4)	107.54(9)
C(8)-C(9)-C(4)	106.35(8)
C(11)-C(10)-C(9)	114.54(9)
C(11)-C(10)-H(10A)	124.7(11)
C(9)-C(10)-H(10A)	120.8(11)
C(10)-C(11)-C(6)	114.53(10)
C(10)-C(11)-H(11A)	123.7(10)
C(6)-C(11)-H(11A)	121.8(10)
C(7)-C(12)-H(12A)	120.4(11)
C(7)-C(12)-H(12C)	120.6(10)
H(12A)-C(12)-H(12C)	119.0(14)

Table 4. Anisotropic displacement parameters ($\text{\AA}^2 \times 10^3$) for cdv71. The anisotropic

displacement factor exponent takes the form: $-2\pi^2 [h^2 a^{*2} U^{11} + \dots + 2 h k a^* b^* U^{12}]$

	U^{11}	U^{22}	U^{33}	U^{23}	U^{13}	U^{12}
O(1)	24(1)	17(1)	36(1)	-7(1)	-6(1)	-1(1)
O(2)	23(1)	24(1)	44(1)	-6(1)	-10(1)	5(1)
O(3)	23(1)	22(1)	29(1)	-6(1)	-11(1)	4(1)
C(1)	20(1)	18(1)	34(1)	-3(1)	-9(1)	-5(1)
C(2)	30(1)	19(1)	33(1)	-5(1)	-12(1)	-4(1)
C(3)	20(1)	18(1)	26(1)	-2(1)	-1(1)	-2(1)
C(4)	16(1)	17(1)	19(1)	0(1)	-2(1)	-1(1)
C(5)	20(1)	23(1)	26(1)	-5(1)	-9(1)	-1(1)
C(6)	18(1)	21(1)	23(1)	-8(1)	1(1)	-7(1)
C(7)	19(1)	18(1)	14(1)	-1(1)	-1(1)	-4(1)
C(8)	15(1)	17(1)	20(1)	-1(1)	-2(1)	-1(1)
C(9)	15(1)	14(1)	18(1)	-2(1)	-3(1)	-2(1)
C(10)	27(1)	18(1)	16(1)	-3(1)	2(1)	-5(1)
C(11)	28(1)	24(1)	23(1)	-7(1)	10(1)	-11(1)
C(12)	24(1)	23(1)	22(1)	-7(1)	2(1)	-5(1)

Table 5. Hydrogen coordinates ($\times 10^3$) and isotropic displacement parameters ($\text{\AA}^2 \times 10^3$)

for cdv71.

	x	y	z	U(eq)
H(3)	-2200(30)	12200(30)	7368(18)	46(5)
H(1A)	-260(30)	6670(20)	7334(15)	29(4)
H(1B)	-610(30)	7840(30)	6002(16)	35(4)
H(2A)	1300(30)	4420(30)	5890(15)	32(4)
H(2B)	2310(20)	5830(20)	5237(15)	25(4)
H(4A)	2410(20)	6820(20)	8860(14)	20(3)
H(5A)	4420(30)	8260(20)	9590(16)	29(4)
H(5B)	5930(30)	7540(30)	8473(16)	37(5)
H(6A)	4630(20)	10980(20)	8320(14)	23(4)
H(8A)	-470(20)	9660(20)	8508(15)	28(4)
H(10A)	2670(30)	8920(30)	5239(16)	32(4)
H(11A)	4710(30)	10660(20)	6080(15)	28(4)
H(12A)	-540(30)	13310(30)	9125(16)	32(4)
H(12C)	1770(30)	13380(20)	9296(15)	30(4)

Table 6. Torsion angles [°] for cdv71.

C(3)-O(1)-C(2)-C(1)	-13.73(18)
C(9)-C(1)-C(2)-O(1)	44.59(15)
C(2)-O(1)-C(3)-O(2)	179.66(12)
C(2)-O(1)-C(3)-C(4)	1.85(18)
O(2)-C(3)-C(4)-C(9)	161.02(11)
O(1)-C(3)-C(4)-C(9)	-21.27(15)
O(2)-C(3)-C(4)-C(5)	35.53(16)
O(1)-C(3)-C(4)-C(5)	-146.75(11)
C(3)-C(4)-C(5)-C(6)	129.05(10)
C(9)-C(4)-C(5)-C(6)	2.90(13)
C(4)-C(5)-C(6)-C(7)	57.87(11)
C(4)-C(5)-C(6)-C(11)	-56.98(12)
C(11)-C(6)-C(7)-C(12)	-125.92(11)
C(5)-C(6)-C(7)-C(12)	118.57(12)
C(11)-C(6)-C(7)-C(8)	54.12(11)
C(5)-C(6)-C(7)-C(8)	-61.39(11)
C(12)-C(7)-C(8)-O(3)	61.14(14)
C(6)-C(7)-C(8)-O(3)	-118.89(10)
C(12)-C(7)-C(8)-C(9)	-179.34(10)
C(6)-C(7)-C(8)-C(9)	0.63(12)
C(2)-C(1)-C(9)-C(10)	57.56(13)
C(2)-C(1)-C(9)-C(8)	-179.46(9)
C(2)-C(1)-C(9)-C(4)	-62.44(12)

O(3)-C(8)-C(9)-C(10)	67.06(11)
C(7)-C(8)-C(9)-C(10)	-55.52(10)
O(3)-C(8)-C(9)-C(1)	-59.88(12)
C(7)-C(8)-C(9)-C(1)	177.54(9)
O(3)-C(8)-C(9)-C(4)	-177.59(9)
C(7)-C(8)-C(9)-C(4)	59.83(11)
C(3)-C(4)-C(9)-C(10)	-73.43(11)
C(5)-C(4)-C(9)-C(10)	52.14(11)
C(3)-C(4)-C(9)-C(1)	50.56(12)
C(5)-C(4)-C(9)-C(1)	176.13(9)
C(3)-C(4)-C(9)-C(8)	171.80(9)
C(5)-C(4)-C(9)-C(8)	-62.63(11)
C(1)-C(9)-C(10)-C(11)	-175.71(10)
C(8)-C(9)-C(10)-C(11)	58.25(12)
C(4)-C(9)-C(10)-C(11)	-55.99(13)
C(9)-C(10)-C(11)-C(6)	-0.22(15)
C(7)-C(6)-C(11)-C(10)	-56.58(13)
C(5)-C(6)-C(11)-C(10)	59.00(13)

Table 7. Hydrogen bonds for cdv71 [\AA and $^\circ$].

D-H...A	d(D-H)	d(H...A)	d(D...A)	\angle (DHA)
O(3)-H(3)...O(2)#1	0.93(2)	1.88(2)	2.8033(13)	174.7(18)

Symmetry transformations used to generate equivalent atoms:

#1 $x-1, y+1, z$